GEOLOGICA ULTRAIECTINA

Mededelingen van de
Faculteit Aardwetenschappen
Universiteit Utrecht

No. 147

Diagenetic and Catagenetic Transformations of Sequestered Biomarkers

Martin P. Koopmans

STELLINGEN

behorend bij het proefschrift
'Diagenetic and Catagenetic Transformations of Sequestered Biomarkers'

1

De afwezigheid van gemethyleerde benz[*b*]thiofenen en dibenz[*b,d*]thiofenen in kunstmatig gematureerde polymeren van polysulfide gebrugde *n*-octyleenheden kan verklaard worden uit de ketenlengte van de gebruikte monomeer.

Aizenshtat Z., Krein E.B., Vairavamurthy M.A. en Goldstein T.P. (1995) In Geochemical Transformations of Sedimentary Sulfur *(Red. M.A. Vairavamurthy en M.A.A. Schoonen), ACS Symposium Series 612, pp. 16-37. Amer. Chem. Soc., Washington.*

Krein E.B. en Aizenshtat Z. (1995) In Geochemical Transformations of Sedimentary Sulfur *(Red. M.A. Vairavamurthy en M.A.A. Schoonen), ACS Symposium Series 612, pp. 110-137. Amer. Chem. Soc., Washington.*

2

Publicatie van de identificatie van bekende verbindingen is nutteloos.

Barakat A.O. en Rullkötter J. (1994) Energy Fuels **8**, *1168-1174.*

Sinninghe Damsté J.S., de Leeuw J.W., Kock-van Dalen A.C., de Zeeuw M.A., de Lange F., Rijpstra W.I.C. en Schenck P.A. (1987) Geochim. Cosmochim. Acta **51**, *2369-2391.*

3

Het nut van een model voor de vorming van pristaan op basis van hypothetisch ethergebonden pristaan moet ernstig worden betwijfeld.

Tang Y.C. en Stauffer M. (1995) Org. Geochem. **23**, *451-460.*

4

De door Schwark en Püttmann (1990) voorgestelde structuur van een C_{39} diarylisoprenoïd met een reguliere kop-staart isoprenoïde keten is onwaarschijnlijk.

Schwark L. en Püttmann W. (1990) Org. Geochem. **16**, *749-761.*

5

De bewering van Summons en Powell (1986), dat de synthese van enkele isomere arylisoprenoïden uit tetrahydro-β-ionon door Ostroukhov *et al.* (1982) bewijst dat β-caroteen niet de voorloper van arylisoprenoïden met een 2,3,6-trimethyl substitutiepatroon in olie kan zijn, berust waarschijnlijk op onvoldoende kennis van aromatiseringsreacties.

Summons R.E. en Powell T.G. (1986) Nature ***319****, 763-765.*

Ostroukhov S.B., Arefev O.A., Makushina V.M., Zabrodina M.N. en Petrov Al.A. (1982) Neftekhimiya ***22****, 723-788.*

6

Het vrijkomen van verborgen moleculaire fossielen uit hoogmoleculaire fracties van sedimentair organisch materiaal als gevolg van milde thermische processen tijdens de diagenese kan tot gevolg hebben dat bij analyse van rijpere sedimentaire gesteentes het belang van het natuurlijke verzwavelingsproces onderschat wordt.

7

Om potentiële speurders niet te demotiveren verdient het aanbeveling de zinsnede "...maar u kunt ook met de plaatselijke politie bellen..." uit politieberichten weg te laten.

8

De titel van het boek *Op JB*, waarin de ontvoering van Martin Bormann door een geheim Engels commando aan het eind van WO II beschreven wordt, suggereert ten onrechte dat de figuur James Bond toen al geschapen was, en is derhalve misleidend.

Christopher Creighton (1996) Op JB. Simon & Schuster, London.

9

Het besluit van de Klimaatcommissie van de Tweede Kamer, dat de stijging van de gemiddelde temperatuur op aarde veroorzaakt wordt door de toenemende CO_2 concentratie in de atmosfeer, kan achteraf als voorbode beschouwd worden voor de plannen van de Minister van Onderwijs en Wetenschappen voor 'politiek-gestuurd' wetenschappelijk onderzoek.

Utrecht, 10 januari 1997 Martin P. Koopmans

GEOLOGICA ULTRAIECTINA

Mededelingen van de
Faculteit Aardwetenschappen
Universiteit Utrecht

No. 147

Diagenetic and Catagenetic Transformations of Sequestered Biomarkers

Diagenetic and catagenetic transformations of sequestered biomarkers

Diagenetische en catagenetische omzettingen van verborgen moleculaire fossielen

(met een samenvatting in het Nederlands)

Proefschrift ter verkrijging van de graad van doctor
aan de Universiteit Utrecht
op gezag van de Rector Magnificus, Prof. Dr. J.A. van Ginkel
ingevolge het besluit van het College van Decanen
in het openbaar te verdedigen
op vrijdag 10 januari 1997 des middags te 14:30 uur

door
Martin Pieter Koopmans
geboren op 27 april 1966, te Amsterdam

Promotor: Prof. Dr. J.W. de Leeuw
Co-promotor: Dr. Ir. J.S. Sinninghe Damsté

This study was partly financed by a studentship from *Shell Research and Technical Services*

ISBN 90-5744-005-9

This thesis is based on the following papers:

Chapter 2. Koopmans M.P., Sinninghe Damsté J.S., Lewan M.D. and de Leeuw J.W. (1995) Thermal stability of thiophene biomarkers as studied by hydrous pyrolysis. *Org. Geochem.* **23**, 583-596.

Chapter 3. Koopmans M.P., de Leeuw J.W., Lewan M.D. and Sinninghe Damsté J.S. (1996) Impact of dia- and catagenesis on sulphur and oxygen sequestration of biomarkers as revealed by artificial maturation of an immature sedimentary rock. *Org. Geochem.* Accepted.

Chapter 4. Koopmans M.P., Rijpstra W.I.C., de Leeuw J.W., Lewan M.D. and Sinninghe Damsté J.S. (1997) Artificial maturation of an immature sulphur- and organic-rich limestone from the Ghareb Formation, Jordan. *Org. Geochem.* Submitted.

Chapter 5. Koopmans M.P., Schaeffer-Reiss C., de Leeuw J.W., Lewan M.D., Maxwell J.R., Schaeffer P. and Sinninghe Damsté J.S. (1997) Sulphur and oxygen sequestration of *n*-C_{37} and *n*-C_{38} unsaturated ketones in an immature kerogen and the release of their carbon skeletons during early stages of thermal maturation. *Geochim. Cosmochim. Acta.* Submitted.

Chapter 6. Koopmans M.P., Rijpstra W.I.C., Klapwijk M.M., de Leeuw J.W., Lewan M.D. and Sinninghe Damsté J.S. (1997) A thermal and chemical degradation approach to decipher pristane and phytane precursors in sedimentary organic matter. In preparation.

Chapter 7. Koopmans M.P., Köster J., van Kaam-Peters H.M.E., Kenig F., Schouten S., Hartgers W.A., de Leeuw J.W. and Sinninghe Damsté J.S. (1996) Diagenetic and catagenetic products of isorenieratene: Molecular indicators for photic zone anoxia. *Geochim. Cosmochim. Acta* **60**, 4467-4496.

Chapter 8. Koopmans M.P., Schouten S., Kohnen M.E.L. and Sinninghe Damsté J.S. (1996) Restricted utility of aryl isoprenoids as indicators for photic zone anoxia. *Geochim. Cosmochim. Acta* **60**, 4873-4876.

Chapter 9. Koopmans M.P., de Leeuw J.W. and Sinninghe Damsté J.S. (1997) Novel cyclised and aromatised diagenetic products of β-carotene in the Green River Shale. *Org. Geochem.* Submitted.

In addition, the author participated in the following research:

Hartgers W.A., Sinninghe Damsté J.S., Koopmans M.P. and de Leeuw J.W. (1993) Sedimentary evidence for a diaromatic carotenoid with an unprecedented aromatic substitution pattern. *J. Chem. Soc., Chem. Commun.*, 1715-1716.

Sinninghe Damsté J.S., Köster J., Baas M., Koopmans M.P., van Kaam-Peters H.M.E., Geenevasen J.A.J. and Kruk C. (1995) Cyclisation and aromatisation of carotenoids during sediment diagenesis. *J. Chem. Soc., Chem. Commun.*, 187-188.

Sinninghe Damsté J.S., Kenig F., Koopmans M.P., Köster J., Schouten S., Hayes J.M. and de Leeuw J.W. (1995) Evidence for gammacerane as an indicator of water column stratification. *Geochim. Cosmochim. Acta* **59**, 1895-1900.

Hoefs M.J.L., van Heemst J.D.H., Gelin F., Koopmans M.P., van Kaam-Peters H.M.E., Schouten S., de Leeuw J.W. and Sinninghe Damsté J.S. (1995) Alternative biological sources for 1,2,3,4-tetramethylbenzene in flash pyrolysates of kerogen. *Org. Geochem.* **23**, 975-979.

van Duin A.C.T., Hollanders B., Smits R.J.A., Baas J.M.A., van de Graaf B., Koopmans M.P. and de Leeuw J.W. (1996) Molecular mechanics calculation of the rotational barriers of 2,2',6-trialkylbiphenyls to explain their GC-elution behaviour. *Org. Geochem.* **24**, 587-591.

Sinninghe Damsté J.S. and Koopmans M.P. (1996) The fate of carotenoids in sediments: An overview. *Pure Appl. Chem.* Submitted.

Sinninghe Damsté J.S., Baas M., Koopmans M.P. and Geenevasen J.A.J. (1996) Cyclisation, aromatisation and expulsion reactions of β-carotene during sediment diagenesis. *J. Chem. Soc., Chem. Commun.* Submitted.

van Duin A.C.T., Sinninghe Damsté J.S., Koopmans M.P., van de Graaf B. and de Leeuw J.W. (1997) A computer simulation method to evaluate diagenetic processes influencing homohopane isomer ratios in sediments: Application in the reconstruction of thermal histories of sedimentary basins. *Geochim. Cosmochim. Acta.* Submitted.

Köster J., van Kaam-Peters H.M.E., Koopmans M.P., de Leeuw J.W. and Sinninghe Damsté J.S. (1997) Sulphurisation of homohopanoids: Effects on carbon number distribution, speciation and 22S/22R epimer ratios. *Geochim. Cosmochim. Acta.* Submitted.

CONTENTS

Summary 11

Samenvatting 15

1. Introduction

1.1 Diagenesis and catagenesis of sedimentary organic matter 19
1.2 Sequestration of biomarkers 20
1.3 Organic sulphur compounds: Origin, occurrence and fate 20
1.4 Carotenoids: Origin, occurrence and fate 22
1.5 Artificial maturation: Hydrous pyrolysis 23
1.6 Scope and framework of the thesis 25

2. Thermal stability of thiophene biomarkers as studied by hydrous pyrolysis

2.1 Abstract 29
2.2 Introduction 29
2.3 Experimental 31
2.4 Results and Discussion 33
2.5 Conclusions 47
2.6 Acknowledgements 48

3. Impact of dia- and catagenesis on sulphur and oxygen sequestration of biomarkers as revealed by artificial maturation of an immature sedimentary rock

3.1 Abstract 49
3.2 Introduction 50
3.3 Experimental 51
3.4 Results 55
3.5 Discussion 79
3.6 Conclusions 96
3.7 Acknowledgements 97

4. Artificial maturation of an immature sulphur- and organic-rich limestone from the Ghareb Formation, Jordan

4.1	Abstract	99
4.2	Introduction	99
4.3	Experimental	100
4.4	Results and Discussion	103
4.5	Conclusions	129
4.6	Acknowledgements	130

5. Sulphur and oxygen sequestration of *n*-C_{37} and *n*-C_{38} unsaturated ketones in an immature kerogen and the release of their carbon skeletons during early stages of thermal maturation

5.1	Abstract	133
5.2	Introduction	134
5.3	Experimental	135
5.4	Results	139
5.5	Discussion	144
5.6	Conclusions	150
5.7	Acknowledgements	151

6. A thermal and chemical degradation approach to decipher pristane and phytane precursors in sedimentary organic matter

6.1	Abstract	153
6.2	Introduction	153
6.3	Experimental	155
6.4	Results	159
6.5	Discussion	175
6.6	Conclusions	181
6.7	Acknowledgements	182

7. Diagenetic and catagenetic products of isorenieratene: Molecular indicators for photic zone anoxia

7.1	Abstract	183
7.2	Introduction	184
7.3	Experimental	187
7.4	Results	189
7.5	Discussion	213
7.6	Conclusions	229
7.7	Acknowledgements	230

8. Restricted utility of aryl isoprenoids as indicators for photic zone anoxia

8.1	Abstract	239
8.2	Introduction	239
8.3	Experimental	240
8.4	Results and Discussion	241
8.5	Conclusions	244
8.6	Acknowledgements	245

9. Novel cyclised and aromatised diagenetic products of β-carotene in the Green River Shale

9.1	Abstract	247
9.2	Introduction	247
9.3	Experimental	248
9.4	Results and Discussion	250
9.5	Conclusions	264
9.6	Acknowledgements	264

References 269

Acknowledgements 301

Curriculum Vitae 303

SUMMARY

In recent years, it has been established that functionalised precursor lipids can be sequestered in high-molecular-weight organic matter fractions of immature sedimentary rocks by reaction with reduced inorganic sulphur species. On the other hand, biomarkers that originate from these precursors are known to occur in a free form in more mature sedimentary rocks and crude oils. The work described in this thesis is directed towards understanding the diagenetic and catagenetic pathways of biomarkers sequestered in high-molecular-weight fractions of immature organic-rich sedimentary rocks, using a combined thermal and chemical degradation approach. In the first part of this thesis (Chapters 2-6), the results of artificial maturation experiments (hydrous pyrolysis) with two immature sulphur-rich sedimentary rocks are described. Analysis of low-molecular-weight hydrocarbons and organic sulphur compounds and chemical degradation of high-molecular-weight organic matter reveals that large changes in biomarker speciation occur already during diagenesis. A distinction can be made between thermally stable forms of biomarkers (*e.g.* hydrocarbons, alkylthiophenes and ketones) and thermally labile forms (*e.g.* sulphur- and oxygen-bound compounds). In the second part of this thesis (Chapters 7-9), a range of novel diagenetic and catagenetic products of the carotenoids isorenieratene and β-carotene is identified, and the reactions that lead to their formation are outlined. The occurrence of carotenoid derivatives in sedimentary rocks up to 450 Ma indicates that the geological preservation potential of carotenoids, which is generally regarded low due to the extended double bond system, is higher than previously thought.

In **Chapter 2**, alkylthiophenes in an artificial maturation series of a sample from the Gessoso-solfifera Formation (Messinian) in Italy are analysed. With increasing thermal maturation, they are formed in large amounts from thermal degradation of the kerogen. The isomer distribution of the alkylthiophenes remains relatively constant during heating so that their use as biomarkers, which was pointed out in previous studies of immature sulphur-rich sedimentary rocks, can now be extended into the oil window. This is exemplified by the specific isomer distributions of alkylthiophenes with *n*-C_{30} and *n*-C_{38} skeletons, which suggest an origin from triacontan-1,15-diol and C_{38} di-unsaturated ketones, respectively.

In **Chapter 3**, a combined thermal and chemical degradation approach is applied to study an immature sulphur-rich sedimentary rock from the Gessoso-solfifera Formation. Biomarkers with different carbon skeletons (*e.g.* *n*-alkanes, isoprenoids, steranes

and hopanes) are followed in several high- and low-molecular-weight fractions as a function of artificial maturation temperature (160-330°C). Phytane and C_{27}-C_{29} steranes, which are present mainly in a sulphur-bound form in the unheated sample, are thermally released at low levels of thermal maturity. Biomarkers originating from multifunctionalised precursors (*e.g.* isorenieratene) are thermally released from the kerogen in a stepwise process. Thermal degradation at relatively low maturation temperatures releases sulphur-linked oligomers into the polar fraction. At higher temperatures, these sulphur links are cleaved as well, and free biomarkers result. Monitoring the speciation of several biomarkers with increasing thermal maturation indicates that alkylthiophenes, ketones, 1,2-di-*n*-alkylbenzenes and free *n*-alkanes are stable thermal degradation products of sulphur- and oxygen-bound carbon skeletons.

In **Chapter 4**, a similar approach is adopted to study a sample from the Ghareb Formation (Late Cretaceous) in Jordan. The results described in Chapters 2 and 3 are generally confirmed, in that hydrocarbons and alkylthiophenes are stable thermal degradation products. The main difference is the abundant formation of alkylthiophenes *vs.* hydrocarbons from the sample from the Ghareb Formation. This is probably due to the larger amount of C-S links per carbon skeleton as compared with the sample from the Gessoso-solfifera Formation. The occurrence of alkylbenzo[*b*]thiophenes and alkyldibenzothiophenes at the highest maturation temperatures (up to 300°C) suggests that they are formed from alkylthiophenes, although experiments at higher temperatures are needed to test this hypothesis.

In **Chapter 5**, the diagenetic pathways of *n*-C_{37} and *n*-C_{38} di- and tri-unsaturated ketones (alkenones) biosynthesised by several Prymnesiophyte algae are deciphered. In the extract of the unheated sample from the Gessoso-solfifera Formation, *n*-C_{37} and *n*-C_{38} skeletons are present in low amounts in a sulphur-bound form. Artificial maturation at temperatures up to 260°C releases large amounts (up to 1 mg/g TOC) of these skeletons from the kerogen, as confirmed by selective chemical degradation experiments with the kerogen of the unheated sample. These results provide another indication that multifunctionalised precursors such as the alkenones are incorporated into the kerogen during early diagenesis, so that in immature samples the presence of the corresponding biomarkers remains unnoticed when only the extract is analysed.

Chapter 6 describes a search for the precursors of the isoprenoid hydrocarbons pristane and phytane in samples from the Gessoso-solfifera, Ghareb, and Green River (Eocene, USA) Formations. Hydrous pyrolysis of these samples yields large amounts of pristane and phytane carbon skeletons, indicating that their precursors are predominantly sequestered in high-molecular-weight fractions. Selective chemical degradation and flash pyrolysis of these fractions suggests a number of precursors, *i.e.* bound tocopherols and pristenes in case of pristane, and phytol and diphytanyl glyceryl ether in case of phytane. The increasing pristane/phytane ratio observed in all three maturation series is due to the higher amount of pristane precursors compared to phytane precursors, and not to the different timing of thermal release of pristane and phytane.

In **Chapter 7**, a suite of novel diagenetic and catagenetic products of the diaromatic carotenoid isorenieratene is identified in a number of sedimentary rocks throughout the Phanerozoic. These compounds are formed by several reactions involving the polyene isoprenoid chain, *i.e.* cyclisation and subsequent aromatisation, expulsion of toluene and *m*-xylene, sulphurisation, C-C bond cleavage, and reduction of double bonds. Isorenieratene is biosynthesised by photosynthetic green sulphur bacteria (*Chlorobiaceae*), organisms that require both light and free H_2S, and is thus an excellent biomarker for photic zone anoxia. *Chlorobiaceae* use the reverse TCA cycle to fix carbon, so that their biomass is enriched in ^{13}C. Therefore, high ^{13}C contents of isorenieratene derivatives are utilised to support their origin from *Chlorobiaceae*. The presence of isorenieratene derivatives in several petroleum source rocks (*e.g.* Duvernay, Exshaw, Schistes Cartons and Kimmeridge Clay Formations) suggests that photic zone anoxia is an important environmental parameter for the preservation of organic matter.

However, care should be taken when identifying diagenetic and catagenetic products of isorenieratene, because similar compounds can also be formed from other carotenoids. This is shown by analysis of a North Sea oil in **Chapter 8**, where aryl isoprenoids with a 2,3,6-trimethyl substitution pattern for the aromatic ring, compounds generally regarded as catagenetic products of isorenieratene, are demonstrated by their ^{13}C content to originate from β-carotene.

The diagenetic products of β-carotene are further described in **Chapter 9**. In a sample from the Green River Formation, a number of β-carotene derivatives is identified that have been formed by the same reactions as the isorenieratene derivatives described in Chapter 7. An additional reaction, however, is aromatisation of the 1,1,5-trimethylcyclohex-5-enyl moieties of β-carotene, which results in 1,2-dimethylbenzene end groups. Despite the identification of a whole range of cyclised and aromatised diagenetic products β-carotene, the large amount of β-carotane indicates that reduction of the double bonds is the most important diagenetic process of β-carotene.

SAMENVATTING

Recent onderzoek heeft uitgewezen dat gefunctionaliseerde lipiden door reactie met gereduceerde anorganische zwavelverbindingen ingebouwd kunnen worden in hoogmoleculaire fracties van het organisch materiaal in onrijpe sedimentaire gesteentes. Ook is het bekend dat moleculaire fossielen die afgeleid zijn van deze gefunctionaliseerde lipiden in rijpere sedimentaire gesteentes en ruwe olie in een vrije vorm voorkomen. Het onderzoek dat in dit proefschrift beschreven wordt is erop gericht om met behulp van thermische en chemische degradatietechnieken de diagenetische en catagenetische reactiepaden te ontrafelen van moleculaire fossielen die verborgen zijn in hoogmoleculaire fracties van onrijpe sedimentaire gesteentes. In het eerste deel van dit proefschrift (Hoofdstuk 2-6) worden de resultaten beschreven van experimenten met twee onrijpe zwavelrijke sedimentaire gesteentes, waarbij de natuurlijke maturatie gesimuleerd wordt door middel van pyrolyse in de aanwezigheid van water. Analyse van laagmoleculaire koolwaterstoffen en organische zwavelverbindingen en chemische degradatie van hoogmoleculair organisch materiaal laat zien dat al tijdens de diagenese grote veranderingen optreden in de verdeling van moleculaire fossielen over verschillende fracties. Er kan onderscheid gemaakt worden tussen thermisch stabiele (bijv. koolwaterstoffen, alkylthiofenen en ketonen) en thermisch labiele (bijv. zwavel- en zuurstofgebonden verbindingen) vormen van moleculaire fossielen. In het tweede deel van dit proefschrift (Hoofdstuk 7-9) wordt een aantal nieuwe diagenetische en catagenetische producten van de carotenoïden isoreniërateen en β-caroteen geïdentificeerd, en hun vormingsreacties worden besproken. Het voorkomen van derivaten van carotenoïden in sedimentaire gesteentes tot 450 miljoen jaar oud geeft aan dat het geologisch preservatiepotentieel van carotenoïden, dat vanwege de vele dubbele bindingen over het algemeen als klein beschouwd wordt, groter is dan tot nog toe werd aangenomen.

In **Hoofdstuk 2** wordt de analyse beschreven van alkylthiofenen in een kunstmatige maturatiereeks van een monster van de Gessoso-solfifera Formatie (Messinien), Italië. Alkylthiofenen worden met toenemende maturatiegraad in grote hoeveelheden gevormd door thermische degradatie van het kerogeen. De isomeerdistributie van de alkylthiofenen blijft relatief constant tijdens de verhitting. Het gebruik van alkylthiofenen als moleculaire fossielen, zoals dat in eerdere studies van onrijpe zwavelrijke sedimentaire gesteentes was gepropageerd, kan nu uitgebreid worden tot de vroege catagenese. Dit wordt verduidelijkt aan de hand van de specifieke isomeerdistributie van alkylthiofenen met n-C_{30} en n-C_{38} skeletten, die wijzen op een oorsprong van respec-

tievelijk triacontaan-1,15-diol en C_{38} tweevoudig onverzadigde ketonen.

In **Hoofdstuk 3** worden thermische en chemische degradatietechnieken toegepast om een onrijp sedimentair gesteente van de Gessoso-solfifera Formatie te bestuderen. Moleculaire fossielen met verschillende koolstofskeletten (bijv. *n*-alkanen, isoprenoïden, steranen en hopanen) die aanwezig zijn in enkele hoog- en laagmoleculaire fracties worden gevolgd als functie van de maturatietemperatuur (160-330°C). Fytaan en C_{27}-C_{29} steranen, die in het onverhitte monster voornamelijk in een zwavelgebonden vorm voorkomen, worden al bij een lage maturatiegraad thermisch vrijgemaakt. Moleculaire fossielen die afgeleid zijn van lipiden met meerdere functionele groepen (bijv. isoreniërateen) worden stapsgewijs thermisch vrijgemaakt uit het kerogeen. Thermische degradatie bij relatief lage maturatietemperaturen resulteert in zwavelgebonden oligomeren die zich in de polaire fractie bevinden. Bij hogere temperaturen worden ook deze zwavelbruggen verbroken, hetgeen resulteert in het vrijkomen van moleculaire fossielen. Registratie van de verdeling van enkele moleculaire fossielen over verschillende fracties met toenemende maturatiegraad geeft aan dat alkylthiofenen, ketonen, 1,2-di-*n*-alkylbenzenen en vrije *n*-alkanen stabiele thermische degradatieproducten zijn van zwavel- en zuurstofgebonden koolstofskeletten.

In **Hoofdstuk 4** wordt een vergelijkbare aanpak gehanteerd voor de bestudering van een monster van de Ghareb Formatie (Boven-Krijt), Jordanië. De resultaten die beschreven zijn in Hoofdstuk 2 en 3, namelijk dat koolwaterstoffen en alkylthiofenen stabiele thermische degradatieproducten zijn, worden over het algemeen bevestigd. Het belangrijkste verschil met de Gessoso-solfifera Formatie is de omvangrijke vorming van alkylthiofenen ten opzichte van koolwaterstoffen, hetgeen waarschijnlijk veroorzaakt wordt door de grotere hoeveelheid C-S bindingen per koolstofskelet in de Ghareb Formatie. De aanwezigheid van alkylbenz[*b*]thiofenen en alkyldibenzthiofenen bij de hoogste maturatietemperaturen (tot 300°C) suggereert dat deze gevormd worden uit alkylthiofenen, hoewel experimenten bij hogere temperaturen nodig zijn om deze hypothese te bevestigen.

In **Hoofdstuk 5** worden de diagenetische reactiepaden ontrafeld van *n*-C_{37} en *n*-C_{38} twee- en drievoudig onverzadigde ketonen (alkenonen) die worden gebiosynthetiseerd door algen van de klasse der *Prymnesiophyceae*. In het extract van het onverhitte monster van de Gessoso-solfifera Formatie zijn *n*-C_{37} en *n*-C_{38} skeletten in lage hoeveelheden aanwezig in een zwavelgebonden vorm. Kunstmatige maturatie bij temperaturen tot 260°C maakt grote hoeveelheden (tot 1 mg/g TOC) van deze skeletten vrij uit het kerogeen. Dit wordt bevestigd door middel van selectieve chemische degradatie van het kerogeen van het onverhitte monster. Deze resultaten vormen een nieuwe aanwijzing dat lipiden met meerdere functionele groepen (zoals alkenonen) tijdens de vroege diagenese worden ingebouwd in het kerogeen, zodat de aanwezigheid van de afgeleide moleculaire fossielen in onrijpe monsters onopgemerkt blijft wanneer alleen het extract wordt geanalyseerd.

In **Hoofdstuk 6** wordt gepoogd de voorlopers van de isoprenoïde koolwaterstoffen

pristaan en fytaan te bepalen in monsters van de Gessoso-solfifera, Ghareb en Green River (Eoceen, VS) Formaties. Kunstmatige maturatie van deze monsters resulteert in grote hoeveelheden van verbindingen met pristaan en fytaan koolstofskeletten, hetgeen aangeeft dat hun voorlopers voornamelijk verborgen zijn in hoogmoleculaire fracties. Selectieve chemische degradatie en flash-pyrolyse van deze fracties wijzen op een aantal mogelijke voorlopers, te weten gebonden tocoferolen en pristenen voor pristaan, en fytol en difytanylglycerylether voor fytaan. De toenemende pristaan/fytaan ratio die in alle drie maturatiereeksen wordt waargenomen is een gevolg van de grotere hoeveelheid voorlopers van pristaan ten opzichte van die van fytaan, en niet van de verschillende temperaturen waarbij pristaan en fytaan thermisch vrijgemaakt worden.

In **Hoofdstuk 7** wordt een reeks van nieuwe diagenetische en catagenetische producten van de diaromatische carotenoïd isoreniërateen geïdentificeerd in een aantal sedimentaire gesteentes uit het Phanerozoïcum. Deze verbindingen zijn gevormd door een aantal reacties van de polyeen isoprenoïde keten, te weten cyclisatie gevolgd door aromatisering, expulsie van tolueen en *m*-xyleen, verzwaveling, verbreking van C-C bindingen, en reductie van dubbele bindingen. Isoreniërateen wordt gebiosynthetiseerd door fotosynthetische groene zwavelbacteriën (*Chlorobiaceae*). Deze organismes hebben zowel licht als vrij H_2S nodig, zodat isoreniërateen een bijzonder geschikt moleculair fossiel is voor het vaststellen van anoxia in de fotische zone. *Chlorobiaceae* gebruiken de omgekeerde TCA cyclus om koolstof te binden, zodat hun biomassa verrijkt is in ^{13}C. Hoge ^{13}C concentraties van derivaten van isoreniërateen worden derhalve gebruikt om hun oorsprong van *Chlorobiaceae* te bevestigen. De aanwezigheid van derivaten van isoreniërateen in enkele oliemoedergesteentes (bijv. van de Duvernay, Exshaw, Schistes Cartons en Kimmeridge Clay Formaties) suggereert dat anoxia in de fotische zone een belangrijke parameter is voor de preservatie van organisch materiaal.

Echter, voorzichtigheid moet betracht worden bij de identificatie van diagenetische en catagenetische producten van isoreniërateen, omdat vergelijkbare producten ook uit andere carotenoïden gevormd kunnen worden. Dit wordt in **Hoofdstuk 8** aangetoond middels analyse van een olie uit het Noordzeegebied. Bepaling van ^{13}C concentraties toont aan dat arylisoprenoïden met een 2,3,6-trimethyl substitutiepatroon van de benzeenring, die over het algemeen voor catagenetische producten van isoreniërateen worden gehouden, afkomstig zijn van β-caroteen.

De diagenetische producten van β-caroteen worden in detail beschreven in **Hoofdstuk 9**. Derivaten van β-caroteen, gevormd door dezelfde reacties als de derivaten van isoreniërateen zoals beschreven in Hoofdstuk 7, zijn geïdentificeerd in een monster van de Green River Formatie. Een additionele reactie van β-caroteen is de aromatisering van de 1,1,5-trimethylcyclohex-5-enyl structuureenheden die resulteert in terminale 1,2-dimethylbenzeenringen. Hoewel een groot aantal gecycliseerde en gearomatiseerde diagenetische producten van β-caroteen is geïdentificeerd, geeft de grote hoeveelheid β-carotaan aan dat reductie van de dubbele bindingen het belangrijkste diagenetische proces is.

CHAPTER 1

Introduction

1.1 Diagenesis and catagenesis of sedimentary organic matter

When organic matter settles on the sea floor, it is subjected to a range of (bio)chemical reactions. A large portion of the sedimentary organic matter is reworked by organisms living on the sea floor or in the top layer of the sediment. A small fraction, however, may escape the biosphere and become part of the geosphere. During geologic time, the organic matter is buried and subjected to increasing subsurface temperatures according to the geothermal gradient (*c.* 25°C/km). Initially, this causes mild chemical transformations known as diagenetic reactions (Peters and Moldowan, 1993). Later, when the consolidated sediment is buried deeper and subjected to higher temperatures, more severe reactions such as C-C bond cleavage ('cracking') of organic matter may take place. This process, which can ultimately lead to the formation of petroleum, is known as catagenesis (Peters and Moldowan, 1993).

Over 90% of the sedimentary organic matter in the geosphere exists in the form of kerogen, a macromolecular substance that is insoluble in water and normal organic solvents (Durand, 1980). Because kerogen is the precursor of crude oils, there have been numerous attempts to elucidate its chemical structure both by thermal (*e.g.* Gallegos, 1975; van de Meent *et al.*, 1980; Larter, 1984; Sinninghe Damsté *et al.*, 1989a) and selective chemical (*e.g.* Michaelis and Albrecht, 1979; Mycke *et al.*, 1987; Hofmann *et al.*, 1992; Richnow *et al.*, 1992) degradation techniques, as summarised by Rullkötter and Michaelis (1990). Marine kerogens are thought to comprise mainly two components (Tegelaar *et al.*, 1989; Gelin *et al.*, 1996b), *i.e.* (i) marine algaenans, the resistant non-hydrolysable macromolecular components of marine algae (Derenne *et al.*, 1992; Gelin *et al.*, 1996a), and (ii) sulphur-rich geomacromolecules formed from the reaction of functionalised lipids and reduced inorganic sulphur species during early diagenesis (Sinninghe Damsté *et al.*, 1988b, 1989c). Not all the organic matter in the geosphere is of high-molecular-weight (> *c.* 800 amu) nature. Low-molecular-weight compounds that are either originally present or that have formed from thermal breakdown of kerogen also undergo chemical transformations during dia- and catagenesis.

1.2 Sequestration of biomarkers

Biomarkers are compounds that are unambiguously related to specific biochemical precursors. This genetic relationship can be determined from three characteristics, *i.e.* (i) the carbon skeleton, (ii) the amount and locations of functional groups, and (iii) the stable carbon isotopic composition. The precursor molecule to which a particular biomarker is related is biosynthesised by a particular source organism, and may thus provide valuable information on chemical (*e.g.* redox conditions), physical (*e.g.* water temperature) and biological (*e.g.* presence of specific organisms) aspects of ancient depositional environments.

In thermally immature sedimentary rocks, the palaeoenvironmental information stored in biomarkers may be obscured because their precursor molecules are sequestered in high-molecular-weight fractions. Compounds with specific functional groups (*e.g.* double bonds and carbonyl moieties) may react with reduced inorganic sulphur species during early diagenesis to form sulphur-rich geomacromolecules (see for a review Sinninghe Damsté and de Leeuw, 1990). These biomarkers are therefore not present in the pool of low-molecular-weight compounds that is routinely analysed. Compounds that are not sequestered will consequently provide a biased view of the assemblage of precursor molecules present during deposition of the sediment (Kohnen *et al.*, 1991c). Alternatively, precursor molecules may be linked by oxygen bonds to become part of high-molecular-weight fractions (*e.g.* Michaelis and Albrecht, 1979; Mycke *et al.*, 1987), although the reactions by which these bonds are formed are not well understood.

In order to understand how the palaeoenvironmental information stored in sequestered biomarkers is affected by the chemical transformations occurring during dia- and catagenesis, detailed information is needed about the behaviour of sequestered biomarkers during increasing thermal maturation. In this study, the dia- and catagenetic fate of organic sulphur compounds and carotenoids is studied in detail.

1.3 Organic sulphur compounds: Origin, occurrence and fate

It is generally accepted that organic sulphur compounds occurring in the geosphere are formed during early diagenesis from the reaction of functionalised lipids with reduced inorganic sulphur species (see for a review Sinninghe Damsté and de Leeuw, 1990). The first indications for this 'natural vulcanisation' reaction came from the identification of organic sulphur compounds with specific carbon skeletons unambiguously related to known precursor lipids (*e.g.* Valisolalao *et al.*, 1984; Brassell *et al.*, 1986b; Sinninghe Damsté *et al.*, 1988b). Additional evidence for the sulphurisation of lipids has been gained from laboratory experiments using alkenes (Fukushima *et al.*, 1992; de Graaf *et al.*, 1992, 1995; Rowland *et al.*, 1993; Schouten *et al.*, 1994; Krein and Aizenshtat, 1995), ketones (Schouten *et al.*, 1993, 1994), aldehydes (Schouten *et al.*,

1993, 1994; Krein and Aizenshtat, 1994), unsaturated aldehydes (Rowland *et al.*, 1993; Schouten *et al.*, 1993, 1994; Krein and Aizenshtat, 1994) and unsaturated alcohols (Fukushima *et al.*, 1992; de Graaf *et al.*, 1992; Schouten *et al.*, 1994; Krein and Aizenshtat, 1994, 1995) as substrates. Sulphurisation can occur (i) intramolecularly, resulting in the formation of low-molecular-weight organic sulphur compounds with *e.g.* thiophene, thiolane or thiane moieties, and (ii) intermolecularly, resulting in the formation of macromolecules consisting of carbon skeletons linked by (poly)sulphide bridges (Sinninghe Damsté *et al.*, 1988b). It has been argued that natural sulphurisation during early diagenesis results (almost) exclusively in the formation of intermolecular C-S bonds, and that low-molecular-weight organic sulphur compounds are subsequently formed during increasing thermal maturation (Aizenshtat *et al.*, 1995; Krein and Aizenshtat, 1995). This cannot, however, explain the occurrence of alkylthiophenes in some thermally immature surface sediments (*e.g.* ten Haven *et al.*, 1990; Fukushima *et al.*, 1992; Wakeham *et al.*, 1995).

The varying amounts and distributions of organic sulphur compounds in different sedimentary rocks and immature crude oils have been interpreted in terms of different input of organic matter, palaeoenvironment and level of thermal maturity (Sinninghe Damsté *et al.*, 1989d). It was shown that in particular alkylthiophenes can be used as biomarkers for chemical, physical and biological aspects of ancient depositional environments (Sinninghe Damsté *et al.*, 1990b; Kohnen *et al.*, 1990c). For instance, the occurrence of enhanced amounts of C_{37} and C_{38} 2,5-di-*n*-alkylthiophenes in several bore hole samples from the Jurf ed Darawish oil shale (Cretaceous) suggested an input into the sediment of C_{37} and C_{38} di- and tri-unsaturated methyl and ethyl ketones biosynthesised by several prymnesiophyte algae (Kohnen *et al.*, 1990c). This assessment could not be made on the basis of hydrocarbon biomarkers, because C_{37} and C_{38} *n*-alkanes were not enhanced compared to the other long-chain alkanes in the $C_{35\text{-}40}$ region (Kohnen *et al.*, 1990c). Much of the work in which organic sulphur compounds are used as biomarkers has been performed with thermally immature sedimentary rocks and 'low thermal stress' crude oils. It is not clear if organic sulphur compounds can still be used as biomarkers in samples with levels of thermal maturity approaching the oil window (*i.e.* the interval in sediment burial representing the main phase of oil formation).

The natural sulphurisation process has been shown to sequester functionalised lipids in high-molecular-weight organic matter, so that the remaining pool of hydrocarbons offers a biased view of the lipids present during deposition (Sinninghe Damsté *et al.*, 1988b; Kohnen *et al.*, 1991c, 1992a,b; Adam *et al.*, 1993; Schaeffer *et al.*, 1995b). In some samples, the amount of sequestered hydrocarbons exceeds the amount of hydrocarbons present as such several times. It is of interest to know at what level of thermal maturity these sulphur-bound carbon skeletons are released. For instance, hydrocarbon assemblages from the relatively immature Mulhouse Basin ($R_o \approx 0.3$-0.4%) contain high amounts of phytane and steranes (Keely *et al.*, 1993; Sinninghe Damsté *et al.*, 1993a), compounds typically present in a sulphur-bound form in more

immature sedimentary rocks (*e.g.* Kohnen *et al.*, 1991c). This may suggest that the sediments of the Mulhouse basin, which contain only low amounts of organically-bound sulphur (Sinninghe Damsté *et al.*, 1993b), have already passed through a 'sulphur stage'.

In general, not much is known about the influence of increasing thermal maturation on sulphur-rich organic matter. The early generation of sulphur-rich oil from sulphur-rich source rocks has been ascribed to the preferential release of organically-bound sulphur at low levels of thermal maturity (*e.g.* Gransch and Posthuma, 1974; Orr, 1986; Baskin and Peters, 1992). This early generation has been discussed in terms of the relative weakness of the C-S bond as compared to the C-C bond (Orr, 1986; Baskin and Peters, 1992). Despite several studies on the abundance and distribution of organically-bound sulphur in artificially matured kerogens (Eglinton *et al.*, 1988b, 1990b), evidence on a molecular level for the role of sulphur in the early generation of hydrocarbons is scarce. Moreover, the discrepancy between the organic sulphur compounds present in immature sedimentary rocks and 'low thermal stress' crude oils (alkylsulphides and alkylthiophenes) on one hand and more mature oils (*e.g.* benzo[*b*]thiophenes and dibenzothiophenes) on the other is still a matter of concern (Sinninghe Damsté *et al.*, 1989a; Sinninghe Damsté and de Leeuw, 1990b).

1.4 Carotenoids: Origin, occurrence and fate

Carotenoids are organic compounds with a conjugated polyene backbone comprising a tail-to-tail isoprenoid chain. They are omnipresent in photosynthetic organisms as accessory pigments and to protect photosynthetic tissue against damage by photosensitised oxidation (Goodwin, 1980). Carotenoids are responsible for the bright colours of many plants and animals (Britton *et al.*, 1995). Up to date, more than 600 structurally different carotenoids have been identified (Britton *et al.*, 1995) which can be divided into carotenes (hydrocarbon carotenoids) and xanthophylls (oxygen-containing carotenoids).

Isorenieratene (**I**; Fig. 1.1) is a diaromatic carotene that is biosynthesised by the brown-coloured photosynthetic green sulphur bacteria (Chlorobiaceae; Liaaen-Jensen, 1965). These organisms need light and free H_2S to perform photosynthesis, and therefore they live in a well defined habitat where anoxic water layers extend into the photic zone. Thus, isorenieratene is a valuable biomarker to indicate photic zone anoxia in past depositional environments. This has been shown by the finding of perhydro-isorenieratene (isorenieratane, **II**) after desulphurisation of recent sediments from the Black Sea, which indicated that periods of photic zone anoxia had existed for the last 6000 years (Sinninghe Damsté *et al.*, 1993d). Chlorobiaceae use the reverse TCA cycle to fix carbon (Sirevåg and Ormerod, 1970), so that their biomass is anomalously enriched in ^{13}C (Quandt *et al.*, 1977; Sirevåg *et al.*, 1977). This has provided additional proof for the identification of isorenieratane (**II**) in sediments from the Black Sea (Sinninghe Damsté *et al.*, 1993d) by compound-specific carbon isotopic measurements (Hayes *et*

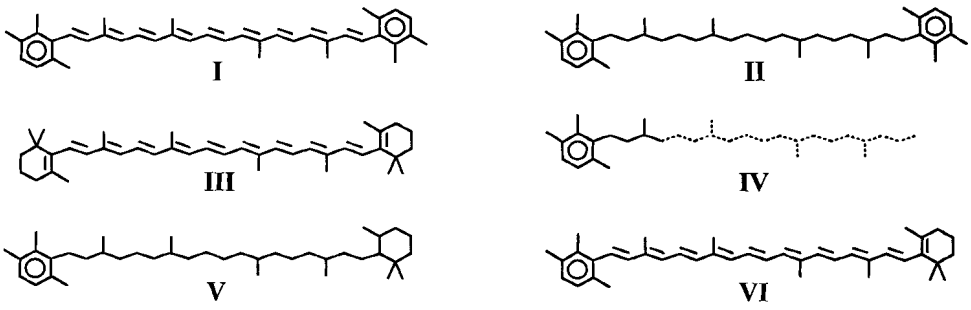

Fig. 1.1. Structures cited in the text.

al., 1990). β-Carotene (**III**) is the most frequently encountered carotene in algae and higher plants, and is therefore much less specific than isorenieratene (**I**). In some algae (*e.g. Dunaliella*), β-carotene (**III**) can amount to more than 10% of the dry weight (Shaish *et al.*, 1992).

Isorenieratene (**I**) and β-carotene (**III**) have been identified in several immature sediments from different depositional environments (*e.g.* Watts *et al.*, 1977; Cardoso *et al.*, 1978). These findings should probably be regarded as relatively rare, because their conjugated double system makes carotenoids susceptible to attack by oxygen and/or light both in the water column and in the top layers of the sediment (Byers and Erdman, 1983). Therefore, low oxygen concentrations in the water column and in the sediment have been regarded as an important factor for the preservation of carotenoids (Sanger, 1988). The geological preservation potential of carotenoids is generally considered to be low (Mackenzie, 1984; Brassell, 1993), despite findings of the perhydro-derivatives of several carotenoids in ancient sedimentary rocks (Murphy *et al.*, 1967; Kimble *et al.*, 1974; Schaeflé *et al.*, 1977; Hartgers *et al.*, 1993). Because the presence of specific carotenoids in the geosphere may provide valuable palaeoenvironmental information (Watts *et al.*, 1977; Sanger, 1988), recognition of carotenoid-derived carbon skeletons and detailed knowledge of the dia- and catagenetic transformations of carotenoids is important.

1.5 Artificial maturation: Hydrous pyrolysis

The dia- and catagenetic fate of sedimentary organic matter is ideally studied in the natural environment. This requires the occurrence of organic-rich rock formations that extend over a depth interval representing a level of thermal maturity from immature into the oil window. However, these natural maturation series are scarce, the Schistes Cartons Formation from the Paris Basin being a notable exception. Consequently, this Formation has been studied extensively for changes in organic matter maturation (*e.g.* Tissot *et al.*, 1971; van Graas *et al.*, 1981; Mackenzie *et al.*, 1980, 1981a). However,

organic facies differences within a particular stratigraphic horizon may hamper the study of organic matter maturation, because the observed differences in organic matter composition cannot be exclusively attributed to the increasing level of thermal maturity. Moreover, the study of the dia- and catagenetic fate of organically-bound sulphur requires a natural maturation series with high amounts of organic sulphur, which is, to the best of our knowledge, not available. In order to simulate the natural maturation process, artificial maturation techniques have been developed. Because the geologic timescales in which these processes take place cannot be copied in the laboratory, experiments are typically conducted at elevated temperatures. Thus, the basic assumption in performing these experiments is that time and temperature are interchangeable. A major advantage of artificial maturation experiments is that the uniformity of the starting material guarantees that the time/temperature conditions under which the experiments are conducted are the only variables.

Artificial maturation basically involves heating an organic-rich sedimentary rock in a closed reactor under an inert atmosphere for a certain amount of time at a certain temperature. Lewan *et al.* (1979) were the first to report an artificial maturation technique (which they called 'hydrous pyrolysis') that involved heating the rock in a reactor filled partly with water. The similarity of the hydrous pyrolysates with natural crude oils led them to suggest that both were formed by similar processes. Heating the rock in the absence of water ('anhydrous pyrolysis') produces compounds (*e.g.* alkenes) not found in petroleum, and is therefore not considered a good simulation of natural petroleum formation (Lewan *et al.*, 1979; Winters *et al.*, 1983). Nevertheless, anhydrous pyrolysis has been widely used as an artificial maturation technique (*e.g.* Mackenzie *et al.*, 1981b; Evans and Felbeck, 1983; Saxby *et al.*, 1986). In addition, other anhydrous techniques have been developed, such as (i) confined pyrolysis (Monthioux *et al.*, 1985; Monthioux, 1988; Landais *et al.*, 1989), where the sample is crushed and confined in a reactor with very little headspace left, and (ii) microscale sealed vessel pyrolysis (MSSV; Horsfield *et al.*, 1989; Horsfield and Düppenbecker, 1991), where the thermal products (of what is essentially a confined pyrolysis experiment) are directly led on a GC column for analysis.

Several studies have compared hydrous and anhydrous pyrolysis (Rullkötter *et al.*, 1984; Comet *et al.*, 1986; Monthioux *et al.*, 1986), and in some cases it was concluded that the presence of water does not play an essential role (Monthioux *et al.*, 1986). However, Lewan (1993) showed that the total amount of pyrolysate after confined pyrolysis of Woodford Shale at 350°C is more than twice lower than the amount generated by hydrous pyrolysis. He also pointed out that the ability of hydrous pyrolysis to generate and expel an oil-like pyrolysate, which enables oil-oil and oil-source rock correlation studies, is a major advantage over anhydrous pyrolysis techniques. In the research described here, hydrous pyrolysis is used because (i) it has proven its usefulness as an artificial maturation technique for the generation of biomarkers from kerogen (*e.g.* Eglinton and Douglas, 1988; Peters *et al.*, 1990), (ii) it allows for the maturation of

relatively large amounts (several hundred grams) of rock, and (iii) it enables fractionation of the pyrolysate, so that different fractions can be analysed and, if desirable, studied by chemical degradation.

The role of water in hydrous pyrolysis experiments has been a matter of debate ever since the technique was first introduced. In particular, the question whether water is just a confining medium or whether it plays a chemical role has been addressed. The thermal degradation of kerogen is retarded in the presence of water (Michels *et al.*, 1995; Lewan, 1997). This has been explained by the role of water as a quencher of radical sites, minimising the role of aromatisation of organic matter as a hydrogen donor (Michels *et al.*, 1995; Lewan, 1997). Hydrous pyrolysis of Woodford Shale at 300, 330 and 350°C for 72 h released much larger amounts of CO_2 than did anhydrous pyrolysis under the same conditions, suggesting an origin from water-derived oxygen (Lewan, 1997). This was supported by experiments using isotopically labeled water (D_2O), which showed that the expelled oil, the bitumen retained in the rock and the kerogen contained significant amounts of deuterium (Lewan, 1997). In addition, hydrous pyrolysis of Kimmeridge Clay kerogen using $H_2{}^{18}O$ yielded alkylated phenols with significant incorporation of ^{18}O (Stalker *et al.*, 1994).

The use of hydrous pyrolysis in organic geochemistry is widespread. It has been applied in the study of (i) kinetics of oil generation (Lewan, 1985; Hunt *et al.*, 1991), (ii) thermal maturity indices such as vitrinite reflectence values (Lewan, 1985; Buchardt and Lewan, 1990), (iii) kerogen/mineral interactions (Eglinton *et al.*, 1986), (iv) isotopic compositions of individual compounds (Bjorøy *et al.*, 1992) and bulk fractions (Lewan, 1983), (v) oil-source rock correlation (Winters *et al.*, 1983; Peters *et al.*, 1989; Moldowan *et al.*, 1992), (vi) thermal transformations of geochemically relevant model compounds (Weres *et al.*, 1988; Smith *et al.*, 1989; Siskin *et al.*, 1990; Navale, 1992, 1994; Leif and Simoneit, 1995) and organisms (Rowland, 1990), (vii) the role of sulphur in the early generation of bitumen and oil from sulphur-rich kerogens (Eglinton *et al.*, 1990b; Baskin and Peters, 1992; Nelson *et al.*, 1995), (viii) biomarker maturity parameter ratios (Lewan *et al.*, 1986; Abbott *et al.*, 1990; Peters *et al.*, 1990), and (ix) biomarker generation from polar fractions (Jones *et al.*, 1988), asphaltenes (Fowler *et al.*, 1988; Jones *et al.*, 1988) and kerogens (Hoering and Navale, 1987; Eglinton and Douglas, 1988; Eglinton *et al.*, 1988a; Abbott *et al.*, 1990; Peters *et al.*, 1990; Huseby *et al.*, 1996). In this study, hydrous pyrolysis is used to induce and investigate dia- and catagenetic transformations of sequestered biomarkers in several immature sedimentary rocks.

1.6 Scope and framework of the thesis

The objective of this research was to investigate the dia- and catagenetic fate of sequestered biomarkers, with special emphasis on organic sulphur compounds and carotenoids. To this end, the natural maturation process was simulated in the laboratory by

hydrous pyrolysis of several immature sedimentary rocks. The free hydrocarbons and low-molecular-weight organic sulphur compounds of the artificially matured samples were analysed, and the high-molecular-weight organic matter was studied by thermal and chemical degradation techniques. These results were then compared with the results obtained from analysis of the unheated sample, which acted as a reference. The resulting combined thermal and chemical degradation approach provides detailed molecular information about the dia- and catagenetic fate of sequestered biomarkers.

The first part of the thesis describes the fate of organic sulphur compounds in the geosphere. In **Chapter 2**, the thermal stability of alkylthiophenes is investigated, in order to assess their applicability as biomarkers at increased levels of thermal maturity. Hydrous pyrolysis of an immature sulphur-rich sedimentary rock from the Gessoso-solfifera Formation generates large amounts of alkylthiophenes from thermal degradation of the kerogen. The isomer distribution of the alkylthiophenes does not change significantly with increasing maturation temperature, so that important information regarding the original positions of functionalities in the precursor molecules is retained. In **Chapter 3**, an integrated thermal and chemical degradation approach is applied to a sample from the Gessoso-solfifera Formation to investigate the dia- and catagenetic fate of organic sulphur compounds and sulphur- and oxygen-bound carbon skeletons. Sulphur-bound skeletons (*e.g.* phytane and steranes) in the polar fraction are released already at low maturation temperatures, and the amounts of the corresponding free hydrocarbons and alkylthiophenes increase simultaneously. These changes occur already at low levels of thermal maturity, as indicated by biomarker maturity parameter ratios. In **Chapter 4**, a similar approach is adopted for a sample from the Ghareb Formation, yielding similar results as described in the previous Chapter. The larger relative amount of alkylthiophenes generated from this sample compared to the sample from the Gessoso-solfifera Formation is ascribed to a higher number of monosulphide links per carbon skeleton. The increasing amounts of alkylbenzo[*b*]thiophenes and alkyldibenzothiophenes allows for a first survey of their formation pathways. In **Chapter 5**, the diagenetic fate of *n*-C_{37} and *n*-C_{38} di- and tri-unsaturated methyl and ethyl ketones (alkenones) biosynthesised by several prymnesiophyte algae is studied in a sample from the Gessoso-solfifera Formation. During early diagenesis, these lipids are incorporated into the kerogen by sulphur and oxygen bonds, as indicated by chemical degradation experiments with the kerogen of the unheated sample. Consequently, the presence of prymnesiophytes in the depositional environment cannot be recognised when only the extractable lipids are taken into account. Hydrous pyrolysis generates large amounts of *n*-C_{37} and *n*-C_{38} carbon skeletons by thermal cleavage of C-S and C-O bonds. These skeletons appear mainly in three forms which are thermally stable, *i.e.* alkanes, 1,2-di-*n*-alkylbenzenes and saturated ketones. In **Chapter 6**, thermal and chemical degradation experiments are described with samples from the Gessoso-solfifera, Ghareb and Green River Formations to identify the precursors of pristane (Pr) and phytane (Ph). Large amounts of Pr and Ph are thermally released by hydrous pyrolysis, indicating that their

precursors are bound in high-molecular-weight fractions. Chemical degradation and flash pyrolysis of high-molecular-weight fractions suggest multiple precursors for both Pr and Ph. The Pr/Ph ratio generally increases with increasing maturation temperature, which is explained in terms of the different amounts of their high-molecular-weight precursors. In summary, the results described in Chapters 2-6 show that sulphur-rich organic matter undergoes thermally induced changes already during diagenesis. These changes can be monitored on a molecular level, and lead to improved assessment of depositional conditions. The thermal stability of alkylthiophenes renders them useful as biomarkers in a maturity interval extending into the oil window.

The second part of the thesis is devoted to the description of the fate of carotenoids in the geosphere. In **Chapter 7**, the identification and occurrence of a whole range of novel dia- and catagenetic products of isorenieratene (**I**) in a suite of samples covering the Phanerozoic is discussed. These compounds have been formed by several processes involving the polyene isoprenoid chain, *i.e.* (i) reaction with reduced inorganic sulphur species, (ii) cyclisation and aromatisation, (iii) expulsion of toluene and *m*-xylene, and (iv) reduction of double bonds. C-C bond cleavage results in the formation of short-chain compounds (*e.g.* aryl isoprenoids, **IV**). Identification is mainly based on NMR, mass spectrometry and stable carbon isotopes. The dia- and catagenetic derivatives of isorenieratene (**I**) can be used as molecular indicators for photic zone anoxia, and are therefore expected to lead to improved recognition of such conditions in ancient sedimentary rocks and crude oils. In **Chapter 8**, β-isorenieratane (**V**) identified in a North Sea oil is shown to be derived from aromatisation of β-carotene (**III**) accompanied by a 1,2-shift of a geminal methyl group, and not from reduction of β-isorenieratene (**VI**) which is biosynthesised by Chlorobiaceae. The aryl isoprenoids (**IV**) have a mixed isotopic signature in the oil, because they can be formed from C-C bond cleavage of both β-isorenieratane (**V**) and isorenieratane (**II**), which was also detected. These results underline the importance of stable carbon isotope measurements for the identification of dia- and catagenetic products of isorenieratene (**I**). In **Chapter 9**, novel cyclised and aromatised diagenetic products of β-carotene (**III**) in the Green River Shale are discussed which are similar to the compounds derived from isorenieratene (**I**). They have been formed by the same reactions, which can be understood because isorenieratene (**I**) and β-carotene (**III**) both contain a polyene isoprenoid chain which enables these reactions. In a number of compounds, both terminal 1,1,5-trimethylcyclo-hex-5-enyl moieties of β-carotene (**III**) have been aromatised, which is accompanied by a rearrangement involving elimination of a methyl group. In summary, the results described in Chapters 7-9 indicate that the geological preservation potential of carotenoids is much larger than previously thought.

CHAPTER 2

Thermal stability of thiophene biomarkers as studied by hydrous pyrolysis

M.P. Koopmans, J.S. Sinninghe Damsté, M.D. Lewan and J.W. de Leeuw

2.1 Abstract

An immature (R_o = 0.25%) sulphur-rich calcareous shale from the Gessoso-solfifera Formation (Messinian) in the Vena del Gesso Basin (northern Italy) was artificially matured by hydrous pyrolysis at constant temperatures ranging from 160 to 330°C for 72 h to study the applicability of alkylthiophenes as molecular indicators during progressive diagenesis and early catagenesis. Artificial maturation at temperatures up to 330°C generated large amounts of alkylthiophenes from the thermal degradation of kerogen. The importance of the kerogen in the production of alkylthiophenes is supported by the observation that the isomer distributions of alkylthiophenes at high temperatures coincide with the isomer distributions of alkylthiophenes in the Curie-point pyrolysate of the isolated kerogen of the original sample. The generation profiles of the thiophenes with a phytane carbon skeleton and the 3,4-di-*n*-alkylthiophenes suggest that continuous degradation of alkylthiophenes is also taking place, so that the overall effect is alkylthiophene concentrations with intermediate values. The structural isomer distribution of linear alkylthiophenes does not change significantly when these compounds are generated at different temperatures. This implies that important information regarding the original positions of functionalities in the precursor molecules is retained and, thus, that alkylthiophenes are useful biomarkers at relatively high levels of thermal maturity (up to R_o $\approx$ 0.95-1.1%).

2.2 Introduction

Several alkylthiophenes bearing an unambiguous link with biochemical precursors have been identified over the last decade (*e.g.* Valisolalao *et al.*, 1984; Brassell *et al.*, 1986b; Sinninghe Damsté *et al.*, 1987a). In these compounds, which are formed by the incorpo-

ration of reduced inorganic sulphur species into functionalised lipids during very early diagenesis (Sinninghe Damsté *et al.*, 1989c; Kohnen *et al.*, 1990b), important information such as the carbon skeleton and the original positions of functional groups has been preserved. This has enabled the use of these organic sulphur compounds as molecular indicators of organic input into, and physical conditions of, the depositional environment (Sinninghe Damsté *et al.*, 1989d, 1990b; Kohnen *et al.*, 1990c). These studies, however, have focused mainly on immature sedimentary rocks ($R_o \leq 0.3\%$). It is presently not known if the use of alkylthiophenes as molecular indicators remains valid in more mature sedimentary rocks and crude oils. However, since alkylthiophenes are much more stable under geological conditions than their biochemical precursors, it has been assumed that the information may be retained even in ancient sedimentary rocks (Sinninghe Damsté *et al.*, 1989c).

There are several aspects to the thermal stability of alkylthiophenes in the geosphere. First, isomerisation of alkylthiophenes, although not very likely, may lead to different structural isomer distributions, which results in loss of important information regarding the original positions of functional groups in the biochemical precursors. Second, thermal degradation of alkylthiophenes may take place by cleavage of side chains (Sinninghe Damsté and de Leeuw, 1990). Third, alteration of alkylthiophenes may occur *via* cyclisation and aromatisation reactions, thereby lowering the amount of alkylthiophenes (Sinninghe Damsté *et al.*, 1989d). In all three cases, the application of alkylthiophenes as molecular indicators has lost its validity, since information about either the original position of functional groups or the carbon skeleton has been lost. Our objective is to study these three aspects of thermal stability, thereby evaluating the use of alkylthiophenes as molecular indicators over a larger maturity interval.

In order to assess the thermal stability of alkylthiophenes, artificial maturation of an immature sulphur-rich sedimentary rock from the Gessoso-solfifera Formation (Messinian) in the Vena del Gesso Basin (northern Italy) was carried out by hydrous pyrolysis over a broad temperature interval (160-330°C). The levels of thermal maturity represented by these experiments were estimated on the basis of vitrinite reflectance values from experimental work by Lewan (1993a) and a kinetic model by Burnham and Sweeney (1989) to be 0.65-0.85% R_o at 300°C, and 0.95-1.1% R_o at 330°C. Hydrous pyrolysis is a technique developed to simulate catagenetic processes such as oil generation and expulsion, using typical experimental temperatures between 300 and 365°C (Lewan *et al.*, 1979; Lewan, 1993b). In a few cases it has been used to establish the effect of diagenesis on relative or absolute changes in concentrations of hydrocarbon biomarkers, using temperatures as low as 200°C (Lewan *et al.*, 1986; Eglinton and Douglas, 1988; Peters *et al.*, 1990). In this work, the main interest was in the applicability of alkylthiophenes as molecular indicators during progressive diagenesis and early catagenesis. Therefore, the temperatures used were relatively low, in order to link the results to previous studies on immature sedimentary rocks (*e.g.* Kohnen *et al.*, 1990c).

2.3 Experimental

Sample. For an extensive description of the geology of the Gessoso-solfifera Formation (Messinian) in the Vena del Gesso Basin (northern Italy), see Vai and Ricci Lucchi (1977) and Sinninghe Damsté *et al.* (1995b). This evaporitic basin comprises a sedimentary sequence, consisting of bituminous marl layers topped by gypsum, that is repeated fourteen times. Three samples covering the complete (1.2 m thick) marl layer of evaporitic cycle IV (*i.e.* IV-1A, IV-1B and IV-1C) were collected from a fresh outcrop in the open-pit gypsum mine at Riolo Terme during a field trip in January 1992. A representative sample of the marl layer of cycle IV, assembled by mixing IV-1A, IV-1B and IV-1C in equal amounts, was used in this study. Rock-Eval pyrolysis yielded a total organic carbon of 1.98 wt.%, a T_{max} of 404°C, and a hydrogen index of 238 mg HC/g TOC. Elemental analyses of the isolated kerogen indicated it was an immature Type II-S kerogen with an atomic H/C ratio of 1.44, an atomic O/C ratio of 0.17, and an atomic S_{org}/C ratio of 0.08.

Hydrous pyrolysis. A detailed description of the experimental procedures of a typical hydrous pyrolysis experiment has been given by Lewan (1993b). In short, a one-litre Hastelloy-C276 reactor is filled with 90 to 100 g of rock chips and 475 g of distilled water. The remaining volume is purged and filled with helium at a pressure of 2.4 bars. Artificial maturation was accomplished by heating aliquots isothermally for 72 h at 160, 180, 200, 220, 239, 260, 280, 300 and 330°C, respectively. The temperatures were continuously monitored during the experiments at 30 s intervals. Standard deviations were between ±0.2 and ±0.3°C for all experiments except for the 160°C experiment which had a standard deviation of ±0.6°C. Experiments at 300 and 330°C generated an expelled oil that was recovered from the water surface with a pipette. The reactor walls and the rock chips were rinsed with benzene to recover any sorbed oil films, which occurred in experiments at 260, 280, 300 and 330°C. 95% or more of the originally loaded rock chips was recovered from all the experiments. The residual rock chips were dried in a vacuum oven ($T \leq 50$°C).

Isolation procedure. The analytical procedure has been described previously by Kohnen *et al.* (1991b). In short, the residual rock chips were freeze-dried and ultrasonically extracted with dichloromethane/methanol (7.5:1 v/v). If a sorbed oil or expelled oil was present, it was combined with the extract. This combined extract was separated into a maltene and an asphaltene fraction by repeated precipitation in *n*-heptane. An aliquot of the maltene fraction (*ca.* 250 mg), to which an alkylthiophene standard was added for quantitative analysis (Kohnen *et al.*, 1990c), was fractionated by column chromatography with alumina into an apolar and a polar fraction by elution with *n*-hexane/dichloromethane (9:1 v/v) and dichloromethane/methanol (1:1 v/v), respectively. Further separation of the apolar fraction by argentatious thin-layer chromatography yielded the alkyl-

thiophene fraction (R_f = 0.4-0.9). The extracted rock residues of the original sample and the sample artificially matured at 300°C were demineralised using standard procedures (Lewan *et al.*, 1986) to yield the isolated kerogens for elemental analyses and Curie-point pyrolysis.

Gas chromatography. Gas chromatography (GC) was performed using a Carlo Erba 5300 instrument, equipped with an on-column injector. A fused silica capillary column (25 m x 0.32 mm) coated with CP Sil-5 (film thickness 0.12 μm) was used with helium as carrier gas. The column effluent was monitored by a flame ionisation detector (FID). The samples were injected at 70°C and the oven was subsequently programmed to 130°C at 20°C/min and then at 4°C/min to 320°C, which was held for 20 min.

Gas chromatography-mass spectrometry. Gas chromatography-mass spectrometry (GC-MS) was carried out on a Hewlett-Packard 5890 gas chromatograph interfaced to a VG Autospec Ultima mass spectrometer operated at 70 eV with a mass range m/z 40-800 and a cycle time of 1.8 s (resolution 1000). The gas chromatograph was equipped with a fused silica capillary column (25 m x 0.32 mm) coated with CP Sil-5 (film thickness 0.12 μm). Helium was used as carrier gas. The samples were injected at 60°C and the oven was subsequently programmed to 130°C at 20°C/min and then at 4°C/min to 310°C, which was held for 20 min.

Curie-point pyrolysis gas chromatography-mass spectrometry. Py-GC-MS analyses were carried out on a Hewlett-Packard 5890 gas chromatograph equipped with a FOM-3LX unit for pyrolysis and interfaced to a VG Autospec Ultima mass spectrometer. The operating conditions for the MS were identical to those described above for GC-MS. The samples were applied to a ferromagnetic wire with a Curie temperature of 610°C. The gas chromatograph, equipped with a cryogenic unit, was programmed from 0°C (5 min) to 320°C (20 min) at a rate of 3°C/min. Separation was achieved using a fused silica capillary column (25 m x 0.32 mm) coated with CP Sil-5 (film thickness 0.4 μm). Helium was used as carrier gas.

Quantitation. Alkylthiophenes were quantified by integration of mass chromatograms of their main fragment ions (m/z 97+98, 111+112, 125+126) and the main fragment ions (m/z 127+128) of the alkylthiophene standard, 2,3-dimethyl-5-(1',1'-d_2-hexadecyl)thiophene. Since mass spectrometric detection of compounds gives a molar response, a factor containing the molecular weights of the alkylthiophene quantified and the alkylthiophene standard was introduced to obtain absolute amounts (μg/g TOC of original rock). Because the alkylthiophenes and the alkylthiophene standard are assumed to have a similar ionisation potential, and because the main fragment ions of the alkylthiophenes and the alkylthiophene standard make up a similar portion of the total ion yield (*ca.* 75%), the calculated amounts of alkylthiopenes are considered to be absolute. However,

because the main fragment ions of mid-chain 2,5-di-*n*-alkylthiophenes (m/z 111+112) represent only *ca.* 25% of the total ion yield (Sinninghe Damsté *et al.*, 1989c), the calculated amounts of mid-chain 2,5-di-*n*-alkylthiophenes were multiplied by three.

Quantification of duplicate experiments at 280 and 300°C indicated that the standard deviation is typically 5-25%. The results for the short-chain alkylthiophenes differed more, probably due to differences in amounts of compounds that volatilised during work-up. The results for the C_{28}-C_{32} and C_{37}-C_{38} 2,5-di-*n*-alkylthiophenes also differed more (standard deviation up to 50%). Reported results for the experiments at 280 and 300°C are averages of the duplicate runs.

2.4 Results and Discussion

An immature (R_o = 0.25%) sulphur-rich sedimentary rock from the Gessoso-solfifera Formation (Messinian) in the Vena del Gesso Basin (northern Italy) was artificially matured by hydrous pyrolysis at 160, 180, 200, 220, 239, 260, 280, 300 and 330°C for 72 h. The artificially matured samples and the original sample, which acted as a reference, were analysed for alkylthiophenes. The analysis was carried out using an internal standard (2,3-dimethyl-5-(1',1'-d_2-hexadecyl)thiophene) to enable quantification of alkylthiophenes.

Alkylthiophenes can be readily analysed by mass chromatography of their main fragment ions, resulting from cleavage β to the thiophene ring. Fig. 2.1 shows six summed mass chromatograms (m/z 97+98+111+112+125+126+139+140) of the alkylthiophene fractions of the original sample (**a**) and the samples artificially matured at 180, 220, 260, 300 and 330°C (**b-f**). The maturity-related changes in abundance and distributions of various classes of alkylthiophenes will be discussed in detail. These classes are (i) linear thiophenes, (ii) thiophenes with a phytane carbon skeleton, (iii) C_{37}-C_{38} 2,5-di-*n*-alkylthiophenes, (iv) C_{28}-C_{32} 2,5-di-*n*-alkylthiophenes and (v) C_{36}-C_{44} 3,4-di-*n*-alkylthiophenes.

Linear thiophenes

This class of alkylthiophenes can be subdivided into four groups based on their chromatographic separation. These groups can be discriminated by their main fragment ions: 2-*n*-alkylthiophenes (m/z 97+98), 2-*n*-alkyl-5-methylthiophenes (m/z 111+112), 2-*n*-alkyl-5-ethylthiophenes (m/z 125+126) and mid-chain 2,5-di-*n*-alkylthiophenes (m/z 111+112). The alkylthiophenes with a particular carbon skeleton will appear as a cluster in the gas chromatogram, in which the coeluting mid-chain 2,5-di-*n*-alkylthiophenes elute first, then the 2-*n*-alkyl-5-ethylthiophene, followed by the 2-*n*-alkyl-5-methylthiophene and finally the 2-*n*-alkylthiophene (Sinninghe Damsté *et al.*, 1989c). In Fig. 2.1**a** and **d** these clusters of linear thiophenes are indicated by numbers that represent the total number of carbon atoms.

In the original sample linear thiophenes are present only in minor amounts (mostly

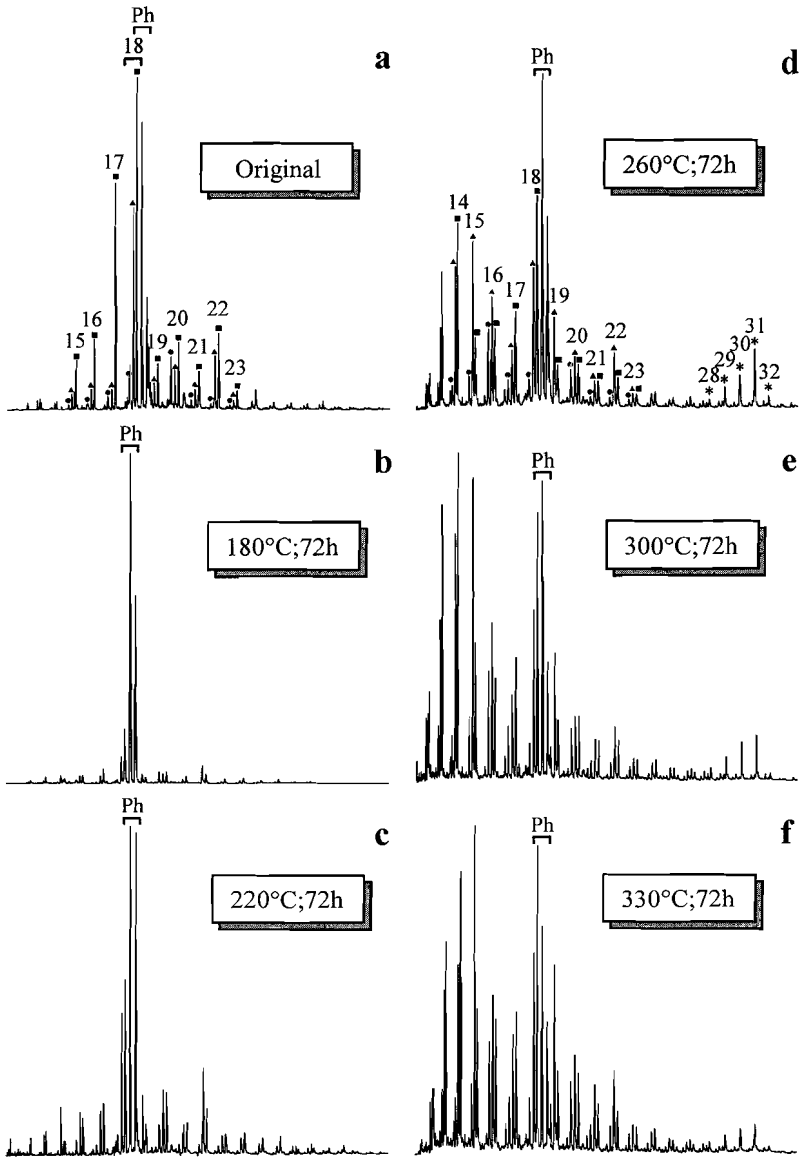

Fig. 2.1. Summed mass chromatograms (m/z 97+98+111+112+125+126+139 +140) of the alkylthiophene fractions of (**a**) the original unheated sample, and the samples subjected to hydrous pyrolysis for 72 h at (**b**) 180°C, (**c**) 220°C, (**d**) 260°C, (**e**) 300°C and (**f**) 330°C. Key: Ph = thiophenes with a phytane carbon skeleton, dots denote 2-*n*-alkyl-5-ethylthiophenes, triangles denote 2-*n*-alkyl-5-methylthiophenes, squares denote 2-*n*-alkylthiophenes and asterisks denote 2,5-di-*n*-alkylthiophenes. Clusters of linear alkylthiophenes are indicated by numbers that represent the total number of carbon atoms.

< 5μg/g TOC). They are dominated by 2-tridecylthiophene, 2-tetradecylthiophene and 2-methyl-5-tridecylthiophene (Fig. 2.1**a**). Artificial maturation at temperatures up to 239°C does not result in significant changes in the amounts of linear thiophenes. This can be seen in Table 2.1 and Fig. 2.2, which shows the summed amounts of C_{14}, C_{17}, C_{20} and C_{26} linear thiophenes as a function of hydrous pyrolysis temperature. Above 239°C large amounts of linear thiophenes are produced (Fig. 2.2). These linear thiophenes are probably derived from the thermal degradation of the kerogen. Curie-point pyrolysis of the isolated kerogen of the original sample yielded linear thiophenes up to C_{26} (Fig. 2.3). Figs. 2.1**c-f** show that the increase in the amounts of short-chain linear thiophenes is larger than the increase in the amounts of long-chain linear thiophenes. This can already be anticipated when the Curie-point pyrolysate of the isolated kerogen of the original sample is studied, because short-chain linear thiophenes are more abundant than long-chain linear thiophenes (Fig. 2.3). At high temperatures, linear thiophenes are present in abundances 20 to 1000 times higher than in the original sample.

In Table 2.2 the isomer distributions of the C_{17} and C_{20} linear thiophenes are given as a function of hydrous pyrolysis temperature. The isomer distribution of the C_{17} linear thiophenes in the original sample is dominated by 2-tridecylthiophene. After thermal treatment at 160°C the relative abundance of 2-dodecyl-5-methylthiophene has increased significantly, which is mainly due to the decreased amount of 2-tridecylthiophene. This results in an isomer distribution that is dominated by 2-tridecylthiophene and 2-methyl-5-dodecylthiophene, whereas 2-ethyl-5-undecylthiophene and the C_{17}

Table 2.1. Absolute amounts (μg/g TOC of original rock) of some linear thiophenes, thiophenes with a phytane carbon skeleton (see for structures Fig. 2.3) and C_{28}-C_{32} mid-chain thiophenes as a function of hydrous pyrolysis temperature.

Compound	original	160°C	180°C	200°C	220°C	239°C	260°C	280°C	300°C	330°C
C_{14} linear thiophenes	0.3	1.1	2.1	1.4	2.5	6.8	$1.0x10^2$	$1.0x10^2$	$2.4x10^2$	$2.6x10^2$
C_{17} linear thiophenes	9.2	4.0	7.2	6.0	10	12	91	$1.0x10^2$	$2.0x10^2$	$2.2x10^2$
C_{20} linear thiophenes	6.6	8.3	16	16	20	24	86	$1.0x10^2$	$1.8x10^2$	$2.4x10^2$
C_{26} linear thiophenes	0.8	0.9	2.3	4.2	4.7	5.5	18	21	35	40
Phytane thiophene I	0.5	4.4	8.9	5.8	10	8.6	49	49	65	60
Phytane thiophene II	11	61	$1.4x10^2$	53	37	19	$2.0x10^2$	$2.2x10^2$	$3.1x10^2$	$1.8x10^2$
Phytane thiophene III	4.2	26	86	49	41	45	$1.2x10^2$	$1.0x10^2$	$1.3x10^2$	$1.1x10^2$
Total phytane thiophenes	16	91	$2.4x10^2$	$1.1x10^2$	88	72	$3.6x10^2$	$3.7x10^2$	$5.0x10^2$	$3.6x10^2$
C_{28} mid-chain thiophenes	0	0	0	1.3	2.0	2.9	12	17	53	39
C_{29} mid-chain thiophenes	0	0	0	2.6	4.1	10	43	33	89	83
C_{30} mid-chain thiophenes	0	0	0	2.8	3.5	12	79	51	$1.3x10^2$	$1.2x10^2$
C_{31} mid-chain thiophenes	0	0	0	4.7	5.9	24	$1.4x10^2$	81	$1.6x10^2$	$1.3x10^2$
C_{32} mid-chain thiophenes	0	0	0	1.8	1.2	3.3	24	18	49	27

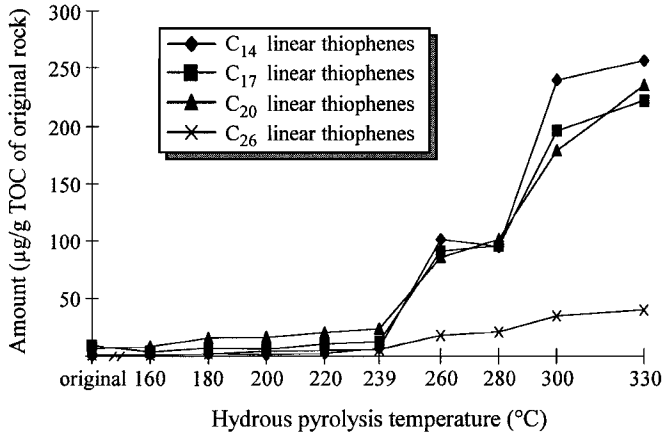

Fig. 2.2. Absolute amounts (µg/g TOC of original rock) of C_{14}, C_{17}, C_{20} and C_{26} linear alkylthiophenes as a function of hydrous pyrolysis temperature.

mid-chain 2,5-di-*n*-alkylthiophenes are significantly less abundant (Table 2.2). Further thermal stress causes a slight decrease in the relative abundance of 2-tridecylthiophene and 2-methyl-5-dodecylthiophene, and a slight increase in the relative abundance of 2-ethyl-5-undecylthiophene and the C_{17} mid-chain 2,5-di-*n*-alkylthiophenes. It is interesting to note that the isomer distribution of the C_{17} linear thiophenes at 330°C is already reflected in the Curie-point pyrolysate of the isolated kerogen of the original sample (Table 2.2). This indicates that the originally present linear thiophenes are diluted by the quantitatively more important thiophenes generated from the bulk of the organic matter (*i.e.* kerogen). There are no indications for the occurrence of isomerisation reactions during hydrous pyrolysis. The compositions of the alkylthiophenes thus reflect the original sites of sulphurisation. The isomer distribution of the C_{20} linear thiophenes shows more variation with temperature (Table 2.2), but the distribution at 330°C does not differ much from the distribution in the Curie-point pyrolysate of the isolated kerogen of the original sample. The high abundance of the linear alkylthiophenes at high maturation temperatures suggests that linear alkylthiophenes are still useful as biomarkers at relatively high levels of thermal maturity ($R_o \approx 0.95$-1.1%), but their original composition may be altered by dilution with thiophenes generated from the kerogen.

Thiophenes with a phytane carbon skeleton

In the alkylthiophene fraction of the original sample three thiophenes with a phytane carbon skeleton (**I-III**; see Fig. 2.3) are major compounds (Fig. 2.1**a**). These isoprenoid thiophenes are widespread in sedimentary rocks and are thought to originate from the incorporation of reduced inorganic sulphur species into chlorophyll-derived phytol or its diagenetic products phytadienes and phytenal (Brassell *et al.*, 1986b; Sinninghe Damsté

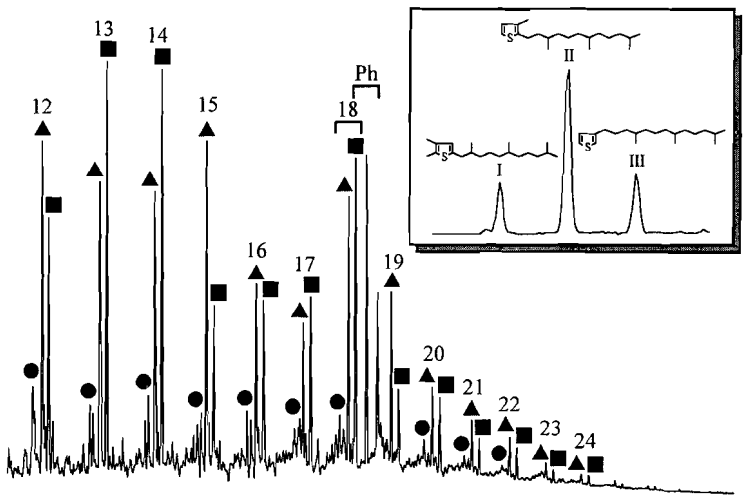

Fig. 2.3. Summed mass chromatogram (m/z 97+98+111+112+125+126) of the flash pyrolysate of the isolated kerogen of the original sample. The insert shows a partial mass chromatogram m/z 308 revealing the distribution of the thiophenes with a phytane carbon skeleton. Key: Ph = thiophenes with a phytane carbon skeleton, dots denote 2-*n*-alkyl-5-ethylthiophenes, triangles denote 2-*n*-alkyl-5-methylthiophenes, and squares denote 2-*n*-alkylthiophenes. Clusters of linear thiophenes are indicated by numbers that represent the total number of carbon atoms.

et al., 1987a; Rullkötter *et al.*, 1988; de Graaf *et al.*, 1992; Schouten *et al.*, 1993, 1994; Krein and Aizenshtat, 1994). Artificial maturation at temperatures as low as 160 and 180°C, respectively, yields a six- and fifteen-fold increase in the total amount of thiophenes with a phytane carbon skeleton. These data are listed in Table 2.1 and shown in Fig. 2.4, in which the generation profiles of the three structural isomers are depicted together with the generation profile of the total amount of thiophenes with a phytane carbon skeleton.

The formation of these isoprenoid thiophenes at relatively low temperatures could result from the thermal decomposition of polysulphide-bound phytanyl units in high-molecular-weight (HMW) fractions of the rock (such as kerogen, asphaltenes and the polar fraction). Schouten *et al.* (1994) found that heating (250°C; 5 min) of oligomeric polysulphide-bound phytane aggregates, formed by the reaction of phytadienes with reduced inorganic polysulphides, yielded C_{20} isoprenoid thiophenes in relatively high abundance. However, the dominant isomer was **I**, and in our experiments at 160°C and 180°C this isomer is still of relatively minor importance. Krein and Aizenshtat (1994) heated (300°C; N_2 flow) oligomeric polysulphide-bound phytanyl units, formed by the reaction of phytenal with reduced inorganic polysulphides, and found only thiophenes **II** and **III** in a 3:1 ratio. These experiments suggest that the formation of HMW fractions

Table 2.2. Relative amounts (%) of structural isomers of C_{17}, C_{20} and C_{31} linear thiophenes as a function of hydrous pyrolysis temperature. Relative amounts of these isomers in the Curie-point pyrolysate of the isolated kerogen of the original sample are listed in the column denoted KER.

Compound	original	160°C	180°C	200°C	220°C	239°C	260°C	280°C	300°C	330°C	KER
2-tridecylthiophene	83	52	56	44	38	37	41	40	37	33	41
2-dodecyl-5-methylthiophene	7	30	32	36	38	37	30	32	31	35	39
2-ethyl-5-undecylthiophene	6	8	7	9	10	14	14	13	16	17	12
C_{17} mid-chain thiophenes	4	10	6	12	14	12	16	15	17	15	9
2-hexadecylthiophene	34	31	32	33	30	20	24	28	29	22	33
2-methyl-5-pentadecylthiophene	25	33	30	44	45	46	38	42	33	42	42
2-ethyl-5-tetradecylthiophene	35	32	34	17	19	28	29	21	26	27	15
C_{20} mid-chain thiophenes	6	5	4	6	7	6	10	10	13	9	10
2-nonyl-5-octadecylthiophene	-	-	-	4	5	4	4	5	6	2	nd[a]
2-decyl-5-heptadecylthiophene	-	-	-	5	5	6	7	10	9	7	nd
2-hexadecyl-5-undecylthiophene	-	-	-	10	12	12	12	14	13	10	nd
2-dodecyl-5-pentadecylthiophene	-	-	-	19	21	17	16	18	17	17	nd
2-tetradecyl-5-tridecylthiophene	-	-	-	62	57	61	61	54	54	64	nd

[a] not detected.

consisting of polysulphide-bound phytanyl units during the earliest stages of diagenesis of the Vena del Gesso sediment involved reaction of reduced inorganic polysulphides with phytenal rather than phytadienes. It is noteworthy that after treatment of the polar fraction of the original sample with MeLi/MeI, a reagent that selectively cleaves S-S bonds and subsequently methylates the produced thiols (Kohnen *et al.*, 1991b), methyl-thioethers of phytane were among the most abundant compounds present (Koopmans *et al.*, unpublished results). This suggests that substantial amounts of polysulphide-bound phytane skeletons are present in the polar fraction.

Artificial maturation at temperatures between 180 and 239°C results in a decrease of the total amount of thiophenes with a phytane carbon skeleton (Fig. 2.4). Further heating at temperatures higher than 239°C again yields increasing amounts of thiophenes with a phytane carbon skeleton, which at 330°C are about 20 times more abundant than in the original sample. These generation profiles suggest that there are two main stages of formation of thiophenes with a phytane carbon skeleton from HMW fractions with different activation energies (low E_A: original to 180°C; high E_A: 239 to 300°C), and that continuous degradation of thiophenes with a phytane carbon skeleton is taking place with notable decreases in absolute abundance between 180 and 200°C. As was stated in the previous paragraph, the formation of thiophenes with a phytane

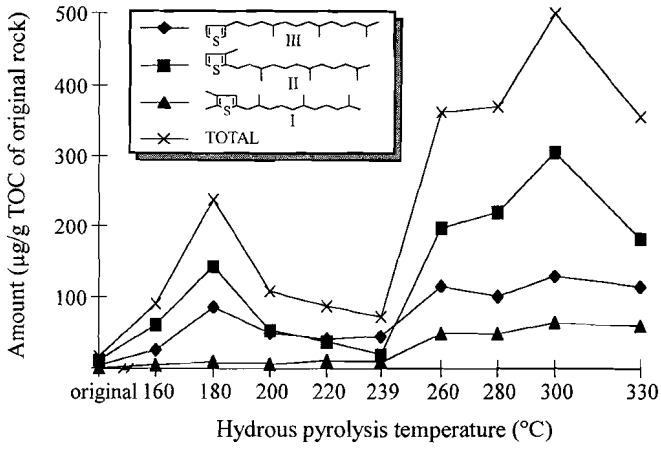

Fig. 2.4. Absolute amounts (µg/g TOC of original rock) of three thiophenes with a phytane carbon skeleton and the total amount of thiophenes with a phytane carbon skeleton as a function of hydrous pyrolysis temperature.

skeleton at low temperatures (first stage of formation) could result from the thermal breakdown of polysulphide-bound phytanyl units in HMW fractions. The second stage of formation of thiophenes with a phytane skeleton could then result from the thermal breakdown of monosulphide-bound phytanyl units in HMW fractions. This coincides with the fact that S-S bonds are weaker than C-S bonds. The similarity of the generation profiles of the linear thiophenes (Fig. 2.2) and the thiophenes with a phytane carbon skeleton (Fig. 2.4) at T > 220°C suggests that they are formed by similar processes. The idea of continuous degradation of thiophenes is supported by two observations. First, 3,4-di-*n*-alkylthiophenes, which have been found in thermally immature sedimentary rocks but whose mid-chain dimethyl carbon skeletons have not been detected upon desulphurisation of HMW fractions (Sinninghe Damsté *et al.*, 1990b; Kohnen *et al.*, 1990a), were present in the original sample but could not be detected after thermal treatment at 220°C (*vide infra*). Second, off-line pyrolysis (400°C; 1 h; N_2 flow) of the isolated kerogen of the original sample yielded phytane skeletons in high amounts (*ca.* 13 mg/g TOC). At 300°C only 5% of the phytane skeletons present in the original kerogen had been converted to free thiophenes with a phytane carbon skeleton, and 10% to free phytane. However, Curie-point pyrolysis of the isolated kerogen of the sample that was artificially matured at 300°C yielded no detectable phytane skeletons (Koopmans *et al.*, 1997c). This indicates that a considerable amount of phytane skeletons is missing, possibly due to the degradation of thiophenes with a phytane carbon skeleton. It is likely that the products of the degradation of the thiophenes with a phytane carbon skeleton are volatilised during work-up.

The isomer distribution of the thiophenes with a phytane carbon skeleton changes

dramatically upon heating. This can be visualised by the isoprenoid thiophene ratio [ITR = (**II+III**)/(**I**+mid-chain thiophenes with a phytane carbon skeleton)], a parameter that is thought to reflect the (hyper)salinity of the depositional environment (Sinninghe Damsté *et al.*, 1989d; Table 2.3). The decline of the ITR from 32 in the original sample to 4.9 at 330°C is probably due to the dilution of the thiophenes with a phytane carbon skeleton already present in the alkylthiophene fraction of the original sample by thiophenes with a phytane carbon skeleton that are liberated from HMW fractions because of increasing thermal stress. This is supported by the composition of the Curie-point pyrolysate of the isolated kerogen of the original sample, comprising the same three thiophenes with a phytane carbon skeleton with a distribution that corresponds to an ITR of 4.2 (Table 2.3; Fig. 2.3). Although the ITR changes considerably with temperature, it does not drop below the critical value of 0.5 which represents the upper limit for hypersaline palaeoenvironments (Sinninghe Damsté *et al.*, 1989d). A similar drop in the ITR with increasing thermal stress has been observed in an evaporite sample using confined pyrolysis (Benalioulhaj *et al.*, 1993).

C_{37}-C_{38} 2,5-di-*n*-alkylthiophenes

Linear C_{37} and C_{38} 2,5-di-*n*-alkylthiophenes are only observed when the rock is matured at 260°C and higher temperatures. This explains why in a previous study of sedimentary rocks from the Vena del Gesso Basin these thiophenes were not discussed (Kohnen *et al.*, 1992a). The C_{37} and C_{38} 2,5-di-*n*-alkylthiophenes are present in relatively minor amounts with a maximum of 27 µg/g TOC at 300°C, and their generation profiles are co-variant as judged from mass chromatograms (m/z 546+560). The C_{38} 2,5-di-*n*-alkylthiophenes occur in slightly higher amounts than the C_{37} 2,5-di-*n*-alkylthiophenes. At 330°C these compounds are not detectable, probably due to the degradation of thiophenes as discussed in the previous section. The C_{37} and C_{38} 2,5-di-*n*-alkylthiophenes are thought to be derived from C_{37} and C_{38} di- and tri-unsaturated methyl and ethyl ketones present in Prymnesiophyceae (Volkman *et al.*, 1980b). Sulphur incorporation into these functionalised lipids has been reported to yield cyclic monosulphides, 2,5-di-*n*-alkylthiophenes (Sinninghe Damsté *et al.*, 1989c, 1990b; Kohnen *et al.*, 1990c) and sulphur-bound *n*-C_{37} and *n*-C_{38} carbon skeletons in HMW fractions (Sinninghe Damsté *et al.*, 1988b; Schouten *et al.*, 1993).

The formation of C_{37} and C_{38} 2,5-di-*n*-alkylthiophenes only at relatively high temperatures (≥ 260°C) can be explained as follows. Because of the large distance between

Table 2.3. Isoprenoid Thiophene Ratio (ITR) as a function of hydrous pyrolysis temperature. The ITR of the Curie-point pyrolysate of the isolated kerogen of the original sample is listed in the column denoted KER.

	original	160°C	180°C	200°C	220°C	239°C	260°C	280°C	300°C	330°C	KER
ITR	32	20	26	18	7.8	7.3	6.4	6.6	6.8	4.9	4.2

the various double bonds and the carbonyl group, which is also available for sulphurisation (Schouten *et al.*, 1993), the incorporation of reduced inorganic sulphur species into C_{37} and C_{38} di- and tri-unsaturated methyl and ethyl ketones occurs predominantly in an intermolecular fashion and is likely to result in multiple sulphur linkages. This leads to the formation of a cross-linked sulphur-rich macromolecular network present in the asphaltene fraction or the kerogen. Artificial maturation at 200°C results in the cleavage of some of these (poly)sulphide bridges, forming sulphur-rich macromolecular aggregates which end up in the polar fraction. This is confirmed by the relatively large amounts of C_{37} and C_{38} *n*-alkanes that were released after desulphurisation of the polar fraction of the sample matured at 200°C, which were an order of magnitude higher than the amounts released after desulphurisation of the polar fraction of the original sample (Koopmans *et al.*, 1997b). At temperatures higher than 220°C, the remaining (poly)sulphide bridges in these macromolecular aggregates will disintegrate, leading to the formation of free C_{37} and C_{38} *n*-alkanes (Koopmans *et al.*, 1997b) and the C_{37} and C_{38} 2,5-di-*n*-alkylthiophenes presently encountered in the alkylthiophene fractions.

The isomer distribution of the C_{38} mid-chain 2,5-di-*n*-alkylthiophenes is not random as judged from an averaged mass spectrum covering the whole peak reflecting the C_{38} mid-chain 2,5-di-*n*-alkylthiophenes (Fig. 2.5**a**). 2-Hexadecyl-5-octadecylthiophene (22%) and 2-nonadecyl-5-pentadecylthiophene (22%) make up a large portion of the total C_{38} mid-chain 2,5-di-*n*-alkylthiophenes, whereas the other isomers are less abundant ($\leq$ 12%). This specific isomer distribution of the C_{38} thiophenes produced after thermal treatment at 260°C is retained when the rock is heated at 280 and 300°C. A similar isomer distribution is observed for the C_{37} mid-chain 2,5-di-*n*-alkylthiophenes, but due to coelution with a more abundant C_{35} hopanoid thiophene it was difficult to quantify. An explanation for this specific isomer distribution can be given on the basis of the number of double bonds present in the precursor lipids. Prymnesiophyceae biosynthesising C_{37} and C_{38} di- and tri-unsaturated methyl and ethyl ketones (Volkman *et al.*, 1980b) adjust the relative amounts of these di- and tri-unsaturated compounds to the temperature of the surrounding water in order to maintain optimal membrane fluidity (Brassell *et al.*, 1986b; Prahl and Wakeham, 1987). This results in an inverse relationship between the overall degree of unsaturation and the surface water temperature (Brassell *et al.*, 1986c; Prahl and Wakeham, 1987). The Vena del Gesso sediments were deposited in an evaporitic environment (Vai and Ricci Lucchi, 1977). Therefore, it can be argued that the surface water temperatures were relatively high when the Prymnesiophyceae bloomed. As a result, these algae biosynthesised mostly di-unsaturated methyl and ethyl ketones. Sulphur incorporation into the C_{38} di-unsaturated methyl and ethyl ketone during the earliest stages of diagenesis can lead to multiple sulphur cross-linking with other functionalised lipids to form a macromolecular structure such as kerogen. Sulphur can be attached to carbon atoms 2, 16, 17, 23 and 24 (methyl ketone) or 3, 16, 17, 23 and 24 (ethyl ketone; Fig. 2.5**b**; Schouten *et al.*, 1993, 1994), assuming that the positions of the double bonds in the methyl ketone are the same as those in the ethyl-

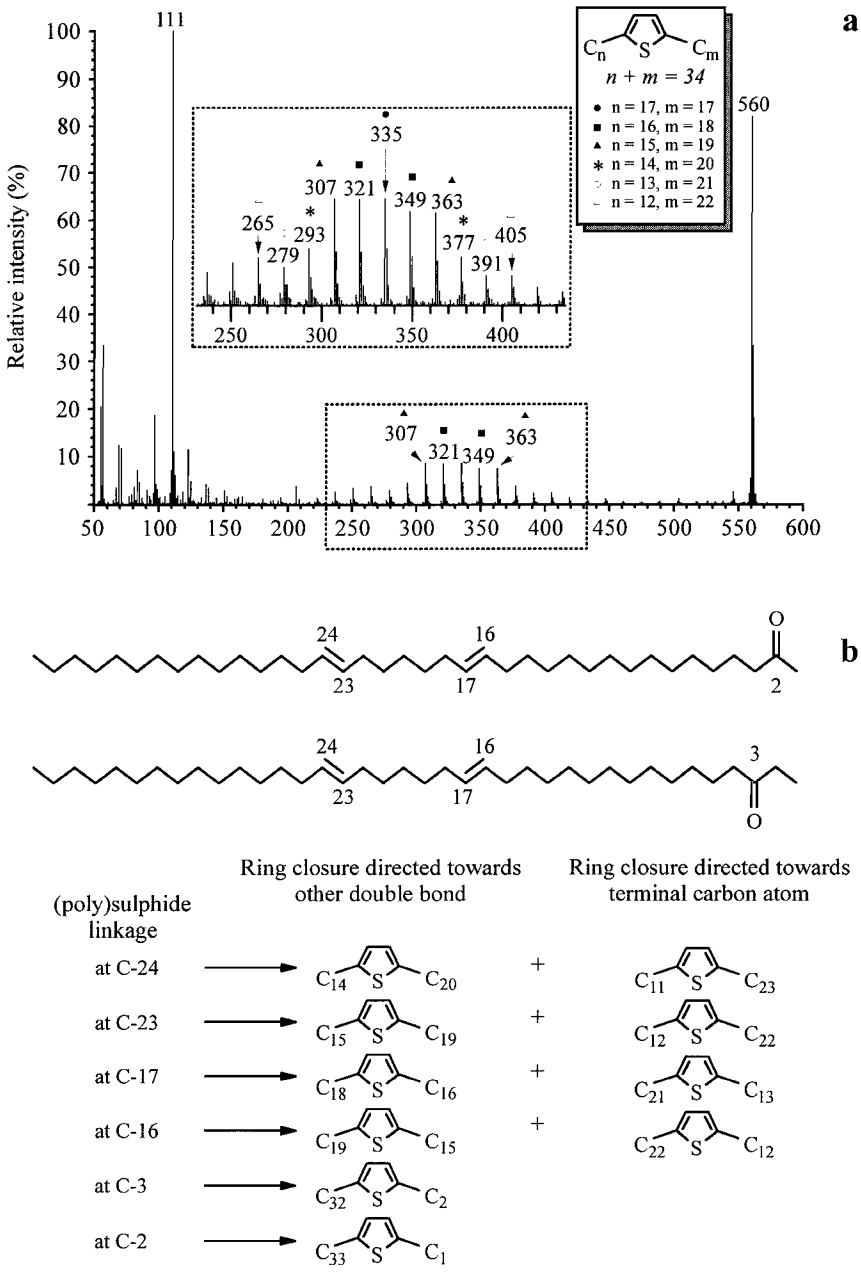

Fig. 2.5. (**a**) Averaged mass spectrum (subtracted for background; averaged over 13 scans) of C_{38} 2,5-di-*n*-alkylthiophenes from the sample artificially matured at 260°C. (**b**) Structures of C_{38} di-unsaturated methyl and ethyl ketones, and possible products of ring closure after cleavage of intermolecular (poly)sulphide linkages.

ketone (de Leeuw *et al.*, 1980).

Artificial maturation at temperatures higher than 220°C leads to degradation of the (poly)sulphide linkages in the macromolecular aggregates in the polar fraction, which may yield C_{38} 2,5-di-*n*-alkylthiophenes as stable products. The dominating isomers, 2-hexadecyl-5-octadecylthiophene and 2-nonadecyl-5-pentadecylthiophene, can only be formed by ring closure directed towards the original position of the second double bond (Fig. 2.5**b**). Theoretically, taking into account all eight possible products of such a ring closure, this should yield 2-hexadecyl-5-octadecylthiophene and 2-nonadecyl-5-pentadecylthiophene in a 1:2 ratio (Fig. 2.5**b**). However, these isomers occur in a 1:1 ratio (both 22% of total C_{38} mid-chain 2,5-di-*n*-alkylthiophenes). The thiophenes that could be formed from ring closure directed towards the terminal carbon atom are represented only by minor peaks in the mass spectrum (Fig. 2.5**a** and **b**). This suggests that the second double bond (or a derivative thereof) plays an important role in ring closure and, therefore, in the production of C_{38} 2,5-di-*n*-alkylthiophenes. It is noteworthy that 2-tetratriacontylthiophene, 2-methyl-5-tritriacontylthiophene and 2-ethyl-5-dotriacontylthiophene, which are present in amounts 20 times lower than the sum of the mid-chain thiophenes, have a relative abundance of 1:4:4. If this ratio is corrected for background (the average relative abundance of 2-*n*-alkylthiophenes, 2-*n*-alkyl-5-methylthiophenes and 2-*n*-alkyl-5-ethylthiophenes is *ca.* 2:2:1), the relative enhancement of 2-methyl-5-tritriacontylthiophene and 2-ethyl-5-dotriacontylthiophene becomes apparent. This is consistent with sulphur incorporation into the keto group at carbon number 2 (methyl ketone) or 3 (ethyl ketone; Schouten *et al.*, 1993) and subsequent ring closure (Fig. 2.5**b**).

The C_{37} and C_{38} 2,5-di-*n*-alkylthiophenes can thus be considered as stabilisation products of multiply (poly)sulphide linked *n*-C_{37} and *n*-C_{38} carbon skeletons derived from unsaturated long-chain ketones. It should be noted that these alkylthiophenes are also present in some relatively immature rocks (Sinninghe Damsté *et al.*, 1989c, 1990b; Kohnen *et al.*, 1990c), suggesting that hydrous pyrolysis simulates natural diagenesis. The explanation for the formation of these thiophenes is basically different from that proposed earlier (Sinninghe Damsté *et al.*, 1989c), and it does not require the unlikely process of double bond isomerisation at the earliest stages of diagenesis as suggested by Sinninghe Damsté *et al.* (1989c). The fact that product-precursor relationships could be made at temperatures up to 300°C (including the confirmation of the original positions of the double bonds of the unsaturated long-chain ketones) underlines the use of alkylthiophenes as molecular indicators during progressive diagenesis and early catagenesis. It should be noted that the C_{37} and C_{38} *n*-alkanes do not reveal information about the presence of original positions of functionalities, and that Curie-point pyrolysis of the isolated kerogen of the original sample did not reveal the C_{37} and C_{38} 2,5-di-*n*-alkylthiophenes.

C_{28}-C_{32} 2,5-di-*n*-alkylthiophenes

At 200°C, 2,5-di-*n*-alkylthiophenes in the C_{28}-C_{32} range are formed. At higher temperatures, large amounts of these compounds are produced with the C_{31} members being the most abundant (Table 2.1; Figs. 2.1 and 2.6). These compounds are not encountered in the alkylthiophene fraction of the original sample, and, therefore, it is not surprising that in a previous study of a similar marl sample from the Vena del Gesso Basin the C_{28}-C_{32} 2,5-di-*n*-alkylthiophenes were not reported (Kohnen *et al.*, 1992a). At 330°C the C_{28}-C_{32} 2,5-di-*n*-alkylthiophenes are still present in considerable quantities.

In Fig. 2.7 an averaged mass spectrum covering the whole peak of the C_{31} mid-chain 2,5-di-*n*-alkylthiophenes is given from the alkylthiophene fraction of the sample matured at 300°C. It is apparent that the distribution of the structural isomers is not random. There is a definite predominance of 2-tetradecyl-5-tridecylthiophene over the other structural isomers. Averaged mass spectra of the other mid-chain 2,5-di-*n*-alkylthiophenes in the C_{28}-C_{32} range also show a definite predominance of the 2-*n*-alkyl-5-tetradecylthiophenes over the other structural isomers. This suggests that the precursors of these compounds had a functional group at C-15. Possible candidates are the C_{30}-C_{32} 1,15-diols and the C_{30}-C_{32} 15-keto-1-ols reported earlier (*e.g.* de Leeuw *et al.*, 1981; ten Haven *et al.*, 1992), although it is known that hydroxyl groups do not react with reduced inorganic sulphur species (Schouten *et al.*, 1993). Reduced inorganic sulphur species could react with the keto group to form a (poly)sulphide linkage with another functionalised lipid (Schouten *et al.*, 1993). Another possibility is the dehydration of the hydroxyl group at C-15 in the C_{30}-C_{32} 1,15-diols, which would yield a double bond either at C-14 or C-15. This allows for the incorporation of sulphur at C-14, C-15 or C-16 in a 1:2:1

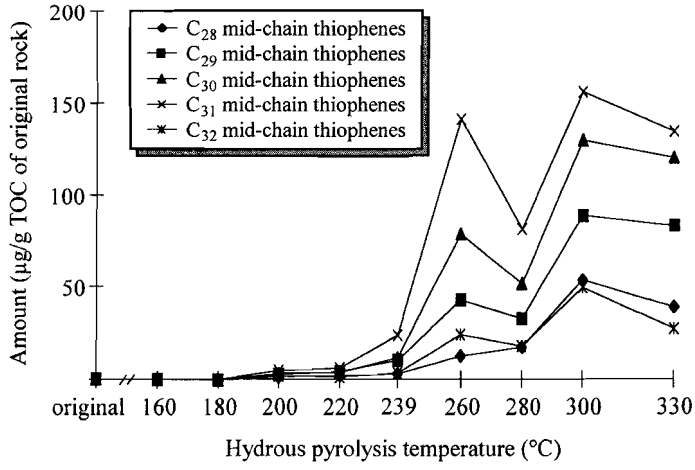

Fig. 2.6. Absolute amounts (µg/g TOC of original rock) of C_{28}-C_{32} 2,5-di-*n*-alkylthiophenes as a function of hydrous pyrolysis temperature.

ratio. Despite these possibilities to form intermolecular (poly)sulphide linkages, it is difficult to imagine how a thiophene could form from such a structure upon increasing thermal stress because no additional functionalities are available near-by. Moreover, the specific isomer distribution of the C_{28}-C_{32} mid-chain 2,5-di-*n*-alkylthiophenes, with the 2-*n*-alkyl-5-tetradecylthiophenes as the dominant isomers, shows that the formation of the thiophene ring is directed preferentially to one side of the carbon chain, thus suggesting that an additional functionality is present between C-16 and the terminal carbon atom. Other possible precursors are the C_{30}-C_{32} di-unsaturated alcohols and the C_{32} mono-unsaturated 1,15-diol found in algae of the class Eustigmatophyceae (Volkman *et al.*, 1992). The position of the double bond in the C_{32} mono-unsaturated 1,15-diol was not determined, although it was proposed that the double bond is located between C-16 and C-32 based on mass spectral data (Volkman *et al.*, 1992). This would coincide with the fact that the formation of the thiophene ring is directed towards that side of the carbon chain. However, the specific carbon number distribution of the C_{28}-C_{32} mid-chain 2,5-di-*n*-alkylthiophenes, with the C_{31} members as the most abundant components, is not reflected in any of the above precursors, which generally have a strong even-over-odd carbon number predominance (Volkman *et al.*, 1992). On the other hand, 2-ethyl-5-pentacosylthiophene, 2-methyl-5-hexacosylthiophene and 2-heptacosylthiophene have a relative abundance of 1:7:2, which after correction for background (see previous section) results in a definite enhancement of 2-methyl-5-hexacosylthiophene over the other two isomers. This suggests that an intermolecular (poly)sulphide linkage was present at C-2, which upon thermal stress formed a thiophene ring. This would be consistent with the presence of a terminal hydroxyl group, which upon dehydration would yield a double bond at C-1 that could react with reduced inorganic sulphur species to form a (poly)sulphide linkage preferentially at C-2 (de Graaf *et al.*, 1992; Schouten *et al.*, 1994).

In Table 2.2 the isomer distribution of the C_{31} mid-chain 2,5-di-*n*-alkylthiophenes is given as a function of hydrous pyrolysis temperature for the range 200°C (when these compounds are first formed) to 330°C. The specific isomer distribution of the C_{31} mid-chain 2,5-di-*n*-alkylthiophenes observed at 200°C is retained at 330°C. Again, this shows that alkylthiophenes maintain their biomarker signatures at relatively high levels of thermal maturity, enabling the link between products and precursors which would not be possible using the corresponding *n*-alkanes, or compounds in the Curie-point pyrolysate of the isolated kerogen of the original sample. The specific isomer distribution also shows that the generation of organic sulphur compounds by the (random) reaction of elemental sulphur with alkanes, as proposed by Schmid *et al.* (1987), during hydrous pyrolysis should be considered highly unlikely. It is important to note that, although the reproducibility of the absolute amounts of C_{28}-C_{32} 2,5-di-*n*-alkylthiophenes is low as determined from duplicate experiments at 280 and 300°C (see Experimental), the reproducibility of the specific isomer distribution is high. Thus, the aspect of the C_{28}-C_{32} 2,5-di-*n*-alkylthiophenes that makes them suitable as molecular indicators is still recog-

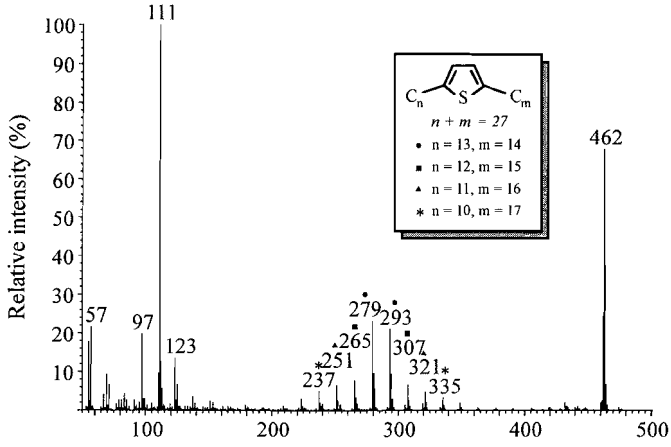

Fig. 2.7. Averaged mass spectrum (subtracted for background; averaged over 13 scans) of C_{31} 2,5-di-*n*-alkylthiophenes from the sample artificially matured at 300°C.

nisable in the duplicate experiments.

C_{36}-C_{44} 3,4-di-*n*-alkylthiophenes

The presence of long mid-chain 3,4-di-*n*-alkylthiophenes has been reported before in immature sedimentary rocks from a.o. the Jurf ed Darawish oil shale in Jordan and the Vena del Gesso Basin (Sinninghe Damsté *et al.*, 1990b; Kohnen *et al.*, 1990a). These reports speculated on the formation of these molecules from specific mid-chain dimethylalkadienes by reaction with reduced inorganic sulphur species. The fact that these carbon skeletons were not reported before was attributed to the instability of the precursor molecule, and it was concluded that the incorporation of sulphur had preserved the carbon skeleton (Sinninghe Damsté *et al.*, 1990b).

In the original unheated rock mid-chain 3,4-di-*n*-alkylthiophenes were found in the C_{36}-C_{44} range. Although the amounts are low (≤ 1 μg/g TOC), a definite even-over-odd carbon number preference is observed. Artificial maturation of the rock results in a gradual decrease of the amounts of C_{36}-C_{44} mid-chain 3,4-di-*n*-alkylthiophenes, and at 220°C these compounds are not detectable. Again, this suggests that the degradation of thiophenes is a process that already takes place at low levels of thermal maturity. It is interesting to note that the C_{36}-C_{44} mid-chain 3,4-di-*n*-alkylthiophenes are the only alkylthiophenes that are *not* generated at increasing temperatures. This observation is consistent with the fact that the corresponding mid-chain dimethylalkanes have never been reported upon desulphurisation of sulphur-rich macromolecular aggregates. This suggests either that their precursors, the mid-chain dimethylalkadienes (Kohnen *et al.*, 1990a), are not incorporated into a macromolecular network such as kerogen from

which they can be liberated upon increasing thermal stress, or that the C_{36}-C_{44} mid-chain 3,4-di-*n*-alkylthiophenes are more labile under geological conditions than their 2,5-di-*n*-alkyl counterparts. The latter is, however, hard to believe from a chemical point of view. It is more likely that the spacing of the original functionalities was appropriate for direct formation of a thiophene moiety.

2.5 Conclusions

After artificial maturation by hydrous pyrolysis at temperatures up to 330°C for 72 h, linear alkylthiophenes and thiophenes with a phytane carbon skeleton are present in much higher concentrations than in the original sample due to their production from HMW fractions, presumably kerogen. The importance of the kerogen in the production of alkylthiophenes is supported by the observation that the isomer distributions of alkylthiophenes at high temperatures coincide with the isomer distributions of alkylthiophenes in the Curie-point pyrolysate of the isolated kerogen of the original sample.

The structural isomer distribution of linear alkylthiophenes does not change significantly when these compounds are generated from HMW fractions at different temperatures. This implies that information regarding the original positions of functional groups in the biochemical precursors is retained at relatively high levels of thermal maturity, indicating that linear alkylthiophenes are useful biomarkers throughout diagenesis and early catagenesis. This is exemplified by the specific isomer distributions of the C_{31} and C_{38} 2,5-di-*n*-alkylthiophenes, which enabled the identification of possible precursor lipids, *i.e.* C_{30}-C_{32} (unsaturated) 1,15-diols or 15-keto-1-ols in case of the C_{31} 2,5-di-*n*-alkylthiophenes and C_{38} di-unsaturated methyl and ethyl ketones in case of the C_{38} 2,5-di-*n*-alkylthiophenes. These long-chain alkylthiophenes are not present in the original (unheated) sample, indicating that hydrous pyrolysis is capable of revealing sequestered information about the depositional environment. The decreasing amounts of mid-chain 3,4-di-*n*-alkylthiophenes suggest that alkylthiophenes are subject to continuous degradation, as can also be concluded from the generation profiles of the thiophenes with a phytane carbon skeleton. This means that the concentrations given here are the collective product of opposing processes involved in the production and degradation of alkylthiophenes. No direct evidence was found for side-chain cleavage, possibly due to loss of volatile compounds during work-up. The absence of (di)benzothiophenes in all samples suggests that cyclisation and aromatisation of alkylthiophenes is not an important 'degradation' pathway.

Generation of organic sulphur compounds by the random reaction of elemental sulphur and alkanes during hydrous pyrolysis is unlikely in view of the highly specific isomer distribution of the C_{31} and C_{38} mid-chain 2,5-di-*n*-alkylthiophenes that does not change significantly upon increasing thermal stress. Hydrous pyrolysis is a useful simulation method to study the thermal stability of alkylthiophenes in the geosphere during diagenesis and early catagenesis. This requires experimental temperatures, however,

that are much lower than the temperatures used to simulate oil generation and expulsion processes.

2.6 Acknowledgements

This work was performed under the auspices of ENOG (European Network of Organic Geochemists) and has benefited from scientific discussions within the group. ENOG comprises Laboratoire de Géochemie, IFP, Rueil Malmaison, France; Institute of Petroleum and Organic Geochemistry, KFA, Jülich, Germany; Laboratoire de Chimie Organiques de Substances Naturelles associé au CNRS, Université Louis Pasteur, Strasbourg, France; Netherlands Institute for Sea Research, Department of Marine Biogeochemistry, Texel, the Netherlands; Department of Environmental Chemistry, CID-CSIC, Barcelona, Spain; Organic Geochemistry Unit, University of Bristol, UK, and receives funding from the European Community (EC contract #ERBSC1*CT91-0736). We thank the Koninklijke/Shell Exploratie en Produktie Laboratorium (Shell Research BV) for providing a research studentship to MPK. We thank Gian Battista Vai, B.C. Schreiber, Brendan Keely, Peter Hofmann, Jan Ebbing, Stefan Schouten, other members of the ENOG group and the management of the gypsum mine for advice and assistance during sampling. Analytical support was provided by Mrs. M. Dekker and Mr. W. Pool. Drs. B. Horsfield and R.L. Patience are thanked for reviewing an earlier version of this manuscript. Dr. J.L. Clayton is acknowledged for constructive comments. This work was partly supported by a PIONIER grant to JSSD from the Netherlands Organisation for Scientific Research (NWO).

CHAPTER 3

Impact of dia- and catagenesis on sulphur and oxygen sequestration of biomarkers as revealed by artificial maturation of an immature sedimentary rock

M.P. Koopmans, J.W. de Leeuw, M.D. Lewan and J.S. Sinninghe Damsté

3.1 Abstract

Hydrous pyrolysis of an immature ($R_o \approx 0.25\%$) sulphur-rich marl from the Gessoso-solfifera Formation (Messinian) in the Vena del Gesso Basin was carried out at $160°C \leq T \leq 330°C$ for 72h, to study the effect of progressive diagenesis and early catagenesis on the abundance and distribution of sulphur-containing and sulphur- and oxygen-linked carbon skeletons in low-molecular-weight and high-molecular-weight fractions (*e.g.* kerogen). To this end, compounds in the saturated hydrocarbon fraction, monoaromatic hydrocarbon fraction, polyaromatic hydrocarbon fraction, alkylsulphide fraction and ketone fraction were quantitated, as well as compounds released after desulphurisation of the polar fraction and $HI/LiAlH_4$ treatment of the desulphurised polar fraction.

Sulphur-bound phytane and (20R)-5α,14α,17α(H) and (20R)-5β,14α,17α(H) C_{27} to C_{29} steranes in the polar fraction become less abundant with increasing maturation temperature, whereas the amount of their corresponding hydrocarbons increases in the saturated hydrocarbon fraction. Carbon skeletons that are bound in the kerogen by multiple bonds (*e.g.* C_{38} *n*-alkane and isorenieratane) are first released into the polar fraction, and then as free hydrocarbons. These changes occur at relatively low levels of thermal maturity ($R_o < 0.6\%$), as evidenced by the 'immature' values of biomarker maturity parameters such as the ββ/(ββ+αβ+βα) C_{35} hopane ratio and the 22S/(22S+22R)-17α,21β(H) C_{35} hopane ratio.

Sulphur- and oxygen-bound moieties present in the polar fraction are not stable with increasing thermal maturation. However, alkylthiophenes, ketones, 1,2-di-*n*-alkylbenzenes and free *n*-alkanes seem to be stable thermal degradation products of these sulphur- and oxygen-bound moieties. Thus, apart from free *n*-alkanes, which are abun-

dantly present in more mature sedimentary rocks and crude oils, alkylthiophenes, 1,2-di-*n*-alkylbenzenes and ketones can also be expected to occur. The positions of the thiophene moiety and the carbonyl group coincide with the original positions of the functional groups of their precursors. Thus, important information about palaeobiochemicals is retained throughout the sequestration/degradation process.

3.2 Introduction

There is considerable evidence that the formation of organic sulphur compounds in the geosphere occurs during the early stages of diagenesis (*e.g.* Sinninghe Damsté *et al.*, 1989c; Kohnen *et al.*, 1989, 1990b; Wakeham *et al.*, 1995). The reactants are lipids bearing functional groups (*e.g.* double bonds or carbonyl groups) and reduced inorganic sulphur species (H_2S, HS_x^-). Laboratory sulphurisation experiments have successfully simulated the natural sulphurisation process under mild conditions using such substrates as alkenes, ketones and aldehydes (*e.g.* Fukushima *et al.*, 1992; de Graaf *et al.*, 1992, 1995; Rowland *et al.*, 1993; Schouten *et al.*, 1993, 1994; Krein and Aizenshtat, 1994).

The intermolecular reaction of reduced inorganic sulphur species with functionalised lipids, leaving saturated hydrocarbons unreacted, affects the biomarker fingerprint by sequestration of these functionalised lipids into high-molecular-weight (HMW) fractions (*i.e.* polar fraction, asphaltenes and kerogen). This has been demonstrated for different carbon skeletons in several sedimentary rocks (Sinninghe Damsté *et al.*, 1988b; Kohnen *et al.*, 1991c, 1992a,b; Adam *et al.*, 1993). Through the sulphur sequestration of these functionalised lipids, important information such as the carbon skeleton and the original positions of functional groups is preserved.

Alternatively, carbon skeletons can also be linked by oxygen bonds (*e.g.* Michaelis and Albrecht, 1979; Chappe *et al.*, 1979; Mycke *et al.*, 1987), although the timing and mechanism of this reaction is not well understood. Recently, it was shown that specific carbon skeletons can be linked by both sulphur and oxygen (Richnow 1992, 1993). Therefore, in this study of the impact of artificial maturation on the amount and distribution of sulphur-bound and sulphur-containing carbon skeletons, the role of oxygen links is also taken into account.

Since S-S, C-S and C-O bonds are weaker than C-C bonds (Claxton *et al.*, 1993), it is likely that the sequestered carbon skeletons are released at relatively low levels of thermal stress, before significant cracking takes place. The timing of the release of biomarkers as hydrocarbons due to the thermal breakdown of relatively weak S-S, C-S and C-O bonds will depend on the amount and type of sulphur and oxygen cross-links, thereby strongly affecting the biomarker fingerprint. It is not known how the distribution of these carbon skeletons over HMW and low-molecular-weight (LMW) fractions changes with increasing thermal stress. Also, it is unclear what the fate of multiply functionalised lipids is, after their incorporation into HMW fractions by multiple C-S and/or C-O bonds.

To address these questions, we originally aimed at analysing a natural maturation set that contains abundant organically-bound sulphur and covers a wide maturity range starting at a low maturity level. However, in the absence of a suitable natural maturation set, we performed artificial maturation experiments with an immature sulphur-rich sedimentary rock from the Vena del Gesso Basin using hydrous pyrolysis. Typically, hydrous pyrolysis is used to simulate catagenetic processes such as oil generation and expulsion, applying experimental temperatures between 300 and 365°C (Lewan *et al.*, 1979; Lewan, 1993b). Only in a few cases has it been used to establish the effect of diagenesis on relative or absolute changes in concentrations of biomarkers, using temperatures as low as 200°C (Lewan *et al.*, 1986; Eglinton and Douglas, 1988; Peters *et al.*, 1990; Koopmans *et al.*, 1995). Since our main interest concerns the effect of low levels of thermal stress on sulphur-rich organic matter, the temperatures used here are relatively low.

3.3 Experimental

Sample description. The sample used in this study is from the Gessoso-solfifera Formation (Messinian) in the Vena del Gesso Basin, Italy. For an extensive description of the geology of the Gessoso-solfifera Formation, see Vai and Ricci Lucchi (1977) and Sinninghe Damsté *et al.* (1995b). Three samples covering the complete (1.2 m thick) marl layer of evaporitic cycle IV (*i.e.* IV-1A, IV-1B and IV-1C) were collected from a fresh outcrop in the open-pit gypsum mine at Riolo Terme during a field trip in January 1993. A representative sample of the marl layer of cycle IV, assembled by mixing IV-1A, IV-1B and IV-1C in equal amounts, was used in this study. The TOC content is 2.0 wt %. Elemental analyses of the isolated kerogen indicate it is an immature Type II-S kerogen with an atomic H/C ratio of 1.44, an atomic O/C ratio of 0.17, and an atomic S_{org}/C ratio of 0.08.

Recently, ten subsamples of this specific marl layer were extensively studied for the abundance and carbon isotopic composition of free and sulphur-bound carbon skeletons in the extracts (Kenig *et al.*, 1995), and the products derived from chemical (Schaeffer *et al.*, 1995a) and thermal (Gelin *et al.*, 1995) degradation of the associated kerogens.

Hydrous pyrolysis. A detailed description of the experimental procedures of a typical hydrous pyrolysis experiment has been given by Lewan (1993b). A one-litre Hastelloy-C276 reactor was filled with 90 to 100 g of rock chips and 475 g of distilled water. The remaining volume was purged and filled with helium at a pressure of 2.4 bars. Artificial maturation was accomplished by heating the rock chips isothermally for 72 h at 160, 180, 200, 220, 239, 260, 280, 300 and 330°C. The temperatures were continuously monitored during the experiments at 30 s intervals. Standard deviations were between ±0.2 and ±0.3°C for all experiments except for the 160°C experiment which had a

standard deviation of ±0.6°C. Experiments at 300 and 330°C generated an expelled oil that was recovered from the water surface with a pipette. The reactor walls and the rock chips were rinsed with benzene to recover any sorbed oil films, which occurred in experiments at 260, 280, 300 and 330°C. 95% or more of the originally loaded rock chips was recovered from all the experiments. The residual rock chips were dried in a vacuum oven ($T \leq 50°C$).

Extraction, fractionation and kerogen preparation. The residual rock chips were freeze-dried and ultrasonically extracted with dichloromethane/methanol (7.5:1 v/v). If a sorbed or expelled oil was present, it was combined with the extract. The combined extract was separated into a maltene and an asphaltene fraction by repeated (3 times) precipitation in heptane. An aliquot of the maltene fraction (*c.* 250 mg), to which four internal standards [6,6-d_2-3-methylhenicosane, 2,3-dimethyl-5-(1',1'-d_2-hexadecyl)thiophene, 2-methyl-2-(4,8,12-trimethyltridecyl)chroman and 2,3-dimethyl-5-(1',1'-d_2-hexadecyl)-thiolane] were added for quantitative analysis, was fractionated by column chromatography with Al_2O_3 into an apolar and a polar fraction by elution with hexane/dichloromethane (9:1 v/v) and dichloromethane/methanol (1:1 v/v), respectively. Further separation of the apolar fraction by argentatious thin-layer chromatography yielded the hydrocarbon fraction (R_f = 0.9-1.0), the monoaromatic hydrocarbon fraction (R_f = 0.4-0.9), the polyaromatic hydrocarbon fraction (R_f = 0.05-0.4) and the alkylsulphide fraction (R_f = 0.0-0.05). Due to the presence of unsaturated compounds in the hydrocarbon fraction after hydrous pyrolysis at 220°C and higher temperatures, this fraction was hydrogenated (Sinninghe Damsté *et al.*, 1988b) to yield the saturated hydrocarbon fraction. The polar fraction was studied by a step-wise chemical degradation procedure (Fig. 3.1) similar to that used by Richnow *et al.* (1992, 1993). The extracted rock residue of the original sample was demineralised using standard procedures (Lewan *et al.*, 1986) to yield the isolated kerogen for elemental analyses and saponification.

Raney Ni degradation. Polar fraction I (Fig. 3.1) was desulphurised with Raney Ni (Sinninghe Damsté *et al.*, 1988b). Before desulphurisation, a known amount of an internal standard [2,3-dimethyl-5-(1',1'-d_2-hexadecyl)thiophene] was added to a known amount (10-20 mg) of the polar fraction. Desulphurisation was accomplished by dissolving the polar fraction in 4 ml of ethanol, and repeatedly (x3) adding a small amount of Raney Ni. The mixture was allowed to reflux for 1.5 h. A sodium chloride solution was added, and the reaction mixture was extensively extracted with dichloromethane. Column chromatography using Al_2O_3 yielded the released hydrocarbons (hexane/dichloromethane 9:1 v/v), which were subsequently hydrogenated (Sinninghe Damsté *et al.*, 1988b), and the residual polar fraction II (dichloromethane/methanol 1:1 v/v).

MeLi/MeI degradation. Polar fraction I (Fig. 3.1) was treated with MeLi/MeI in order to selectively cleave S-S bonds and form the methylthioethers of the released compounds

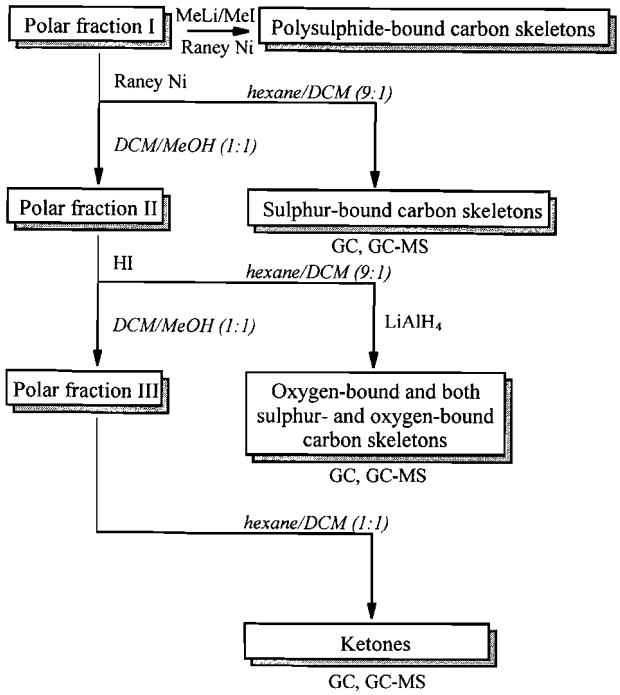

Fig. 3.1. Analytical scheme applied to the polar fractions. A step-wise chemical degradation procedure was followed to allow for the quantitative analysis of (i) polysulphide-bound carbon skeletons, (ii) sulphur-bound carbon skeletons, (iii) oxygen-bound and both sulphur- and oxygen-bound carbon skeletons, and (iv) ketones.

(Kohnen *et al.*, 1991b). First, a known amount of an internal standard [2,3-dimethyl-5-(1',1'-d_2-hexadecyl)thiophene] was added to a known amount (*c.* 40 mg) of the polar fraction. The mixture was dissolved in 4 ml of diethylether. After adding 1.5 ml of MeLi, the mixture was stirred for 1 min. Then, 1 ml of MeI was gradually added, and the mixture was stirred for 15 min. After the addition of water to deactivate any excess MeI, the reaction mixture was extensively extracted with diethylether. Column chromatography using Al_2O_3 yielded the methylthioethers of the released hydrocarbons (hexane/dichloromethane 9:1 v/v), and a residual polar fraction (dichloromethane/methanol 1:1 v/v). The methylthioether fraction was then desulphurised with Raney Ni and subsequently hydrogenated as described above.

HI degradation. Polar fraction II (Fig. 3.1) was treated with HI in order to cleave C-O bonds (March, 1985). A known amount of an internal standard [2,3-dimethyl-5-(1',1'-d_2-hexadecyl)thiophene] was added to a known amount (10-20 mg) of polar fraction. Cleavage of C-O bonds was accomplished by dissolving the polar fraction in 4 ml of a

57% solution of HI in water, and refluxing for 1 h. The reaction mixture was allowed to cool, and was neutralised with excess water and a 5% $Na_2S_2O_3$ solution in water before it was extensively extracted with hexane. Column chromatography using Al_2O_3 yielded the released alkyliodides (hexane/dichloromethane 9:1 v/v), and the residual polar fraction III (dichloromethane/methanol 1:1 v/v).

$LiAlH_4$ reduction. The alkyliodides released after HI treatment of polar fraction II were reduced using $LiAlH_4$ (Johnson *et al.*, 1948) (Fig. 3.1). The sample was dissolved in 4 ml of 1,4-dioxane, and subsequently 75 mg of $LiAlH_4$ was added. The mixture was allowed to reflux for 1.5 h. After the reaction mixture had cooled, ethyl acetate was added to destroy any excess $LiAlH_4$. Then water was added, and the reaction mixture was extensively extracted with hexane. Column chromatography using Al_2O_3 yielded the alkanes (hexane/dichloromethane 9:1 v/v). $LiAlH_4$ treatment quantitatively modified the deuterated internal standard [2,3-dimethyl-5-(1',1'-d_2-hexadecyl)thiophene] to 2,3-dimethyl-5-hexadecylthiophene.

Isolation of ketones. The residual polar fraction III was fractionated by column chromatography using Al_2O_3 into the ketone fraction (hexane/dichloromethane 1:1 v/v) and a residual fraction (Fig. 3.1).

Saponification. The kerogen of the original sample was saponified as described previously (Goossens *et al.*, 1989). A standard [2,3-dimethyl-5-(1',1'-d_2-hexadecyl)thiophene] was added for quantitative analysis.

Gas chromatography. Gas chromatography (GC) was performed using a Hewlett-Packard 5890 instrument, equipped with an on-column injector and a flame ionisation detector (FID). A fused silica capillary column (25 m x 0.32 mm) coated with CP Sil-5 (film thickness 0.12 μm) was used with helium as carrier gas. The samples were injected at 70°C and the oven was subsequently programmed to 130°C at 20°C/min and then at 4°C/min to 320°C, at which it was held for 20 min.

Gas chromatography-mass spectrometry. Gas chromatography-mass spectrometry (GC-MS) was carried out on a Hewlett-Packard 5890 gas chromatograph interfaced to a VG Autospec Ultima mass spectrometer operated at 70 eV with a mass range m/z 40-800 and a cycle time of 1.8 s (resolution 1000). The gas chromatograph was equipped with a fused silica capillary column (25 m x 0.32 mm) coated with CP Sil-5 (film thickness 0.12 μm). Helium was used as carrier gas. The samples were injected at 60°C and the oven was subsequently programmed to 130°C at 20°C/min and then at 4°C/min to 310°C, at which it was held for 20 min.

Quantitation. Quantitation of saturated hydrocarbons was accomplished by integration

of their peak areas and that of the internal standard (6,6-d_2-3-methylhenicosane) in the FID trace. Compounds released after desulphurisation of polar fraction I (Fig. 3.1) were quantitated by integration of their peak areas and that of the internal standard (6,6-d_2-3-methylhenicosane) in the FID trace. Compounds released after HI/$LiAlH_4$ treatment of polar fraction II (Fig. 3.1) were quantitated by integration of their peak areas and that of the modified internal standard (2,3-dimethyl-5-hexadecylthiophene) in the FID trace.

Quantitation of alkylthiophenes has been described before (Koopmans *et al.*, 1995). Alkylsulphides were quantitated by integration of mass chromatograms of their main fragment ion (m/z 87, 101, 115) and the main fragment ion (m/z 115) of the alkylsulphide standard, 2,3-dimethyl-5-(1',1'-d_2-hexadecyl)thiolane. Other compounds in the monoaromatic and polyaromatic hydrocarbon fraction were quantitated by integration of mass chromatograms of their main fragment ion and the main fragment ion of the appropriate standard. Saturated methyl, ethyl and mid-chain ketones were quantitated by integration of mass chromatograms of the fragment ion m/z 58 and the main fragment ion (m/z 127) of the standard [2,3-dimethyl-5-(1',1'-d_2-hexadecyl)thiophene]. A correction was made to account for the intensity of the fragment ions relative to the total ion current in the spectra of the compounds quantitated and the standard. Since mass spectrometric detection of compounds gives a molar response, a factor was introduced taking into account the molecular weights of the compounds quantitated and the standard, in order to obtain absolute amounts (μg/g TOC of original rock).

Quantitation of duplicate experiments at 280 and 300°C indicated that the standard deviation is typically *c.* 25%, although the results for some fractions differed more. Reported results for the experiments at 280 and 300°C are averages of the duplicate runs, unless stated otherwise.

3.4 Results

An immature (R_o = 0.25%; Kohnen *et al.*, 1991b) sulphur-rich marl from the Messinian Gessoso-solfifera Formation in the Vena del Gesso Basin (Italy) was artificially matured using hydrous pyrolysis at different temperatures (160, 180, 200, 220, 239, 260, 280, 300 and 330°C; 72h) to study the effect of progressive diagenesis and early catagenesis on the abundance and distribution of hydrocarbons, LMW organic sulphur compounds, and sulphur-rich geomacromolecules. In this section, the fractions containing these compounds are described.

Apolar fraction

Saturated hydrocarbon fraction

Absolute amounts of *n*-alkanes, acyclic isoprenoid alkanes and steranes in the original sample and the artificially matured samples are listed in Table 3.1. Absolute amounts of triterpanes are listed in Table 3.2. These data correlate well with data from a recent

Table 3.1. Absolute amounts (μg/g TOC of original rock) of *n*-alkanes, acyclic isoprenoid alkanes and steranes in the saturated hydrocarbon fraction of the original sample and the artificially matured samples.

	original	160°C	180°C	200°C	220°C	239°C	260°C	280°C	300°C	330°C
n-C_{15}	4	25	23	10	12	10	66	$1.4x10^2$	$2.8x10^2$	$3.6x10^2$
n-C_{16}	5	33	33	10	16	22	$1.2x10^2$	$1.9x10^2$	$3.4x10^2$	$4.8x10^2$
n-C_{17}	33	35	39	46	60	48	$2.0x10^2$	$2.8x10^2$	$5.0x10^2$	$7.7x10^2$
n-C_{18}	25	18	18	44	62	54	$1.7x10^2$	$2.5x10^2$	$3.8x10^2$	$6.7x10^2$
n-C_{19}	17	13	15	29	42	50	$1.5x10^2$	$2.5x10^2$	$3.9x10^2$	$6.8x10^2$
n-C_{20}	8	10	14	20	53	98	$2.3x10^2$	$3.0x10^2$	$4.4x10^2$	$7.0x10^2$
n-C_{21}	17	18	16	23	35	64	$1.6x10^2$	$2.4x10^2$	$4.1x10^2$	$6.5x10^2$
n-C_{22}	9	14	16	18	45	85	$2.0x10^2$	$3.0x10^2$	$4.3x10^2$	$6.3x10^2$
n-C_{23}	35	25	25	30	45	72	$1.6x10^2$	$2.8x10^2$	$4.3x10^2$	$6.7x10^2$
n-C_{24}	8	9	9	15	27	58	$1.4x10^2$	$2.2x10^2$	$3.3x10^2$	$5.0x10^2$
n-C_{25}	42	33	30	40	49	76	$1.6x10^2$	$2.4x10^2$	$3.7x10^2$	$5.7x10^2$
n-C_{26}	9	10	10	14	23	46	$1.2x10^2$	$1.7x10^2$	$2.5x10^2$	$3.7x10^2$
n-C_{27}	57	59	53	66	73	89	$1.9x10^2$	$2.5x10^2$	$3.6x10^2$	$5.0x10^2$
n-C_{28}	12	13	12	19	25	39	$1.1x10^2$	$1.6x10^2$	$2.2x10^2$	$3.2x10^2$
n-C_{29}	95	$1.2x10^2$	$1.1x10^2$	$1.3x10^2$	$1.4x10^2$	$1.8x10^2$	$3.8x10^2$	$4.6x10^2$	$6.5x10^2$	$1.1x10^3$
n-C_{30}	12	14	15	20	26	54	$2.0x10^2$	$2.4x10^2$	$3.9x10^2$	$5.8x10^2$
n-C_{31}	$1.2x10^2$	$1.6x10^2$	$1.7x10^2$	$1.7x10^2$	$1.9x10^2$	$2.1x10^2$	$3.7x10^2$	$3.3x10^2$	$3.6x10^2$	$5.1x10^2$
n-C_{32}	6	10	11	12	19	42	93	$1.1x10^2$	$1.3x10^2$	$1.8x10^2$
n-C_{33}	47	62	65	72	77	83	$1.5x10^2$	$1.4x10^2$	$1.5x10^2$	$2.0x10^2$
n-C_{34}	2	3	3	5	5	10	27	41	67	91
n-C_{35}	4	9	1	8	14	21	48	56	74	97
n-C_{36}	0	0	0	1	2	4	13	18	19	43
n-C_{37}	0	0	2	2	7	67	$2.6x10^2$	$1.6x10^2$	$1.6x10^2$	$1.8x10^2$
n-C_{38}	0	0	0	0	4	86	$3.4x10^2$	$1.8x10^2$	$1.8x10^2$	$2.0x10^2$
n-C_{39}	0	0	0	0	2	17	59	33	30	41
HBI C_{20}	6	7	5	3	4	0	0	0	0	0
Pr[a]	2	14	21	16	45	67	$3.5x10^2$	$5.5x10^2$	$7.8x10^2$	$5.2x10^2$
Ph[a]	6	$1.3x10^2$	$1.6x10^2$	$1.6x10^2$	$3.2x10^2$	$3.9x10^2$	$1.3x10^3$	$1.1x10^3$	$1.3x10^3$	$7.3x10^2$
PME	10	15	11	10	7	10	28	26	42	97
Squalane	5	4	3	7	18	17	24	19	20	0
Lycopane	27	37	36	39	37	34	30	23	16	0
(20R)-βαα C_{27}[b]	0	0	1	6	13	68	86	43	36	22
(20R)-ααα C_{27}[b]	0	0	3	14	35	$1.3x10^2$	$2.4x10^2$	$1.5x10^2$	$1.2x10^2$	48
(20R)-βαα C_{28}[b]	0	0	1	2	6	35	72	37	25	8
(20R)-ααα C_{28}[b]	0	0	1	6	27	$1.2x10^2$	$2.4x10^2$	$1.3x10^2$	89	31
(20R)-βαα C_{29}[b]	0	0	2	7	18	$1.0x10^2$	$1.3x10^2$	70	54	25
(20R)-ααα C_{29}[b]	0	0	3	17	47	$1.8x10^2$	$3.7x10^2$	$2.3x10^2$	$1.7x10^2$	37

[a] Pr and Ph represent the summed amount of saturated and unsaturated Pr and Ph in both the saturated hydrocarbon fraction and the monoaromatic hydrocarbon fraction.

[b] Sterane.

study by Kenig *et al.* (1995), who quantitated free and sulphur-bound biomarkers in ten subsamples of the marl layer of evaporitic cycle IV of the Vena del Gesso Basin.

n-*Alkanes.* Gas chromatograms of the saturated hydrocarbon fractions of the original sample and the samples artificially matured at 220, 260 and 330°C are shown in Fig. 3.2. In the original sample the *n*-alkanes show a bimodal distribution, maximising at C_{17} and C_{31}. The long-chain *n*-alkanes have a strong odd-over-even carbon number predominance ($CPI_{24\text{-}34}$ = 8.1; Bray and Evans, 1961), typically attributed to input of higher plant epicuticular waxes (Eglinton and Hamilton, 1967). When the sample is heated, the

Table 3.2. Absolute amounts (μg/g TOC of original rock) of gammacerane and hopanes in the hydrocarbon fraction of the original sample and the artificially matured samples. The amounts listed for the 280 and 300°C experiments are not averages of the duplicate runs.

	original	220°C	239°C	260°C	280°C	300°C	330°C
Gammacerane[a]	0	1	8	10	19	9	4
(22S)-αß C_{31}	0	0	1	6	6	11	10
(22R)-αß C_{31}	0	1	4	23	34	53	16
(22S+R)-ßα C_{31}	0	1	3	15	23	38	16
(22R)-ßß C_{31}	2	7	9	11	5	0	0
(22S)-αß C_{32}	0	0	1	2	3	4	4
(22R)-αß C_{32}	0	1	1	7	12	15	6
(22S)-ßα C_{32}	0	0	0	1	1	2	3
(22R)-ßα C_{32}	0	0	1	8	12	12	7
(22R)-ßß C_{32}	0	2	3	5	2	0	0
(22S)-αß C_{33}	0	0	0	2	4	5	3
(22R)-αß C_{33}	0	0	1	11	13	12	5
(22S)-ßα C_{33}	0	0	1	4	4	4	3
(22R)-ßα C_{33}	0	0	2	13	16	17	5
(22R)-ßß C_{33}	0	2	5	7	2	0	0
(22S)-αß C_{34}	0	0	0	2	5	9	5
(22R)-αß C_{34}	0	0	3	12	26	28	8
(22S)-ßα C_{34}	0	0	0	4	8	12	5
(22R)-ßα C_{34}	0	0	1	16	27	30	7
(22R)-ßß C_{34}	0	3	6	12	4	0	0
(22S)-αß C_{35}	0	0	0	1	2	2	2
(22R)-αß C_{35}	0	0	3	7	10	7	3
(22S)-ßα C_{35}	0	0	0	2	2	1	2
(22R)-ßα C_{35}	0	0	1	6	7	5	2
(22R)-ßß C_{35}	0	2	5	5	1	0	0

[a] Gammacerane represents the summed amount of gammacerane and gammacer-2-ene.

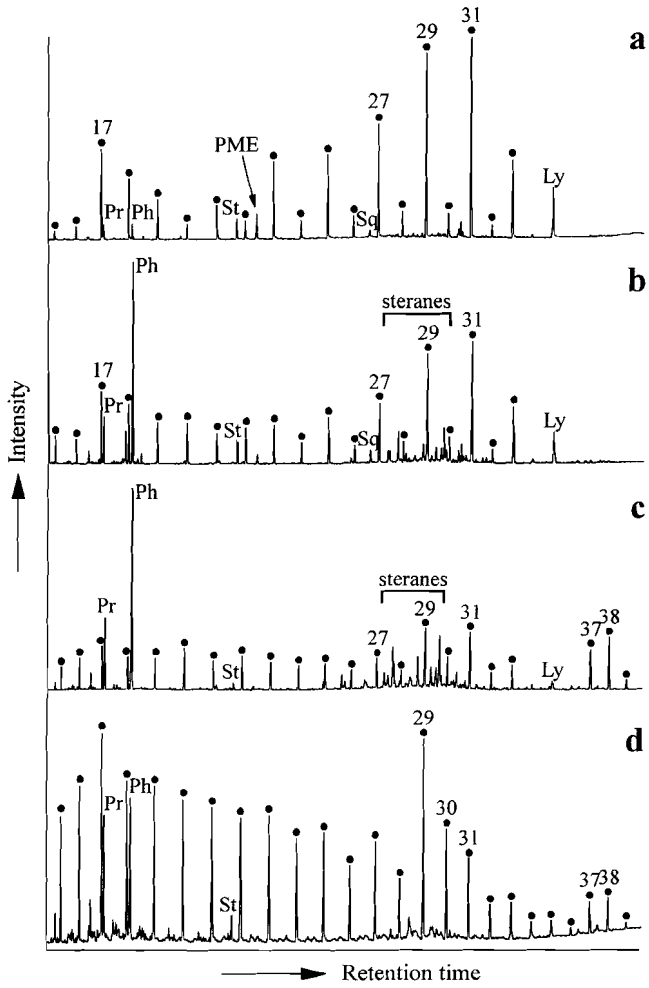

Fig. 3.2. Gas chromatogram of the saturated hydrocarbon fraction of (**a**) the original sample, and the samples artificially matured at (**b**) 220°C, (**c**) 260°C, and (**d**) 330°C. Key: dots = *n*-alkanes (numbers indicate number of carbon atoms), Pr = pristane, Ph = phytane, St = internal standard, PME = 2,6,10,15,19-pentamethyleicosane, Sq = squalane, Ly = lycopane.

CPI decreases steadily due to the massive production (factor 10-50) of even as well as odd *n*-alkanes. At 330°C the CPI is 1.7, and the *n*-alkane distribution is relatively smooth except for two features: (i) the C_{29} *n*-alkane is very abundant (*c.* 1.1 mg/g TOC of original rock) compared to the other long-chain *n*-alkanes, and (ii) the C_{37} and C_{38} *n*-alkanes are clearly increased. The latter is even more apparent at 260°C, where C_{37} and C_{38} are among the most abundant *n*-alkanes (Fig. 3.2**c**).

Acyclic isoprenoid alkanes. In the original sample, lycopane is the most abundant isoprenoid hydrocarbon (Fig. 3.2**a**). Other isoprenoids that can be distinguished are pristane (Pr), phytane (Ph), 2,6,10,15,19-pentamethylicosane (PME) and squalane. It should be noted that the peak denoted 'Pr' in Fig. 3.2**a** is actually a coelution of Pr and 2,6,10-trimethyl-7-(3-methylbutyl)dodecane, the C_{20} highly branched isoprenoid (HBI). Both Pr and Ph are produced in large amounts (*c.* 1.3 mg/g TOC of original rock for Ph) when the sample is heated. The concentrations of C_{20} HBI, squalane and lycopane are essentially constant with increasing maturation temperature, suggesting that these carbon skeletons are not present in HMW fractions from which they can be liberated upon increasing thermal stress. This was already recognised by Kohnen *et al.* (1992a,b), who found free but no sulphur- or oxygen-bound C_{20} HBI and lycopane in another marl from the Vena del Gesso Basin.

The acyclic isoprenoid hydrocarbons appear to be thermally less stable than the *n*-alkanes, since their absolute amounts are rapidly decreasing at 330°C whereas the *n*-alkanes are still increasing. This is probably due to the relative weakness of the bonds between secondary and tertiary carbon atoms in isoprenoids (*c.* 340 kJ/mol), compared to the bonds between two secondary carbon atoms in *n*-alkanes (*c.* 370 kJ/mol; Claxton *et al.*, 1993).

Steranes. In the original sample, no steranes could be detected. Upon thermal maturation up to 260°C, considerable amounts of (20R)-5α,14α,17α(H) and (20R)-5β,14α,17α(H) C_{27} to C_{29} steranes are produced (Table 3.1). At higher temperatures their amounts decrease, probably due to thermal degradation of the sterane carbon skeleton. The sterane distribution remains largely unchanged throughout the temperature range: (i) 5α isomers are more abundant than 5β isomers, and (ii) C_{29} steranes predominate over C_{27} and C_{28} steranes (Fig. 3.3**a**). The 20S/(20S+20R)-5α,14α,17α(H) C_{29} sterane ratio, which is often used as a maturity parameter and has an equilibrium value of 0.55 (Seifert and Moldowan, 1986) corresponding to a vitrinite reflectance of *c.* 0.8% (Peters and Moldowan, 1993, p. 226), increases gradually to 0.19 at 330°C (Fig. 3.3**b**). This suggests that the hydrous pyrolysis temperatures applied represent relatively mild levels of thermal maturity. It should be noted, however, that significant amounts of expelled oil (up to 110 mg/g TOC of original rock) were collected after hydrous pyrolysis at temperatures higher than 260°C.

Triterpanes. The only hopane identified in the original sample is (22R)-17β,21β(H) C_{31} hopane. When the sample is artificially matured at 220°C, low amounts of C_{31} to C_{35} hopanes [mainly (22R)-17β,21β(H) isomers] are produced. At temperatures up to 280°C more hopanes are produced, including (22R)- and (22S)-17α,21β(H) and 17β,21α(H) isomers. At temperatures higher than 280°C their amounts decrease, probably due to thermal degradation of the hopane carbon skeleton. The 22S/(22S+22R)-17α,21β(H) C_{35} hopane ratio, an often used maturity parameter with an equilibrium value of

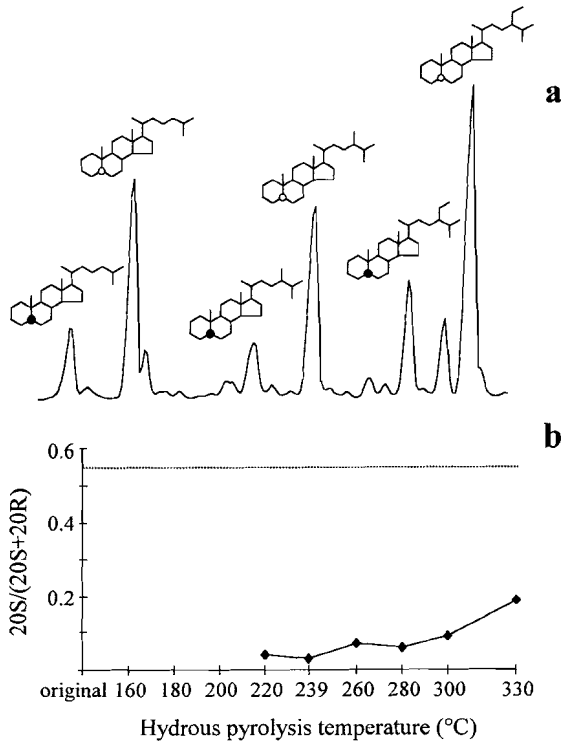

Fig. 3.3. (**a**) Partial m/z 217 mass chromatogram of the saturated hydrocarbon fraction of the sample artificially matured at 260°C, showing the distribution of the C_{27} to C_{29} steranes. (**b**) Diagram showing the 20S/(20S+20R)-5α,14α,17α(H) C_{29} sterane ratio as a function of maturation temperature. The thermodynamic equilibrium value of 0.55 (Seifert and Moldowan, 1986) is indicated with a stippled line.

c. 0.6, reaches 0.43 at 330°C (Fig. 3.4), suggesting that the sample has barely entered the catagenetic stage. At 280°C, the thermodynamically unstable 17β,21β(H) isomer of C_{35} hopane is still present (Fig. 3.4), which is another indication of the relatively low level of thermal maturity represented by these artificial maturation experiments.

The summed absolute amounts of all isomers of any hopane skeleton reach a maximum at higher temperatures than those of the sterane skeletons. Their maximum amounts, however, are an order of magnitude lower than those of the steranes. This could suggest that the hopane carbon skeleton is more resistant to thermal stress than the sterane carbon skeleton. Similar results were reported by Eglinton and Douglas (1988) for hydrous pyrolysis of an immature kerogen from the Kimmeridge Clay Formation, although their optimum temperatures are *c.* 30°C higher.

Gammacerane (**I**; see Appendix) could not be detected in the original sample, but is produced when the sample is heated at 220°C and higher temperatures (Table 3.2).

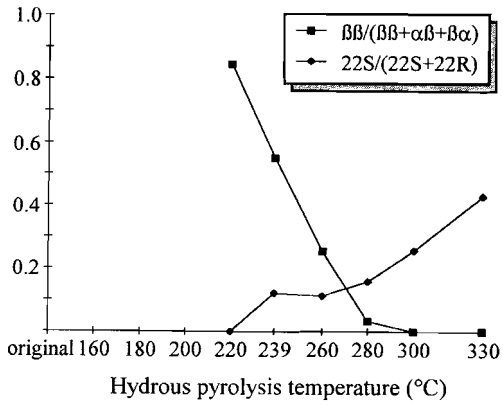

Fig. 3.4. Diagram showing two hopane maturity parameters, the ββ/(ββ+αβ+βα) C_{35} hopane ratio (squares) and the 22S/(22S+22R)-17α,21β(H) C_{35} hopane ratio (diamonds), as a function of maturation temperature. The thermodynamic equilibrium values are 0 and 0.6, respectively (Seifert and Moldowan, 1986).

Recently, a new route for the formation of gammacerane from tetrahymanol (**II**) was proposed (Sinninghe Damsté *et al.*, 1995c) based partly on data presented here. This route involves the incorporation of tetrahymanol (or its derivatives gammacer-2-ene and gammacer-3-one) in a sulphur-rich macromolecular network, from which it is liberated as free gammacerane after moderate thermal stress is applied.

Monoaromatic hydrocarbon fraction

Absolute amounts of selected compounds in the monoaromatic hydrocarbon fraction of the original sample and the artificially matured samples are listed in Table 3.3. Absolute amounts of alkylthiophenes have been reported elsewhere (Koopmans *et al.*, 1995).

In a recent study of the thermal stability of alkylthiophene biomarkers, the abundance and isomer distribution of alkylthiophenes as a function of maturation temperature was already discussed (Koopmans *et al.*, 1995). In short, large amounts of linear alkylthiophenes (C_{12}-C_{26}) are generated from the kerogen upon artificial maturation at temperatures higher than 239°C (Fig. 3.5). Thiophenes with a Ph carbon skeleton (**III-V**) are particularly abundant (up to 500 μg/g TOC of original rock), and they are partly released already at the lowest temperatures (160-180°C). The specific isomer distributions of the C_{31} and C_{38} mid-chain 2,5-di-*n*-alkylthiophenes are retained over a large maturation temperature interval, indicating that alkylthiophenes are useful as biomarkers during progressive diagenesis. These isomer distributions enabled the identification of possible precursors, *i.e.* C_{30}-C_{32} (unsaturated) 1,15-diols or 15-keto-1-ols for the C_{31} 2,5-di-*n*-alkylthiophenes and C_{38} di-unsaturated methyl and ethyl ketones for the C_{38} 2,5-di-*n*-alkylthiophenes (Koopmans *et al.*, 1995). A C_{35} hopanoid thiophene with the

Table 3.3. Absolute amounts (μg/g TOC of original rock) of selected compounds in the monoaromatic hydrocarbon fraction and the polyaromatic hydrocarbon fraction of the original sample and the artificially matured samples. Also indicated is the chroman ratio (Sinninghe Damsté *et al.*, 1987b, 1989d). Roman numbers refer to structures in the Appendix.

	original	160°C	180°C	200°C	220°C	239°C	260°C	280°C	300°C	330°C
VI	18	31	19	51	46	24	16	0	0	0
C_{30} 1,2-DAB[a]	0	0	0	0	0	5	16	26	52	62
C_{31} 1,2-DAB	0	0	0	2	4	14	45	34	92	86
C_{37} 1,2-DAB	0	0	0	0	0	1	9	14	22	31
C_{38} 1,2-DAB	0	0	0	0	0	1	11	18	28	41
VIIa	0	0	0	7	14	16	39	20	8	0
VIIb	0	0	0	0	1	11	36	18	10	0
Isorenieratane	0	1	3	12	14	$1.1x10^2$	79	$1.1x10^2$	57	9
VIIIa	0	0	0	0	0	0	1	1	0	0
VIIIb	2	1	2	4	4	4	7	8	6	0
VIIIc	7	4	5	9	12	17	24	28	16	2
Chroman ratio	0.8	0.7	0.8	0.7	0.8	0.8	0.8	0.8	0.7	na[b]

[a] DAB = di-*n*-alkylbenzenes.

[b] Not applicable due to low amounts of methylated chromans.

17β,21β(H) configuration (**VI**) is present in the original sample (Fig. 3.5**a**). Its concentration increases up to 220°C, after which it decreases and is zero at 280°C. The decrease is partly due to isomerisation of the 17β,21β(H) configuration to the thermodynamically more stable 17α,21β(H) and 17β,21α(H) configurations.

Apart from alkylthiophenes, abundant C_{27} to C_{29} sterenes, steradienes and A- and C-ring monoaromatic steroids are present in this fraction (Fig. 3.5). These compounds become relatively less abundant with increasing thermal maturation. 1,2-Di-*n*-alkylbenzenes with C_{30} and C_{31}, and C_{37} and C_{38} skeletons are produced after heating at 200 and 239°C, respectively. The C_{31} 1,2-di-*n*-alkylbenzenes are dominated by one isomer, 1-dodecyl-2-tridecylbenzene, just as the C_{31} mid-chain 2,5-di-*n*-alkylthiophenes are dominated by 2-tetradecyl-5-tridecylthiophene (Koopmans *et al.*, 1995). Possible precursors for 2-tetradecyl-5-tridecylthiophene are thought to have a functional group at C-15 (*e.g.* C_{30}-C_{32} 1,15-diols or 15-keto-1-ols), more so because the other mid-chain 2,5-di-*n*-alkylthiophenes in the C_{28}-C_{32} range also showed a predominance of the 2-alkyl-5-tetradecylthiophene (Koopmans *et al.*, 1995). However, the predominance of 1-dodecyl-2-tridecylbenzene, when compared with recent work by Behar *et al.* (1995), suggests a functional group at C-13 or C-14. The less abundant C_{30} 1,2-di-*n*-alkylbenzenes mainly consist of 1-tridecyl-2-undecylbenzene, suggesting a functional group at C-14. The intensity of the C_{37} and C_{38} 1,2-di-*n*-alkylbenzenes was too low to determine their isomer

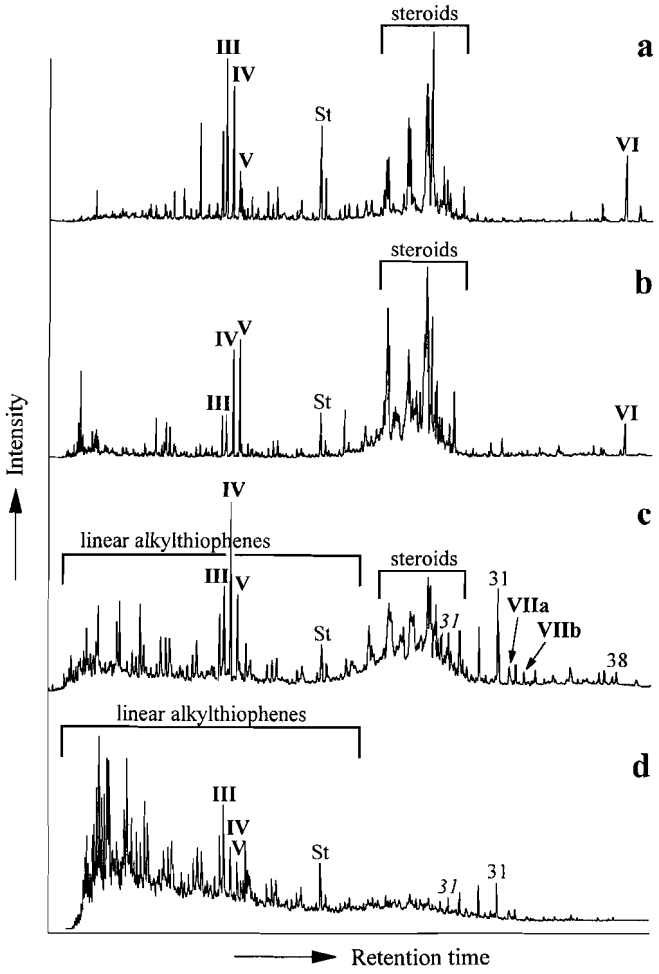

Fig. 3.5. Gas chromatogram of the monoaromatic hydrocarbon fraction of (**a**) the original sample, and the samples artificially matured at (**b**) 220°C, (**c**) 260°C, and (**d**) 330°C. Key: St = internal standard. Regular numbers indicate number of carbon atoms of mid-chain 2,5-di-*n*-alkylthiophenes. Italic numbers indicate number of carbon atoms of 1,2-di-*n*-alkylbenzenes. Roman numbers refer to structures in the Appendix.

distribution. A number of benzohopanes (**VII**) is produced when the sample is heated at 200°C and higher temperatures. Their generation profiles are similar to those of the hopanes in the hydrocarbon fraction (cf. Tables 3.2 and 3.3).

Polyaromatic hydrocarbon fraction

Absolute amounts of selected compounds in the polyaromatic hydrocarbon fraction of the original sample and the artificially matured samples are listed in Table 3.3. Gas chromatograms of the polyaromatic hydrocarbon fraction of the original sample and the samples artificially matured at 220, 260 and 300°C are shown in Fig. 3.6. The polyaromatic hydrocarbon fraction is very complex. It contains LMW diaromatics (naphtha-

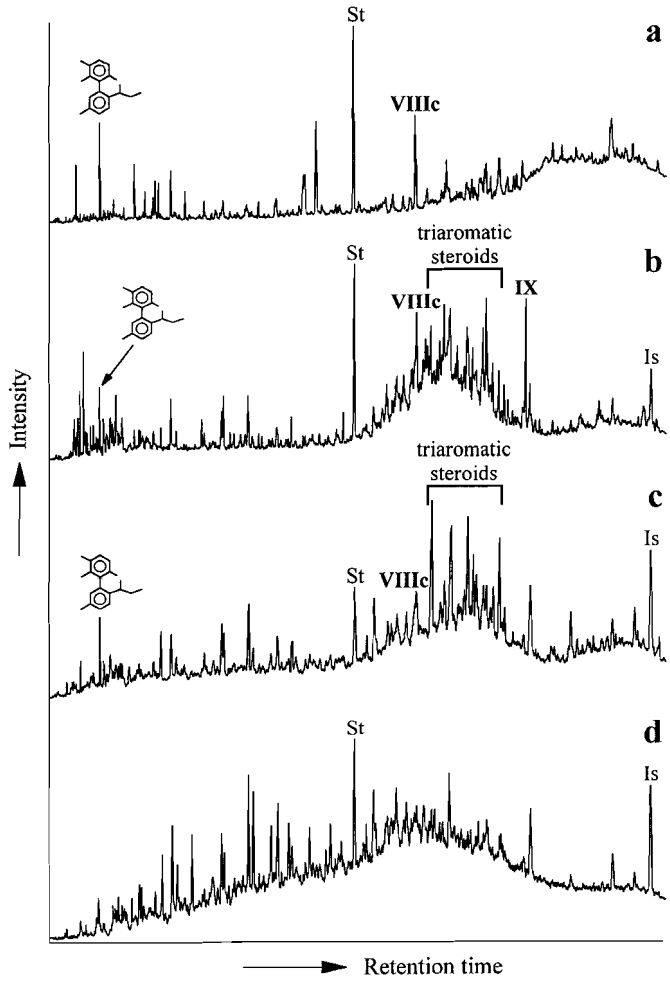

Fig. 3.6. Gas chromatogram of the polyaromatic hydrocarbon fraction of (**a**) the original sample, and the samples artificially matured at (**b**) 220°C, (**c**) 260°C, and (**d**) 300°C. Key: St = internal standard, Is = isorenieratane. Roman numbers refer to structures in the Appendix. The indicated alkylated biphenyl is one of the diagenetic products of isorenieratene (**X**) (Koopmans *et al.*, 1996a).

lenes and biphenyls), C_{27} to C_{29} triaromatic steroids, methylated 2-methyl-2-(4,8,12-trimethyltridecyl)chromans (**VIII**), a benzohopane (**IX**), and polyaromatic derivatives of the diaromatic carotenoid isorenieratene (**X**).

The biological origin of the methylated chromans is unknown (Sinninghe Damsté *et al.*, 1993c). Therefore, it is interesting that their concentrations increase with increasing maturation temperature (Table 3.3), which suggests that they are released from, and thus were incorporated into, a HMW fraction. The relative abundance of the methylated chromans, expressed as the chroman ratio [**VIIIc/(VIIIa+VIIIb+VIIIc)**], has been proposed as an indicator for palaeosalinity (Sinninghe Damsté *et al.*, 1987b, 1989d). It has been used successfully in a study of a large sample set from the Mulhouse Basin (Sinninghe Damsté *et al.*, 1993c). From our data it follows that the chroman ratio is essentially constant over the maturity interval investigated (Table 3.3), suggesting that the chroman ratio can be used for sedimentary rocks that have undergone progressive diagenesis ($0.25\% \leq R_o < 0.6\%$; *vide infra*). The use of the chroman ratio is probably restricted to an upper maturity level, due to thermal degradation of the skeletons of the methylated chromans (Table 3.3). The chroman ratio is probably a better indicator for palaeosalinity than the isoprenoid thiophene ratio (Sinninghe Damsté *et al.*, 1989d), which has been shown to be strongly maturity dependent in the same maturity interval (Koopmans *et al.*, 1995).

The polyaromatic derivatives of isorenieratene (**X**) present in this fraction have recently been identified, and the generation profiles of some of these compounds have been described (Koopmans *et al.*, 1996a). These diagenetic products of isorenieratene include C_{40}, C_{33}, C_{32} and short-chain compounds. The reactions by which they are formed are (i) sulphurisation, (ii) cyclisation and subsequent aromatisation of the polyene isoprenoid chain, and (iii) expulsion of *m*-xylene and toluene from the polyene isoprenoid chain. C-C bond cleavage takes place during catagenesis, resulting in the formation of short-chain compounds (*e.g.* aryl isoprenoids).

Alkylsulphide fraction

Absolute amounts of alkylthiolanes, alkylthianes and alkyl-1,2-dithianes in the alkylsulphide fraction of the original sample and the artificially matured samples are listed in Table 3.4. Gas chromatograms of the alkylsulphide fraction of the original sample and the samples artificially matured at 220, 260 and 300°C are shown in Fig. 3.7.

In the original sample three 1,2-dithianes are present with a *n*-C_{18}, Ph and (22R)-17β,21β(H) C_{35} hopane carbon skeleton, respectively. After artificial maturation at 160°C their concentrations decrease dramatically, probably due to the weakness of the S-S bond. After heating at 200°C these disulphides could not be detected. These results strongly suggest that macromolecularly polysulphide-bound compounds in the polar fraction will be released at similarly low temperatures. Another compound bearing two sulphur atoms (**XI**) is present in the original sample. **XI** was recently identified by Schouten *et al.* (1995d), who reported that it was difficult to desulphurise with Raney

Ni. They ascribed this to the shielding of the sulphur atoms by the quaternary carbon atoms of **XI**. Thermal stress probably causes rapid degradation of **XI**, since the thermally induced homolytic cleavage of the C-S bonds will result in relatively stable tertiary radicals. Indeed, **XI** does not survive heating at 239°C, suggesting it is thermally unstable. However, it is not possible to compare the generation profiles of **XI** and other alkylsulphides directly, since **XI** is probably not produced upon heating whereas most alkylsulphides are.

Alkylthiolanes and alkylthianes are hardly present in the original sample, with the exception of a thiane with a squalane carbon skeleton (**XII**) first identified by Kohnen *et al.* (1992b). In general, alkylthiolanes and alkylthianes are formed in significant amounts when the sample is heated at 239°C. Their concentrations maximise between 260 and 280°C, whilst at 330°C they have disappeared. In comparison to the abundance and carbon number distribution of the alkylthiophenes (Koopmans *et al.*, 1995), the alkylthiolanes and alkylthianes are *c.* 5-10 times less abundant and seem to be more restricted to shorter-chain carbon skeletons. Alkylthiophenes are still abundantly present at 330°C, whereas the alkylsulphides (*i.e.* alkylthiolanes and alkylthianes) have disappeared at that temperature, suggesting that alkylthiophenes are thermally more stable. The generation profiles of alkylthiophenes and alkylsulphides are broadly similar, suggesting that they are formed from a HMW fraction by similar processes. No evidence is found that alkylthiophenes are formed from aromatisation of alkylsulphides, as proposed in the early literature (for a review see Sinninghe Damsté and de Leeuw, 1990).

It is remarkable that no alkylsulphides were detected with *n*-C_{30}, *n*-C_{31}, *n*-C_{37} and *n*-C_{38} skeletons, since these skeletons were abundantly present in the monoaromatic fraction as mid-chain 2,5-di-*n*-alkylthiophenes and 1,2-di-*n*-alkylbenzenes. Alkylsulphides with *n*-C_{37} and *n*-C_{38} skeletons have been reported before (Sinninghe Damsté *et al.*, 1989c; Rullkötter *et al.*, 1990; Barakat and Rullkötter, 1994). Our results suggest that the thermal release of *n*-C_{30}, *n*-C_{31}, *n*-C_{37} and *n*-C_{38} skeletons from HMW fractions predominantly yields alkylthiophenes and alkylbenzenes as stable products.

Apart from alkylsulphides, this fraction also contains some polyaromatic derivatives of isorenieratene (**X**) (Koopmans *et al.*, 1996a).

Polar fraction

The polar fraction, which contains both LMW polar compounds (*e.g.* ketones, alcohols and carboxylic acids) and geomacromolecules containing heteroatoms, has been extensively studied for sulphur- and oxygen-bound moieties by several chemical degradation techniques. These include (i) Raney Ni desulphurisation (cleavage of C-S bonds), (ii) MeLi/MeI treatment (cleavage of S-S bonds), (iii) HI/$LiAlH_4$ treatment (cleavage of C-O bonds), and (iv) isolation of ketones. They are schematically shown in Fig. 3.1. These fractions are discussed hereafter.

Sulphur-bound carbon skeletons

Absolute amounts of *n*-alkanes, acyclic isoprenoid alkanes, steranes, triterpanes and other compounds released after Raney Ni desulphurisation and subsequent hydrogena-

Table 3.4. Absolute amounts (µg/g TOC of original rock) of alkylthiolanes, alkylthianes and alkyl-1,2-dithianes with indicated carbon skeletons in the alkylsulphide fraction of the original sample and the artificially matured samples. Roman numbers refer to structures in the Appendix.

	original	160°C	180°C	200°C	220°C	239°C	260°C	280°C	300°C	330°C
Alkylthiolanes:										
n-C_{13}	0	nd[a]	nd	0	0	0	3	3	2	0
n-C_{14}	0	nd	nd	0	0	1	17	11	8	0
n-C_{15}	0	nd	nd	0	0	1	31	20	12	0
n-C_{16}	1	nd	nd	0	0	3	34	19	13	0
n-C_{17}	0	nd	nd	0	0	1	12	16	7	0
n-C_{18}	0	nd	nd	0	1	5	25	30	10	0
n-C_{19}	0	nd	nd	0	0	2	6	10	4	0
n-C_{20}	0	nd	nd	0	1	3	6	10	4	0
n-C_{21}	0	nd	nd	0	0	1	0	6	3	0
n-C_{22}	0	nd	nd	0	1	6	4	10	4	0
n-C_{23}	0	nd	nd	0	0	0	0	1	0	0
n-C_{24}	0	nd	nd	0	0	0	0	2	0	0
Ph	0	nd	nd	6	4	15	94	94	28	0
Alkylthianes:										
n-C_{14}	0	nd	nd	0	0	1	11	5	4	0
n-C_{15}	0	nd	nd	0	0	1	15	7	4	0
n-C_{16}	0	nd	nd	0	0	2	19	6	4	0
n-C_{17}	0	nd	nd	0	0	0	0	1	0	0
n-C_{18}	0	nd	nd	0	0	0	5	5	2	0
n-C_{20}	0	nd	nd	0	0	0	0	2	1	0
n-C_{22}	0	nd	nd	0	0	0	0	2	1	0
Squalane	9	nd	nd	7	7	6	3	4	2	0
XI	11	nd	nd	4	4	0	0	0	0	0
Alkyl-1,2-dithianes:										
n-C_{18}	4	nd	nd	0	0	0	0	0	0	0
Ph	6	nd	nd	0	0	0	0	0	0	0
(22S) ßß C_{35}[b]	10	1	1	0	0	0	0	0	0	0

[a] Not determined due to absence of standard.

[b] Hopane.

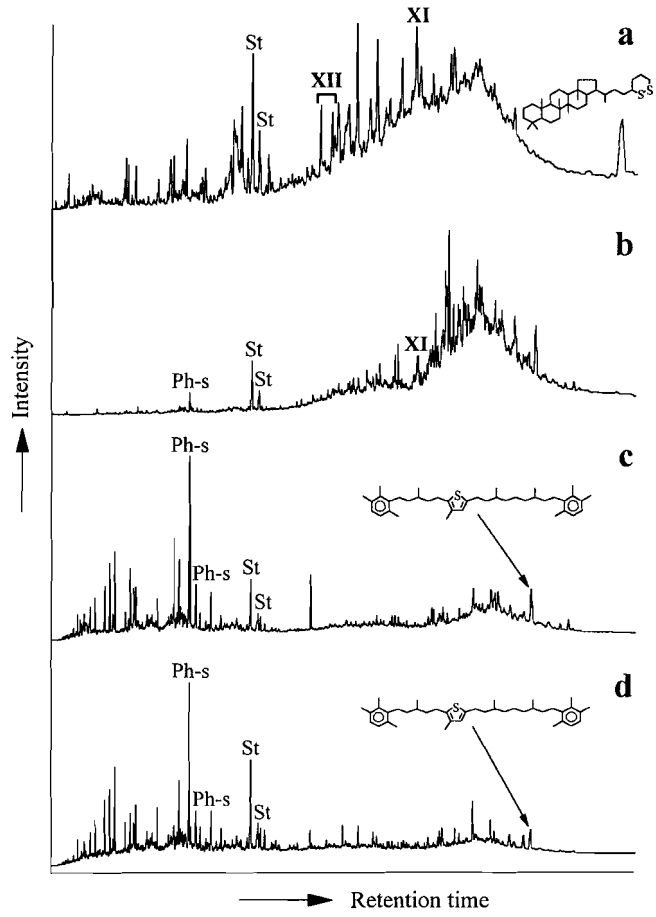

Fig. 3.7. Gas chromatogram of the alkylsulphide fraction of (**a**) the original sample, and the samples artificially matured at (**b**) 220°C, (**c**) 260°C, and (**d**) 300°C. Key: Ph-s = alkylthiolane with a Ph carbon skeleton, St = internal standard. Roman numbers refer to structures in the Appendix. The diaromatic compound in (**c**) and (**d**) is one of the diagenetic products of isorenieratene (**X**) (Koopmans *et al.*, 1996a). It should be noted that alkylthiolanes (including the standard) and alkylthianes elute as a doublet of *cis* and *trans* isomers (Sinninghe Damsté *et al.*, 1987c).

tion of polar fraction I (see Fig. 3.1) of the original sample and the artificially matured samples are listed in Table 3.5. These data correlate well with data from a recent study by Kenig *et al.* (1995), who quantitated free and sulphur-bound biomarkers in ten subsamples of the marl layer of evaporitic cycle IV of the Vena del Gesso Basin. Gas chromatograms of the hydrogenated desulphurised polar fractions of the original sample and the samples artificially matured at 220, 260 and 300°C are shown in Fig. 3.8.

Table 3.5. Absolute amounts (μg/g TOC of original rock) of compounds released after desulphurisation and subsequent hydrogenation of polar fraction I of the original sample and the artificially matured samples.

	original	160°C	180°C	200°C	220°C	239°C	260°C	280°C	300°C	330°C
n-C_{16}	12	28	20	20	34	34	58	20	47	37
n-C_{17}	27	37	33	35	44	55	67	29	54	52
n-C_{18}	79	72	68	86	94	$1.1x10^2$	$1.1x10^2$	52	68	71
n-C_{19}	28	28	22	41	40	51	55	28	38	41
n-C_{20}	54	52	49	75	65	67	56	28	32	42
n-C_{21}	25	23	24	41	39	45	43	20	29	31
n-C_{22}	52	46	46	64	54	60	47	18	25	43
n-C_{23}	25	16	16	33	30	31	29	13	17	25
n-C_{24}	29	26	26	45	35	38	30	11	14	22
n-C_{25}	18	13	13	30	25	23	27	11	13	17
n-C_{26}	30	29	25	43	33	32	24	10	10	14
n-C_{27}	14	11	11	23	19	20	20	7	7	10
n-C_{28}	36	29	28	48	37	35	29	11	15	10
n-C_{29}	23	22	28	50	40	57	47	11	11	18
n-C_{30}	62	85	$1.3x10^2$	$1.8x10^2$	83	$1.5x10^2$	92	19	17	21
n-C_{31}	29	47	68	92	72	$1.5x10^2$	$1.2x10^2$	19	17	17
n-C_{32}	20	33	50	74	45	$1.0x10^2$	54	10	7	7
n-C_{33}	14	15	14	35	25	28	23	6	4	3
n-C_{34}	4	10	9	26	20	20	15	5	3	1
n-C_{35}	11	12	14	27	19	30	25	6	4	1
n-C_{36}	3	6	5	17	5	18	8	3	1	0
n-C_{37}	18	32	41	$1.6x10^2$	95	97	40	11	5	1
n-C_{38}	14	42	50	$1.7x10^2$	$1.0x10^2$	$1.2x10^2$	39	11	6	1
n-C_{39}	0	5	5	19	16	20	5	2	1	0
Pr	7	10	11	11	15	11	19	9	14	6
Ph	$4.1x10^2$	$3.2x10^2$	$3.2x10^2$	$3.4x10^2$	$3.0x10^2$	$2.1x10^2$	$2.6x10^2$	$1.2x10^2$	$1.5x10^2$	$2.0x10^2$
HBI C_{25}	6	8	6	10	5	3	4	5	0	0
Squalane	13	18	19	45	25	16	25	6	4	0
(20R)-βαα C_{27}[a]	55	50	54	81	47	25	14	4	0	0
(20R)-ααα C_{27}[a]	$2.0x10^2$	$1.3x10^2$	$1.4x10^2$	$2.0x10^2$	$1.1x10^2$	58	19	3	0	0
(20R)-βαα C_{28}[a]	$1.1x10^2$	40	40	76	44	21	13	4	0	0
(20R)-ααα C_{28}[a]	$2.3x10^2$	78	77	$1.5x10^2$	73	49	17	3	0	0
(20R)-βαα C_{29}[a]	$1.9x10^2$	78	73	$1.3x10^2$	74	39	26	9	0	0
(20R)-ααα C_{29}[a]	$3.4x10^2$	$1.5x10^2$	$1.5x10^2$	$2.4x10^2$	$1.3x10^2$	79	30	5	0	0
Gammacerane	33	12	10	20	11	0	1	0	0	0
(22R)-ββ C_{35}[b]	45	39	32	48	35	14	6	0	0	0
Isorenieratane	66	$6.1x10^2$	$7.7x10^2$	$1.0x10^3$	$4.6x10^2$	$4.2x10^2$	$5.5x10^2$	58	7	0

[a] Sterane.
[b] Hopane.

n-*Alkanes.* The *n*-alkanes are relatively minor compounds in the desulphurised polar fraction I of the original sample. They show a bimodal distribution, maximising at C_{18} and C_{30}. A moderate even-over-odd carbon number predominance of the long-chain *n*-alkanes is noted ($CPI_{24\text{-}34}$ = 0.6). With increasing thermal maturation the amounts of even as well as odd *n*-alkanes released after desulphurisation of polar fraction I typically increase, so that the CPI approaches unity. The increase in the amounts of released *n*-alkanes is probably caused by the thermal breakdown of the kerogen discharging relatively small sulphur-linked moieties, amongst others containing *n*-alkane carbon skeletons, into the polar fraction. This phenomenon also causes the sudden appearance of the C_{37} and C_{38} *n*-alkanes at 200°C (Figs. 3.8**b** and **c**). These carbon skeletons are not present in the desulphurised polar fraction I of the original sample, since sulphurisation of their precursors (C_{37} and C_{38} di- and tri-unsaturated ketones from Prymnesiophyte algae), containing a relatively large number of widely spaced functional groups, sequesters these skeletons in the kerogen (Koopmans *et al.*, 1997b).

Acyclic isoprenoid alkanes. Ph is the most abundant compound in the desulphurised polar fraction of the original sample (Fig. 3.8**a**). Other acyclic isoprenoids, *i.e.* Pr, 2,6,10,14-tetramethyl-7-(3-methylpentyl)pentadecane (C_{25} HBI) and squalane are present in minor amounts. When the sample is heated, the amount of Ph gradually decreases until at 330°C it is *c.* 50% of its original value. The amounts of the other acyclic isoprenoids first increase, after which they approach zero at 330°C.

Steranes. (20R)-5α,14α,17α(H) and (20R)-5β,14α,17α(H) C_{27} to C_{29} steranes are abundant in the desulphurised polar fraction of the original sample (Fig. 3.8**a**). With increasing thermal maturation their amounts decrease, and at 300°C they are not detectable, suggesting that the sulphur-bound steranes have been released as free steranes and steroids. The gradually decreasing amounts of sulphur-bound steranes in the polar fraction also suggest that in the original sample steranes are mainly present in the polar fraction and not in the kerogen, contrary to the *n*-alkanes (Table 3.5).

In the original sample and after mild thermal treatment, the sterane distribution is similar to that of the saturated hydrocarbon fraction (cf. Fig. 3.3**a**), *i.e.* 5α-isomers are more abundant than 5β-isomers. At 280°C, however, 5β-isomers are slightly more dominant than 5α-isomers (Table 3.5). Since 5α-steranes are more stable than 5β-steranes (Mackenzie *et al.*, 1980; van Graas *et al.*, 1982), this suggests that sulphur-bound 5α-steranes are released at a higher rate than 5β-steranes.

Triterpanes. In the original sample, the triterpanes are dominated by gammacerane (**I**) and (22R)-17β,21β(H) C_{35} hopane, whereas the C_{31} to C_{34} 17β,21β(H) homologues are much less abundant. With increasing thermal maturation the amount of gammacerane decreases until it is undetectable at 239°C. This suggests that sulphur-bound gammacerane, like the steranes but unlike most *n*-alkanes, is not released from the kerogen into

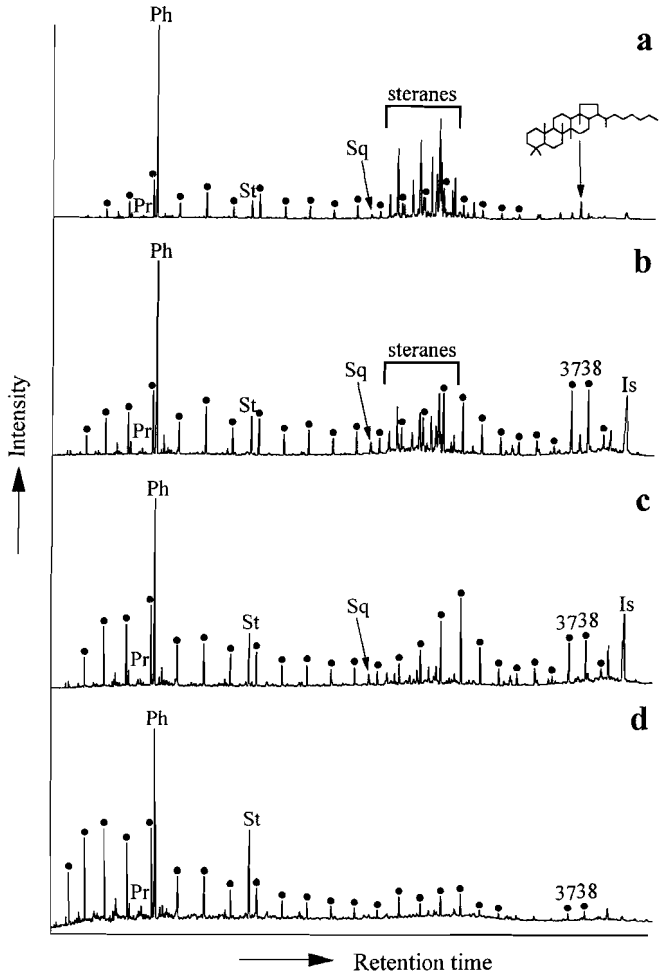

Fig. 3.8. Gas chromatogram of the desulphurised polar fraction I of (**a**) the original sample, and the samples artificially matured at (**b**) 220°C, (**c**) 260°C, and (**d**) 300°C. Key: dots = *n*-alkanes (numbers indicate number of carbon atoms), Pr = pristane, Ph = phytane, St = internal standard, Sq = squalane, Is = isorenieratane.

the polar fraction with increasing thermal stress. This is in line with the finding by Schouten *et al.* (1995b) that gammacerane is bound to other moieties by only one sulphur bridge in the polar fraction of a marl from the Vena del Gesso Basin. Because the precursor of gammacerane, tetrahymanol (**II**), has only one functional group, the chance that it becomes part of a sulphur-rich HMW fraction upon natural sulphurisation is small.

Throughout the maturation series, the C_{35} homologues remain the most abundant

hopanes in the desulphurised polar fraction. The amount of (22R)-17β,21β(H) C_{35} hopane gradually decreases with increasing maturation until it is undetectable at 280°C. At 160°C, (22R)-17α,21β(H) and 17β,21α(H) C_{35} hopane are already present in low amount.

Other compounds. Diagenetic products of isorenieratene (**X**) enter the polar fraction after mild thermal treatment (Fig. 3.8**b**). They are dominated by isorenieratane, whereas small amounts of C_{32} and C_{33} diaryl isoprenoids, and C_{40} diaryl isoprenoids with an additional benzene ring are also present. Their generation profiles have been discussed in detail elsewhere (Koopmans *et al.*, 1996a). The amount of isorenieratane present in the 200°C experiment is *c.* 15 times higher than in the original sample, indicating that sulphur-bound isorenieratane is released from the kerogen into the polar fraction.

Polysulphide-bound carbon skeletons

Polar fraction I of the original sample and the samples heated at 160-280°C was checked for the presence of S-S bonds by treatment with MeLi/MeI, which selectively cleaves S-S bonds, producing methylthioethers (Kohnen *et al.*, 1991b). These were desulphurised with Raney Ni and subsequently hydrogenated before their carbon skeletons were analysed by GC and GC-MS.

The distribution of compounds released after MeLi/MeI treatment of polar fraction I of the original sample is similar to that released after desulphurisation of polar fraction I (cf. Fig. 3.8**a**). Ph and (20R)-5α,14α,17α(H) and 5β,14α,17α(H) C_{27} to C_{29} steranes are dominant compounds, and *n*-alkanes are present in moderate amounts. The main difference between the two fractions is the high abundance of gammacerane (**I**) in the MeLi/MeI treated polar fraction, an anomaly also noted by Schouten *et al.* (1995b) for another marl sample from the Vena del Gesso Basin.

The relative amount of polysulphide-bound *vs.* total sulphur-bound carbon skeletons typically increases at low maturation temperatures (Fig. 3.9). At first, this result may be puzzling because S-S bonds are weaker than C-S bonds and, therefore, one intuitively expects the relative amount of polysulphide-bound skeletons to decrease with increasing thermal stress. However, the increasing relative amount of polysulphide-bound carbon skeletons is perfectly logical. Assume that during natural sulphurisation of a given multifunctionalised lipid mono- and polysulphidic inorganic sulphur species are available in a ratio x:y. Then, every functional group that undergoes natural sulphurisation has a chance of [y/(x+y)] * 100% of becoming polysulphide-linked. Thus, when one sulphur link is present, MeLi/MeI treatment will result in a [y/(x+y)] * 100% yield. When two sulphur links are present, the yield will be [y/(x+y) * y/(x+y)] * 100%, and in the general case of n sulphur links the yield will be $[y^n/(x+y)^n]$ * 100%, since only carbon skeletons that are exclusively polysulphide-bound contribute to the yield obtained by MeLi/MeI treatment. Consequently, the yield of the MeLi/MeI treatment decreases with increasing number of sulphur links. This is supported by the results of the MeLi/

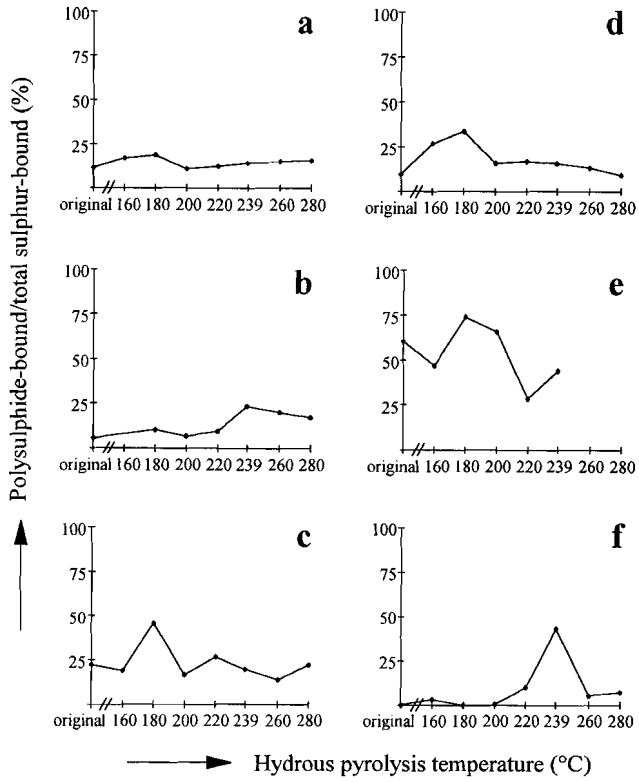

Fig. 3.9. Relative amount (%) of polysulphide-bound *vs.* total sulphur-bound (**a**) *n*-C_{22}, (**b**) *n*-C_{38}, (**c**) squalane, (**d**) (20R)-5α,14α,17α(H) C_{29} sterane, (**e**) gammacerane, and (**f**) isorenieratane as a function of hydrous pyrolysis temperature. The missing data points in (**e**) are due to the absence of sulphur-bound gammacerane. The data points of the 280°C experiment are not averages of the duplicate runs.

MeI treatment of polar fraction I of the original sample (Fig. 3.9). Only a very small portion of the carbon skeletons known to be derived from multifunctionalised precursors prone to multiple sulphur-linking is exclusively polysulphide-bound (*e.g.* C_{38} *n*-alkane: 6%, isorenieratane: 0%).

When thermal stress is applied, sulphur links will be cleaved. Assuming that mono- and polysulphide links are equally weak, the chance that a monosulphide link is thermally cleaved equals the chance that a polysulphide link is thermally cleaved. If n sulphur links are originally present, the number of links after one thermal cleavage is (n-1), and MeLi/MeI treatment will result in a $[y^{(n-1)}/(x+y)^{(n-1)}]$ * 100% yield. Therefore, the yield after one cleavage divided by the original yield equals [(x+y)/y]. Since in a typical example x (the relative amount of monosulphide links) is greater than 0, [(x+y)/y] is greater than 1 and, thus, the relative amount of polysulphide-bound carbon

skeletons increases after thermal cleavage of one sulphur link. By analogy, the yield will increase after each successive cleavage.

Since S-S bonds are actually weaker than C-S bonds, it is more realistic to introduce a relative probability for the cleavage of monosulphide links (p) and polysulphide links (q). If a given moiety is linked by n sulphur links, the MeLi/MeI yield after thermal cleavage of one sulphur link equals:

$$\{[y^n/(x+y)^n] + [np/(p+(n-1)q) * xy^{(n-1)}/(x+y)^n]\} * 100\%.$$

The first term in square brackets equals the original yield. The second term in square brackets is greater than 0, even when p approaches 0 and q approaches 1. Therefore, the yield after one thermal cleavage is greater than the original yield. By analogy, the yield will increase after each successive cleavage.

Fig. 3.9 shows that the relative amount of polysulphide-bound carbon skeletons, as a function of maturation temperature, differs greatly for different carbon skeletons. This is probably a result of the different number of functionalities of their precursors. Compounds originating from precursors containing multiple functional groups, *i.e.* the C_{38} *n*-alkane (Fig. 3.9**b**) from C_{38} di-and tri-unsaturated methyl and ethyl ketones and isorenieratane (Fig. 3.9**f**) from isorenieratene (**X**), show an increase in the relative amount of polysulphide-bound carbon skeletons at relatively high temperatures. Compounds originating from precursors probably bearing only one or two functional groups, *i.e.* the C_{22} *n*-alkane (Fig. 3.9**a**) and (20R)-5α,14α,17α(H) C_{29} sterane (Fig. 3.9**d**), show an increase in the relative amount of polysulphide-bound carbon skeletons at relatively low temperatures. These two different types of profiles can be directly related to the number of sulphur links and thus to the number of functional groups of the precursor lipids, since more thermal stress is needed if a larger number of sulphur links is present. Therefore, the assessment of the maturity dependence of the relative amount of polysulphide-bound carbon skeletons can give information about the amount of functionalities of possible precursors.

The profiles of squalane (Fig. 3.9**c**) and gammacerane (Fig. 3.9**e**) are more difficult to understand. The precursor of sulphur-bound squalane might be squalene, which contains six double bonds. Based on this precursor, a profile similar to that of the C_{38} *n*-alkane and isorenieratane is expected, which is, however, not observed. Another possible precursor for sulphur-bound squalane would be octahydrosqualene (**XIII**), which was tentatively identified in particulate organic matter of the Cariaco trench (Wakeham, 1990). This precursor would explain why only one thiane with a squalane carbon skeleton (**XII**) was identified in the alkylsulphide fraction (Fig. 3.7), whereas the reaction of squalene with inorganic sulphur species can yield a multitude of alkylsulphides (Schouten *et al.*, 1994). The precursor of sulphur-bound gammacerane is probably tetrahymanol (or its derivatives gammacer-2-ene and gammacer-3-one; Richnow *et al.*, 1993; Sinninghe Damsté *et al.*, 1995c). This precursor contains only one functional group.

Since S-S bonds are weaker than C-S bonds, the relative amount of polysulphide-bound gammacerane is expected to decrease with increasing maturation temperature. Broadly, this trend is indeed observed. The fact that S-S bonds are weaker than C-S bonds is probably also the reason that the profiles in Fig. 3.9 generally show a downward trend at high maturation temperatures.

Oxygen-bound and both sulphur- and oxygen-bound carbon skeletons

To check for the presence of oxygen-bound moieties, polar fractions II were treated with HI/$LiAlH_4$, a method that cleaves C-O bonds and thus converts dialkylethers and alcohols to the corresponding alkanes. It should be noted that compounds originally sequestered by both sulphur and oxygen are also included in this fraction. Absolute amounts of selected compounds released from polar fraction II of the original sample and the artificially matured samples are listed in Table 3.6. Gas chromatograms of the HI/$LiAlH_4$ treated polar fractions II of the original sample and the samples artificially matured at 220, 260 and 330°C are shown in Fig. 3.10.

The HI/$LiAlH_4$ treated polar fraction II of the original sample contains abundant Ph, a series of *n*-alkanes with a strong even-over-odd carbon number predominance of the long-chain *n*-alkanes (CPI_{24-34} = 0.2) and abundant *n*-C_{30}, (20R)-5α,14α,17α(H) C_{27} to C_{29} steranes, relatively low amounts of (22R)-17β,21β(H) hopanes dominated by the

Table 3.6. Absolute amounts (µg/g TOC of original rock) of selected compounds released after HI/$LiAlH_4$ treatment of polar fraction II of the original sample and the artificially matured samples. Roman numbers refer to structures in the Appendix.

	original	160°C	180°C	200°C	220°C	239°C	260°C	280°C	300°C	330°C
n-C_{22}	$1.7x10^2$	84	$1.1x10^2$	$1.1x10^2$	63	62	$1.4x10^2$	90	$1.4x10^2$	68
n-C_{29}	$1.2x10^2$	86	94	$1.8x10^2$	$1.3x10^2$	$1.4x10^2$	$1.9x10^2$	$1.3x10^2$	$1.8x10^2$	$1.1x10^2$
n-C_{30}	$7.6x10^2$	$9.1x10^2$	$1.2x10^3$	$1.2x10^3$	$3.5x10^2$	$4.0x10^2$	$2.8x10^2$	$1.3x10^2$	$1.6x10^2$	$1.2x10^2$
n-C_{31}	81	94	$1.3x10^2$	$2.3x10^2$	$1.5x10^2$	$2.3x10^2$	$3.5x10^2$	87	$1.2x10^2$	42
n-C_{37}	0	28	32	$1.6x10^2$	95	$1.7x10^2$	$1.9x10^2$	62	69	18
n-C_{38}	0	32	43	$1.9x10^2$	$1.2x10^2$	$2.0x10^2$	$2.3x10^2$	71	82	17
Pr	1	1	2	2	4	4	4	8	15	0
Ph	$6.6x10^2$	$1.9x10^2$	$3.0x10^2$	$3.5x10^2$	$4.1x10^2$	$2.5x10^2$	$1.9x10^2$	$1.4x10^2$	$1.3x10^2$	42
(20R) ααα C_{29}[a]	$2.8x10^2$	$2.1x10^2$	$2.8x10^2$	$4.2x10^2$	$3.4x10^2$	$2.5x10^2$	$1.3x10^2$	48	29	7
(22R) ßß C_{35}[b]	4	5	8	14	11	6	5	0	0	0
XIV	$3.9x10^2$	$1.8x10^2$	$3.1x10^2$	$3.4x10^2$	$3.8x10^2$	$3.9x10^2$	$2.2x10^2$	58	0	0
XV	71	44	64	88	$1.2x10^2$	82	48	0	0	0
XVI	97	70	$1.0x10^2$	$1.4x10^2$	$1.5x10^2$	87	44	0	0	0
XVII	93	69	97	$1.3x10^2$	$1.3x10^2$	88	40	0	0	0
Isorenieratane	15	14	17	42	18	22	19	4	1	0

[a] Sterane.

[b] Hopane.

C_{31} and C_{32} components, and four C_{40} biphytanes with 0-3 cyclopentyl moieties (**XIV-XVII**) which were identified by their mass spectra (de Rosa and Gambacorta, 1988; Schouten, unpublished results) (Fig. 3.10**a**). To check if these carbon skeletons are present as free alcohols or as oxygen-bound moieties, polar fraction I of the original sample was derivatised with BSTFA. This yielded mainly trimethylsilyl (TMS) derivatives of (i) *n*-C_{22}, *n*-C_{24}, *n*-C_{26} and *n*-C_{28} alcohols, (ii) triacontan-1,15-diol and triacontan-15-one-1-ol, (iii) C_{27} to C_{29} sterols, (iv) (22R)-17β,21β(H) C_{31} and C_{32} hopanols, and (v) diphytanyl glyceryl ether (**XVIII**). Thus, Ph and the biphytanes released by HI/$LiAlH_4$ treatment are predominantly present as oxygen-bound or both sulphur- and oxygen-bound moieties, and not as free alcohols. As confirmed by the presence of **XVIII**, their precursors are most likely glyceryl ether lipids from methanogenic bacteria (de Rosa and Gambacorta, 1988; Kohnen *et al.*, 1992a,b). The presence of triacontan-1,15-diol and triacontan-15-one-1-ol in the sediment was already anticipated in an earlier study (Koopmans *et al.*, 1995).

When the sample is artificially matured, the distribution of the compounds in the HI/$LiAlH_4$ treated polar fraction II changes considerably (Fig. 3.10). At low temperatures, (20R)-5β,14α,17α(H) C_{27} to C_{29} steranes are released by HI/$LiAlH_4$ treatment. At 220°C, the even-over-odd predominance of the *n*-alkanes has largely disappeared, and the C_{37} and C_{38} *n*-alkanes are abundant compared to the other *n*-alkanes in the $C_{35\text{-}40}$ region (Fig. 3.10**b**). At 260°C, the *n*-alkanes have become more pronounced compared to the isoprenoids and the steranes, and the high abundance of the C_{29} to C_{31}, and C_{37} and C_{38} components is remarkable (Fig. 3.10**c**). At 330°C, HI/$LiAlH_4$ treatment predominantly releases *n*-alkanes, with a relatively high abundance of the C_{29} and C_{30} components (Fig. 3.10**d**). The different generation profiles of oxygen-bound and both sulphur- and oxygen-bound C_{29} to C_{31} *n*-alkanes (Table 3.6) suggest that these compounds may have different precursors.

Polar fraction I of the sample heated at 260°C was also directly subjected to HI/$LiAlH_4$ treatment, yielding compounds that were exclusively oxygen-bound. Thus, a distinction could be made between (i) sulphur-bound carbon skeletons, (ii) oxygen-bound carbon skeletons, and (iii) carbon skeletons bound by both sulphur and oxygen links. Relative amounts of selected carbon skeletons in these three compartments are given in Table 3.7. A high percentage of the *n*-alkanes is both sulphur- and oxygen-bound. A relatively high percentage of Ph is exclusively oxygen-bound, probably originating from the diphytanyl glyceryl ether **XVIII**. However, the major part of the Ph skeletons in the polar fraction is exclusively sulphur-bound, probably due to the reaction of phytol with reduced inorganic sulphur species during early diagenesis. The four C_{40} biphytanes (**XIV-XVII**), which were not detected in the desulphurised polar fraction I, are almost exclusively oxygen-bound, suggesting an origin from methanogenic bacteria (de Rosa and Gambacorta, 1988; Kohnen *et al.*, 1992a,b).

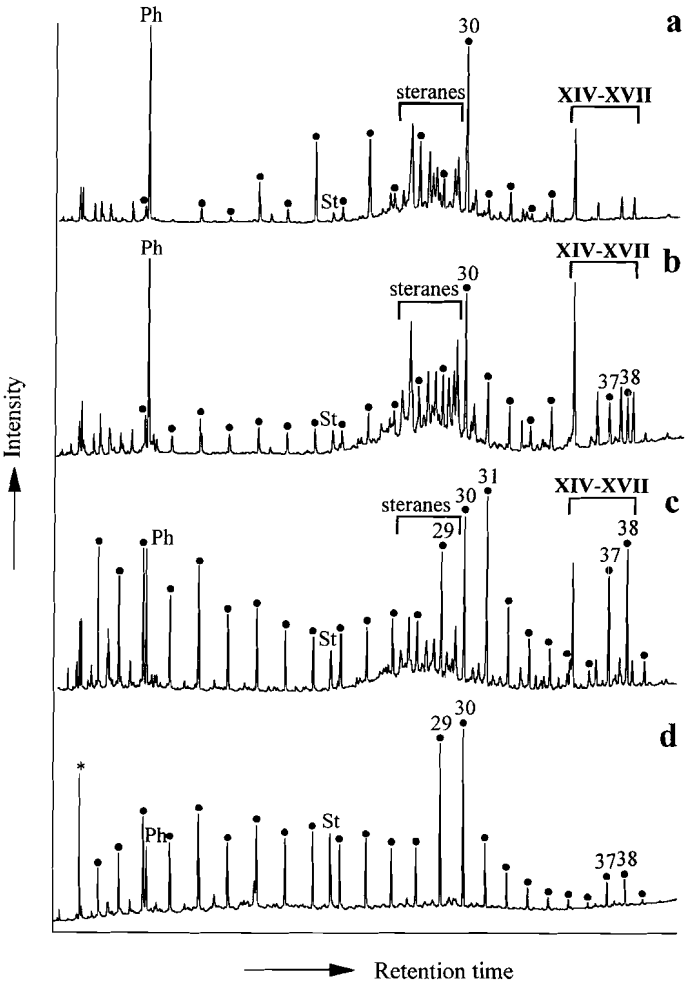

Fig. 3.10. Gas chromatogram of the HI/$LiAlH_4$ treated polar fraction II of (**a**) the original sample, and the samples artificially matured at (**b**) 220°C, (**c**) 260°C, and (**d**) 330°C. Key: dots = *n*-alkanes (numbers indicate number of carbon atoms), Ph = phytane, St = internal standard, * = contaminant. Roman numbers refer to structures in the Appendix.

Ketones

Heating experiments by flash pyrolysis (Gelin *et al.*, 1993, 1994) and off-line pyrolysis (Behar *et al.*, 1995) of ether lipids isolated from the green microalga *Botryococcus braunii* containing several oxygen-linked alkyl chains have shown that ketones can be formed as thermal degradation products. The position of the carbonyl group in the alkyl chain coincides with the position of the oxygen-linked carbon atom in the ether lipid. In

Table 3.7. Relative amounts (%) of sulphur-bound, oxygen-bound, and both sulphur- and oxygen-bound carbon skeletons for selected compounds in the polar fraction of the sample artificially matured at 260°C. Roman numbers refer to structures in the Appendix.

	S-bound	O-bound	both S- and O-bound
n-C_{22}	26%	21%	53%
n-C_{29}	20%	16%	63%
n-C_{30}	25%	29%	47%
n-C_{31}	26%	8%	66%
n-C_{37}	18%	10%	73%
n-C_{38}	15%	10%	76%
Ph	57%	27%	16%
(20R)-ααα C_{29}[a]	18%	21%	60%
XIV	0%	69%	31%
XV	0%	92%	8%
XVI	0%	91%	9%
XVII	0%	88%	12%
Isorenieratane	97%	4%	0%

[a] Sterane.

order to gain insight in the distribution of all recognisable thermal degradation products of sulphur- and oxygen-bound carbon skeletons, ketones present in polar fraction III (Fig. 3.1) of the original sample and the artificially matured samples were analysed. Absolute amounts of selected ketones are given in Table 3.8.

In the ketone fraction of the original sample, 1-iodotriacontan-15-one is present in moderate amounts (45 μg/g TOC). This iodine-containing compound elutes in polar fraction III after column chromatography of the products of the HI treatment of polar fraction II (Fig. 3.1) because of the relatively polar carbonyl group. In the ketone fraction of the sample heated at 160°C a large amount (370 μg/g TOC of original rock) of 1-iodotriacontan-15-one is present, probably originating from thermal breakdown of the asphaltenes and/or the kerogen. This thermal breakdown can be envisaged in two ways: (i) oxygen-linked (at C-15) triacontan-1,15-diol is thermally released as free triacontan-15-one-1-ol, or (ii) oxygen-linked (at C-1) triacontan-15-one-1-ol is thermally released as free triacontan-15-one-1-ol. The first hypothesis is unlikely, since it would involve the formation of an oxygen link selectively at C-15, whereas formation of an oxygen link at C-1 is also possible. The corresponding 15-iodotriacontanal was not found. The second hypothesis may involve thermal release of ester-bound (at C-1) triacontan-15-one-1-ol from the asphaltenes and/or the kerogen. Ester bonds are relatively weak (310 kJ/mol; Claxton *et al.*, 1993), and may be subject to hydrolysis in hydrous pyrolysis

Table 3.8. Absolute amounts (μg/g TOC of original rock) of selected ketones with indicated carbon skeletons in the original sample and the artificially matured samples.

	original	160°C	180°C	200°C	220°C	239°C	260°C	280°C	300°C	330°C
n-C_{22}	2	11	16	15	38	48	42	53	$1.0x10^2$	82
n-C_{29}	0	11	17	36	85	$1.8x10^2$	$1.4x10^2$	$2.0x10^2$	$3.1x10^2$	$4.5x10^2$
n-C_{30}[a]	45	$4.0x10^2$	$5.0x10^2$	$3.0x10^2$	$1.4x10^2$	$3.1x10^2$	$1.6x10^2$	$1.7x10^2$	$2.7x10^2$	$3.1x10^2$
n-C_{31}	13	67	92	60	$1.3x10^2$	$3.3x10^2$	$2.2x10^2$	$1.2x10^2$	$1.7x10^2$	$1.6x10^2$
n-C_{37}	0	13	24	58	$1.2x10^2$	$3.3x10^2$	$2.2x10^2$	$1.3x10^2$	$1.3x10^2$	$1.1x10^2$
n-C_{38}	0	17	28	87	$1.8x10^2$	$5.5x10^2$	$3.7x10^2$	$1.8x10^2$	$1.8x10^2$	$1.3x10^2$
Ph	2	13	22	17	35	32	50	26	70	12
Isorenieratane	71	46	35	79	34	49	41	18	12	0

[a] Includes ketones with an *n*-C_{30} skeleton and 1-iodotriacontan-15-one.

experiments. Indeed, hydrous pyrolysis of Kimmeridge oil shale showed the activation energy for the generation of organic acids (*c.* 20 kJ/mol) to be much lower than the activation energy for the generation of hydrocarbons (*c.* 70 kJ/mol; Barth *et al.*, 1989). The early thermal release of ester-bound triacontan-15-one-1-ol also coincides with the early generation of oxygen-containing C_{30} skeletons as indicated by HI/$LiAlH_4$ treatment of polar fraction II (Table 3.6), which might be due to the release of ester-bound (at C-1 and/or C-15) triacontan-1,15-diol from the asphaltenes and/or the kerogen. To check for the presence of ester-bound moieties in the kerogen of the original sample, it was saponified and the released products were derivatised and analysed by GC-MS. This released a total amount of triacontan-1,15-diol and triacontan-15-one-1-ol of *c.* 510 μg/g TOC, accounting, at least partly, for the increase of oxygen-containing C_{30} skeletons at low maturation temperatures (Tables 3.6 and 3.8).

When the sample is artificially matured at temperatures higher than 160°C, large amounts of *n*-C_{29} to *n*-C_{31}, and *n*-C_{37} and *n*-C_{38} ketones are formed (Table 3.8), dominated by mid-chain ketones (Fig. 3.11**b**). At 260°C, the carbon skeleton distribution of the ketones is similar to that of the compounds released after HI/$LiAlH_4$ treatment of polar fraction II (Fig. 3.11). This shows the close relationship between these two fractions, *i.e.* their components ultimately derive from oxygen-bound moieties.

3.5 Discussion

Generation profiles of specific carbon skeletons

In this section, the distribution of selected carbon skeletons over the fractions discussed above as a function of maturation temperature will be discussed. The 'summed amount' of a particular carbon skeleton refers to the sum of the amounts in all fractions.

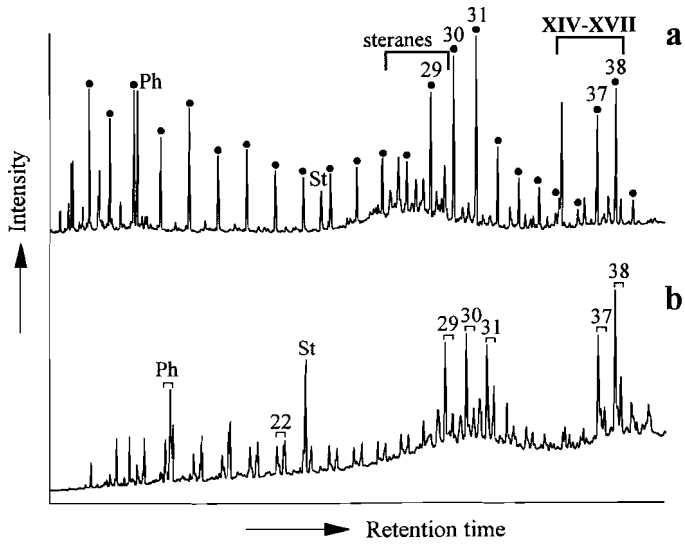

Fig. 3.11. Gas chromatogram of (**a**) the HI/$LiAlH_4$ treated polar fraction II, and (**b**) the ketones isolated from polar fraction III of the sample artificially matured at 260°C. Key: dots = *n*-alkanes, Ph = compound with a phytane carbon skeleton, St = internal standard. Numbers indicate number of carbon atoms of *n*-alkanes (**a**) and ketones (**b**). Roman numbers refer to structures in the Appendix. The first eluting peak in each cluster of ketones represents the mid-chain ketones.

C_{22} *n*-alkane

This compound is a typical example of an *n*-alkane having one or several unknown precursors. However, based on the relative amount of polysulphide-bound *vs.* total sulphur-bound *n*-C_{22} skeletons with increasing thermal maturation as revealed by MeLi/MeI treatment of polar fractions I (Fig. 3.9**a**), it can be stated that sulphur-bound *n*-C_{22} skeletons are, on average, linked by more than one sulphur link. The summed amount of *n*-C_{22} skeletons as a function of maturation temperature is shown in Fig. 3.12. This generation profile is typical for *n*-alkanes that do not have a specific precursor. Note that the generation profile of the *n*-C_{22} skeleton differs greatly from the generation profiles of the *n*-C_{30} and *n*-C_{38} skeletons, which have a limited number of very specific precursors (*vide infra*).

The amount of free C_{22} *n*-alkane increases gradually from 9 μg/g TOC in the original sample to *c.* 630 μg/g TOC of original rock at 330°C (Table 3.1). This increase cannot be explained only by thermal degradation of sulphur-bound *n*-C_{22}, since (i) the amount of sulphur-bound *n*-C_{22} in the polar fraction is an order of magnitude lower than the maximum amount of C_{22} *n*-alkane generated (cf. Tables 3.1 and 3.5), and (ii) the amount of sulphur-bound *n*-C_{22} in the kerogen is only twice as high as that in the polar

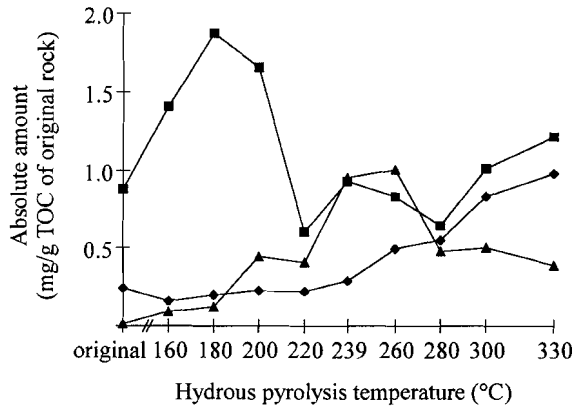

Fig. 3.12. Summed absolute amounts (mg/g TOC of original rock) of n-C_{22} (diamonds), n-C_{30} (squares) and n-C_{38} (triangles) skeletons as a function of hydrous pyrolysis temperature.

fraction (Schaeffer *et al.*, 1995a), and thus too low to explain the maximum amount of free C_{22} n-alkane. Moreover, sulphur-bound n-C_{22} in the polar fraction and the kerogen is probably the major precursor of the generated C_{22} alkylthiophenes. An origin of free C_{22} n-alkane from oxygen-bound n-C_{22} is also not very likely, since the major part of n-C_{22} released by HI/$LiAlH_4$ treatment of polar fraction II probably results from the reduction of free n-C_{22} alcohols. Therefore, another HMW precursor of C_{22} n-alkane must be inferred, from which it is probably formed by (random) C-C bond cleavage. Possible candidates are the recently discovered highly aliphatic marine algaenans, isolated from, amongst others, the marine microalgae *Nannochloropsis salina* and *Nannochloropsis* sp. (Gelin *et al.*, 1996a).

C_{30} n-alkane

The precursor of a large part of the n-C_{30} skeletons is probably triacontan-1,15-diol or triacontan-15-one-1-ol, whose TMS derivatives were identified in polar fraction I of the original sample. These compounds have been previously identified in sediments (*e.g.* de Leeuw *et al.*, 1981; Morris and Brassell, 1988; ten Haven *et al.*, 1992). Ester-bound triacontan-1,15-diol and mono-unsaturated triacontanol have been released by acid and base hydrolyses of polar lipids of the marine microalga *Nannochloropsis salina* (Volkman *et al.*, 1992). This corroborates our finding of ester-bound triacontan-1,15-diol in the kerogen.

The summed amount of n-C_{30} skeletons as a function of maturation temperature is shown in Fig. 3.12. This generation profile can be roughly divided into two maturity intervals, *i.e.* from the original sample to 220°C, and from 220°C to 330°C. The generation profile of the summed amount of n-C_{30} skeletons in the first maturity interval is go-

verned by the thermal release of ester-bound triacontan-1,15-diol and triacontan-15-one-1-ol (Fig. 3.13**a**). The early release of these compounds is probably due to the weakness of the ester bond as discussed in a previous section. The sudden decrease of the summed amount of *n*-C_{30} skeletons between 180 and 220°C, which is presumably related to the sudden decrease of ester-bound triacontan-1,15-diol and triacontan-15-one-1-ol (Fig. 3.13**a**), is difficult to understand. This decrease suggests that, due to the slightly higher temperatures, ester-bound triacontan-1,15-diol and triacontan-15-one-1-ol are not released as C_{30} compounds, but are possibly degraded to compounds with other carbon skeletons. The generation profile of the summed amount of *n*-C_{30} skeletons in the second maturity interval is broadly related to the generation profile of the free C_{30} *n*-alkane (Fig. 3.13**a**). However, in this second maturity interval C_{30} 2,5-di-*n*-alkylthiophenes are also generated (Koopmans *et al.*, 1995), as well as 1,2-di-*n*-alkylbenzenes and free ketones (Tables 3.3 and 3.8).

To get a better understanding of the relationship between *n*-C_{30} skeletons in different fractions, the relative amounts of these skeletons as a function of maturation temperature are shown in Fig. 3.13**b**. The relative amount of oxygen-bound and both sulphur- and oxygen-bound *n*-C_{30} (indicated by double crosses) decreases rapidly with increasing thermal maturation. At temperatures higher than 239°C the relative amount of sulphur-bound *n*-C_{30} (crosses) also decreases, suggesting that oxygen- and sulphur-bound *n*-C_{30} are thermally unstable. On the other hand, the relative amounts of mid-chain 2,5-di-*n*-alkylthiophenes (squares), 1,2-di-*n*-alkylbenzenes (triangles) and ketones (dots) with a *n*-C_{30} skeleton are constant at high temperatures. It is likely that the mid-chain 2,5-di-*n*-alkylthiophenes and the ketones are stable thermal degradation products of sulphur- and oxygen-linked *n*-C_{30} skeletons, respectively (Gelin *et al.*, 1993, 1994, 1996a; Behar *et al.*, 1995; Koopmans *et al.*, 1995). The formation of the C_{30} 1,2-di-*n*-alkylbenzenes is not completely understood, but it may involve thermal degradation of sulphur- and oxygen-linked *n*-C_{30} skeletons. This would imply a new route for the formation of 1,2-di-*n*-alkylbenzenes in relatively immature sedimentary rocks (cf. Sinninghe Damsté *et al.*, 1991). The relative amount of the C_{30} *n*-alkane (diamonds) increases with increasing maturation temperature, suggesting that, at high temperatures, generation of the free *n*-alkane may be a favoured pathway.

C_{38} *n*-alkane

The *n*-C_{37} and *n*-C_{38} skeletons identified in the fractions described above probably originate from C_{37} and C_{38} di- and tri-unsaturated methyl and ethyl ketones (alkenones) biosynthesised by several Prymnesiophyte algae. Since the relative amount of di- and tri-unsaturated ketones in these algae is directly related to growth temperature, sedimentary alkenone distributions have been used to infer palaeo sea surface temperatures (for a review see Brassell, 1993).

The summed amount of *n*-C_{38} skeletons as a function of maturation temperature is shown in Fig. 3.12. This generation profile is clearly different from those of the *n*-C_{22}

and n-C_{30} skeletons. In the original sample, only a small amount (14 μg/g TOC) of n-C_{38} skeletons was detected in the apolar and polar fraction. The far greater part of the n-C_{38} skeletons is sulphur- and oxygen-bound in the kerogen (Koopmans *et al.*, 1997b). When the sample is heated at temperatures up to 260°C, large amounts of n-C_{38} skeletons are released (up to 1 mg/g TOC of original rock) from the kerogen, as suggested by the increase in the summed amount of n-C_{38} skeletons in the apolar and polar fraction (Fig. 3.12). These carbon skeletons are released as sulphur-bound n-C_{38}, oxygen-bound n-C_{38}, both sulphur- and oxygen-bound n-C_{38}, saturated n-C_{38} methyl, ethyl and mid-chain ketones, C_{38} mid-chain 2,5-di-n-alkylthiophenes, C_{38} 1,2-di-n-alkylbenzenes, and free C_{38} n-alkanes. At temperatures higher than 260°C the summed amount of n-C_{38} skeletons decreases (Fig. 3.12), probably due to thermal degradation of free n-C_{38} skeletons or their bound precursors.

The relationships between these different compounds bearing the n-C_{38} skeleton

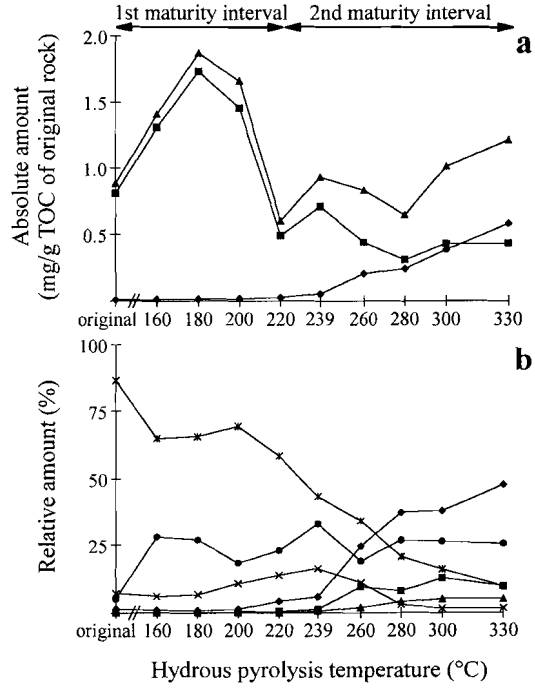

Fig. 3.13. (**a**) Generation profiles of the n-C_{30} skeleton in the HI/$LiAlH_4$ treated polar fraction II plus the ketone fraction (squares), the saturated hydrocarbon fraction (diamonds), and the summed amount of n-C_{30} skeletons (triangles). (**b**) Relative amounts (%) of the n-C_{30} skeleton in the saturated hydrocarbon fraction (diamonds), monoaromatic hydrocarbon fraction (squares: mid-chain 2,5-di-n-alkylthiophenes; triangles: 1,2-di-n-alkylbenzenes), desulphurised polar fraction I (crosses), HI/$LiAlH_4$ treated polar fraction II (double crosses), and ketone fraction (dots).

can be understood if their relative amounts are plotted against maturation temperature (Fig. 3.14). The relative amounts of sulphur-bound n-C_{38} (crosses) on the one hand and oxygen-bound and both sulphur- and oxygen-bound n-C_{38} (double crosses) on the other generally decrease with increasing maturation temperature, suggesting that sulphur- and oxygen-bound n-C_{38} skeletons are thermally unstable. On the other hand, the relative amounts of n-C_{38} methyl, ethyl and mid-chain ketones (dots), C_{38} 1,2-di-n-alkylbenzenes (triangles) and free C_{38} n-alkanes (diamonds) are constant, or increase, at high maturation temperatures. This suggests that these compounds are stable thermal degradation products of originally both sulphur- and oxygen-bound n-C_{38} skeletons in the kerogen.

Pristane

The isoprenoid hydrocarbons Pr and Ph are two of the first and most frequently used biomarkers. It is, therefore, surprising that there is still a lot of controversy as to their exact origin. The classical viewpoint is that both Pr and Ph originate from the phytyl side chain of chlorophyll (see for a review Volkman and Maxwell, 1986). Later, additional precursors were proposed, *i.e.* tocopherols (Goossens *et al.*, 1984) and macromolecularly-bound methylated 2-methyl-2-(4,8,12-trimethyltridecyl)chromans (Li *et al.*, 1995) as precursors of Pr, and archaebacterial ether lipids as precursors of both Pr and Ph (*e.g.* Risatti *et al.*, 1984; Rowland, 1990; Navale, 1994).

Pr was identified in the saturated hydrocarbon fraction, after desulphurisation of

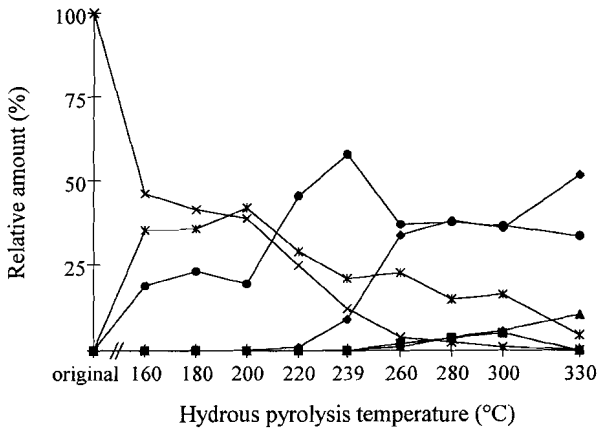

Fig. 3.14. Relative amounts (%) of the n-C_{38} skeleton in the saturated hydrocarbon fraction (diamonds), monoaromatic hydrocarbon fraction (squares: mid-chain 2,5-di-n-alkylthiophenes; triangles: 1,2-di-n-alkylbenzenes), desulphurised polar fraction I (crosses), HI/$LiAlH_4$ treated polar fraction II (double crosses), and ketone fraction (dots).

polar fraction I, and after HI/$LiAlH_4$ treatment of polar fraction II. The absolute amount of Pr in these fractions and the summed amount of Pr as a function of maturation temperature are shown in Fig. 3.15. In the original sample, free Pr is present in very low amounts. When the sample is heated, a large amount of free Pr is generated (up to 780 µg/g TOC of original rock). Throughout the maturation series, free Pr strongly dominates the distribution of the Pr carbon skeleton. Sulphur- and oxygen-bound Pr are present in very low relative amounts. Moreover, Li/$EtNH_2$ desulphurisation of (unheated) kerogens from the marl layer of evaporitic cycle IV of the Vena del Gesso Basin yielded no detectable Pr (Schaeffer *et al.*, 1995a). These results indicate that (i) the generated free Pr derives from a precursor that is present in a HMW fraction outside our analytical window (*e.g.* kerogen), and (ii) the precursor of free Pr is not sulphur- or oxygen-bound Pr. Thus, these results support the propositions that macromolecularly-bound tocopherols and archaebacterial ether lipids may be the major precursors of Pr (Goossens *et al.*, 1984; Risatti *et al.*, 1984; Rowland, 1990; Navale, 1994).

When the sample is heated at 330°C the amount of free Pr decreases, due to thermal degradation of free Pr. This is probably caused by the relative weakness of the bonds between tertiary and secondary carbon atoms (Claxton *et al.*, 1993), which makes the Pr carbon skeleton (and isoprenoid hydrocarbons in general) more prone to thermal degradation than *n*-alkanes.

Phytane

In contrast to the distribution of the Pr carbon skeleton, the Ph carbon skeleton is

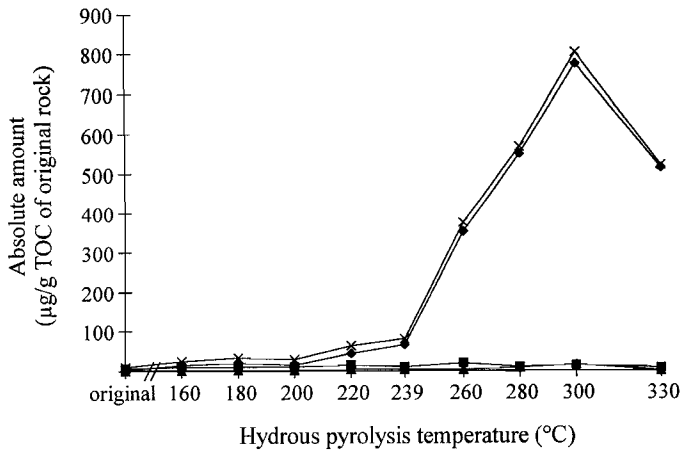

Fig. 3.15. Generation profiles of Pr in the saturated hydrocarbon fraction (diamonds), desulphurised polar fraction I (squares), and HI/$LiAlH_4$ treated polar fraction II (triangles). The summed amount of Pr is represented by crosses.

present in almost all fractions (Table 3.9). For example, the finding of increasing amounts of alkylthiophenes and, to a lesser extent, ketones with a Ph carbon skeleton with increasing maturation temperature suggests that thermal degradation of sulphur- and oxygen-bound Ph is an important generation pathway of free Ph skeletons. This would imply that Pr and Ph have different precursors, since sulphur- and oxygen-bound Pr play a negligible role in the formation of free Pr skeletons (see previous section).

The generation profile of the summed amount of Ph is relatively simple (Table 3.9). At low temperatures, the summed amount of Ph is relatively constant, although large changes occur within individual fractions. With increasing thermal maturation, the summed amount of Ph suddenly increases from *c.* 1.0 mg/g TOC of original rock at 239°C to *c.* 2.3 mg/g TOC of original rock at 260°C, after which it is relatively constant before decreasing at 330°C. The sudden increase in the summed amount of Ph is reflected in the generation profiles of free Ph and the thiophenes with a Ph carbon skeleton (**III-V**), suggesting that the increase is caused by thermal degradation of sulphur-bound Ph in HMW fractions (*e.g.* kerogen). However, $Li/EtNH_2$ desulphurisation of unheated kerogens from the marl layer of evaporitic cycle IV of the Vena del Gesso Basin released only *c.* 530 µg/g TOC of Ph (Schaeffer *et al.*, 1995a), which cannot explain the large increase in Ph at 260°C. Also, the amount of sulphur-bound Ph in the polar fraction decreases gradually, which is not in accordance with the sudden increase in the summed amount of Ph at 260°C.

The relative amount of Ph skeletons in individual fractions as a function of hydrous pyrolysis temperature is shown in Fig. 3.16. At temperatures lower than 220°C the relationship between these generation profiles is obscure, but at temperatures higher than 220°C several distinct features can be discerned. The relative amount of oxygen-bound and both sulphur- and oxygen-bound Ph (double crosses) decreases with increasing maturation temperature, but this is not accompanied by an increase in the relative

Table 3.9. Absolute amounts (µg/g TOC of original rock) of the Ph carbon skeleton in different fractions as a function of hydrous pyrolysis temperature. Roman numbers refer to structures in the Appendix.

	original	160°C	180°C	200°C	220°C	239°C	260°C	280°C	300°C	330°C
Free Ph	6	$1.3x10^2$	$1.6x10^2$	$1.6x10^2$	$3.2x10^2$	$3.9x10^2$	$1.3x10^3$	$1.1x10^3$	$1.3x10^3$	$7.3x10^2$
Ph thiophenes (**III-V**)	16	91	$2.4x10^2$	$1.1x10^2$	88	72	$3.6x10^2$	$3.7x10^2$	$5.0x10^2$	$3.6x10^2$
Ph sulphides	6	nd[a]	nd[a]	6	4	15	94	94	28	0
Sulphur-bound Ph	$4.1x10^2$	$3.2x10^2$	$3.2x10^2$	$3.4x10^2$	$3.0x10^2$	$2.1x10^2$	$2.6x10^2$	$1.2x10^2$	$1.5x10^2$	$2.0x10^2$
Oxygen-bound Ph[b]	$6.6x10^2$	$1.9x10^2$	$3.0x10^2$	$3.5x10^2$	$4.1x10^2$	$2.5x10^2$	$1.9x10^2$	$1.4x10^2$	$1.3x10^2$	42
Phytanone	2	13	22	17	35	32	50	26	70	12
TOTAL	$\mathbf{1.1x10^3}$	$\mathbf{7.5x10^2}$	$\mathbf{1.0x10^3}$	$\mathbf{9.9x10^2}$	$\mathbf{1.2x10^3}$	$\mathbf{9.7x10^2}$	$\mathbf{2.3x10^3}$	$\mathbf{1.9x10^3}$	$\mathbf{2.2x10^3}$	$\mathbf{1.3x10^3}$

[a] Not determined due to absence of standard.

[b] Includes both sulphur- and oxygen-bound carbon skeletons.

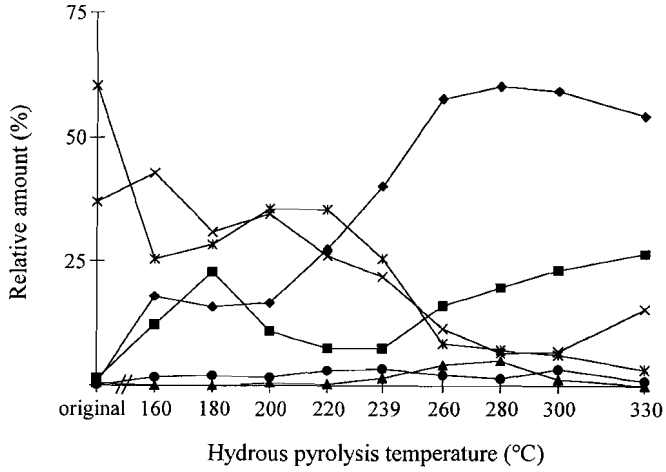

Fig. 3.16. Relative amounts (%) of the Ph carbon skeleton in the saturated hydrocarbon fraction (diamonds), monoaromatic hydrocarbon fraction (squares: alkylthiophenes), alkylsulphide fraction (triangles), desulphurised polar fraction I (crosses), $HI/LiAlH_4$ treated polar fraction II (double crosses), and ketone fraction (dots).

amount of ketones/aldehydes with a Ph carbon skeleton (dots), as seen with the n-C_{30} and n-C_{38} skeletons. This can be explained by an origin from **XVIII**, which probably produces phytene, and not phytenal, upon thermal maturation. The relative amount of sulphur-bound Ph (crosses) also decreases with increasing maturation temperature, but at 330°C it seems to increase again. This is difficult to understand, since the relative weakness of C-S bonds compared to C-C bonds is expected to lead to a continuously decreasing relative amount of sulphur-bound Ph. The relative amount of alkylthiophenes (squares) increases as expected, since these compounds are considered stable thermal degradation products of sulphur-bound moieties. The relative amount of free Ph (diamonds) decreases at temperatures higher than 280°C, probably due to the low thermal stability of the isoprenoid chain as compared to straight chains (see previous section on Pr).

The Ph carbon skeleton may have several different precursors (phytol, oxygen-bound Ph from methanogenic ether lipids), which can be bound in HMW fractions in different ways (sulphur-, ether- and ester-bound), explaining the complex generation profiles of the Ph carbon skeleton. The origin and fate of Pr and Ph carbon skeletons in this and three other maturation series of samples from both marine and lacustrine depositional environments will be further elaborated elsewhere.

C_{40} biphytanes XIV-XVII

The C_{40} biphytanes with 0-3 cyclopentyl moieties (**XIV-XVII**) form an interesting

group of compounds, since they are almost exclusively ether-bound in the polar fraction (Table 3.7). Their generation profiles are largely covariant (Table 3.6), suggesting that they are produced from a similar precursor (*i.e.* archaebacterial ether lipids). Their amount reaches a maximum in the interval 200-239°C, after which they decrease rapidly and are not detectable at 300°C. Thermally induced cleavage of the C-O bonds linking **XIV-XVII** to the glyceryl carbon skeleton may cause this early decrease, although **XIV-XVII** were not detected in the saturated hydrocarbon fraction. Alternatively, the early decrease of ether-bound biphytanes may be caused by their intrinsic thermal lability due to the presence of 8-11 tertiary carbon atoms. The biphytanes with one or more cyclopentyl moieties (**XV-XVII**) contain two adjacent tertiary carbon atoms, making them especially labile. Indeed, **XV-XVII** seem to be degraded at a lower temperature than the acyclic biphytane.

(20R)-5α,14α,17α(H) C_{29} sterane

The (20R)-5α,14α,17α(H) C_{29} sterane is regarded as representative for the (20R)- and (20S)-5α,14α,17α(H) and 5β,14α,17α(H) C_{27} to C_{29} steranes, since the generation profiles of the steranes are largely covariant. Generally, (20R)-5α,14α,17α(H) C_{29} sterane is the most abundant.

The absolute amounts of the (20R)-5α,14α,17α(H) C_{29} sterane skeleton in the saturated hydrocarbon fraction, the desulphurised polar fraction I, and the HI/$LiAlH_4$ treated polar fraction II as a function of maturation temperature are shown in Fig. 3.17. The absolute amount of (both) sulphur- and oxygen-bound (20R)-5α,14α,17α(H) C_{29} sterane (including free sterols that are reduced by the HI/$LiAlH_4$ treatment) generally decreases with increasing maturation temperature. Formation of alkylthiophenes and ketones with a (20R)-5α,14α,17α(H) C_{29} sterane skeleton is probably not a favourable thermal degradation pathway, as suggested by the absence of these compounds after heating. Instead, a large amount of free (20R)-5α,14α,17α(H) C_{29} sterane is formed with increasing thermal maturation. At temperatures higher than 260°C the absolute amount of free (20R)-5α,14α,17α(H) C_{29} sterane decreases, probably due to thermal degradation of the carbon skeleton. This is not surprising, since the sterane carbon skeleton contains two quaternary and at least seven tertiary carbon atoms, making the bonds between these and other carbon atoms relatively weak. This explanation agrees with the observation that free *n*-alkanes, Pr and Ph, and (20R)-5α,14α,17α(H) C_{29} sterane are degraded at progressively lower temperatures. Alternatively, aromatisation of one or more of the six-membered rings may be an important 'degradation' pathway of the (20R)-5α,14α,17α(H) C_{29} sterane skeleton.

(22R)-17β,21β(H) C_{35} hopane

In contrast to the (20R)-5α,14α,17α(H) C_{29} sterane skeleton, the (22R)-17β,21β(H) C_{35} hopane skeleton is also encountered as alkylthiophene (**VI**) and alkyldisulphide. The reason for this is that the precursor of the (22R)-17β,21β(H) C_{35} hopane skeleton, bac-

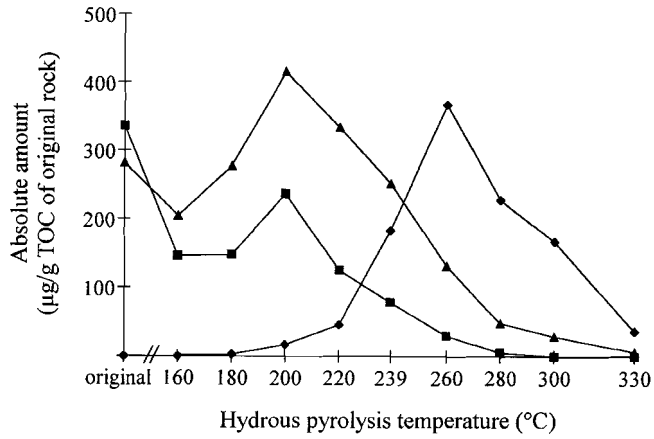

Fig. 3.17. Generation profiles of the (20R)-5α,14α,17α(H) C_{29} sterane skeleton in the saturated hydrocarbon fraction (diamonds), desulphurised polar fraction I (squares), and HI/$LiAlH_4$ treated polar fraction II (triangles).

teriohopanetetrol (**XIX**), has four functional groups in the side-chain which facilitates a direct intramolecular reaction with reduced inorganic sulphur species to form LMW organic sulphur compounds. The functional groups of the precursor of the (20R)-5α,14α,17α(H) C_{29} sterane skeleton are generally too far apart for direct formation of LMW organic sulphur compounds, although LMW steroid thiolanes have been reported (*e.g.* Sinninghe Damsté *et al.*, 1989d). At 260°C, a much higher proportion of the (20R)-5α,14α,17α(H) C_{29} sterane skeleton is encountered as free alkane (69%) compared to the (22R)-17β,21β(H) C_{35} hopane skeleton (16%). This is probably a direct result of the different number of functional groups of their precursors, and the different number of possible degradation pathways of both skeletons.

The absolute amount of the (22R)-17β,21β(H) C_{35} hopane skeleton in several fractions is shown in Fig. 3.18. The summed amount of (22R)-17β,21β(H) C_{35} hopane skeletons (dots) decreases rapidly at temperatures higher than 200°C, and is virtually zero at 280°C. This is at least partly due to isomerisation of the 17β,21β(H) configuration to the thermodynamically more stable 17α,21β(H) and 17β,21α(H) configurations (cf. Fig. 3.4). The relatively high amount of the alkylthiophene **VI**, which was first identified in an immature sedimentary rock (Valisolalao *et al.*, 1984), in the original sample is probably due to direct sulphur incorporation into bacteriohopanetetrol or a diagenetic derivative, and not to thermal degradation of sulphur-bound (22R)-17β,21β(H) C_{35} hopane, since similar thiophenic degradation products of other sulphur-bound moieties are only produced after mild thermal treatment (Koopmans *et al.*, 1995). The increasing amount of oxygen-bound and both sulphur- and oxygen-bound (22R)-17β,21β(H) C_{35} hopane (double crosses) with increasing thermal maturation up to

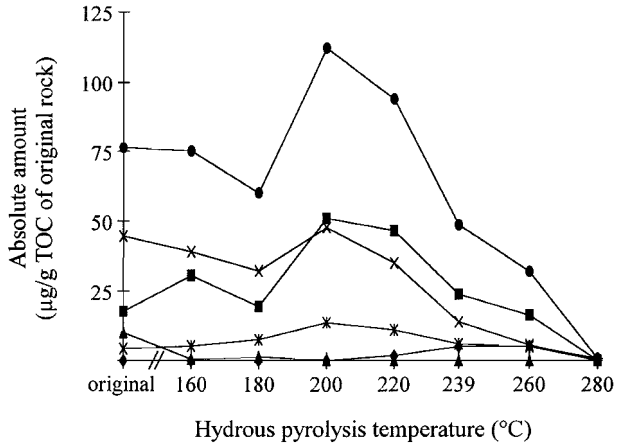

Fig. 3.18. Generation profiles of the (22R)-17β,21β(H) C_{35} hopane skeleton in the hydrocarbon fraction (diamonds), monoaromatic hydrocarbon fraction (squares: alkylthiophenes), alkylsulphide fraction (triangles), desulphurised polar fraction I (crosses), and HI/$LiAlH_4$ treated polar fraction II (double crosses). The summed amount of the (22R)-17β,21β(H) C_{35} hopane skeleton is represented by dots. Note that the temperature on the x-axis ranges to 280°C, because at higher temperatures (22R)-17β,21β(H) C_{35} hopane skeletons could not be detected.

200°C is probably due to the release of these moieties from HMW fractions (*e.g.* kerogen). Due to its four hydroxyl groups, bacteriohopanetetrol can be linked to the kerogen by up to four oxygen bonds (Mycke *et al.*, 1987).

Isorenieratane

The maturity-related changes in the amount and distribution of the diagenetic products of isorenieratene (**X**) in the marl layer of evaporitic cycle IV of the Vena del Gesso Basin have been discussed elsewhere (Koopmans *et al.*, 1996a). Here, we will focus on the relationship between the intact isorenieratane carbon skeletons in several fractions. The absolute amounts of the isorenieratane carbon skeleton in the polyaromatic hydrocarbon fraction, desulphurised polar fraction I, HI/$LiAlH_4$ treated polar fraction II, and the ketone fraction are listed in Table 3.10, together with the summed amount of isorenieratane.

The summed amount of isorenieratane carbon skeletons increases dramatically from the original sample to the sample heated at 200°C. This increase is reflected in the increasing amount of isorenieratane released after desulphurisation of polar fraction I. The increasing amount of sulphur-bound isorenieratane in polar fraction I with increasing temperature is probably due to the release of relatively small sulphur-linked geomacromolecules containing sulphur-bound isorenieratane from the kerogen. At tempera-

Table 3.10. Absolute amounts (μg/g TOC of original rock) of the isorenieratane carbon skeleton in different fractions as a function of hydrous pyrolysis temperature.

	original	160°C	180°C	200°C	220°C	239°C	260°C	280°C	300°C	330°C
Free isorenieratane	0	1	3	12	14	$1.1x10^2$	79	$1.1x10^2$	57	9
Sulphur-bound	66	$6.1x10^2$	$7.7x10^2$	$1.0x10^3$	$4.6x10^2$	$4.2x10^2$	$5.5x10^2$	58	7	0
Oxygen-bound[a]	15	14	17	42	18	22	19	4	1	0
Isorenieratanone[b]	71	46	35	79	34	49	41	18	12	0
TOTAL	**$1.5x10^2$**	**$6.7x10^2$**	**$8.3x10^2$**	**$1.2x10^3$**	**$5.3x10^2$**	**$5.9x10^2$**	**$6.9x10^2$**	**$1.9x10^2$**	**77**	**9**

[a] Includes both sulphur- and oxygen-bound hydrocarbons.

[b] Mainly one isomer (**XX**).

tures higher than 200°C the amount of sulphur-bound isorenieratane decreases, but this is not reflected in a direct increase in the amount of free isorenieratane. Instead, a wide variety of polyaromatic and sulphur-containing isorenieratene derivatives is formed (Koopmans *et al.*, 1996a), which probably should be regarded as stable thermal degradation products.

Keely *et al.* (1995) have shown that the marl layer of evaporitic cycle IV of the Vena del Gesso Basin contains *c.* 300 μg/g TOC of free isorenieratene (**X**), that will make up part of polar fraction I. Raney Ni 'desulphurisation' of olefins is known to yield saturated hydrocarbons (March, 1985). However, Raney Ni is probably not able to fully hydrogenate the conjugated double bonds of isorenieratene. Therefore, only part (66 μg/g TOC) of the free isorenieratene present in polar fraction I is 'released' as free isorenieratane. It cannot be established what portion of isorenieratane released by Raney Ni desulphurisation of polar fraction I of the original sample represents free isorenieratene, and what portion represents sulphur-bound isorenieratane.

$HI/LiAlH_4$ treatment of polar fraction II released small amounts of isorenieratane. The ketone fraction also contains a relatively small amount of isorenieratanone (Table 3.10). Isorenieratanone in the original sample, which comprises mainly a single isomer (**XX**), probably originates from direct oxidation of isorenieratene, and not from thermal degradation of oxygen-bound isorenieratane, because similar degradation products of other carbon skeletons are typically formed only after mild thermal treatment.

Role of HMW fractions

In this study, the focus is on free and bound biomarkers in relatively LMW fractions, *i.e.* the apolar and polar fraction. It is clear from the summed generation profiles of several carbon skeletons (*e.g.* Figs. 3.12 and 3.15, Tables 3.9 and 3.10) that the mass balance (amount present in the original sample minus amount present after heating) is generally negative. Thus, HMW fractions outside our analytical window, *i.e.* the asphal-

tene fraction and the kerogen, play an important role in the release/production of LMW carbon skeletons. Thermally induced cleavages of S-S, C-S, C-O and C-C bonds are important in this respect. Due to differences in bond strengths, these bonds will be cleaved at different levels of thermal stress. Before the effect of increasing thermal stress on HMW fractions can be discussed, the structure of these fractions should be considered.

The marl sample used in this study is extremely organic-sulphur-rich (kerogen atomic S_{org}/C ratio is 0.08). The structure of HMW sulphur-rich organic matter has been the subject of numerous studies (for a review see Sinninghe Damsté and de Leeuw, 1990). Schaeffer *et al.* (1995a) desulphurised kerogens of ten subsamples of the marl layer of evaporitic cycle IV of the Vena del Gesso Basin, and found similar product distributions as Kenig *et al.* (1995) who desulphurised the corresponding polar and asphaltene fractions. Kohnen *et al.* (1991b) desulphurised the alkylsulphide fraction (which may also contain HMW organic matter), and the polar and asphaltene fractions of an immature marl from the Vena del Gesso Basin, and found similar product distributions. MeLi/MeI treatment of these fractions indicated that the number of sulphur links was positively correlated with the average molecular weight (Kohnen *et al.*, 1991b). These data led them to propose a model, elaborating on earlier work by Sinninghe Damsté *et al.* (1990a), in which the increasing average molecular weight of sulphur-rich fractions is a direct result of the increasing number of sulphur cross-links. Thus, the sulphur-rich fractions can be regarded as part of a continuum comprised of similar carbon skeletons, only differing in the amount of sulphur links.

The sample also contains abundant oxygen (kerogen atomic O/C ratio is 0.17), possibly partly in the form of the selectively preserved remains of marine algaenans. The algaenans of the marine microalgae *Nannochloropsis salina* and *Nannochloropsis* sp. consist mainly of ether-linked straight chain C_{28}-C_{34} skeletons (Gelin *et al.*, 1996a). Alternatively, ether links may have formed in the water column (Harvey *et al.*, 1983) or during diagenesis, although the mechanisms by which these links are formed are much less well understood than the mechanisms of sulphur incorporation. It was shown that ester bonds are present in the kerogen as well. Ester-bound C_{30}-C_{36} alkandiols and C_{30}-C_{32} alkenols have been released by acid and base hydrolyses of extracts of *Nannochloropsis salina* (Volkman *et al.*, 1992; Gelin *et al.*, 1996a).

Several workers have reported the preferential release of alkylthiophenes compared to alkanes/alkenes in flash pyrolysates of kerogens with increasing levels of thermal maturity (Eglinton *et al.*, 1988b, 1990a,b; Tomic *et al.*, 1995; Nelson *et al.*, 1995). Sinninghe Damsté *et al.* (1990a) explained this early release of alkylthiophenes by proposing that alkylthiophenes are attached to the kerogen by multiple sulphur links. However, they fail to explain which are the multifunctionalised precursors needed to form such highly sulphur cross-linked moieties in the kerogen. X-ray absorption near edge structure spectroscopy (XANES) of artificially matured kerogens isolated from Monterey Shale indicates that the relative amount of (poly)sulphide sulphur decreases signifi-

cantly with increasing thermal maturation, whereas the relative amount of thiophenic sulphur remains relatively constant (Nelson *et al.*, 1995). Flash pyrolysis of the same kerogens indicates that alkylthiophenes are preferentially removed from the kerogen with increasing thermal maturation compared to alkanes/alkenes (Nelson *et al.*, 1995). We interpret these results to suggest that sulphide-bound moieties in the kerogen give rise to alkylthiophenes upon flash pyrolysis. This explains why 'alkylthiophenes' are preferentially removed from the kerogen with increasing thermal maturation, since S-S and C-S bonds are weaker than C-C bonds and are thus expected to be cleaved at lower levels of thermal maturity.

Recent heating experiments ('anhydrous pyrolysis') of synthetic sulphide-linked polymers yielded alkylthiophenes as stable thermal degradation products (Krein and Aizenshtat, 1994, 1995; Schouten *et al.*, 1994), providing further evidence for the role of sulphide-linked moieties in the production of alkylthiophenes during artificial maturation. It is important to note in this respect that the position of the thiophene ring in the alkyl chain still points to the position of the original functional group in the precursor. Thus, important information about the precursor is preserved. This was also shown by Koopmans *et al.* (1995), who inferred the presence of several palaeobiochemicals in the depositional environment of the Vena del Gesso Basin from specific isomer distributions of alkylthiophenes produced by hydrous pyrolysis.

In the maturation set under study the relative amount of alkylthiophenes is constant, or even increases, at high maturation temperatures (Fig. 3.19). Thus, the results obtained by hydrous pyrolysis support the evidence obtained by flash pyrolysis (Nelson *et al.*, 1995) and anhydrous pyrolysis (Krein and Aizenshtat, 1994, 1995; Schouten *et al.*, 1994) that alkylthiophenes are formed as stable degradation products when sulphide-linked moieties are subjected to thermal stress. Therefore, it is anticipated that a

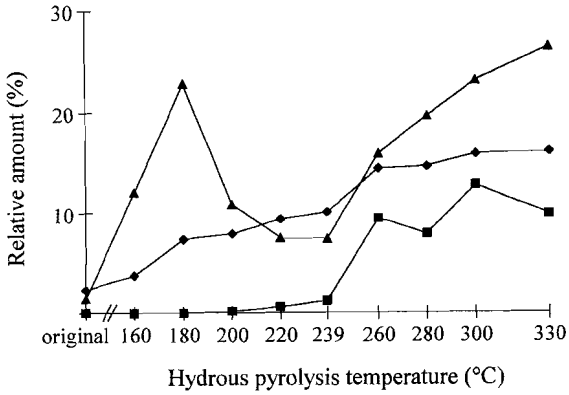

Fig. 3.19. Relative amounts (%) of alkylthiophenes with a *n*-C_{22} (diamonds), *n*-C_{30} (squares), and Ph skeleton (triangles) as a function of maturation temperature.

similar production of alkylthiophenes occurs in the natural situation, and that alkylthiophenes in sedimentary rocks that have undergone progressive diagenesis originate, at least partly, from thermal degradation of sulphide-linked carbon skeletons. The absolute amount of free C_{22} *n*-alkane and Ph released after desulphurisation of kerogens of subsamples from the marl layer of evaporitic cycle IV of the Vena del Gesso Basin (Schaeffer *et al.*, 1995a) is almost the same as the absolute amount of C_{22} *n*-alkylthiophenes and alkylthiophenes with a Ph carbon skeleton produced upon thermal maturation (Koopmans *et al.*, 1995). It is tempting to suggest that sulphur-bound C_{22} *n*-alkane and Ph in the kerogen are quantitatively converted to free alkylthiophenes, but this approach is probably too simplistic. An alkyl chain (R) that is linked to the kerogen by one monosulphide bridge can be thermally released in two ways, *i.e.* by the homolytic cleavage of both C-S bonds, yielding either an RS• radical or an R• radical. Therefore, it is likely that a significant proportion of sulphur-bound C_{22} *n*-alkane and Ph is converted to free alkanes.

Oxygen atoms in the kerogen can link carbon skeletons through ether as well as ester bonds. Recently it has been shown that thermal maturation of ether-linked carbon skeletons in HMW organic matter produces, amongst other compounds, ketones (Gelin *et al.*, 1993, 1994, 1996a; Behar *et al.*, 1995). These ketones can probably be regarded as stable thermal degradation products of ether-linked moieties, much in the same way as alkylthiophenes are stable thermal degradation products of sulphur-linked moieties. The position of the carbonyl group is identical to the position of the ether-linked carbon atom in the alkyl chain, so that important information about the original position of functional groups is retained. Ester bonds are easily hydrolysed at low levels of thermal stress, as evidenced by the early release of ester-bound triacontan-1,15-diol and triacontan-15-one-1-ol. This is in agreement with calculated activation energies for the generation of organic acids (*c.* 20 kJ/mol) and hydrocarbons (*c.* 70 kJ/mol) during hydrous pyrolysis of Kimmeridge oil shale (Barth *et al.*, 1989).

In conclusion, the role of the kerogen during thermal maturation is probably that it releases thermally labile sulphur- and oxygen-linked carbon skeletons as alkylthiophenes, ketones, and free *n*-alkanes at relatively low temperatures. C-C bond cleavage at higher temperatures ($T > 300°C$) results in the release of high amounts of primarily *n*-alkanes.

Comparison with naturally matured samples

In order to be able to make a comparison between the artificially matured samples and samples that have undergone natural maturation, the temperatures used during hydrous pyrolysis should be translated to vitrinite reflectance values. The vitrinite reflectance value (R_o) of the unheated marl is *c.* 0.25% (Kohnen *et al.*, 1991b). Due to the presence of only trace amounts of vitrinite, the vitrinite reflectance values of the heated samples were estimated by comparing several biomarker maturity parameter ratios, *i.e.* the

$\beta\beta/(\beta\beta+\alpha\beta+\beta\alpha)$ C_{35} hopane ratio and the 22S/(22S+22R)-17α,21β(H) C_{35} hopane ratio, to the ratios of samples whose vitrinite reflectance value has been measured. At 300°C the $\beta\beta/(\beta\beta+\alpha\beta+\beta\alpha)$ C_{35} hopane ratio equals 0 (Fig. 3.4), corresponding to $R_o \approx 0.4\%$ (Mackenzie, 1984; Peters and Moldowan, 1993). At 330°C the 22S/(22S+22R)-17α, 21β(H) C_{35} hopane ratio equals 0.43 (Fig. 3.4), corresponding to $R_o < 0.6\%$ (Mackenzie, 1984; Peters and Moldowan, 1993). Thus, the hydrous pyrolysis experiments represent only a narrow maturity interval ($0.25\% \leq R_o < 0.6\%$). It should be noted that these vitrinite reflectance values are much lower than those previously reported (Koopmans *et al.*, 1995), which were based on vitrinite reflectance values of shales that had undergone hydrous pyrolysis under the same conditions.

Homohopanes with a 17β,21β(H) configuration are usually absent from sedimentary rocks that have undergone mild diagenesis. In the light of the results presented here, this suggests that dramatic changes in the molecular composition of these samples have already occurred in the maturity interval $0.25\% \leq R_o < 0.4\%$. For instance, (i) S-S and C-S bonds in the kerogen are already cleaved at T < 200°C, releasing large amounts of sulphur-linked carbon skeletons, originating from multifunctionalised lipids (*e.g.* isorenieratene and C_{37} and C_{38} alkenones), into the polar fraction, which at a later stage (but still at $R_o < 0.4\%$) are released as free hydrocarbons, (ii) ester bonds are hydrolysed at low levels of thermal stress (T < 180°C), (iii) 1,2-dithianes are degraded at T < 200°C indicating the weakness of S-S bonds, and (iv) the large amount of both sulphur- and oxygen-linked *n*-C_{38} skeletons sequestered in the kerogen is already released at 260°C. All these reactions occur when homohopanes with a 17β,21β(H) configuration are still present. The weakness of the S-S bond, which is cleaved at $R_o << 0.4\%$, sheds new light on sulphur-rich oils containing abundant S-S bonds, such as the Rozel Point and Amposta oils (Schouten *et al.*, 1995b). These 'oils' are probably not oils in a true sense, *i.e.* formed by the cleavage of C-C bonds, which occurs mainly at T > 300°C ($R_o > 0.4\%$). More likely, they are low maturity bitumens formed by cleavage of S-S and C-S bonds.

A relatively immature setting ($R_o \approx 0.3$-0.4%) with which the hydrous pyrolysis results may be compared is the Mulhouse Basin. The organic geochemistry of the Mulhouse Basin has recently been jointly studied (*e.g.* Hofmann *et al.*, 1993; Keely *et al.*, 1993; Sinninghe Damsté *et al.*, 1993a). Saturated hydrocarbon fractions of samples from this evaporitic sequence are characterised by high amounts of Ph and steranes, and a low $CPI_{24\text{-}34}$. The suite of compounds in the saturated hydrocarbon fractions from the Mulhouse Basin is similar to that present in (i) the desulphurised polar fraction I of the unheated marl from the Vena del Gesso Basin (Fig. 3.8**a**), and (ii) the saturated hydrocarbon fraction of the artificially matured marl (260°C) from the Vena del Gesso Basin (Fig. 3.2**c**). These results strongly suggest that the organic matter of the Mulhouse Basin has passed through a 'sulphur stage' and that large changes must have already occurred, despite the fact that these sediments are typically described as immature.

In general, sequestration of functionalised lipids by sulphur and oxygen may not be recognised in most sedimentary rocks that have undergone mild thermal maturation,

as the corresponding carbon skeletons have already been released as *n*-alkanes, alkylthiophenes, ketones, and alkylbenzenes. Thus, the process of sulphur and oxygen sequestration, which is probably important for the geological preservation of functionalised lipids, is likely to be overlooked. Our results indicate that special care has to be taken when samples are studied whose level of thermal maturity is comparable to that of the marl from the Vena del Gesso Basin.

3.6 Conclusions

Hydrous pyrolysis experiments (160°C < T < 330°C) with an immature ($R_o \approx 0.25\%$) sulphur-rich sedimentary rock represent a narrow maturity interval ($R_o < 0.6\%$), as indicated by biomarker maturity parameter ratios [*i.e.* the $\beta\beta/(\beta\beta+\alpha\beta+\beta\alpha)$ C_{35} hopane ratio and the 22S/(22S+22R)-17α,21β(H) C_{35} hopane ratio]. Heating at relatively low temperatures (≤ 260°C) already has a large impact on the amounts and distributions of saturated hydrocarbons present as such, and sulphur-bound hydrocarbons in the polar fraction. Phytane and (20R)-5α,14α,17α(H) and (20R)-5β,14α,17α(H) C_{27} to C_{29} steranes, originally hardly present in the saturated hydrocarbon fraction, are released from the polar fraction through thermal cleavage of relatively weak S-S and C-S bonds. Compounds known to be not sequestered by sulphur and oxygen (*e.g.* lycopane) are not released. These results suggest that similar reactions occur in the natural situation. Indeed, saturated hydrocarbon fractions of the slightly more mature Mulhouse Basin ($R_o \approx 0.3$-0.4%) are characterised by relatively high amounts of Ph and steranes, and a low carbon preference index, suggesting that the organic matter has already passed through a 'sulphur stage'.

Alkylthiophenes are formed in large amounts upon maturation. No evidence was found for the transformation of alkylthiolanes to alkylthiophenes, as proposed in the early literature (for a review see Sinninghe Damsté and de Leeuw, 1990). The generation profiles of the methylated chromans suggest that they are produced from, and thus were sequestered in, high-molecular-weight fractions. The chroman ratio, which is an indicator of palaeosalinity, is constant in the maturity range studied, suggesting that it can be used for sedimentary rocks throughout diagenesis.

Specific carbon skeletons originating from multifunctionalised lipids (*e.g.* C_{38} alkenones, isorenieratene) only enter the polar fraction after mild thermal treatment. Due to their multiple functional groups these lipids are likely to be incorporated into the kerogen. Upon thermal maturation they are released first into the polar fraction, and then as free hydrocarbons, due to cleavage of S-S, C-S and C-O bonds. The relative amount of polysulphide-bound *vs.* total sulphur-bound carbon skeletons as a function of maturation temperature can give information about the number of functional groups in possible precursors. For instance, it is shown that the precursor of sulphur-bound squalane is probably octahydrosqualene, and not squalene.

The distribution of oxygen-bound and both sulphur- and oxygen-bound hydrocar-

bons on the one hand and ketones on the other in the sample heated at 260°C is similar, with abundant C_{29}-C_{31}, C_{37} and C_{38} *n*-alkane skeletons, suggesting a close relationship. The early release of triacontan-1,15-diol and triacontan-15-one-1-ol into the polar fraction suggests that relatively weak ester bonds in the kerogen are hydrolysed at low levels of thermal maturity, as supported by saponification of the kerogen of the original sample.

The distribution of selected carbon skeletons over all low and high-molecular-weight fractions as a function of maturation temperature shows that sulphur- and oxygen-bound skeletons are thermally labile. On the other hand, alkylthiophenes, ketones, *n*-alkanes and, when formed, 1,2-di-*n*-alkylbenzenes are thermally stable, suggesting that similar compounds are formed in the natural situation. Pristane is formed in high amounts as free hydrocarbon, and is not present in a sulphur- or oxygen-bound form, suggesting that it is formed from its precursor(s) by C-C bond cleavage.

Thermal degradation of sulphur- and oxygen-linked carbon skeletons in high-molecular-weight fractions seems to yield mainly alkylthiophenes and ketones as stable thermal degradation products. This explains the observation made by flash pyrolysis GC (Eglinton *et al.*, 1988b, 1990a,b; Tomic *et al.*, 1995; Nelson *et al.*, 1995) that, with increasing thermal maturation, alkylthiophenes are preferentially removed from the kerogen compared to *n*-alkanes/*n*-alkenes. The position of the thiophene moiety and the carbonyl group coincides with the original position of the functional group in the precursor. Therefore, important information about the biochemicals present in the depositional environment is retained.

3.7 Acknowledgements

We thank Shell International Exploration and Production for providing a research studentship to MPK. Analytical support was provided by Mrs. W.I.C. Rijpstra. GC-MS analyses were carried out by Mrs. M. Dekker and Mr. W. Pool. Mr. T.A. Daws is thanked for TOC measurements. Dr. C.A. Lewis and an anonymous referee are thanked for constructive comments. This work was partly supported by a PIONIER grant to JSSD from the Netherlands Organisation for Scientific Research (NWO).

Appendix

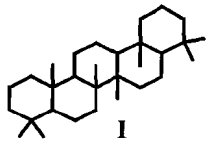

I

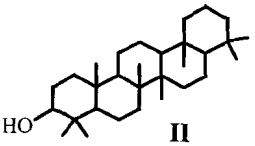

II

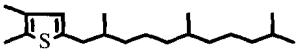

III

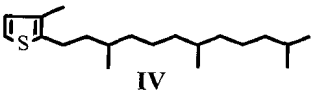

IV

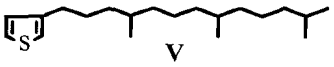

V

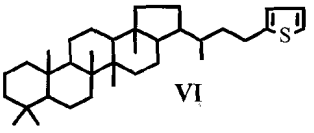

VI

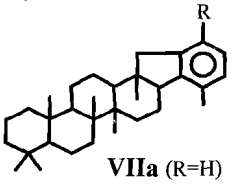

VIIa (R=H)
VIIb (R=Me)

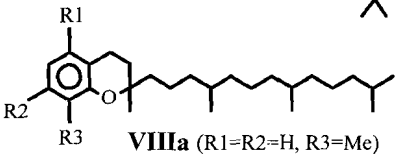

VIIIa (R1=R2=H, R3=Me)
VIIIb (R1=R3=Me, R2=H)
VIIIc (R1=R2=R3=Me)

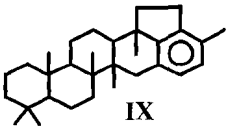

IX

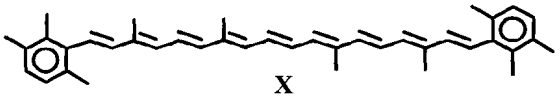

X

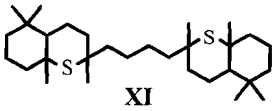

XI

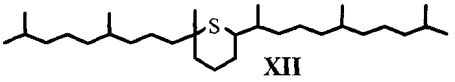

XII

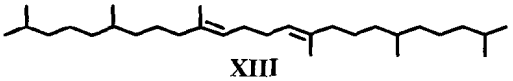

XIII

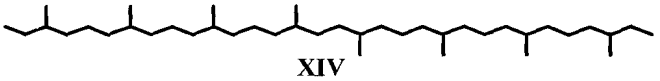

XIV

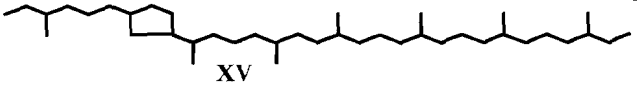

XV

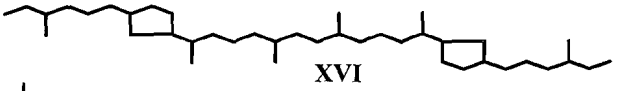

XVI

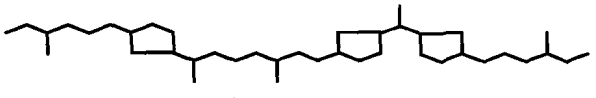

XVII

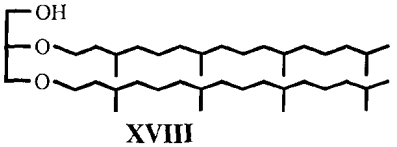

XVIII

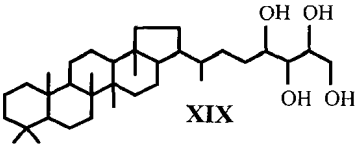

XIX

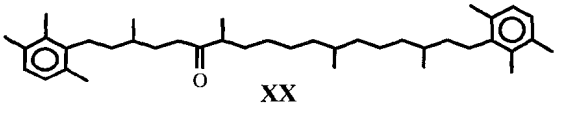

XX

CHAPTER 4

Artificial maturation of an immature sulphur- and organic-rich limestone from the Ghareb Formation, Jordan

M.P. Koopmans, W.I.C. Rijpstra, J.W. de Leeuw, M.D. Lewan
and J.S. Sinninghe Damsté

4.1 Abstract

An immature (R_o = 0.39%), sulphur-rich (S_{org}/C = 0.07), organic-rich (17.9 wt.% TOC) limestone from the Ghareb Formation (Upper Cretaceous) in Jordan was artificially matured by hydrous pyrolysis (200-300°C; 72h) to study the effect of progressive diagenesis and early catagenesis on the amounts and distributions of hydrocarbons, organic sulphur compounds and sulphur-rich geomacromolecules. The use of internal standards allowed the determination of absolute amounts.

With increasing thermal maturation, large amounts of alkanes and alkylthiophenes with predominantly linear carbon skeletons are generated from a high-molecular-weight fraction. The alkylthiophene isomer distributions do not change significantly with increasing thermal maturation, indicating the applicability of alkylthiophenes as biomarkers at relatively high levels of thermal maturity. For a given carbon skeleton, the saturated hydrocarbon, alkylthiophenes and alkylbenzo[*b*]thiophenes are stable forms at higher temperatures, whereas the alkylsulphides are not stable. The large amount of alkylthiophenes produced compared to the alkanes may be explained by a relatively high number of monosulphide links per carbon skeleton. These results are in good agreement with those obtained previously for an artificial maturation series of an immature sulphur-rich sample from the Gessoso-solfifera Formation.

4.2 Introduction

In the past decade, the geochemical research of organic sulphur compounds (OSC) has evolved from the identification of numerous series of new compounds (see for a review Sinninghe Damsté and de Leeuw, 1990) to the application of OSC as indicators of

biological, chemical and physical conditions of past depositional environments (*e.g.* Sinninghe Damsté *et al.*, 1989d, 1990b; Kohnen *et al.*, 1990c; Kenig *et al.*, 1995). This biomarker concept is based on the observation that sulphurisation of lipids occurs at functionalised sites (*e.g.* Valisolalao *et al.*, 1984; Brassell *et al.*, 1986b), as was later confirmed by laboratory sulphurisation experiments (*e.g.* Fukushima *et al.*, 1992; de Graaf *et al.*, 1992, 1995; Rowland *et al.*, 1993; Schouten *et al.*, 1993, 1994; Krein and Aizenshtat, 1994). Thus, the position of the sulphur atom in an OSC reveals information about the position of the functional group of the precursor molecule. Most of the OSC work has focused on thermally immature sedimentary rocks ($R_o \leq 0.3\%$) and "low thermal stress" crude oils. There are three reasons to expand the study of OSC and sulphur-rich geomacromolecules to thermally more mature samples. First, alkylthiophenes with a known biochemical precursor can be followed in a maturation series to investigate if they retain their palaeoenvironmental information. Second, the importance of sulphur-bound carbon skeletons in the early generation of crude oil can be evaluated. Third, the generation of benzo[*b*]thiophenes and dibenzothiophenes, which are important components of natural crude oils but whose formation pathways are poorly understood (Sinninghe Damsté *et al.*, 1989a; Aizenshtat *et al.*, 1995), can be monitored.

Recently, this approach was followed in the study of an artificial maturation series of an immature sulphur-rich marl from the Gessoso-solfifera Formation (Messinian) in the Vena del Gesso Basin, Italy. Throughout a maturity interval representing the diagenetic stage ($0.25\% \leq R_o < 0.6\%$), the isomer distribution of the alkylthiophenes remained essentially constant so that important palaeoenvironmental information could still be extracted (Koopmans *et al.*, 1995). Sulphur-bound phytane and steranes were thermally released as free hydrocarbons before significant C-C bond cleavage occurred, indicating the importance of sulphur-bound carbon skeletons in the early generation of specific carbon skeletons (Koopmans *et al.*, 1996b).

The aim of this work is to study the amounts and distributions of hydrocarbons, OSC and sulphur-rich geomacromolecules in a maturation series of a sample from the Ghareb Formation (Upper Cretaceous) at El Lajjun, Jordan. This sample contains more complex distributions of OSC than the sample from the Gessoso-solfifera Formation studied previously, and may therefore provide additional insights in the fate of organically-bound sulphur during dia- and catagenesis. The Ghareb Formation at El Lajjun is stratigraphically equivalent to the Lower Member of the Jurf ed Darawish oil shale. A sample from the latter (JED-156) has been the subject of many detailed molecular organic geochemical investigations (Sinninghe Damsté *et al.*, 1988b, 1989b,c,d, 1990a, 1995a; Kohnen *et al.*, 1990c; Hofmann *et al.*, 1992; Schouten *et al.*, 1995e).

4.3 Experimental

Sample description. The sample used in this study is a limestone from the Ghareb Formation (Upper Cretaceous) at El Lajjun, Jordan. The TOC content is 17.9 wt.%.

Elemental analysis of the isolated kerogen indicates it is an immature Type II-S kerogen with an atomic H/C ratio of 1.38, an atomic O/C ratio of 0.07, and an atomic S_{org}/C ratio of 0.07.

Hydrous pyrolysis. A detailed description of the experimental procedures of a typical hydrous pyrolysis experiment has been given by Lewan (1993b). A one-litre Hastelloy-C276 reactor was filled with 300 g of rock chips and 350 g of distilled water. The remaining volume was purged and filled with helium at a pressure of 2.4 bar. Artificial maturation was accomplished by heating the rock chips isothermally for 72 h at 200, 220, 240, 260, 280 and 300°C. The temperatures were continuously monitored during the experiments at 30 s intervals. Standard deviations were between ±0.1 and ±0.4°C for all experiments. Experiments at 280 and 300°C generated an expelled oil that was recovered from the water surface with a pipette. The reactor walls and the rock chips were rinsed with benzene to recover any sorbed oil films, which occurred in experiments at 260, 280 and 300°C. The residual rock chips were dried in a vacuum oven ($T \leq 50$°C).

Extraction, fractionation and kerogen preparation. An aliquot (*c.* 10 g) of the residual rock chips was freeze-dried and Soxhlet extracted with dichloromethane/methanol (7.5:1 v/v). If a sorbed or expelled oil was present, proportional amounts were combined with the extract. The combined extract was separated into maltene and asphaltene fractions by repeated (3 times) precipitation in heptane. An aliquot of the maltene fraction (*c.* 250 mg), to which four internal standards [6,6-d_2-3-methylhenicosane, 2,3-dimethyl-5-(1',1'-d_2-hexadecyl)thiophene, 2-methyl-2-(4,8,12-trimethyltridecyl)chroman and 2,3-dimethyl-5-(1',1'-d_2-hexadecyl)thiolane] were added for quantitative analysis, was fractionated by column chromatography with Al_2O_3 into an apolar and a polar fraction by elution with hexane/dichloromethane (9:1 v/v) and dichloromethane/methanol (1:1 v/v), respectively (Fig. 4.1). The amounts of asphaltenes and the apolar and polar fractions were determined gravimetrically. Further separation of the apolar fraction by argentatious thin-layer chromatography yielded the A1 fraction (saturated hydrocarbons; R_f = 0.9-1.0), the A2 fraction (alkylthiophenes; R_f = 0.4-0.9), the A3 fraction (bi-, di-, benzo[*b*]- and dibenzothiophenes; R_f = 0.05-0.4), and the A4 fraction (alkylsulphides; R_f = 0.0-0.05) (Fig. 4.1). The extracted rock residue of the original sample was demineralised using standard procedures (Lewan *et al.*, 1986) to yield the isolated kerogen for elemental analysis.

$LiAlH_4$ reduction of alkylsulphoxides. The polar fraction was treated with $LiAlH_4$ to reduce alkylsulphoxides to alkylsulphides (Payzant *et al.*, 1983; Schouten *et al.*, 1995e). Before the reaction, a known amount of an internal standard [2,3-dimethyl-5-(1',1'-d_2-hexadecyl)thiophene] was added to a known amount (20-40 mg) of the polar fraction. After the reduction, the reaction mixture was fractionated by column chromatography

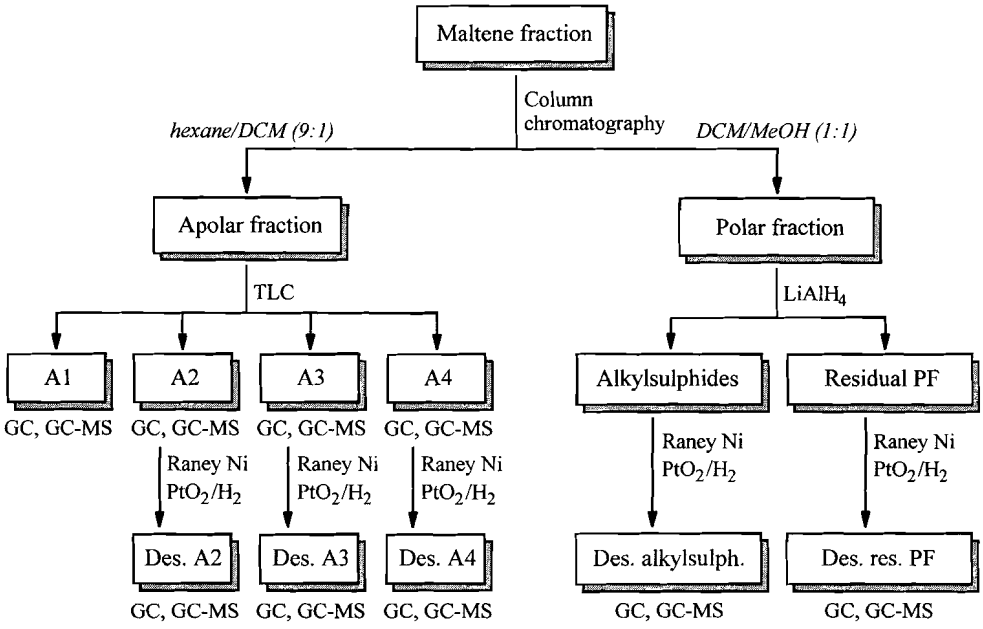

Fig. 4.1. Analytical flow diagram applied to the maltene fractions.

with Al_2O_3 into an alkylsulphide fraction and a residual polar fraction by elution with hexane/dichloromethane (9:1 v/v) and dichloromethane/methanol (1:1 v/v), respectively (Fig. 4.1).

Raney Ni degradation. The A2, A3 and A4 fractions, as well as the alkylsulphide and the residual polar fraction obtained after reduction of the polar fraction were desulphurised with Raney Ni (Sinninghe Damsté *et al.*, 1988b) (Fig. 4.1). Before desulphurisation of the residual polar fraction, a known amount of an internal standard [2,3-dimethyl-5-(1',1'-d_2-hexadecyl)thiophene] was added to a known amount (10-20 mg) of the residual polar fraction. Desulphurisation was accomplished by dissolving the fractions in 4 ml of ethanol, and repeatedly (x3) adding a small amount of Raney Ni. The mixture was allowed to reflux for 1.5 h. A sodium chloride solution was added, and the reaction mixture was extensively extracted with dichloromethane. Column chromatography using Al_2O_3 yielded an apolar fraction (hexane/dichloromethane 9:1 v/v), which was subsequently hydrogenated (Sinninghe Damsté *et al.*, 1988b).

Gas chromatography. Gas chromatography (GC) was performed using a Hewlett-Packard 5890 instrument equipped with an on-column injector. A fused silica capillary column (25 m x 0.32 mm) coated with CP Sil-5 (film thickness 0.12 μm) was used with

helium as carrier gas. The column effluent was monitored by both a flame ionisation (FID) and a sulphur-selective flame photometric (FPD) detector, using a stream-splitter at the end of the column (split ratio FID:FPD = 1:2). Samples were injected at 70°C and the oven was programmed to 130°C at 20°C/min and then at 4°C/min to 320°C, at which it was held for 20 min.

Gas chromatography-mass spectrometry. Gas chromatography-mass spectrometry (GC-MS) was carried out on a Hewlett-Packard 5890 gas chromatograph interfaced to a VG Autospec Ultima mass spectrometer operated at 70 eV with a mass range m/z 40-800 and a cycle time of 1.8 s (resolution 1000). The gas chromatograph was equipped with a fused silica capillary column (25 m x 0.32 mm) coated with CP Sil-5 (film thickness 0.12 μm). Helium was used as carrier gas. The samples were injected at 60°C and the oven was subsequently programmed to 130°C at 20°C/min and then at 4°C/min to 310°C, at which it was held for 20 min.

Quantitation. Quantitation of compounds in the A1 fraction and the desulphurised A2, A4, reduced alkylsulphoxide, and residual polar fractions was accomplished by integration of mass chromatograms of their main fragment ion and the main fragment ion of the standard, 6,6-d_2-3-methylhenicosane. Compounds in the desulphurised A3 fraction were quantitated by integration of mass chromatograms of their main fragment ion and the main fragment ion of the standard, 2-methyl-2-(4,8,12-trimethyltridecyl)chroman. A correction was made to account for the intensity of the fragment ions relative to the total ion current. Because mass spectrometric detection of compounds gives a molar response, a factor was introduced taking into account the molecular weights of the compounds quantitated and the standard to obtain absolute amounts (μg/g TOC of original rock).

4.4 Results and Discussion

A thermally immature (R_o = *c.* 0.39%; Koopmans *et al.*, 1997c) sulphur- and organic-rich limestone from the Upper Cretaceous Ghareb Formation at El Lajjun, Jordan, was artificially matured by hydrous pyrolysis at different temperatures (200, 220, 240, 260, 280 and 300°C; 72h) to study the effect of progressive diagenesis and early catagenesis on the amounts and distributions of hydrocarbons, OSC and sulphur-rich geomacromolecules. The original, unheated sample was also analysed and acted as a reference.

In addition to the techniques mentioned in the Experimental section, HI/$LiAlH_4$ degradation (cleavage of C-O bonds) and MeLi/MeI degradation (cleavage of S-S bonds) experiments were carried out on the polar fraction of the original sample and the sample heated at 260°C (only HI/$LiAlH_4$), because analysis of an artificial maturation series of a sample from the Gessoso-solfifera Formation indicated that relatively large amounts of carbon skeletons could be released in this way (Koopmans *et al.*, 1996b).

However, the amounts released are low, and it is concluded that only low amounts of carbon skeletons are sequestered *via* C-O or S-S bonds.

The amounts of several bulk fractions (asphaltenes, polar and apolar fraction) as a function of hydrous pyrolysis temperature are shown in Fig. 4.2, expressed as a percentage of total organic matter of the original sample (calculated from the elemental composition and the TOC content). With increasing maturation temperature, the amount of extractable organic matter increases significantly to 89% of total organic matter at 300°C. This implies that almost all the insoluble organic matter (kerogen) in the original sample is solubilised at 300°C. The relative amounts of the polar and apolar fraction increase progressively at high temperature, whereas the relative amount of asphaltenes decreases at 300°C. This suggests that the asphaltenes are thermally degraded at temperatures higher than 280°C, leading to formation of compounds in the polar and apolar fraction.

Apolar fraction

A1 fraction

Absolute amounts of selected saturated hydrocarbons in the A1 fraction of the original sample and the artificially matured samples are given in Table 4.1.

In the original sample, the *n*-alkane distribution maximises at C_{29} (Fig. 4.3**a**). The

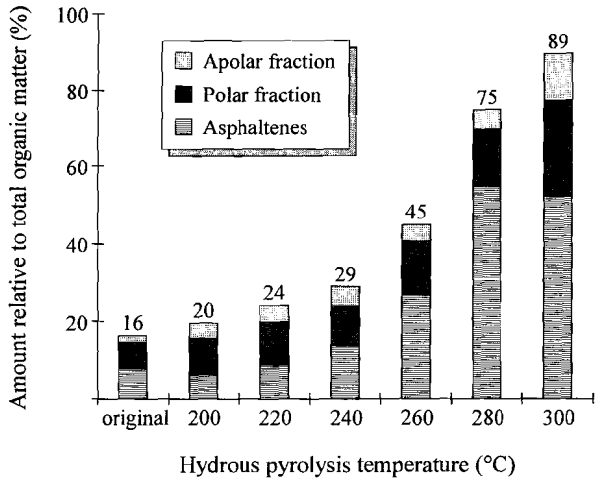

Fig. 4.2. Bar diagram showing the relative amounts of asphaltenes, polar and apolar fraction (expressed as a percentage of total organic matter of the original sample) as a function of hydrous pyrolysis temperature. Numbers indicate the summed relative amount of the three fractions, and equal the percentage of extractable organic matter.

long-chain *n*-alkanes have a moderate odd-over-even carbon number predominance (CPI_{24-34} = 1.7; Bray and Evans, 1961). With increasing thermal maturation, the CPI decreases until it is 1.0 at 300°C, due to the production (factor 5-15) of *n*-alkanes mainly at 260-300°C (Table 4.1). Short-chain *n*-alkanes are produced in higher amounts than long-chain *n*-alkanes, and at 300°C the *n*-alkanes maximise at C_{16} (Fig. 4.4**a**).

2,6,10-Trimethyltridecane, nor-pristane, pristane (Pr) and phytane (Ph) are the most abundant branched alkanes in the original sample (Fig. 4.3**a**). In addition, small amounts of 2,6,10,14-tetramethyl-7-(3-methylpentyl)pentadecane (HBI C_{25}) and lycopane are present. With increasing thermal maturation, large amounts of these isoprenoids are produced (factor 6-30; Table 4.1). The Pr/Ph ratio, which is 0.3 in the original sample, increases up to 1.5 at 300°C (Fig. 4.4**a**), a phenomenon discussed in detail elsewhere (Koopmans *et al.*, 1997c).

The sterane distribution in the original sample consists mainly of (20R)-5α,14α, 17α(H) and (20R)- and (20S)-5α,14β,17β(H) C_{27}-C_{29} steranes, with small amounts of (20R)-5β,14α,17α(H) C_{27}-C_{29} steranes, pregnane (**I**; see Appendix), 4-methylpregnane, homopregnane and bishomopregnane (Fig. 4.5**a**). The (20R)-5α,14α,17α(H) steranes are dominated by the C_{27} and C_{29} members. The (20R)- and (20S)-5α,14β,17β(H) steranes, however, are dominated by the C_{28} member, suggesting a significant input into the sediment of Δ^7 C_{28} sterols, because Δ^7 sterols are known to be transformed to (20R)- and (20S)-5α,14β,17β(H) steranes during relatively early stages of diagenesis (ten Haven *et al.*, 1986; Peakman *et al.*, 1989). With increasing thermal maturation the ste-

Table 4.1. Absolute amounts (μg/g TOC of original rock) of selected compounds in the A1 fraction of the original sample and the artificially matured samples. Also indicated are the Pr/Ph ratio and the CPI. Roman numbers refer to structures in the Appendix.

	original	200°C	220°C	240°C	260°C	280°C	300°C
n-C_{18}	32	36	48	43	$1.2x10^2$	$2.4x10^2$	$4.6x10^2$
n-C_{28}	53	51	52	73	$1.2x10^2$	$2.0x10^2$	$3.7x10^2$
n-C_{38}	3	2	2	3	6	10	15
9-methyloctadecane	0	0	1	1	4	9	16
Pr	21	18	20	15	93	$2.7x10^2$	$6.4x10^2$
Ph	73	67	65	47	$1.5x10^2$	$2.7x10^2$	$4.4x10^2$
HBI C_{25}	3	2	2	2	5	14	21
(20R)-5α,14α,17α(H) C_{29} sterane	21	49	55	95	$2.7x10^2$	$3.8x10^2$	$1.7x10^2$
Pregnane (**I**)	0	2	2	4	21	50	$1.1x10^2$
17α,21β(H) C_{35} hopanes	4	6	8	13	31	62	67
13α(H),14β(H) C_{20} tricyclic terpane (**III**)	0	2	2	3	15	44	69
Gammacerane (**II**)	4	19	27	40	$1.3x10^2$	$2.2x10^2$	$1.9x10^2$
Pr/Ph	0.3	0.3	0.3	0.3	0.6	1.0	1.5
CPI	1.7	1.7	1.6	1.4	1.2	1.1	1.0

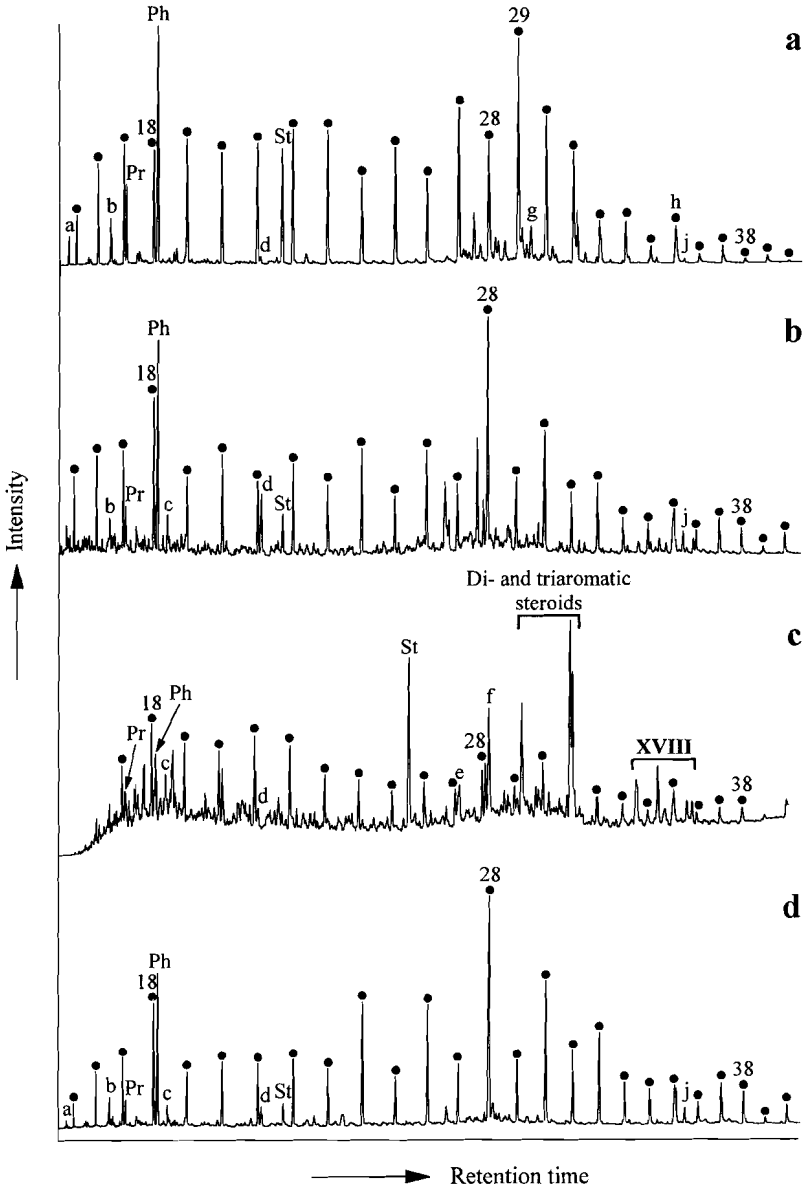

Fig. 4.3. TIC of (**a**) the A1 fraction and the desulphurised (**b**) A2, (**c**) A3 and (**d**) A4 fractions of the original sample. Key: dots = *n*-alkanes (numbers indicate number of carbon atoms), Pr = pristane, Ph = phytane, St = standard, a = 2,6,10-trimethyltridecane, b = nor-pristane, c = 9-methyloctadecane, d = HBI C_{25}, e = 2,5,8-trimethyl-2-(4,8,12-trimethyltridecyl)chroman (**XVIIb**), f = 2,5,7,8-tetramethyl-2-(4,8,12-trimethyltridecyl)chroman (**XVIIc**), g = (20R)-5α,14α,17α(H) C_{29} sterane, h = lycopane, j = (22R)-17α,21β(H) C_{35} hopane.

rane distribution remains largely unchanged (Fig. 4.5), but at 300°C it has become much more complex with higher relative amounts of (20S)-5α,14α,17α(H) steranes, (20R)- and (20S)-5α,14β,17β(H) steranes, and pregnanes (Fig. 4.5**d**). The amount of pregnane (**I**) has also increased in an absolute sense (Table 4.1), which is interesting in the light of the decreasing absolute amount of (20R)-5α,14α,17α(H) C_{29} sterane at high maturation temperatures. A (20R)-5α,14α,17α(H) C_{29} sterane generation profile similar to that found in this study (Table 4.1) has been reported for an artificial maturation series of a sample from the Gessoso-solfifera Formation (Koopmans *et al.*, 1996b).

The 20S/(20S+20R)-5α,14α,17α(H) C_{29} sterane ratio, which is often used as a maturity parameter and has an equilibrium value of 0.55 (Seifert and Moldowan, 1986) corresponding to a vitrinite reflectance of *c.* 0.8% (Peters and Moldowan, 1993), increases from 0.03 in the original sample to 0.50 at 300°C (Fig. 4.6**a**). The increase of the 20S/(20S+20R)-5α,14α,17α(H) C_{29} sterane ratio with increasing level of thermal maturity has classically been ascribed to isomerisation of the chiral center at C-20 (*e.g.* Mackenzie *et al.*, 1980; Mackenzie, 1984; Seifert and Moldowan, 1986). Our approach allows us to determine absolute amounts of the individual isomers, so that the presumed isomerisation at C-20 can be tested. The absolute amounts of (20S)- and (20R)-5α,14α, 17α(H) C_{29} sterane are shown in Fig. 4.6**b**. In the original sample, the biological (20R)-isomer is much more abundant than the (20S)-isomer, hence the low 20S/(20S+20R)-ratio. Up to 280°C, both isomers are thermally generated from a high-molecular-weight (HMW) fraction in more or less comparable amounts, so that the 20S/(20S+20R)-ratio increases. At 300°C the absolute amount of the (20R)-isomer decreases dramatically whereas the (20S)-isomer remains constant, so that the 20S/(20S+20R)-ratio increases further and approaches its equilibrium value (Fig. 4.6**a**). Similar generation profiles of (20S)- and (20R)-5α,14α,17α(H) C_{29} sterane have been reported for natural (Bishop and Abbott, 1993) and artificial (Abbott *et al.*, 1990; Peters *et al.*, 1990) maturation series. In summary, (i) the generation of the (20S)-isomer from a HMW fraction indicates that isomerisation at C-20 does occur, because this isomer is not biosynthesised, (ii) the generation profiles of the (20R)- and (20S)-isomers do not show any indication for the direct conversion of free (20R)- into (20S)-isomers, and (iii) the (20S)-isomer appears to be thermally more stable than the (20R)-isomer.

The carbon number distribution and speciation of the homohopanoids has been discussed in detail elsewhere (Köster *et al.*, 1997). In the original sample, the hopanes are dominated by 17α,21β(H) isomers, with small amounts of 17β,21α(H) isomers (Fig. 4.7**a**). The carbon number distribution ranges from C_{27} to C_{35}, with the C_{30} and C_{31} members being the most abundant. With increasing thermal maturation, the C_{29} member becomes relatively more abundant, and the 22S/(22S+22R)-17α,21β(H) ratios of the extended hopanes approach their equilibrium values (*c.* 0.6; Mackenzie, 1984; Peters and Moldowan, 1993) (Fig. 4.7). This increase has been ascribed to the isomerisation of the chiral center at C-22 (*e.g.* Ensminger *et al.*, 1974; Seifert and Moldowan, 1986). The absolute amounts of the (22S)- and (22R)-17α,21β(H) C_{35} hopanes as a function of

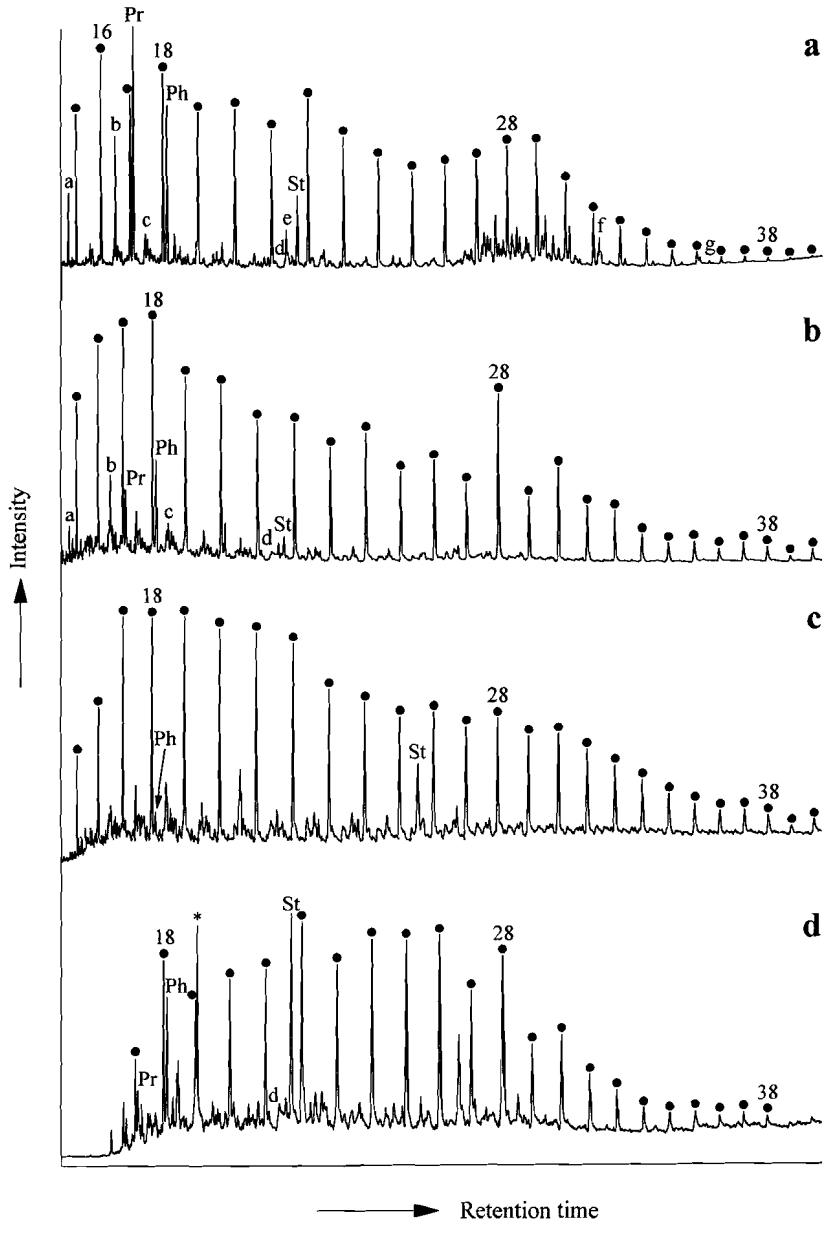

Fig. 4.4. TIC of (**a**) the A1 fraction and the desulphurised (**b**) A2, (**c**) A3 and (**d**) A4 fractions of the sample heated at 300°C. Key: dots = *n*-alkanes (numbers indicate number of carbon atoms), Pr = pristane, Ph = phytane, St = standard, a = 2,6, 10-trimethyltridecane, b = nor-pristane, c = 9-methyloctadecane, d = HBI C_{25}, e = pregnane (**I**), f = gammacerane (**II**), g = (22R)-17α,21β(H) C_{35} hopane, * = contaminant.

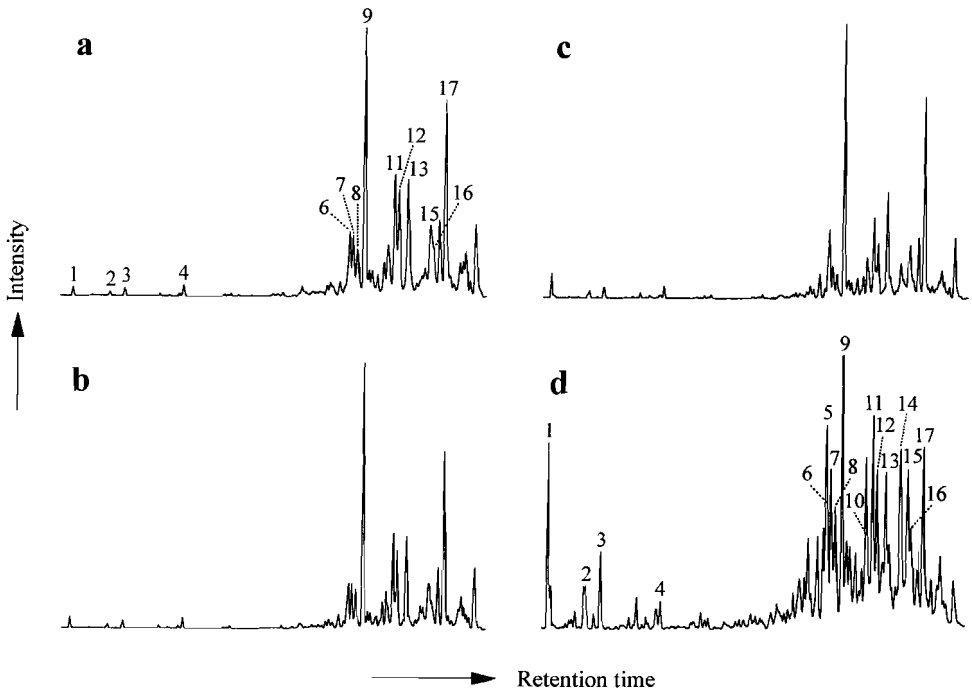

Fig. 4.5. Partial summed m/z 217+218+231+232 mass chromatogram of the A1 fraction of (**a**) the original sample, and the samples artificially matured at (**b**) 200°C, (**c**) 260°C and (**d**) 300°C. Identification of numbered compounds is given in Table 4.2.

maturation temperature are shown in Fig. 4.8. Both isomers are thermally generated from a HMW fraction with increasing maturation temperature, but at 300°C the (22S)-isomer still increases while the (22R)-isomer levels off. Thus, our results suggest a lower thermal stability of the (22R)- compared to the (22S)-isomer, in agreement with results of Bishop and Abbott (1993) for a natural maturation series. At 300°C the summed amount of the (22S)- and (22R)-17α,21β(H) C_{35} hopanes still increases, suggesting that hopanes are more resistant to thermal degradation than steranes (Table 4.1), in accordance with results from other studies (Eglinton and Douglas, 1988; Koopmans *et al.*, 1996b).

Gammacerane (**II**), which is present in low abundance in the original sample, is formed in high amounts (factor 50) upon increasing thermal maturation (Table 4.1). At 260°C, it is the most abundant triterpane in the m/z 191 mass chromatogram (Fig. 4.7**c**). The occurrence of free gammacerane in this maturation series is probably governed by an early diagenetic sulphurisation/desulphurisation pathway of tetrahymanol, as described by Sinninghe Damsté *et al.* (1995c).

A whole suite of tri- and, to a lesser extent, tetracyclic terpanes is formed during hydrous pyrolysis, of which the 13α(H),14β(H) C_{20} component (**III**) is the most abundant (Fig. 4.7). This component was identified by comparison of its mass spectrum and relative retention time with data from the literature (Chicarelli *et al.*, 1988). Its amount increases more sharply than that of the 17α,21β(H) C_{35} hopanes (Table 4.1). A relative increase of tricyclic terpanes compared to hopanes with increasing thermal maturation has been observed before in heating experiments with immature sedimentary rocks and crude oils (Aquino Neto *et al.*, 1983; Peters *et al.*, 1990).

A2 fraction

The A2 fractions are dominated by several series of *n*-alkylthiophenes, as determined from summed m/z 97+111+125 mass chromatograms (cf. Sinninghe Damsté *et al.*, 1986). Therefore, these fractions were desulphurised to enable quantitation of alkylthiophene carbon skeletons. Absolute amounts of selected compounds in the desulphurised A2 fraction of the original sample and the artificially matured samples are given in Table 4.3. The A2 fractions were also analysed before desulphurisation to determine the alkylthiophene isomer distributions, and to study the amounts and distributions of alkylbenzenes and alkylbenzo[*b*]thiophenes separately, because the latter are converted to

Table 4.2. Steranes identified by GC-MS in the A1 fraction of the original sample and the artificially matured samples (Fig. 4.5).

Peak number	Compound
1	5α,14β C_{21} sterane (pregnane; **I**)
2	4-methyl-5α,14β C_{21} sterane
3	5α,14β C_{22} sterane
4	5α,14β C_{23} sterane
5	(20S)-5α,14α,17α(H) C_{27} sterane
6	(20R)-5β,14α,17α(H) C_{27} sterane
7	(20R)-5α,14β,17β(H) C_{27} sterane
8	(20S)-5α,14β,17β(H) C_{27} sterane
9	(20R)-5α,14α,17α(H) C_{27} sterane
10	(20S)-5α,14α,17α(H) C_{28} sterane
11	(20R)-5α,14β,17β(H) C_{28} sterane
12	(20S)-5α,14β,17β(H) C_{28} sterane
13	(20R)-5α,14α,17α(H) C_{28} sterane
14	(20S)-5α,14α,17α(H) C_{29} sterane
15	(20R)-5α,14β,17β(H) C_{29} sterane
16	(20S)-5α,14β,17β(H) C_{29} sterane
17	(20R)-5α,14α,17α(H) C_{29} sterane

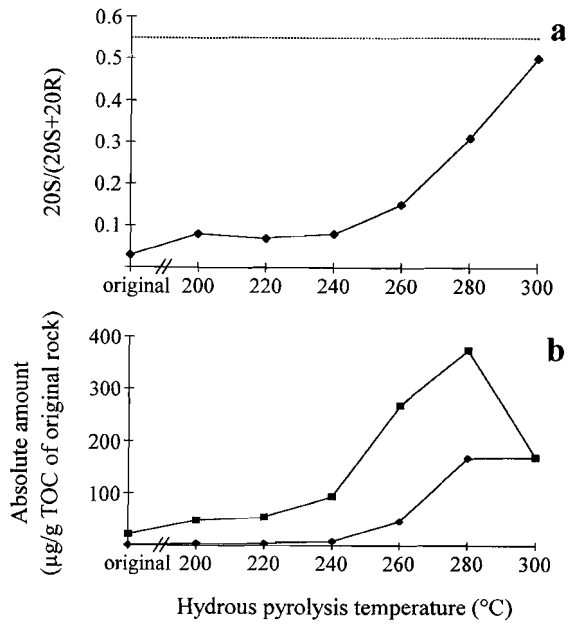

Fig. 4.6. (**a**) Diagram showing the 20S/(20S+20R)-5α,14α,17α(H) C_{29} sterane ratio as a function of maturation temperature. The thermodynamic equilibrium value of 0.55 (Seifert and Moldowan, 1986) is indicated with a stippled line. (**b**) Generation profiles of (20S)- (diamonds) and (20R)- (squares) 5α,14α,17α(H) C_{29} steranes.

alkylbenzenes upon desulphurisation.

The desulphurised A2 fraction of the original sample contains predominantly *n*-alkanes and Ph, with smaller amounts of Pr, 9-methyloctadecane, HBI C_{25}, and 17α,21β(H) hopanes dominated by the C_{35} isomers (Fig. 4.3**b**). The *n*-alkanes show a distinct even-over-odd carbon number predominance ($CPI_{24\text{-}34}$ = 0.5) which is most pronounced at *n*-C_{28}. The A2 fraction contains three alkylthiophenes with a Pr carbon skeleton which have been identified as **VI-VIII** (Koopmans *et al.*, 1997c). The 2-3‰ difference in $\delta^{13}C$ value of Pr in the desulphurised A2 fraction and free Pr in the A1 fraction (Koopmans *et al.*, 1997c) suggests different precursors, *e.g.* pristenes, pristadienes and pristatrienes known to occur in zooplankton (Blumer and Thomas, 1965; Blumer *et al.*, 1969) for the alkylthiophenes, and bound tocopherols for free Pr (Goossens *et al.*, 1984). Comparison of the hydrocarbon distribution of the desulphurised A2 fraction with that of the A1 fraction reveals the high relative abundance of 9-methyloctadecane and HBI C_{25} in the former (Figs. 4.3**a** and **b**). These originate from desulphurisation of specific alkylthiophene isomers with 9-methyloctadecane (**IX-XI**) and HBI C_{25} (**XII** and **XIII**) skeletons first identified by Sinninghe Damsté *et al.* (1989b,c). Alkyl-

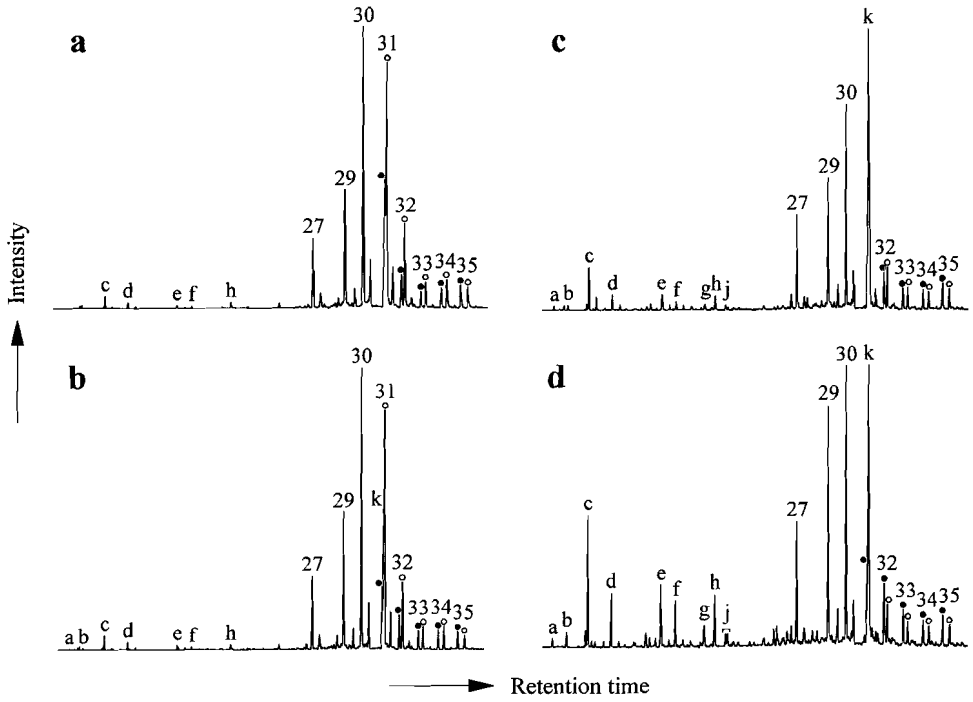

Fig. 4.7. Partial m/z 191 mass chromatogram of the A1 fraction of (**a**) the original sample, and the samples artificially matured at (**b**) 200°C, (**c**) 260°C and (**d**) 300°C, showing the terpane distributions. Key: numbers indicate carbon number of hopanes, solid dots indicate (22S)-17α,21β(H) isomers, open dots indicate (22R)-17α, 21β(H) isomers, a = 13β(H) C_{19} tricyclic terpane, b = 14α(H) C_{19} tricyclic terpane, c = 13α(H),14β(H) C_{20} tricyclic terpane (**III**), d = 13α(H),14β(H) C_{21} tricyclic terpane, e = C_{23} tricyclic terpane, f = C_{24} tricyclic terpane, g = (22S+R) C_{25} tricyclic terpanes, h = C_{24} tetracyclic terpane, j = (22S+R) C_{26} tricyclic terpanes, k = gammacerane.

benzenes are minor compounds in the original sample, with the most prominent components, icosylbenzene and 1,2-dimethyl-4-phytanylbenzene (**IV**), amounting to *c.* 10 μg/g TOC. The latter component was identified by comparison of its mass spectrum and relative retention time with data from the literature (Sinninghe Damsté *et al.*, 1988a). In addition, several series of C_2 to C_{17} alkylated benzo[*b*]thiophenes are present in similar amounts as the alkylbenzenes (Table 4.3). A monoaromatic hopanoid (**V**), which was identified by comparison of its mass spectrum with data from the literature (Greiner *et al.*, 1977), and some monoaromatic steroids are also present.

Artificial maturation results in increasing amounts of alkylthiophenes with linear and, to a lesser extent, isoprenoid carbon skeletons (factor 3-10), especially at 260-

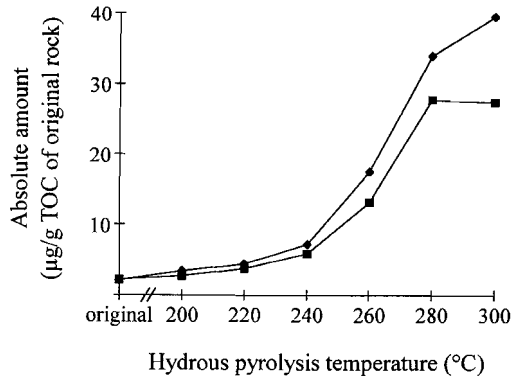

Fig. 4.8. Generation profiles of (22S)- (diamonds) and (22R)- (squares) 17α, 21β(H) C_{35} hopanes in the A1 fraction.

300°C (Table 4.3). Similar results have been reported in previous studies (Koopmans *et al.*, 1995, 1996b), in which it was reasoned that alkylthiophenes are stable thermal degradation products of sulphur-bound carbon skeletons in HMW fractions, an interpretation shared by Aizenshtat *et al.* (1995). Alkylbenzenes are produced in low amounts (factor 2-3), so that at 300°C they are negligible compared to the alkylthiophenes. Alkylbenzo[*b*]thiophenes, however, are produced in very large amounts: at 300°C the amounts of the C_{11} members are two orders of magnitude higher than in the original sample (Table 4.3). The carbon number distributions of the alkylbenzenes and alkylbenzo[*b*]thiophenes change to lower carbon numbers with increasing maturation, as follows from the generation profiles of the C_3 and C_{10} alkylated benzo[*b*]thiophenes (Table 4.3). Inspection of the A2 fractions of the artificially matured samples reveals that the sterane and gammacerane carbon skeletons are represented mainly by Δ^2 sterenes and gammacer-2-ene, respectively, and not by alkylthiophenes.

Now that the generation profiles of the alkylthiophenes with an acyclic carbon skeleton have been determined, it is interesting to see if the production of these compounds influences their isomer distribution, because specific distributions can reveal information about the input of particular palaeobiochemicals into the sediment (*e.g.* Sinninghe Damsté *et al.*, 1989d, 1990b; Kohnen *et al.*, 1990c). With increasing thermal maturation, the relative amounts of the 2-*n*-alkylthiophenes increase slightly while the relative amounts of the mid-chain 2,5-di-*n*-alkylthiophenes (in which both alkyl side chains contain at least 3 C atoms) decrease slightly (Fig. 4.9). Similar results have been reported for an artificial maturation series of a sample from the Gessoso-solfifera Formation (Koopmans *et al.*, 1995). In that study, the isomer distribution of the C_{31} and C_{38} alkylthiophenes in the sample heated at 330°C was still dominated by particular isomers that were already the major isomers in the original sample, indicating that information

Table 4.3. Absolute amounts (μg/g TOC of original rock) of selected carbon skeletons in the A2 fraction of the original sample and the artificially matured samples. Also indicated are the Pr/Ph ratio and the CPI. Roman numbers refer to structures in the Appendix.

	original	200°C	220°C	240°C	260°C	280°C	300°C
n-C_{18}	$1.2x10^2$	$1.7x10^2$	$2.2x10^2$	$2.4x10^2$	$5.8x10^2$	$7.9x10^2$	$1.2x10^3$
n-C_{28}	$2.8x10^2$	$4.7x10^2$	$6.4x10^2$	$6.5x10^2$	$1.7x10^3$	$1.6x10^3$	$1.7x10^3$
n-C_{38}	42	70	$1.1x10^2$	74	$1.8x10^2$	$1.6x10^2$	$2.7x10^2$
9-methyloctadecane	11	13	16	16	31	36	43
Pr	38	53	69	53	$1.7x10^2$	$2.3x10^2$	$3.3x10^2$
Ph	$2.0x10^2$	$2.3x10^2$	$2.7x10^2$	$2.7x10^2$	$4.0x10^2$	$4.5x10^2$	$5.8x10^2$
HBI C_{25}	71	61	70	82	84	$1.2x10^2$	77
(20R)-5α,14α,17α(H) C_{29} sterane	7	21	44	59	58	17	0
17α,21β(H) C_{35} hopanes	90	94	$1.3x10^2$	$1.0x10^2$	$1.1x10^2$	$1.1x10^2$	40
Gammacerane (**II**)	2	11	24	35	76	50	27
C_3 alkylated benzo[*b*]thiophenes[a]	7	35	28	81	$1.6x10^2$	$3.3x10^2$	$1.1x10^3$
C_{10} alkylated benzo[*b*]thiophenes	16	33	36	46	88	98	$2.9x10^2$
Monoaromatic hopanoid (**V**)	13	23	28	21	27	13	12
Pr/Ph	0.2	0.2	0.3	0.2	0.4	0.5	0.6
CPI	0.5	0.5	0.5	0.5	0.8	0.6	0.7

[a] Summed amount of C_3 alkylated benzo[*b*]thiophenes in the A2 and A3 fractions.

about the original positions of functional groups of precursor molecules was retained at the highest temperature. Here, the isomer distribution of the C_{28} alkylthiophenes may provide a valuable testcase, because studies of the related Jurf ed Darawish oil shale have indicated that the C_{28} alkylthiophenes are dominated by two particular isomers, *i.e.* 2-hexadecyl-5-octylthiophene and 2-nonyl-5-pentadecylthiophene (Sinninghe Damsté *et al.*, 1989c; Kohnen *et al.*, 1990c). These isomers have been ascribed to sulphur incorporation into a octacosa-9,12-diene precursor (Sinninghe Damsté *et al.*, 1989c; Kohnen *et al.*, 1990c). In the original sample, 2-hexadecyl-5-octylthiophene and 2-nonyl-5-pentadecylthiophene make up 25 and 18% of the C_{28} mid-chain 2,5-di-*n*-alkylthiophenes, respectively, whereas the other isomers represent 11% or less. With increasing thermal maturation, their relative abundance decreases to 20 and 16%, respectively, as compared to 12% or less for the other isomers. Thus, although the predominance of 2-hexadecyl-5-octylthiophene and 2-nonyl-5-pentadecylthiophene becomes less marked with increasing thermal maturation, they are still the major mid-chain isomers, still suggesting a octacosa-9,12-diene precursor that is incorporated into the kerogen by reaction with reduced inorganic sulphur species and thermally released as alkylthiophene.

The isomer distribution of the alkylthiophenes with a Ph carbon skeleton can be expressed as the isoprenoid thiophene ratio (ITR), which is defined as the sum of 3-

(4,8,12-trimethyltridecyl)thiophene (**XIV**) and 2-(3,7,11-trimethyldodecyl)-3-methylthiophene (**XV**), divided by the sum of 2,3-dimethyl-5-(2,6,10-trimethylundecyl)thiophene (**XVI**) and the mid-chain isomers. The ITR has been used as an indicator for palaeosalinity (Sinninghe Damsté *et al.*, 1989d), with values < 0.5 indicating hypersalinity. In the maturation series under study, the ITR increases from 0.07 in the original sample to 0.39 at 300°C (Fig. 4.9**d**). Although this interval falls in the hypersalinity range, the ITR is clearly maturity dependent. A similar maturity dependence was observed for an artificial maturation series of a sample from the Gessoso-solfifera Formation, where the ITR dropped from 32 in the original sample to 4.9 at 330°C (Koopmans *et al.*, 1995). The fact that for both maturation series the ITR approaches unity with increasing maturation temperature may be due to dilution of the alkylthiophenes already present in the extract with alkylthiophenes thermally released from the kerogen.

A3 fraction

The A3 fractions were analysed both before and after desulphurisation. Absolute amounts of selected compounds in the desulphurised A3 fraction of the original sample and the artificially matured samples are given in Table 4.4.

The A3 fraction of the original sample contains methylated 2-methyl-2-(4,8,12-trimethyltridecyl)chromans (MTTCs; **XVIIa-c**; Sinninghe Damsté *et al.*, 1987b), a series of C_{32}-C_{35} benzohopanes (**XVIII**) first identified by Hussler *et al.* (1984), and di- and triaromatic steroids. C_3-C_5 alkylated benzo[*b*]thiophenes are present in small amounts. Apparently, the benzo[*b*]thiophenes are present in both the A2 and A3 fractions, although the longer chain components, which are slightly less polar, are only detected in the A2 fraction. Acyclic carbon skeletons are present as well, as revealed by desulphurisation of the A3 fraction (Fig. 4.3**c**). These probably derive from alkylbithiophenes (containing two conjugated thiophene moieties) and/or alkyldithiophenes (containing two non-conjugated thiophene moieties). Indeed, three bithiophenes with a Ph carbon skeleton (**XIX-XXI**) were identified by comparison of their mass spectra with those reported in the literature (Sinninghe Damsté and de Leeuw, 1987; Sinninghe Damsté *et al.*, 1987c).

With increasing thermal maturation, the absolute amounts of linear carbon skeletons generally increase. Artificial maturation results in the production of relatively large amounts of a di- (**XXII**) and triaromatic hopanoid (**XXIII**; Table 4.4) first identified by Greiner *et al.* (1976, 1977). The latter is the most abundant compound in the A3 fraction of the samples heated at 200-260°C. In addition, dibenzothiophene and C_1-C_3 alkylated dibenzothiophenes are produced during heating, especially at 300°C (Table 4.4). The methylated MTTC generation profiles are rather flat, so that it is not clear if these compounds are generated during thermal maturation from HMW precursors as observed in a study of an artificially matured sedimentary rock from the Gessoso-solfifera Formation (Koopmans *et al.*, 1996b). The distribution of the methylated MTTCs can be expressed as the chroman ratio (Sinninghe Damsté *et al.*, 1987b, 1989d), *i.e.* 2,5,7,8-

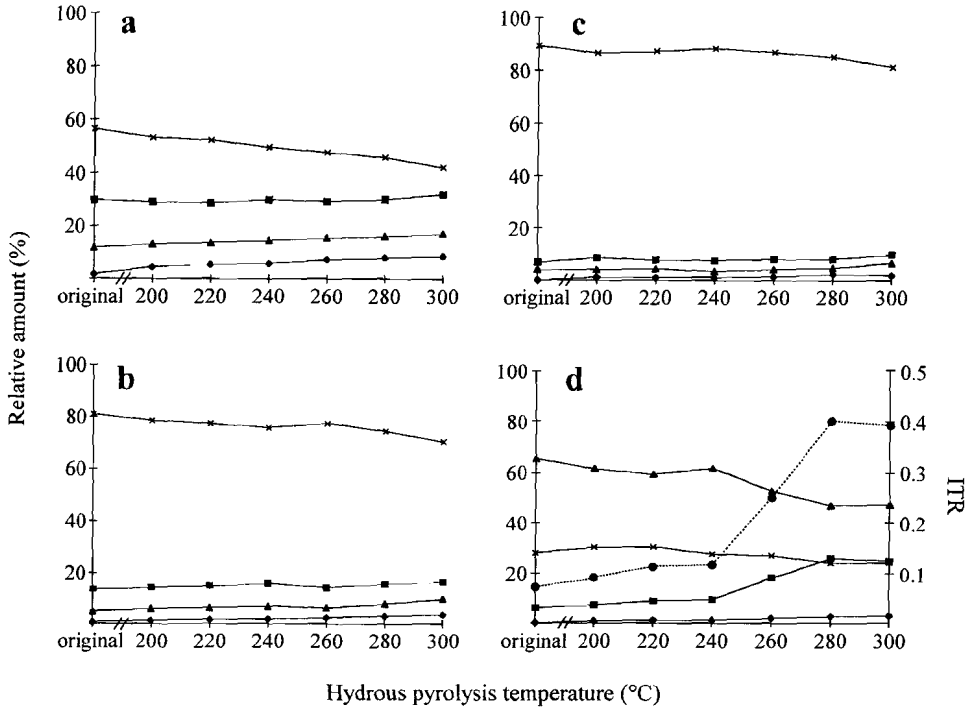

Fig. 4.9. Relative amounts of the alkylthiophene isomers with an (**a**) *n*-C_{18}, (**b**) *n*-C_{28}, (**c**) *n*-C_{38} and (**d**) Ph carbon skeleton as a function of maturation temperature. In (**a-c**), diamonds represent 2-alkylthiophenes, squares represent 2-alkyl-5-methylthiophenes, triangles represent 2-alkyl-5-ethylthiophenes, and crosses represent mid-chain 2,5-dialkylthiophenes. In (**d**), diamonds represent 3-(4,8,12-trimethyltridecyl)thiophene (**XIV**), squares represent 2-(3,7,11-trimethyldodecyl)-3-methylthiophene (**XV**), triangles represent 2,3-dimethyl-5-(2,6,10-trimethylundecyl)thiophene (**XVI**), and crosses represent the mid-chain isomers. The isoprenoid thiophene ratio (ITR) is indicated in (**d**) by a stippled line.

tetramethyl-2-(4,8,12-trimethyltridecyl)chroman (**XIIc**) divided by the summed amount of methylated MTTCs. This ratio has been used as an indicator for palaeosalinity (Sinninghe Damsté *et al.*, 1993c), and was shown to be independent of the level of thermal maturity of an artificially matured sedimentary rock from the Gessoso-solfifera Formation (Koopmans *et al.*, 1996b). In the maturation set under study the chroman ratio is virtually constant (Table 4.4), thus corroborating these results.

A4 fraction

The A4 fractions contain predominantly alkylsulphides with linear carbon skeletons, as determined from summed m/z 87+101+115 mass chromatograms (cf. Sinninghe Damsté

Table 4.4. Absolute amounts (μg/g TOC of original rock) of selected carbon skeletons in the A3 fraction of the original sample and the artificially matured samples. Also indicated are the Pr/Ph and chroman ratio and the CPI. Roman numbers refer to structures in the Appendix.

	original	200°C	220°C	240°C	260°C	280°C	300°C
n-C_{18}	8	18	13	85	31	$1.1x10^2$	$2.2x10^2$
n-C_{28}	9	64	32	$1.6x10^2$	40	$1.4x10^2$	$2.6x10^2$
n-C_{38}	4	16	11	51	7	55	59
9-methyloctadecane	2	1	1	6	1	2	0
Pr	2	5	3	20	4	16	25
Ph	8	13	5	79	5	25	41
HBI C_{25}	3	6	3	21	2	10	11
(20R)-5α,14α,17α(H) C_{29} sterane	0	4	6	0	0	0	0
C_{32} benzohopane (**XVIII**)	10	24	31	14	27	35	19
Diaromatic hopanoid (**XXII**)	0	6	6	6	1	6	0
Triaromatic hopanoid (**XXIII**)	0	88	81	90	77	23	26
C_1 alkylated dibenzothiophenes	0	8	6	10	13	7	64
Monomethyl MTTC (**XVIIa**)	1	2	2	2	2	2	0
Dimethyl MTTC (**XVIIb**)	12	10	10	11	12	12	9
Trimethyl MTTC (**XVIIc**)	24	30	27	33	33	33	17
Pr/Ph	0.2	0.4	0.5	0.2	0.7	0.6	0.6
Chroman ratio	0.7	0.7	0.7	0.7	0.7	0.7	0.6
CPI	0.9	0.9	0.7	0.9	0.8	0.9	1.0

et al., 1986). No attempt was made to study the isomer distributions of the alkylsulphides with linear carbon skeletons, because the complex mass spectral fragmentation behaviour of these compounds, whose isomers almost coelute, makes it difficult to determine relative amounts of different isomers (Sinninghe Damsté *et al.*, 1987c). Instead, the A4 fractions were desulphurised to enable quantitation of carbon skeletons. However, several alkylsulphides with cyclic carbon skeletons were directly identified in the A4 fraction. Absolute amounts of selected carbon skeletons in the A4 fraction of the original sample and the artificially matured samples are given in Table 4.5. Absolute amounts of alkylsulphoxides, which are believed to be formed from alkylsulphides by post-depositional oxidation or by oxidation during sample storage (Payzant et al., 1983; Kohnen *et al.*, 1990b; Schouten *et al.*, 1995e), are included in the amounts listed in Table 4.5. The analysis of the alkylsulphoxides is briefly discussed in the next section.

The desulphurised A4 fraction of the original sample consists mainly of Ph and *n*-alkanes with a strong even-over-odd carbon number predominance (CPI_{24-34} = 0.4; Fig. 4.3**d**), and, in fact, strongly resembles the desulphurised A2 fraction (Fig. 4.3**b**). Small amounts of nor-pristane, Pr, 9-methyloctadecane, HBI C_{25} and hopanes dominated by the 17α,21β(H) C_{35} isomers are also present. Steranes are present in low amounts, and

Table 4.5. Absolute amounts (μg/g TOC of original rock) of selected carbon skeletons in the A4 fraction and the reduced alkylsulphoxide fraction as a function of maturation temperature. Also indicated is the Pr/Ph ratio. Roman numbers refer to structures in the Appendix.

	original	200°C	220°C	240°C	260°C	280°C	300°C
n-C_{18}	$3.7x10^2$	$4.0x10^2$	$5.6x10^2$	$3.2x10^2$	$3.0x10^2$	$1.9x10^2$	$1.6x10^2$
n-C_{28}	$9.9x10^2$	$1.5x10^3$	$1.8x10^3$	$1.1x10^3$	$1.0x10^3$	$4.5x10^2$	$2.8x10^2$
n-C_{38}	$1.7x10^2$	$2.7x10^2$	$2.6x10^2$	$1.2x10^2$	$1.7x10^2$	53	37
9-methyloctadecane	19	13	17	14	14	4	2
Pr	49	38	59	32	41	35	34
Ph	$3.7x10^2$	$3.1x10^2$	$4.1x10^2$	$2.0x10^2$	$2.4x10^2$	$1.4x10^2$	$1.0x10^2$
HBI C_{25}	44	34	47	18	16	28	15
(20R)-5α,14α,17α(H) C_{29} sterane	9	27	26	10	20	19	5
Pregnane (**I**)	0	0	0	0	1	1	0
17α,21β(H) C_{35} hopanes	$2.0x10^2$	$1.4x10^2$	$1.4x10^2$	78	$1.3x10^2$	28	12
C_{23} tricyclic terpane	10	14	18	3	17	27	9
Gammacerane (**II**)	2	7	3	2	4	1	0
Pr/Ph	0.1	0.1	0.1	0.2	0.2	0.3	0.3

their distribution differs from that in the A1 fraction in that (20R)- and (20S)-5α,14β,17β(H) steranes are relatively more abundant (cf. Fig. 4.5**a**). The C_{23} tetracyclic terpenoid sulphide **XXIV**, first identified by Payzant *et al.* (1983, 1988), is present in small amounts in the A4 fraction. Four compounds with unidentified C_{15}, C_{20}, C_{25} and C_{30} skeletons were recognised by mass spectrometry as polycyclic alkylsulphides. Their mass spectra show a major fragment ion at m/z 169, and each compound occurs as a 1:1 doublet in the m/z 169 mass chromatogram (not shown).

When the sample is heated up to 220°C, the amounts of alkylsulphides with linear carbon skeletons increase significantly (Table 4.5). This is in sharp contrast with the results obtained for the A1 and desulphurised A2 fractions, where the amounts of compounds with linear carbon skeletons strongly increase only at 260-300°C. Moreover, while the concentrations in the A1 and desulphurised A2 fractions increase continuously until 300°C (Tables 4.1 and 4.3), the generation profiles of the alkylsulphides reach a maximum at 220°C after which they decrease (Table 4.5). This indicates that alkylsulphides are not stable under the conditions used, and may suggest the transformation of alkylsulphides to alkylthiophenes. Interestingly, quite different results were obtained for artificially matured samples from the Gessoso-solfifera Formation (Koopmans *et al.*, 1996b), where the alkylsulphide and alkylthiophene generation profiles were largely co-variant and no indications were found for a conversion of alkylsulphides to alkylthiophenes.

Polar fraction

The polar fraction contains sulphur-rich macromolecular aggregates as well as low-molecular-weight (LMW) alkylsulphoxides. To separate these two, in order to make a distinction between sulphur cross-linked carbon skeletons and oxidised alkylsulphides, the polar fractions were first reduced with $LiAlH_4$. Two fractions (reduced sulphoxide and residual polar fraction) were then obtained by column chromatography, which were both desulphurised and will now be discussed.

Reduced alkylsulphoxide fraction

Like the A4 fractions, the reduced alkylsulphoxide fractions were desulphurised to enable quantitation of carbon skeletons. The desulphurised reduced alkylsulphoxide fraction of the original sample (Fig. 4.10**a**) is similar in composition to the desulphurised A4 fraction (Fig. 4.3**d**), which confirms their common origin. Absolute amounts of selected carbon skeletons in the desulphurised reduced alkylsulphoxide fraction of the original sample and the artificially matured samples, together with the absolute amounts of these carbon skeletons in the A4 fractions, are listed in Table 4.5.

Residual polar fraction

Absolute amounts of selected carbon skeletons in the desulphurised residual polar fraction are listed in Table 4.6.

The original sample is dominated by Ph and *n*-alkanes with a moderate even-over-odd carbon number predominance ($CPI_{24\text{-}34}$ = 0.6; Fig. 4.10**b**). In addition, smaller amounts of nor-pristane, Pr, 9-methyloctadecane, HBI C_{25}, squalane, (20R)-5α,14α, 17α(H) and (20R)- and (20S)-5α,14β,17β(H) C_{27}-C_{29} steranes, hopanes dominated by the 17α,21β(H) C_{35} isomers, tricyclic terpanes dominated by the C_{23} isomers, and gammacerane are present.

With increasing thermal maturation, the amounts of these carbon skeletons first decrease, but at 260°C they increase again to reach a maximum at 280°C (Table 4.6). This is hard to understand in the light of the weakness of the C-S bond (300 kJ/mol) compared to the C-C bond (370 kJ/mol; Claxton *et al.*, 1993), which is expected to lead to more or less continuously decreasing amounts of sulphur-bound carbon skeletons in the polar fraction. In a study of a maturation series of a sample from the Gessoso-solfifera Formation, the amounts of most sulphur-bound carbon skeletons in the polar fraction were relatively constant with increasing thermal maturation (Koopmans *et al.*, 1996b), which was ascribed to the 'intermediate' character of the polar fraction: it is filled with sulphur-rich macromolecular aggregates from thermal breakdown of the kerogen, and simultaneously releases free hydrocarbons due to thermal cleavage of C-S bonds. The amounts of some carbon skeletons even increased in the polar fraction, but this was invariably the case only at relatively low temperatures for carbon skeletons whose precursors contain multiple functionalities (Koopmans *et al.*, 1996b). A problem

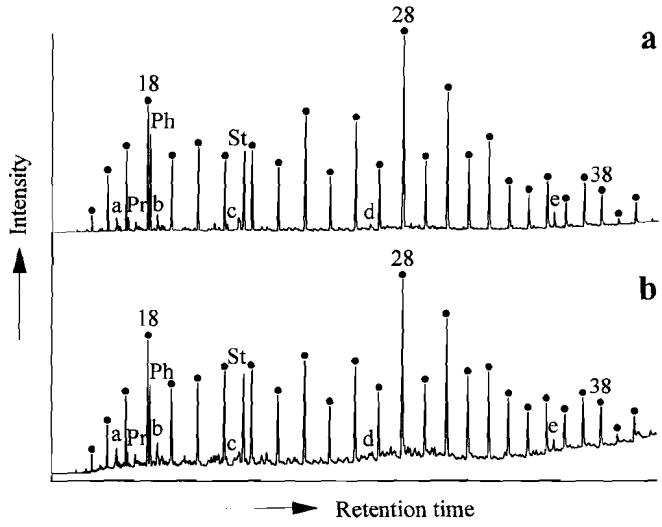

Fig. 4.10. TIC of (**a**) the desulphurised reduced sulphoxide fraction and (**b**) the desulphurised residual polar fraction. Key: dots = *n*-alkanes (numbers indicate number of carbon atoms), Pr = pristane, Ph = phytane, St = standard, a = nor-pristane, b = 9-methyloctadecane, c = HBI C_{25}, d = squalane, e = (22R)-17α,21β(H) C_{35} hopane.

with the $LiAlH_4$ reduction of the polar fraction, which might leave alkylsulphoxides unreduced and thus in the residual polar fraction, is not very likely because the generation profiles are generally very smooth (*e.g.* *n*-C_{28}; Table 4.6).

Carbon skeleton speciation as a function of maturation temperature

Now that the absolute amounts of a selection of carbon skeletons in all fractions studied as a function of maturation temperature are known, their relative amounts can be calculated in order to determine which compound classes are thermally stable and which are not. Linear, branched and cyclic carbon skeletons are discussed below. Alkylsulphides will be presented as a combined fraction (*i.e.* alkylsulphides present as such and as alkylsulphoxides; cf. Table 4.5).

Linear carbon skeletons

The summed amount of *n*-C_{18} skeletons is relatively constant at low maturation temperatures and increases significantly only at 260°C. At 300°C it amounts to *c.* 2.5 mg/g TOC of original rock (Table 4.7). The relative amount of the *n*-C_{18} skeleton in all fractions is shown in Fig. 4.11**a**. In the original sample, it is mainly present in the form of alkylsulphides (crosses). With increasing thermal maturation, the relative amount of

Table 4.6. Absolute amounts (μg/g TOC of original rock) of selected carbon skeletons in the desulphurised residual polar fraction of the original sample and the artificially matured samples. Also indicated are the Pr/Ph ratio and the CPI. Roman numbers refer to structures in the Appendix.

	original	200°C	220°C	240°C	260°C	280°C	300°C
n-C_{18}	$1.1x10^2$	$1.1x10^2$	56	45	83	$2.7x10^2$	$1.7x10^2$
n-C_{28}	$2.9x10^2$	$2.0x10^2$	96	92	$1.8x10^2$	$7.2x10^2$	$2.5x10^2$
n-C_{38}	71	61	32	33	68	$1.5x10^2$	$1.4x10^2$
9-methyloctadecane	9	5	2	1	4	4	0
Pr	12	13	6	5	10	39	32
Ph	72	49	22	17	36	$1.3x10^2$	70
HBI C_{25}	5	0	0	0	3	0	0
(20R)-5α,14α,17α(H) C_{29} sterane	13	21	11	6	7	5	0
Pregnane (**I**)	1	0	0	0	1	0	0
17α,21β(H) C_{35} hopanes	50	19	7	4	27	37	0
C_{23} tricyclic terpane	6	0	0	0	3	3	0
Gammacerane (**II**)	8	0	0	0	4	0	0
Pr/Ph	0.2	0.3	0.3	0.3	0.3	0.3	0.5
CPI	0.6	0.7	0.8	0.8	0.6	0.6	0.7

alkylsulphides decreases, suggesting that this form of the *n*-C_{18} skeleton is thermally unstable. On the other hand, the relative amounts of the free hydrocarbon (diamonds), alkylthiophenes (squares) and alkylbenzo[*b*]thiophenes (dots) increase, suggesting that these forms are thermally stable. Saturated hydrocarbons and alkylthiophenes have been noted before as thermally stable compound classes under hydrous pyrolysis conditions (Koopmans *et al.*, 1995, 1996b, 1997b).

The *n*-C_{28} skeleton is by far the most abundant carbon skeleton in the extract of the original sample (*c.* 1.6 mg/g TOC; Table 4.7). Its summed amount increases already at low temperatures, and at 280°C it is *c.* 3.1 mg/g TOC of original rock. The relative amounts of the *n*-C_{28} skeleton in the alkylsulphide, saturated hydrocarbon and alkylthiophene fractions show similar changes with maturation temperature as the *n*-C_{18} skeleton (cf. Figs. 4.11**a** and **b**).

The distributions of the *n*-alkanes in all fractions of the original sample show slightly increased amounts of the C_{37} and C_{38} components compared to the other long-chain *n*-alkanes in the C_{35}-C_{40} region (Figs. 4.3 and 4.10). This carbon number distribution suggests an origin for these skeletons from *n*-C_{37} and *n*-C_{38} di- and tri-unsaturated ketones (alkenones) biosynthesised by several Prymnesiophyte algae, as was concluded previously for a sample from the related Jurf ed Darawish oil shale (Sinninghe Damsté *et al.*, 1988b, 1989c; Kohnen *et al.*, 1990c). Recently, the speciation of the *n*-C_{37} and *n*-C_{38} skeletons in an artificial maturation series of a sample from the Gessoso-solfifera

Formation was discussed in detail (Koopmans *et al.*, 1997b). It appeared that, due to the reaction of reduced inorganic sulphur species with the multiple functionalities of the alkenones, these compounds became sulphur-bound in the kerogen so that *n*-C_{37} and *n*-C_{38} skeletons could not be detected in the extract of the original sample. After mild thermal treatment, the amounts of these skeletons in the polar fraction increased, due to thermal breakdown of sulphur-linked moieties in the kerogen. After heating at higher temperatures, the *n*-C_{37} and *n*-C_{38} skeletons were released as free hydrocarbons, alkylthiophenes and saturated ketones, which were shown to be stable thermal degradation products (Koopmans *et al.*, 1997b). In the sample under study, these effects are not observed. First, in the extract of the original sample *n*-C_{38} skeletons are already present, amounting to *c.* 0.29 mg/g TOC (Table 4.7), which may be due to the higher level of thermal maturity of the sample from the Ghareb Formation (R_o = 0.39%) compared to the sample from the Gessoso-solfifera Formation (R_o = 0.25%). Second, the relative amount of the desulphurised residual polar fraction (double crosses; Fig. 4.11**c**) follows a different trend, decreasing at low and increasing at high maturation temperatures. Third, the production of the free hydrocarbon (diamonds) is marginal, amounting to 3% at 300°C (Fig. 4.11**c**), whereas in the case of the sample from the Gessoso-solfifera Formation the free hydrocarbon represented 36% at 300 and 52% at 330°C (Koopmans *et al.*, 1997b). Fourth, the production of the alkylthiophenes (squares) is significant in the sample under study (53% at 300°C; Fig. 4.11**c**), whereas it was marginal in the sample from the Gessoso-solfifera Formation. Thus, while artificial maturation of sulphur-rich organic matter in the sample from the Gessoso-solfifera Formation produces mainly C_{38} *n*-alkanes, in the sample from the Ghareb Formation it produces mainly C_{38} *n*-alkylthiophenes. One obvious difference between the samples is the presence of abundant oxygen-linked *n*-C_{38} skeletons in the sample from the Gessoso-solfifera Formation (Koopmans *et al.*, 1997b), although it is not clear how this would influence the formation of alkanes *vs.* alkylthiophenes. In fact, the relative amount of the *n*-C_{38} skeleton in all fractions changes with maturation temperature in a similar fashion as the *n*-C_{18} and *n*-C_{28} skeletons. Thus, there is no indication from these relative generation profiles that these linear carbon skeletons have dissimilar precursors.

Branched carbon skeletons

The exact origin of the acyclic isoprenoids Pr and Ph is still controversial. Apart from the classical viewpoint that chlorophyll *a* is their precursor (see for a review Volkman and Maxwell, 1986), several other precursors have been suggested, *i.e.* bound tocopherols (Goossens *et al.*, 1984) and bound methylated MTTCs (Li *et al.*, 1995) as precursors of Pr, and archaebacterial ether lipids as precursors of both Pr and Ph (*e.g.* Risatti *et al.*, 1984; Rowland, 1990; Navale, 1994). In a combined thermal and chemical degradation approach to decipher Pr and Ph precursors in sedimentary organic matter, Koopmans *et al.* (1997c) identified free and bound (archaebacterial) diphytanyl glyceryl ether and sulphur-bound Ph (probably originating from phytol) as precursors of free Ph

Table 4.7. Summed absolute amounts (μg/g TOC of original rock) of selected carbon skeletons in all fractions as a function of maturation temperature. Roman numbers refer to structures in the Appendix.

	original	200°C	220°C	240°C	260°C	280°C	300°C
n-C_{18}[a]	$6.6x10^2$	$7.7x10^2$	$9.3x10^2$	$7.7x10^2$	$1.2x10^3$	$1.7x10^3$	$2.5x10^3$
n-C_{28}	$1.6x10^3$	$2.2x10^3$	$2.7x10^3$	$2.0x10^3$	$3.0x10^3$	$3.1x10^3$	$2.9x10^3$
n-C_{38}	$2.9x10^2$	$4.2x10^2$	$4.2x10^2$	$2.8x10^2$	$4.4x10^2$	$4.4x10^2$	$5.1x10^2$
9-methyloctadecane	40	31	36	38	54	55	60
Pr	$1.2x10^2$	$1.3x10^2$	$1.6x10^2$	$1.2x10^2$	$3.2x10^2$	$5.9x10^2$	$1.1x10^3$
Ph	$7.2x10^2$	$6.7x10^2$	$7.7x10^2$	$6.1x10^2$	$8.3x10^2$	$1.0x10^3$	$1.2x10^3$
HBI C_{25}	$1.3x10^2$	$1.0x10^2$	$1.2x10^2$	$1.2x10^2$	$1.1x10^2$	$1.7x10^2$	$1.2x10^2$
(20R)-5α,14α,17α(H) C_{29} sterane	50	$1.2x10^2$	$1.4x10^2$	$1.7x10^2$	$3.5x10^2$	$4.2x10^2$	$1.8x10^2$
17α,21β(H) C_{35} hopanes	$3.4x10^2$	$2.5x10^2$	$2.8x10^2$	$2.0x10^2$	$3.0x10^2$	$2.4x10^2$	$1.2x10^2$
Gammacerane (**II**)	16	37	53	77	$2.1x10^2$	$2.7x10^2$	$2.2x10^2$

[a] Includes C_{10} alkylated benzo[*b*]thiophenes (see Table 4.3).

formed in high amounts upon artificial maturation of a sample from the Gessoso-solfifera Formation. However, in the Green River Shale the precursor of free Ph could not be identified, although Ph is among the most abundant hydrocarbons (up to 2.4 mg/g TOC) in the artificially matured samples.

The generation profile of the summed amount of the Pr carbon skeleton is rather similar to that of the *n*-C_{18} skeleton (Table 4.7). However, at 260-300°C the summed amount of the Pr carbon skeleton increases at a higher rate. The relative amount of the Pr carbon skeleton in all fractions changes similarly with maturation temperature as the linear carbon skeletons: at high temperatures, the free hydrocarbon (diamonds) and, to a lesser extent, the alkylthiophenes (squares) are thermally stable (Fig. 4.11**d**). These results are in sharp contrast with those previously reported for an artificial maturation series of a sample from the Gessoso-solfifera Formation (Koopmans *et al.*, 1996b), where the Pr carbon skeleton was almost exclusively found as free hydrocarbon. This was taken as an indication that bound tocopherols and archaebacterial ether lipids were the major precursors of Pr. Clearly, in the Ghareb Formation sulphur-bound Pr, possibly originating from pristenes, pristadienes and pristatrienes known to occur in zooplankton (Blumer and Thomas, 1965; Blumer *et al.*, 1969), plays an important role as well.

The generation profile of the Ph carbon skeleton covaries with that of the Pr carbon skeleton (Table 4.7). However, when Pr and Ph are produced at 260-300°C, Ph is produced at a lower rate, hence the increasing Pr/Ph ratios in all fractions. Again, the relative amount of the Ph carbon skeleton as a function of maturation temperature indicates that the free hydrocarbon (diamonds) and the alkylthiophenes (squares) are thermally stable (Fig. 4.11**e**).

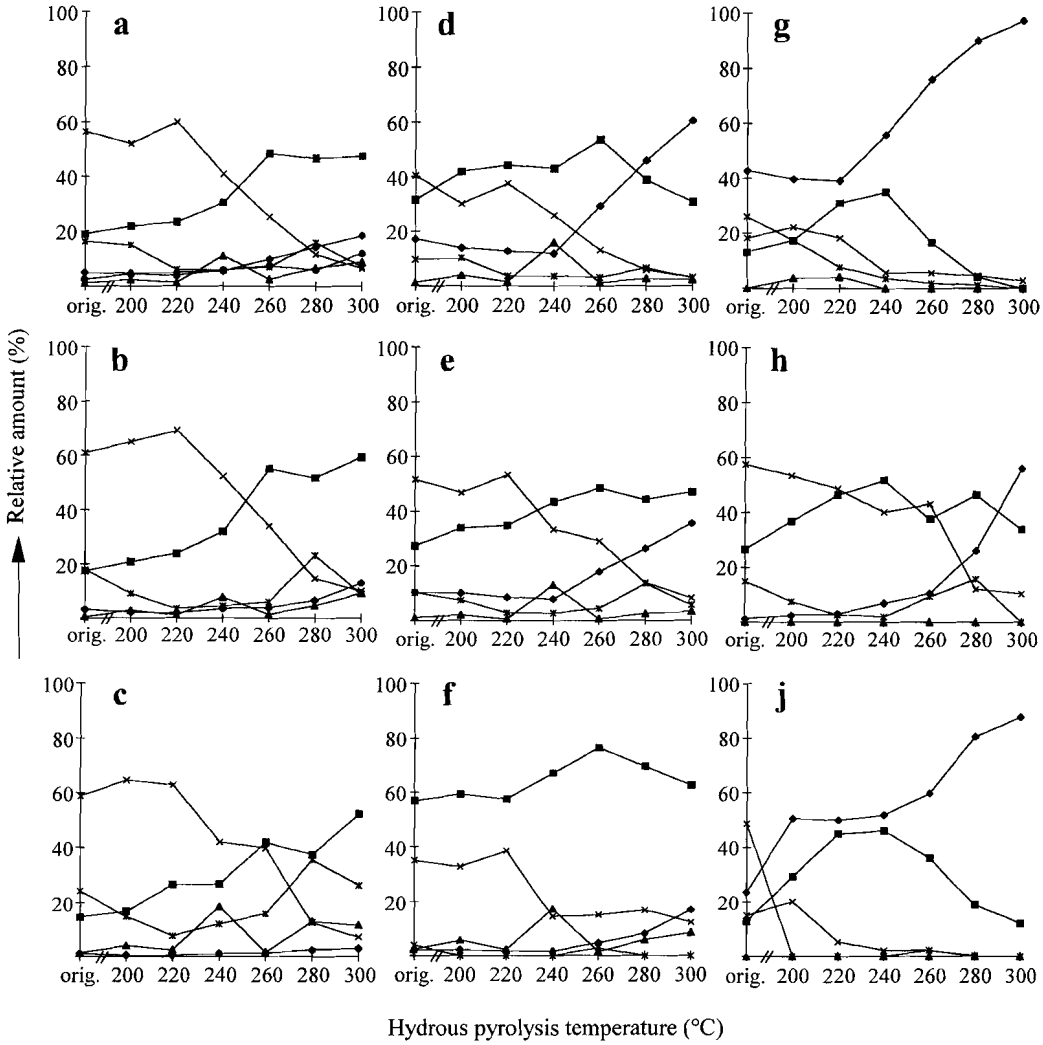

Fig. 4.11. Relative amounts (%) of the carbon skeletons of (**a**) *n*-C_{18} (**b**) *n*-C_{28}, (**c**) *n*-C_{38}, (**d**) Pr, (**e**) Ph, (**f**) HBI C_{25} (**g**), (20R)-5α,14α,17α(H) C_{29} sterane, (**h**) (22R)-17α,21β(H) C_{35} hopane, and (**j**) gammacerane in the A1 fraction (diamonds), A2 fraction (squares), A3 fraction (triangles), A4 plus reduced alkylsulphoxide fraction (cf. Table 4.5; crosses), and desulphurised residual polar fraction (double crosses). Alkylbenzo[*b*]thiophenes in (**a**) are represented by dots.

The HBI C_{25} skeleton differs from the other acyclic carbon skeletons in that its summed amount remains relatively constant throughout the maturation series (Table 4.7). This may be an indication that the HBI C_{25} skeleton is not sequestered in the

kerogen from which it can be thermally released. This would then suggest that the changes in the relative amount of the HBI C_{25} skeleton in different fractions with maturation temperature are due to interconversion of different forms of this carbon skeleton. The alkylthiophenes (squares) are much more abundant at high temperatures than the other forms (Fig. 4.11**f**), although they do not seem to be particularly stable.

Cyclic carbon skeletons

The (20R)-5α,14α,17α(H) C_{29} sterane skeleton is taken as representative for all C_{27}-C_{29} steranes, because it is typically one of the most abundant isomers in all fractions. Its summed amount increases to *c.* 0.42 mg/g TOC of original rock at 280°C, after which it decreases to become *c.* 0.18 mg/g TOC of original rock at 300°C (Table 4.7). This may reflect the intrinsic lability of the sterane carbon skeleton, which contains two quaternary and at least seven tertiary carbon atoms, making the bonds with the secondary carbon atoms relatively weak. The question remains what are the sterane degradation products. The absolute amount of the pregnanes in the A1 fraction is doubled between 280 and 300°C (Table 4.1). This would argue against the reasoning that the relatively high amount of labile bonds in the sterane carbon skeleton causes its degradation, because the pregnane skeleton also contains these weak bonds and is not degraded. However, pregnanes may themselves be thermal degradation products of steranes by cleavage of C-C bonds in the sterane side chain. This cleavage may be enhanced by cross-linking of the sterane carbon skeleton *via* the side chain, which may weaken the C-C bonds in the side chain. Chemical degradation of the kerogen of the related Jurf ed Darawish oil shale using $Li/EtND_2$ indicated that the steranes were sulphur-linked *via* the A-ring and the side chain (Hofmann *et al.*, 1992). However, thermal degradation of steranes that are sulphur-linked in the side chain should also yield steroid thiophenes, which were not observed. Moreover, decreasing summed amounts of steranes in an artificial maturation series of a sample from the Gessoso-solfifera Formation were not accompanied by increasing amounts of pregnanes (Koopmans *et al.*, 1996b). Therefore, it seems not very likely that pregnanes are thermal degradation products of (bound) steranes. An alternative 'degradation' pathway of the sterane carbon skeleton may be aromatisation of the ring system.

Fig. 4.11**g** shows the relative amount of the (20R)-5α,14α,17α(H) C_{29} sterane skeleton as a function of maturation temperature. The free hydrocarbon (diamonds) is the only stable form at high temperatures, approaching 100%. At temperatures lower than 240°C, both steranes (diamonds) and Δ^2 sterenes (squares) are formed, whereas at higher temperatures mainly steranes are formed. This may indicate that the formation of Δ^2 sterenes, supposedly from thermal degradation of sterane skeletons sulphur-bound *via* C-3 in HMW fractions (cf. Adam *et al.*, 1991; Kohnen *et al.*, 1993), is only favourable at relatively low temperatures. Apparently, the quenching of radical sites (formed by thermal cleavage of C-S bonds) by water-derived hydrogen (Lewan, 1997) is more efficient at higher temperatures.

The carbon number distribution, speciation and 22S/22R isomer ratios of the extended hopanes as a function of maturation temperature have recently been discussed in detail by Köster *et al.* (1997). Here, we will focus on the fate of the (22S)- and (22R)-17α,21β(H) C_{35} isomers. The summed amount of the 17α,21β(H) C_{35} hopanes in all fractions decreases with increasing maturation temperature (Table 4.7). In the original sample, they are almost exclusively present in a sulphur-bound form (Fig. 4.11**h**). With increasing thermal maturation, the alkylsulphides (crosses) are not stable, whereas the free hydrocarbons (diamonds) are. The fate of the alkylthiophenes (squares) is not clear, but at high temperatures they seem relatively stable at 40%. These generation profiles are similar to those of the *n*-alkanes, but quite different from those of the steranes. The reason for this is probably that hopanes, like *n*-alkanes, easily form LMW OSC with sulphide and thiophene moieties in the side chain, whereas steranes do not.

Gammacerane (**II**) is present only in low amounts in the extract of the original sample (Table 4.7). Upon heating, large amounts of gammacerane are formed from thermal degradation of a HMW fraction (Table 4.7). Li/$EtNH_2$ desulphurisation of the kerogen from the related Jurf ed Darawish oil shale released relatively large amounts of gammacerane (Hofmann *et al.*, 1992), suggesting that sulphur-bound gammacerane in the kerogen, formed by natural sulphurisation of tetrahymanol (**XXV**) or its diagenetic products (Richnow *et al.*, 1993; Sinninghe Damsté *et al.*, 1995c), may be the source of gammacerane in the extract at higher temperatures. The relative amount of the gammacerane carbon skeleton in different fractions (Fig. 4.11**j**) changes with maturation temperature in a similar fashion as the (20R)-5α,14α,17α(H) C_{29} sterane skeleton (Fig. 4.11**g**): at temperatures lower than 240°C gammacerane (diamonds) and gammacer-2-ene (squares) are formed, but at higher temperatures gammacerane prevails. These similar relative generation profiles are probably due to the identical mode of bonding (sulphur-bound at C-3; cf. Adam *et al.*, 1993) of the (20R)-5α,14α,17α(H) C_{29} sterane and gammacerane carbon skeletons in HMW fractions.

Tricyclic terpanes are thought to be derived from biochemical cyclisation of C_{30} or C_{40} polyprenols present in prokaryotic membranes (Ourisson *et al.*, 1982; Aquino Neto *et al.*, 1983). They have also been found in the extracts and kerogen pyrolysates of tasmanite oil shales (*e.g.* Philp *et al.*, 1982; McCaffrey *et al.*, 1994; Revill *et al.*, 1994). They are omnipresent in crude oils with the C_{23} isomers usually being dominant (Aquino Neto *et al.*, 1983). In this study, C_{19}-C_{26} tricyclic terpanes were identified in the A1 fraction and the desulphurised A4, reduced alkylsulphoxide and residual polar fractions, with different carbon number distributions. In the A1 fraction, the 13α(H),14β(H) C_{20} component (**III**) is the dominant isomer (peak denoted c in Fig. 4.7), whereas in the desulphurised A4, reduced alkylsulphoxide and residual polar fractions the C_{23} components are the most abundant. The generation profile of 13α(H),14β(H) C_{20} tricyclic terpane in the A1 fraction shows increasing amounts at 260-300°C (Table 4.1), whereas the amounts of sulphur-bound and sulphur-containing C_{23} tricyclic terpane in the other three fractions are relatively constant with increasing maturation temperature (Tables

4.5 and 4.6). The different generation profiles and carbon number distributions of the tricyclic terpanes in the A1 fraction on the one hand and the desulphurised A4, reduced alkylsulphoxide and residual polar fractions on the other suggest that they have different precursors.

Comparison with natural samples and other artificial maturation series

In order to be able to compare these results with other naturally and artificially matured samples, the level of thermal maturity of the Ghareb maturation series should be determined. The original, unheated rock has an estimated vitrinite reflectance value of 0.39% R_o (Koopmans *et al.*, 1997c). The vitrinite reflectance values of the artificially matured samples can be estimated by comparing several biomarker maturity parameter ratios. The 17β,21α(H)/[17α,21β(H)+17β,21α(H)] C_{30} hopane ratio, which has an equilibrium value of *c.* 0.05 representing a vitrinite reflectance value of *c.* 0.7% R_o (Mackenzie *et al.*, 1980; Seifert and Moldowan, 1980; Peters and Moldowan, 1993), is constant at *c.* 0.15 in the maturity range covered. This may indicate that the equilibrium value has yet to be reached, and thus that $R_o < 0.7\%$ for the sample heated at 300°C. The 22S/(22S+22R)-17α,21β(H) C_{35} hopane ratio, which has an equilibrium value of *c.* 0.6 representing a vitrinite reflectance value of *c.* 0.6% R_o (Mackenzie, 1984; Seifert and Moldowan, 1986; Peters and Moldowan, 1993), increases from 0.49 in the original sample to 0.59 at 300°C. The 20S/(20S+20R)-5α,14α,17α(H) C_{29} sterane ratio, which has an equilibrium value of *c.* 0.55 representing a vitrinite reflectance value of *c.* 0.8% R_o (Seifert and Moldowan, 1986; Peters and Moldowan, 1993), increases from 0.03 in the original sample to 0.50 at 300°C (Fig. 4.6). These data suggest that the sample heated at 300°C has a vitrinite reflectance value of $0.6\% \leq R_o < 0.7\%$. Therefore, the hydrous pyrolysis experiments at temperatures of 200-300°C (72h) represent a relatively narrow maturity interval of *c.* 0.4 to 0.6-0.7% R_o.

The original sample contains immature Type II-S kerogen with an atomic S_{org}/C ratio of 0.07. The amount of organic sulphur is comparable to that of a sample from the Gessoso-solfifera Formation (S_{org}/C ratio = 0.08) which has previously been the subject of artificial maturation studies (Koopmans *et al.*, 1995, 1996b, 1997b). However, the latter sample is less mature (R_o = 0.25%) and contains abundant S-S linked carbon skeletons (Koopmans *et al.*, 1996b). Artificial maturation of this sample at relatively low temperatures (T < 300°C), corresponding to vitrinite reflectance values of < 0.4% R_o, resulted in cleavage of these weak S-S bonds (Koopmans *et al.*, 1996b). The sample from the Ghareb Formation contains only small amounts of S-S linked carbon skeletons, which seems to be in agreement with its estimated vitrinite reflectance value of 0.39% R_o. Consequently, the similarity of the S_{org}/C ratios of both samples suggests that the sample from the Ghareb Formation contains a larger amount of C-S links per carbon skeleton. This seems to be in agreement with the increasing amount of extractable organic matter with increasing thermal maturation (Fig. 4.2). A kerogen consisting of highly

sulphur cross-linked LMW carbon skeletons will thermally degrade at relatively low temperature to LMW (= soluble) organic matter through cleavage of relatively weak C-S bonds. The different nature and amount of sulphide links of the samples from the Ghareb and Gessoso-solfifera Formations may explain the different thermal behaviour of the sulphide-linked carbon skeletons in these samples. In the Ghareb Formation acyclic carbon skeletons are predominantly released as alkylthiophenes (Fig. 4.11), whereas in the Gessoso-solfifera Formation they are predominantly released as alkanes (Koopmans *et al.*, 1996b). Evidence is accumulating that alkylthiophenes are formed as thermally stable compounds from thermal degradation of (poly)sulphide-linked carbon skeletons (Krein and Aizenshtat, 1994, 1995; Schouten *et al.*, 1994; Aizenshtat *et al.*, 1995; Koopmans *et al.*, 1995, 1996b). Thus, it seems likely that a carbon skeleton linked by a larger amount of C-S bonds has a greater chance to be thermally transformed to an alkylthiophene. This is in agreement with the observations for the samples from the Ghareb and Gessoso-solfifera Formations.

Artificial maturation of the sample from the Ghareb Formation results in the formation of abundant alkylbenzo[*b*]thiophenes and, to a lesser extent, alkyldibenzothiophenes (Tables 4.3 and 4.4). These compounds were not detected in the artificial maturation series of the sample from the Gessoso-solfifera Formation, which may be due to the lower level of thermal maturity covered by those experiments ($0.25\% \leq R_o < 0.6\%$; Koopmans *et al.*, 1996b), although the small difference in the maturity range of the two samples does not make this a likely possibility. Rather, the abundant formation of alkylthiophenes, which are the presumed precursors of alkylbenzo[*b*]thiophenes and alkyldibenzothiophenes (Sinninghe Damsté *et al.*, 1989a), in the sample from the Ghareb Formation compared to the relatively meagre formation of alkylthiophenes in the sample from the Gessoso-solfifera Formation may explain the abundance of alkylbenzo[*b*]-thiophenes and alkyldibenzothiophenes in the former. Benzo[*b*]thiophenes and dibenzothiophenes are major compounds in natural crude oils (Ho *et al.*, 1974), so it seems that hydrous pyrolysis is indeed simulating the formation of crude oil from immature organic-rich sedimentary rocks (cf. Lewan *et al.*, 1979). This is supported by the 'oil-like' distributions of the *n*-alkanes (*i.e.* a shift to lower carbon numbers and a decreasing CPI) in the A1 and desulphurised A2 and A3 fractions which develop with increasing thermal maturation (cf. Figs. 4.3 and 4.4). The discrepancy between the OSC present in immature sedimentary rocks and crude oils (alkylsulphides and alkylthiophenes) and more mature oils (*e.g.* benzo[*b*]thiophenes and dibenzothiophenes) is still a matter of concern (Sinninghe Damsté *et al.*, 1989a; Sinninghe Damsté and de Leeuw, 1990). This discrepancy has been explained by the formation of benzo[*b*]thiophenes and dibenzothiophenes *via* cyclisation and aromatisation of the alkyl side chains of alkylthiophenes present as free compounds or bound in the kerogen (Sinninghe Damsté *et al.*, 1989a), although the exact mechanism of this reaction is still unknown (Aizenshtat *et al.*, 1995). The maturity set under study is potentially valuable in this respect, because it allows the quantitative analysis of both precursors (alkylthiophenes) and products (benzo[*b*]thio-

phenes and dibenzothiophenes) of this reaction. However, the relative amounts of the alkylthiophenes and alkylbenzo[*b*]thiophenes with *e.g.* the *n*-C_{18} skeleton both increase with increasing maturation temperature (Fig. 4.11**a**), suggesting that both are thermally stable under the conditions used, and showing no indication that one is converted into the other. It seems that higher experimental temperatures are required to study this reaction. Samples from the Ghareb Formation that were heated for 72h at temperatures between 300 and 365°C are presently under study.

4.5 Conclusions

Hydrous pyrolysis experiments (200-300°C; 72h) with an immature sulphur- and organic-rich limestone from the Ghareb Formation represent a relatively narrow maturity interval (R_o = 0.4 to 0.6-0.7%). Quantitative analysis of the heated samples indicates that large changes in abundance and distribution of carbon skeletons occur under these conditions.

In the original sample, *n*-alkane carbon skeleton distributions are dominated by odd *n*-alkanes in the free hydrocarbon fraction and even *n*-alkanes in sulphur-containing fractions. With increasing maturation temperature, the *n*-alkane distributions become rather smooth due to the generation of even as well as odd *n*-alkane carbon skeletons. Short-chain *n*-alkane carbon skeletons are produced in higher amounts than long-chain *n*-alkane carbon skeletons, resulting in 'oil-like' distributions. The increase of the 20S/(20S+20R)-5α,14α,17α(H) C_{29} sterane ratio and the 22S/(22S+22R)-17α,21β(H) C_{35} hopane ratio is due to (i) generation of S-isomers from HMW fractions at relatively low maturation temperatures, and (ii) preferential destruction of R-isomers at higher maturation temperatures. No evidence is found for direct conversion of free R- to free S-isomers.

Alkylthiophenes with predominantly linear carbon skeletons are abundant in the original sample. With increasing maturation temperature, alkylthiophenes with linear carbon skeletons are generated in high amounts, which leaves their isomer distributions relatively constant. The use of alkylthiophenes as biomarkers at relatively high levels of thermal maturity is exemplified by the high relative abundance of 2-hexadecyl-5-octylthiophene and 2-nonyl-5-pentadecylthiophene at 300°C, suggesting a octacosa-9,12-diene precursor. The isomer distribution of the alkylthiophenes with a Ph carbon skeleton, expressed as the ITR, changes from 0.07 in the original sample to 0.39 at 300°C. The chroman ratio, however, is constant at 0.7. Desulphurisation of the alkylsulphide fraction and the reduced alkylsulphoxide fraction yields similar hydrocarbon distributions, suggesting that the alkylsulphoxides are formed by oxidation of the alkylsulphides.

The distribution of linear and isoprenoid carbon skeletons over all fractions changes dramatically with maturation temperature. Saturated hydrocarbons, alkylthiophenes and alkylbenzo[*b*]thiophenes are stable with increasing maturation temperature, where-

as alkylsulphides are not. At low maturation temperatures, sterane and gammacerane carbon skeletons are generated partly as alkane and partly as alk-2-ene. At higher temperatures, the alkane is predominantly formed, which may indicate the importance of water as a source of hydrogen at higher temperatures.

The sample from the Ghareb Formation contains only low amounts of polysulphide-bound carbon skeletons. Therefore, the high S_{org}/C ratio suggests a relatively large amount of monosulphide links per carbon skeleton. This may explain the generation of large amounts of alkylthiophenes compared to alkanes. Artificial maturation also results in the generation of large amounts of alkylbenzo[*b*]thiophenes and, to a lesser extent, alkyldibenzothiophenes. To fully understand their possible genetic relationship with alkylthiophenes, samples artificially matured at temperatures higher than 300°C are presently analysed.

4.6 Acknowledgements

We thank Shell International Exploration and Production for providing a research studentship to MPK. The Natural Resources Authority of Jordan is gratefully acknowledged for their assistance in helping the authors collect a sample of the Ghareb Formation from the El Lajjun quarry. GC-MS analyses were carried out by Mrs. M. Dekker and Mr. W. Pool. This work was partly supported by a PIONIER grant to JSSD from the Netherlands Organisation for Scientific Research (NWO).

Appendix

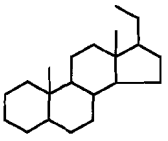

I

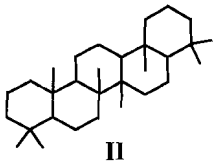

II

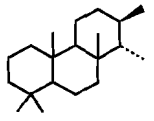

III

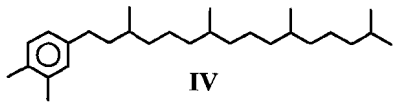

IV

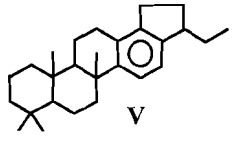

V

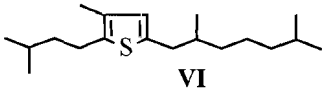

VI

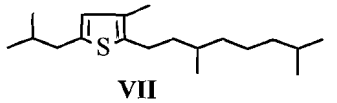

VII

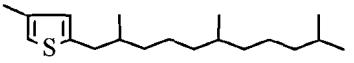

VIII

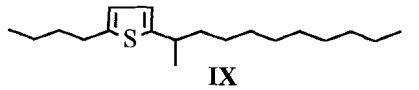

IX

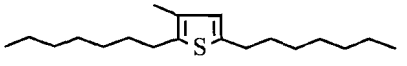

X

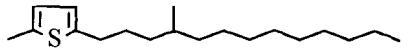

XI

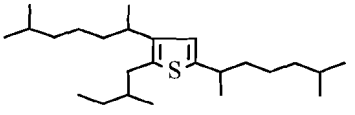

XII

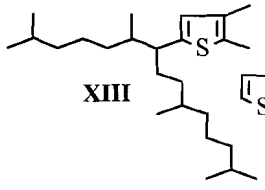

XIII

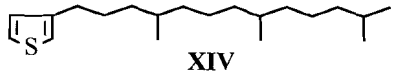

XIV

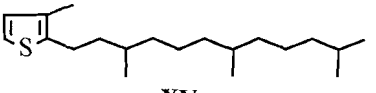

XV

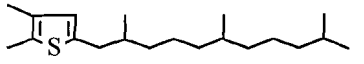

XVI

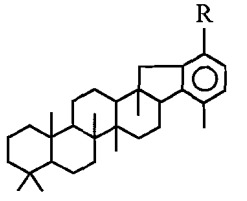

XVIII (R=H, Me, Et, Pr)

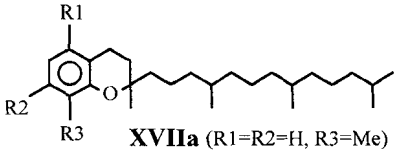

XVIIa (R1=R2=H, R3=Me)
XVIIb (R1=R3=Me, R2=H)
XVIIc (R1=R2=R3=Me)

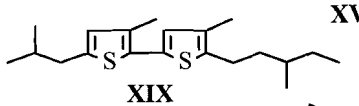

XIX

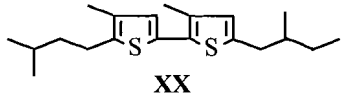

XX

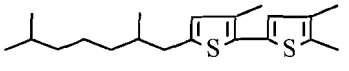

XXI

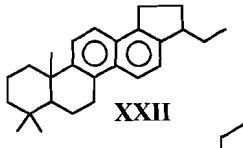

XXII

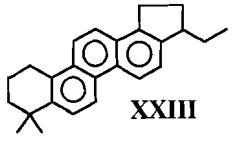

XXIII

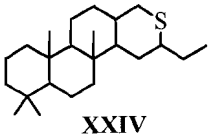

XXIV

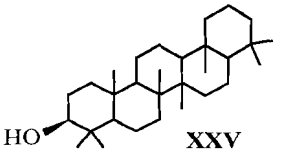

XXV

CHAPTER 5

Sulphur and oxygen sequestration of *n*-C_{37} and *n*-C_{38} unsaturated ketones in an immature kerogen and the release of their carbon skeletons during early stages of thermal maturation

M.P. Koopmans, C. Schaeffer-Reiss, J.W. de Leeuw, M.D. Lewan, J.R. Maxwell, P. Schaeffer and J.S. Sinninghe Damsté

5.1 Abstract

A sedimentary rock from the Gessoso-solfifera Formation (Messinian) in the Vena del Gesso Basin (northern Italy) containing immature (R_o = 0.25%) S-rich organic matter was artificially matured by hydrous pyrolysis at temperatures from 160 to 330°C for 72 h to study the diagenetic fate of *n*-C_{37} and *n*-C_{38} di- and tri-unsaturated methyl and ethyl ketones (alkenones) biosynthesised by several prymnesiophyte algae. During early diagenesis, the alkenones are incorporated into the kerogen by both sulphur and oxygen cross-linking as indicated by chemical degradation experiments with the kerogen of the unheated sample. Heating at temperatures between 160 and 260°C, which still represents early stages of thermal maturation, produces large amounts (up to 1 mg/g TOC) of S-bound, O-bound and both S- and O-bound *n*-C_{37} and *n*-C_{38} skeletons, saturated *n*-C_{37} and *n*-C_{38} methyl, ethyl and mid-chain ketones, C_{37} and C_{38} mid-chain 2,5-di-*n*-alkylthiophenes, C_{37} and C_{38} 1,2-di-*n*-alkylbenzenes, and C_{37} and C_{38} *n*-alkanes. With increasing thermal maturation, three forms of the *n*-C_{37} and *n*-C_{38} skeletons are relatively stable (saturated hydrocarbons, 1,2-di-*n*-alkylbenzenes and saturated ketones), whereas the S- and O-bound skeletons are relatively labile. These results suggest that in natural situations saturated ketones with an *n*-C_{37} and *n*-C_{38} skeleton can be expected as well as the corresponding hydrocarbons.

5.2 Introduction

The use of lipid biomarkers in molecular biogeochemistry as indicators of biological, chemical and physical aspects of ancient depositional environments is mainly restricted to saturated and aromatic hydrocarbons which, in most cases, derive from functionalised precursors (see for a review Peters and Moldowan, 1993). In recent years it has become clear, however, that reaction of reduced inorganic sulphur species with functionalised lipids (natural sulphurisation) during early diagenesis can result in selective sequestration of carbon skeletons into macromolecular fractions, which can bias interpretations of the sedimentary record (*e.g.* Kohnen *et al.* 1991c, 1992a). Therefore, S-bound biomarkers in polar and asphaltene fractions and in kerogen should also be examined to allow more effective conclusions about palaeoenvironmental conditions to be made. Furthermore, specific carbon skeletons can be linked to a macromolecular structure by oxygen bonds (*e.g.* Michaelis and Albrecht, 1979; Chappe *et al.*, 1979; Mycke *et al.*, 1987; Richnow *et al.*, 1992, 1993), although the mechanisms by which such links are formed are not well understood.

Functionalised lipids that are widely used as biomarkers in immature sediments include specific *n*-C_{37} and *n*-C_{38} di- and tri-unsaturated methyl and ethyl ketones (alkenones; Fig. 5.1; Boon *et al.*, 1978; de Leeuw *et al.*, 1980; Volkman *et al.*, 1980a,b; Rechka and Maxwell, 1988a,b). These alkenones, biosynthesised by algae of the family Gephyrocapsaceae belonging to the class Prymnesiophyceae (Marlowe *et al.*, 1984, 1990; Farrimond *et al.*, 1986; Conte *et al.*, 1994; Volkman *et al.*, 1980a,b, 1995), are of particular importance since their relative abundance is directly related to growth temperature (Brassell *et al.*, 1986a,c; Prahl and Wakeham, 1987; Prahl *et al.*, 1988). Hence, numerous studies have inferred palaeo sea surface temperatures from sedimentary al-

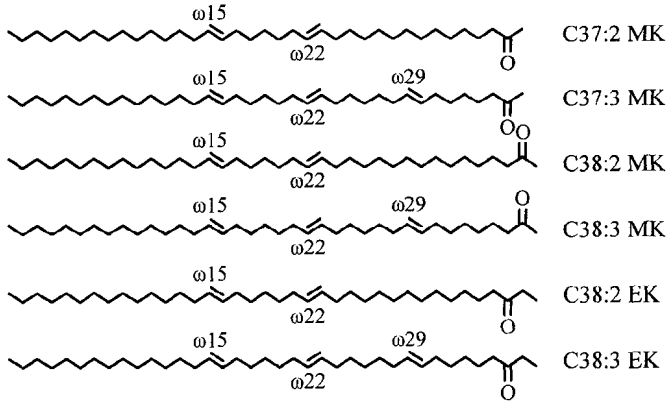

Fig. 5.1. Structures of *n*-C_{37} and *n*-C_{38} di- and tri-unsaturated methyl (MK) and ethyl (EK) ketones with positions of double bonds indicated.

kenone distributions (for a review see Brassell, 1993).

Laboratory sulphurisation experiments with geochemically relevant model compounds have shown that C-C double bonds and carbonyl groups are susceptible to reaction with reduced inorganic sulphur species under relatively mild conditions (de Graaf *et al.*, 1992; Schouten *et al.*, 1993, 1994). Therefore, C_{37} and C_{38} alkenones can be expected to react readily with reduced inorganic sulphur species during early diagenesis. Indeed, there have been several reports on (i) C_{37} and C_{38} cyclic monosulphides and 2,5-di-*n*-alkylthiophenes in immature sedimentary rocks and 'low thermal stress' crude oils (Sinninghe Damsté *et al.*, 1989c, 1990b; Kohnen *et al.*, 1990c; Rullkötter *et al.*, 1990; Barakat and Rullkötter, 1994), (ii) C_{37} and C_{38} *n*-alkanes released after desulphurisation of polar fractions of such samples (Sinninghe Damsté *et al.*, 1988b, 1990a; Rullkötter and Michaelis, 1990; Richnow *et al.*, 1992; Schouten *et al.*, 1993; Hefter *et al.*, 1995), and (iii) C_{37} and C_{38} *n*-alkanes released after desulphurisation of immature kerogens (Schaeffer *et al.*, 1995a). Thus, sulphurisation of alkenones may bias palaeoenvironmental reconstructions.

Here, we report on a 'double bias' in the sedimentary record from sulphur and oxygen sequestration of alkenones in the kerogen. At an early stage of thermal maturation, the *n*-C_{37} and *n*-C_{38} skeletons are released into the polar fraction by thermal cleavage of sulphur and oxygen bonds. With increasing thermal maturation, the *n*-C_{37} and *n*-C_{38} skeletons are released from the polar fraction predominantly as saturated hydrocarbons and saturated ketones, so that the presence of prymnesiophytes in the depositional environment can be recognised.

5.3 Experimental

Sample description. The sample is a marlstone with immature (R_o = 0.25%) organic matter from the Gessoso-solfifera Formation (Messinian) in the Vena del Gesso Basin, Italy. For an extensive description of the geology of the formation, see Vai and Ricci Lucchi (1977). The sample was taken from the marl layer of evaporitic cycle IV (Sinninghe Damsté *et al.*, 1995b). The TOC content is 2.0 wt%. Elemental analysis of the kerogen indicates that it is a Type II-S kerogen with an atomic H/C ratio of 1.44, an atomic O/C ratio of 0.17, and an atomic S_{org}/C ratio of 0.08.

Hydrous pyrolysis. A detailed description of the experimental procedures has been given by Lewan (1993b). A one-litre Hastelloy-C276 reactor was filled with 90 to 100 g of rock chips and 475 g of distilled water. The remaining volume was purged and filled with helium at a pressure of 2.4 bar. Artificial maturation was accomplished by heating isothermally for 72 h at 160, 180, 200, 220, 239, 260, 280, 300 and 330°C. Temperatures were monitored at 30 s intervals. Standard deviations were between ±0.2 and ±0.3°C except for the 160°C experiment (±0.6°C). Experiments at 300 and 330°C generated an expelled oil that was recovered from the water surface with a pipette. Reactor

walls and rock chips were rinsed with benzene to recover any sorbed oil films, which occurred in experiments at 260, 280, 300 and 330°C. ≥ 95% of the rock chips was recovered from all experiments. Residual chips were dried in a vacuum oven (T ≤ 50°C).

Extraction, fractionation and kerogen preparation. Residual rock chips were freeze-dried and ultrasonically extracted with dichloromethane/methanol (7.5:1 v/v). Any sorbed or expelled oil was combined with the extract. The combined extract was separated into a maltene and an asphaltene fraction by repeated (x3) precipitation in heptane. An aliquot of the maltene fraction (*c.* 250 mg), to which two standards [6,6-d_2-3-methylhenicosane and 2,3-dimethyl-5-(1',1'-d_2-hexadecyl)thiophene] were added for quantitative analysis, was fractionated by column chromatography with Al_2O_3 into an apolar and a polar fraction ('polar fraction I') by elution with hexane/dichloromethane (9:1 v/v) and dichloromethane/methanol (1:1 v/v), respectively (Fig. 5.2). Further separation of the apolar fraction by argentatious thin-layer chromatography yielded the saturated hydrocarbon fraction (R_f = 0.9-1.0) and the alkylthiophene fraction (R_f = 0.4-0.9). The extracted residue of the original sample was demineralised using standard procedures (Lewan *et al.*, 1986) to yield the kerogen.

Attempted isolation of biopolymer from Emiliania huxleyi *and* Isochrysis galbana. The algal cultures were ultrasonically extracted with mixtures of methanol and dichloromethane, and the residues were treated subsequently with 1N KOH/methanol (reflux, 1 h). The residue of *Emiliania huxleyi* was further treated with 2N HCl (reflux, 8 h), 6N H_2SO_4 (20°C, 2 h) and 0.5 N H_2SO_4 (reflux, 16 h). After each treatment the released products were removed by extraction.

Chemical degradation of polar fractions. The sequential chemical degradation of the polar fractions is shown in Fig. 5.2. Polar fraction I (10-20 mg), to which a known amount of a synthetic standard [2,3-dimethyl-5-(1',1'-d_2-hexadecyl)thiophene] was added, was desulphurised with Raney Ni (Sinninghe Damsté *et al.*, 1988b). Small amounts of Raney Ni were added repeatedly (x3) in 30 min intervals to the polar fraction (dissolved in 4 ml of ethanol), and the mixture was refluxed for 1.5 h. The reaction mixture was allowed to cool, and a sodium chloride solution was added, after which the reaction mixture was extensively extracted with dichloromethane. Column chromatography using Al_2O_3 yielded the released hydrocarbons (hexane/dichloromethane 9:1 v/v), which were subsequently hydrogenated (Sinninghe Damsté *et al.*, 1988b), and residual polar fraction II (dichloromethane/methanol 1:1 v/v).

Polar fraction II (10-20 mg), to which a known amount of a synthetic standard [2,3-dimethyl-5-(1',1'-d_2-hexadecyl)thiophene] was added, was treated with HI in order to cleave C-O bonds (March, 1985). Polar fraction II was dissolved in 4 ml of a 57% solution of HI in water, and refluxed for 1 h. The reaction mixture was allowed to cool, and was neutralised with excess water and a 5% $Na_2S_2O_3$ solution in water before being

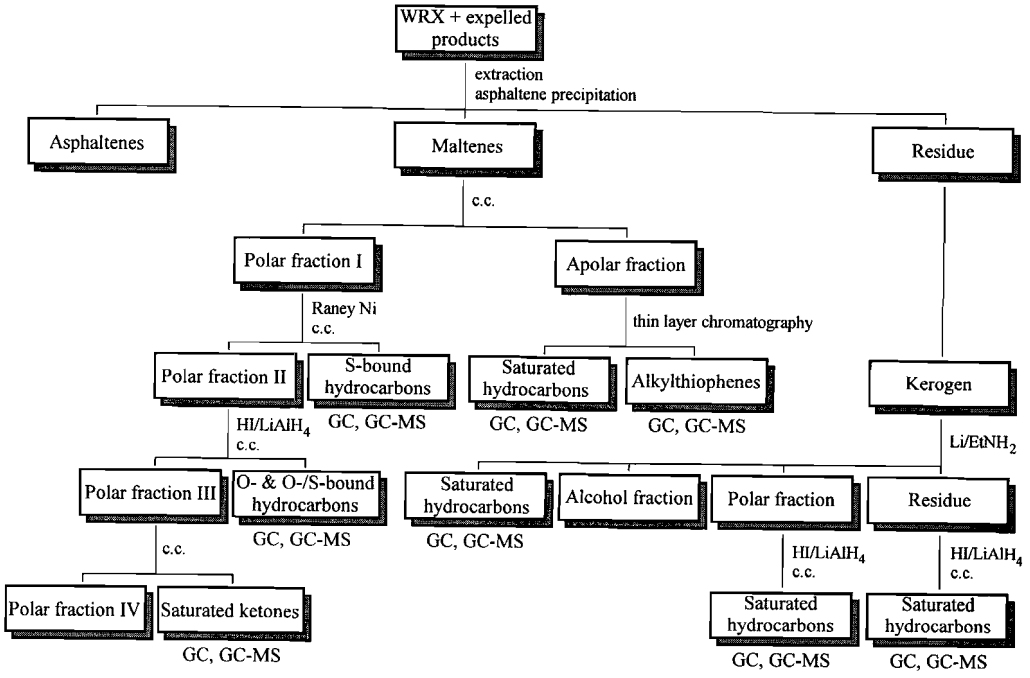

Fig. 5.2. Analytical flow diagram displaying the fractionation and sequential chemical degradation procedures. Key: c.c. = column chromatography.

extensively extracted with hexane. Column chromatography using Al_2O_3 yielded the released alkyl iodides (hexane/dichloromethane 9:1 v/v), and residual polar fraction III (dichloromethane/methanol 1:1 v/v). To reduce the released alkyl iodides to the corresponding saturated hydrocarbons, they were dissolved in 4 ml of 1,4-dioxane, after which 75 mg of $LiAlH_4$ was added (Johnson *et al.*, 1948). The mixture was allowed to reflux for 1.5 h. After the reaction mixture had cooled, ethyl acetate was added to destroy any excess $LiAlH_4$. Water was added, and the reaction mixture was extensively extracted with hexane. Column chromatography using Al_2O_3 yielded the alkanes (hexane/dichloromethane 9:1 v/v).

Polar fraction III, to which a known amount of a synthetic standard [2,3-dimethyl-5-(1',1'-d_2-hexadecyl)thiophene] was added, was fractionated by column chromatography using Al_2O_3 into a saturated ketone fraction (hexane/dichloromethane 1:1 v/v) and a residual polar fraction IV.

Chemical degradation of the kerogen. The sequential chemical degradation of the kerogen of the original sample is shown in Fig. 5.2. The kerogen was treated with Li in ethylamine ($Li/EtNH_2$). A detailed description of the procedure has been given else-

where (Hofmann *et al.*, 1992). Dry ethylamine (*c.* 30 ml) was distilled under nitrogen into a round bottom flask (cooled at -78°C) containing the kerogen (*c.* 100 mg) and a known amount of a synthetic standard (androstane). During the distillation powdered Li was added until a blue colour was obtained. The mixture was stirred under nitrogen (0°C; 2 h) during which Li was regularly added to maintain the blue colour. Excess Li was removed by slow addition of methanol. Acidic water was added (until pH < 2) to dissolve the Li salts formed and to hydrolyse the amides which are by-products of the reaction (Schaeffer *et al.*, 1995a). The supernatant was recovered after centrifugation and extracted with dichloromethane. The residue was washed with distilled water (x3) and acetone (x2), and ultrasonically extracted (15 min) with dichloromethane/methanol (1:1 v/v, x5). The organic extracts were combined and fractionated by column chromatography over silica gel, yielding a saturated hydrocarbon fraction (hexane), an alcohol fraction (dichloromethane), and a polar fraction (dichloromethane/methanol 1:1 v/v).

HI degradation of the polar fraction released after Li/$EtNH_2$ treatment of the kerogen of the original sample was carried out as described above. HI degradation of the residue after Li/$EtNH_2$ treatment of the kerogen of the original sample and of the residues of *Emiliania huxleyi* and *Isochrysis galbana* was achieved by the same reaction scheme (24 h).

Gas chromatography. Gas chromatography (GC) was performed using a Hewlett-Packard 5890 instrument, equipped with an on-column injector. A fused silica capillary column (25 m x 0.32 mm) coated with CP Sil-5 (film thickness 0.12 μm) was used with helium as carrier gas. The column effluent was monitored by a flame ionisation detector (FID). Samples were injected at 70°C and the oven was subsequently programmed to 130°C at 20°C/min and then at 4°C/min to 320°C, at which it was held for 20 min.

Gas chromatography-mass spectrometry. Gas chromatography-mass spectrometry (GC-MS) was carried out on a Hewlett-Packard 5890 gas chromatograph interfaced to a VG Autospec Ultima mass spectrometer operated at 70 eV with a mass range m/z 40-800 and a cycle time of 1.8 s (resolution 1000). GC conditions were as above.

Quantitation. Quantitation of saturated hydrocarbons was accomplished by integration of their peak areas and that of the standard (6,6-d_2-3-methylhenicosane) in the FID trace. Quantitation of alkylthiophenes has been described before (Koopmans *et al.*, 1995). 1,2-Di-*n*-alkylbenzenes were quantitated by integration of mass chromatograms of the fragment ion at m/z 105 and the main fragment ion (m/z 127) of the standard [2,3-dimethyl-5-(1',1'-d_2-hexadecyl)thiophene]. Compounds released after desulphurisation of polar fraction I and after HI/$LiAlH_4$ treatment of polar fraction II were quantitated by integration of their peak areas and that of the standard in the FID trace. Saturated methyl, ethyl and mid-chain ketones were quantitated by integration of mass chromatograms of the fragment ion at m/z 58 and the main fragment ion (m/z 127) of the

standard [2,3-dimethyl-5-(1',1'-d_2-hexadecyl)thiophene]. Compounds released after chemical degradation of the kerogen were quantitated by integration of their peak areas and that of the standard (androstane) in the FID trace.

When quantitating compounds by integrating mass chromatograms, a correction was made to account for the intensity of the fragment ions used relative to the total ion current in the spectra of the compounds quantitated and the standard. Because mass spectrometric detection of compounds gives a molar response, a factor comprising the molecular weights of the compounds quantitated and the standard was introduced to obtain absolute amounts (μg/g TOC of original rock).

Quantitation of duplicate hydrous pyrolysis experiments at 280 and 300°C indicated that the standard deviation was typically < 25%. However, the results for some fractions differed more, especially for the 300°C experiments. Reported results for the experiments at 280 and 300°C are averages of the duplicate runs.

5.4 Results

Separate aliquots of a marlstone from the Gessoso-solfifera Formation were heated isothermally for 72 h at temperatures between 160 and 330°C by hydrous pyrolysis. Absolute amounts (μg/g TOC of original rock) of compounds with *n*-C_{37} and *n*-C_{38} skeletons in the original sample and the artificially matured samples are listed in Table 5.1.

Apolar fractions

In the saturated hydrocarbon fraction of the original sample, *n*-C_{37} and *n*-C_{38} alkanes could not be detected (Fig. 5.3). After heating at 220°C, formation of *n*-C_{37} and *n*-C_{38} alkanes is still insignificant. At 239°C and higher temperatures, relatively large amounts are released, presumably from high-molecular-weight fractions. When their concentrations reach a maximum at 260°C (Table 5.1), they are among the most abundant *n*-alkanes (Fig. 5.3). Their generation profiles show a high positive correlation (R^2 = 0.988), with an average C_{37}/C_{38} ratio of 0.81. At temperatures > 260°C short-chain *n*-alkanes become dominant (Koopmans *et al.*, 1996b).

The generation profiles of the mid-chain alkylthiophenes with *n*-C_{37} and *n*-C_{38} skeletons have been described before (Koopmans *et al.*, 1995). They are formed when the sample is heated at 260°C and above, although they are not detectable at 330°C. The specific isomer distribution of the C_{38} mid-chain 2,5-di-*n*-alkylthiophenes at 260°C is maintained at 300°C, and is consistent with sulphur incorporation at the ω15 and ω22 double bonds of di-unsaturated C_{38} methyl and ethyl ketones (Fig. 5.1) biosynthesised by several prymnesiophytes, suggesting an origin from these algae (Koopmans *et al.*, 1995).

C_{37} and C_{38} 1,2-di-*n*-alkylbenzenes are formed at 239°C and above. They were identified by a main fragment ion at m/z 105, resulting from cleavage β to both sides of

Table 5.1. Absolute amounts (μg/g TOC of original rock) of *n*-C_{37} and *n*-C_{38} skeletons in various fractions as a function of hydrous pyrolysis temperature.

n-C_{37}	original	160°C	180°C	200°C	220°C	239°C	260°C	280°C	300°C	330°C
Apolar fraction										
alkanes	0	0	2	2	7	67	$2.6x10^2$	$1.6x10^2$	$1.6x10^2$	$1.8x10^2$
2,5-di-*n*-alkylthiophenes	0	0	0	0	0	0	15	13	18	0
1,2-di-*n*-alkylbenzenes	0	0	0	0	0	1	9	14	22	31
Polar fraction										
S-bound (PF I)[a]	18	32	41	$1.6x10^2$	95	97	40	19	5	1
O- and O/S-bound (PF II)[b]	0	28	32	$1.6x10^2$	95	$1.7x10^2$	$1.9x10^2$	62	69	18
mid-chain ketones (PF III)[c]	0	8	13	42	83	$2.4x10^2$	$1.9x10^2$	$1.1x10^2$	$1.1x10^2$	89
methyl ketone (PF III)[c]	0	5	11	16	34	91	37	23	21	20
TOTAL	**18**	**73**	**99**	**$3.8x10^2$**	**$3.1x10^2$**	**$6.6x10^2$**	**$7.3x10^2$**	**$4.0x10^2$**	**$4.1x10^2$**	**$3.4x10^2$**

n-C_{38}	original	160°C	180°C	200°C	220°C	239°C	260°C	280°C	300°C	330°C
Apolar fraction										
alkanes	0	0	0	0	4	86	$3.4x10^2$	$1.8x10^2$	$1.8x10^2$	$2.0x10^2$
2,5-di-*n*-alkylthiophenes	0	0	0	0	0	0	20	14	20	0
1,2-di-*n*-alkylbenzenes	0	0	0	0	0	1	11	18	28	41
Polar fraction										
S-bound (PF I)[a]	14	42	50	$1.7x10^2$	$1.0x10^2$	$1.2x10^2$	39	17	6	1
O- and O/S-bound (PF II)[b]	0	32	43	$1.9x10^2$	$1.2x10^2$	$2.0x10^2$	$2.3x10^2$	71	82	17
mid-chain ketones (PF III)[c]	0	13	17	61	$1.1x10^2$	$3.3x10^2$	$2.6x10^2$	$1.2x10^2$	$1.3x10^2$	99
(m)ethyl ketone (PF III)[c]	0	5	11	25	73	$2.2x10^2$	$1.1x10^2$	56	53	31
TOTAL	**14**	**92**	**$1.2x10^2$**	**$4.5x10^2$**	**$4.1x10^2$**	**$9.6x10^2$**	**$1.0x10^3$**	**$4.8x10^2$**	**$5.0x10^2$**	**$3.9x10^2$**

[a] PF I = polar fraction I (Fig. 5.2).
[b] PF II = polar fraction II (Fig. 5.2).
[c] PF III = polar fraction III (Fig. 5.2).

the benzene ring, and by a series of minor ions, resulting from cleavage β to one side of the benzene ring (cf. Sinninghe Damsté *et al.*, 1991). Their absolute amounts increase gradually with increasing maturation temperature.

Polar fractions

Polar fractions were studied by sequential chemical degradation, in order to analyse both S- and O-bound moieties (Fig. 5.2). A similar, albeit qualitative, approach was followed by Richnow *et al.* (1992, 1993).

Desulphurisation of polar fraction I of the original sample yields relatively low amounts of *n*-C_{37} and *n*-C_{38} alkanes (Fig. 5.3). After heating at 200°C, *n*-C_{37} and *n*-C_{38} dominate the *n*-alkane distribution (Fig. 5.3) in amounts an order of magnitude higher than in the original sample (Table 5.1). Above 200°C, the amounts of S-bound *n*-C_{37} and *n*-C_{38} alkanes decrease (Table 5.1), probably due to thermal cleavage of relatively weak S-S and C-S bonds. Their generation profiles show a high positive correlation (R^2 = 0.991), with an average C_{37}/C_{38} ratio of 0.91.

HI/$LiAlH_4$ treatment of polar fraction II of the original sample does not yield detectable amounts of *n*-C_{37} and *n*-C_{38} alkanes (Table 5.1). HI/$LiAlH_4$ treatment of polar fraction II of the heated samples yields, however, relatively high amounts (Fig. 5.3). These products may include *n*-C_{37} and *n*-C_{38} skeletons that were sequestered by multiple bonds involving both sulphur and oxygen: Raney Ni treatment of polar fraction I cleaves the sulphur bonds of these multiply linked skeletons, which are only released after their remaining oxygen bonds are cleaved by HI treatment of polar fraction II. The largest amounts are released at 260°C (Table 5.1). The generation profiles of O-linked and both S- and O-linked *n*-C_{37} and *n*-C_{38} alkanes show a high positive correlation (R^2 = 0.999), with an average C_{37}/C_{38} ratio of 0.83. To determine the proportion of *n*-C_{38} skeletons bound solely by oxygen, polar fraction I of the sample heated at 260°C was treated with HI/$LiAlH_4$, which released 25 μg/g TOC of *n*-C_{38} alkane (not shown in Table 5.1). Comparison of this amount and the amounts released after desulphurisation of polar fraction I and HI/$LiAlH_4$ treatment of polar fraction II reveals that 76% of the sequestered *n*-C_{38} skeletons is linked by both sulphur and oxygen. Richnow *et al.* (1992) found that *n*-alkane and hopanoid skeletons were in part linked by both sulphur and oxygen in macromolecular fractions of a Monterey oil. However, *n*-C_{37} and *n*-C_{38} skeletons were linked only by sulphur, as indicated by their presence after desulphurisation and absence after subsequent C-O bond cleavage (Richnow *et al.*, 1992).

In polar fraction III of the original sample, ketones with *n*-C_{37} or *n*-C_{38} skeletons could not be detected. However, saturated *n*-C_{37} methyl ketones and *n*-C_{38} methyl and ethyl ketones are relatively abundant in the heated samples, as are saturated *n*-C_{37} and *n*-C_{38} mid-chain ketones (Fig. 5.4). The highest amounts of ketones are found after heating at 239°C (Table 5.1). Their generation profiles show a high positive correlation (R^2 = 0.988), with an average C_{37}/C_{38} ratio of 0.60. Interestingly, the carbonyl group of

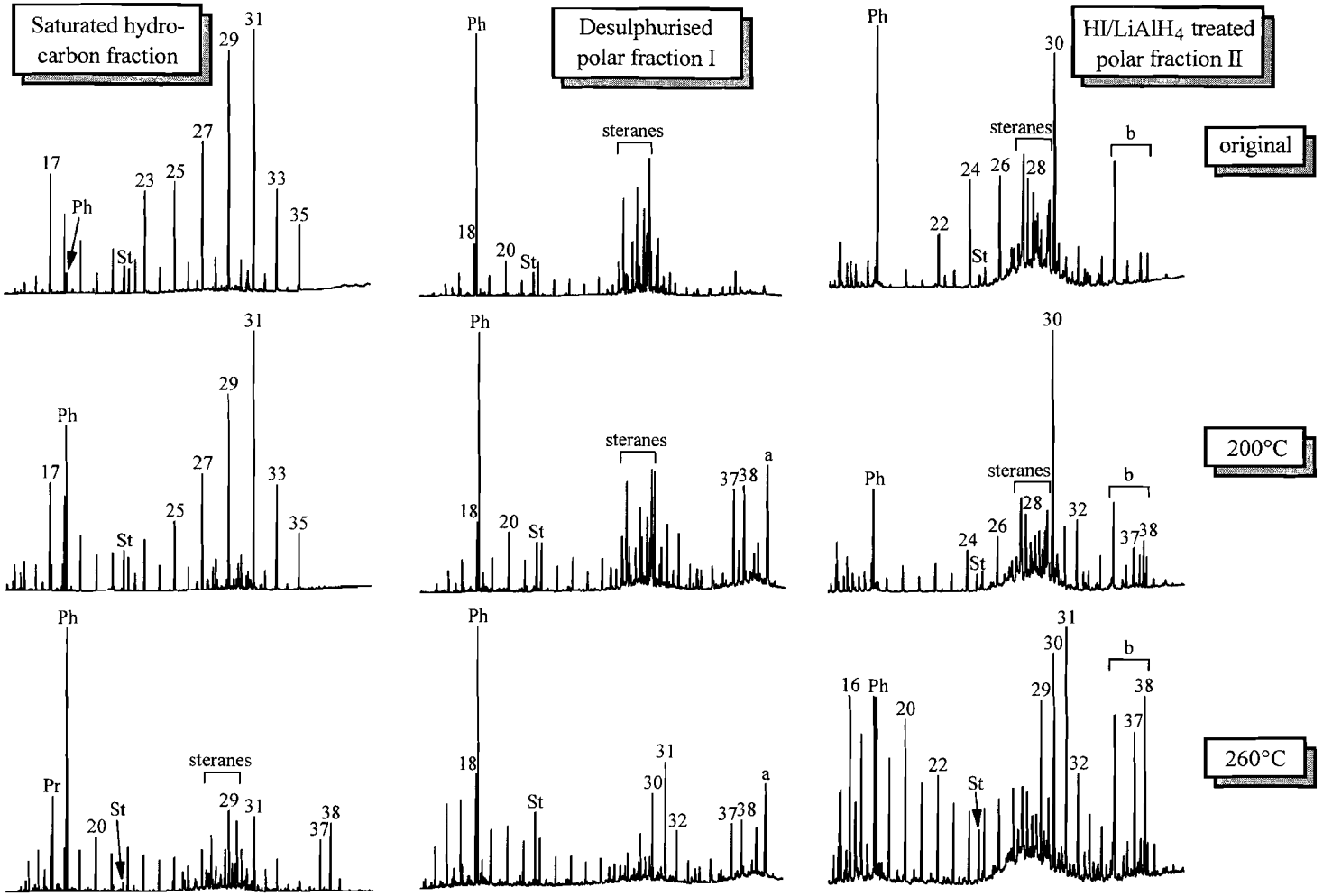
Saturated hydro-carbon fraction
Desulphurised polar fraction I
HI/LiAlH4 treated polar fraction II
original
200°C
260°C
Ph
St
Pr
steranes
a
b
16
17
18
20
22
23
24
25
26
27
28
29
30
31
32
33
35
37
38

the n-C_{37} mid-chain ketones is located predominantly at C-15 (*i.e.* ω15 and ω23) and C-16 (*i.e.* ω16 and ω22) as determined from an averaged mass spectrum (Fig. 5.5). These positions correspond to the ω15 and ω22 double bonds of the di-unsaturated n-C_{37} methyl ketone (Fig. 5.1) as determined by de Leeuw *et al.* (1980). The position of the carbonyl group of the n-C_{38} mid-chain ketones is also mainly restricted to the original double bond positions.

Polar fraction IV of the sample heated at 260°C was derivatised with BSTFA. Because analysis did not reveal any GC amenable compounds, polar fractions IV of the other samples were not further studied.

Kerogen of the original sample

The summed amounts of n-C_{37} and n-C_{38} skeletons in the apolar and polar fractions as a function of maturation temperature are shown in Fig. 5.6. In the original sample these amounts are low, but at 260°C large amounts of n-C_{37} and n-C_{38} skeletons are produced (up to 1 mg/g TOC), apparently from the kerogen. At temperatures higher than 260°C the summed amounts decrease, probably due to thermal degradation of free n-C_{37} and n-C_{38} skeletons or their bound precursors.

In order to investigate the presence of n-C_{37} and n-C_{38} skeletons in the kerogen of the original sample, chemical degradation experiments were conducted. First, the kerogen was treated with Li/$EtNH_2$ which reductively cleaves C-S bonds (Hofmann *et al.*, 1992). Then, the released polar fraction and the residue were treated with HI/$LiAlH_4$ to cleave C-O bonds. The results are given in Table 5.2. The amounts of n-C_{37} and n-C_{38} alkanes released from the kerogen are an order of magnitude higher than the amounts of n-C_{37} and n-C_{38} skeletons in the apolar and polar fractions of the original sample (cf. Tables 5.1 and 5.2). This indicates that the bulk of the n-C_{37} and n-C_{38} skeletons in the original sample is sequestered in the kerogen. However, the amounts of n-C_{37} and n-C_{38} alkanes released from the kerogen by chemical degradation are lower than the amounts generated by hydrous pyrolysis. This may be caused by the macromolecular nature of the kerogen, hampering the access of the chemical reagents.

Fig. 5.3. Gas chromatograms of the saturated hydrocarbon fraction, desulphurised polar fraction I, and HI/$LiAlH_4$ treated polar fraction II of the original sample and the samples artificially matured at 200 and 260°C. Key: Pr = pristane, Ph = phytane, St = standard, a = isorenieratane, b = C_{40} biphytanes with 0-3 cyclopentyl rings. The most abundant n-alkanes are indicated by numbers that represent the number of carbon atoms.

5.5 Discussion

Origin of *n*-C_{37} and *n*-C_{38} skeletons

The high correlation coefficients of the generation profiles of the summed amounts of *n*-C_{37} and *n*-C_{38} skeletons ($R^2 = 0.986$) and of the amounts of *n*-C_{37} and *n*-C_{38} skeletons in individual fractions ($R^2 > 0.98$) suggest that they originate from similar precursors and were sequestered by the same processes. The specific carbon number distributions in several fractions (Figs. 5.3 and 5.4), with the *n*-C_{37} and *n*-C_{38} skeletons being much more abundant than other long-chain homologues, suggest an input of *n*-C_{37} and *n*-C_{38} alkenones into the sediment. The average ratio of the summed amounts of *n*-C_{37} and *n*-C_{38} skeletons (0.71) is similar to the ratio of total *n*-C_{37} methyl ketones and total *n*-C_{38} methyl and ethyl ketones found in *Gephyrocapsa oceanica* (0.62 - Conte *et al.*, 1994; 0.70 - Volkman *et al.*, 1995), but differs significantly from the ratio in *Emiliania huxleyi* (1.46 - Prahl *et al.*, 1988; 1.15 - Conte *et al.*, 1994). This is consistent with the fact that *Emiliania huxleyi* did not exist during the Late Miocene (Thierstein *et al.*, 1977), when the sediments of the Gessoso-solfifera Formation were deposited.

The only lipids with an *n*-C_{37} or *n*-C_{38} skeleton known to be biosynthesised by prymnesiophytes are (i) di-, tri- and tetra-unsaturated ketones (Volkman *et al.*, 1980a,b;

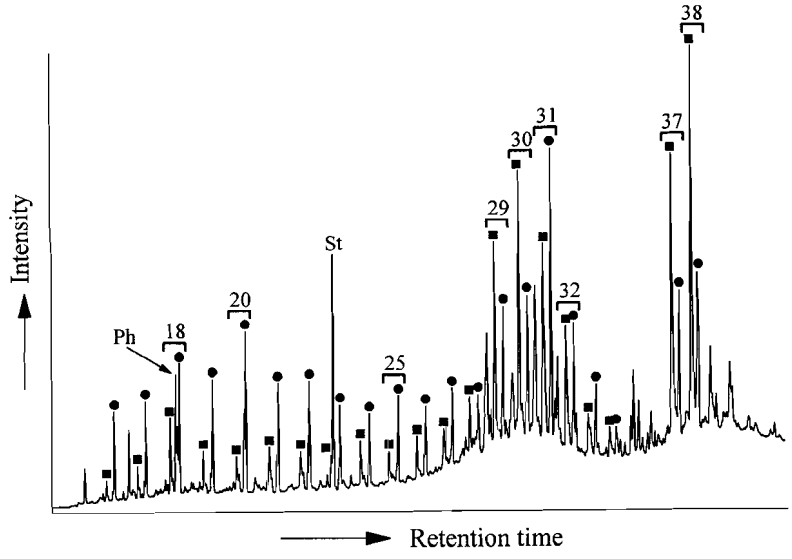

Fig. 5.4. Gas chromatogram of the ketone fraction of the sample artificially matured at 239°C. Key: Ph = ketone with a Ph carbon skeleton, St = internal standard. Dots indicate (co-eluting) methyl and ethyl ketones, squares indicate (co-eluting) mid-chain ketones. Numbers indicate number of carbon atoms.

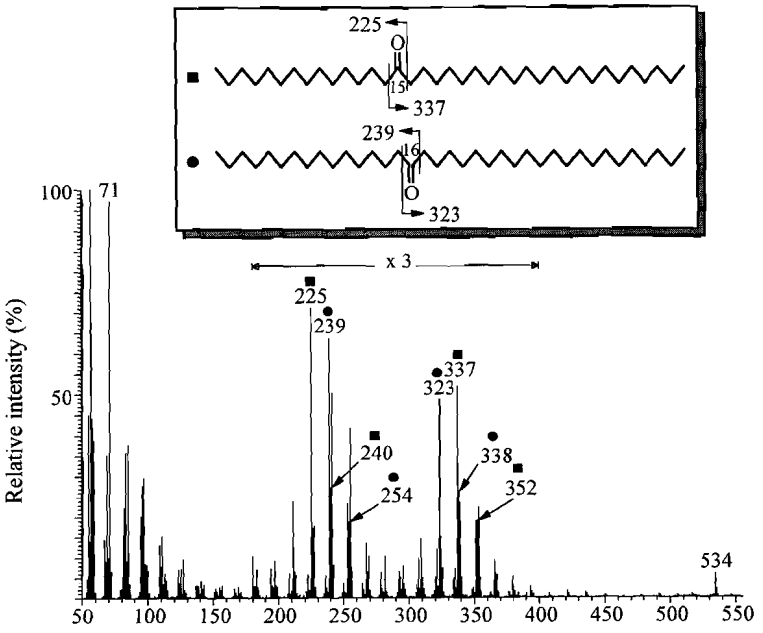

Fig. 5.5. Averaged mass spectrum (subtracted for background; averaged over 17 scans) of n-C_{37} mid-chain ketones from the sample artificially matured at 239°C. Even m/z values correspond to McLafferty fragment ions (fragmentations not indicated in insert).

Marlowe *et al.*, 1984), and (ii) alkatrienes and alkatetraenes (Volkman *et al.*, 1980a,b; Sikes and Volkman, 1993). These compounds may be the precursors of the C_{37} and C_{38} n-alkanes, mid-chain 2,5-di-n-alkylthiophenes and saturated methyl and ethyl ketones encountered in the artificially matured samples. They can also be the precursors of S-bound n-C_{37} and n-C_{38} skeletons in the polar fraction and the kerogen, because laboratory sulphurisation experiments have shown that hydrocarbons with double bonds or carbonyl groups react readily with reduced inorganic sulphur species (de Graaf *et al.*, 1992; Schouten *et al.*, 1993, 1994). However, it is difficult to understand how the lipids of prymnesiophytes could be the precursors of O-bound n-C_{37} or n-C_{38} skeletons or saturated mid-chain ketones.

A possible formation pathway of O-bound n-C_{37} and n-C_{38} skeletons is the reaction of the double bonds of the prymnesiophyte lipids with oxygen under the influence of light (cf. Harvey *et al.*, 1983). Another explanation would be the existence of a biopolymer in prymnesiophytes comprising an O-linked network of hydrocarbons including high amounts of n-C_{37} and n-C_{38} skeletons. Such a biopolymer would resemble the structure of the algaenan of the microalga *Nannochloropsis salina* recently reported by Gelin *et al.* (1996a). Flash pyrolysis of this algaenan yielded high amounts of mid-chain

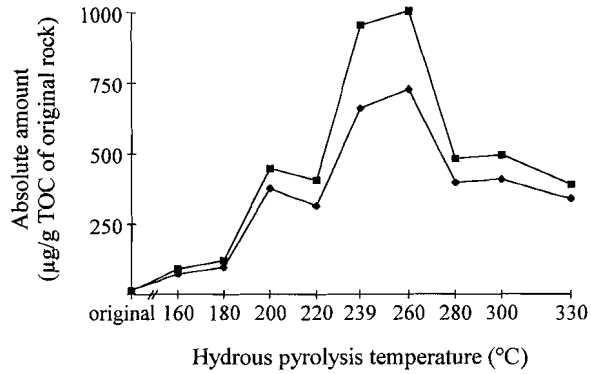

Fig. 5.6. Summed amounts (µg/g TOC of original rock) of n-C_{37} (diamonds) and n-C_{38} (squares) skeletons in the apolar and polar fractions as a function of hydrous pyrolysis temperature.

ketones (Gelin *et al.*, 1996a), consistent with our findings of mid-chain ketones in the artificially matured samples. Flash (Gelin *et al.*, 1993, 1994) and off-line pyrolysis (Behar *et al.*, 1995) of ether lipids isolated from the green microalga *Botryococcus braunii* yielded high amounts of mid-chain ketones with carbon skeletons corresponding to the constituent alkyl chains, indicating that ether lipids can produce mid-chain ketones upon thermal stress.

In order to check for the presence of such a biopolymer in prymnesiophytes, an extracted culture of *Emiliania huxleyi* was subjected to successive base and acid hydrolyses. This yielded an insoluble macromolecular substance (*c.* 0.5‰ of extracted biomass), but HI/$LiAlH_4$ treatment did not release n-C_{37} or n-C_{38} alkanes. Accordingly, HI/$LiAlH_4$ treatment of an extracted culture of *Isochrysis galbana* did not release n-C_{37} or n-C_{38} alkanes. These findings suggest that prymnesiophytes do not biosynthesise an oxygen cross-linked biomacromolecule containing relatively large amounts of n-C_{37} and n-C_{38} skeletons. Therefore, it is likely that the O-bound n-C_{37} and n-C_{38} skeletons and the mid-chain ketones encountered in the polar fractions of the heated samples have a diagenetic origin, with the latter probably deriving from thermal breakdown of the former (cf. Gelin *et al.*, 1993, 1994, 1996a).

Diagenetic pathways of n-C_{37} and n-C_{38} skeletons

Chemical degradation experiments showed that 76% of the n-C_{38} skeletons sequestered in polar fraction I of the sample heated at 260°C is linked by both sulphur and oxygen bonds. Because thermal stress is expected to cleave C-S as well as C-O bonds, it is likely that the proportion of the n-C_{38} skeleton linked by both sulphur and oxygen bonds decreases with increasing maturation temperature. Alternatively, at temperatures lower

Table 5.2. Absolute amounts (μg/g TOC) of *n*-C_{37} and *n*-C_{38} alkanes released from the kerogen of the original sample.

	$Li/EtNH_2$ on kerogen[a]	$HI/LiAlH_4$ on residue[a]	$HI/LiAlH_4$ on released polar fraction[a]	**TOTAL**
n-C_{37}	75	$1.5x10^2$	81	**$3.0x10^2$**
n-C_{38}	72	$1.7x10^2$	93	**$3.4x10^2$**

[a] See Fig. 5.2 for flow diagram of chemical degradation of the kerogen.

than 260°C this proportion might be higher than 76%, especially in the original sample. Such a highly cross-linked structure is probably present in the kerogen, because the number of (sulphur) cross-links and the average molecular weight of geomacromolecules are positively correlated (Sinninghe Damsté *et al.*, 1990a; Kohnen *et al.*, 1991b; Schouten *et al.*, 1995a). Indeed, chemical degradation experiments with the kerogen of the original sample yielded high amounts of *n*-C_{37} and *n*-C_{38} alkanes compared to the amounts in the apolar and polar fraction (Tables 5.1 and 5.2). In the following discussion of diagenetic pathways, attention is focused on the *n*-C_{38} skeleton.

In Fig. 5.7**a**, the absolute amount of the *n*-C_{38} skeleton in the apolar and polar fractions is shown as a function of maturation temperature. In the original sample, *n*-C_{38} alkane is only encountered after desulphurisation of polar fraction I (triangles in Fig. 5.7**a**). Heating at 160°C results in the production of low amounts of S-bound *n*-C_{38} alkane (triangles), O-bound and/or both S- and O-bound *n*-C_{38} alkane (crosses), and *n*-C_{38} saturated ketones (double crosses). Generation of S- and O-bound *n*-C_{38} can be ascribed to cleavage of C-S bonds, which are weaker than C-O bonds (Claxton *et al.*, 1993), in the kerogen. However, the presence of *n*-C_{38} mid-chain ketones can only be explained by the cleavage of oxygen bonds in the kerogen (cf. Gelin *et al.*, 1993, 1994, 1996a). Therefore, cleavage of both C-S and C-O bonds seems to occur already at the lowest maturation temperature applied. Substantial amounts of *n*-C_{38} alkane (diamonds) are encountered only at 239°C. This is consistent with the assumption that the far greater part of the *n*-C_{38} skeleton in the original sample is both S- and O-linked in the kerogen, so that for the thermal release of *n*-C_{38} alkane at least one C-S and at least one C-O bond should be cleaved. At temperatures higher than 260°C the absolute amounts of the *n*-C_{38} skeleton in all fractions generally decrease, probably due to thermal degradation of these skeletons or their bound precursors. It should be noted that these processes occur at relatively low levels of thermal maturity, because 25% of the pentakishomohopanes still have the biologically inherited and thermodynamically unstable 17β,21β(H)-configuration at 260°C (Koopmans *et al.*, 1996b).

In order to unravel further the diagenetic pathways of the *n*-C_{38} skeleton, its relative amount in various fractions is plotted in Fig. 5.7**b**. In the original sample it is exclusively S-bound in the polar fraction (triangles). The relative amount of S-bound *n*-C_{38} gradually decreases with increasing temperature, attesting to the labile character of

C-S and S-S bonds. The relative amount of O-bound n-C_{38} increases up to 200°C after which it gradually decreases (crosses). After the first formation of n-C_{38} alkane (diamonds) at 220°C, its relative abundance increases to 52% at 330°C. The relative amount of C_{38} 1,2-di-n-alkylbenzenes (squares) increases steadily to 10% at 330°C. Although the C_{38} 1,2-di-n-alkylbenzenes are obviously stable thermal degradation products of macromolecularly-bound n-C_{38} skeletons, it is presently not clear how they are formed. The relative amount of n-C_{38} saturated ketones (double crosses) maximises at 239°C, after which it decreases slightly to stay relatively constant at *c.* 35%. These generation profiles suggest that there are three relatively stable forms of the n-C_{38} skeleton (saturated hydrocarbon, 1,2-di-n-alkylbenzenes and saturated ketones), and two relatively labile forms (S-bound and O-bound; Fig. 5.8). These results suggest that in sedimentary rocks with more mature organic matter containing abundant n-C_{37} and n-C_{38} skeletons, saturated ketones might be expected to occur besides saturated hydrocarbons.

'Double bias' of the sedimentary record from sulphur and oxygen sequestration of n-C_{37} and n-C_{38} skeletons

Reaction of functionalised lipids with reduced inorganic sulphur species results in selective removal of specific carbon skeletons from the pool of low-molecular-weight compounds, and leads to incomplete assessments of depositional environments. This bias can be lifted by taking into account S-bound carbon skeletons in the polar fraction (Kohnen *et al.*, 1991c, 1992a). From the present study it follows that a 'double bias' of the sedimentary record of the Gessoso-solfifera Formation is caused by sulphur and oxygen sequestration of n-C_{37} and n-C_{38} alkenones in the kerogen. Interestingly, the work by Kohnen *et al.* (1991c, 1992a) was partly based on an unheated marl from the Gessoso-solfifera Formation, in which they did not detect free or S-bound n-C_{37} and n-C_{38} alkanes.

An important question is whether sulphur and oxygen sequestration of alkenones affects the relative amounts of di- and tri-unsaturated ketones ($U^{K'}_{37}$) used to infer palaeo sea surface temperatures. Oxidative degradation of alkenones in sediments lowers their total amount, but does not alter the $U^{K'}_{37}$ (Prahl *et al.*, 1989). Not much attention has been paid to the effect of sulphurisation on the $U^{K'}_{37}$, although the occurrence of S-bound and S-containing n-C_{37} and n-C_{38} skeletons has been described before (Sinninghe Damsté *et al.*, 1988b, 1989c, 1990a,b; Kohnen *et al.*, 1990c; Rullkötter and Michaelis, 1990; Rullkötter *et al.*, 1990; Richnow *et al.*, 1992; Schouten *et al.*, 1993; Barakat and Rullkötter, 1994; Koopmans *et al.*, 1995; Hefter *et al.*, 1995). Sulphurisation of either the di- or tri-unsaturated ketones sequesters these compounds into high-molecular-weight fractions and, thus, might directly affect the $U^{K'}_{37}$ which is based on free di- and tri-unsaturated ketones. Therefore, formation of the first C-S bond is the important step. Because di-unsaturated ketones contain three functionalities available for sulphurisation and tri-unsaturated ketones contain four, we anticipate that both

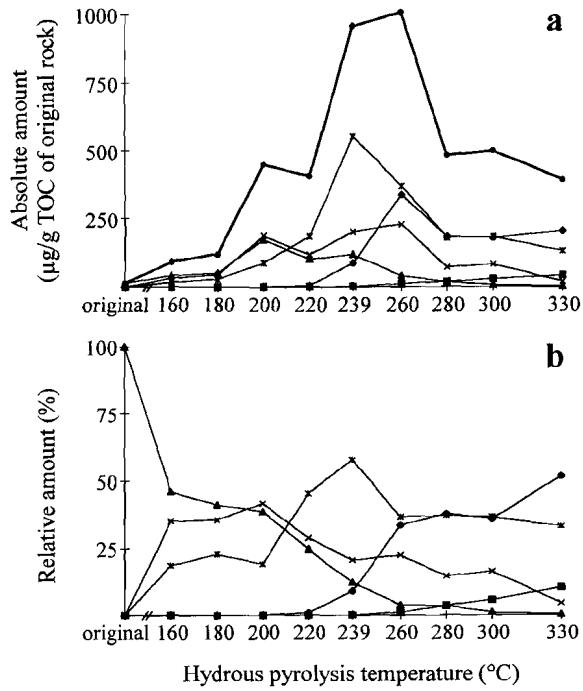

Fig. 5.7. (**a**) Absolute and (**b**) relative amounts of the *n*-C_{38} skeleton in the saturated hydrocarbon fraction (diamonds), alkylthiophene fraction (1,2-dialkylbenzenes: squares), desulphurised polar fraction I (triangles), HI/$LiAlH_4$ treated polar fraction II (crosses), and ketone fraction (double crosses) as a function of hydrous pyrolysis temperature. The fat line marked with circles in (**a**) indicates the total amount of *n*-C_{38} skeletons in the apolar and polar fractions as a function of hydrous pyrolysis temperature. Alkylthiophenes are not shown.

would react with reduced inorganic sulphur species at approximately the same rate. Therefore, the $U^{K'}_{37}$ may be unaffected. Although the mechanism by which alkenones become O-linked is unknown, our results suggest that the functional groups are involved. Therefore, the same argument applies as with the sulphurisation reaction, and the $U^{K'}_{37}$ is probably unaffected.

It might be expected that multiply-functionalised lipids other than the alkenones are also subject to both sulphur and oxygen sequestration, especially when functionalities are too far apart for direct formation of cyclic sulphides or thiophenes (Sinninghe Damsté *et al.*, 1989c). Evidence for both S- and O-linking of pentakishomohopane was provided by Richnow *et al.* (1992, 1993). Such a 'double bias' will severely influence the perception of biochemicals present during sediment deposition. It should be noted, however, that this 'double bias' will be more pronounced in immature sediments and sedimentary rocks, which have not experienced the thermal stress needed for cleavage

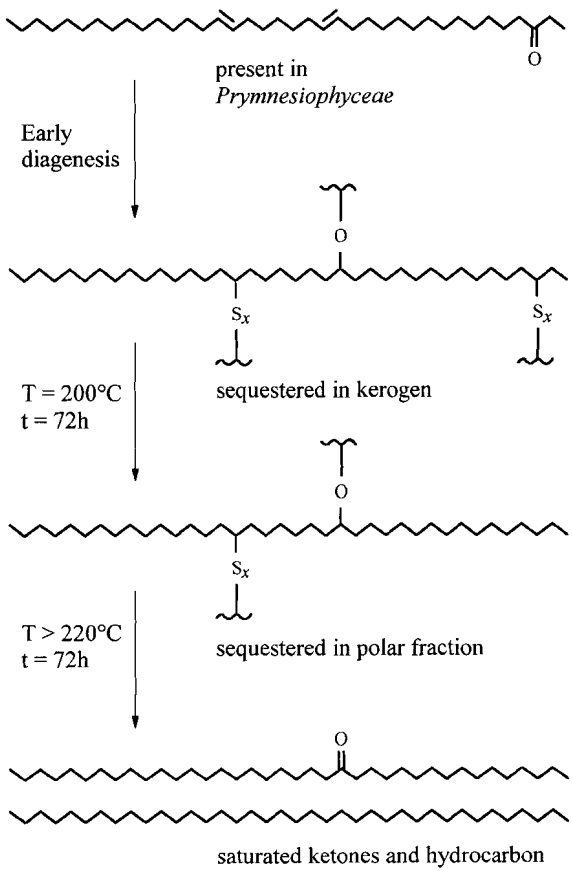

Fig. 5.8. Diagenetic scheme of *n*-C_{38} di-unsaturated ketones. Formation of 1,2-di-*n*-alkylbenzenes and 2,5-di-*n*-alkylthiophenes is not shown.

of C-S and C-O bonds.

5.6 Conclusions

Hydrous pyrolysis of a sedimentary rock with immature (R_o = 0.25%) S-rich organic matter from the Gessoso-solfifera Formation at temperatures between 160 and 260°C results in the production of large amounts of S- and O-bound *n*-C_{37} and *n*-C_{38} alkanes, saturated *n*-C_{37} and *n*-C_{38} methyl, ethyl and mid-chain ketones, C_{37} and C_{38} mid-chain 2,5-di-*n*-alkylthiophenes, C_{37} and C_{38} 1,2-di-*n*-alkylbenzenes and C_{37} and C_{38} *n*-alkanes. The high correlation coefficients ($R^2 > 0.98$) of the generation profiles of the *n*-C_{37} and *n*-C_{38} skeletons suggest that these compounds originate from similar precursors, *i.e.* *n*-C_{37} and *n*-C_{38} di- and tri-unsaturated alkenones biosynthesised by several prymnesio-

phyte algae. The large increase (*c.* 1 mg/g TOC) in the summed amounts of *n*-C_{37} and *n*-C_{38} skeletons upon thermal maturation suggests that these are formed from the kerogen, which is supported by chemical degradation experiments with the kerogen of the unheated sample.

The finding of O-bound *n*-C_{37} and *n*-C_{38} alkanes and saturated *n*-C_{37} and *n*-C_{38} mid-chain ketones with the carbonyl group predominantly at C-15 and C-16, corresponding to the double bond positions of the alkenones, indicates that the alkenones are also sequestered by oxygen bonds. The far greater part of the *n*-C_{37} and *n*-C_{38} skeletons is probably linked by both sulphur and oxygen bonds. The absence of an O-linked biopolymer containing *n*-C_{37} and *n*-C_{38} skeletons in *Emiliania huxleyi* and *Isochrysis galbana* suggests that prymnesiophytes do not biosynthesise such a biopolymer, and, thus, that the O-linked *n*-C_{37} and *n*-C_{38} skeletons have a diagenetic origin.

The relative amounts of *n*-C_{38} skeletons in various fractions as a function of hydrous pyrolysis temperature suggest that there are three thermally stable forms (saturated hydrocarbon, 1,2-di-*n*-alkylbenzenes and saturated ketones), and two thermally labile forms (S-bound and O-bound). It is proposed that the stable forms originate from the thermal breakdown of the labile forms at relatively low levels of thermal maturity.

The sequestration of the alkenones by both sulphur and oxygen results in a 'double bias' of the sedimentary record. However, hydrous pyrolysis is capable of lifting this 'double bias' by cleaving C-S and C-O bonds in the kerogen and releasing *n*-C_{37} and *n*-C_{38} skeletons. The 'double bias' will probably not affect the $U^{K'}_{37}$, since the di-and tri-unsaturated ketones are expected to react with reduced inorganic sulphur species at comparable rates.

5.7 Acknowledgements

We thank Shell International Exploration and Production for providing a research studentship to MPK. Analytical support was provided by Mrs. M. Dekker and Mr. W. Pool. Mr. R. Kempers and Mrs. M. Kok are kindly thanked for growing and extracting the *Emiliania huxleyi* culture. This work was partly supported by a PIONIER grant to JSSD from the Netherlands Organisation for Scientific Research (NWO). This work was performed under the auspices of ENOG (European Network of Organic Geochemists) and has benefited from scientific discussions within the group. ENOG comprises Laboratoire de Géochimie, IFP, Rueil-Malmaison, France; Institute of Petroleum and Organic Geochemistry, KFA, Jülich, Germany; Geologisches Institut der Universität Köln, Germany; Laboratoire de Chimie Organiques de Substances Naturelles associé au CNRS, Université Louis Pasteur, Strasbourg, France; Netherlands Institute for Sea Research, Department of Marine Biogeochemistry and Toxicology, Texel, Netherlands; Department of Environmental Chemistry, CID-CSIC, Barcelona, Spain; Organic Geochemistry Unit, University of Bristol, UK, and receives funding from the European Community (EC contract # CHRX-CT94-0474).

CHAPTER 6

A thermal and chemical degradation approach to decipher pristane and phytane precursors in sedimentary organic matter

M.P. Koopmans, W.I.C. Rijpstra, M.M. Klapwijk, J.W. de Leeuw, M.D. Lewan and J.S. Sinninghe Damsté

6.1 Abstract

A thermal and chemical degradation approach was followed to determine the precursors of pristane (Pr) and phytane (Ph) in three samples from the Gessoso-solfifera, Ghareb and Green River Formations. Hydrous pyrolysis of these samples yields large amounts of Pr and Ph carbon skeletons, indicating that their precursors are predominantly sequestered in high-molecular-weight fractions. Chemical degradation of the polar fraction and the kerogen of the unheated samples generally does not release large amounts of Pr and Ph. Additional information on the precursors of Pr and Ph is obtained from flash pyrolysis analyses of kerogens and residues after hydrous pyrolysis and after chemical degradation. In this way, multiple precursors for Pr and Ph are recognised in these three samples, which explains the observation that the generation of Pr and Ph can be described in terms of activation energy distributions instead of a single set of kinetic parameters. The main increase of the Pr/Ph ratio with increasing maturation temperature, which is associated with strongly increasing amounts of Pr and Ph, is probably due to the higher amount of precursors of Pr compared to Ph, and not to the different timing of generation of Pr and Ph.

6.2 Introduction

The acyclic isoprenoid hydrocarbons pristane (Pr) and phytane (Ph) are ubiquitous in sedimentary rocks, crude oils and coals (see for reviews Volkman and Maxwell, 1986; Peters and Moldowan, 1993). The Pr/Ph ratio has been proposed as an indicator for the

oxicity of the depositional environment based on the assumption that both Pr and Ph originate from the phytol side chain of chlorophyll *a* (Brooks *et al.*, 1969; Powell and McKirdy, 1973; Didyk *et al.*, 1978). In the presence of oxygen, phytol would be oxidised to phytenic acid, yielding Pr after decarboxylation. In the absence of oxygen, phytol would be dehydrated, yielding phytadiene which eventually would be hydrogenated to Ph (Didyk *et al.*, 1978). Therefore, Pr/Ph ratios less than one were associated with anoxic depositional environments, whereas Pr/Ph ratios greater than one were ascribed to oxic depositional environments (Didyk *et al.*, 1978).

The Pr/Ph ratio is widely used both in organic and petroleum geochemistry. There are, however, three major problems concerning its use (ten Haven *et al.*, 1987). First, chlorophyll *a* is not the only source of Pr and Ph. Alternative precursors for Pr are bound tocopherols (Goossens *et al.*, 1984), archaebacterial ether lipids (Rowland, 1990; Navale, 1994), Pr and its mono-, di-, and tri-unsaturated counterparts in zooplankton (Blumer *et al.*, 1963, 1969; Blumer and Thomas, 1965), and bound methylated 2-methyl-2-(4,8,12-trimethyltridecyl)chromans, although these compounds are thought to be formed from the reaction of phytol with bound phenols (Li *et al.*, 1995). Archaebacterial ether lipids have been suggested as precursors for Ph (Risatti *et al.*, 1984; Rowland, 1990; Navale, 1994). Second, sulphur-bound Ph has been shown to be abundant in polar fractions, asphaltenes and kerogens of immature sedimentary rocks and 'low thermal stress' crude oils (see for a review Sinninghe Damsté and de Leeuw, 1990). These sequestered Ph skeletons probably originate from natural sulphurisation of phytol or its diagenetic derivatives (Brassell *et al.*, 1986b; Kohnen *et al.*, 1992a), as supported by laboratory sulphurisation experiments (de Graaf *et al.*, 1992; Krein and Aizenshtat, 1994). Maturation of these immature samples may induce preferential thermal cleavage of relatively weak C-S bonds, resulting in the formation of free Ph and organic sulphur compounds (OSC) with a Ph carbon skeleton (*e.g.* alkylthiophenes; Krein and Aizenshtat, 1994; Schouten *et al.*, 1994; Koopmans *et al.*, 1995, 1996b, 1997d), thus strongly influencing the Pr/Ph ratio. Third, the Pr/Ph ratio has been demonstrated to change significantly with increasing thermal stress both in laboratory experiments (Connan, 1974; Lewan *et al.*, 1979; Alexander *et al.*, 1981; Evans and Felbeck, 1983) and in natural maturity sequences (Brooks *et al.*, 1969; Tissot *et al.*, 1971; Rashid, 1979; Radke *et al.*, 1980; Snowdon, 1980; Requejo, 1994; Dzou *et al.*, 1995). However, absolute concentrations of Pr and Ph are not always reported, which makes it difficult to determine the cause of this change.

In this study, we aim at (i) determining the precursors of Pr and Ph in several sedimentary rocks from different depositional environments, and (ii) investigating the maturity dependence of the Pr/Ph ratio. To this end, we first determine the Pr and Ph potential of the unheated rocks by hydrous pyrolysis experiments. Then, the high-molecular-weight (HMW) precursors of Pr and Ph are characterised by selective chemical degradation of the polar fraction and the kerogen of the unheated samples, and their amounts are compared to the Pr and Ph potential. In addition, flash pyrolysis analyses of

(i) kerogens, (ii) residues after extraction of artificially matured samples, and (iii) residues after chemical degradation of the kerogen of the unheated samples are carried out to identify HMW precursors of Pr and Ph.

6.3 Experimental

Samples. The samples used in this study are from the (i) Gessoso-solfifera Formation (Late Miocene), (ii) Ghareb Formation (Late Cretaceous), and (iii) Green River Formation (Late Eocene). The first two samples represent marine settings, the last represents a lacustrine setting. A description of the samples, including some key references, is given in Table 6.1.

Hydrous pyrolysis. The experimental procedures of a typical hydrous pyrolysis experiment have been described elsewhere (Lewan, 1993b). A one-litre Hastelloy-C276 reactor was filled with rock chips and distilled water. The remaining volume was purged and filled with helium at a pressure of 2.4 bar. Artificial maturation was accomplished by heating rock chips isothermally for 72 h. The experimental conditions used for each sample are described in Table 6.2. Temperatures were continuously monitored at 30 s intervals. Standard deviations were between ±0.2 and ±0.3°C for all experiments except for the 160°C experiment which had a standard deviation of ±0.6°C. Any expelled oil was recovered from the water surface with a pipette. Reactor walls and rock chips were rinsed with benzene to recover any sorbed oil films. Residual rock chips were dried in a vacuum oven ($T \leq 50°C$).

Extraction, fractionation and kerogen preparation. Residual rock chips were freeze-dried and ultrasonically or Soxhlet extracted with dichloromethane/methanol (7.5:1

Table 6.1. Sample description.

Formation name	*Location*	*Age*	*Lithology*	*Setting*
Gessoso-solfifera	Italy	Late Miocene	Marlstone	Lagoonal
Ghareb	Jordan	Late Cretaceous	Limestone	Shallow marine
Green River	USA	Late Eocene	Dolomitic marlstone	Lacustrine

Formation name	*Kerogen Type*	*TOC (%)*	*R_o (%)*	*Reference*
Gessoso-solfifera	II-S	2.0	0.25	Vai and Ricci Lucchi (1977)
Ghareb	II-S	17.9	0.39[a]	Hufnagel (1984)
Green River	I	15.2	0.44[a]	Katz (1995)

[a] Determined from the Pristane Formation Index (Goossens *et al.*, 1988a,b).

Table 6.2. Experimental conditions during hydrous pyrolysis.

Sample	*Rock chips (g)*	*Distilled water (g)*	*T (°C)*
Gessoso-solfifera Fm.	90-100	450	160, 180, ..., 300, 330
Ghareb Fm.	300	350	200, 220, ..., 360
Green River Fm.	200	400	240, 255, ..., 300, 330, 350

v/v). If a sorbed or expelled oil was present, it was combined with the extract. For some samples, the combined extract was directly fractionated by column chromatography with Al_2O_3 to obtain the saturated hydrocarbon fraction (hexane/dichloromethane 9:1 v/v). For other samples, a more laborious fractionation scheme was followed. First, the combined extract was separated into a maltene and an asphaltene fraction by repeated (x3) precipitation in heptane (40-fold excess). Then, an aliquot of the maltene fraction (*c.* 250 mg), to which four internal standards [6,6-d_2-3-methylhenicosane, 2,3-dimethyl-5-(1',1'-d_2-hexadecyl)thiophene, 2-methyl-2-(4,8,12-trimethyltridecyl)chroman and 2,3-dimethyl-5-(1',1'-d_2-hexadecyl)thiolane] were added for quantitative analysis, was fractionated by column chromatography with Al_2O_3 into an apolar and a polar fraction by elution with hexane/dichloromethane (9:1 v/v) and dichloromethane/methanol (1:1 v/v), respectively (Fig. 6.1). Further separation of the apolar fraction by argentatious thin-layer chromatography yielded the saturated hydrocarbon fraction (R_f = 0.9-1.0), the alkylthiophene fraction (R_f = 0.4-0.9), the benzothiophene fraction (R_f = 0.05-0.4), and the alkylsulphide fraction (R_f = 0.0-0.05) (Fig. 6.1).

The extracted rock residues of the original samples from the Gessoso-solfifera and Green River Formations were demineralised using standard procedures (Lewan *et al.*, 1986) to yield the kerogens. The extracted rock residue of the original sample from the Ghareb Formation was decalcified by reaction with HCl. The extracted rock residues of several heated samples were re-extracted ultrasonically with methanol (x1), methanol/dichloromethane (1:1 v/v; x1), and dichloromethane (x3) for flash pyrolysis GC analysis.

Chemical degradation of polar fractions. Polar fractions were desulphurised with Raney Ni (Sinninghe Damsté *et al.*, 1988b) (Fig. 6.1). Before desulphurisation, a known amount of a synthetic standard [2,3-dimethyl-5-(1',1'-d_2-hexadecyl)thiophene] was added to a known amount (10-20 mg) of polar fraction. Desulphurisation was accomplished by dissolving the polar fraction in 4 ml of ethanol, and repeatedly (x3) adding a small amount of Raney Ni. The mixture was allowed to reflux for 1.5 h. A sodium chloride solution was added, and the reaction mixture was extensively extracted with dichloromethane. Column chromatography using Al_2O_3 yielded the released hydrocarbons (hexane/dichloromethane 9:1 v/v) which were subsequently hydrogenated (Sinninghe Damsté *et al.*, 1988b), and the residual polar fraction (dichloromethane/methanol 1:1 v/v).

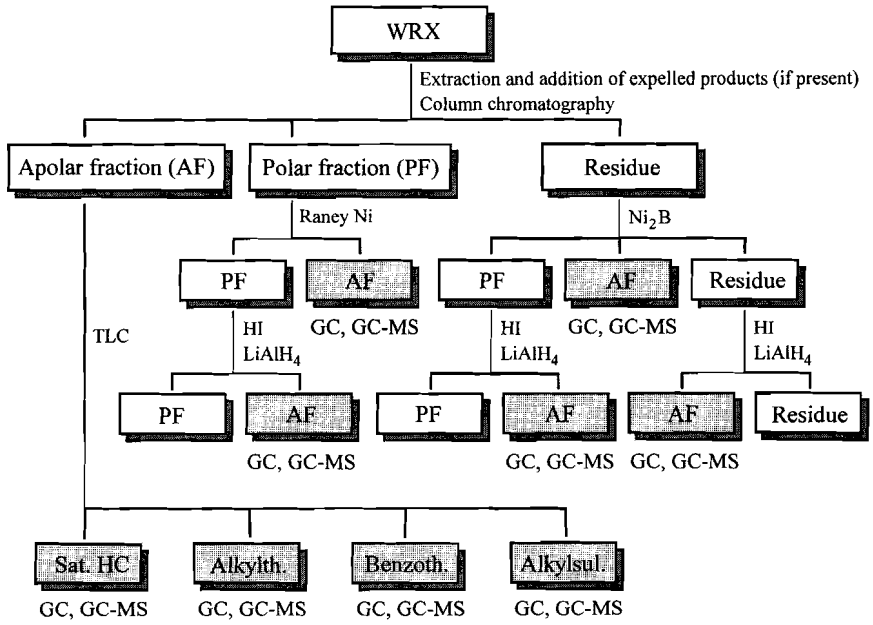

Fig. 6.1. Analytical flow diagram. The hatched boxes indicate fractions analysed by GC and GC-MS.

Residual polar fractions were treated with HI in order to cleave C-O bonds (March, 1985) (Fig. 6.1). A known amount of a synthetic standard [2,3-dimethyl-5-(1',1'-d_2-hexadecyl)thiophene] was added to a known amount (10-20 mg) of residual polar fraction. Cleavage of C-O bonds was accomplished by dissolving the residual polar fraction in 4 ml of a 57% solution of HI in water, and refluxing for 1 h. The reaction mixture was allowed to cool, and was neutralised with excess water and a 5% $Na_2S_2O_3$ solution in water before it was extensively extracted with hexane. Column chromatography using Al_2O_3 yielded the released alkyliodides (hexane/dichloromethane 9:1 v/v), and a residual fraction (dichloromethane/methanol 1:1 v/v).

Alkyliodides released after HI treatment of residual polar fractions were reduced using $LiAlH_4$ (Johnson *et al.*, 1948) (Fig. 6.1). The sample was dissolved in 4 ml of 1,4-dioxane, and subsequently 75 mg of $LiAlH_4$ was added. The mixture was allowed to reflux for 1.5 h. After the reaction mixture had cooled, ethyl acetate was added to destroy any excess $LiAlH_4$. Then water was added, and the reaction mixture was extensively extracted with hexane. Column chromatography using Al_2O_3 yielded the alkanes (hexane/dichloromethane 9:1 v/v). $LiAlH_4$ treatment modified the deuterated internal standard, 2,3-dimethyl-5-(1',1'-d_2-hexadecyl)thiophene, to 2,3-dimethyl-5-hexadecylthiophene.

Chemical degradation of kerogens. Kerogens were desulphurised with Ni_2B instead of

Raney Ni (Fig. 6.1), because the efficiency of Ni_2B for the desulphurisation of geomacromolecules is higher (Schouten *et al.*, 1993; Hefter *et al.*, 1995). Before desulphurisation, a known amount of a synthetic standard [2,3-dimethyl-5-(1',1'-d_2-hexadecyl)thiophene] was added to a known amount (*c.* 50 mg) of kerogen. After the addition of 10 ml of a tetrahydrofuran/methanol (1:1 v/v) mixture, desulphurisation was accomplished by adding 500 mg of $NiCl_2$ and 500 mg of $NaBH_4$. The mixture was allowed to reflux for 24 h. A sodium chloride solution was added, and the reaction mixture was extensively extracted with dichloromethane. Column chromatography using Al_2O_3 yielded the released hydrocarbons (hexane/dichloromethane 9:1 v/v) and the released polar fraction (dichloromethane/methanol 1:1 v/v). The released polar fraction was then treated with $HI/LiAlH_4$ as described in the previous section.

The residue was treated with HNO_3 (65 %) to dissolve Ni salts. HI degradation of the residual organic matter was achieved following the procedure described above (24 h). A standard [2,3-dimethyl-5-(1',1'-d_2-hexadecyl)thiophene] was added for quantitative analysis. The released alkyliodides were reduced with $LiAlH_4$ as described above (Fig. 6.1). Residues after chemical degradation were re-extracted ultrasonically with methanol (x1), methanol/dichloromethane (1:1 v/v; x1), and dichloromethane (x3) for flash pyrolysis GC analysis.

In addition, the kerogen from the Gessoso-solfifera Formation was saponified as described previously (Goossens *et al.*, 1989). A standard [2,3-dimethyl-5-(1',1'-d_2-hexadecyl)thiophene] was added for quantitative analysis.

Gas chromatography. Gas chromatography (GC) was performed using a Hewlett-Packard 5890 instrument, equipped with an on-column injector. A fused silica capillary column (25 m x 0.32 mm) coated with CP Sil-5 (film thickness 0.12 μm) was used with helium as carrier gas. The column effluent was monitored by a flame ionisation detector (FID). Samples were injected at 70°C and the oven was subsequently programmed to 130°C at 20°C/min and then at 4°C/min to 320°C, at which it was held for 20 min.

Gas chromatography-mass spectrometry. Gas chromatography-mass spectrometry (GC-MS) was carried out on a Hewlett-Packard 5890 gas chromatograph interfaced to a VG Autospec Ultima mass spectrometer operated at 70 eV with a mass range m/z 40-800 and a cycle time of 1.8 s (resolution 1000). The gas chromatograph was equipped with a fused silica capillary column (25 m x 0.32 mm) coated with CP Sil-5 (film thickness 0.12 μm). Helium was used as carrier gas. Samples were injected at 60°C and the oven was subsequently programmed to 130°C at 20°C/min and then at 4°C/min to 310°C, at which it was held for 20 min.

Flash pyrolysis gas chromatography-mass spectrometry. Py-GC-MS analyses were carried out on a Hewlett-Packard 5890 gas chromatograph equipped with a FOM-31X unit for pyrolysis and interfaced to a VG Autospec Ultima mass spectrometer. The

operating conditions for the MS were identical to those described above for GC-MS. The samples were applied to a ferromagnetic wire with a Curie temperature of 610°C. The gas chromatograph, equipped with a cryogenic unit, was programmed from 0°C (5 min) to 320°C (20 min) at a rate of 3°C/min. Separation was achieved using a fused silica capillary column (25 m x 0.32 mm) coated with CP Sil-5 (film thickness 0.4 μm). Helium was used as carrier gas.

Isotope-ratio-monitoring gas chromatography-mass spectrometry. The DELTA-C irm-GC-MS system is, in principle, similar to the DELTA-S system described previously (Hayes *et al.*, 1990). The gas chromatograph (Hewlett-Packard 5890) was equipped as for GC-MS analyses with helium as carrier gas. Hydrocarbon fractions were chromatographed over silica-lite with cyclohexane to remove linear alkanes. They were subsequently injected on-column at 70°C and the oven was programmed as for GC analyses. Isotopic values were calculated by integrating the mass 44, 45 and 46 ion currents of the peaks produced by combustion of the chromatographically separated compounds and of CO_2-spikes generated by admitting CO_2 of a known ^{13}C content at regular intervals into the mass spectrometer. Values were determined at least in duplicate. Results were averaged to obtain mean values and to calculate standard deviations. The stable carbon isotope compositions are reported in the delta notation against the PDB ^{13}C standard.

Quantitation. Pr and Ph present in saturated hydrocarbon fractions and released after desulphurisation of polar fractions and kerogens were quantitated by integration of their peak areas and that of the internal standard (6,6-d_2-3-methylhenicosane) in the FID trace. Pr and Ph released after HI/$LiAlH_4$ treatment of residual polar fractions and kerogens were quantitated by integration of their peak areas and that of the modified internal standard (2,3-dimethyl-5-hexadecylthiophene) in the FID trace. Results reported for the 260 and 280°C experiments with the sample from the Gessoso-solfifera Formation are averages of duplicate runs (Koopmans *et al.*, 1996b). The standard deviation is typically *c.* 25%, although the results for some fractions differed more.

6.4 Results

Absolute amounts of Pr and Ph carbon skeletons

Free Pr and Ph in the saturated hydrocarbon fraction

Full descriptions of the saturated hydrocarbon fractions of the samples from the Gessoso-solfifera, Ghareb and Green River Formations have been given elsewhere (Koopmans *et al.*, 1996b, 1997a,d). Here, we will focus on the maturity-related abundance of Pr and Ph. They are present in different amounts in the unheated samples (Fig. 6.2). Artificial maturation up to a certain 'critical' temperature (T_c; indicated in Fig. 6.2 with a stippled line) leaves the amounts of Pr and Ph relatively constant (Fig. 6.2). For

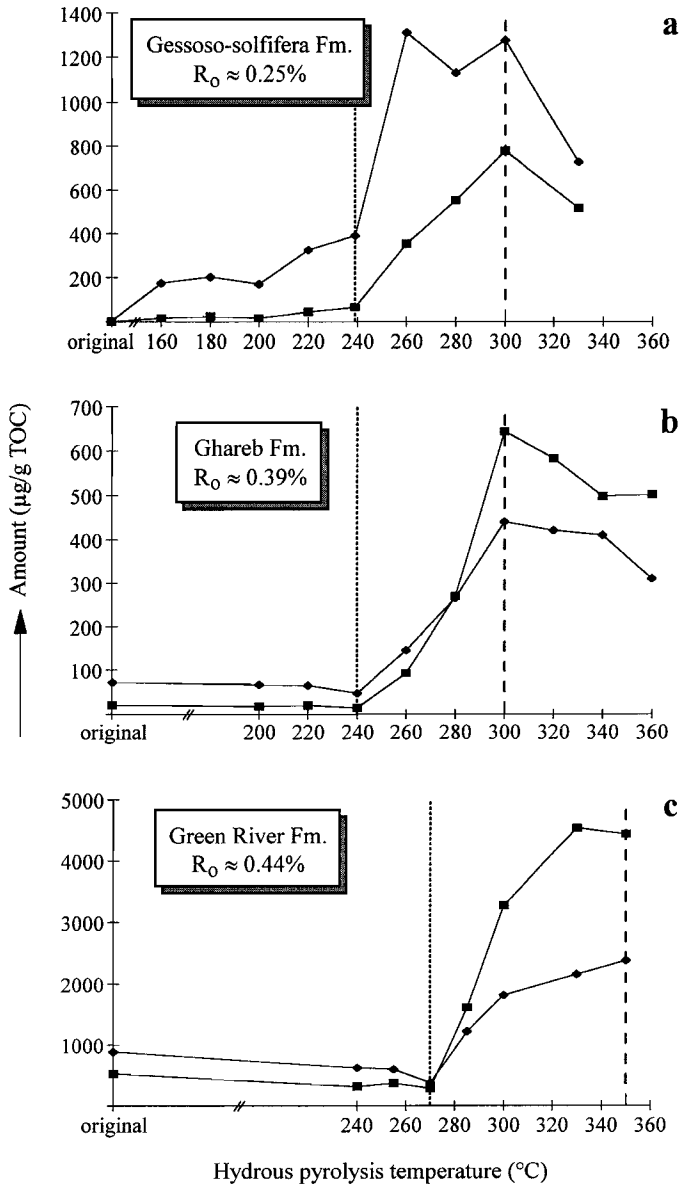

Fig. 6.2. Generation profiles of Pr (squares) and Ph (diamonds) in the samples from the (**a**) Gessoso-solfifera, (**b**) Ghareb, and (**c**) Green River Formations. The stippled line indicates the 'critical temperature' T_c, after which the amounts of Pr and Ph increase abundantly. The dashed line indicates T_{max}, the temperature at which the Pr and Ph concentrations reach their maximum values. In (**a**), T_c refers to the generation profile of Pr only, because generation of Ph has already occurred at 160°C, so that $T_{c\,(Ph)} < 160°C$.

the sample from the Gessoso-solfifera Formation, it should be noted that the indicated T_c refers only to Pr (Fig. 6.2**a**), because abundant generation of Ph has already occurred at 160°C, so that $T_{c\,(Ph)} < 160°C$. For the samples from the Ghareb and Green River Formations, the amounts of Pr and Ph actually decrease slightly up to T_c. Therefore, the water collected from several hydrous pyrolysis experiments was extracted with dichloromethane to check if Pr and Ph had dissolved in it. However, no hydrocarbons could be detected. T_c is different for each sample and positively correlated with (i) the level of thermal maturity, and (ii) the amount of Pr and Ph already present in the original sample relative to the maximum amount of Pr and Ph generated (Fig. 6.2). When the samples are heated at $T > T_c$, large amounts of Pr and Ph are generated. At the highest maturation temperatures, the amounts of Pr and Ph are relatively constant or decrease.

OSC with Pr and Ph carbon skeletons

The generation of alkylthiophenes and alkylsulphides with the Ph carbon skeleton in the maturation series of the sample from the Gessoso-solfifera Formation has been described in detail elsewhere (Koopmans *et al.*, 1995, 1996b). The alkylthiophenes with the Ph carbon skeleton, whose relative amounts increase with increasing thermal maturation, were considered to be stable thermal degradation products of sulphur-bound Ph (Koopmans *et al.*, 1996b). OSC with the Pr carbon skeleton were not detected. The summed amount of low-molecular-weight (LMW) Pr and Ph carbon skeletons (free hydrocarbons plus OSC) in the Gessoso-solfifera maturation series is shown in Fig. 6.3**a** and **b**. The Pr and Ph potential, which is defined as the maximum amount of LMW Pr and Ph carbon skeletons generated minus the amount present in the original sample, is indicated with a doubleheaded arrow.

In the Ghareb maturation series, OSC with Pr and Ph carbon skeletons were encountered in the alkylthiophene, alkylbenzothiophene and alkylsulphide fractions, as described elsewhere (Koopmans *et al.*, 1997d). The alkylthiophene fraction contains three alkylthiophenes with a Pr carbon skeleton, which were tentatively identified by mass spectrometry as **I-III** (Fig. 6.4). Of these, only **II** has been reported before (Sinninghe Damsté *et al.*, 1987c). The isomer distribution of the alkylthiophenes with a Pr carbon skeleton does not change significantly with increasing thermal maturation. These compounds may be formed from sulphur incorporation into pristenes, pristadienes and pristatrienes known to occur in zooplankton (Blumer and Thomas, 1965; Blumer *et al.*, 1969). The compounds in the benzothiophene fraction are probably di- and/or bithiophenes, because desulphurisation of this fraction yielded free Pr and Ph, amongst other saturated hydrocarbons (Koopmans *et al.*, 1997d). Three bithiophenes with a Ph carbon skeleton were indeed identified (Koopmans *et al.*, 1997d). The increasing relative amounts of alkylthiophenes with a Ph carbon skeleton suggested that they can be regarded as stable thermal degradation products of sulphur-bound phytane (Koopmans *et al.*, 1997d). The summed amount of LMW Pr and Ph carbon skeletons in the Ghareb maturation series is shown in Fig. 6.3**c** and **d**. Alkylsulphoxides, which are believed to be

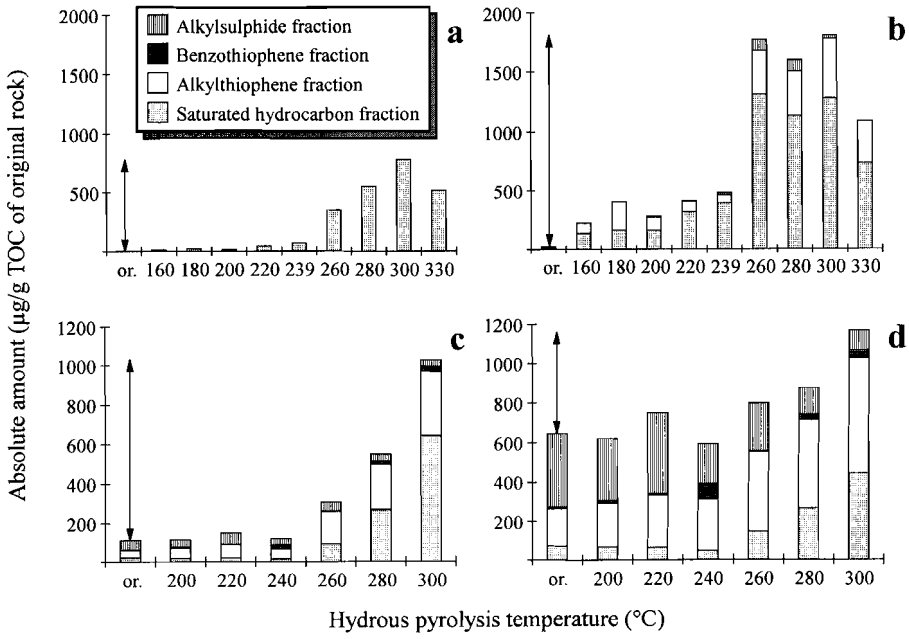

Fig. 6.3. Bar plots showing summed amount of LMW Pr and Ph carbon skeletons (free hydrocarbons plus OSC). (**a**) Pr in the Gessoso-solfifera Formation, (**b**) Ph in the Gessoso-solfifera Formation, (**c**) Pr in the Ghareb Formation, (**d**) Ph in the Ghareb Formation. Doubleheaded arrows indicate the Pr and Ph potential.

formed from alkylsulphides by post-depositional oxidation or by oxidation during sample storage (Payzant *et al.*, 1983; Kohnen *et al.*, 1990b; Schouten *et al.*, 1995e), are included with the alkylsulphides. The Pr and Ph potential is indicated by a doubleheaded arrow.

In the original sample from the Green River Formation, OSC with Pr and Ph carbon skeletons could not be detected. Therefore, the artificially matured samples were not investigated for these compounds.

Pr and Ph carbon skeletons sequestered in the polar fraction

Polar fractions of the unheated samples and several artificially matured samples from the Gessoso-solfifera, Ghareb and Green River Formations were studied by sequential chemical degradation using Raney Ni and HI/$LiAlH_4$, to analyse sulphur-bound carbon skeletons, and oxygen-bound and both sulphur- and oxygen-bound carbon skeletons, respectively. Absolute amounts of Pr and Ph released are listed in Tables 6.3 and 6.4. The total amounts released from the polar fractions of the unheated samples are illustrated in Fig. 6.5 by the hatched bars.

The amount of Ph released from the polar fraction of the original sample from the

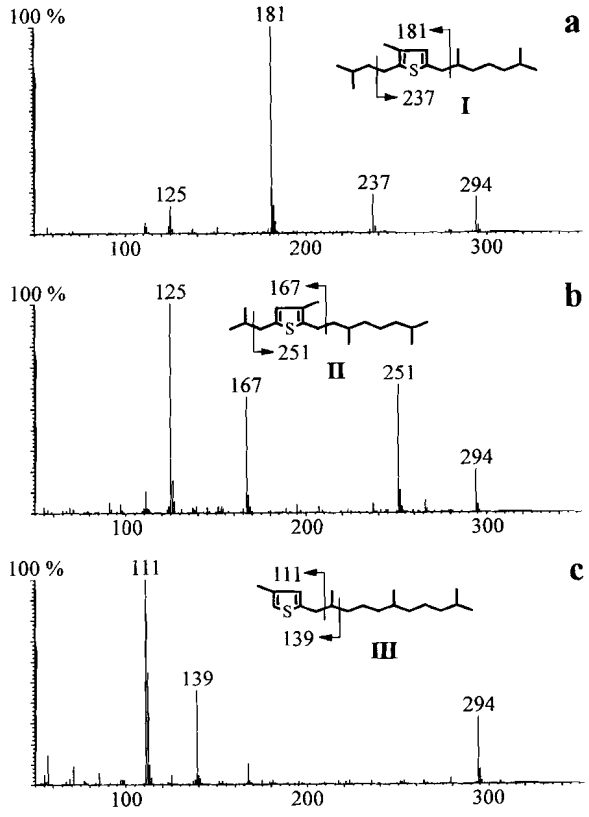

Fig. 6.4. Mass spectra (subtracted for background) of three alkylthiophenes with a Pr carbon skeleton in the alkylthiophene fraction of the sample of the Ghareb Formation heated at 200°C. The high relative intensity of the fragment ion at m/z 125 in (**b**) is due to coelution with 2-ethyl-5-undecylthiophene.

Gessoso-solfifera Formation exceeds the amount of Pr by two orders of magnitude (Fig. 6.5**a**). The amount of Ph released after desulphurisation of the polar fraction decreases with increasing maturation temperature (Table 6.3), suggesting that sulphur-bound Ph is thermally released already at low temperatures. The polar fraction of the unheated sample from the Gessoso-solfifera Formation was also derivatised with BSTFA. This yielded the TMS ether of dihydrophytol (*c.* 70 μg Ph/g TOC) and diphytanyl glyceryl ether (*c.* 680 μg Ph/g TOC). The latter compound is a known constituent of archaebacteria (de Rosa and Gambacorta, 1988), and a suspected source of both Pr and Ph (Risatti *et al.*, 1984; Rowland, 1990; Navale, 1994). The summed amount of the Ph carbon skeleton in these two compounds compares well with the amount of Ph released after treatment of the desulphurised polar fraction with $HI/LiAlH_4$, which also reduces alcohols.

The amounts of Pr and Ph released from the polar fraction of the unheated sample

Table 6.3. Absolute amounts (μg/g TOC of original rock) of Pr and Ph released by Raney Ni treatment of the polar fraction as a function of hydrous pyrolysis temperature (°C).

		original	160	180	200	220	239	240	260	270	280	285	300	330
Gessoso-	*Pr*	7	10	11	11	15	11	na[a]	19	na	9	na	14	6
solfifera Fm.	*Ph*	$4.1x10^2$	$3.2x10^2$	$3.2x10^2$	$3.4x10^2$	$3.0x10^2$	$2.1x10^2$	na	$2.6x10^2$	na	$1.2x10^2$	na	$1.5x10^2$	$2.0x10^2$
Ghareb	*Pr*	12	na	na	13	6	na	5	10	na	39	na	32	na
Fm.	*Ph*	72	na	na	49	22	na	17	36	na	$1.3x10^2$	na	70	na
Green River	*Pr*	3	na	na	na	na	na	nd[b]	na	3	na	3	nd	nd
Fm.	*Ph*	14	na	na	na	na	na	nd	na	12	na	16	nd	nd

[a] na = not applicable.

[b] nd = not determined.

from the Ghareb Formation are low (Fig. 6.5**b**), as is the case for the Green River Formation (Fig. 6.5**c**). Note that, especially for the Green River Formation, the amounts of Pr and Ph released from the polar fraction are much smaller than the Pr and Ph potential (indicated by the double-headed arrows in Fig. 6.5), which is defined as the maximum amount of free Pr and Ph generated minus the amount present in the original sample.

Pr and Ph carbon skeletons sequestered in the kerogen

Kerogens of the unheated samples from the Gessoso-solfifera, Ghareb and Green River Formations were studied by chemical degradation using Ni_2B and $HI/LiAlH_4$, to analyse sulphur-bound carbon skeletons, and oxygen-bound and both sulphur- and oxygen-bound carbon skeletons, respectively. Amounts of Pr and Ph released are listed in Table 6.5 and visualised in Fig. 6.5. In addition, (i) the kerogens of the unheated samples, (ii) the residues after chemical degradation of the kerogens of the unheated samples, and (iii) the re-extracted residues obtained after extraction of the artificially matured rock samples were studied by flash pyrolysis.

For the Gessoso-solfifera Formation, the chemical degradation results of the kerogen of the unheated sample are similar to those of the polar fraction, *i.e.* large amounts of Ph and only small amounts of Pr are released (Fig. 6.5**a**). Saponification of the kerogen and derivatisation of the released products yielded the TMS ethers of dihydrophytol (*c.* 200 μg Ph/g TOC) and diphytanyl glyceryl ether (*c.* 380 μg Ph/g TOC). The summed amount of the Ph carbon skeleton in these two compounds compares well with the amount of Ph released from the kerogen by $HI/LiAlH_4$ treatment (*c.* 850 μg Ph/g TOC; Table 6.5), which also reduces the alcohol part of esters. Flash pyrolysis of the kerogen of the unheated sample yields abundant prist-1-ene and phytenes, and a smaller amount of prist-2-ene (Fig. 6.6**a**). After hydrous pyrolysis at 200°C, the phytenes have decreased dramatically relative to the *n*-alkenes/*n*-alkanes (Fig. 6.6**b**). With increasing level of thermal maturity, the relative amount of prist-1-ene decreases gradually until it is

Table 6.4. Absolute amounts (μg/g TOC of original rock) of Pr and Ph released by HI/$LiAlH_4$ treatment of the desulphurised polar fraction as a function of hydrous pyrolysis temperature (°C).

		original	160	180	200	220	239	260	270	280	285	300	330
Gessoso-solfifera	*Pr*	1	1	2	2	4	4	4	na[a]	8	na	15	0
Formation	*Ph*	$6.6x10^2$	$1.9x10^2$	$3.0x10^2$	$3.5x10^2$	$4.1x10^2$	$2.5x10^2$	$1.9x10^2$	na	$1.3x10^2$	na	$1.3x10^2$	42
Ghareb	*Pr*	4	na	na	nd[b]	nd	na	12	na	nd	na	nd	na
Formation	*Ph*	13	na	na	nd	nd	na	37	na	nd	na	nd	na
Green River	*Pr*	7	na	na	na	na	na	na	2	na	4	nd	nd
Formation	*Ph*	11	na	na	na	na	na	na	4	na	5	nd	nd

[a] na = not applicable.

[b] nd = not determined.

not detectable anymore in the sample heated at 300°C (Fig. 6.6). Flash pyrolysis of the residue after Ni_2B desulphurisation of the kerogen of the unheated sample yields pristenes and phytenes in approximately the same relative amount as in the flash pyrolysate of the untreated kerogen (not shown). This is in contrast with results obtained by Gelin *et al.* (1996b), who desulphurised kerogens from the Gessoso-solfifera Formation with $Li/EtNH_2$ and noted a selective removal of phytenes from the flash pyrolysate after desulphurisation. This may indicate that the Ni_2B desulphurisation of the kerogen was not effective. Subsequent HI/$LiAlH_4$ treatment of the desulphurised kerogen removes the precursors of prist-1-ene and the phytenes, as evidenced by their absence in the flash pyrolysate, although the relative amount of prist-2-ene remains unchanged (Fig. 6.7**b**). Flash pyrolysis of the residue after direct HI/$LiAlH_4$ treatment of the kerogen of the unheated sample yields decreased amounts of prist-1-ene and the phytenes, and a relatively unchanged amount of prist-2-ene (Fig. 6.7**c**). Thus, the relative amounts of prist-1-ene and prist-2-ene are unaffected by Ni_2B desulphurisation, but HI/$LiAlH_4$ treatment decreases the relative amount of prist-1-ene while the relative amount of prist-2-ene remains constant.

Chemical degradation of the kerogen of the unheated sample from the Ghareb Formation releases comparable amounts of Pr and Ph (Fig. 6.5**b**). Flash pyrolysis of the kerogen of the unheated sample yields prist-1-ene, but no phytenes (Fig. 6.8**a**). With increasing level of thermal maturity, flash pyrolysis of the extracted residues yields lower amounts of prist-1-ene, particularly at maturation temperatures in the 260-300°C range (Fig. 6.8). Flash pyrolysis of the residue after Ni_2B desulphurisation of the kerogen of the unheated sample does not yield prist-1-ene (Fig. 6.9), and subsequent HI/$LiAlH_4$ treatment does not alter this.

The amounts of Pr and Ph released by chemical degradation of the kerogen of the unheated sample from the Green River Formation are much lower than the Pr and Ph potential (Fig. 6.5**c**). Flash pyrolysis of the kerogen of the unheated sample yields abun-

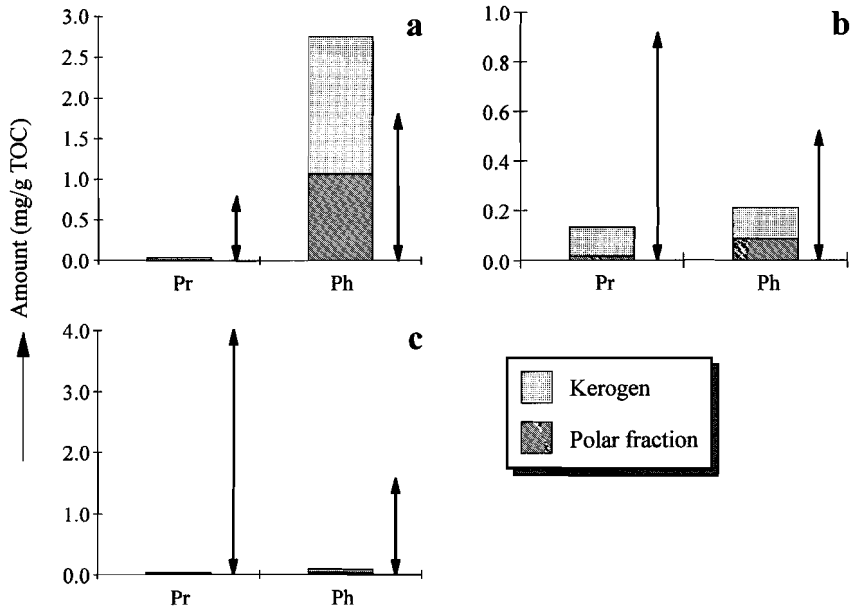

Fig. 6.5. Absolute amounts (mg/g TOC) of Pr and Ph released by chemical degradation from the polar fraction and the kerogen of the unheated samples from the (**a**) Gessoso-solfifera, (**b**) Ghareb, and (**c**) Green River Formations. The double-headed arrows indicate the Pr and Ph potential (see Fig. 6.3).

dant prist-1-ene, and a smaller amount of prist-2-ene (Fig. 6.10**a**). With increasing level of thermal maturity, the relative amounts of prist-1-ene and prist-2-ene decrease (Fig. 6.10). Flash pyrolysis of the residue after Ni_2B desulphurisation of the kerogen of the unheated sample lowers the relative amount of prist-1-ene considerably (Fig. 6.11**b**). Flash pyrolysis of the residue after subsequent HI/$LiAlH_4$ treatment leaves the relative amount of prist-1-ene unchanged, whereas the relative amount of prist-2-ene increases (Fig. 6.11**c**). Flash pyrolysis of the residue after direct HI/$LiAlH_4$ treatment of the kerogen of the unheated sample also lowers the relative amount of prist-1-ene, whereas the relative amount of prist-2-ene increases abundantly (Fig. 6.11**d**).

^{13}C contents of Pr and Ph

Although $\delta^{13}C$ values of Pr and Ph in more mature sedimentary rocks and crude oils are often virtually identical (*e.g.* Collister *et al.*, 1992; Kenig *et al.*, 1994; Li *et al.*, 1995; Hughes *et al.*, 1995), stable carbon isotope measurements of Pr and Ph in immature sedimentary rocks have led to recognition of distinct sources (Freeman *et al.*, 1990; Hughes *et al.*, 1995; Schouten *et al.*, 1996). Therefore, $\delta^{13}C$ values of free and bound Pr

Table 6.5. Amounts (μg/g TOC) of Pr and Ph released by chemical degradation from the kerogen of the unheated samples.

		KG/NB[a]	KG/NB/PF/HI[b]	KG/NB/RES/HI[c]
Gessoso-solfifera Formation	*Pr*	17	6	11
	Ph	$8.3x10^2$	$1.5x10^2$	$7.0x10^2$
Ghareb Formation	*Pr*	3	6	$1.1x10^2$
	Ph	10	4	$1.1x10^2$
Green River Formation	*Pr*	1	5	13
	Ph	9	13	36

[a] Ni_2B desulphurisation of the kerogen.

[b] $HI/LiAlH_4$ treatment of the polar fraction released after desulphurisation of the kerogen.

[c] $HI/LiAlH_4$ treatment of the residue after desulphurisation of the kerogen.

and Ph in the samples from the Gessoso-solfifera, Ghareb and Green River Formations were determined.

Saturated hydrocarbon fractions

$\delta^{13}C$ values of Pr and Ph as a function of maturation temperature in the samples from the Gessoso-solfifera, Ghareb and Green River Formations are shown in Fig. 6.12.

The $\delta^{13}C$ value of Pr in the Gessoso-solfifera Formation is influenced by coelution with 2,6,10-trimethyl-7-(3-methylbutyl)dodecane. However, the latter is not generated during hydrous pyrolysis (Koopmans *et al.*, 1996b), so that its abundance relative to that of Pr decreases with increasing maturation temperature. Knowing the amounts of Pr and 2,6,10-trimethyl-7-(3-methylbutyl)dodecane in the original sample and after heating at 220°C (Koopmans *et al.*, 1996b), and assuming that the $\delta^{13}C$ value of Pr does not change significantly upon heating at this low temperature, the $\delta^{13}C$ value of Pr in the original sample can be estimated at -28.3‰. Ph in the Gessoso-solfifera Formation becomes enriched in ^{13}C with increasing maturation temperature, suggesting an input from an isotopically relatively heavy HMW source. It should be noted, however, that destruction of the Ph carbon skeleton, which takes place between 300 and 330°C (Fig. 6.2), is probably accompanied by a kinetic isotope effect resulting in relatively heavy Ph (Fig. 6.12), as observed previously by Bjorøy *et al.* (1992).

The $\delta^{13}C$ values of Pr and Ph in the Ghareb and Green River Formations do not change significantly with increasing maturation temperature (Fig. 6.12), suggesting that the HMW precursors of Pr and Ph have similar $\delta^{13}C$ values as the free Pr and Ph originally present. The enriched values of Pr and Ph in the Green River Formation at 350°C as compared to the values at 330°C may be due to destruction of their carbon skeletons, although their generation profiles show no sign of such a process (Fig. 6.2).

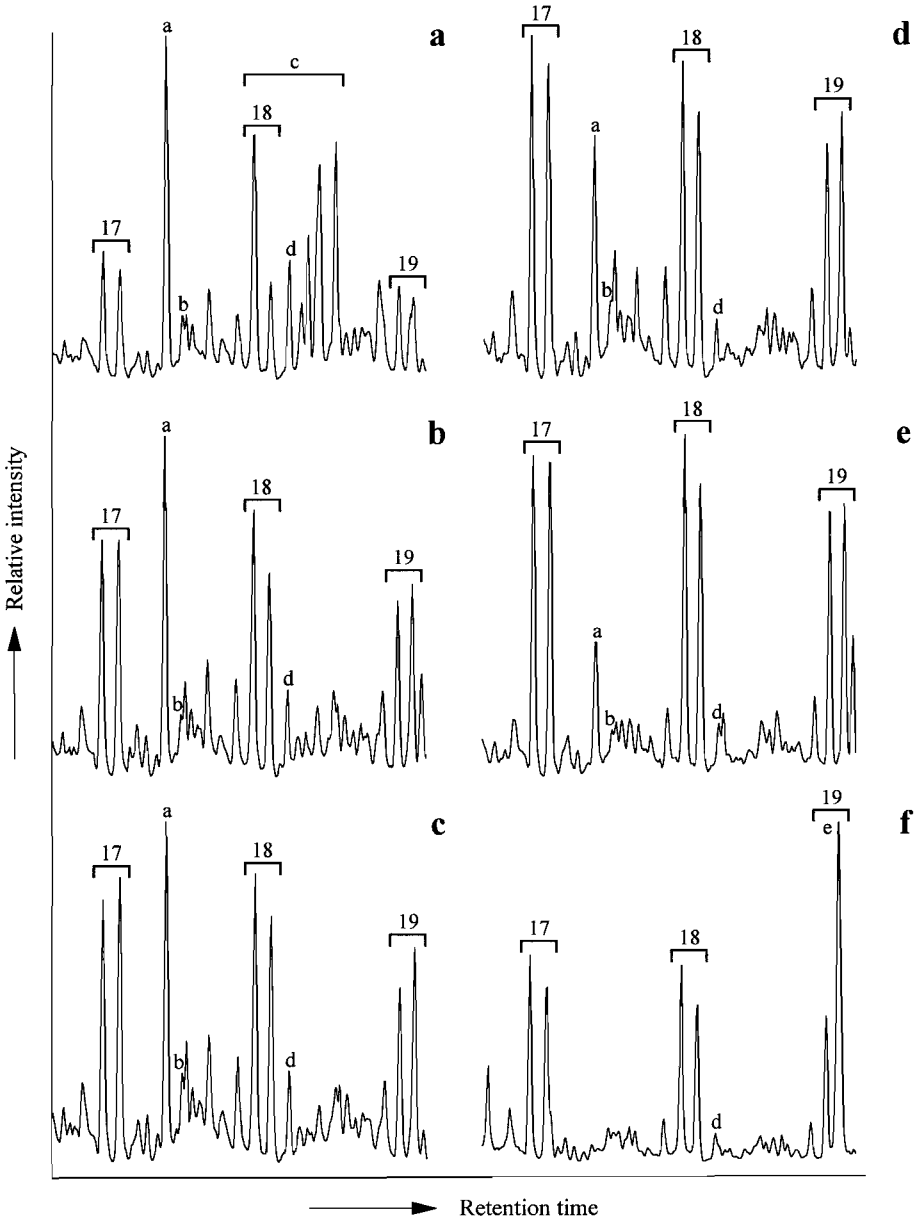

Fig. 6.6. Partial TIC of the flash pyrolysate of (**a**) the kerogen of the unheated sample from the Gessoso-solfifera Formation, and the residues after extraction of the samples artificially matured at (**b**) 200, (**c**) 220, (**d**) 260, (**e**) 280 and (**f**) 300°C. Key: numbers indicate number of carbon atoms of *n*-alk-1-ene/*n*-alkane doublets, a = prist-1-ene, b = prist-2-ene, c = phytene, d = Ph, e = elemental sulphur

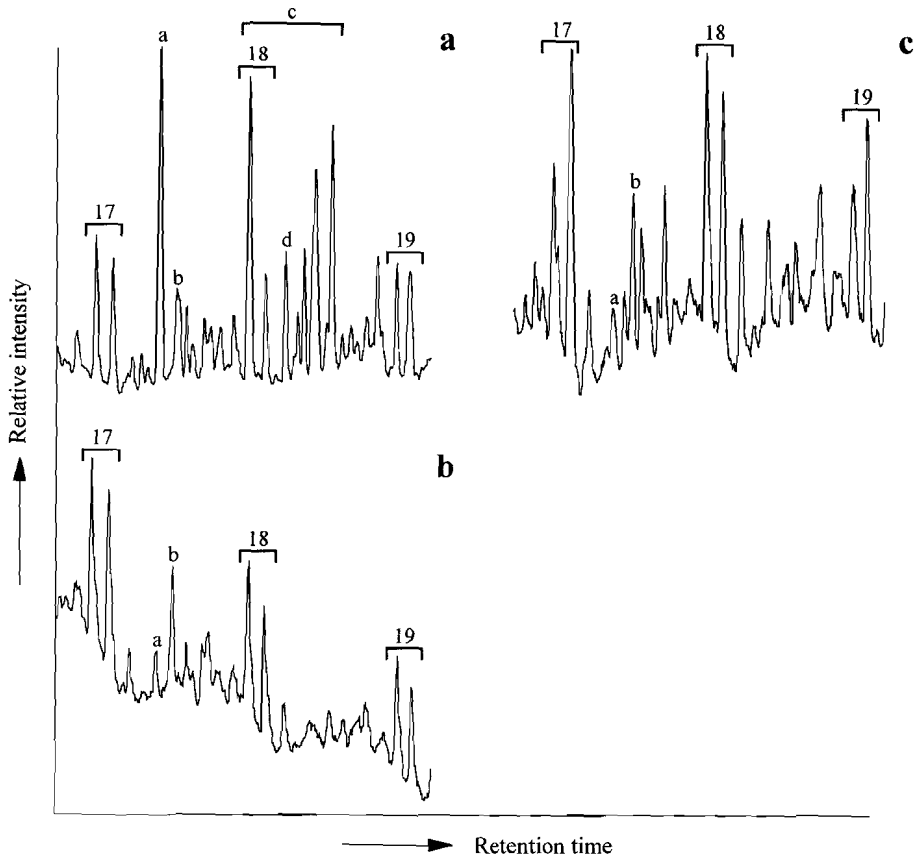

Fig. 6.7. Partial flash pyrolysis gas chromatograms of (**a**) the kerogen of the unheated sample from the Gessoso-solfifera Formation, (**b**) the residue after HI/ $LiAlH_4$ treatment of the desulphurised kerogen, and (**c**) the residue after direct HI/ $LiAlH_4$ treatment of the kerogen. Key: numbers indicate number of carbon atoms of *n*-alk-1-ene/*n*-alkane doublets, a = prist-1-ene, b = prist-2-ene, c = phytene, d = Ph.

LMW OSC

Compound specific carbon isotope analysis of Pr in the desulphurised alkylthiophene fraction of the original sample from the Ghareb Formation and the samples heated at 260 and 300°C reveal a consistent enrichment in ^{13}C of 2-3‰ compared to free Pr in the saturated hydrocarbon fraction. A similar isotopic difference for the Ph carbon skeleton in different fractions of a sample from the Gessoso-solfifera Formation was ascribed to different precursors (Kohnen *et al.*, 1992a). This may indicate different precursors for the alkylthiophenes with a Pr carbon skeleton (**I-III**), *e.g.* pristenes, pristadienes and pristatrienes found in zooplankton (Blumer and Thomas, 1965; Blumer *et al.*, 1969), and free Pr, *e.g.* bound tocopherols (Goossens *et al.*, 1984).

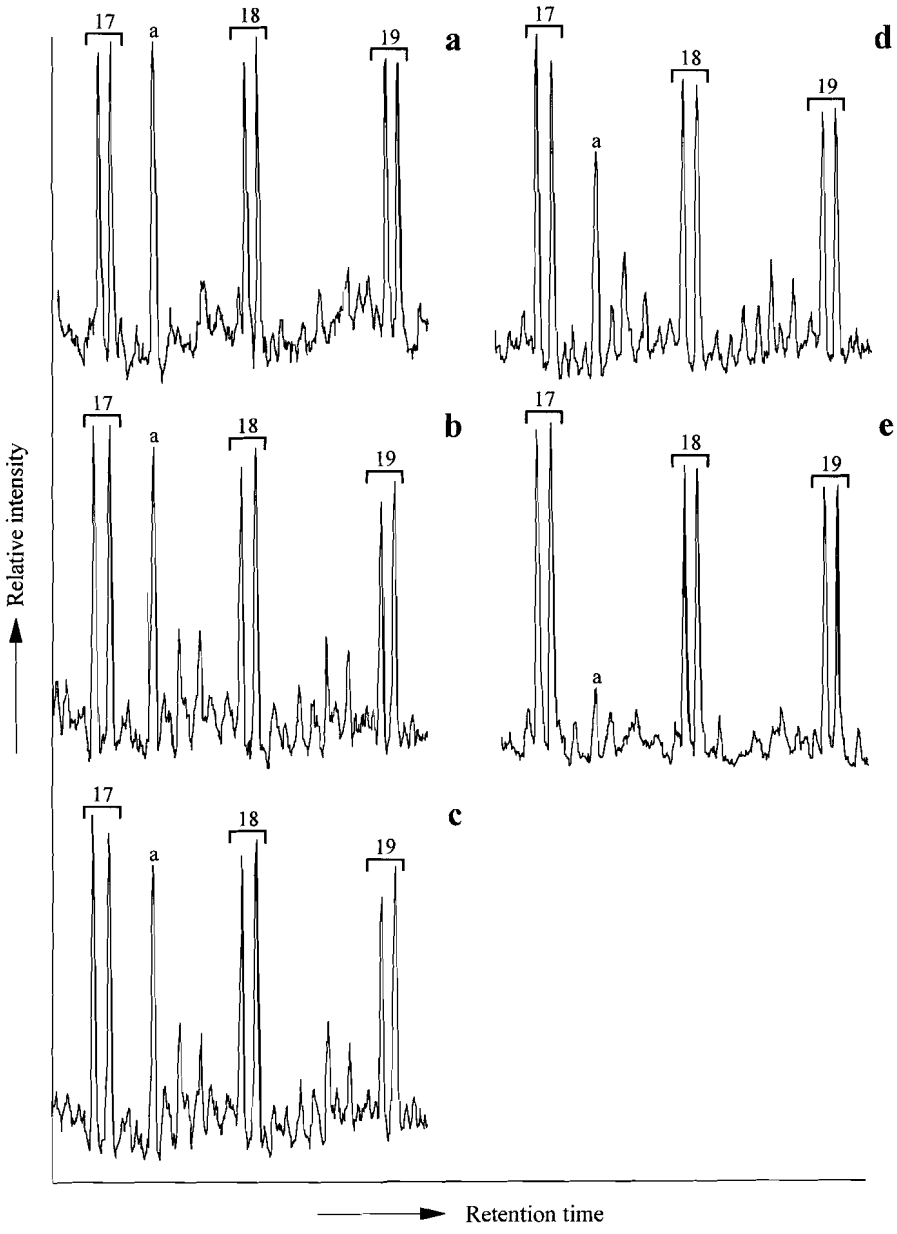

Fig. 6.8. Partial flash pyrolysis gas chromatograms of (**a**) the kerogen of the unheated sample from the Ghareb Formation, and the residues after extraction of the samples artificially matured at (**b**) 200, (**c**) 240, (**d**) 260 and (**e**) 300°C. Key: numbers indicate number of carbon atoms of *n*-alk-1-ene/*n*-alkane doublets, a = prist-1-ene.

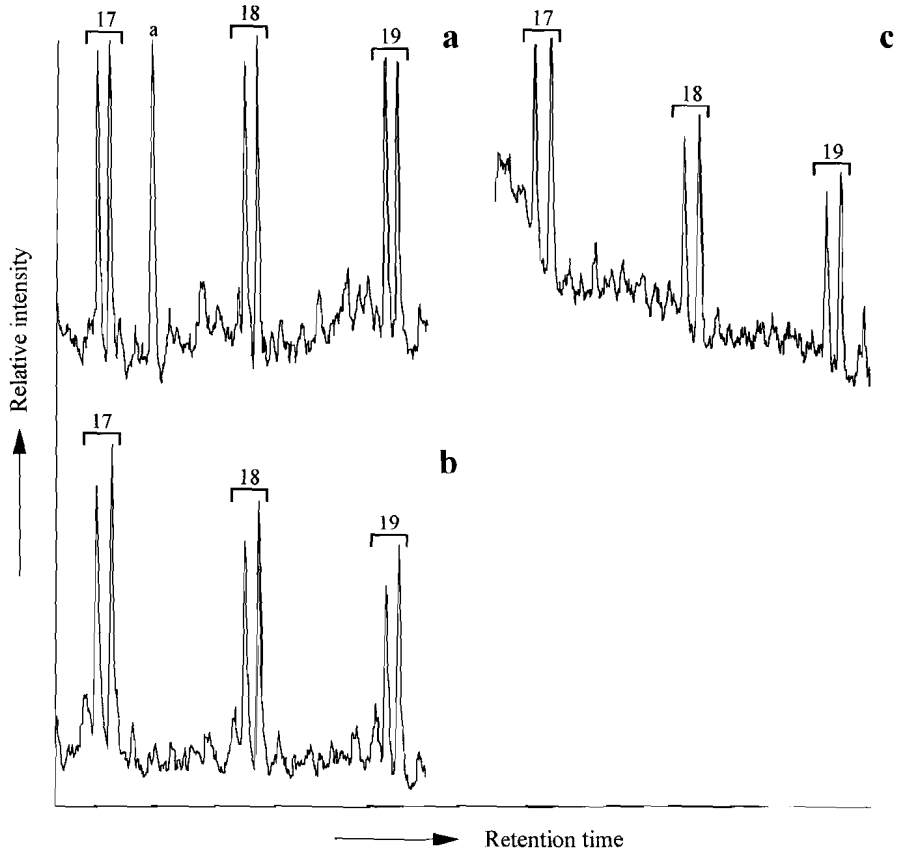

Fig. 6.9. Partial flash pyrolysis gas chromatograms of (**a**) the kerogen of the unheated sample from the Ghareb Formation, (**b**) the residue after Ni_2B desulphurisation, and (**c**) the residue after subsequent $HI/LiAlH_4$ treatment. Key: numbers indicate number of carbon atoms of *n*-alk-1-ene/*n*-alkane doublets, a = prist-1-ene.

Polar fractions

$\delta^{13}C$ values of Ph released by chemical degradation of the polar fraction of the unheated samples from the Gessoso-solfifera, Ghareb and Green River Formations are listed in Table 6.6. The amounts of Pr released were too low to determine the $\delta^{13}C$ value.

The $\delta^{13}C$ values of Ph released from the polar fraction of the Gessoso-solfifera Formation by Raney Ni and $HI/LiAlH_4$ differ by *c.* 10‰, which clearly suggests a different source for sulphur-bound Ph on the one hand, and oxygen-bound and both sulphur- and oxygen-bound Ph on the other. The $\delta^{13}C$ value of oxygen-bound and both sulphur- and oxygen-bound Ph is similar to that of the C_{40} biphytanes with one to three cyclopentyl moieties that are also released by $HI/LiAlH_4$ treatment of the polar fraction (Koopmans *et al.*, 1996b). These carbon skeletons probably originate from methanogenic

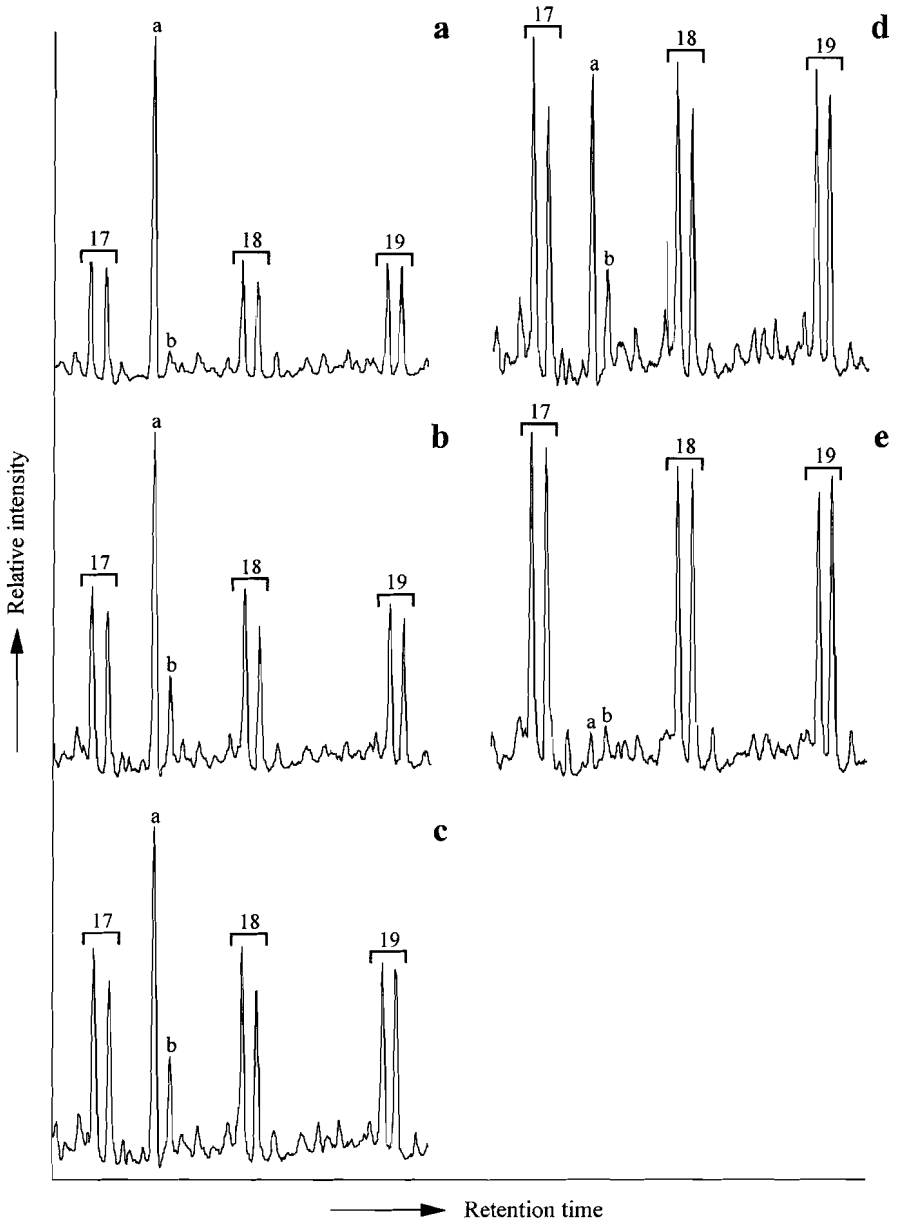

Fig. 6.10. Partial flash pyrolysis gas chromatograms of (**a**) the kerogen of the unheated sample from the Green River Formation, and the residues after extraction of the samples artificially matured at (**b**) 240, (**c**) 270, (**d**) 285 and (**e**) 330°C. Key: numbers indicate number of carbon atoms of *n*-alk-1-ene/*n*-alkane doublets, a = prist-1-ene, b = prist-2-ene.

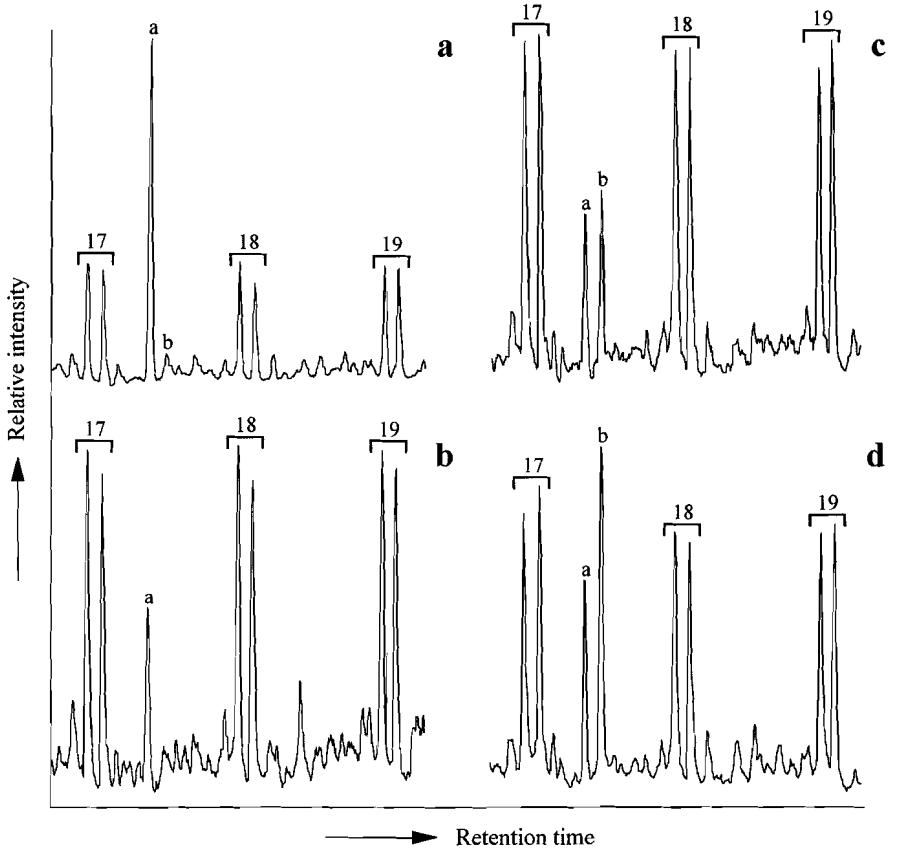

Fig. 6.11. Partial flash pyrolysis gas chromatograms of (**a**) the kerogen of the unheated sample from the Green River Formation, (**b**) the residue after Ni_2B desulphurisation, (**c**) the residue after subsequent $HI/LiAlH_4$ treatment, and (**d**) the residue after direct $HI/LiAlH_4$ treatment of the kerogen. Key: numbers indicate number of carbon atoms of *n*-alk-1-ene/*n*-alkane doublets, a = prist-1-ene, b = prist-2-ene.

bacteria (Kohnen *et al.*, 1992a), and it is therefore likely that oxygen-bound and both sulphur- and oxygen-bound Ph has the same source, *i.e.* diphytanyl glyceryl ether that was identified in the polar fraction.

Kerogens

The amounts of Pr and Ph released from the kerogen of the Ghareb and Green River Formations by chemical degradation were too low to determine the $\delta^{13}C$ values (Table 6.5). $\delta^{13}C$ values of Ph released from the kerogen of the Gessoso-solfifera Formation are listed in Table 6.6.

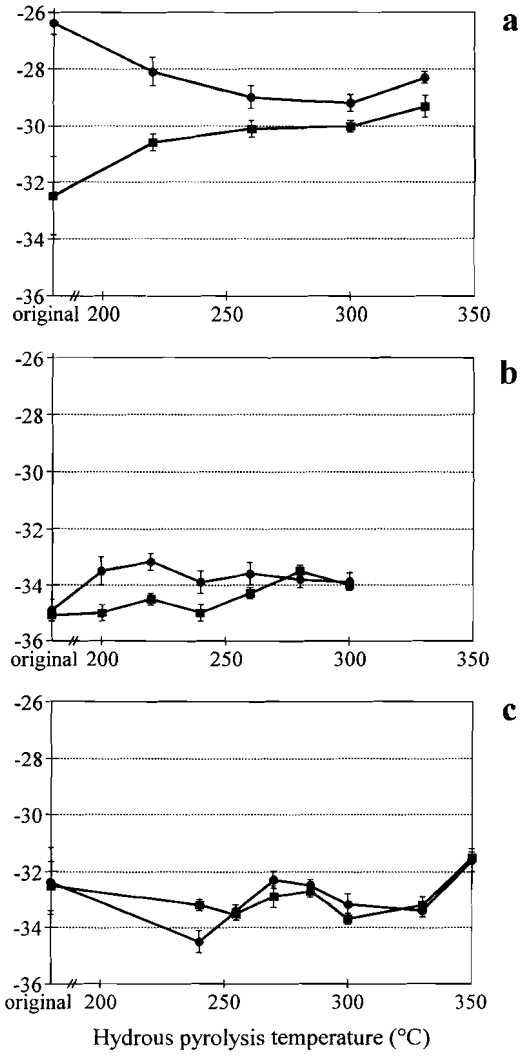

Fig. 6.12. $\delta^{13}C$ values (‰) of Pr (dots) and Ph (squares) in the saturated hydrocarbon fractions of the samples from the (**a**) Gessoso-solfifera, (**b**) Ghareb, and (**c**) Green River Formations as a function of maturation temperature.

The $\delta^{13}C$ value of Ph released after desulphurisation of the kerogen of the Gessoso-solfifera Formation is similar to that of Ph released after desulphurisation of the polar fraction, suggesting a similar source, *i.e.* phytol. The $\delta^{13}C$ value of Ph released after HI/$LiAlH_4$ treatment of the polar fraction obtained after desulphurisation of the kerogen is intermediate between the $\delta^{13}C$ values of Ph released after desulphurisation

Table 6.6. $\delta^{13}C$ values (‰) of Pr and Ph released by chemical degradation from polar fractions and kerogens of the original samples.

		PF/RN[a]	PF/HI[b]	KG/NB[c]	KG/NB/PF/HI[d]
Gessoso-solfifera Formation	*Ph*	-32.0±0.2	-22.4±0.1	-31.5±0.5	-26.4±0.5
Ghareb Formation	*Ph*	-31.8±0.3	-30.1±0.7	nd[e]	nd
Green River Formation	*Ph*	-32.5±0.2	nd	nd	nd

[a] Raney Ni desulphurisation of the polar fraction.

[b] $HI/LiAlH_4$ treatment of the desulphurised polar fraction.

[c] Ni_2B desulphurisation of the kerogen.

[d] $HI/LiAlH_4$ treatment of the polar fraction released after desulphurisation of the kerogen.

[e] nd = not determined because the amount was too low.

and subsequent $HI/LiAlH_4$ treatment of the polar fraction, suggesting a mixed source from phytol and diphytanyl glyceryl ether. This is in agreement with the results obtained after saponification of the kerogen, which yielded comparable amounts of dihydrophytol and diphytanyl glyceryl ether.

6.5 Discussion

Precursors of Pr and Ph

The artificial maturation experiments clearly show that for all samples studied the amounts of Pr and Ph after heating are much higher than the amounts originally present (Fig. 6.2). This suggests that Pr and Ph are present as bound moieties in HMW fractions of the unheated samples from which they are liberated upon increasing thermal stress. The release of Pr and Ph suggests that cleavage of relatively weak C-S and C-O bonds is involved, because cleavage of C-C bonds would also lead to degradation of the Pr and Ph carbon skeletons themselves, which could then of course not be identified as such. Therefore, selective C-S and C-O bond cleavage by chemical degradation experiments with HMW fractions of the unheated samples seems to be a good method to identify the precursors of Pr and Ph.

Gessoso-solfifera Formation

Chemical degradation experiments with the polar fraction and the kerogen of the Gessoso-solfifera Formation show that a large amount of Ph and only a small amount of Pr is released (Fig. 6.5**a**). The amount of Pr released is much smaller than the Pr potential. These results can be understood if distinct precursors for Pr and Ph are inferred, *i.e.* bound tocopherols and (possibly) archaebacterial ether lipids for Pr, and phytol and archaebacterial ether lipids for Ph.

Bound tocopherols can thermally generate prist-1-ene *via* a retro-Diels-Alder reaction (Goossens *et al.*, 1984). Although this reaction involves cleavage of a C-C bond (Fig. 6.13**a**), the concerted mechanism requires only a relatively low activation energy (Sauer and Sustmann, 1980). Chemical degradation of bound tocopherols cannot release Pr, in agreement with our results. Flash pyrolysis of the kerogen of the unheated sample from the Gessoso-solfifera Formation yields abundant prist-1-ene, suggesting an origin from bound tocopherols (Fig. 6.6). The decreasing relative amount of prist-1-ene with increasing maturation temperature correlates well with the increasing amounts of Pr in the saturated hydrocarbon fraction (cf. Figs. 6.2 and 6.6). This correlation has been noted before for two natural maturation series (van Graas *et al.*, 1981; Goossens *et al.*, 1988a), and it was taken as evidence that the precursor of prist-1-ene in the flash pyrolysate is also the precursor of free Pr. Flash pyrolysis of the residues after chemical degradation of the kerogen of the unheated sample indicates that the precursor of prist-1-ene is not sulphur-, but oxygen-bound and/or sulphur- and oxygen-bound in the kerogen (Fig. 6.7), in agreement with the tocopherol hypothesis. However, tocopherols were not among the products released after HI treatment of the kerogen. The different behaviour of prist-2-ene in the flash pyrolysates of the chemically degraded kerogen (Fig. 6.7) suggests that prist-1-ene and prist-2-ene have different precursors. Interestingly, prist-1-ene and prist-2-ene have been proposed to have the same precursor, with prist-2-ene being formed in the presence of clay (Regtop *et al.*, 1986). The Pr carbon skeleton could also be thermally generated from diphytanyl glyceryl ether (Fig. 6.13**b**), because the C-C bond adjacent to the C-O bond is much weaker than the other C-C bonds that constitute the Ph carbon skeleton (Claxton *et al.*, 1993). This is supported by flash pyrolysis of 1,2-di-O-*n*-C_{16} glycerol, which yielded, apart from hexadecanal and hexadecan-1-ol, large amounts of hexadec-1-ene and pentadec-1-ene, whereas shorter-chain alk-1-enes were much less abundant (Fig. 6.14). By analogy this would suggest, however, that dihydrophytol and phytanal are important compounds in the flash pyrolysate of the kerogen of the unheated sample, but these compounds were not observed. Hydrous pyrolysis of the methanogen *Methanosarcina barkeri* for 72 h at 330°C yielded Pr and Ph in a 2:1 ratio, suggesting that Pr is formed from diphytanyl glyceryl ether in higher amounts than Ph (Rowland, 1990). However, Navale (1992) showed that hydrous pyrolysis of diphytanyl glyceryl ether at 330°C yielded mainly dihydrophytol and phytene.

Ph is released after desulphurisation and C-O bond cleavage of both the polar fraction and the kerogen (Tables 6.3, 6.4 and 6.5). Ph released after desulphurisation probably originates from phytol (Brassell *et al.*, 1986b; Kohnen *et al.*, 1992a), whose diagenetic products phytadiene and phytenal have been shown to react readily with inorganic sulphur species in laboratory sulphurisation experiments (de Graaf *et al.*, 1992; Schouten *et al.*, 1993, 1994; Krein and Aizenshtat, 1994). Flash pyrolysis of the kerogen of the unheated sample and the residues of the artificially matured samples reveals the early thermal loss of phytenes from the kerogen (Fig. 6.6), which may be due to thermal cleavage of relatively weak C-S and S-S bonds. At comparatively low temperatures,

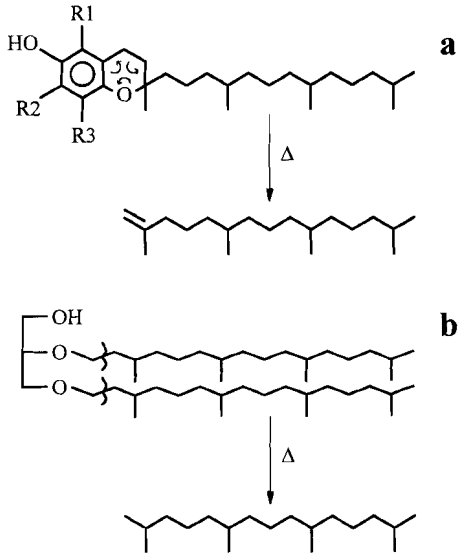

Fig. 6.13. Thermal generation of the Pr carbon skeleton from (**a**) tocopherols and (**b**) diphytanyl glyceryl ether.

alkylthiophenes with the Ph carbon skeleton as well as free Ph, which both can be regarded as stable thermal degradation products of sulphur-bound Ph (Koopmans *et al.*, 1996b), are formed in relatively high abundance (up to *c.* 400 μg/g TOC of original rock; Fig. 6.3**b**). However, the flash pyrolysates of the kerogen of the unheated sample and the residue after Ni_2B desulphurisation of the kerogen of the unheated sample show similar relative amounts of phytenes, suggesting that sulphur-bound Ph is not the precursor of the phytenes found upon flash pyrolysis. These results are in contrast, however, with results obtained by Gelin *et al.* (1996b), who noted a selective removal of phytenes from the flash pyrolysate after Li/$EtNH_2$ desulphurisation of kerogens from the Gessoso-solfifera Formation. Thus, our results from flash pyrolysis of the desulphurised kerogen should probably be viewed with caution. Direct HI treatment of the kerogen of the unheated sample removes the precursor of the phytenes from the kerogen (Fig. 6.7**c**), suggesting that oxygen-bound Ph is the precursor of the phytenes. Saponification of the kerogen released diphytanyl glyceryl ether and dihydrophytol in comparable amounts, suggesting that ester-bound diphytanyl glyceryl ether and ester-bound phytol are the main source for oxygen-bound Ph in the kerogen. This is supported by the $\delta^{13}C$ value of Ph released after HI/$LiAlH_4$ treatment of the polar fraction obtained after desulphurisation of the kerogen, which is intermediate between the $\delta^{13}C$ values of phytol and diphytanyl glyceryl ether as determined from chemical degradation of the polar fraction (Table 6.6).

In summary, in the Gessoso-solfifera Formation the precursors of Pr are probably

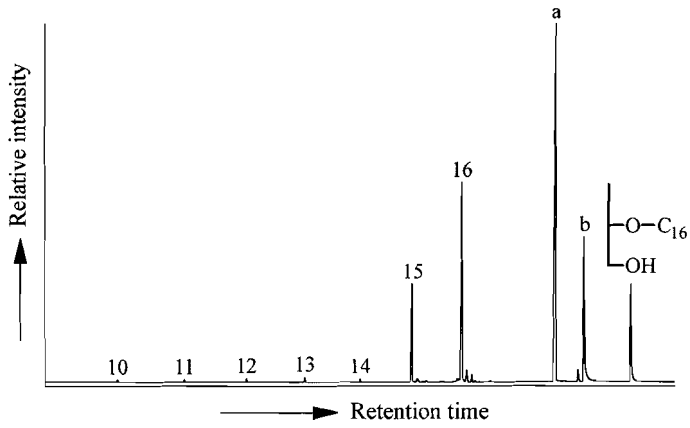

Fig. 6.14. Partial TIC of the flash pyrolysate of 1,2-di-O-*n*-C_{16} glycerol. Key: numbers indicate carbon numbers of alk-1-enes, a = hexadecanal, b = hexadecan-1-ol. The identification of the 1-O-*n*-C_{16} glycerol derivative is tentative.

predominantly bound tocopherols and the (unknown) precursors of prist-2-ene found in the flash pyrolysates. The precursors of Ph are mainly phytol and diphytanyl glyceryl ether.

Ghareb Formation

Chemical degradation of the polar fraction and the kerogen of the Ghareb Formation released Pr as well as Ph, albeit in lower amounts than their respective potential (Fig. 6.5**b**). The low amounts released from the kerogen may be explained by its highly sulphur cross-linked nature (Koopmans *et al.*, 1997d), which hampers the release of these skeletons because more bonds have to be cleaved.

The sample from the Ghareb Formation is the only one studied from which Pr was released in significant amounts by chemical degradation (Fig. 6.5). This is probably due to the presence of sulphur-bound Pr in the kerogen, as suggested by the abundant formation of three alkylthiophenes with a Pr carbon skeleton during hydrous pyrolysis (Fig. 6.3**c**). Sulphur-bound Pr probably originates from sulphur incorporation into pristenes, pristadienes and pristatrienes known to occur in zooplankton (Blumer and Thomas, 1965; Blumer *et al.*, 1969). Flash pyrolysis of the kerogen of the unheated sample yields prist-1-ene (Fig. 6.9**a**), suggesting the presence of bound tocopherols. However, the absence of prist-1-ene in the flash pyrolysate of the desulphurised kerogen (Fig. 6.9**b**), is a strong indication that sulphur-bound Pr is the precursor of the free Pr formed during hydrous pyrolysis. It is not clear why sulphur-bound Pr carbon skeletons with predominantly mid-chain C-S links in the kerogen, as suggested by the formation of the mid-chain alkylthiophenes **I-III** (Fig. 6.4), yield the terminal alkene prist-1-ene upon flash

pyrolysis. Isomerisation of double bonds during flash pyrolysis may possibly explain the formation of the terminal alkene prist-1-ene.

The precursor of Ph in the sample from the Ghareb Formation may be sulphur- or oxygen-bound Ph, as indicated by the chemical degradation experiments (Tables 6.3, 6.4 and 6.5). The absence of phytenes in the flash pyrolysates of the kerogen, the residues of the heated samples and the residues after chemical degradation does not reveal additional information in this respect (Figs. 6.8 and 6.9). The formation of increasing relative amounts of alkylthiophenes with a Ph carbon skeleton with increasing thermal maturation (Fig. 6.3**d**) suggests an origin from sulphur-bound Ph in HMW fractions.

In summary, the precursors of Pr and Ph in the Ghareb Formation are probably sulphur-bound Pr and Ph in HMW fractions.

Green River Formation

Chemical degradation experiments with the polar fraction and the kerogen of the sample from the Green River Formation show that the amounts of Pr and Ph generated by hydrous pyrolysis cannot be retrieved by chemical degradation, indicating that both Pr and Ph are neither sulphur- nor oxygen-bound (Fig. 6.5**c**).

Additional information about the precursor of Pr comes from flash pyrolysis analyses. Flash pyrolysis of the kerogen of the unheated sample yields abundant prist-1-ene and some prist-2-ene (Fig. 6.10**a**). With increasing thermal maturation, their amounts relative to the *n*-alkenes/*n*-alkanes decrease (Fig. 6.10). Flash pyrolysis of the residue after desulphurisation of the kerogen of the unheated sample yields decreased amounts of prist-1-ene (Fig. 6.11**b**), suggesting that its precursor is at least partly sulphur-bound. Flash pyrolysis of the residue after HI/$LiAlH_4$ treatment of the kerogen of the unheated sample also yields decreased amounts of prist-1-ene (Fig. 6.11**d**), suggesting an oxygen-bound precursor, *e.g.* bound tocopherols. However, analysis of the released products did not reveal the presence of tocopherols. In addition, a large relative amount of prist-2-ene is present in the flash pyrolysate (Fig. 6.11**d**), which is also present in the flash pyrolysate of the residue after HI/$LiAlH_4$ treatment of the desulphurised kerogen (Fig. 6.11**c**). Thus it seems that prist-2-ene is 'formed' upon HI/$LiAlH_4$ treatment.

Flash pyrolysis does not provide information on the precursors of Ph, because no phytenes could be detected. Thus, although Ph is formed abundantly upon hydrous pyrolysis (*c.* 1.5 mg/g TOC of original rock; Fig. 6.2**c**), our combined thermal and chemical degradation approach cannot reveal the nature of its HMW precursor.

In summary, the precursor of Pr in the Green River Formation is probably partly sulphur- and partly oxygen-bound Pr, in addition to the (unknown) precursor of prist-2-ene found in the flash pyrolysates. The precursor of Ph is not known.

Maturity dependence of the Pr/Ph ratio

The Pr/Ph ratio changes with increasing maturation temperature for all three samples (Fig. 6.15). In order to investigate the variation of the Pr/Ph ratio with increasing thermal maturation, three different maturation temperature intervals should be distinguished, *i.e.* (i) $T \leq T_c$, (ii) $T_c \leq T \leq T_{max}$, and (iii) $T \geq T_{max}$, where T_{max} is the temperature at which the Pr and Ph concentrations reach their maximum values (indicated in Fig. 6.2 with a dashed line).

It should be noted that T_c and T_{max} are different for different samples (Fig. 6.2). The positive correlation of T_c with (i) the level of thermal maturity, and (ii) the amount of Pr and Ph already present in the original sample relative to the maximum amount of Pr and Ph generated, can be understood in terms of an activation energy distribution for the generation of Pr and Ph. Such an approach has been advocated by Burnham (1989) for the generation of pristane. A sample that has reached a certain level of thermal maturity will first generate the portion of Pr and Ph that requires the lowest activation energy. At a slightly higher level of thermal maturity, the portion with the next lowest activation energy will be generated, and so on. If the sample is then artificially matured, Pr and Ph will only be generated at an artificial maturation temperature equivalent to the level of thermal maturity already attained in the natural situation, hence the correlation of T_c and R_o. The theoretical basis for the use of activation energy distributions instead of single activation energies is that more than one reaction is responsible for the generation of Pr (Burnham, 1989). This is in agreement with our finding of several precursors for Pr and Ph.

At $T \leq T_c$, the Pr and Ph concentrations of all three samples are relatively constant (Fig. 6.2), so that the Pr/Ph ratios do not change significantly with increasing maturation temperature (Fig. 6.15). The generation profile of Ph in the Gessoso-solfifera Formation shows relatively abundant formation of Ph already at 160°C (Fig. 6.2**a**), which results in a drop of the Pr/Ph ratio (Fig. 6.15). The absence of this initial increase in the Ph generation profiles of the samples from the Ghareb and Green River formations supports the concept of an activation energy distribution, because these samples have probably already passed through the natural maturation stage at which this early generation of Ph (which is associated with a low activation energy) occurs. At $T_c \leq T \leq T_{max}$, when both Pr and Ph are generated in large amounts (Fig. 6.2), the increase of the Pr/Ph ratio is most pronounced (Fig. 6.15). This increase cannot be ascribed to the different timing of Pr and Ph formation, because the generation profiles of Pr and Ph in the samples which show the largest variation in the Pr/Ph ratio (from the Ghareb and Green River Formations) are highly correlated in this temperature interval ($R^2 > 0.96$). Rather, the Pr/Ph ratio increases because the ratio of the precursors of Pr and Ph in the HMW fractions is higher than the ratio of Pr and Ph already present in the saturated hydrocarbon fraction. At $T \geq T_{max}$, when destruction of the Pr and Ph carbon skeleton outcompetes their generation (Fig. 6.2), the increase of the Pr/Ph ratio tends to level off (Fig. 6.15). Simi-

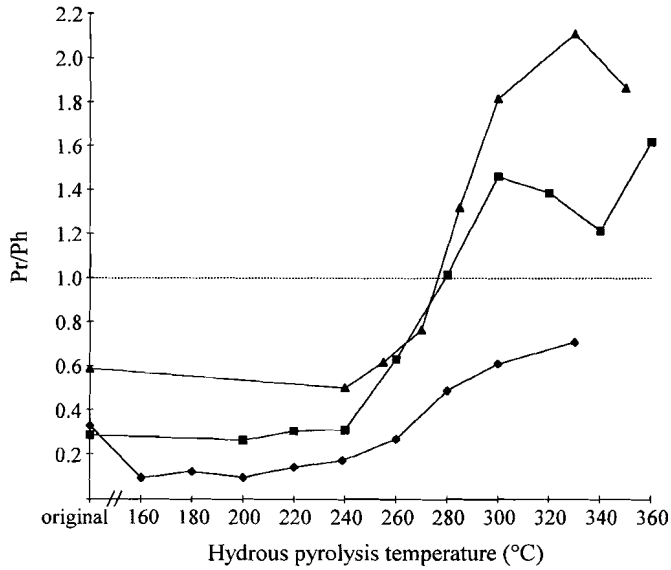

Fig. 6.15. Pr/Ph ratio as a function of hydrous pyrolysis temperature for the samples from the Gessoso-solfifera (diamonds), Ghareb (squares) and Green River (triangles) Formations.

lar results were reported for an artificial maturation series of a sample from the Mahogany Zone of the Green River Shale (Evans and Felbeck, 1983), with a gradual increase of the Pr/Ph ratio from 0.3 in the unheated sample to 1.4 at T_{max}, after which the Pr/Ph ratio was variable.

For the samples from the Ghareb and Green River Formations the Pr/Ph ratio changes from a value smaller than unity to a value greater than unity. This is particularly interesting, because such values are typically attributed to reducing and oxidising depositional environments, respectively (Didyk *et al.*, 1978). These results indicate that it is dangerous to use the Pr/Ph ratio for samples with a relatively low level of thermal maturity ($R_o \leq 0.4\%$). In fact, the diversity of the origins for Pr and Ph in the samples investigated here leads us to discourage the use of the Pr/Ph ratio to assess the oxicity of the depositional environment.

6.6 Conclusions

Artificial maturation of three immature sedimentary rocks generates large amounts of Pr and Ph carbon skeletons, indicating that their precursors are bound in high-molecular-weight fractions. For some samples, the formation of abundant alkylthiophenes with Pr and Ph carbon skeletons provides a clue to sulphur-bound HMW precursors. However,

chemical degradation experiments with high-molecular-weight fractions of the unheated samples generally do not release large amounts of Pr and Ph. This is especially true for the sample from the Green River Formation, where only a few percent of the Pr and Ph generated by artificial maturation can be released by chemical degradation.

Additional information about the precursors of Pr and Ph is provided by flash pyrolysis of kerogens of the unheated samples, and residues after heating and after chemical degradation. Prist-1-ene and prist-2-ene present in several flash pyrolysates seem to have different precursors, contrary to the prevailing belief that prist-2-ene is formed from prist-1-ene in the presence of clay.

In the Gessoso-solfifera Formation, bound tocopherols and the (unknown) precursor of prist-2-ene are the precursors of Pr, and sulphur-bound Ph (probably originating from phytol or its diagenetic products) and diphytanyl glyceryl ether are the precursors of Ph. In the Ghareb Formation, sulphur-bound Pr and Ph are the precursors of free Pr and Ph. In the Green River Formation, sulphur- and oxygen-bound Pr and the (unknown) precursor of prist-2-ene are the precursors of Pr, whereas the precursor of Ph remains obscure.

The lowest artificial maturation temperature (T_c) at which large amounts of Pr and Ph are formed is positively correlated with the level of thermal maturity of the unheated samples. This can be explained in terms of activation energy distributions, which also fits with the finding of multiple precursors for Pr and Ph.

6.7 Acknowledgements

Dr. T.E. Ruble (US Geological Survey, USA) is gratefully acknowledged for providing several artificially matured samples from the Green River Formation. Dr. S. Schouten is thanked for irm-GC-MS measurements. Analytical support was provided by Mrs. M. Dekker and Mr. W. Pool. We thank Shell International Exploration and Production for providing a research studentship to MPK, and for financial support for the irm GC-MS facility. This work was partly supported by a PIONIER grant to JSSD from the Netherlands Organisation for Scientific Research (NWO).

CHAPTER 7

Diagenetic and catagenetic products of isorenieratene: Molecular indicators for photic zone anoxia

M.P. Koopmans, J. Köster, H.M.E. van Kaam-Peters, F. Kenig, S. Schouten, W.A. Hartgers, J.W. de Leeuw and J.S. Sinninghe Damsté

7.1 Abstract

A wide range of novel dia- and catagenetic products of the diaromatic carotenoid isorenieratene, a pigment of the photosynthetic green sulphur bacteria Chlorobiaceae, has been identified in a number of sedimentary rocks ranging from Ordovician to Miocene. Compound identification is based on NMR, mass spectrometry, the presence of atropisomers, and stable carbon isotopes. Atropisomers contain an axially chiral centre which, in combination with other chiral centres, results in two or more diastereomers that can be separated on a normal GC column. Chlorobiaceae use the reverse TCA cycle to fix carbon, so that their biomass is enriched in ^{13}C. High ^{13}C contents of isorenieratene derivatives therefore support their inferred origins.

Isorenieratene derivatives include C_{40}, C_{33} and C_{32} diaryl isoprenoids and short-chain aryl isoprenoids with additional aromatic and/or sulphur-containing rings. C_{33} and C_{32} compounds are diagenetic products of C_{33} and C_{32} 'carotenoids' formed from isorenieratene during early diagenesis through expulsion of toluene and *m*-xylene, respectively. Cyclisation of the polyene acyclic isoprenoid chain can proceed *via* an intramolecular Diels-Alder reaction, followed by aromatisation of the newly formed ring. Sulphurisation is also an important process during early diagenesis, competing with expulsion and cyclisation. Sulphur-bound isorenieratane is released during progressive diagenesis, due to cleavage of relatively weak S-S and C-S bonds. Cleavage of C-C bonds during aromatisation of newly formed rings and during catagenesis yields short-chain compounds. The inherent presence of a conjugated double bond system in carotenoids implies that similar dia- and catagenetic reactions can occur with all carotenoids.

Chlorobiaceae live at or below the oxic/anoxic boundary layer and require both light and H_2S. The presence of isorenieratene or its dia- and catagenetic products in

ancient sedimentary rocks and crude oils is therefore an excellent indication for photic zone anoxia in the depositional environment. Dia- and catagenetic products of isorenieratene are expected to find applications in reconstruction of palaeoenvironments and in oil-oil and oil-source rock correlation studies. Their presence in several petroleum source rocks suggests that anoxia is an important environmental parameter for the preservation of organic matter.

7.2 Introduction

It is generally accepted that anoxic depositional environments favour the preservation of organic matter (Demaison and Moore, 1980), albeit that Pedersen and Calvert (1990) have recently challenged this. Anoxic conditions in the marine environment occur when the supply of oxygen in bottom waters is limited by restricted water circulation arising from density or temperature stratification, or by contact of an oxygen-minimum layer with the sea floor (*e.g.* on continental shelves and slopes). Since anoxia and, thus, preservation of organic matter can lead to formation of petroleum source rocks, it is important to be able to recognise (ancient) anoxic basins. Hence, recognition of biomarkers in sedimentary rocks and oils that are unambiguously related to anoxic depositional conditions is a challenge for petroleum geochemistry and organic geochemistry alike.

Green sulphur bacteria (Chlorobiaceae) are photoautotrophic organisms that are strictly anaerobic and require both light and H_2S. Their presence attests to an anoxic water layer reaching into the photic zone, and euxinic conditions. Chlorobiaceae produce two types of characteristic pigments (bacteriochlorophylls and isorenieratene) that can be used to trace their distribution in the geological record. The bacteriochlorophylls *c*, *d* and *e* are unique compared to other (bacterio)chlorophylls in that their tetrapyrrole nucleus can contain as many as 38 C atoms (Scheer, 1991). The diaromatic carotenoid isorenieratene (**I**; see Appendix I) comprises an irregular (tail-to-tail) isoprenoid chain, and a specific 1-alkyl-2,3,6-trimethyl substitution pattern for both its aromatic rings (Liaaen-Jensen, 1978a,b). The high ^{13}C content of isorenieratene and the bacteriochlorophylls *c*, *d* and *e* determined, respectively, from octadecahydroisorenieratene (or isorenieratane; **II**) (Kohnen *et al.*, 1992a; Sinninghe Damsté *et al.*, 1993d; Hartgers *et al.*, 1994c) and the breakdown products of the extended porphyrins (Grice *et al.*, 1995), can be attributed to carbon fixation *via* the reverse tricarboxylic acid (TCA) cycle used by Chlorobiaceae (Quandt *et al.*, 1977; Sirevåg *et al.*, 1977; Schidlowski *et al.*, 1984). Isorenieratene and the bacteriochlorophylls *c*, *d* and *e* and their dia- and catagenetic products are, therefore, excellent biomarkers for anoxic depositional environments with a relatively shallow oxic water column.

Isorenieratene has been identified in several immature marine sediments (Cardoso *et al.*, 1978; Brassell *et al.*, 1983; Repeta, 1993; Keely *et al.*, 1995). The fossilisation potential of the isorenieratene carbon skeleton was first shown by Schaeflé *et al.* (1977), who described the isolation and identification (by synthesis of an authentic standard) of

isorenieratane (**II**) from a Jurassic shale from the Paris Basin. They proposed that isorenieratane originated from isorenieratene by saturation of the double bonds in the isoprenoid chain. Isorenieratane (Requejo *et al.*, 1992; Hartgers *et al.*, 1994b,c) and diaryl isoprenoids with unspecified aromatic substitution patterns (Chou and Wood, 1986; Schwark and Püttmann, 1990; Requejo *et al.*, 1992) have subsequently been reported in various samples. In an Uzbek oil of unspecified age, Ostroukhov *et al.* (1982) tentatively identified a series of 1-alkyl-2,3,6-trimethylbenzenes (**III**). Summons and Powell (1986, 1987) identified 1-alkyl-2,3,6-trimethylbenzenes in oils of Palaeozoic age by synthesis of authentic standards, and found them to be enriched in ^{13}C by 7-8‰ compared to alkanes in the same oils. These carbon isotopic data, together with a distribution pattern ranging from C_{13} to C_{31}, wherein the C_{17}, C_{23} and C_{28} members are present only in low abundance, led them to propose an origin from isorenieratene for these aryl isoprenoids. Hartgers *et al.* (1994c) have shown that aryl isoprenoids are derived from thermal breakdown of isorenieratene incorporated into high-molecular-weight (HMW) organic matter, rather than from thermal breakdown of free isorenieratane. Several other workers have recognised 1-alkyl-2,3,6-trimethylbenzenes (Clark and Philp, 1989; Yu Xinke *et al.*, 1990; Fowler, 1992; Requejo *et al.*, 1992; Hartgers *et al.*, 1994b) and alkyltrimethylbenzenes with other or unspecified aromatic substitution patterns (Schwark and Püttmann, 1990; Clayton *et al.*, 1992; Requejo *et al.*, 1992, 1995; Hartgers *et al.*, 1994b; Guthrie and Pratt, 1995) in sedimentary rocks and crude oils. Summons and Powell (1992) claimed the identification of a variety of aryl isoprenoid isomers in Siberian Platform oils of Late Proterozoic age, a finding of particular interest because it would represent the oldest report of Chlorobiaceae in the fossil record. However, evidence for the identification is poor, and the inferred isomerisation of the isoprenoid chain (Summons and Powell, 1992) seems unlikely.

The nine conjugated double bonds of isorenieratene make it highly susceptible to reaction with reduced inorganic sulphur species (*e.g.* de Graaf *et al.*, 1992; Schouten *et al.*, 1994) that are present in abundance in the anoxic water column and the top layers of the sediment. Incorporation of sulphur into isorenieratene results in the formation of multiply sulphur-linked isorenieratane moieties in HMW fractions such as the polar and asphaltene fractions and the kerogen during early diagenesis (Sinninghe Damsté *et al.*, 1989c; Kohnen *et al.*, 1990b). In the maltene fraction of immature ($R_o \approx 0.25\%$) marlstones from the Vena del Gesso Basin in northern Italy diaryl isoprenoids were present solely as sulphur-bound moieties in macromolecular aggregates (Kohnen *et al.*, 1991c; Kenig *et al.*, 1995). A similar observation was made for β-carotane by Adam *et al.* (1993), who liberated this compound after desulphurisation of a HMW fraction of a sulphur-rich oil that did not contain free β-carotane in the saturated hydrocarbon fraction. The early diagenetic fate of isorenieratene can be reconstructed from studies in the Black Sea. Chlorobiaceae were isolated from the chemocline and were shown to contain isorenieratene (Overmann *et al.*, 1992), which was also identified in suspended particulate organic matter from waters at and below the chemocline (Repeta *et al.*,

1989). In the top layers of the sediment, both free isorenieratene (Repeta, 1993) and isorenieratene sulphur-bound in geomacromolecules (Sinninghe Damsté *et al.*, 1993d; Wakeham *et al.*, 1995) were identified. The portion of isorenieratene sequestered in sulphur-rich geomacromolecules increases from 15% in the top sediment layer (Unit I) to 95% at 40-60 cm depth (Unit IIb), suggesting a progressive sulphurisation of isorenieratene with increasing depth (cf. Sinninghe Damsté *et al.*, 1993d; Repeta, 1993; Wakeham *et al.*, 1995).

Sulphur sequestration of isorenieratene has also been observed in other samples. There are various reports on the identification of isorenieratane (Kohnen *et al.*, 1992a; Kenig *et al.*, 1995; Schaeffer *et al.*, 1995a,b; Sinninghe Damsté *et al.*, 1993d, 1995b) and diaryl isoprenoids with unspecified aromatic substitution patterns (Sinninghe Damsté *et al.*, 1990a; Kohnen *et al.*, 1991b,c) in sulphur-rich geomacromolecules. Several studies have reported a high abundance of 1,2,3,4-tetramethylbenzene (TMB) in flash pyrolysates of kerogens (Douglas *et al.*, 1991; Hartgers *et al.*, 1991, 1994a,b,c; Requejo *et al.*, 1992; Gelin *et al.*, 1995), and proposed that it is formed by β-cleavage of a benzene ring of a diaromatic carotenoid incorporated into the kerogen. In a comparative study of immature kerogens and coals, Hartgers *et al.* (1994a,c) proposed that TMB is a 'pyrolytic' biomarker for macromolecularly bound diaromatic carotenoids. However, the ^{13}C content of TMB in flash pyrolysates of kerogens isolated from Indian Ocean surface sediments is identical to that of algal lipids, excluding an origin from isorenieratene (Hoefs *et al.*, 1995). Moreover, it should be noted that TMB is not a biomarker for macromolecularly bound isorenieratene *per sé*. β-cleavage of a benzene ring of macromolecularly bound renieratene and renierapurpurin, diaromatic carotenoids with a 2,3,4/2,3,6- and 2,3,4/2,3,4-trimethyl substitution pattern for their aromatic rings, respectively, or of the monoaromatic carotenoid chlorobactene also yields TMB. However, a distinction between the aromatic carotenoids can be made based on the $\delta^{13}C$ values of the β- and γ-cleavage products, and the distribution of γ-cleavage products in the flash pyrolysates. Hartgers *et al.* (1994b,c) found that TMB and 1-ethyl-2,3,6-trimethylbenzene (γ-cleavage product of isorenieratane) released after off-line pyrolysis of a kerogen isolated from the Duvernay Formation had anomalously high ^{13}C contents. 1-Ethyl-2,3,6-trimethylbenzene is often a dominant C_5 alkylbenzene in kerogens containing macromolecularly bound isorenieratene (Hartgers *et al.*, 1994a,c).

Here, we report on the discovery of a wide range of unprecedented dia- and catagenetic products of isorenieratene in rock samples from different geographical locations ranging through the Phanerozoic. They include sulphur-containing compounds, polyaromatic compounds with up to four additional aromatic rings, shorter-chain analogues with a C_{32} or C_{33} carbon skeleton, and aryl isoprenoids with additional aromatic rings or sulphur-containing moieties. These compounds are all related to isorenieratene and can therefore be regarded as indicators for photic zone anoxia in ancient depositional environments. The effect of progressive diagenesis and early catagenesis on the amounts and distributions of these compounds was studied by hydrous pyrolysis of an immature

($R_o \approx 0.25\%$) sulphur-rich sedimentary rock from the Gessoso-solfifera Formation (Messinian) that contains abundant macromolecularly bound isorenieratene.

7.3 Experimental

Hydrous pyrolysis. A sample of the 1.2 m thick marl layer of evaporitic cycle IV of the Gessoso-solfifera Formation (Messinian) in the Vena del Gesso Basin (northern Italy) was subjected to artificial maturation by hydrous pyrolysis, as described by Lewan (1993b). In short, a one-litre Hastelloy-C276 reactor was filled with rock chips (90-100 g) and distilled water (475 g). The remaining volume was purged and filled with helium (2.4 bar). Aliquots of the marl sample were heated isothermally for 72 h at 160, 180, 200, 220, 239, 260, 280, 300 and 330°C, respectively, with their temperatures monitored at 30 s intervals. Standard deviations were between ±0.2 and 0.3°C (±0.6°C at 160°C). The experiments at 300 and 330°C generated an expelled oil that was recovered from the water surface with a pipette. The reactor walls and the rock chips were rinsed with benzene to recover any sorbed oil films, which occurred in experiments at 260°C and higher temperatures. 95% or more of the originally loaded rock chips was recovered from all experiments. The residual rock chips were dried in a vacuum oven ($T \leq 50°C$).

Extraction and fractionation. Samples were freeze-dried and ultrasonically or Soxhlet extracted with dichloromethane/methanol (7.5:1 v/v). For the artificially matured samples, the sorbed oil and expelled oil (if present) were combined with the extract. Extracts were separated into a maltene and an asphaltene fraction by repeated (3 times) precipitation in *n*-heptane. An aliquot of the maltene fraction (*ca.* 250 mg), with an added standard [2-methyl-2-(4,8,12-trimethyltridecyl)chroman] for quantitative analysis, was fractionated by column chromatography with alumina into an apolar and a polar fraction by elution with *n*-hexane/dichloromethane (9:1 v/v) and dichloromethane/methanol (1:1 v/v), respectively. Further separation of the apolar fraction by argentatious thin-layer chromatography, using *n*-hexane as a developer, yielded the polyaromatic fraction ($R_f = 0.0\text{-}0.4$). When less complex fractions were required (*e.g.* for isotope-ratio-monitoring gas chromatography-mass spectrometry), two separate fractions were collected (A3 and A4 fraction; $R_f = 0.05\text{-}0.4$ and $R_f = 0.0\text{-}0.05$, respectively).

Desulphurisation. Polar fractions were desulphurised with Raney Ni and subsequently hydrogenated (Sinninghe Damsté *et al.*, 1988b). Before desulphurisation, a known amount of a synthetic standard [2,3-dimethyl-5-(1',1'-d_2-hexadecyl)thiophene] was added to 10-20 mg of the polar fraction. The released hydrocarbons were isolated from the desulphurised polar fraction by column chromatography using alumina.

Gas chromatography. Gas chromatography (GC) was performed using a Hewlett-Packard 5890 instrument equipped with an on-column injector. A fused silica capillary

column (25 m x 0.32 mm) coated with CP Sil-5 (film thickness 0.12 μm) was used with helium as carrier gas. The column effluent was monitored by both a flame ionisation (FID) and a sulphur-selective flame photometric (FPD) detector, using a stream-splitter at the end of the column (split ratio FID:FPD = 1:2). Samples were injected at 70°C and the oven was programmed to 130°C at 20°C/min and then at 4°C/min to 320°C, at which it was held for 20 min.

Gas chromatography-mass spectrometry. Gas chromatography-mass spectrometry (GC-MS) was carried out on a Hewlett-Packard 5890 gas chromatograph interfaced to a VG Autospec Ultima mass spectrometer operated at 70 eV with a mass range m/z 40-800 and a cycle time of 1.8 s (resolution 1000). The gas chromatograph was equipped with a fused silica capillary column (25 m x 0.32 mm) coated with CP Sil-5 (film thickness 0.12 μm). Helium was used as carrier gas. Samples were injected at 60°C and the oven was programmed to 130°C at 20°C/min and then at 4°C/min to 310°C, at which it was held for 20 min.

Isotope-ratio-monitoring gas chromatography-mass spectrometry. The DELTA-C irm-GC-MS system is, in principle, similar to the DELTA-S system described previously (Hayes *et al.*, 1990). The gas chromatograph (Hewlett-Packard 5890) was equipped as for GC-MS analyses above with helium as carrier gas. Samples were injected on-column at 70°C and the oven was programmed as for GC analyses above. Isotopic values were calculated by integrating the mass 44, 45 and 46 ion currents of the peaks produced by combustion of the chromatographically separated compounds and of CO_2-spikes generated by admitting CO_2 of a known ^{13}C content at regular intervals into the mass spectrometer. Values were determined at least in duplicate. Results were averaged to obtain mean values and to calculate standard deviations. The stable carbon isotope compositions are reported in the delta notation against the PDB ^{13}C standard.

Quantitation. Dia- and catagenetic products of isorenieratene in the polyaromatic fraction and those released after desulphurisation of the polar fraction were quantitated by integration of a summed mass chromatogram of their major fragment ions (m/z 133+237+287) and the main fragment ions of the standards, 2-methyl-2-(4,8,12-trimethyltridecyl)-chroman (m/z 147) and 6,6-d_2-3-methylheneicosane (m/z 57), respectively. Corrections were made to account for the intensity of the fragment ions relative to the total ion current in the spectra of the compounds quantitated and of the standard. Since mass spectrometric detection of compounds gives a molar response, a factor was introduced taking into account the molecular weights of the compounds quantitated and the standard to obtain absolute amounts (μg/g TOC).

7.4 Results

The rock samples used in this study originate from different depositional environments and geographical locations and range from Ordovician to Miocene. They were selected because previous work in our laboratory had shown that they contain abundant isorenieratene derivatives. An overview of the samples, some selected characteristics and references are given in Table 7.1. Our aim was to identify as many dia- and catagenetic products of isorenieratene as possible, in order to extend the use of isorenieratene as indicator for photic zone anoxia in ancient depositional environments. The many novel isorenieratene derivatives encountered can be divided into three groups according to their carbon number, namely (i) C_{40}, (ii) C_{32} and C_{33} and (iii) short-chain compounds, respectively. Further groupings were based on the presence of additional aromatic rings and sulphur-containing rings.

Structural identifications

A detailed description of the identification of dia- and catagenetic products of isorenieratene is given in Appendix II. To avoid duplications, the various aspects of the identifications are discussed in the text only once. Identification is based on mass spectrometry, NMR, co-injection with an authentic standard, and the presence of atropisomers. For clarity we use the numbering system of Fresenius (1989) to denote specific carbon atoms of the isorenieratene skeleton (cf. **I** in Appendix I).

Atropisomers

Before discussing the structures of the dia- and catagenetic products of isorenieratene, an important aspect of their structural identification should be introduced, *i.e.* the recognition of atropisomers. The term atropisomers refers to stereoisomeric compounds that result from restricted rotation around a C-C single bond, which are configurationally stable at room temperature (Mislow, 1966; March, 1985). Some of the isorenieratene derivatives contain a biphenyl or phenyl-naphthyl moiety. Rotation around the phenyl-phenyl or phenyl-naphthyl C-C bond in these molecules is severely hindered because of the presence of *ortho*, and, to a lesser extent (Theilacker and Hopp, 1959; Ling and Harris, 1964; Wolf *et al.*, 1995), *meta* and *para* methyl and/or alkyl groups. These substituents cause excessive nonbonded interactions when they are forced to 'pass' each other in the transition state. As a result, two stable configurations exist in which the two aromatic ring systems are almost perpendicular. Neither the phenyl nor naphthyl groups possess a mirror plane perpendicular to the plane of the aromatic ring, given the 2,3,6-trimethyl substitution pattern for the aromatic rings and the isoprenoid character of the chain. Thus, the two stable configurations are atropisomers and the molecule is axially chiral (Mislow, 1966; March, 1985). If it also contains an asymmetric carbon atom, two diastereomers result which may be separated on a capillary GC column with a normal

Table 7.1. Sample description.

Formation name	*Location*	*Age*	*Lithology*	*Setting*	*Kerogen Type*	*TOC (%)*	*R_o (%)*	*Reference*
Gessoso-solfifera	Italy	Late Miocene	Marlstone	Lagoonal	II-S	2.0	0.25	Vai and Ricci Lucchi (1977)
Menilite	Poland	Oligocene	Black shale	Flysch	I/I-S	17.2	±0.25	Köster *et al.* (1995a)
Canje	Guyana	Late Cretaceous	Calcareous shale	Shallow marine	II	3.3	±0.5	
Kimmeridge Clay	UK	Late Jurassic	Oil shale	Shallow marine	II-S	28.9	0.42[a]	Oschmann (1991)
Calcaires en Plaquettes	France	Late Jurassic	Laminated limestone	Carbonate platform	I-S	6.2	±0.3	Tribovillard *et al.* (1992)
Oxford Clay	UK	Late Jurassic	Claystone/shale	Shallow marine	II	16.6	0.38[a]	Kenig *et al.* (1994)
Schistes Cartons (G6-5-6)	France	Early Jurassic	Marlstone	Shallow marine	II	8.4	0.43[a]	MacKenzie *et al.* (1980)
Schistes Cartons (JAA)[b]	France	Early Jurassic	Laminated black shale	Shallow marine	II	12.2	0.42[a]	MacKenzie *et al.* (1980)
Allgäu	Germany	Early Jurassic	Marlstone	Restricted local basin	II	11.0	0.43[a]	Köster *et al.* (1995b)
Hauptdolomit	Germany	Late Triassic	Laminated black marlstone	Carbonate platform	I-S	28.8	±0.4[c]	Köster *et al.* (1988)
Kössen Marl	Hungary	Late Triassic	Marlstone	Shallow marine	II-S	5.3	±0.4[c]	Clayton and Koncz (1994)
Minnelusa	USA	Late Carboniferous	Marlstone	Shallow marine	II-S	20.9	±0.6[c]	Clayton *et al.* (1992)
Exshaw	Canada	Early Carboniferous	Black shale	Shallow marine	II	15.9	0.43	Allen and Creaney (1991)
Duvernay	Canada	Late Devonian	Laminated limestone	Marine	II	9.0	±0.4	Requejo *et al.* (1992)
Boas Oil Shale	Canada	Late Ordovician	Oil shale	Shallow marine	II	6.3	0.47[a]	McCracken and Nowlan (1989)
Womble	USA	Ordovician	Laminated cherty shale	Marine	II	14.6	na[d]	Douglas *et al.* (1991)

[a] Estimated value determined from the Pristane Formation Index (Goossens *et al.*, 1988a,b).

[b] Jouy-aux-Arches.

[c] Approximate value determined from several independent measures of thermal maturity.

[d] Not applicable.

apolar stationary phase, appearing as peaks of approximately equal intensity.

The high activation energy barrier that separates atropisomers results in restricted interconversion, at a rate that depends on the activation energy and the temperature. Molecular mechanics calculations indicate that the activation energies for rotation around the phenyl-phenyl C-C bond in 2,3,5',6-tetramethyl-2'-(2-butyl)biphenyl (**IV**) and the phenyl-naphthyl C-C bond in 3,8-dimethyl-1-(2,3,6-trimethylphenyl)naphthalene (**V**) are 138-168 and 180-210 kJ/mol, respectively (van Duin *et al.*, 1996). The latter value is higher, probably due to the enhanced rigidity of **V** compared to **IV**. A pseudohomologous series of 2,3,5',6-tetramethyl-2'-alkylbiphenyls was identified in the Allgäu Formation (see below), which can be recognised by the main fragment ion at m/z 237, corresponding to cleavage β to the biphenyl moiety (Fig. 7.1). The C_{20} component and the higher pseudohomologues of this series contain an asymmetric carbon atom at C-13, which, in combination with the axially chiral biphenyl moiety, results in two diastereomers that are separated in GC analysis (Fig. 7.1). Thus, the elution temperature of these compounds (159-180°C) is insufficient to overcome the high activation energy barrier for rotation around the phenyl-phenyl C-C bond. It should be noted that separation of the atropisomers is dependent on both the activation energy for rotation and differences in their physical properties. An axially chiral centre seems important for separation of these diastereomers, because acyclic compounds with two (or more) asym-

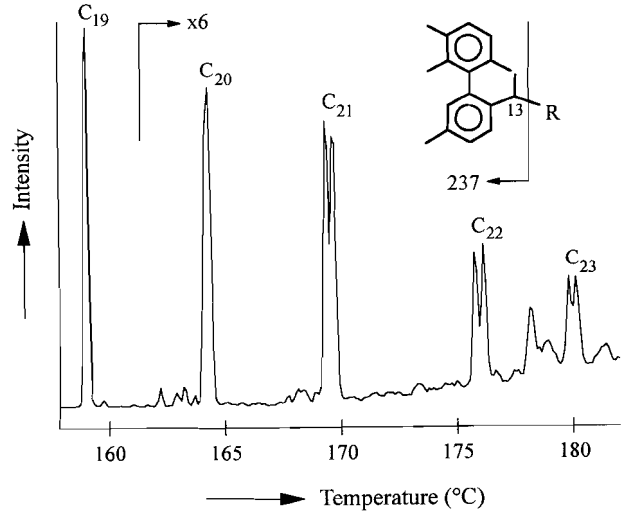

Fig. 7.1. Partial m/z 237 mass chromatogram of the polyaromatic fraction of the sample from the Allgäu Formation, showing the gas chromatographic separation of the atropisomers of the C_{20}-C_{23} members of the 2,3,5',6-tetramethyl-2'-alkylbiphenyls in an approximate 1:1 ratio. The C_{19} (R = CH_3) member is reflected by one peak because it does not contain an asymmetric carbon atom.

metric carbon atoms (*e.g.* squalane) are not or hardly separated by capillary GC using a normal apolar stationary phase.

Competition between the half-life and the retention time of atropisomers will determine their appearance in the GC. This was shown by König *et al.* (1993), who carried out isothermal GC using capillary columns coated with modified cyclodextrins, allowing separation of enantiomeric structures, and determined the separation of the two atropisomers of 2,2'-diisopropylbiphenyl as a function of column temperature.

C_{40} compounds

Isorenieratane. We encountered isorenieratane (**II**) in all samples, except that from the Gessoso-solfifera Formation. Schwark and Püttmann (1990) detected 'isorenieratane or its positional isomers' as a broadened peak, and concluded that this was caused by decomposition reactions during GC analysis. However, peak broadening probably resulted from the GC operating in the isothermal (T = 300°C) mode during elution of the diaryl isoprenoid, and from the presence of numerous diastereomers. Isorenieratane isolated from the Exshaw Formation also showed peak broadening during GC analysis, and was shown by NMR to contain 4 isomerised chiral carbon atoms (Hartgers and Sinninghe Damsté, unpublished results).

Diaryl isoprenoids with one additional aromatic ring. Two diaryl isoprenoids with one additional aromatic ring have been identified (**VI** and **VII**). The position of the additional aromatic ring in **VI** was established by ^{1}H and ^{13}C NMR (Sinninghe Damsté *et al.*, 1995d). In the mass spectrum of **VII** (Fig. 7.2**a**), the higher intensity of the fragment ion at m/z 237 *vs.* that at m/z 133 is explained by the fact that it is also α to the tertiary carbon atom C-13. The fragment ions at m/z 222 and 207 probably result from consecutive loss of CH_3• from the main fragment ion at m/z 237. Polychlorinated biphenyls (PCB's) can lose Cl• or even Cl_2 consecutively during mass spectral fragmentation, and the corresponding fragment ions have a higher relative intensity if the PCB contains at least two chlorine atoms in *ortho* positions (Safe and Hutzinger, 1971, 1972). This is probably due to the production, upon electron impact, of ions with a high internal energy caused by steric strain associated with restricted rotation around the phenyl-phenyl C-C bond. Consecutive loss of Cl• or Cl_2 results in an energy gain through release of steric strain (Safe and Hutzinger, 1971, 1972). Alkylated biphenyls that exhibit hindered rotation around the phenyl-phenyl C-C bond show consecutive loss of methyl or alkyl radicals from their molecular ions (Wolf, 1993; Wolf *et al.*, 1995).

Diaryl isoprenoids with two additional aromatic rings. These compounds can be divided into four groups: those with (i) two additional benzene rings (**VIII** and **IX**), (ii) a naphthalene moiety (**X-XIII**), (iii) an acenaphthene moiety (**XIV**), and (iv) a naphthalene moiety and a cyclohexadienyl moiety (**XV** and **XVI**). Mass spectra of **VIII** and **X** are shown in Fig. 7.2**b** and **c**, respectively. The similarity of the distribution of the

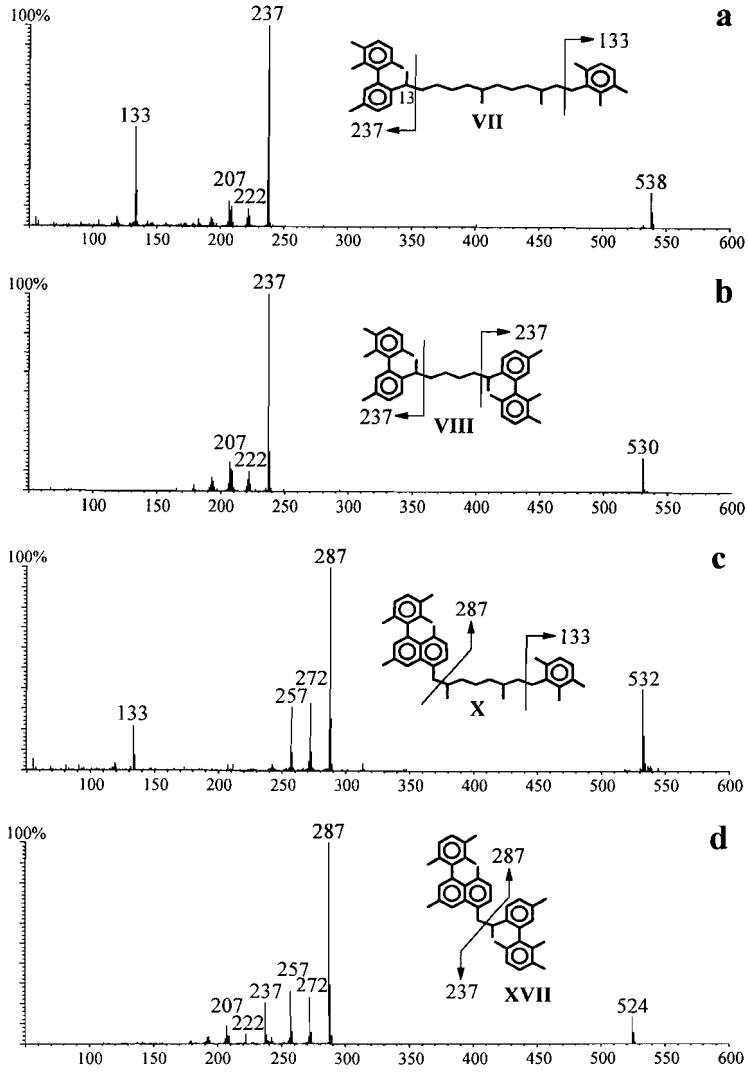

Fig. 7.2. Mass spectra (subtracted for background) of some C_{40} cyclised and aromatised diagenetic products of isorenieratene.

diastereomers of **VIII** and **IX** in three samples from different locations, and of variable age and maturity (Fig. 7.3) indicates that they represent atropisomers.

Identification of a naphthalene moiety in **X**, **XII** and **XIII** is supported by their accurate masses, which differ from that of isorenieratane by 14.10 amu. This is consistent with a difference of 14 H atoms, and not a methylene group, which would have resulted in a difference of 14.02 amu. Schwark and Püttmann (1990) reported a C_{39}

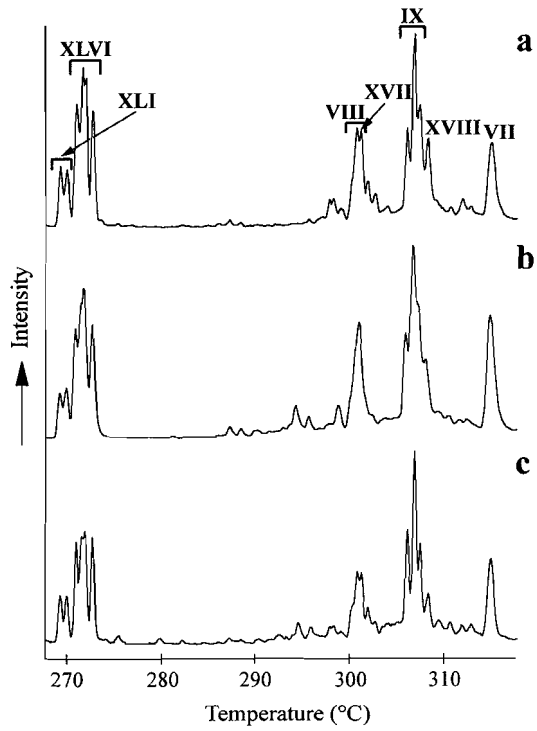

Fig. 7.3. Partial m/z 237 mass chromatograms of the polyaromatic fractions of the samples from the (**a**) Allgäu, (**b**) Kimmeridge Clay, and (**c**) Schistes Cartons (G6-5-6) Formations, showing compounds containing a biphenyl moiety. The gas chromatographic separation of the atropisomers of **VIII**, **IX**, **XLI** and **XLVI** can be discerned. Roman numbers refer to structures in Appendix I.

diaryl isoprenoid with a regular head-to-tail isoprenoid chain and an unknown substitution pattern for the aromatic rings in the Permian Kupferschiefer. Their tentative assignment was based on mass spectral data that revealed a molecular ion at m/z 532. However, it seems more likely that this compound is a C_{40} diaryl isoprenoid with an additional naphthalene moiety, since loss of a methylene group from the acyclic isoprenoid chain seems improbable. The intensity of the molecular ion in their mass spectrum (55%) is much higher than that of the C_{40} diaryl isoprenoid they report (21%), despite the structural similarity of the presumed C_{39} and C_{40} diaryl isoprenoids. This supports the presence of an additional naphthalene moiety in their compound, which is further substantiated by a small (7%) fragment ion at m/z 183.

The m/z 287 mass chromatogram of the polyaromatic fraction of the sample from the Kimmeridge Clay Formation (Fig. 7.4**a**) shows that the peaks attributed to **X** and **XI** do not occur in the 1:1 distribution expected for two atropisomers. Moreover, different

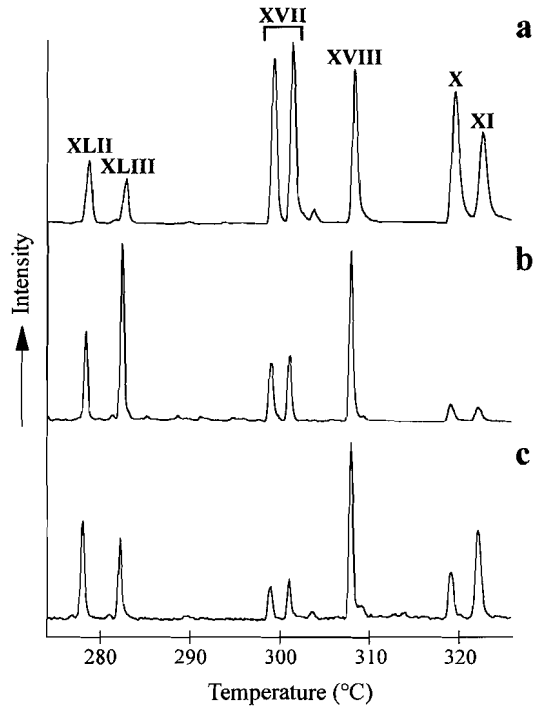

Fig. 7.4. Partial m/z 287 mass chromatograms of the polyaromatic fractions of the samples from the (**a**) Kimmeridge Clay, (**b**) Allgäu, and (**c**) Schistes Cartons (G6-5-6) Formations, showing compounds containing a phenyl-naphthyl moiety. The gas chromatographic separation of the atropisomers of **XVII** in a consistent approximate 1:1 distribution can be discerned. Roman numbers refer to structures in Appendix I.

distributions are found in the Allgäu Formation (Fig. 7.4**b**) and in sample G6-5-6 from the Schistes Cartons Formation (Fig. 7.4**c**), thereby fully excluding the possibility that **X** and **XI** are atropisomers. Their peak assignments were made based on the intensity of the fragment ions at m/z 272 and 257 relative to that at m/z 287. The main fragment ion at m/z 287 has a high internal energy because of restricted rotation around the phenyl-naphthyl C-C bond. The 1-phenylnaphthalene backbone of **X** is anticipated to have a higher rotational energy barrier than the 2-phenylnaphthalene backbone of **XI**, because of the hindering position of C-20 in **X**. Therefore, the fragment ions at m/z 272 and 257 are expected to have a higher intensity relative to m/z 287 in the mass spectrum of **X**. It was thus concluded that the last eluting peak in the m/z 287 mass chromatogram corresponds to **XI** (Fig. 7.4).

Diaryl isoprenoids with three additional aromatic rings. These compounds can be divi-

ded into two groups: compounds with a naphthalene moiety and an additional benzene ring (**XVII** and **XVIII**), and those with a condensed aromatic ring system (**XIX** and **XX**). The mass spectrum of **XVII** is shown in Fig. 7.2**d**.

The peak assignments of **XVII** and **XVIII** were made based on the presence of atropisomers and the intensity of the fragment ions at m/z 272 and 257 relative to that at m/z 287 (cf. **X** and **XI**). The m/z 287 mass chromatogram shows three peaks with a molecular ion at m/z 524, attributed to **XVII** and **XVIII** (Fig. 7.4). The mass spectra of the first two are virtually identical, but that of the third has less intense fragment ions at m/z 257 and 272. The similarity in the mass spectra of the first two peaks, combined with their approximate 1:1 distribution in three samples of different locations, age and maturity (Fig. 7.4) strongly suggests that they are atropisomers. Thus, the third peak represents the other structure containing a naphthalene moiety and an additional benzene ring. Both structures comprise an asymmetric carbon atom and a biphenyl moiety with restricted rotation around the phenyl-phenyl C-C bond. Rotation around the phenyl-naphthyl C-C bond in the 1-phenylnaphthyl moiety of **XVII** is severely hindered, but in the 2-phenylnaphthyl moiety of **XVIII** it can rotate more freely due to lack of direct interaction of bulky *ortho* groups. Therefore, **XVIII** is probably represented by the third peak in the cluster with molecular ion at m/z 524 in the m/z 287 mass chromatogram, whereas the axially chiral centre in **XVII** results in the first two separate peaks (Fig. 7.4). This identification is supported by the relative intensities of the fragment ions at m/z 257 and 272 in their mass spectra, associated with restricted rotation around the phenyl-naphthyl C-C bond (cf. **X** and **XI**). Also, peak assignments of **XVII** and **XVIII** are consistent with those of **X** and **XI**, in that the compounds with the 1-phenylnaphthyl moiety elute before their counterparts with the 2-phenylnaphthyl moiety.

Diaryl isoprenoids with four additional aromatic rings. In this group, one compound has been identified (**XXI**). Comparison of the accurate masses of the molecular ions of isorenieratane and **XXI** (m/z 520) reveals a difference of 0.18 amu, corresponding to 22 H atoms. Within experimental error, this is consistent with an elemental formula $C_{40}H_{40}$.

Diaryl isoprenoids with non-aromatic rings. Several compounds were recognised with major fragment ions that resembled those of compounds discussed above, but with mass spectra that did not match any diaryl isoprenoids with additional aromatic rings. We believe that they represent structures intermediate between isorenieratene and its aromatic derivatives, containing one or more (unsaturated) cyclohexyl moieties, possibly in combination with aromatic rings. A typical example of a diaryl isoprenoid with a saturated cyclohexyl moiety is **XXII**, which has a molecular ion at m/z 528 and major fragment ions at m/z 237 and 291. These ions suggest a structure like **XXII** based on its similarity to **XVII**.

Diaryl isoprenoids containing one sulphur atom. Compounds identified with one sul-

phur atom include a thiane (**XXIII**), five thiophenes (**XXIV-XXVIII**), two benzo[*b*]-thiophenes (**XXIX** and **XXX**) and a compound with a thiophene ring and a benzene ring (**XXXI**). The identification of these compounds is mainly based on mass spectrometry (*e.g.* Fig. 7.5) and detection with a sulphur-selective detector (FPD).

XXIII is reflected by two peaks in the gas chromatogram, corresponding to *cis-trans* isomers. Their elution order is assumed to be the same as that of the *cis-trans*

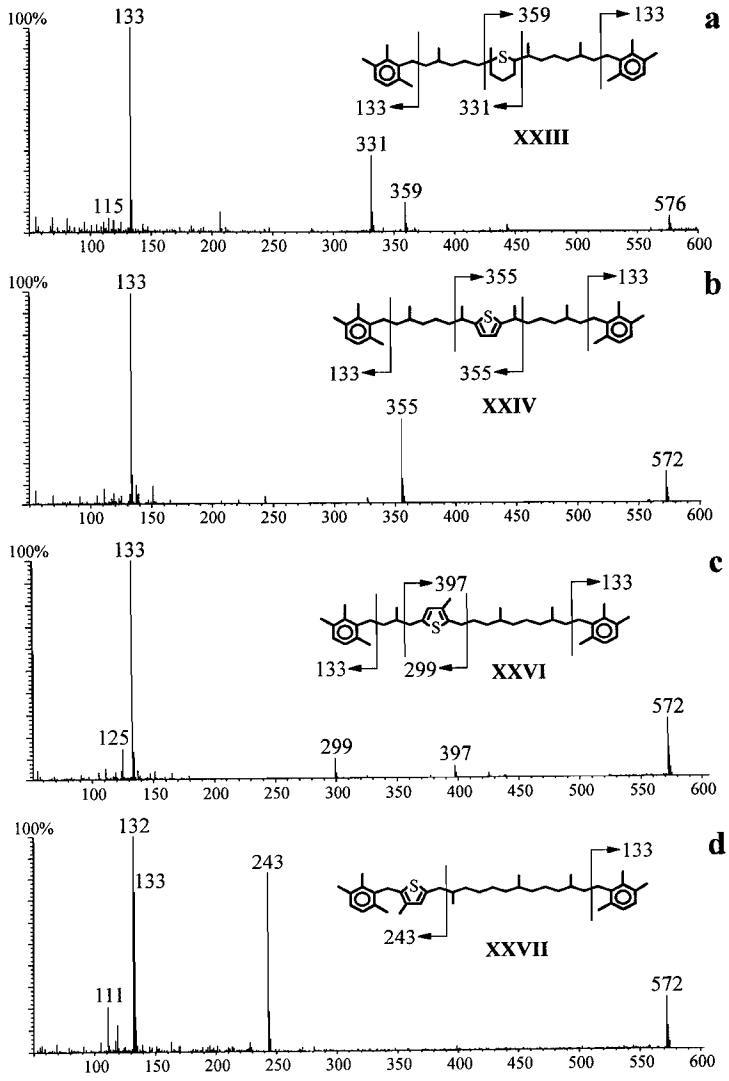

Fig. 7.5. Mass spectra (subtracted for background) of some C_{40} sulphur-containing diagenetic products of isorenieratene.

isomers of 2,6-di-*n*-alkylthianes (Sinninghe Damsté *et al.*, 1987c), *i.e. cis* elutes before *trans*. The sulphur atom is attached at one side to a tertiary carbon atom, consistent with Markovnikov's rule (de Graaf *et al.*, 1992). Formation of a thiane with sulphur attached to two tertiary carbon atoms apparently does not take place, although Markovnikov's rule favours this reaction.

Formation of the fragment ion at m/z 132, the base peak in the mass spectrum of **XXVII**, is thought to result from a McLafferty rearrangement involving H transfer from the benzene ring to the thiophene ring (Fig. 7.6). This rearrangement also occurs in methylated diphenylmethanes where the ion intensity is proportional to the number of *ortho* methyl groups, probably due to increased availability of H atoms (McLafferty and Stauffer, 1989).

The fragment ion at m/z 308 in the mass spectrum of **XXX** results from a McLafferty rearrangement favoured by a vacant *ortho* and *para* position of the benzene ring and the tertiary carbon atom C-13' to which the γ-H atom is attached (cf. Kingston *et al.*, 1988; Sinninghe Damsté *et al.*, 1988a).

Diaryl isoprenoids containing two sulphur atoms. This group comprises two dithiophenes (**XXXII** and **XXXIII**), a thieno[3,2-*b*]thiophene (**XXXIV**), a compound containing a benzo[*b*]thiophene moiety and a thiophene ring (**XXXV**), and a 1,2-dithiane (**XXXVI**).

The fragment ion at m/z 194 in the mass spectrum of **XXXIV** results from cleavage β to both sides of the thieno[3,2-*b*]thiophene moiety, and is analogous to the fragment ion at m/z 220 in the mass spectrum of a bithiophene with a phytane carbon skeleton (Sinninghe Damsté and de Leeuw, 1987). Stabilisation energy associated with the fully conjugated fragment ion favours the double cleavage.

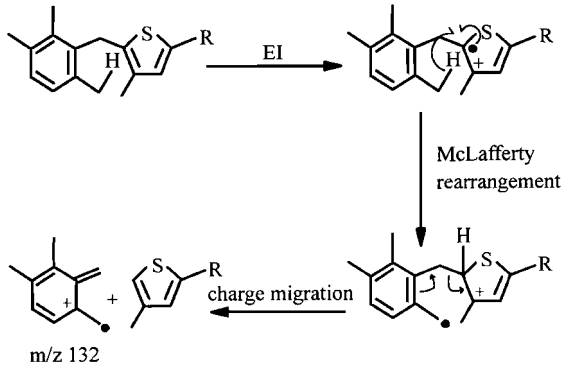

Fig. 7.6. McLafferty rearrangement leading to the fragment ion at m/z 132 in the mass spectra of **XXVII**, **XXX-XXXIII**, **XXXV**, **XLIX**, **L**, **LXI** and **LXII**.

C_{32} and C_{33} compounds

Several compounds were encountered with mass spectral characteristics (*e.g.* m/z 133, 237, 287) that suggest structures similar to those described above, but with molecular ions ($420 \leq M^{+\bullet} \leq 474$) consistent with diagenetic products of C_{32} and C_{33} 'carotenoids' (**XXXVII** and **XXXVIII**) formed from isorenieratene by expulsion of *m*-xylene and toluene, respectively (see below). The carbon numbering system (Fresenius, 1989) for isorenieratene is applied in a modified form to **XXXVII** and **XXXVIII**, based on their structural similarities. This does not imply that the absent carbon atoms are necessarily the atoms lost upon expulsion.

C_{32} compounds. C_{32} diagenetic products of **XXXVII** include a diaryl isoprenoid (**XXXIX**), two compounds with an additional benzene ring (**XL** and **XLI**), two compounds with a naphthalene moiety (**XLII** and **XLIII**), and a thiophene (**XLIV**). Mass spectra of **XXXIX-XLI** and **XLIII** are shown in Fig. 7.7.

XXXIX was recently reported after desulphurisation of polar fractions and kerogens of immature marlstones from the Gessoso-solfifera Formation (Kenig *et al.*, 1995; Schaeffer *et al.*, 1995a). The relative intensity of the fragment ion at m/z 134 in the mass spectrum of **XXXIX** is lower than in those of isorenieratane and the C_{33} diaryl isoprenoid (see below). This is due to the absence of methyl group C-19', so that the γ-H atom is attached to a secondary instead of a tertiary carbon atom, favouring the McLafferty rearrangement in isorenieratane and the C_{33} diaryl isoprenoid (cf. Kingston *et al.*, 1988; Sinninghe Damsté *et al.*, 1988a).

XLI appears as two peaks of equal intensity in the m/z 237 mass chromatogram (Fig. 7.3). These diastereomers result from its axial chirality and an asymmetric carbon atom. The high activation energy for rotation around the phenyl-phenyl C-C bond (138-168 kJ/mol; van Duin *et al.*, 1996) and the relatively low elution temperature (269-270°C) prevent interconversion of the atropisomers. The constant 1:1 distribution of the diastereomers in samples from different geographical locations, age and maturity (Fig. 7.3) further supports their identification as atropisomers. Schwark and Püttmann (1990) reported an unknown compound with a molecular ion at m/z 426 and a fragment ion at m/z 133 in the Permian Kupferschiefer. This may be **XL**, because they tentatively identified isorenieratane in the same sample.

The GC separation of the two atropisomers of **XLI** enabled determination of the activation energy for rotation around the phenyl-phenyl C-C bond, using the approach of König *et al.* (1993). They employed isothermal GC using capillary columns coated with modified cyclodextrins, which separated enantiomeric structures, to calculate the rate of interconversion of the two atropisomers of 2,2'-diisopropylbiphenyl as a function of temperature. Their data and the activation energy for rotation around the phenyl-phenyl C-C bond of 2,2'-diisopropylbiphenyl determined by Wolf (1993) make it possible to distinguish three stages of atropisomer peak separation and their respective ratios of half-life ($t_{½}$) to retention time (t_r), namely: (i) plateau between peaks ≤ 10% of peak

height ($t_{½} \geq 2*t_r$), (ii) plateau between peaks $\cong$ 50% of peak height ($t_{½} \cong t_r$) and (iii) one peak ($t_{½} \leq 0.5*t_r$). Thus, the peak shapes at different temperatures enable estimation of the half-life of the atropisomers which is related to the activation energy by the equation:

$$t_{½} = (\ln 2/A)*e^{(E/RT)}$$

where $t_{½}$ = half-life, A = frequency factor, E = activation energy, R = gas constant, and T = column temperature. Isothermal GC analyses of the polyaromatic fraction of the sample from the Kimmeridge Clay Formation at eight temperatures from 260 to 320°C showed that at 260°C the two peaks are fully separated, at 270°C the plateau between the peaks is approximately 10% of the peak height, at 300°C the plateau is approximately 50% of the peak height, and at 320°C one broad peak results (Fig. 7.8). Given A, which is known from molecular mechanics calculations (van Duin *et al.*, 1996), the activation energy is 155 kJ/mol, within the range (138-168 kJ/mol) calculated for **IV** using molecular mechanics (van Duin *et al.*, 1996). Apparently, the elongated alkyl chain present in **XLI** but absent in **IV** has little influence on the activation energy for rotation around the phenyl-phenyl C-C bond.

Neither **XLII** nor **XLIII** contains an asymmetric carbon atom in addition to the axially chiral centre at the phenyl-naphthyl C-C bond, so that they do not occur as diastereomers. The m/z 287 mass chromatogram reveals **XLII** and **XLIII** with variable relative intensities for different samples, proving that they are not atropisomers (Fig. 7.4). As with **X** and **XI**, peak assignment of **XLII** and **XLIII** is based on the intensity of the secondary fragment ions at m/z 257 and 272 relative to the main fragment ion at m/z 287. The mass spectrum of the first eluting compound has more intense fragment ions at m/z 257 and 272 than that of the second, suggesting that it is **XLII**. This proposed elution order for **XLII** and **XLIII** matches those of **X** and **XI** and **XVII** and **XVIII**, where the compound with a 1-phenylnaphthyl moiety elutes before that with a 2-phenylnaphthyl moiety.

C_{33} compounds. C_{33} diagenetic products of **XXXVIII** comprise a C_{33} diaryl isoprenoid (**XLV**), a C_{33} diaryl isoprenoid with an additional benzene ring (**XLVI**), and four thiophenes (**XLVII-L**). Mass spectra of **XLV-XLVII** and **XLIX** are shown in Fig. 7.9.

XLV was recently reported after desulphurisation of polar fractions and kerogens of immature marlstones from the Gessoso-solfifera Formation (Kenig *et al.*, 1995; Schaeffer *et al.*, 1995a). The McLafferty fragment ion at m/z 134 has a higher relative intensity than in the mass spectrum of **XXXIX**, and approximately the same as in isorenieratane (see above).

XLVI comprises an axially chiral centre and two asymmetric carbon atoms giving rise to four diastereomers, reflected in the m/z 237 mass chromatogram by four peaks of approximately equal intensity (Fig. 7.3). The absence of C_{33} diaryl isoprenoids with an

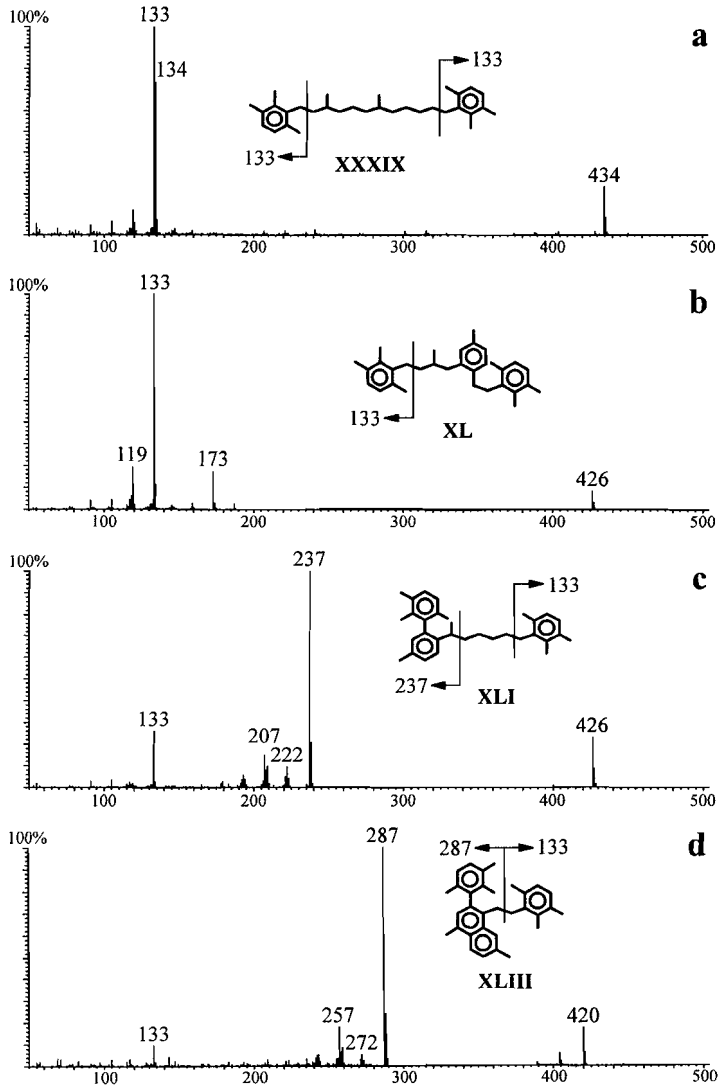

Fig. 7.7. Mass spectra (subtracted for background) of some C_{32} diagenetic products of isorenieratene.

additional benzene ring involving C-11 to C-9' and with a naphthalene moiety is due to the C-20 and C-19' methyl groups that preclude aromatisation.

The absence of a centre of symmetry in the C_{33} diaryl isoprenoid carbon skeleton leads to different compounds from formation of thiophene rings at C-8 to C-11 (**XLIX**) *vs.* C-14 to C-8' (**L**). Upon cleavage β to the thiophene ring, the former yields a fragment ion at m/z 243 and the latter at m/z 257. In **L** this cleavage is also α to a tertiary

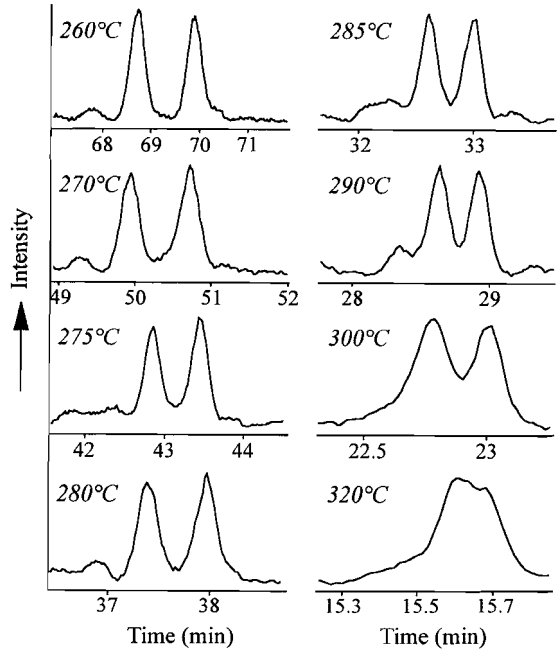

Fig. 7.8. Isothermal, partial gas chromatograms of the polyaromatic fraction of the sample from the Kimmeridge Clay Formation at various temperatures, showing the increasing height of the plateau between the peaks representing the atropisomers of **XLI** with increasing temperature.

carbon atom, which may explain its higher relative intensity.

Short-chain compounds

This group consists of compounds derived from C-C bond cleavage of C_{32}, C_{33} and C_{40} compounds. They will be differentiated as (i) aryl isoprenoids (**III**), (ii) aryl isoprenoids with additional aromatic rings (**LI-LX**), and (iii) sulphur-containing aryl isoprenoids (**LXI** and **LXII**). Mass spectra of **LI**, **LIII**, **LX** and **LXII** are shown in Fig. 7.10.

Aryl isoprenoids. A pseudohomologous series of aryl isoprenoids occurred in almost all samples with a distribution pattern containing low abundances of C_{12}, C_{17} and C_{23} members. Summons and Powell (1992) claimed identification of a variety of C_{14}-C_{20} aryl isoprenoid isomers in Siberian Platform oils of Late Proterozoic age. To explain the large number of isomers, they suggested methyl shifts in the isoprenoid chain. In the present study, however, no evidence was found for such isomerisations of aryl isoprenoids. Recently, we found evidence for the formation of aryl isoprenoids from β-carotene *via* aromatisation of a cyclohexenyl moiety and subsequent C-C bond cleavage of

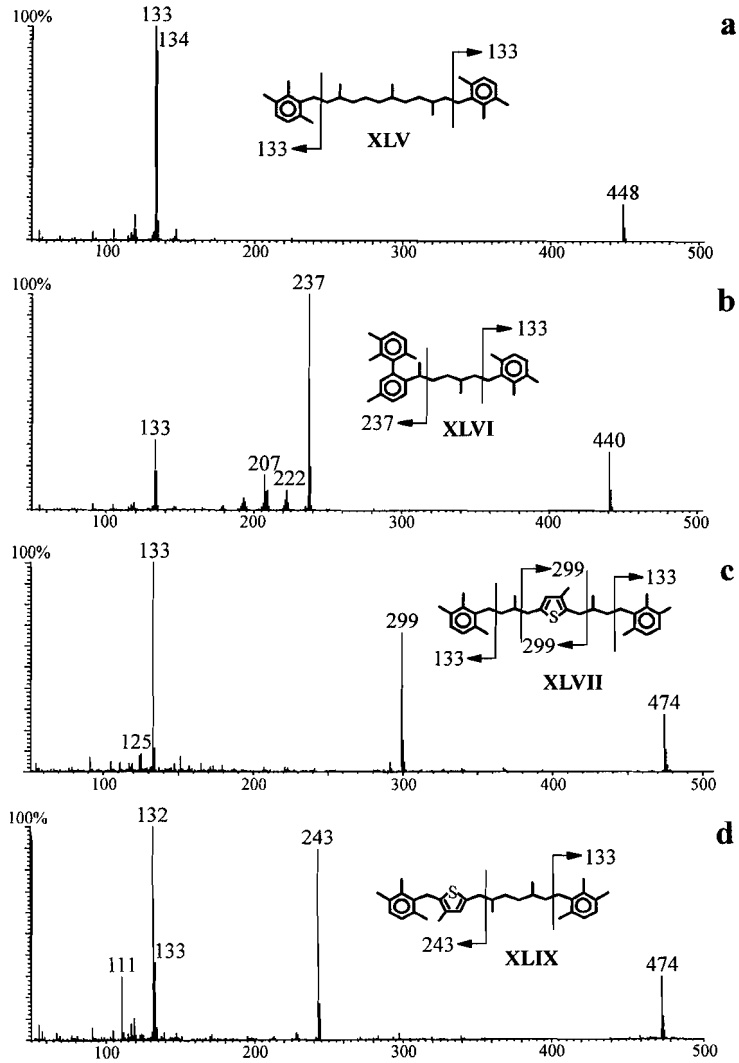

Fig. 7.9. Mass spectra (subtracted for background) of some C_{33} diagenetic products of isorenieratene.

the isoprenoid chain (Koopmans *et al.*, 1996c). This indicates that aryl isoprenoids can only be taken as catagenetic products of isorenieratene when they are significantly enriched in ^{13}C (by *c.* 15‰) compared to algal lipids.

Aryl isoprenoids containing one additional aromatic ring. These compounds can be divided in four groups that differ in the position of the additional benzene ring in the

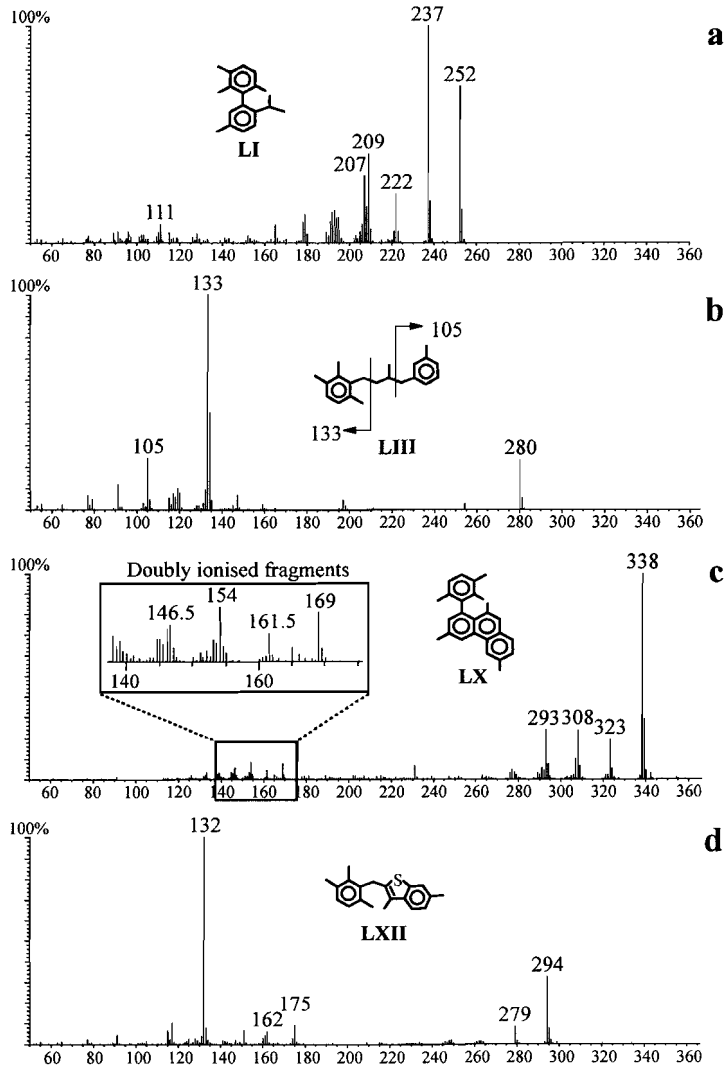

Fig. 7.10. Mass spectra (subtracted for background) of some short-chain isorenieratene derivatives.

isoprenoid chain and in their carbon skeleton, dependent on their formation from C_{32}, C_{33} and C_{40} precursors. The first group has an additional benzene ring in the 'biphenyl position' (**LI**). The other three groups have an additional benzene ring at various positions in the isoprenoid chain (**LII-LIV**).

LI include C_{19}-C_{23} components easily distinguished in a mass chromatogram of their main fragment ion at m/z 237 (Fig. 7.1), and C_{16}-C_{18} components recognised from

their retention times and characteristic (alkylated biphenyl-like) mass spectra, which contain fragment ions generated by consecutive loss of methyl radicals from the molecular ion (Wolf, 1993; Wolf *et al.*, 1995). The doubly ionised fragments, for instance at $(M^{+\bullet}\text{-n*15})/2$, in the mass spectra of **LI** are diagnostic of polyaromatic hydrocarbons (Safe and Hutzinger, 1973). The C_{20}-C_{23} components possess both an axially chiral centre and an asymmetric carbon atom, which gives rise to two diastereomers. For the C_{21}-C_{23} components these are separated by gas chromatography in a 1:1 distribution typical of atropisomers, whereas the C_{20} diastereomers almost coelute, as judged from the slightly broadened peak (Fig. 7.1).

C_{18} (R = H) and C_{19} (R = CH_3) components of **LII**, C_{21} (R = H), C_{22} (R = CH_3) and C_{24} (R = C_3H_7) components of **LIII**, and C_{26} (R = H) and C_{27} (R = CH_3) components of **LIV** were identified. Their mass spectra show enhanced peaks at m/z 105 or 119 resulting from cleavage β to one or both sides of the additional benzene ring. Four unknown compounds with molecular ions at m/z 266, 280, 294 and 336 in the m/z 133 mass chromatogram of the aromatic fraction of a sample from the Permian Kupferschiefer have been reported (Schwark and Püttmann, 1990). The second component ($M^{+\bullet}$ = 280) was the most prominent and appears to be the C_{21} diaryl isoprenoid **LIII** (R = H), because (i) no other major fragment ions were reported, which excludes the possibility of a biphenyl structure, (ii) it is prominent in our samples as well, and (iii) isorenieratane was also tentatively identified. Diaryl isoprenoids **LIII** with molecular ions at m/z 280, 294 and 322 were also found in a Devonian oil from the Pripyat Basin (Belorussia) that contains abundant aryl isoprenoids (J.L. Clayton, personal communication).

Aryl isoprenoids containing two additional aromatic rings. These compounds can be divided into two groups: aryl isoprenoids with a naphthalene moiety involving (i) C-7 to C-15' (**LV** and **LVI**), and (ii) C-11 to C-11' (**LVII-LIX**).

Mass spectra of **LV** and **LVI** show no major fragment ions indicative of the structural moieties encountered in other isorenieratene derivatives (*e.g.* m/z 133 and 237). However, three features are typical of alkylated polyaromatic hydrocarbons (Safe and Hutzinger, 1973). First, the molecular ion is the base peak, which testifies to the stability of the molecule under electron impact. Second, a number of doubly ionised fragments is observed (*e.g.* at m/z 137 and 144). Third, the spectra exhibit strong ($M^{+\bullet}$-n*15) fragment ions from consecutive loss of methyl radicals. All four compounds contain an axially chiral centre, but there are no diastereomers because none contains an asymmetric carbon atom. They elute in the order **LVI** (R = H), **LVI** (R = CH_3), **LV** (R = H), **LV** (R = CH_3), based on the intensity of the fragment ions ($M^{+\bullet}$-n*15) relative to the molecular ion (see also identifications of **X**, **XI**, **XVII**, **XVIII**, **XLII** and **XLIII**). The elution order of **LV** and **LVI**, with the 2-phenylnaphthyl compounds eluting prior to their 1-phenylnaphthyl counterparts, differs from that of the corresponding C_{32} (**XLII** and **XLIII**) and C_{40} (**X** and **XI**) compounds. Perhaps the structural difference between the isomers is more pronounced for the short-chain compounds, whereas for the C_{32} and C_{40} com-

pounds the retention time is predominantly influenced by the alkyl chain.

Aryl isoprenoids containing three additional aromatic rings. One aryl isoprenoid with a phenanthrene moiety has been identified (**LX**). Its mass spectrum (Fig. 7.10**c**) shows characteristics similar to those of **LV** and **LVI** (cf. Safe and Hutzinger, 1973), indicative of alkylated polyaromatic hydrocarbons. No diastereomers exist due to the absence of asymmetric carbon atoms.

Sulphur-containing aryl isoprenoids. This group of compounds is mainly comprised of aryl isoprenoids with a thiophene ring or cyclic sulphide moiety, although one compound with a benzo[*b*]thiophene (**LXII**) moiety has been identified. The sulphur-containing ring occurs at various positions in the isoprenoid chain, yielding different families of compounds. Identification of these compounds in the Calcaires en Plaquettes Formation is supported by production of abundant aryl isoprenoids upon desulphurisation, as discussed elsewhere (van Kaam-Peters *et al.*, 1997b).

One family of aryl isoprenoids with a thiophene ring (**LXI**) is easy to recognise by an abundant fragment ion at m/z 132 (Fig. 7.6) and a fragment ion at m/z 243 resulting from cleavage β to the thiophene ring. It cannot be presumed that the alkyl side chain of **LXI** is a tail-to-tail isoprenoid chain (cf. **XXVII**), because it may be formed by C-C bond cleavage of **XLIX** or **L**, which possess different alkyl chains. Cleavage products of **L**, however, would be distinguished by a fragment ion at m/z 257.

Isorenieratene derivatives in polar fractions

Comparison of sulphur-bound isorenieratene derivatives present in the polar fractions of samples from the Gessoso-solfifera, Schistes Cartons, Allgäu and Boas Oil Shale Formations was made after Raney Ni desulphurisation followed by GC-MS analysis of the released hydrocarbons. The distributions of these products are revealed by partial summed mass chromatograms of fragments (m/z 133+237+287) that represent the most important ions in the mass spectra of most isorenieratene derivatives (Fig. 7.11).

Released hydrocarbons include a series of aryl isoprenoids (C_{15}-C_{27}), diaryl isoprenoids (**II**, **XXXIX** and **XLV**), and diaryl isoprenoids with an additional benzene ring (**VI** and **VII**). C_{32} and C_{33} diaryl isoprenoids with an additional benzene ring and diaryl isoprenoids with more than one additional aromatic ring are present in low amounts.

^{13}C content of dia- and catagenetic products of isorenieratene

Important circumstantial evidence for the genetic relationship of **II-LXII** with isorenieratene is provided by their ^{13}C content (Table 7.2). Comparison of δ^{13}C values of **II-LXII** and components [phytane and 2,5,7,8-tetramethyl-2-(4,8,12-trimethyltridecyl)-chroman] presumed to be derived from algae living in the upper part of the water

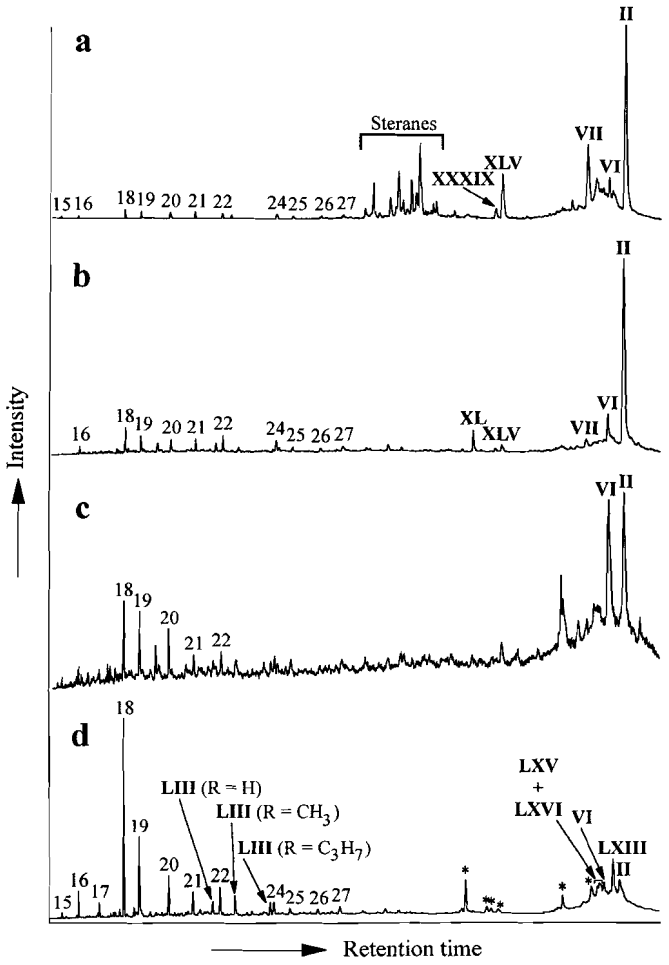

Fig. 7.11. Summed (m/z 133+237+287) mass chromatograms of the desulphurised polar fractions of the samples from the (**a**) Gessoso-solfifera, (**b**) Schistes Cartons, (**c**) Allgäu, and (**d**) Boas Oil Shale Formations. Aryl isoprenoids are indicated by numbers that represent the total number of carbon atoms. Roman numbers refer to structures in Appendix I. Compounds with an unidentified aromatic substitution pattern are denoted with an asterisk.

column (Sinninghe Damsté *et al.*, 1993c) and using Rubisco for CO_2 fixation (Hayes, 1993) reveals a consistent enrichment of *ca.* 15‰ for **II-LXII** in samples ranging from Ordovician to Recent (Table 7.2 and Fig. 7.12).

The complex composition of the A3 and A4 fractions (see Experimental) containing the dia- and catagenetic products of isorenieratene may introduce several problems during isotope-ratio-monitoring GC-MS. First, coelution of compounds will complicate

Table 7.2. $\delta^{13}C$ values (‰) of dia- and catagenetic products of isorenieratene.

	Kimmeridge Clay Fm.	Calcaires en Plaquettes Fm.	Allgäu Fm.	Gessoso-solfifera Fm.[a]	Gessoso-solfifera Fm.[b]	Boas Oil Shale Fm.
II	-16.6±0.3	-19.0±0.8	-19.0±0.3	-16.4±1.0	-13.7±0.8	
III (C_{16})						-18.9±0.3
VI	-16.3±0.2		-18.7±0.7			
VII	-17.3±0.3					
VIII+XVII	-17.9±0.4					
IX	-15.3±0.5					
X+XIV	-19.9±1.4					
XVIII	-14.7±0.5		-21.3±1.2			
XXIV		-19.2±0.3				
XXV		-19.6±0.6				
XXVI		-21.2±0.5				
XXXIX					-13.5±3.0	
XL			-19.0±1.1			
XLIII			-20.8±0.4			
XLV	-15.9±0.3			-15.8±0.8	-13.4±1.0	
XLVI	-17.7±0.8					
LI (R=H)					-16.2±0.7	
LI (R=*i*-Pr)					-15.9±1.0	
LIII (R=H)	-16.3±0.2					
LV (R=H)	-18.6±1.8					
LXIII						-17.2±1.1
Phytane	-31.2±0.2	-30.5±0.1	-33.5±0.2	-30.1±0.3[c]	-29.3±0.7	-34.2±0.3
Chroman[d]	-33.1±0.5	-32.6±0.2	-33.6±0.2	-28.7±0.3	-26.3±0.2	

[a] Polyaromatic fraction of the sample artificially matured by hydrous pyrolysis at 239°C.

[b] Desulphurised polar fraction of unheated sample.

[c] Phytane in the sample artificially matured by hydrous pyrolysis at 260°C.

[d] 2,5,7,8-Tetramethyl-2-(4,8,12-trimethyltridecyl)chroman.

peak definition (Ricci *et al.*, 1994). Coelution of the dia- and catagenetic products of isorenieratene and compounds not originating from Chlorobiaceae may introduce errors of up to several ‰, although GC-MS analyses indicate that such coelutions are rare. Second, subtraction of the appropriate background value is difficult when peaks elute in a 'hump'. In both cases systematic errors will be made, *i.e.* a low standard deviation does not guarantee that the value is reliable. However, the difference in $\delta^{13}C$ values between dia- and catagenetic products of isorenieratene and compounds derived from algae (*ca.* 15‰) is much larger than these errors, so they can still be used to characterise an origin from Chlorobiaceae.

$\delta^{13}C$ values of dia- and catagenetic products of isorenieratene in each sample fall

within a 2-3‰ range. Thus, there are no systematic differences in $\delta^{13}C$ values between compounds with different carbon skeletons or type or number of sulphur-containing or aromatic rings. This is in agreement with the findings of Freeman *et al.* (1994) and Sinninghe Damsté *et al.* (1995d) that diagenetic aromatisation is not accompanied by isotopic fractionation.

Schouten *et al.* (1995c) found that laboratory hydrosulphurisation of a model compound (1-decene) was accompanied by a kinetic isotope effect, producing sulphur compounds that were initially depleted in ^{13}C. They argued that a lack of fractionation effects in other studies of free and sulphurised sedimentary lipids (Kohnen *et al.*, 1992a; Schouten *et al.*, 1996) could be explained by complete sulphurisation of functionalised lipids, in agreement with our results. Hartgers *et al.* (1994c) found that free isorenieratane was enriched in ^{13}C relative to its macromolecularly-bound counterpart by *ca.* 12‰, a difference ascribed to a kinetic isotope effect during formation of geomacromolecules. The lack of such a difference here may indicate that all available isorenieratene has been incorporated into macromolecules from which it is only released at a later stage of diagenesis. The absence of free isorenieratane in immature sedimentary rocks ($R_o \approx 0.25\%$) from the Vena del Gesso Basin (northern Italy), and the high amounts of isorenieratane released after desulphurisation of polar fractions, asphaltenes and kerogen (Kohnen *et al.*, 1991c; Kenig *et al.*, 1995; Schaeffer *et al.*, 1995a; Koopmans *et al.*, 1996b) supports this interpretation.

Diagenetic products of a diaromatic carotenoid with a 3,4,5-/2,3,6-trimethyl substitution pattern

Recently, Hartgers *et al.* (1993) identified a C_{40} diaryl isoprenoid with an unprecedented 3,4,5-/2,3,6-trimethyl substitution pattern for the aromatic rings (**LXIII**) in the Mississippian Exshaw Formation. This compound is thought to derive from a diaromatic carotenoid with the same carbon skeleton (**LXIV**), biosynthesised by photosynthetic sulphur bacteria that may be extinct (Hartgers *et al.*, 1993, 1994c). Because **LXIV** possesses a conjugated double bond system identical to that of isorenieratene, we anticipate that dia- and catagenetic products analogous to those formed from isorenieratene can be identified.

Both isorenieratane and **LXIII** were identified in the Boas Oil Shale, Womble, Exshaw and Duvernay Formations. An origin for **LXIII** from photosynthetic sulphur bacteria is supported by its high ^{13}C content ($\delta^{13}C = -17.2 \pm 1.1$‰; Table 7.2) in the Boas Oil Shale Formation. This sample also contains two diaryl isoprenoids with a 3,4,5-/2,3,6-trimethyl substitution pattern and an additional aromatic ring (**LXV** and **LXVI**). These elute earlier than **VI**, compatible with the elution order of the diaryl isoprenoids **LXIII** and isorenieratane. **LXIII**, **LXV** and **LXVI** were also released after desulphurisation of the polar fraction of the sample from the Boas Oil Shale Formation (Fig. 7.11**d**).

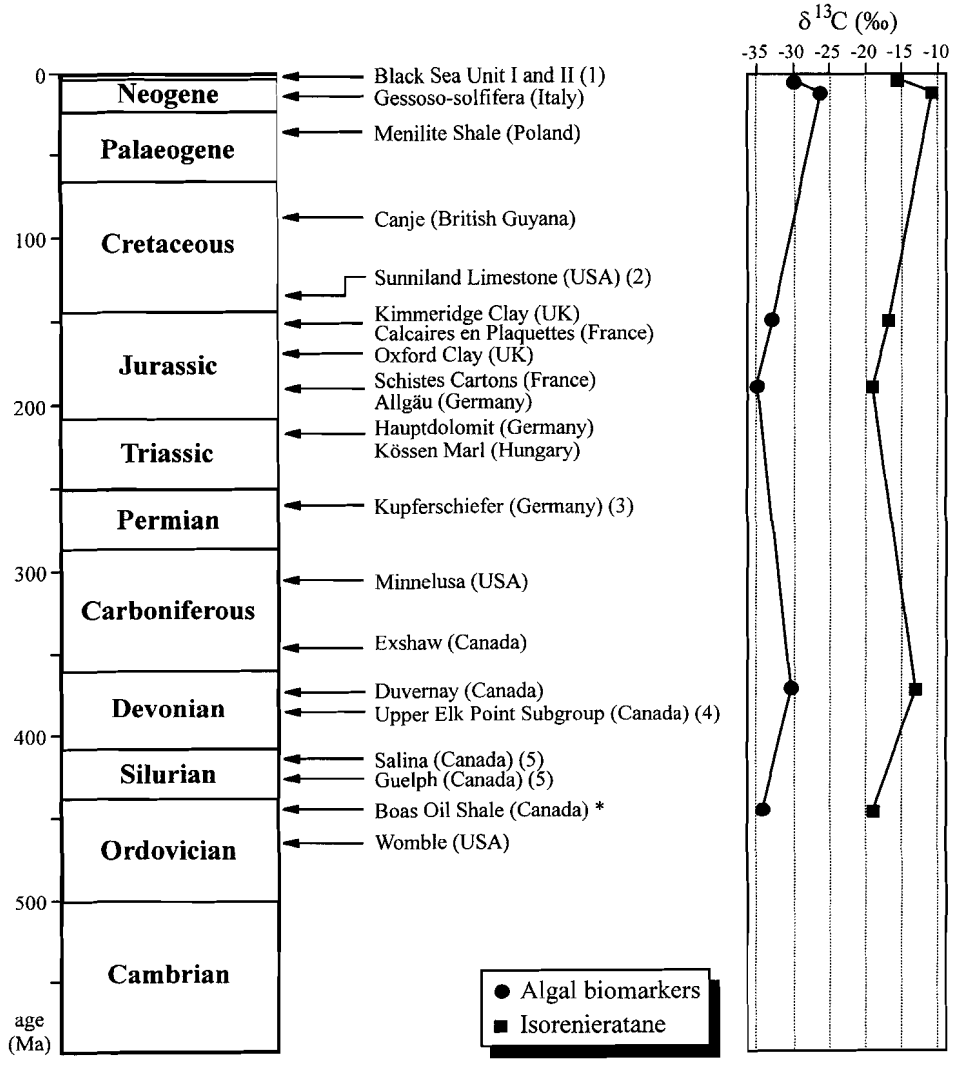

Fig. 7.12. Occurrence of isorenieratene derivatives through time. $\delta^{13}C$ values of isorenieratane and algal biomarkers [phytane and 2,5,7,8-tetramethyl-2-(4,8,12-trimethyltridecyl)chroman] in samples of different age display a constant difference of *ca.* 15‰. Key: * = isotope value of C_{16} aryl isoprenoid. Numbers in brackets refer to previous studies: (1) Sinninghe Damsté *et al.* (1993d); (2) Yu Xinke *et al.* (1990); (3) Schwark and Püttmann (1990); (4) Clark and Philp (1989); (5) Summons and Powell (1987).

Because of the asymmetric carbon skeleton of **LXIV**, different compounds result when an additional aromatic ring is present at either C-11 to C-15' or C-15 to C-11'

(**LXV** and **LXVI**). This complication also applies to other diagenetic products of **LXIV**. The input of two structurally distinct diaromatic carotenoids (**I** and **LXIV**) into the sediment, one with an asymmetric carbon skeleton, severely complicates identification and distinction of their dia- and catagenetic products.

Artificial maturation experiments

To study the influence of thermal maturity on the amounts and distributions of isorenieratene derivatives in polyaromatic and HMW fractions, artificial maturation experiments were conducted with a marl sample from the Gessoso-solfifera Formation using hydrous pyrolysis at temperatures between 160 and 330°C.

Partial summed (m/z 133+237+287) mass chromatograms of the polyaromatic fractions of the original sample and the samples artificially matured at 160, 260 and 300°C are shown in Fig. 7.13. The distribution of isorenieratene derivatives in the original sample is dominated by **VII** (3 μg/g TOC), whereas isorenieratane (**II**) is absent (Fig. 7.13**a**). Mild heating (160°C) results in release of low amounts of isorenieratene derivatives with molecular ions 2 or 4 amu less than expected, suggesting the presence of additional rings or double bonds (Fig. 7.13**b**). These compounds disappeared upon hydrogenation of the A3 fraction of the sample heated at 200°C whereas the relative amount of isorenieratane increased, indicating that they are unsaturated isorenieratene derivatives. After heating between 239 and 300°C, isorenieratane (**II**) is the most abundant isorenieratene derivative (79 and 61 μg/g TOC at 260 and 300°C, respectively; Fig. 7.13**c** and **d**). A wide range of polyaromatic diagenetic products of isorenieratene and some sulphur-containing compounds are also present. At 330°C only small amounts of isorenieratene derivatives remain, presumably due to their thermal degradation.

Summed (m/z 133+237+287) mass chromatograms of the desulphurised polar fractions of the same samples are shown in Fig. 7.14. Desulphurisation of the polar fraction of the original sample yields isorenieratane (66 μg/g TOC), intermediate amounts of **VI**, **VII** and the C_{32} and C_{33} diaryl isoprenoids **XXXIX** and **XLV**, and low amounts of C_{15}-C_{27} aryl isoprenoids (Fig. 7.14**a**). As temperatures are raised to 300°C, the amounts of these compounds first increase and then decrease, but no other isorenieratene derivatives with more than one additional aromatic ring are released. However, at 300°C **IX** is present in low abundance (6 μg/g TOC). At 330°C no isorenieratene derivatives could be detected. The concentration of isorenieratane is highest at 200°C ($1.0*10^3$ μg/g TOC; Fig. 7.15**a**). It is the most abundant compound below 300°C, but at higher temperatures **VI** predominates. The relative amounts of aryl isoprenoids increase progressively, but their absolute amounts remain low (C_{18} = 7 μg/g TOC at 300°C). They are dominated by C_{16} and C_{18} members.

In the original sample isorenieratane is solely present as a sulphur-bound moiety in the polar fraction (Fig. 7.15**a**) and in other HMW fractions (*i.e.* asphaltenes and kerogen). The thermal release of sulphur-bound isorenieratane can be examined by plotting

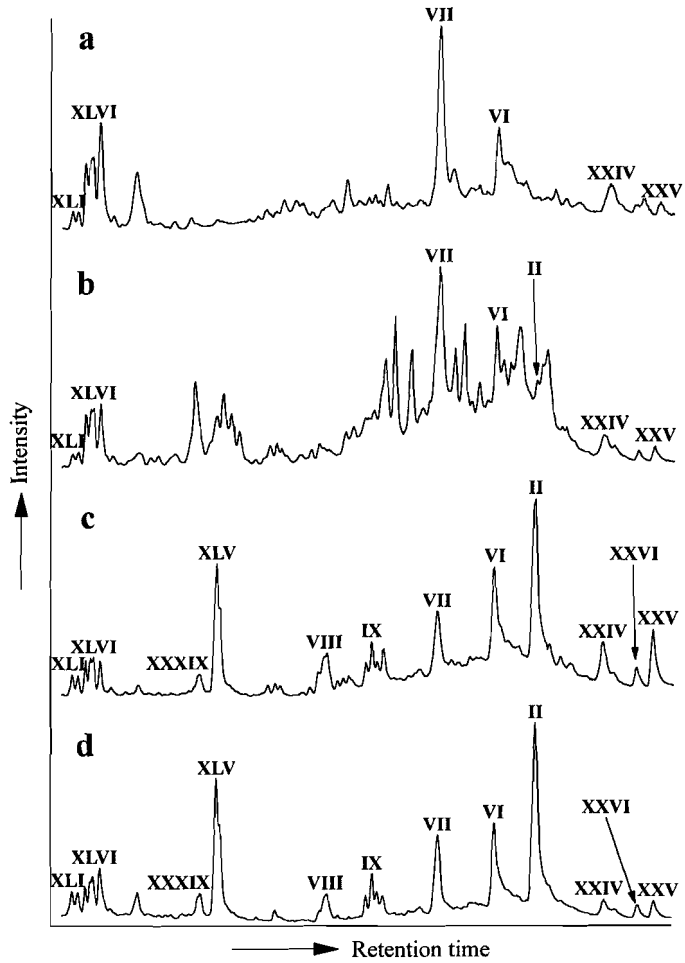

Fig. 7.13. Partial summed (m/z 133+237+287) mass chromatograms of the polyaromatic fractions of (**a**) the original sample from the Gessoso-solfifera Formation, and the samples artificially matured at (**b**) 160°C, (**c**) 260°C, and (**d**) 300°C. Roman numbers refer to structures in Appendix I.

the ratio [polar S-bound]/[polar S-bound + free] for isorenieratane against maturation temperature (Fig. 7.15**b**). Isorenieratane is predominantly present as a sulphur-bound moiety up to 239°C. At higher temperatures it is released, so that the percentage of sulphur-bound isorenieratane decreases rapidly to zero at 330°C.

7.5 Discussion

Dia- and catagenetic pathways of isorenieratene

Hartgers *et al.* (1994c) presented a concise schematic overview of dia- and catagenetic pathways of isorenieratene, stating that it is predominantly (> 99%) incorporated into macromolecular substances *via* multiple S-, O- and/or C-links. Progressive dia- and

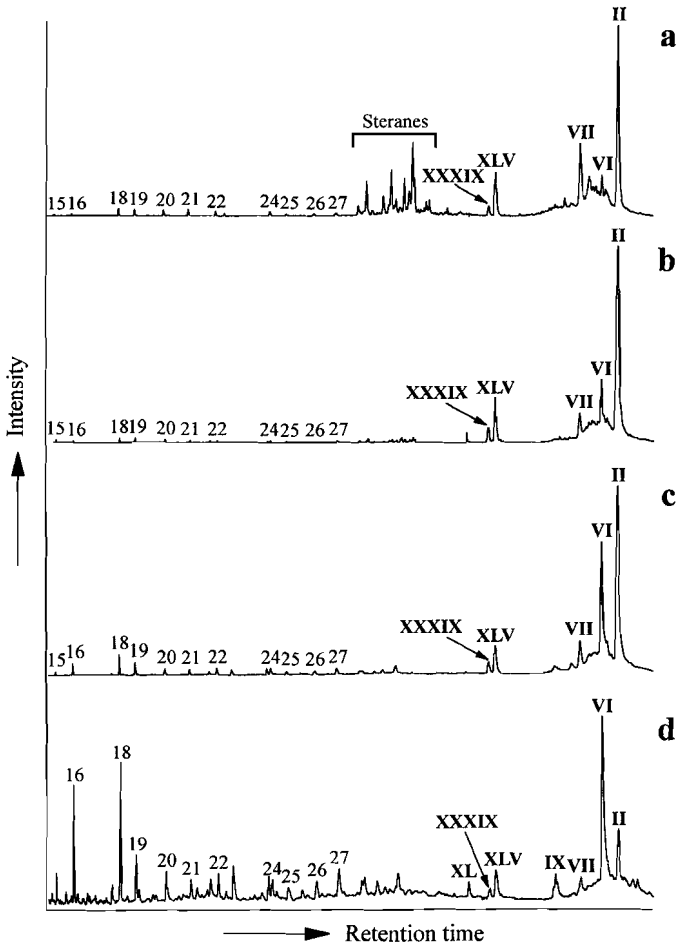

Fig. 7.14. Summed (m/z 133+237+287) mass chromatograms of the desulphurised polar fractions of (**a**) the original sample from the Gessoso-solfifera Formation, and the samples artificially matured at (**b**) 160°C, (**c**) 260°C, and (**d**) 300°C. Aryl isoprenoids are indicated by numbers that represent the total number of carbon atoms. Roman numbers refer to structures in Appendix I.

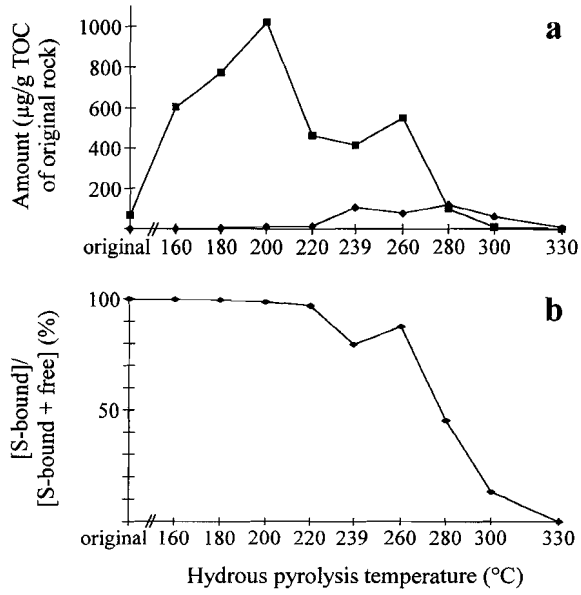

Fig. 7.15. (**a**) Generation profiles of free isorenieratane in the polyaromatic fraction (diamonds) and sulphur-bound isorenieratane in the polar fraction (squares) of artificially matured samples from the Gessoso-solfifera Formation as a function of maturation temperature. (**b**) [Polar sulphur-bound]/[polar sulphur-bound + free] ratio for isorenieratane as a function of maturation temperature.

catagenesis results in the release of aryl isoprenoids from these HMW substances. The small percentage of isorenieratene not incorporated into HMW fractions was held to account for the free isorenieratane in sedimentary rocks and crude oils (Hartgers *et al.*, 1994c). This scheme does not include LMW sulphur-containing or aromatised C_{32}, C_{33} or C_{40} compounds, which is our aim here.

There are three principal early diagenetic pathways for isorenieratene. First, cyclisation with subsequent aromatisation of the isoprenoid chain can occur. Second, toluene or *m*-xylene can be expelled yielding C_{33} or C_{32} 'carotenoids'. Third, reduced inorganic sulphur species (either mono- or polysulphides) can react with isorenieratene in an intra- and intermolecular fashion to generate LMW and HMW products (Sinninghe Damsté *et al.*, 1989c, 1993d; de Graaf *et al.*, 1992; Kohnen *et al.*, 1992a; Schouten *et al.*, 1994; Kenig *et al.*, 1995; Schaeffer *et al.*, 1995a). In the following sections these reactions will be discussed, together with C-C bond cleavage that occurs during later stages of maturation.

Cyclisation and aromatisation

Formation of additional aromatic rings in isorenieratene derivatives seems to take place

at specific sites in the acyclic isoprenoid chain. Five different diaryl isoprenoids with one additional aromatic ring can be anticipated (Sinninghe Damsté *et al.*, 1995d), but only two are encountered as major components (**VI** and **VII**). It appears that they form from isorenieratene by cyclisation and aromatisation of a part of the acyclic isoprenoid chain. Cyclisation probably proceeds in two steps (Fig. 7.16). First, *trans-cis* isomerisation of one double bond within the all-*trans* conjugated double bond system of isorenieratene must occur to form a six-membered ring transition state. Such isomerisation reactions do occur during diagenesis, given the presence of isorenieratene and one of its stereoisomers, containing one *cis* double bond, in an immature marlstone from the Gessoso-solfifera Formation (Keely *et al.*, 1995). Second, an intramolecular Diels-Alder reaction takes place where the diene and the dienophile are adjacent double bonds in the six-membered ring transition state, as proposed earlier for the thermal degradation of polyvinyl chloride (*e.g.* Tüdös *et al.*, 1974; O'Mara, 1977; Starnes and Edelson, 1979) and β-carotene (Ishiwatari, 1980). The resulting cyclohexadienyl moieties probably aromatise fast because of the energy gain associated with restoration of a fully conjugated double bond system. The Diels-Alder reaction can only result in cyclisation involving C-11 to C-15' and C-7 to C-12, yielding compounds with a ring in the isoprenoid chain at the position found in **VI** and **VII** (Fig. 7.16). The dominance of **VI** over **VII** usually observed is probably due to steric hindrance associated with formation of the latter. The positions of the additional benzene rings in **VIII** and **IX** are identical to those in **VII** and **VI**. Thus, even when two additional benzene rings are present they occupy the two preferred positions discussed above, suggesting that they form by the same cyclisation process.

It can be argued, however, that the double bonds in the isoprenoid chain of isorenieratene form a conjugated system and are therefore not localised as depicted in Fig. 7.16. Delocalisation of double bonds would, in principle, enable cyclisation involving C-10 to C-15 and C-12 to C-14', even though the six-membered ring transition states only comprise two double bonds. The six-membered ring transition states of the cyclisation reactions involving C-10 to C-15 and C-12 to C-14' are thought to have higher activation energies than those involving C-7 to C-12 and C-11 to C-15', however, because they imply that the molecule is either a biradical or an ionic species. Indeed, C_{40} diaryl isoprenoids with an additional aromatic ring involving C-10 to C-15 and C-12 to C-14' have only been found in low abundance in the Kimmeridge Clay Formation (van Kaam-Peters *et al.*, 1997a). It can therefore be assumed that cyclisation *via* six-membered ring transition states that contain three double bonds represent the major formation pathway of additional aromatic rings in isorenieratene. Cyclisation involving C-20 to C-14' is improbable because C-20 is sp^3 hybridised and not part of the conjugated system.

Formation of diaryl isoprenoids with an additional naphthalene moiety probably occurs in a similar fashion (Fig. 7.17). The cyclisation products shown in Fig. 7.16 serve as precursors. First, a *trans-cis* isomerisation reaction must occur to form a six-

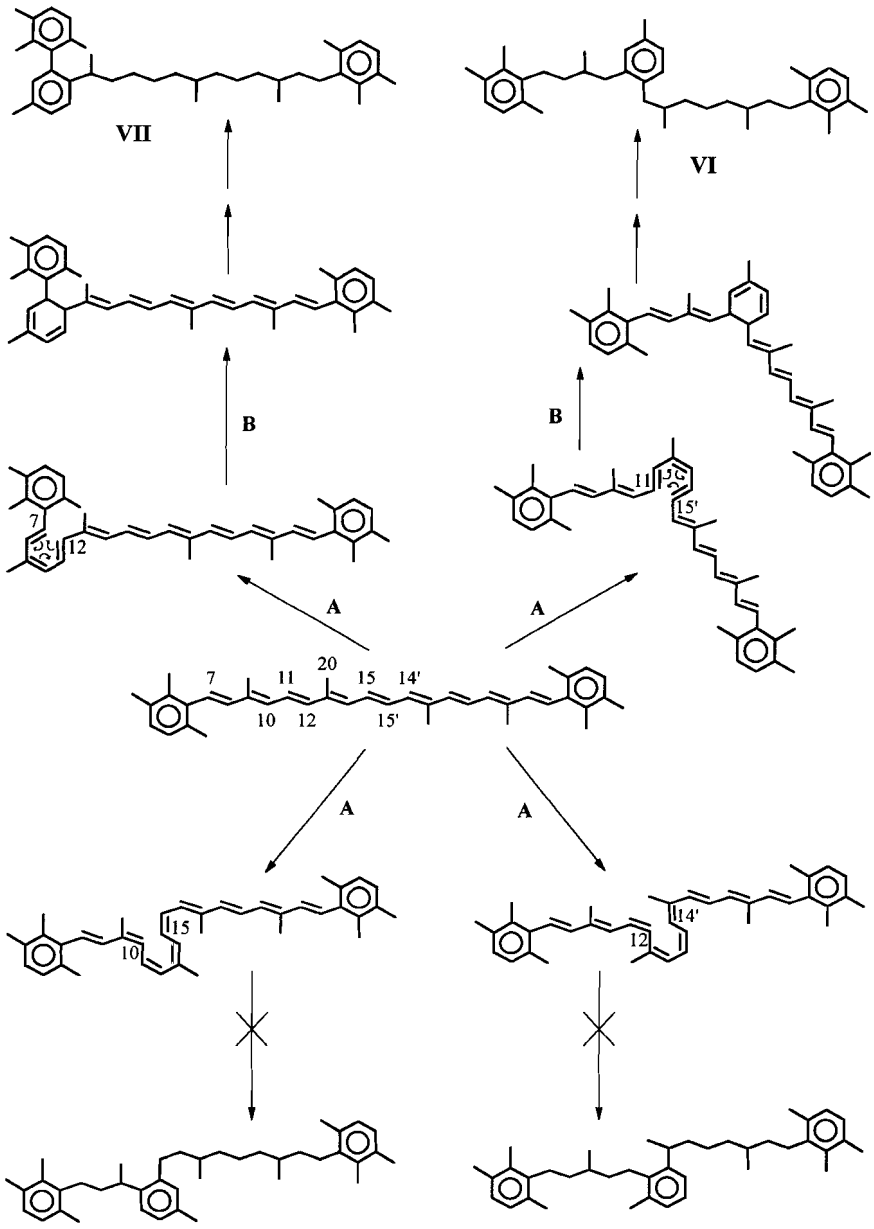

Fig. 7.16. Formation of diaryl isoprenoids with an additional benzene ring. Cyclisation of isorenieratene proceeds in two steps: (**A**) *trans-cis* isomerisation of a double bond, (**B**) intramolecular Diels-Alder reaction. It is unlikely that the Diels-Alder reaction proceeds *via* the other two six-membered ring transition states, because these have a high activation energy due to the unfavourable positions of the double bonds.

membered ring transition state. Second, the double bonds in the cyclohexadienyl moiety must shift to form a conjugated system and enable a Diels-Alder reaction. Alternatively, and more likely, the ring may have aromatised, which also enables a Diels-Alder reaction. **X** can form from the precursors of both **VI** and **VII**, whereas **XII** can only form from the precursor of **VI** (Fig. 7.17). **XI** and **XIII** cannot form from either precursor. They require a ten-membered ring transition state and are probably formed directly from isorenieratene (Fig. 7.18). **XI** is abundant in the Kimmeridge Clay Formation, and is more abundant than **X** in sample G6-5-6 from the Schistes Cartons Formation (Fig. 7.4), indicating the importance of its formation pathway. However, direct comparison of the amounts of **XI** and **X** is inherently dangerous, because the precursor of **X** can undergo more subsequent cyclisation reactions. The factors controlling formation of compounds with either a 1- or 2-phenylnaphthalene moiety (*e.g.* **X** and **XI**) are presently unclear.

Formation of the diaryl isoprenoid with a phenanthrene moiety (**XX**) from the aromatised precursor of **IX**, **X** or **XII** (Fig. 7.19) requires a sequence of reactions similar to that responsible for formation of diaryl isoprenoids with a naphthalene moiety from the aromatised precursors of **VI** and **VII** (cf. Fig. 7.17). We propose, following identification of **VII**, **X**, **XVII** and **XX**, that the diaryl isoprenoid with four additional aromatic rings (**XXI**) is the expected end point of the cyclisation and aromatisation process described above (see Figs. 7.16, 7.17 and 7.19).

The cyclohexadienyl moiety of **XV** and **XVI** is probably also the product of a Diels-Alder reaction. Subsequent aromatisation of this ring is precluded by the quaternary carbon atom C-9'. A similar observation is made for **XIV**, where the quaternary carbon atom C-13' seems to preclude aromatisation of the acenaphthene moiety. However, **XIX** is probably the aromatised counterpart of **XIV**, formed *via* loss of methyl group C-20'. Corresponding aromatised counterparts of **XV** and **XVI** were not found.

The cyclisation and aromatisation reactions of isorenieratene are summarised in Fig. 7.20. The double bonds indicated are actually absent in the diagenetic products. They must be hydrogenated at some stage of diagenesis.

Expulsion of *m*-xylene and toluene

Mild heating of β-carotene (**LXVII**) produces C_{32} (philene; **LXVIII**) and C_{33} (lexene; **LXIX**) 'carotenoids' plus *m*-xylene and toluene, respectively (*e.g.* Kuhn and Winterstein, 1933; Day and Erdman, 1963; Edmunds and Johnstone, 1965; Byers and Erdman, 1983). Jiang and Fowler (1986) tentatively identified fully hydrogenated lexene (or lexane; **LXX**), the C_{33} pseudohomologue of β-carotane (**LXXI**), in an oil from NW China. **LXX** and a series of 2,2,6-trimethyl-1-alkylcyclohexanes were identified in Canadian oils (Fowler *et al.*, 1993). The identical ^{13}C compositions of **LXX** and **LXXI** in the saturated hydrocarbon fraction of a gilsonite (Utah) suggested a common C_{40} carotenoid precursor (Schoell *et al.*, 1994). The fragment ions at m/z ($M^{+\bullet}$-106) and ($M^{+\bullet}$-92) in the mass spectrum of β-carotene are thought to originate from loss of *m*-xylene and toluene, respectively, either during mass spectral fragmentation, or during

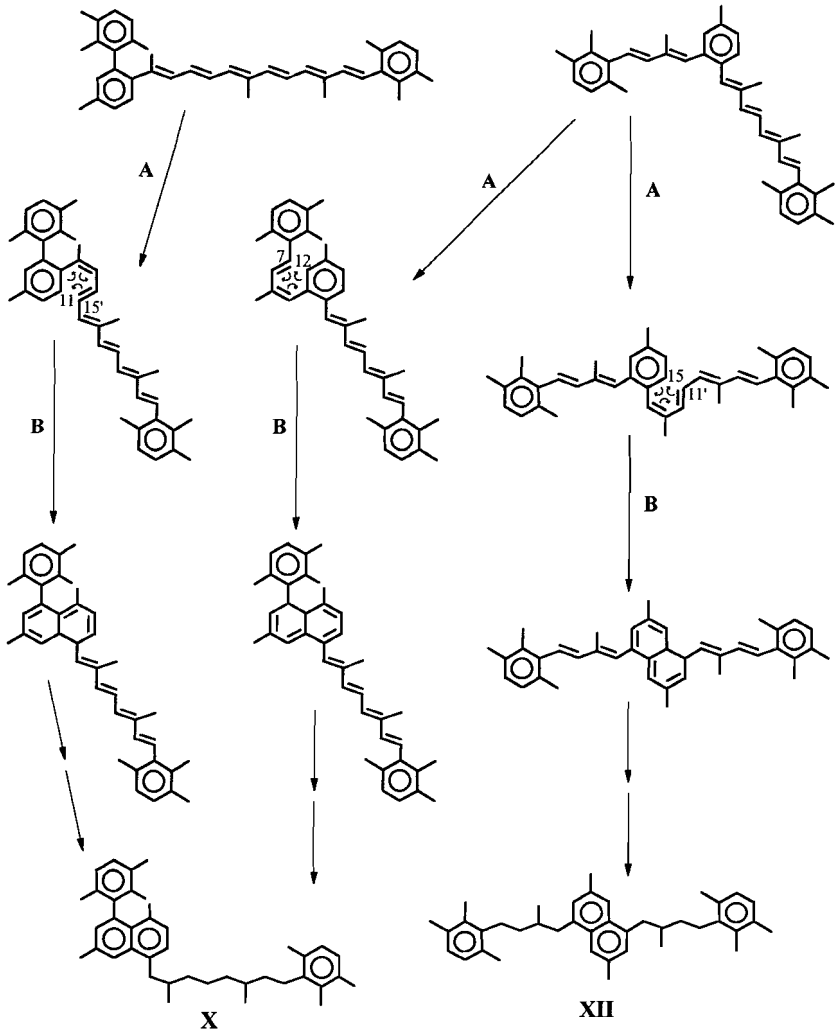

Fig. 7.17. Formation of diaryl isoprenoids with a naphthalene moiety. Cyclisation of the aromatised precursors of **VI** and **VII**, which serve as starting products, proceeds in two steps: (**A**) *trans-cis* isomerisation of a double bond, (**B**) intramolecular Diels-Alder reaction.

heating in the ion source and subsequent ionisation of the degradation products (*e.g.* Vetter *et al.*, 1971; Enzell and Wahlberg, 1980).

A pericyclic reaction *via* an eight-membered ring transition state comprising carbon atoms from the acyclic isoprenoid chain leads to expulsion of *m*-xylene and toluene from β-carotene (Vetter *et al.*, 1971; Byers and Erdman, 1983). Since this mechanism

does not involve the cyclohexenyl moieties, isorenieratene can undergo similar reactions, as proposed recently by Kenig *et al.* (1995). Cleavage only occurs between carbon atoms linked by double bonds in the polyene isoprenoid chain (Vetter *et al.*, 1971), which, for isorenieratene, implies that only one C_{32} (**XXXVII**) and one C_{33} 'carotenoid' (**XXXVIII**) can be formed. There are four possibilities for the expulsion of toluene from isorenieratene, and only two for *m*-xylene (cf. Vetter *et al.*, 1971; Enzell and Wahlberg, 1980). Although steric hindrance associated with formation of the eight-membered ring transition state may also be influential, in most samples C_{33} compounds are indeed more abundant than C_{32} compounds. The cyclisation, aromatisation and sulphurisation reactions that led to the C_{40} diagenetic products of isorenieratene can also occur with **XXXVII** and **XXXVIII**. Further expulsion of *m*-xylene or toluene from **XXXVII** and **XXXVIII** is less likely because only six double bonds remain in the isoprenoid chain, complicating formation of a sterically unhindered eight-membered ring transition state (Vetter *et al.*, 1971). Thermal degradation of philene (**LXVIII**) and lexene (**LXIX**) under laboratory conditions indeed proceeds considerably slower than thermal degradation of β-carotene (**LXVII**) (Byers and Erdman, 1983). A C_{28} 'carotenoid' may be formed *via* a similar reaction, involving expulsion of either 1,5- or 1,6-dimethylnaphthalene *via* a twelve-membered ring transition state. Small amounts of dimethylnaphthalenes were reported in thermal degradation experiments with β-carotene (Day and Erdman, 1963; Byers and Erdman, 1983). Schaeffer *et al.* (1995a) found small amounts of a C_{28} diaryl isoprenoid after desulphurisation of a sulphur-rich kerogen.

The additional benzene rings in the C_{32} and C_{33} compounds **XL**, **XLI** and **XLVI** are in the same positions as in the C_{40} compounds **VI** and **VII**, suggesting either that (i) cyclisation and aromatisation occurs at preferred parts of the isoprenoid chain which are 'recognisable' in C_{32} and C_{33} 'carotenoids', or (ii) the conjugated double bond system remaining after cyclisation of isorenieratene is large enough to facilitate expulsion of *m*-xylene or toluene. The first explanation is consistent with proposed cyclisation reactions for isorenieratene (Fig. 7.16), whereas in the second cyclisation of isorenieratene may produce the unsaturated 'precursor' of **VI**, leaving a conjugated double bond system that is insufficient to enable expulsion of *m*-xylene or toluene (Vetter *et al.*, 1971). Therefore, **XL**, **XLI** and **XLVI** are held to form through cyclisation and aromatisation of **XXXVII** and **XXXVIII** (cf. Fig. 7.16), *i.e.* after expulsion of *m*-xylene or toluene from isorenieratene.

Sulphurisation

No carotenoids of biological origin with sulphur directly bound to their carbon skeleton have been reported (Liaaen-Jensen, 1990), suggesting that sulphur-containing diaryl isoprenoids are diagenetic products of isorenieratene. Reaction of isorenieratene with reduced inorganic sulphur species during early diagenesis (sulphurisation) is probably particularly efficient because isorenieratene contains nine conjugated double bonds all available for reaction (Sinninghe Damsté *et al.*, 1989c; de Graaf *et al.*, 1992; Schouten

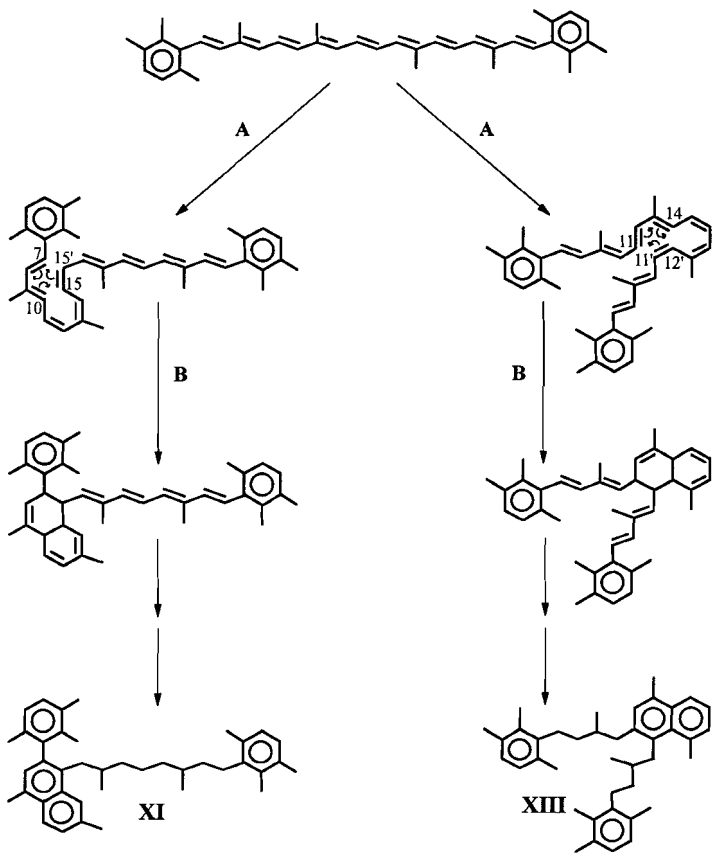

Fig. 7.18. Formation of diaryl isoprenoids with a naphthalene moiety *via* a ten-membered ring transition state. Cyclisation of isorenieratene occurs in two steps: (**A**) three *trans-cis* isomerisation reactions of double bonds, (**B**) intramolecular Diels-Alder reaction.

et al., 1994). Sulphurisation can proceed in an intermolecular and/or an intramolecular fashion.

Intermolecular sulphurisation of isorenieratene results in the formation of cross-linked structures that make up part of geomacromolecules. The nine conjugated double bonds of isorenieratene allow for abundant formation of sulphur links. The number of sulphur links and the average molecular weight of geomacromolecules are positively correlated (Sinninghe Damsté *et al.*, 1990a; Kohnen *et al.*, 1991b), so that isorenieratene is probably mainly incorporated into the kerogen. This is supported by the artificial maturation experiments with the marl sample from the Gessoso-solfifera Formation. Desulphurisation of the polar fraction of the unheated sample yields relatively low

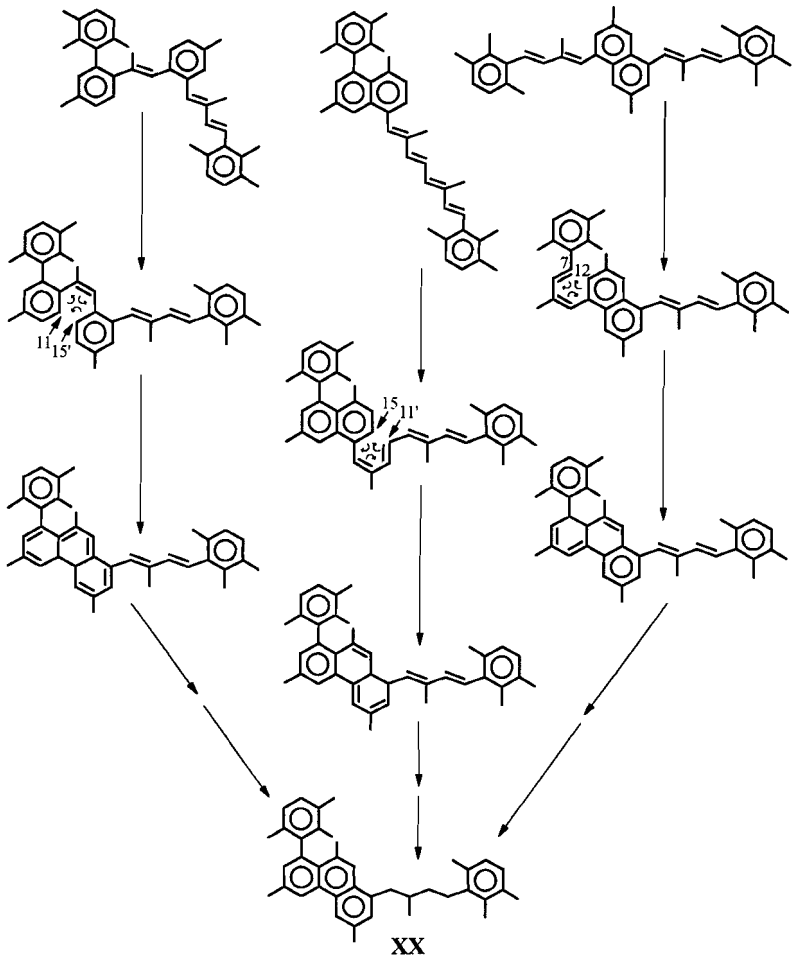

Fig. 7.19. Formation of a diaryl isoprenoid with a phenanthrene moiety. Cyclisation of the aromatised precursors of **IX**, **X** and **XII**, which serve as starting products, proceeds in two steps: (**A**) *trans-cis* isomerisation of a double bond, (**B**) intramolecular Diels-Alder reaction.

amounts of isorenieratane (Fig. 7.15**a**). When the sample is heated to 200°C, large amounts of sulphur-bound isorenieratane are present in the polar fraction. This increase suggests that sulphur-bound isorenieratane in the kerogen is released as part of smaller sulphur-linked structures that reside in the polar fraction, by the thermal cleavage of relatively weak S-S and C-S bonds (Koopmans *et al.*, 1996b).

Intramolecular sulphurisation can yield free isorenieratene derivatives containing one or more sulphur atoms (*e.g.* thiophenes). However, it seems more likely that intra- and intermolecular sulphurisation occur simultaneously, so that free sulphur-containing

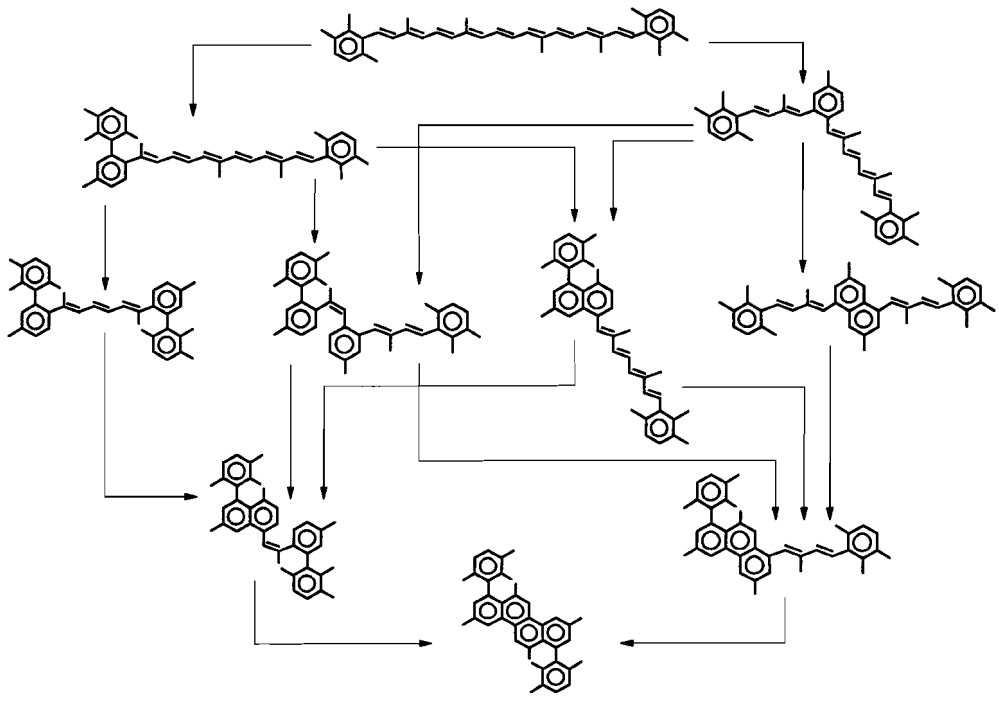

Fig. 7.20. Overview of formation pathways of C_{40} cyclised and aromatised diagenetic products of isorenieratene. This scheme does not include compounds comprising naphthalene moieties formed *via* ten-membered ring transition states. Their formation pathways are outlined in Fig. 7.18.

isorenieratene derivatives are not expected to be abundant. Indeed, such compounds have not been reported, whereas isorenieratane has been released after desulphurisation of the polar fraction of several samples (Kohnen *et al.*, 1992a; Sinninghe Damsté *et al.*, 1993d, 1995b; Kenig *et al.*, 1995; Schaeffer *et al.*, 1995a,b). An alternative formation pathway of free sulphur-containing isorenieratene derivatives is *via* thermal degradation of (poly)sulphide-bound isorenieratane, which can yield alkylthiophenes (cf. Krein and Aizenshtat, 1994; Schouten *et al.*, 1994; Koopmans *et al.*, 1995).

Five structural isomers of diaryl isoprenoids with one thiophene ring (**XXIV-XXVIII**) were identified. These represent all possible isomers, if thiophenes involving C-19, C-20, C-19' and C-20' are disregarded. This suggests that many di- and even terthiophenes can be expected to form during diagenesis. Although a maximum of 15 dithiophene isomers can be formed, only two were identified (**XXXII** and **XXXIII**). This may be due to their low abundance which makes identification difficult. Moreover, several of the dithiophene isomers will probably not elute from the capillary column.

Comparison of distributions of sulphur-bound isorenieratene derivatives in the

polar fraction of samples from the Gessoso-solfifera, Schistes Cartons, Allgäu and Boas Oil Shale Formations (Fig. 7.11) reveals that C_{32} and C_{33} diaryl isoprenoids with an additional aromatic ring and diaryl isoprenoids with more than one additional aromatic ring are present in low amounts, probably because the sulphur bridges that link their precursors to the macromolecular network prevent cyclisation reactions. Isorenieratane (**II**) is much more abundant than other isorenieratene derivatives compared to the polyaromatic fractions of the same samples (see below), which may indicate that the conjugated double bond system of sulphurised isorenieratene is too small to enable expulsion or cyclisation reactions. Alternatively, the number of double bonds in isorenieratene (compared to its cyclised diagenetic products) makes it more susceptible to incorporation into a sulphur-rich macromolecular network.

Interplay of early diagenetic reactions

Studies of Recent Black Sea sediments have shown that incorporation of isorenieratene into a sulphur-rich macromolecular network proceeds quickly in the upper sediment layers (cf. Sinninghe Damsté *et al.*, 1993d; Repeta, 1993; Wakeham *et al.*, 1995). Identification of **VI**, **VII**, **XXXIX** and **XLV** in the desulphurised polar fraction of an immature marlstone from the Gessoso-solfifera Formation (Fig. 7.14**a**) suggests that cyclisation and expulsion can occur before sulphurisation, although it cannot exclude such reactions after incorporation into a macromolecular network. However, **XXX**, **XXXV** and **LXII** strongly suggest that sulphurisation preceded cyclisation, which is unlikely to proceed through C-10 to C-15 in isorenieratene (Fig. 7.16). Thus, cyclisation with subsequent aromatisation, expulsion, and sulphurisation are probably competing processes during early diagenesis, probably dependent on the availability of reduced inorganic sulphur species which may 'quench' isorenieratene before any pericyclic reactions (expulsion and cyclisation) can occur. However, sulphur is not a prerequisite for expulsion and cyclisation reactions, because cyclised and aromatised diagenetic products of β-carotene have been identified in a sample from the Green River Formation that contains only small amounts of organic sulphur (Koopmans *et al.*, 1997a). In summary, the three competing processes probably succeed each other. For instance, **XLI** may be formed *via* several different pathways (Fig. 7.21). These pathways should include one cyclisation and one expulsion reaction. Sulphurisation is not required, but can occur at any stage of the process (Fig. 7.21).

The dia- and catagenetic products of isorenieratene identified in this study mark the first recognition of cyclisation and aromatisation of poly-unsaturated acyclic moieties in biomarkers during sediment diagenesis. These reactions are not restricted to isorenieratene. The conjugated double bond systems of other carotenoids are anticipated to experience similar diagenetic reactions, as observed here for the diaromatic carotenoid with the 3,4,5-/2,3,6-trimethyl substitution pattern. Analysis of a sample from the Green River Formation (Mahogany Zone) reveals a wide range of previously unrecognised cyclised and aromatised diagenetic products of β-carotene that are structurally similar to

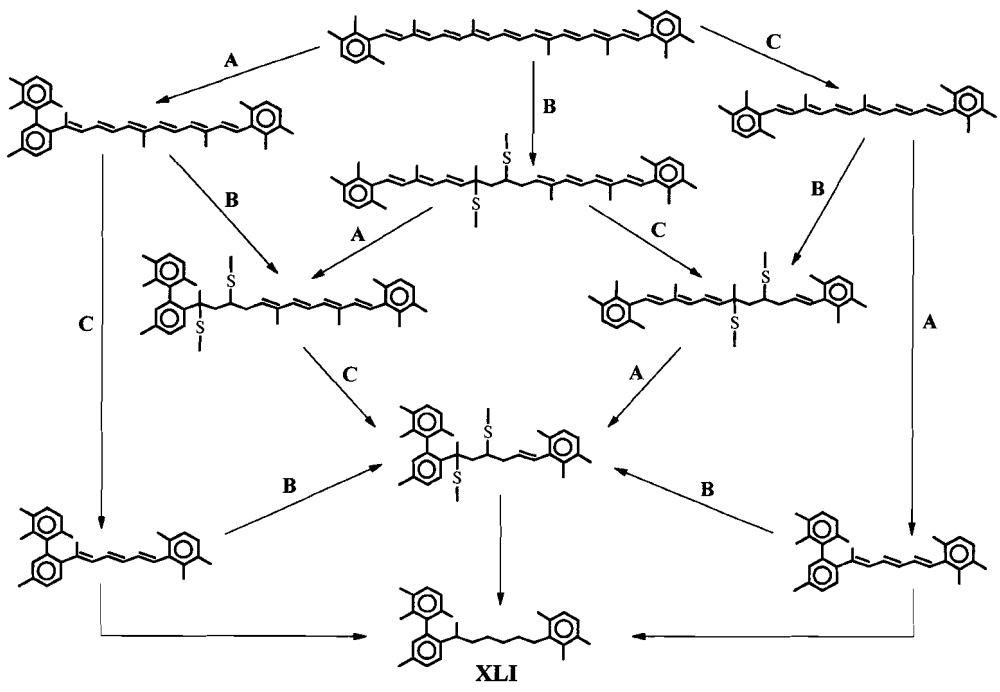

Fig. 7.21. Possible formation pathways of **XLI**, including (**A**) cyclisation, (**B**) sulphurisation and (**C**) expulsion reactions.

the compounds described here (Koopmans *et al.*, 1997a). These are likely formed by comparable pathways.

C-C bond cleavage

It appears that short-chain compounds form from C-C bond cleavage of C_{32}, C_{33} and C_{40} isorenieratene derivatives. For example, **LII** probably originates from the C-11 to C-1' part of **XL**, and **LIV** can only be formed from C-C bond cleavage of **VI**. Random C-C bond cleavage probably only takes place at relatively high levels of thermal maturity (Requejo *et al.*, 1992), comparable to the formation of alkanes and aromatics from kerogen, although perhaps facilitated by methyl branches and aromatic moieties in the isoprenoid chain. Aryl isoprenoids typically represent the only discernible remnants of isorenieratene in mature sedimentary rocks and crude oils (*e.g.* Ostroukhov *et al.*, 1982; Summons and Powell, 1986, 1987), although they also occur in immature sedimentary rocks as part of sulphur-rich geomacromolecules (Hartgers *et al.*, 1994c).

C_{12}, C_{17} and C_{23} aryl isoprenoids cannot be formed by single C-C bond cleavage of isorenieratane. However, in **XXXIX** and **XLV** single C-C bond cleavage results in aryl isoprenoids with isoprenoid chains different from those formed from isorenieratane. For

example, C_{12} and C_{17} aryl isoprenoids can result from thermal breakdown of **XXXIX**, and C_{17} and C_{23} aryl isoprenoids may be similarly derived from **XLV**. Compounds comprising additional aromatic rings preclude formation of aryl isoprenoids with up to 31 carbon atoms. For instance, C-C bond cleavage of **VI** can, at most, yield a C_{18} aryl isoprenoid.

There is a discrepancy between the distributions of aryl isoprenoids and their counterparts with additional aromatic rings. For the former a typical pattern includes compounds in the range C_{13}-C_{31} with the short-chain components dominant (Summons and Powell, 1986, 1987), a distribution that seems to indicate random C-C bond cleavage. For the latter the distributions are restricted to compounds apparently formed by α (R = H) and β (R = CH_3) cleavage (see Appendix I). This suggests that they form from C_{32}, C_{33} and C_{40} precursors by two principal processes: (i) cleavage of an alkyl side chain associated with aromatisation of unsaturated rings (cf. Starnes and Edelson, 1979), and (ii) C-C bond cleavage β to the aromatic ring system.

Maturity-related changes in abundance and distribution of isorenieratene derivatives

The increasing amount of sulphur-bound isorenieratane in the polar fraction of the sample from the Gessoso-solfifera Formation with increasing artificial maturation temperature up to 200°C (Fig. 7.15**a**) is probably due to the cleavage of relatively weak S-S and C-S bonds in the kerogen, resulting in the release of smaller sulphur-linked structures that contain isorenieratane and end up in the polar fraction (Koopmans *et al.*, 1996b). After heating at temperatures higher than 200°C, the amount of sulphur-bound isorenieratane in the polar fraction decreases, probably due to the thermal cleavage of the remaining S-S and C-S bonds. This process can be monitored by plotting the ratio [polar S-bound]/[polar S-bound + free] as a function of temperature (Fig. 7.15**b**), which shows that considerable release of sulphur-bound isorenieratane only occurs at 280°C and higher temperatures. It is obvious from Fig. 7.15**a** that sulphur-bound isorenieratane is not thermally released exclusively as free isorenieratane. The far greater part is probably released as cyclised and aromatised or sulphur-containing derivative of isorenieratene as a means of stabilisation.

Isorenieratane (**II**) and **VI** are abundantly present in the desulphurised polar fractions of the samples from the artificial maturation series (Fig. 7.14). **II** is presumed to be linked *via* more sulphur bonds than **VI** because of the greater number of double bonds in isorenieratene compared to the precursor of **VI**, suggesting that the **VI/II** ratio in the desulphurised polar fraction would decrease with increasing maturation temperature. However, it increases from 0.1 in the original sample to 2.4 at 300°C. There are two possible explanations for this discrepancy. First, thermal cleavage of sulphur bonds linking isorenieratene may produce radical sites within the isoprenoid chain that may induce cyclisation and subsequent aromatisation as a means of stabilisation. This stabili-

sation reaction may be enhanced at higher temperatures, yielding greater amounts of diaryl isoprenoids with an additional aromatic ring upon desulphurisation. However, it is unlikely that this process would yield **VI** exclusively, because the radical sites would be expected at various positions. Second, if the polar fraction contains isorenieratene or its partly hydrogenated counterparts, increasing maturation temperatures may induce the cyclisation reactions shown in Fig. 7.16. Keely *et al.* (1995) found isorenieratene in immature marlstones from the Gessoso-solfifera Formation. Desulphurisation and subsequent hydrogenation of a polar fraction containing isorenieratene or its partly hydrogenated counterparts would yield isorenieratane. However, the ratio of **VII** to **II** does not increase with increasing temperature, nor does the ratio **(XXXIX+XLV)/II**, which could serve as an indicator for the extent of expulsion.

The maturity-related trends in the amounts and distributions of isorenieratene derivatives deduced from the artificial maturation experiments can be compared to those in natural samples by examination of polyaromatic and desulphurised polar fractions of four samples with different degrees of thermal maturity. These are from the (i) Gessoso-solfifera ($R_o \approx 0.25\%$), (ii) Schistes Cartons (Paris Basin G6-5-6; $R_o = 0.43\%$), (iii) Allgäu ($R_o = 0.43\%$), and (iv) Boas Oil Shale Formations ($R_o = 0.47\%$). Vitrinite reflectance values for the last three samples were determined *via* the Pristane Formation Index (Goossens *et al.*, 1988a,b).

Partial summed (m/z 133+237+287) mass chromatograms of the polyaromatic fractions of these four samples (Fig. 7.22) reveal no obvious trends. The absence of isorenieratane in the Gessoso-solfifera Formation is attributed to its initial incorporation *via* sulphur-linkages in HMW fractions. The other three samples do not contain Type II-S kerogen, so that it is unclear whether the presence of isorenieratane in their polyaromatic fractions reflects their lower sulphur contents or higher levels of thermal maturity. Samples from the Schistes Cartons and Allgäu Formations possess similar distributions of isorenieratene derivatives (Fig. 7.22**b** and **c**), but the amounts of C_{32} and C_{33} compounds relative to isorenieratane in the latter is *ca.* twice that in the former. It also contains *ca.* twice the amount of C_{40} cyclised and aromatised isorenieratene derivatives relative to isorenieratane, suggesting that pericyclic reactions (*i.e.* expulsion and cyclisation) were more prominent during early diagenesis of the Allgäu than of the Schistes Cartons Formation. The ratio of C_{40} compounds to C_{32} and C_{33} compounds is probably not a function of thermal maturity, because it is fixed during early diagenesis given the low activation energy of the expulsion reaction (Byers and Erdman, 1983). The proportion of cyclised and aromatised products relative to diaryl isoprenoids is probably governed by similar controls, because cyclisation and expulsion are both pericyclic reactions. In the Boas Oil Shale Formation, concentrations of C_{32}, C_{33} and C_{40} isorenieratene derivatives are low (< 30 μg/g TOC). The abundance of aryl isoprenoids (C_{15} = 41 μg/g TOC; not shown in Fig. 7.22**d**) may be related to the higher level of thermal maturity, because aryl isoprenoids are the only recognisable remains of isorenieratene previously identified in ancient sedimentary rocks and crude oils (*e.g.* Summons and

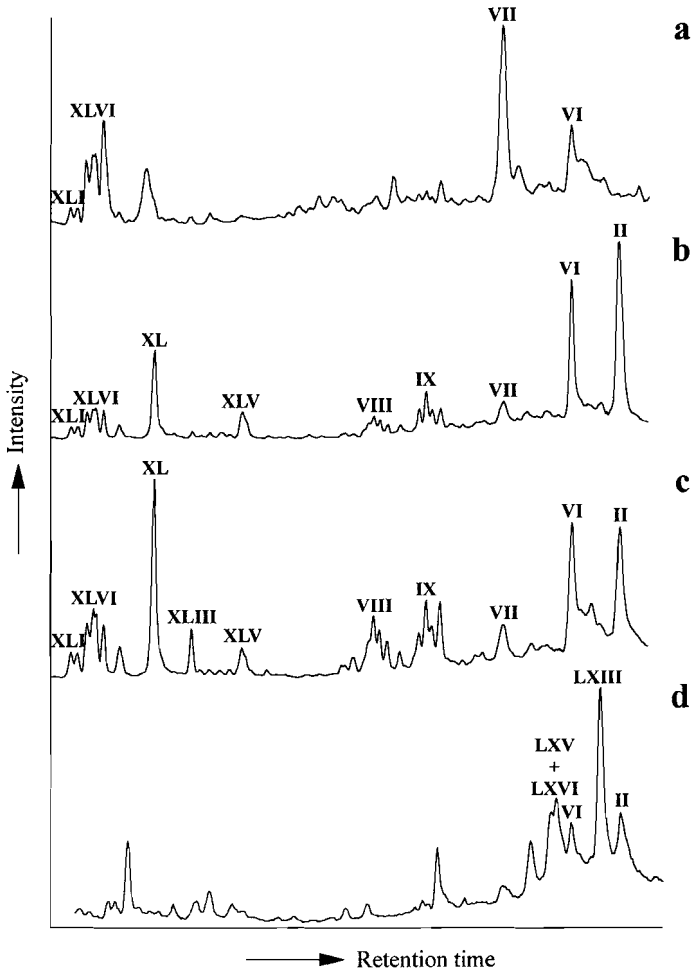

Fig. 7.22. Partial summed (m/z 133+237+287) mass chromatograms of the polyaromatic fractions of the samples from the (**a**) Gessoso-solfifera, (**b**) Schistes Cartons, (**c**) Allgäu, and (**d**) Boas Oil Shale Formations. Roman numbers refer to structures in Appendix I.

Powell, 1986, 1987). The high amount of aryl isoprenoids in the Boas Oil Shale suggests that C-C bond cleavage is more important with increasing thermal maturity, in agreement with data of Requejo *et al.* (1992).

Summed mass chromatograms (m/z 133+237+287) of the desulphurised polar fractions (Fig. 7.11) show an increase in short-chain compounds, particularly aryl isoprenoids, with increasing thermal maturity. The **VI/II** ratio does not increase with increasing thermal maturity as in the maturation series from the Gessoso-solfifera For-

mation (Fig. 7.14). 30% of isorenieratane in the Schistes Cartons Formation and 7% in the Allgäu Formation is sulphur-bound. For the C_{40} diaryl isoprenoid **LXIII** in the Boas Oil Shale Formation this percentage is 21. These values suggest that these samples represent a level of thermal maturity comparable to the sample from the Gessoso-solfifera Formation artificially matured at temperatures higher than 280°C (cf. Fig. 7.15**b**). However, the amount of reduced sulphur species present during early diagenesis of these sediments may also influence these percentages.

Palaeoenvironmental significance of isorenieratene derivatives

Dia- and catagenetic products of isorenieratene provide important information on the anoxic conditions of the depositional environment, especially in sedimentary rocks and crude oils that do not contain isorenieratane. They are potentially valuable tools in oil-oil and oil-source rock correlation and biomarker studies because of their specific carbon skeletons and anomalously high ^{13}C contents. Molecular palaeontology (*i.e.* recognition of biological sources of sedimentary organic compounds) is severely complicated by the diagenetic reactions of isorenieratene, because it is the precursor of many products. Precise identifications of carbon skeletons and ^{13}C contents of these products is required, because other carotenoids (*e.g.* β-carotene) can undergo the same diagenetic transformations leading to similar, albeit not identical, suites of diagenetic products (Koopmans *et al.*, 1997a).

In the present study, isorenieratene derivatives have been identified in sedimentary rocks ranging from Ordovician to Miocene (Fig. 7.12). This suggests that in the past anoxygenic photosynthesis has been a more common process. The only contemporary example of a marine basin where anoxygenic photosynthesis takes place is the Black Sea (Repeta *et al.*, 1989). The presence of isorenieratene derivatives in the samples studied also shows that anoxic conditions can be associated with formation of organic-rich sediments, given that all samples contain more than 5% TOC except those from the Gessoso-solfifera and Canje Formations. Petroleum source rocks containing isorenieratene derivatives are from the Duvernay, Exshaw, Schistes Cartons, Kimmeridge Clay and Menilite Formations (Klemme and Ulmishek, 1991). Thus, euxinic conditions with anoxia extending into the photic zone favour preservation of organic matter, and can accompany formation of petroleum source rocks. However, our data cannot resolve the relative importance of anoxia and productivity for the preservation of organic matter (cf. Demaison and Moore, 1980; Pedersen and Calvert, 1990).

Several sedimentological (*e.g.* presence of lamination), geochemical (*e.g.* S/C ratio, degree of pyritisation, trace metal concentrations) and palaeontological (*e.g.* biofacies analysis) indicators are commonly used to assess bottom water anoxia (see Arthur and Sageman, 1994 and Wignall, 1994 for reviews). However, these indicators cannot provide information on the thickness of the oxic and anoxic part of the water column. The strength of the isorenieratene derivatives as palaeoenvironmental indicators is that

they give an indication of the position of the chemocline in the water column (cf. Black Sea; Sinninghe Damsté *et al.*, 1993d), because light penetration is limited to a certain depth depending on local conditions. A relatively small oxic water column implies degradation of organic matter at a relatively low rate, and thus enhanced preservation of organic matter, because it is generally believed that the rate of aerobic degradation is lower than the rate of anaerobic degradation (*e.g.* Peters and Moldowan, 1993). The palaeoenvironmental significance of isorenieratene derivatives in relation to the geological setting of the samples studied will be further elaborated in a separate paper.

7.6 Conclusions

A wide range of novel dia- and catagenetic products of the diaromatic carotenoid isorenieratene has been identified in a number of sedimentary rocks ranging from Ordovician to Miocene. Their identification is based on NMR, mass spectrometry, the presence of atropisomers, and stable carbon isotopes. $\delta^{13}C$ values of dia- and catagenetic products of isorenieratene and compounds derived from algae living in the upper part of the water column show a consistent difference of *ca.* 15‰ throughout the Phanerozoic. This supports an origin from Chlorobiaceae because these organisms use the reverse TCA cycle to fix carbon, leading to biomass anomalously enriched in ^{13}C.

Dia- and catagenetic products of isorenieratene include C_{40}, C_{33} and C_{32} diaryl isoprenoids and short-chain aryl isoprenoids with additional aromatic and/or sulphur-containing rings. The reactions by which these compounds are formed include cyclisation with subsequent aromatisation, expulsion, sulphurisation, hydrogenation, and C-C bond cleavage. Cyclisation of the acyclic isoprenoid chain is proposed to occur *via* an intramolecular Diels-Alder reaction. C_{33} and C_{32} compounds are diagenetic products of C_{33} and C_{32} 'carotenoids' formed from isorenieratene by expulsion of toluene and *m*-xylene, respectively. Sulphurisation during early diagenesis sequesters isorenieratene predominantly in the kerogen, from which it is released during progressive diagenesis as indicated by artificial maturation experiments. C-C bond cleavage of isorenieratene derivatives is governed by two processes: (i) cleavage β to the additional aromatic ring system, and (ii) loss of an alkyl chain associated with aromatisation of a newly formed ring. Similar reactions can occur with other carotenoids, as shown by the identification of novel diagenetic products of a diaromatic carotenoid with a 3,4,5-/2,3,6-trimethyl substitution pattern for the aromatic rings.

Sulphurisation, expulsion, and cyclisation with subsequent aromatisation are probably competing processes during early diagenesis. Incorporation of (partly cyclised) isorenieratene into a sulphur-rich macromolecular network diminishes the possibilities for further expulsion and cyclisation reactions due to lack of a conjugated double bond system sufficiently large for these reactions. Therefore, the availability of reduced inorganic sulphur species during early diagenesis may (partly) determine the fate of isorenieratene. The extent of expulsion and cyclisation with subsequent aromatisation is

probably already established during early diagenesis, and increasing maturation does not profoundly influence the product distribution.

Since isorenieratene is uniquely biosynthesised by the photosynthetic green sulphur bacteria Chlorobiaceae, the presence of any dia- and catagenetic products of isorenieratene in sedimentary rocks and crude oils indicates photic zone anoxia in the depositional environment. These compounds are expected to be useful in palaeoenvironmental reconstruction and in oil-oil and oil-source rock correlation studies. Their presence in several petroleum source rocks suggests that anoxia is important for the preservation of organic matter.

7.7 Acknowledgements

The following persons are kindly thanked for providing samples: Drs. J.L. Clayton (Kössen Marl and Minnelusa Formations), M.G. Fowler (Boas Oil Shale and Womble Formations), R.G. Friedt (Exshaw Formation), H.L. ten Haven (Canje Formation), A.Y. Huc (Schistes Cartons Formation), M.E.L. Kohnen (Calcaires en Plaquettes and Kimmeridge Clay Formations) and A.G. Requejo (Duvernay Formation). We thank Dr. M.D. Lewan (USGS, Denver) for permission to conduct hydrous pyrolysis experiments in his laboratory. Drs. J.A.J. Geenevasen and C. Kruk are thanked for their help in providing and analysing the NMR data. Analytical support was provided by Mrs. M. Baas, Mrs. M. Dekker, Mr. W.G. Pool and Mr. A. Dijkhuizen. Drs. A.G. Requejo and J.M. Guthrie are thanked for constructive reviews. Dr. S.C. Brassell's assistance in streamlining an earlier version of the manuscript is greatly appreciated. We thank the Koninklijke/Shell Exploratie en Productie Laboratorium (Shell Research BV) and the Netherlands Organisation for Scientific Research (NWO) for providing studentships to MPK and HMEvK-P, respectively. This work was supported by a PIONIER grant to JSSD from NWO. Shell Internationale Petroleum Maatschappij is gratefully acknowledged for financial support for the irm GC-MS facility.

Appendix I

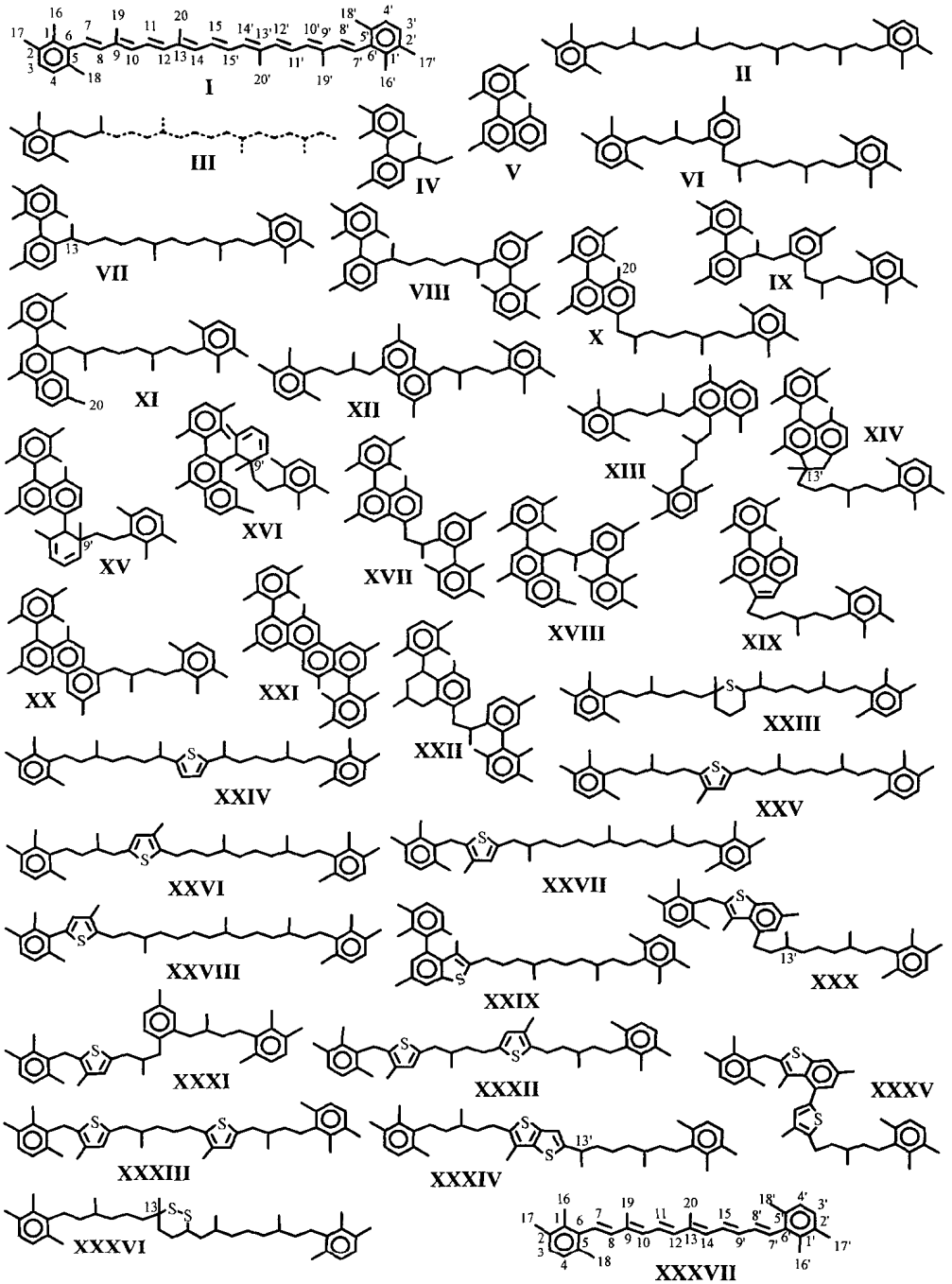
I
II
III
IV
V
VI
VII
VIII
IX
X
XI
XII
XIII
XIV
XV
XVI
XVII
XVIII
XIX
XX
XXI
XXII
XXIII
XXIV
XXV
XXVI
XXVII
XXVIII
XXIX
XXX
XXXI
XXXII
XXXIII
XXXIV
XXXV
XXXVI
XXXVII

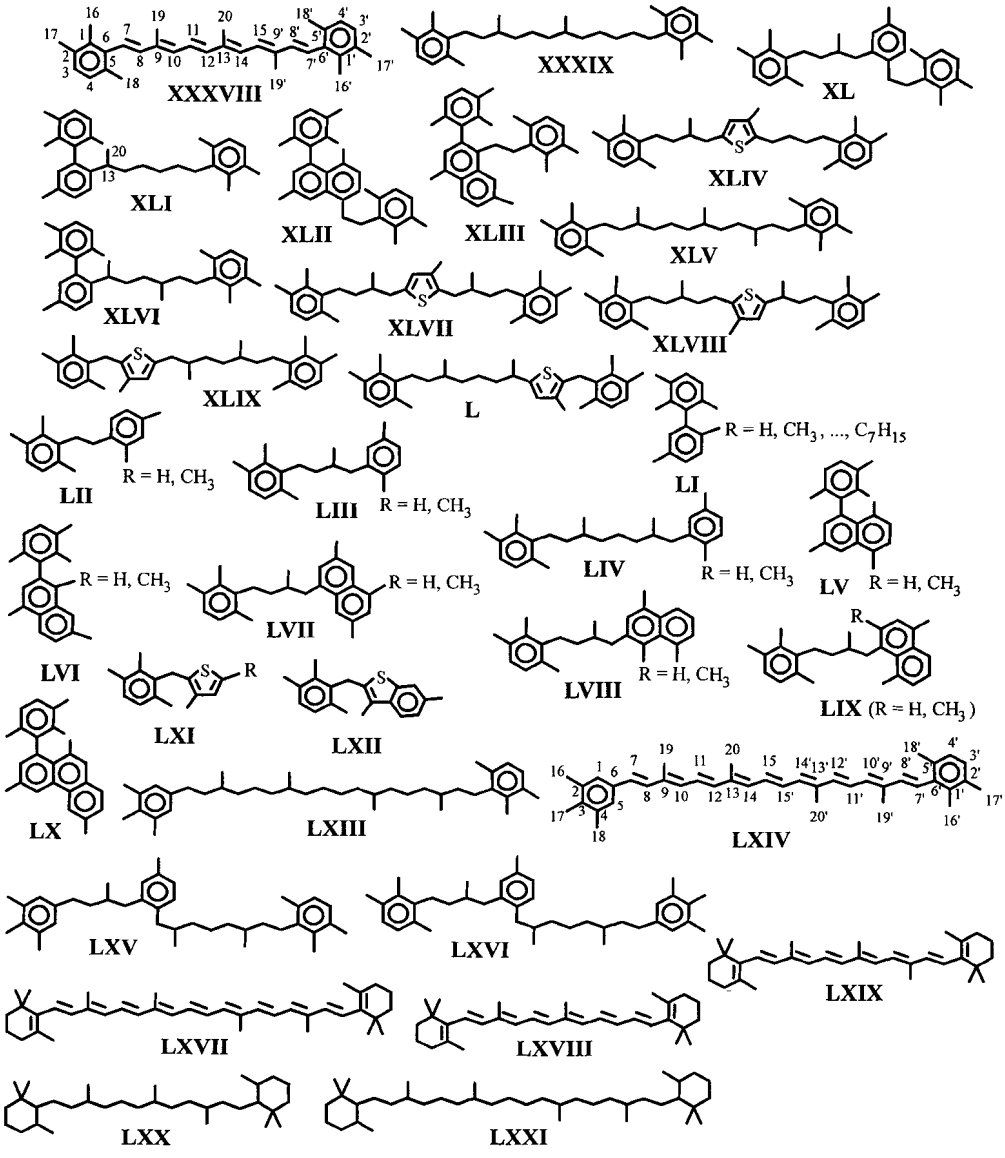
XXXVIII
XXXIX
XL
XLI
XLII
XLIII
XLIV
XLV
XLVI
XLVII
XLVIII
XLIX
L
LI
R = H, CH3, ..., C7H15
LII
R = H, CH3
LIII
R = H, CH3
LIV
R = H, CH3
LV
R = H, CH3
LVI
R = H, CH3
LVII
R = H, CH3
LVIII
R = H, CH3
LIX (R = H, CH3)
LX
LXI
LXII
LXIII
LXIV
LXV
LXVI
LXVII
LXVIII
LXIX
LXX
LXXI

Appendix II. Details of structural identifications of **II-LXII**.

Structure	*Formula*	*M+•*	*Diagnostic fragment ions (intensity)*	*Cyclisation*[a]	*Atropisomers*	*Further details*
C 40 compounds						
II	$C_{40}H_{66}$	546(29)	133[b](100), 134[c](91)	No	No	Co-injection with authentic standard
VI	$C_{40}H_{58}$	538(20)	119[d](22), 133[b](100), 134[c](36), 173(12)	11-15' (Fig. 7.16)	No	^{1}H and ^{13}C NMR (see Appendix III and Sinninghe Damsté *et al.*, 1995d)
VII	$C_{40}H_{58}$	538(17)	133[b](49), 207[e](12), 222[f](9), 237[g](100)	7-12 (Fig. 7.16)	No[h]	Mass spectrum in Fig. 7.2**a**
VIII	$C_{40}H_{50}$	530(17)	207[e](15), 222[f](10), 237[g](100)	7-12 (Fig. 7.16)	Yes[i]	Mass spectrum in Fig. 7.2**b**
IX	$C_{40}H_{50}$	530(1)	133[b](17), 207[e](11), 222[f](7), 237[g](100), 294[j](2)	7-12, 15-11' (Fig. 7.16)	Yes (1:2:1)[k]	
X	$C_{40}H_{52}$	532(40)	133[b](22), 257[e](31), 272[f](33), 287[l](100)	7-12, 11-15' (Fig. 7.17)	No[h]	Mass spectrum in Fig. 7.2**c**
XI	$C_{40}H_{52}$	532(76)	133[b](37), 257[e](23), 272[f](7), 287[l](100)	7-15', 10-15 (Fig. 7.18)	No[h]	
XII	$C_{40}H_{52}$	532(54)	133[b](100), 183[m](65)	11-15', 15-11' (Fig. 7.17)	No	
XIII	$C_{40}H_{52}$	532(9)	133[b](100), 183[m](26)	11-11', 14-12' (Fig. 7.18)	No	
XIV	$C_{40}H_{50}$	530(37)	133[b](59), 283[e](13), 298[f](6), 313[n](100)	7-12, 11-15' (Fig. 7.17), 10-13' [o]	No[h]	
XV	$C_{40}H_{46}$	526(8)	133[b](59), 147[p](28), 235(13), 379[p](100)	7-12, 11-15' (Fig. 7.17), 14'-9'[i]	Yes (1:1)[q]	
XVI	$C_{40}H_{46}$	526(9)	133[b](58), 147[p](22), 235(8), 379[p](100)	7-15', 10-15 (Fig. 7.18), 14'-9'	Yes (1:1)[q]	
XVII	$C_{40}H_{44}$	524(13)	207[e](9), 222[f](5), 237[g](20), 257[e](26), 272[f](23), 287[l](100)	7-12, 11-15' (Fig. 7.17), 12'-7' (Fig. 7.16)	Yes (1:1)	Mass spectrum in Fig. 7.2**d**
XVIII	$C_{40}H_{44}$	524(23)	207[e](18), 222[f](9), 237[g](64), 257[e](15), 272[f](5), 287[l](100)	7-15', 10-15 (Fig. 7.18), 12'-7' (Fig. 7.16)	No[r]	
XIX	$C_{39}H_{46}$	514[s,t](100)	133[b](12), 280[e](8), 295[f](14), 310[u](29), 325(10)	7-12, 11-15' (Fig. 7.17), 10-13' [o]	No[h]	
XX	$C_{40}H_{46}$	526[t](100)	133[b](67), 321[e](17), 336[f](1), 351[v](71)	7-12, 11-15', 15-11' (Fig. 7.19)	No[h]	
XXI	$C_{40}H_{40}$	520[t](100)	nd[w]	7-12, 11-15', 15-11', 12'-7'	No[h]	
XXII	$C_{40}H_{48}$	528(12)	207[e](27), 222[f](11), 237[g](100), 261[e](12), 276[f](11), 291[x](92)	7-12, 11-15' (Fig. 7.17), 12'-7' (Fig. 7.16)	Yes[y]	Similarity to **XVII**; see also van Kaam-Peters *et al.* (1997a)
XXIII[z]	$C_{40}H_{64}S$	576(6)	115[aa](7), 133[b](100), 331[ab](36), 359[ab](14)	No	No	Mass spectrum in Fig. 7.5**a**
XXIV	$C_{40}H_{60}S$	572(14)	133[b](100), 355[ac](40)	No	No	Mass spectrum in Fig. 7.5**b**
XXV	$C_{40}H_{60}S$	572(31)	125[ad](23), 133[b](100), 313[ac](3), 314[c](3), 327(4), 383[ac](5)	No	No	
XXVI	$C_{40}H_{60}S$	572(26)	125[ad](14), 133[b](100), 299[ac](9), 397[ac](6)	No	No	Mass spectrum in Fig. 7.5**c**
XXVII	$C_{40}H_{60}S$	572(23)	111[ae](20), 132[af](100), 133[b](74), 243[ac](82)	No	No	Mass spectrum in Fig. 7.5**d**
XXVIII	$C_{40}H_{60}S$	572(63)	132[ag](55), 133[b](71), 229[ac](100)	No	No	
XXIX	$C_{40}H_{54}S$	566(38)	133[b](100), 293[ah](17)	7-12 (Fig. 7.16)	No[h]	
XXX	$C_{40}H_{54}S$	566(90)	132[af](53), 133[b](100), 175[ai](15), 307[ah](11), 308[c](11)	10-15	No	
XXXI	$C_{40}H_{52}S$	564(37)	119[d](6), 132[af](13), 133[b](100), 243[ac](13), 244[c](17), 389[b](5)	15-11' (Fig. 7.16)	No	

XXXII	$C_{40}H_{54}S_2$	598(31)	111[ae](33), 132[af](55), 133[b](100), 243[ac](59), 409[ac](7)	No	No	
XXXIII	$C_{40}H_{54}S_2$	598(45)	111[ae](31), 132[af](59), 133[b](100), 243[ac](72), 299[ac](20), 423[ac](24)	No	No	
XXXIV	$C_{40}H_{56}S_2$	600(55)	133[b](100), 194[aj](16), 383[ak](56), 411[ak](10)	No	No	
XXXV	$C_{40}H_{48}S_2$	592[l](100)	132[af](9), 133[b](65), 403[ac](26), 460[al](6)	10-15	No	
XXXVI	$C_{40}H_{64}S_2$	608(2)	133[b](100), 359[am](2), 575[an](5)	No	No	
C_{32} compounds						
XXXIX	$C_{32}H_{50}$	434(23)	133[b](100), 134[c](73)	No	No	Mass spectrum in Fig. 7.7**a**
XL	$C_{32}H_{42}$	426(7)	119[d](18), 133[b](100), 173(17)	11-9' (cf. Fig. 7.16)	No	Mass spectrum in Fig. 7.7**b**
XLI	$C_{32}H_{42}$	426(22)	133[b](25), 207[e](14), 222[f](9), 237[g](100)	7-12 (cf. Fig. 7.16)	Yes (1:1)	Mass spectrum in Fig. 7.7**c**
XLII	$C_{32}H_{36}$	420(21)	133[b](?)[ao], 257[e](20), 272[f](6), 287[l](100)	7-12, 11-9' (cf. Fig. 7.17)	No	
XLIII	$C_{32}H_{36}$	420(17)	133[b](9), 257[e](17), 272[f](5), 287[l](100)	7-9', 10-15 (cf. Fig. 7.18)	No	Mass spectrum in Fig. 7.7**d**
XLIV	$C_{32}H_{44}S$	460(67)	133[b](100), 285[ac](66), 299[ac](25)	No	No	
C_{33} compounds						
XLV	$C_{33}H_{52}$	448(16)	133[b](100), 134[c](88)	No	No	Mass spectrum in Fig. 7.9**a**
XLVI	$C_{33}H_{44}$	440(26)	133[b](31), 207[e](15), 222[f](8), 237[g](100)	7-12 (cf. Fig. 7.16)	Yes (1:1:1:1)	Mass spectrum in Fig. 7.9**b**
XLVII	$C_{33}H_{46}S$	474(27)	125[ad](9), 133[b](100), 299[ac](66)	No	No	Mass spectrum in Fig. 7.9**c**
XLVIII	$C_{33}H_{46}S$	474(40)	133[b](100), 139[ad](16), 285[ac](9), 327[ac](57), 341[ap](38)	No	No	
XLIX	$C_{33}H_{46}S$	474(28)	111[ae](29), 132[af](100), 133[b](36), 243[ac](90)	No	No	Mass spectrum in Fig. 7.9**d**
L	$C_{33}H_{46}S$	474(35)	125[aq](42), 132[af](75), 133[b](57), 257[ac](100)	No	No	
Short-chain compounds						
LI	$C_{16}H_{17}R^{ar}$	252(72)	111[as](8), 207[at](30), 209[au](41), 222[av](22), 237[aw](100)	7-12 (cf. Fig. 7.16)	Yes[ax] (1:1)	Mass spectrum in Fig. 7.10**a**
LII	$C_{18}H_{21}R^{ay}$	252(22)	119[b](79), 133[b](100)	11-9' (cf. Fig. 7.16)	No	
LIII	$C_{21}H_{27}R^{az}$	280(23)	105[b](24), 133[b](100)	11-15' (cf. Fig. 7.16)	No	Mass spectrum in Fig. 7.10**b**
LIV	$C_{26}H_{37}R^{ay}$	364(11)	119[b](61), 133[b](100)	15-11' (cf. Fig. 7.16)	No	
LV	$C_{21}H_{21}R^{ay}$	288(100)	144[as](11), 243[at](32), 258[av](29), 273[aw](43)	7-12, 11-15' (cf. Fig. 7.17)	No	
LVI	$C_{21}H_{21}R^{ay}$	288(100)	144[as](3), 243[at](28), 258[av](17), 273[aw](32)	7-15', 10-15 (cf. Fig. 7.18)	No	
LVII-LIX[ba]	$C_{26}H_{31}R^{bb}$	344(47)	133[b](54), 169[l](100), 170[c](26)	11-15', 15-11' (cf. Fig. 7.17); 11-11', 14-12' (cf. Fig. 7.18); 11-11', 12-14' (cf. Fig. 7.18)	No	
LX	$C_{26}H_{26}$	338(100)	154[as](9), 169[as](8), 293[at](23), 308[av](23), 323[aw](19)	7-12, 11-15', 15-11' (cf. Fig. 7.19)	No	Mass spectrum in Fig. 7.10**c**
LXI	$C_{15}H_{17}SR^{bc}$	272(22)	132[af](100), 243[ac](8)	No	No	
LXII	$C_{20}H_{22}S$	294(32)	132[af](100), 162[al](6), 175[ah](9), 279[bd](7)	10-15	No	Mass spectrum in Fig. 7.10**d**

[a] Carbon atoms connected by a C-C bond formed by cyclisation are indicated by their carbon number (cf. **I** in Appendix I).

[b] Cleavage ß to benzene ring.

[c] McLafferty rearrangement.

[d] Cleavage ß to both sides of additional benzene ring.

[e] Loss of two $\bullet CH_3$'s from the main fragment ion, indicating severely hindered rotation around a C-C single bond (cf. Safe and Hutzinger, 1971, 1972; Wolf, 1993; Wolf *et al.*, 1995).

[f] Loss of $\bullet CH_3$ from the main fragment ion, indicating severely hindered rotation around a C-C single bond (cf. Safe and Hutzinger, 1971, 1972; Wolf, 1993; Wolf *et al.*, 1995).

[g] Cleavage ß to biphenyl moiety.

[h] Despite the presence of several chiral centres this compound appears as a single peak in the gas chromatogram, probably due to the high elution temperature that causes rapid interconversion of the atropisomers.

[i] **VIII** contains two biphenyl moieties and two asymmetric carbon atoms. It appears as a broad, asymmetric peak in the m/z 237 mass chromatogram (Fig. 7.3), which indicates that its biphenyl moieties still maintain some axially chiral character at the elution temperature (301°C).

[j] M/z ($M^{+\bullet}$-236): loss of biphenyl moiety *via* a McLafferty rearrangement.

[k] Distribution arising from partial coelution of two of four diastereomers.

[l] Cleavage ß to naphthalene moiety.

[m] Cleavage ß to both sides of naphthalene moiety.

[n] Cleavage α to acenaphthene moiety and carbon atom C-13', explaining the high intensity of this fragment ion compared to that at m/z 133.

[o] The mechanism of formation of the five-membered ring is presently not understood.

[p] Cleavage α to cyclohexadienyl moiety.

[q] Similar 1:1 distributions are found for the samples from the Kimmeridge Clay and Schistes Cartons Formations, and for an artificially matured sample (239°C) from the Gessoso-solfifera Formation, supporting their identification as atropisomers.

[r] Due to the lower rotational barrier of the 2- compared to the 1-phenylnaphthalene moiety (cf. **XVII**), the number of diastereomers is twice as low, resulting in one peak in the m/z 287 mass chromatogram (Fig. 7.4).

[s] The molecular mass of **XIX** is lower than that of a fully aromatised C_{40} diaryl isoprenoid. Therefore, it is concluded that **XIX** is a C_{39} compound.

[t] The high intensity of the molecular ion is indicative of polyaromatic character (Safe and Hutzinger, 1973).

[u] Cleavage ß to acenaphthylene moiety.

[v] Cleavage ß to phenanthrene moiety.

[w] Interference from other isorenieratene derivatives made it difficult to obtain a pure mass spectrum.

[x] Cleavage ß to tetrahydronaphthalene moiety.

[y] The m/z 291 mass chromatogram contains several peaks with a molecular at m/z 528. Due to the presence of three asymmetric carbon atoms and two axially chiral centres, it is unclear if these peaks represent atropisomers. However, the elution temperature (279-282°C) is probably low enough to prevent rapid interconversion of atropisomers.

[z] *Trans* isomer.

[aa] Cleavage α to both sides of thiane ring.

[ab] Cleavage α to thiane ring.

[ac] Cleavage ß to thiophene ring.

[ad] Cleavage ß to both sides of thiophene ring.

[ae] M/z (243-132).

[af] McLafferty rearrangement, indicating the presence of an aromatic moiety separated from a terminal benzene ring by a methylene group (Fig. 7.6).

[ag] This fragment ion is probably due to coelution with **XXVII**.

[ah] Cleavage ß to benzo[*b*]thiophene moiety.

[ai] M/z (307-132).

[aj] Cleavage ß to both sides of thieno[3,2-*b*]thiophene moiety.

[ak] Cleavage ß to thieno[3,2-*b*]thiophene moiety. The fragment ion at m/z 383 has a higher intensity than that at m/z 411, because it is α to the quaternary carbon atom C-13'.

[al] M/z ($M^{+\bullet}$-132): McLafferty rearrangement followed by charge retention instead of charge migration (cf. Fig. 7.6).

[am] Cleavage α to 1,2-dithiane moiety and α to quaternary carbon atom C-13, after loss of HS• radical.

[an] M/z ($M^{+\bullet}$-33): loss of HS•, a fragmentation characteristic of 1,2-dithianes (Kohnen *et al.*, 1991a).

[ao] The relative intensity of the fragment ion at m/z 133 could not be determined due to coelution with the more abundant **XL**.

[ap] M/z ($M^{+\bullet}$-133).

[aq] M/z (257-132).

[ar] R = H, ..., C_7H_{15}. Listed mass spectrum belongs to R = $CH(CH_3)_2$ component.

[as] Doubly ionised fragment ion, diagnostic of polyaromatic hydrocarbons (Safe and Hutzinger, 1973).

[at] Loss of three •CH_3's from the molecular ion, indicating severely hindered rotation around a C-C single bond (cf. Safe and Hutzinger, 1971, 1972; Wolf, 1993; Wolf *et al.*, 1995).

[au] M/z ($M^{+\bullet}$-43): loss of isopropyl moiety.

[av] Loss of two •CH_3's from the molecular ion, indicating severely hindered rotation around a C-C single bond (cf. Safe and Hutzinger, 1971, 1972; Wolf, 1993; Wolf *et al.*, 1995).

[aw] Loss of •CH_3 from the molecular ion, indicating severely hindered rotation around a C-C single bond (cf. Safe and Hutzinger, 1971, 1972; Wolf, 1993; Wolf *et al.*, 1995).

[ax] The C_{20}-C_{23} components possess both an axially chiral centre and an asymmetric carbon atom, which gives rise to two diastereomers. The C_{16}-C_{19} components do not have an asymmetric carbon atom, hence they occur as a single peak in the gas chromatogram.

[ay] R = H, CH_3. Listed mass spectrum belongs to R = CH_3 component.

[az] R = H, CH_3, C_3H_7. Listed mass spectrum belongs to R = H component.

[ba] **LVII-LIX** are represented in the gas chromatogram by a broad, asymmetric peak (not shown), which suggests that they are coeluting.

[bb] R = H, CH_3. Listed mass spectrum belongs to R = H component.

[bc] Listed mass spectrum belongs to R = C_3H_7 component.

[bd] M/z ($M^{+\bullet}$-15).

Appendix III: ^{1}H and ^{13}C NMR data of **VI**.[a]

carbon atom		chemical shift	
		$\delta^{1}H$ (ppm)	$\delta^{13}C$ (ppm)[b]
CH3	C-16	2.17 (s)[c]	15.2[d]
	C-17	2.23 (s)^	20.7[#,d,e]
	C-18	2.27 (s)^	19.9[#,e]
	C-19	1.00 (d, J = 6.7 Hz)	19.5[*,f]
	C-20	2.23 (s)	21.0[e,g]
	C-16'	2.19 (s)[c,h]	15.2[d]
	C-17'	2.25 (s)[Ø,h]	20.7[#,d,e]
	C-18'	2.29 (s)[Ø,h]	19.9[#,e]
	C-19'	0.97 (d, J = 6.7 Hz)[i,j]	19.6[*,f]
	C-20'	0.85 (d, J = 6.7 Hz)[j]	19.5[*,f]
CH2	C-7	2.60 (m), 2.76 (m)[k]	27.9
	C-8	1.36 (m), 1.53 (m)[k]	n.d.[l]
	C-10	2.42 (m), 2.71 (m)[k]	40.0
	C-7'	2.57 (m), 2.66 (m)[k,m]	27.6
	C-8'	1.37 (m), 1.53 (m)[k]	n.d.
	C-10'	1.19 (m), 1.40 (m)[k]	n.d.
	C-11'	1.28 (m), 1.47 (m)[k]	24.7[n]
	C-12'	1.19 (m), 1.40 (m)[k]	n.d.
	C-14'	2.34 (m), 2.63 (m)[k]	n.d.
CH	C-3	6.89 (s)[o]	127.1[■,c,d]
	C-4	6.89 (s)[o]	127.4[■,c,d]
	C-9	1.86 (m)[k]	34.7[◊]
	C-12	6.94 (bm)	130.6[♦,c,g]
	C-14	6.92 (dd, J = 7.7&1.6 Hz)	126.2[g]
	C-15	6.99 (d, J = 7.7 Hz)	130.1[♦,g]
	C-3'	6.89 (s)[o]	127.1[■,c,d]
	C-4'	6.89 (s)[o]	127.4[■,c,d]
	C-9'	1.52 (m)[k]	33.6[p]
	C-13'	1.70 (m)[k]	35.4[◊]
C	C-1	-	133.3[q]
	C-2	-	134.7[∇,q]
	C-5	-	134.3[∇,q]
	C-6	-	139.4 [,q]
	C-11	-	139.7

C-13	-	134.4[▽,g]
C-1'	-	133.3[q]
C-2'	-	134.7[▽,q]
C-5'	-	134.3[▽,q]
C-6'	-	139.2[□,q]
C-15'	-	136.6

[illegible] Assignments may be interchanged.

[a] Determined on a Bruker AMX-400 Mhz NMR spectrometer in $CDCl_3$.

[b] Multiplicity of signals assessed by an attached proton test.

[c] Determined by a ^{1}H-^{13}C correlation.

[d] In agreement with shifts of 1,2,3,4-tetramethylbenzene: CH_3 at C-1 (20.5), CH_3 at C-2 (15.6), C-5 and C-6 (126.9).

[e] ^{1}H-^{13}C correlation shows correlation with aromatic methyl.

[f] ^{1}H-^{13}C correlation shows correlation with aliphatic methyl.

[g] In agreement with the shifts of 1,2,4-trimethylbenzene: CH_3 at C-4 (20.9), C-3 (130.5), C-4 (135.1), C-5 (126.6) and C-6 (129.6).

[h] In agreement with δ aromatic CH_3 's of 1-isopentyl-2,3,6-trimethylbenzene (δ = 2.28, 2.24, 2.20; Summons and Powell, 1987), aryl isoprenoids (δ = 2.30, 2.25, 2.20; Summons and Powell, 1987) and isorenieratane (δ = 2.28, 2.23, 2.20; Schaeflé *et al.*, 1977).

[i] In agreement with δ CH_3 at C-3' of 1-isopentyl-2,3,6-trimethylbenzene (d, δ = 0.98; Summons and Powell, 1987), aryl isoprenoids (d, δ = 0.98; Summons and Powell, 1987) and isorenieratane (d, δ = 0.98; Hartgers *et al.*, 1993).

[j] Average of four doublets due to the presence of four diastereomers.

[k] Assignments established by a COSY spectrum and long-range ^{1}H-^{1}H correlations.

[l] n.d. = not determined.

[m] In agreement with δ CH_2 at C-1' of 1-isopentyl-2,3,6-trimethylbenzene (δ = 2.61; Summons and Powell, 1987) and isorenieratane (δ = 2.64; Hartgers *et al.*, 1993).

[n] In agreement with δ CH_2 at C-5', C-9', C-11' in 1-methyl-3-phytanylbenzene (δ = 24.4-24.8; Sinninghe Damsté *et al.*, 1988a).

[o] In agreement with δ aromatic protons of 1-ethyl-2,3,6-trimethylbenzene (s, δ = 6.90; Hartgers *et al.*, 1993), 1-isopentyl-2,3,6-trimethylbenzene (s, δ = 6.89; Summons and Powell, 1987), aryl isoprenoids (s, δ = 6.91; Summons and Powell, 1987) and isorenieratane (s, δ = 6.92; Schaeflé *et al.*, 1977).

[p] In agreement with δ CH at C-3' in 1-methyl-3-phytanylbenzene (δ = 33.4; Sinninghe Damsté *et al.*, 1988a).

[q] In agreement with shifts calculated by the additivity principle and using the shifts of 1,2,3,4-tetramethylbenzene, 1,3-dimethylbenzene and 1-methyl-3-phytanylbenzene (Sinninghe Damsté *et al.*, 1988a): C-1 (132.8), C-2 (134.8), C-3 (126.8), C-4 (126.7), C-5 (133.7) and C-6 (139.2).

CHAPTER 8

Restricted utility of aryl isoprenoids as indicators for photic zone anoxia

M.P. Koopmans, S. Schouten, M.E.L. Kohnen and J.S. Sinninghe Damsté

8.1 Abstract

In a North Sea oil, the carotenoid derivatives β-carotane, β-isorenieratane and isorenieratane were identified, together with a series of aryl isoprenoids with a 2,3,6-trimethyl substitution pattern for the aromatic ring. The $\delta^{13}C$ values of β-carotane and β-isorenieratane are similar, whereas isorenieratane is *c.* 15‰ heavier. This suggests that β-isorenieratane is not derived from β-isorenieratene biosynthesised by Chlorobiaceae, but from aromatisation of β-carotene. This was confirmed by laboratory aromatisation of partially hydrogenated β-carotene, which yielded β-isorenieratane as the main product. The aryl isoprenoids, which can be formed by C-C bond cleavage of both isorenieratane and β-isorenieratane, have a mixed isotopic signature in the oil. These results indicate that mere identification of aryl isoprenoids, without determination of their $\delta^{13}C$ values, cannot be used to assess the presence of Chlorobiaceae, and, thus, photic zone anoxia in the depositional environment.

8.2 Introduction

The occurrence of aryl isoprenoids with a 2,3,6-trimethyl substitution pattern for the aromatic ring and a tail-to-tail isoprenoid chain (**I**; see Appendix) in sedimentary rocks and crude oils is often taken as an indication for the presence of brown-coloured photosynthetic green sulphur bacteria (Chlorobiaceae) and photic zone anoxia in the depositional environment (Summons and Powell, 1986, 1987; Clark and Philp, 1989; Yu Xinke *et al.*, 1990; Fowler, 1992; Requejo *et al.*, 1992; Hartgers *et al.*, 1994b,c; Koopmans *et al.*, 1996a). The aryl isoprenoids are thought to form from C-C bond cleavage of the isoprenoid chain of isorenieratene (**II**) and β-isorenieratene (**III**), both biosynthesised by Chlorobiaceae (Liaaen-Jensen, 1978a,b; de Wit and Caumette, 1995), that are bound in

high-molecular-weight organic matter fractions (*e.g.* kerogen) of the sediment (Requejo *et al.*, 1992; Hartgers *et al.*, 1994c). The origin of aryl isoprenoids from Chlorobiaceae can be confirmed by their ^{13}C contents, because Chlorobiaceae fix CO_2 *via* the reverse tricarboxylic acid cycle (Sirevåg and Ormerod, 1970) leading to biomass anomalously enriched in ^{13}C (Quandt *et al.*, 1977; Sirevåg *et al.*, 1977). However, ^{13}C contents of aryl isoprenoids are seldom reported because these compounds are usually present only in low abundance in complex mixtures.

Here, we reveal a diagenetic origin of β-isorenieratane (**IV**) from the ubiquitous carotenoid β-carotene (**V**). Evidence comes from (i) stable carbon isotope measurements of β-carotane (**VI**), β-isorenieratane and isorenieratane (**VII**) in a North Sea oil, and (ii) laboratory formation of β-isorenieratane from β-carotene. Because C-C bond cleavage of both macromolecularly-bound isorenieratane and β-isorenieratane yields aryl isoprenoids, these compounds have a mixed origin as confirmed by their ^{13}C content in the oil. This indicates that aryl isoprenoids cannot be used as markers for Chlorobiaceae and, thus, photic zone anoxia, unless they are significantly enriched in ^{13}C compared to algal lipids.

8.3 Experimental

Fractionation. 40.1 mg of a North Sea oil, to which a mixture of three standards was added for quantitative analysis, was chromatographed with Al_2O_3 to obtain the apolar fraction (hexane/dichloromethane 9:1 v/v). Further separation of the apolar fraction by argentatious thin-layer chromatography yielded the saturated hydrocarbon fraction (R_f = 0.78-1.00), the monoaromatic hydrocarbon fraction (R_f = 0.29-0.78), and the polyaromatic hydrocarbon fraction (R_f = 0.06-0.29). For stable carbon isotope measurements, some fractions were further chromatographed. The saturated hydrocarbon fraction was eluted over silica-lite with cyclohexane to remove linear alkanes. The monoaromatic hydrocarbon fraction was first eluted over silica-lite with cyclohexane to remove linear alkylbenzenes, and then over Al_2O_3 with hexane and hexane/dichloromethane (9:1 v/v). The latter fraction contained the aryl isoprenoids and some C_{40} carotenoid derivatives.

Laboratory formation of β-isorenieratane from β-carotene. 4.5 mg of β-carotene (Acros Chimica) was hydrogenated with H_2/PtO_2 for 4 h. Column chromatography using Al_2O_3 (hexane/dichloromethane 1:1 v/v) yielded the hydrogenated products (78%). These were dissolved in dry toluene, and 26.0 mg of 2,3-dichloro-5,6-dicyano-1,4-benzoquinone (DDQ) was added. The mixture was allowed to reflux for 24 h. The reaction mixture was chromatographed with hexane/dichloromethane (9:1 v/v) over Al_2O_3.

Gas chromatography. Gas chromatography (GC) was performed using a Hewlett-Packard 5890 instrument, equipped with an on-column injector. A fused silica capillary column (25 m x 0.32 mm) coated with CP Sil-5 (film thickness 0.12 μm) was used with

helium as carrier gas. For the co-injection experiments, a capillary column (30 m x 0.25 mm) coated with DB-1701 (film thickness 0.25 μm) was also used. The column effluent was monitored by a flame ionisation detector. Samples were injected at 70°C and the oven was subsequently programmed to 130°C at 20°C/min and then at 4°C/min to 320°C, at which it was held for 20 min.

Gas chromatography-mass spectrometry. Gas chromatography-mass spectrometry (GC-MS) was carried out on a Hewlett-Packard 5890 gas chromatograph interfaced to a VG Autospec Ultima mass spectrometer operated at 70 eV with a mass range m/z 40-800 and a cycle time of 1.8 s (resolution 1000). The configuration and conditions of the gas chromatograph were the same as for GC described above.

Isotope-ratio-monitoring gas chromatography-mass spectrometry. The DELTA-C irm-GC-MS system is, in principle, similar to the DELTA-S system described previously (Hayes *et al.*, 1990). The gas chromatograph (Hewlett-Packard 5890) was equipped as for GC analyses with helium as carrier gas. Fractions were injected on-column at 70°C and the oven was programmed as for GC analyses. Isotopic values were calculated by integrating the mass 44, 45 and 46 ion currents of the peaks produced by combustion of the chromatographically separated compounds and of CO_2-spikes generated by admitting CO_2 of a known ^{13}C content at regular intervals into the mass spectrometer. Values were determined at least in duplicate. Results were averaged to obtain mean values and to calculate standard deviations. The stable carbon isotope compositions are reported in the delta notation against the PDB ^{13}C standard.

8.4 Results and Discussion

The oil was fractionated by column chromatography into a saturated hydrocarbon fraction, a monoaromatic hydrocarbon fraction, and a polyaromatic hydrocarbon fraction. The saturated hydrocarbon fraction contains a substantial amount (Table 8.1) of β-carotane, and a series of 1-alkyl-2,2,6-trimethylcyclohexanes (**VIII**) first identified by Anders and Robinson (1971). The monoaromatic hydrocarbon fraction contains β-isorenieratane (**IV**), an aromatised diagenetic product of β-carotene (**IX**), and a series of aryl isoprenoids with a distribution similar to that of the 1-alkyl-2,2,6-trimethylcyclohexanes. The polyaromatic hydrocarbon fraction contains isorenieratane.

After further chromatographic steps (see Experimental), the ^{13}C contents of β-carotane, β-isorenieratane, isorenieratane, **IX** and the C_{19}-C_{21} aryl isoprenoids were measured (Fig. 8.1). The $\delta^{13}C$ values of β-carotane and its aromatic counterpart **IX** are almost identical. The $\delta^{13}C$ values of isorenieratane and phytane, which is taken as a marker for algae living in the upper part of the water column and using Rubisco for CO_2 fixation (Hayes, 1993), differ by *c.* 16‰. This is in agreement with values obtained from a suite of carbonaceous rocks throughout the Phanerozoic (Koopmans *et al.*,

Table 8.1. Absolute amounts of several carotenoid derivatives. Roman numbers refer to structures in the Appendix.

Compound	Amount (μg/g oil)
β-carotane (**VI**)	$1.1x10^3$
β-isorenieratane (**IV**)	$1.3x10^2$
IX	$2.6x10^2$
Isorenieratane (**VII**)	$2.1x10^2$
C_{19} aryl isoprenoid (**I**)	$2.7x10^2$
C_{19} cyclohexane (**VIII**)	$4.3x10^2$

1996a). However, the $\delta^{13}C$ value of β-isorenieratane, which was expected to be similar to that of isorenieratane because their unsaturated counterparts β-isorenieratene and isorenieratene are biosynthesised by Chlorobiaceae, is close to that of β-carotane. In addition, the C_{19}, C_{20} and C_{21} aryl isoprenoids are *c.* 10‰ lighter than isorenieratane.

In order to explain the similarity of the $\delta^{13}C$ values of β-carotane and β-isorenieratane, an attempt was made to form β-isorenieratane from β-carotene in the laboratory (Fig. 8.2). β-carotene was hydrogenated, which yielded β-carotane and a suite of mono- and di-unsaturated counterparts. This mixture was aromatised with DDQ, which yielded β-isorenieratane (10%) as the main product. β-isorenieratane was identified by comparison of its mass spectrum with that of an authentic standard, and by co-injection experiments using two different capillary columns. Apparently, a geminal methyl group of the cyclohexenyl moiety has shifted exclusively from the 2 to the 3 position during aromatisation (Fig. 8.2), in agreement with literature data on aromatisation reactions with DDQ of similar compounds (Braude *et al.*, 1960; Fu and Harvey, 1978). These results indicate that β-isorenieratane present in sedimentary rocks and crude oils cannot be used as a marker for Chlorobiaceae. It should be noted that, in principle, isorenieratane can be formed from β-carotene by aromatisation of both cyclohexenyl moieties. However, the different $\delta^{13}C$ values of β-carotane and isorenieratane in the North Sea oil (Fig. 8.1) indicate that this is not an important process.

Aryl isoprenoids with a 2,3,6-trimethyl substitution pattern for the aromatic ring are thought to form from C-C bond cleavage of the isoprenoid chain of macromolecularly-bound isorenieratene and β-isorenieratene (Requejo *et al.*, 1992; Hartgers *et al.*, 1994c). Thus, our results suggest that aryl isoprenoids can be formed indirectly from β-carotene during sediment burial, as supported by their $\delta^{13}C$ values in the oil (Fig. 8.1). This implies that the occurrence of aryl isoprenoids in sedimentary rocks and crude oils cannot be taken as an indication for the presence of Chlorobiaceae in the depositional environment, unless they are significantly enriched in ^{13}C compared to algal lipids. Interestingly, β-carotene was originally proposed as the precursor of the aryl isopre-

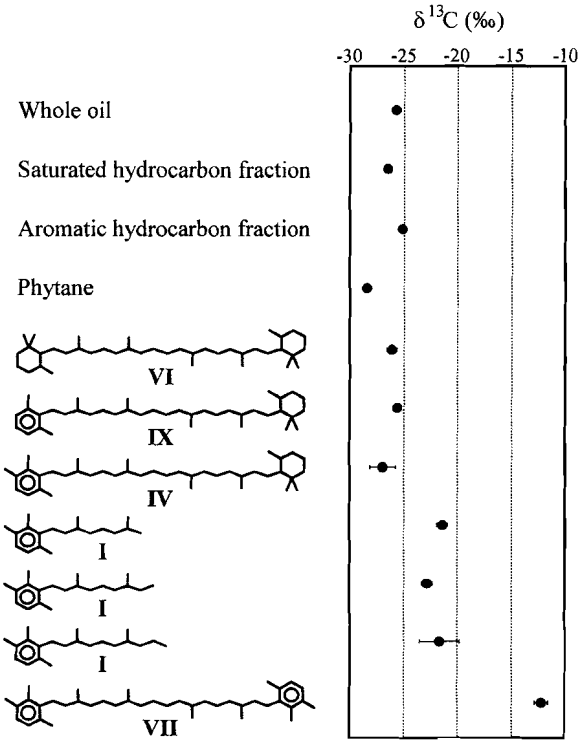

Fig. 8.1. $\delta^{13}C$ values of β-carotane, β-isorenieratane, isorenieratane, **IX**, phytane, several aryl isoprenoids, and bulk fractions. When error bars are not shown, the standard deviation (n = 2) falls within the range given by the markers. The $\delta^{13}C$ value of β-isorenieratane is similar to that of β-carotane, but differs strongly from that of isorenieratane. The aryl isoprenoids have values intermediate between those of β-isorenieratane and isorenieratane.

noids (Ostroukhov *et al.*, 1982). This hypothesis was later questioned (Summons and Powell, 1986), because synthesis of aryl isoprenoids by aromatisation of β-ionone (Ostroukhov *et al.*, 1982) resulted in two isomers with different trimethyl substitution patterns for the aromatic ring. However, the fate of geminal methyl groups during aromatisation reactions is merely a result of the reagent used (Fu and Harvey, 1978).

Our results also could explain two apparent anomalies. First, the C_{31} aryl isoprenoid is present in the oil under study and has been reported before as the ultimate member of the series in other sedimentary rocks and crude oils (Summons and Powell, 1986, 1987; Requejo *et al.*, 1992), although the formation of this component from isorenieratane requires an unlikely cleavage α to the benzene ring. However, cleavage α to the cyclohexyl moiety of β-isorenieratane is facile, and results in the formation of the C_{31} aryl isoprenoid. Second, the difference in $\delta^{13}C$ values of the aryl isoprenoids and the

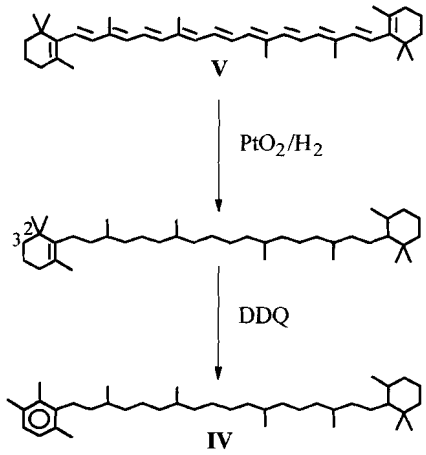

Fig. 8.2. Scheme for the laboratory transformation of β-carotene into β-isorenieratane.

saturated hydrocarbon fraction reported by Summons and Powell (1986) is only 6-9‰. A similar difference is found in this study (4-5‰), but it is much smaller than the difference expected when the aryl isoprenoids would be exclusively formed from isorenieratane (*c.* 15‰; Koopmans *et al.*, 1996a). This can be explained by the formation of aryl isoprenoids from β-isorenieratane, and thus, indirectly, from β-carotene. Therefore, it seems likely that the aryl isoprenoids reported by Summons and Powell (1986) were partly derived from β-carotene.

8.5 Conclusions

$\delta^{13}C$ values of β-carotane, β-isorenieratane and isorenieratane in a North Sea oil suggest a genetic relationship of β-carotane and β-isorenieratane. This is supported by laboratory aromatisation of β-carotene, which yielded β-isorenieratane. The $\delta^{13}C$ values of the aryl isoprenoids with a 2,3,6-trimethyl substitution pattern for the aromatic ring are intermediate between those of β-isorenieratane and isorenieratane, suggesting a mixed source. These results indicate that aryl isoprenoids in sedimentary rocks and crude oils do not indicate the presence of Chlorobiaceae, and, thus, photic zone anoxia in the depositional environment, unless they are significantly enriched in ^{13}C compared to algal lipids. Particularly the co-occurrence of aryl isoprenoids and β-carotane should be viewed with caution.

8.6 Acknowledgements

We thank Shell International Exploration and Production for providing the oil sample and a research studentship to MPK. Shell International Exploration and Production is also gratefully acknowledged for financial support for the irm-GC-MS facility. Analytical support was provided by Mrs. M. Dekker and Mr. W. Pool. Two anonymous reviewers are thanked for their constructive comments. This work was partly supported by a PIONIER grant to JSSD from the Netherlands Organisation for Scientific Research (NWO).

Appendix

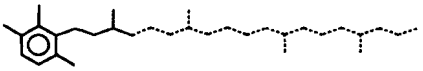

I

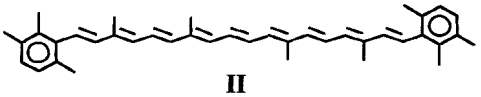

II

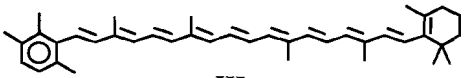

III

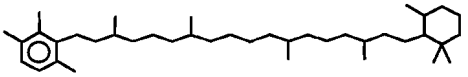

IV

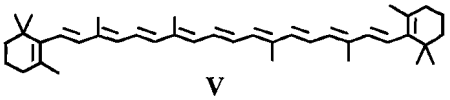

V

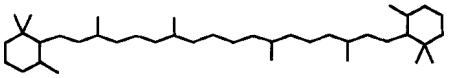

VI

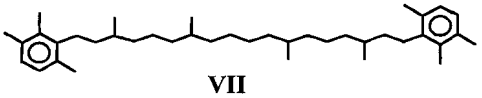

VII

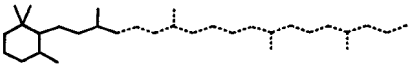

VIII

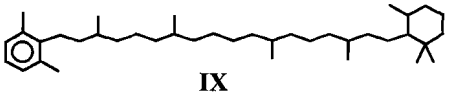

IX

CHAPTER 9

Novel cyclised and aromatised diagenetic products of ß-carotene in the Green River Shale

M.P. Koopmans, J.W. de Leeuw and J.S. Sinninghe Damsté

9.1 Abstract

A suite of novel diagenetic products of β-carotene has been identified in an extract of a sample from the Green River Shale. Identification is mainly based on comparison of mass spectra with those of diagenetic products of another carotenoid, isorenieratene. These compounds were formed by (i) cyclisation and aromatisation of the polyene isoprenoid chain, (ii) expulsion of toluene and *m*-xylene from the polyene isoprenoid chain, and (iii) aromatisation of the 1,1,5-trimethylcyclohex-5-enyl moieties resulting in 1,2-dimethylbenzene end groups. Reduction of the double bonds of β-carotene is the most important diagenetic process, however, as judged from the high relative amount of β-carotane (63% of quantitated diagenetic products of β-carotene). These results indicate that the fossilisation potential of carotenoids is larger than previously thought.

9.2 Introduction

The tetraterpenoid hydrocarbon β-carotane (perhydro-β-carotene; **I**, see Appendix I) has been identified for the first time in a sedimentary rock from the Green River Shale (Murphy *et al.*, 1967). It was considered to be a diagenetic product of the carotenoid β-carotene (**II**), from which it was supposedly formed through reduction of the conjugated double bonds during diagenesis (Murphy *et al.*, 1967). Later, β-carotane has been found in numerous sedimentary rocks and crude oils (*e.g.* Shi Ji-Yang *et al.*, 1982; Hall and Douglas, 1983; Jiang and Fowler, 1986; Brassell *et al.*, 1988; Fu Jiamo *et al.*, 1988; Mello *et al.*, 1988; Clark and Philp, 1989; Peters *et al.*, 1989; Philp *et al.*, 1992; Keely *et al.*, 1993; Yawanarajah *et al.*, 1993). Desulphurisation of polar fractions of immature sedimentary rocks and 'low thermal stress' crude oils has yielded β-carotane (Sinninghe Damsté *et al.*, 1990a, 1993b,d; Kohnen *et al.*, 1991c; Adam *et al.*, 1993). Desulphuri-

sation of a non-extracted crushed rock from Gibellina (Italy) yielded sulphur-containing compounds with the β-carotane carbon skeleton (Schaeffer *et al.*, 1995b).

Despite the findings in ancient sedimentary rocks of β-carotane (Murphy *et al.*, 1967), isorenieratane (**III**; Schaeflé *et al.*, 1977) and other diaryl isoprenoids originating from diaromatic carotenoids (Schaeflé *et al.*, 1977; Hartgers *et al.*, 1993), the geological preservation potential of carotenoids is generally considered to be low (Mackenzie, 1984; Brassell, 1993). However, Koopmans *et al.* (1996a) have recently shown that the diaromatic carotenoid isorenieratene (**IV**) can survive diagenesis through a number of reactions involving the polyene isoprenoid chain. These include (i) sulphurisation, (ii) cyclisation and subsequent aromatisation, (iii) expulsion of *m*-xylene and toluene, and (iv) reduction of double bonds. C-C bond cleavage takes place during catagenesis, resulting in short-chain compounds (*e.g.* aryl isoprenoids). It was hypothesised that similar diagenetic reactions could occur with other carotenoids (Koopmans *et al.*, 1996a), since carotenoids comprise by definition a conjugated double bond system that enables these reactions.

Isorenieratene (**IV**) and β-carotene (**II**) differ by their terminal ring systems. Isorenieratene has two aromatic rings with a 1,2,5-trimethyl substitution pattern (see Appendix I for carbon numbering system of carotenoids), whereas β-carotene contains two 1,1,5-trimethylcyclohex-5-enyl moieties. Cyclisation and aromatisation of the polyene isoprenoid chain of isorenieratene leaves the methyl substitution pattern for the terminal aromatic rings intact (Koopmans *et al.*, 1996a). Aromatisation of the 1,1,5-trimethylcyclohex-5-enyl moiety of β-carotene, however, will affect the methyl substitution pattern, because C-1 is a quaternary carbon atom which cannot bear two methyl groups and at the same time form part of a benzene ring.

Here, we report on a range of novel diagenetic products of β-carotene in the Green River Shale that have apparently been formed by reactions similar to those decribed for isorenieratene (Koopmans *et al.*, 1996a). These results indicate that the fossilisation potential of an important class of natural products (*i.e.* carotenoids) is higher than previously thought.

9.3 Experimental

Sample description. The sample used in this study is from the Parachute Creek Member (Mahogany Zone) of the Green River Shale. Rock-Eval pyrolysis yielded a total organic carbon of 15.3 wt.%, a T_{max} of 438°C, a hydrogen index of 962 mg HC/g TOC, and an oxygen index of 27 mg CO_2/g TOC (Type I kerogen). The estimated R_o value is 0.44%, as determined from the Pristane Formation Index (Goossens *et al.*, 1988a,b).

Extraction and fractionation. The sample was freeze-dried, pulverised in a rotary disc mill, and Soxhlet extracted with dichloromethane/methanol (7.5:1 v/v). The extract was separated into a maltene and an asphaltene fraction by repeated (3 times) precipitation

in heptane (40-fold excess). An aliquot of the maltene fraction (*c.* 250 mg), to which two standards [6,6-d_2-3-methylhenicosane and 2-methyl-2-(4,8,12-trimethyltridecyl)-chroman] were added for quantitative analysis, was fractionated by column chromatography (Al_2O_3; 20 x 2 cm) into an apolar and a polar fraction by elution with hexane/dichloromethane (9:1 v/v) and dichloromethane/methanol (1:1 v/v), respectively. Further separation of the apolar fraction by argentatious thin-layer chromatography (TLC), using hexane as developer, yielded the saturated hydrocarbon fraction (R_f = 0.9-1.0) and the aromatic hydrocarbon fraction (R_f = 0.0-0.9).

Gas chromatography. Gas chromatography (GC) was performed using a Hewlett-Packard 5890 instrument, equipped with an on-column injector. A fused silica capillary column (25 m x 0.32 mm) coated with CP Sil-5 (film thickness 0.12 μm) was used with helium as carrier gas. The column effluent was monitored by a flame ionisation detector (FID). The samples were injected at 70°C and the oven was subsequently programmed to 130°C at 20°C/min and then at 4°C/min to 320°C, at which it was held for 20 min.

Gas chromatography-mass spectrometry. Gas chromatography-mass spectrometry (GC-MS) was carried out on a Hewlett-Packard 5890 gas chromatograph interfaced to a VG Autospec Ultima mass spectrometer operated at 70 eV with a mass range m/z 40-800 and a cycle time of 1.8 s (resolution 1000). The gas chromatograph was equipped with a fused silica capillary column (25 m x 0.32 mm) coated with CP Sil-5 (film thickness 0.12 μm). Helium was used as carrier gas. The samples were injected at 60°C and the oven was subsequently programmed to 130°C at 20°C/min and then at 4°C/min to 310°C, at which it was held for 20 min.

Quantitation. Quantitation of β-carotane and other diagenetic products of β-carotene in the saturated hydrocarbon fraction was accomplished by integration of mass chromatograms of their major fragment ions and the main fragment ion (m/z 57) of the internal standard, 6,6-d_2-3-methylhenicosane. Aromatic diagenetic products of β-carotene in the aromatic hydrocarbon fraction were quantitated by integration of mass chromatograms of their major fragment ions (m/z 119, 120, 223, 273, and the molecular ion) and the main fragment ion (m/z 147) of the standard, 2-methyl-2-(4,8,12-trimethyltridecyl)-chroman. A correction was made to account for the intensity of the fragment ions relative to the total ion current in the spectra of the quantitated compounds and the spectrum of the standard. Because mass spectrometric detection of compounds gives a molar response, a factor was introduced taking into account the molecular weights of the quantitated compounds and the standard to obtain absolute amounts (μg/g TOC of original rock).

9.4 Results and Discussion

Saturated hydrocarbon fraction

The saturated hydrocarbon fraction contains large amounts of pristane, phytane, steranes dominated by the (20R)-5α,14α,17α(H) C_{27}-C_{29} components, hopanes, and gammacerane (Fig. 9.1). Recently, gammacerane was proposed as an indicator for water column stratification (Sinninghe Damsté *et al.*, 1995c). Thus, the presence of gammacerane supports the 'stratified lake model' used to describe the depositional setting of the Green River Shale (*e.g.* Johnson, 1981; Katz, 1995). Normal alkanes are minor components in the saturated hydrocarbon fraction. This seems to be a characteristic of samples from the Parachute Creek Member of the Green River Shale (Ruble *et al.*, 1994).

The abundant presence of β-carotane (*c.* 1.7 mg/g TOC; Table 9.1) suggests a large input of β-carotene in the depositional environment. Lexane (**V**), the C_{33} pseudohomologue of β-carotane which partly coelutes with 17α,21β(H) hopane, and γ-carotane (**VI**), which often co-occurs with β-carotane but generally in lower amounts (*e.g.* Anders and Robinson, 1971; Hall and Douglas, 1983; Jiang and Fowler, 1986), are also present.

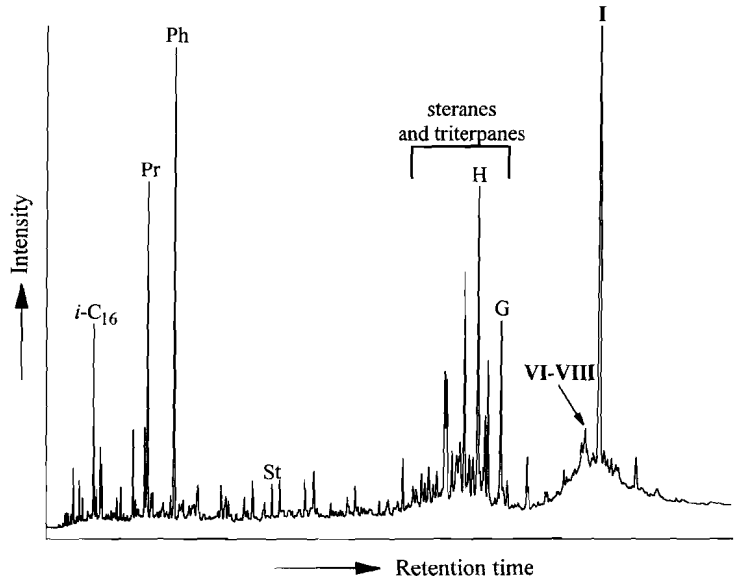

Fig. 9.1. Gas chromatogram of the saturated hydrocarbon fraction. Key: *i*-C_{16} = 2,6,10-trimethyltridecane, Pr = pristane, Ph = phytane, St = standard (6,6-d_2-3-methylhenicosane), H = 17α,21β(H) C_{30} hopane, G = gammacerane. Roman numbers refer to structures in Appendix I.

Aromatic hydrocarbon fraction

The aromatic hydrocarbon fraction contains some low-molecular-weight aromatics (*e.g.* naphthalenes), abundant 2,5,7,8-tetramethyl-2-(4,8,12-trimethyltridecyl)chroman, and a suite of polyaromatic compounds that were identified as diagenetic products of β-carotene (Fig. 9.2). Two components, 1,1,6-trimethyl-1,2,3,4-tetrahydronaphthalene and a monoaromatic tricyclic hydrocarbon, were tentatively identified based on the similarity of their mass spectra with those reported in the literature (Anders *et al.*, 1973). Laboratory studies have shown that 1,1,6-trimethyl-1,2,3,4-tetrahydronaphthalene is an important thermal degradation product of β-carotene (Day and Erdman, 1963; Byers and Erdman, 1983).

Identification of diagenetic products of β-carotene

The identification of the aromatic diagenetic products of β-carotene is mainly based on comparison of their mass spectra with those of the polyaromatic diagenetic products of isorenieratene reported previously (Koopmans *et al.*, 1996a). Aromatisation of the 1,1,5-trimethylcyclohex-5-enyl moieties of β-carotene results in a 1,2-dimethyl substitution pattern for the terminal aromatic rings, as recently demonstrated for one compound by isolation and subsequent NMR analysis (Sinninghe Damsté *et al.*, 1996). Therefore, the aromatic diagenetic products of β-carotene show the following mass spectral characteristics compared to their isorenieratene counterparts: (i) fragment ions are 14 amu lower, and (ii) molecular ions are 28 amu lower.

Absolute and relative amounts of some selected diagenetic products of β-carotene

Table 9.1. Absolute and relative amounts of diagenetic products of β-carotene in the Green River Shale. Roman numbers refer to structures in Appendix I.

Compound	Absolute amount (μg/g TOC)	Relative amount (%)
I	$1.7x10^3$	63
V	$2.4x10^2$	8.8
VII+VIII	$3.4x10^2$	13
X	$6.2x10^1$	2.3
XI	$7.5x10^1$	2.8
XII	$8.2x10^1$	3.0
XIII	$3.3x10^1$	1.2
XIV	$7.5x10^1$	2.8
XX	$3.8x10^1$	1.4
XXI	$2.8x10^1$	1.0
XXIII	$4.0x10^1$	1.5

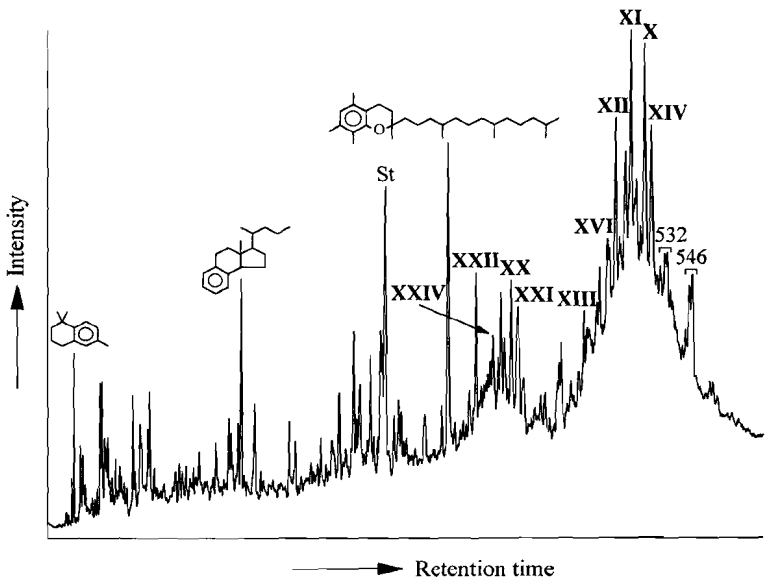

Fig. 9.2. Gas chromatogram of the aromatic hydrocarbon fraction. Key: St = standard [2-methyl-2-(4,8,12-trimethyltridecyl)chroman], 532 = cluster of compounds with a molecular mass of 532, 546 = cluster of compounds with a molecular mass of 546. Roman numbers refer to structures in Appendix I.

are listed in Table 9.1. The aromatic diagenetic products of β-carotene will be discussed according to the number of carbon atoms (*i.e.* C_{40}, C_{38}, C_{30} and C_{31}, and other carbon numbers). A detailed description of the identification of the diagenetic products of β-carotene is given in Appendix II.

C_{40} compounds

Two monoaromatic diagenetic products of β-carotene were identified in the saturated hydrocarbon fraction (**VII** and **VIII**). All other aromatic diagenetic products of β-carotene were encountered in the aromatic hydrocarbon fraction. The difference of eight amu between the molecular ion (m/z 550) of **VII** and **VIII** and the molecular ion of β-carotane suggests the presence of an aromatic ring in the isoprenoid chain of **VII** and **VIII**. This is confirmed by the main fragment ion at m/z 119 in the mass spectrum of **VII** (Appendix II), which results from cleavage β to both sides of the aromatic ring. The McLafferty fragment ions at m/z 300 and 370 in the mass spectrum of **VII** indicate that this ring is at C-11 to C-15'. **VII** partly coelutes with the less abundant **VIII**, which makes it difficult to obtain a good mass spectrum of the latter. However, a prominent fragment ion at m/z 243 can be discerned, suggesting an aromatic ring at C-7 to C-12. Koopmans *et al.* (1996a) have shown that additional aromatic rings in the polyene iso-

prenoid chain of isorenieratene (**IV**) are formed by intramolecular Diels-Alder reactions, resulting in only two possible positions for the additional aromatic ring, *i.e.* at C-7 to C-12 and at C-11 to C-15'. Because β-carotene contains a conjugated double bond system similar to that of isorenieratene, it is likely that the formation of aromatic rings in the polyene isoprenoid chain of β-carotene occurs in a similar manner, which is indeed observed as shown by the identification of **VII** and **VIII**. Before aromatic rings at C-7 to C-12 and at C-11 to C-15' in β-carotene can be formed, *trans-cis* isomerisation reactions of the double bonds at C-9 and C-13, respectively, of *all-trans*-β-carotene are required (Fig. 9.3). Interestingly, the C-9 and C-13 double bonds of β-carotene are known to isomerise much faster than the other double bonds (Doering *et al.*, 1995), and some algae even contain 9-*cis*-β-carotene in high relative amounts (Ben-Amotz *et al.*, 1989).

A C_{40} compound with two terminal 1,1,5-trimethylcyclohexyl moieties and a

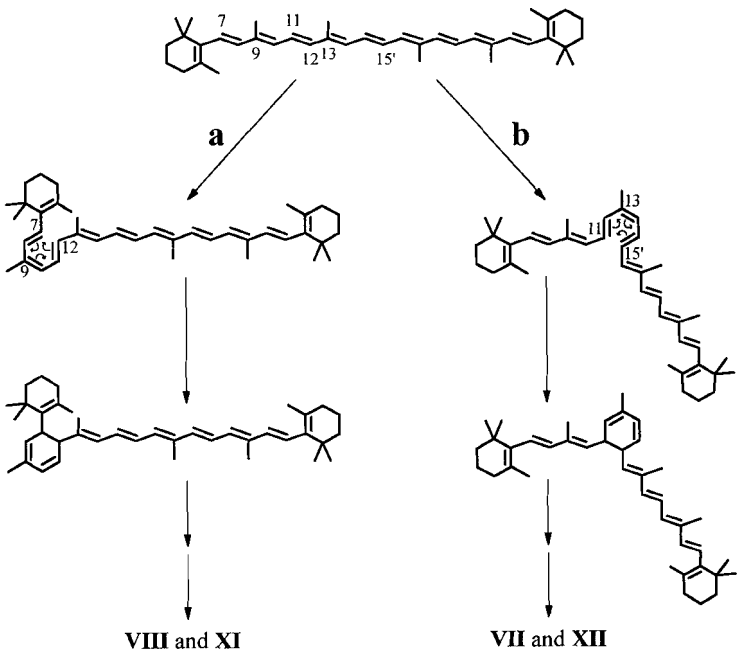

Fig. 9.3. Formation of additional aromatic rings in the polyene isoprenoid chain of β-carotene may occur (**a**) at C-7 to C-12 and (**b**) at C-11 to C-15', following *trans-cis* isomerisation reactions of the double bonds at C-9 and C-13, respectively. The newly formed cyclohexadienyl moieties are thought to aromatise fast because of the energy gain associated with restoration of a conjugated double bond system (cf. Koopmans *et al.*, 1996a). Subsequent diagenetic reactions (*e.g.* reduction of double bonds) will ultimately lead to compounds **VII**, **VIII**, **XI** and **XII**.

naphthalene moiety in the isoprenoid chain (**IX**) has been identified based on its mass spectrum. The molecular ion of **IX** is 14 amu lower than that of β-carotane, suggesting either the loss of a methyl group or the presence of a naphthalene moiety. The accurate masses of the molecular ions of **IX** and β-carotane differ by 14.11 amu, concurrent with a difference of 14 H atoms. The loss of a methyl group would have resulted in a difference of 14.02 amu. Koopmans *et al.* (1996a) have shown that formation of naphthalene moieties in the polyene isoprenoid chain of isorenieratene can only occur in two positions, *i.e.* at C-7 to C-15' or at C-11 to C-11'. Since the naphthalene moiety is not at C-7 to C-15', as deduced from the absence of a fragment ion at m/z 293, it must be at C-11 to C-11'. This is supported by the fragment ion at m/z 183, resulting from cleavage β to both sides of the naphthalene moiety.

C_{38} compounds

One of the major compounds in the aromatic hydrocarbon fraction is the diaryl isoprenoid **X**. Its mass spectrum (Fig. 9.4**a**) shows fragment ions 14 amu lower and a molecular ion 28 amu lower than the corresponding ions in the mass spectrum of the isorenieratene counterpart (isorenieratane; Fig. 9.4**e**). The McLafferty fragment ion at m/z 120 in the mass spectrum of **X** (Fig. 9.4**a**) has a higher relative intensity than the McLafferty fragment ion at m/z 134 in the mass spectrum of isorenieratane (Fig. 9.4**e**), because the terminal benzene rings of **X** have a free *ortho* and *para* position to transfer a H atom to, whereas the terminal benzene rings of isorenieratane have only a free *para* position (Kingston *et al.*, 1988). The relative intensity of the McLafferty fragment ions in these mass spectra is in good agreement with the relative intensity of the McLafferty fragment ions of several methylated phytanylbenzenes reported by Sinninghe Damsté *et al.* (1988a).

Two diaryl isoprenoids with an additional aromatic ring in the isoprenoid chain have been identified (**XI** and **XII**). **XI** has an additional aromatic ring at C-7 to C-12 ('biphenyl position'), as determined from the similarity of its mass spectrum (Fig. 9.4**b**) with that of its isorenieratene counterpart (Fig. 9.4**f**). Because the formation of additional aromatic rings can occur only at two positions (at C-7 to C-12 and at C-11 to C-15'; Koopmans *et al.*, 1996a), the additional aromatic ring in the isoprenoid chain of **XII** is at C-11 to C-15'.

Two diaryl isoprenoids containing two additional aromatic rings in the isoprenoid chain have been identified (**XIII** and **XIV**). The structure of **XIII** was determined based on the similarity of its mass spectrum (Fig. 9.4**c**) with that of its isorenieratene counterpart (Fig. 9.4**g**). The molecular ion and the major fragment ion of **XIV** indicate that it contains a naphthalene moiety at C-7 to C-15'.

One compound with two additional condensed rings (**XV**) was tentatively identified from its mass spectrum. The molecular ion and the main fragment ion at m/z 221 in the mass spectrum of **XV** are two amu lower than the corresponding ions in the mass spectrum of the structurally related compound **XI** (Fig. 9.4**b**). In both mass spectra,

secondary fragment ions are present resulting from the consecutive loss of methyl radicals from the main fragment ion (cf. Wolf, 1993; Wolf *et al.*, 1995; Koopmans *et al.*, 1996a). This suggests that the structure of **XV** is similar to that of **XI**, with an additional ring or double bond in the biphenyl moiety. We propose that an additional ring is present in the form of a 9,10-dihydrophenanthrene moiety, because it is not possible to introduce a double bond into the biphenyl moiety. At present it is not clear by what mechanism this 9,10-dihydrophenanthrene moiety is formed.

One diaryl isoprenoid containing three additional aromatic rings in the isoprenoid chain (**XVI**) has been identified based on the similarity of its mass spectrum (Fig. 9.4**d**) with that of its isorenieratene counterpart (Fig. 9.4**h**). The isorenieratene counterpart of **XVI** is represented by two peaks of approximately equal intensity in the m/z 287 mass chromatogram of the polyaromatic fraction of several sedimentary rocks, due to the presence of two axially chiral centers and one asymmetric carbon atom (Koopmans *et al.*, 1996a). **XVI**, however, has no axially chiral centers, so that no diastereomers exist. Therefore, **XVI** is reflected in the m/z 273 mass chromatogram by only one peak (not shown).

One compound with a 9,10-dihydrophenanthrene moiety and an additional aromatic ring (**XVII**) was tentatively identified by comparison of its mass spectrum with that of **XV**. The fragment ion at m/z 223 indicates that the additional aromatic ring is in the 'biphenyl position' (cf. Figs. 9.4**b** and **c**). The fragment ion at m/z 221 is more intense than that at m/z 223, probably because the former represents cleavage α to a quaternary carbon atom.

C_{30} and C_{31} compounds

Laboratory heating experiments have shown that expulsion of *m*-xylene and toluene from the polyene isoprenoid chain of β-carotene, yielding philene (**XVIII**) and lexene (**XIX**), respectively, is one of the major degradation pathways of β-carotene (*e.g.* Kuhn and Winterstein, 1933; Day and Erdman, 1963; Edmunds and Johnstone, 1965; Byers and Erdman, 1983). Saturated lexene (lexane; **V**), the C_{33} pseudohomologue of β-carotane, has been found in small amounts in several oils (Jiang and Fowler, 1986; Fowler *et al.*, 1993; Vorob'yeva *et al.*, 1993) and a bitumen (Schoell *et al.*, 1994) that also contained significant amounts of β-carotane. Similar C_{32} and C_{33} diagenetic products of isorenieratene were released after desulphurisation of polar fractions and kerogens from the Vena del Gesso Basin (Kenig *et al.*, 1995; Schaeffer *et al.*, 1995a). In addition, Koopmans *et al.* (1996a) identified C_{32} and C_{33} diagenetic products of isorenieratene with additional aromatic rings in the aromatic hydrocarbon fractions of some well known petroleum source rocks (*e.g.* Schistes Cartons and Kimmeridge Clay Formations).

In the present study, two diaryl isoprenoids (**XX** and **XXI**) were identified that were formed by expulsion of *m*-xylene and toluene, respectively, from the polyene isoprenoid chain of β-carotene, and aromatisation of the 1,1,5-trimethylcyclohex-5-enyl

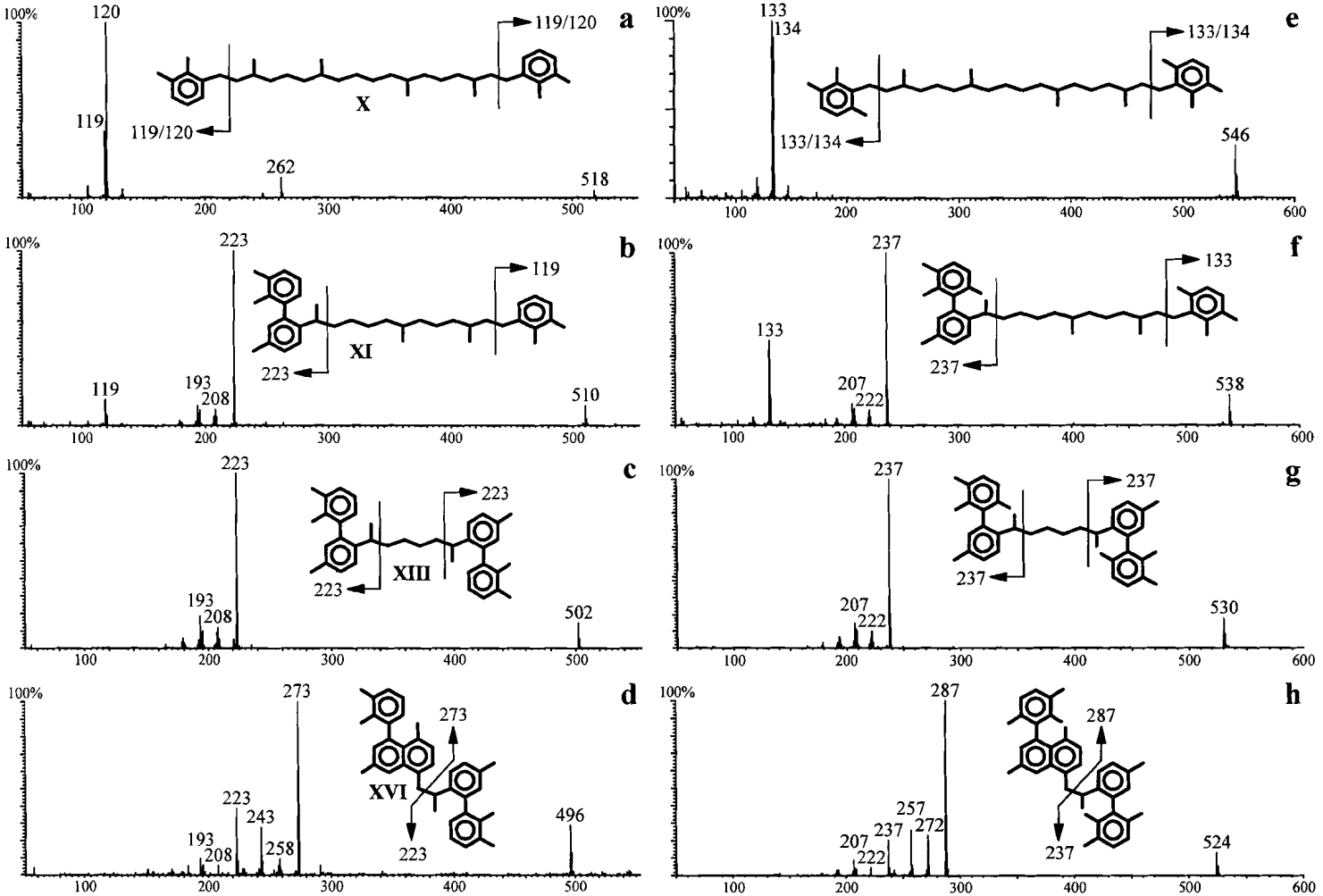
a
100%
120
119
119/120
262
518
X
b
223
119
193
208
510
XI
c
223
193
208
502
XIII
d
273
223
243
193
208
258
496
XVI
e
133
134
133/134
546
f
237
133
207
222
538
g
237
207
222
530
h
287
257
237
272
207
222
524

moieties. Their mass spectra (Figs. 9.5**a** and **b**) are similar to those of their isorenieratene counterparts (Figs. 9.5**e** and **f**). The high relative intensity of the fragment ion at m/z 120 in the mass spectra of **XX** and **XXI** (Figs. 9.5**a** and **b**) compared to the relative intensity of the corresponding ion at m/z 134 in the mass spectra of their isorenieratene counterparts (Figs. 9.5**e** and **f**) is due to the presence of a free *ortho* and *para* position at the aromatic rings.

Three diaryl isoprenoids with a $C_{30/31}$ carbon skeleton and an additional aromatic ring in the isoprenoid chain have been identified (**XXII-XXIV**). **XXII** (mass spectrum shown in Fig. 9.5**c**) was isolated and identified by NMR (Sinninghe Damsté *et al.*, 1996). The structure of **XXIII** was determined based on the similarity of its mass spectrum (Fig. 9.5**d**) with that of its isorenieratene counterpart (Fig. 9.5**h**). The mass spectrum of **XXIV** is also similar to that of its isorenieratene counterpart reported earlier (Koopmans *et al.*, 1996a). The isorenieratene counterparts of **XXIII** and **XXIV** contain an axially chiral center and one and two asymmetric carbon atoms, respectively. Consequently, they are represented in the m/z 237 mass chromatogram by two peaks in an approximate 1:1 ratio, and by four peaks in an approximate 1:1:1:1 ratio, respectively (Fig. 9.6**a**). **XXIII** and **XXIV**, however, do not contain an axially chiral center, while the number of asymmetric carbon atoms is the same as for their isorenieratene counterparts. Thus, **XXIII** and **XXIV** are represented in the m/z 223 mass chromatogram by one peak, and by two peaks in an approximately 1:1 ratio, respectively (Fig. 9.6**b**).

One C_{30} compound with a 9,10-dihydrophenanthrene moiety (**XXV**) was tentatively identified by comparison of its mass spectrum with that of **XV**.

Compounds with other carbon numbers

Two clusters of compounds, with molecular masses of 532 and 546, are present in the gas chromatogram of the aromatic hydrocarbon fraction (Fig. 9.2). Averaged mass spectra of these clusters indicate that they represent diaryl isoprenoids with a dimethyl/trimethyl and a trimethyl/trimethyl substitution pattern for the terminal aromatic rings, respectively. Co-injection experiments with authentic standards indicate that the two major peaks in the 546 cluster coelute with renieratane (**XXVI**) and octadecahydrorenierapurpurin (**XXVII**), and that isorenieratane (**III**) is not present. Two origins are conceivable for the compounds that make up these two clusters.

First, they could originate from β-carotene through aromatisation of the 1,1,5-trimethylcyclohex-5-enyl moieties, accompanied by either the shift of a geminal methyl

Fig. 9.4. Mass spectra (subtracted for background) of (**a**) **X**, (**b**) **XI**, (**c**) **XIII**, and (**d**) **XVI**, and (**e-h**) their isorenieratene counterparts. The structural difference between **X**, **XI**, **XIII** and **XVI** and their isorenieratene counterparts is the 1,2,5-trimethyl substitution pattern of the terminal aromatic rings of the latter. The fragment ion at m/z 262 in (**a**) is probably due to a co-eluting compound.

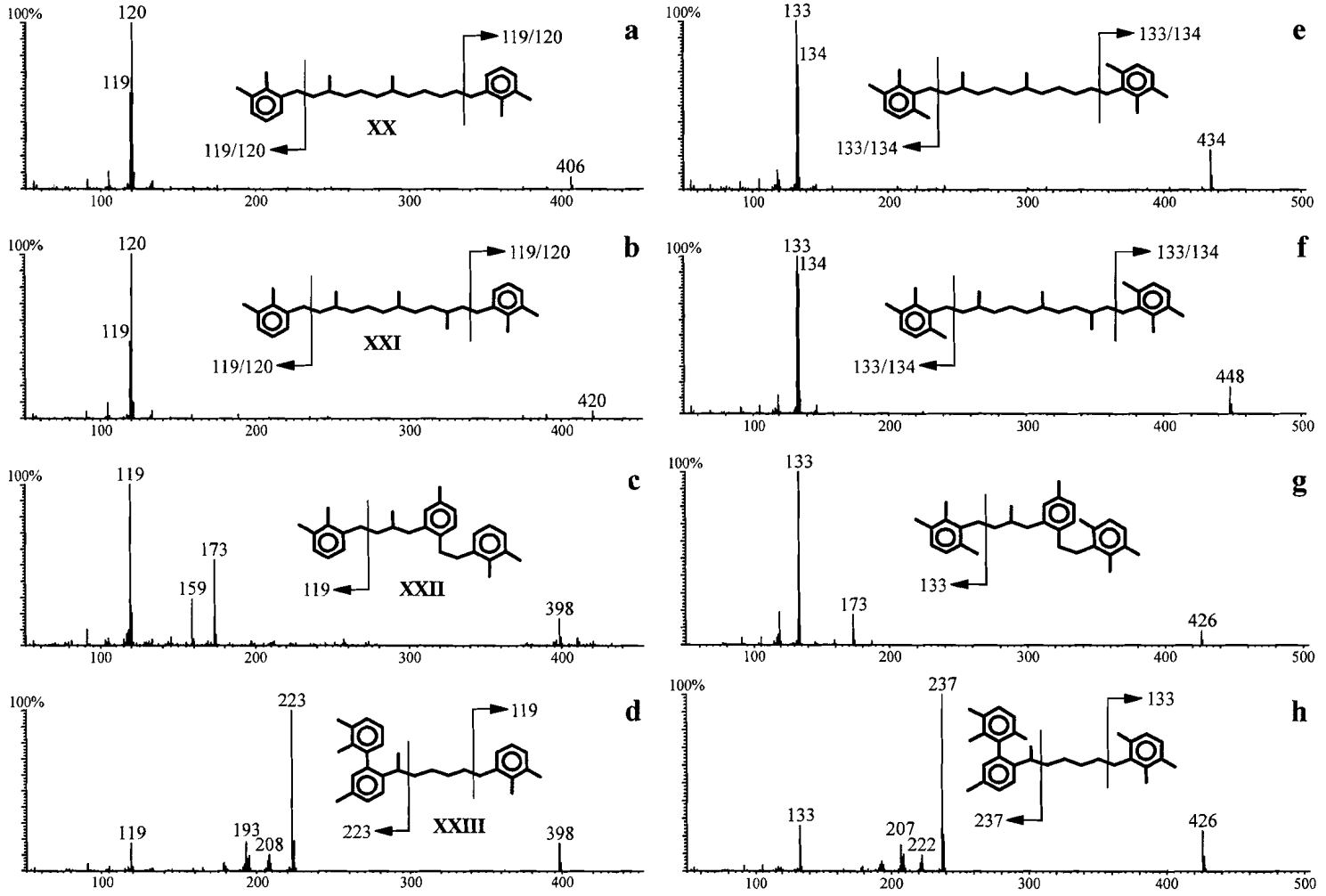
a
100%
120
119
119/120
119/120
406
XX
b
100%
120
119
119/120
119/120
420
XXI
c
100%
119
173
159
119
398
XXII
d
100%
223
119
193
208
223
398
XXIII
e
100%
133
134
133/134
133/134
434
f
100%
133
134
133/134
133/134
448
g
100%
133
133
173
426
h
100%
237
133
133
207
222
237
426
100
200
300
400
500

group, or a rearrangement of methyl groups involving elimination of a methyl group. Recently, it was shown that β-isorenieratane (**XXVIII**) can be formed from aromatisation of β-carotene both in the laboratory and in Nature (Koopmans *et al.*, 1996c). However, only 1,2-shifts have been described in the literature (Braude *et al.*, 1960; Fu and Harvey, 1978), which severely limits the number of possible aromatisation products. In effect, aromatisation of the 1,1,5-trimethylcyclohex-5-enyl moieties of β-carotene can theoretically result in three different diaryl isoprenoids (Fig. 9.7). Aromatisation with a 1,2-shift of a geminal methyl group in both rings ultimately leads to formation of isorenieratane (**III**; Fig. 9.7**a**), which is not present. Aromatisation with a 1,2-shift in one ring, and a rearrangement of methyl groups involving elimination of a methyl group in the other ultimately leads to a compound with molecular mass 532 (Fig. 9.7**b**), which may be present in the 532 cluster. Aromatisation with a rearrangement of methyl groups involving elimination of a methyl group in both rings ultimately leads to formation of **X** (Fig. 9.7**c**), which is a major compound in the aromatic hydrocarbon fraction (Fig. 9.2). Therefore, β-carotene is not the precursor of any compound in the 546 cluster, and may be the precursor of one compound in the 532 cluster.

Second, the compounds in the two clusters could originate from carotenoids other than β-carotene. The two major peaks in the 546 cluster that coelute with renieratane (**XXVI**) and octadecahydrorenierapurpurin (**XXVII**) probably originate from renieratene (**XXIX**) and renierapurpurin (**XXX**), diaromatic carotenoids biosynthesised by photosynthetic purple sulphur bacteria (Liaaen-Jensen, 1978b), through reduction of the double bonds in the isoprenoid chain. Aromatisation of the 1,1,5-trimethylcyclohex-5-enyl moiety of β-isorenieratene (**XXXI**), a pigment of the brown-coloured photosynthetic green sulphur bacteria (Liaaen-Jensen, 1965), accompanied by a 1,2-shift of a geminal methyl group would lead to isorenieratane (**III**), which is not present. Aromatisation of the 1,1,5-trimethylcyclohex-5-enyl moiety of β-isorenieratene with a rearrangement of methyl groups involving elimination of a methyl group would ultimately result in a compound with a molecular mass of 532. However, this compound would be identical to that formed from β-carotene (Fig. 9.7**b**), and thus cannot explain the occurrence of more than one compound with a molecular mass of 532 (Fig. 9.2).

In summary, the two major peaks in the 546 cluster are most likely renieratane (**XXVI**) and octadecahydrorenierapurpurin (**XXVII**), originating from reduction of renieratene (**XXIX**) and renierapurpurin (**XXX**). One of the compounds in the 532 cluster may originate from β-carotene (**II**) or β-isorenieratene (**XXXI**). The structure and origin of the other compounds in the 532 cluster is not known.

Fig. 9.5. Mass spectra (subtracted for background) of (**a**) **XX**, (**b**) **XXI**, (**c**) **XXII**, and (**d**) **XXIII**, and (**e-h**) their isorenieratene counterparts. The structural difference between **XX-XXIII** and their isorenieratene counterparts is the 1,2,5-trimethyl substitution pattern of the terminal aromatic rings of the latter.

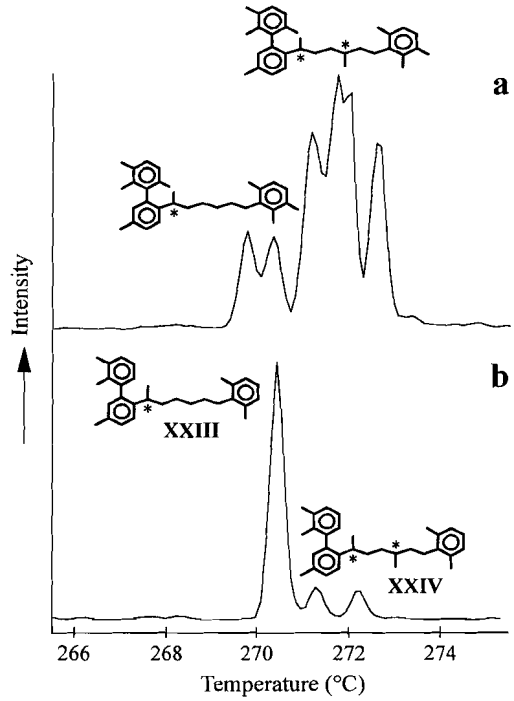

Fig. 9.6. (**a**) Partial m/z 237 mass chromatogram of the aromatic hydrocarbon fraction of a sample from the Allgäu Formation, showing the gas chromatographic separation of the atropisomers of the isorenieratene counterparts of **XXIII** and **XXIV** (after Koopmans *et al.*, 1996a). (**b**) Partial m/z 223 mass chromatogram of the aromatic hydrocarbon fraction of the sample from the Green River Shale, showing the gas chromatographic separation of the isomers of **XXIII** and **XXIV**. The absence of an axially chiral center in **XXIII** and **XXIV** causes the number of diastereomers, and thus the number of peaks that can be separated, to be twice as low as for the isorenieratene counterparts. Asymmetric carbon atoms are indicated by an asterisk.

Diagenetic pathways of β-carotene

The diagenetic products of β-carotene discussed so far can be divided into three groups according to their degree of aromaticity. The first group comprises β-carotane and lexane (**V**), which are fully saturated and represent 71% of the quantitated diagenetic products of β-carotene (Table 9.1). The second group consists of compounds with two saturated 1,1,5-trimethylcyclohexyl moieties and an aromatic moiety in the isoprenoid chain (**VII-IX**; 13% of quantitated diagenetic products of β-carotene). The third group consists of compounds containing two terminal 1,2-dimethyl substituted benzene rings (**X-XVII**, **XX-XXV**). Although this group contains by far the most compounds, it repre-

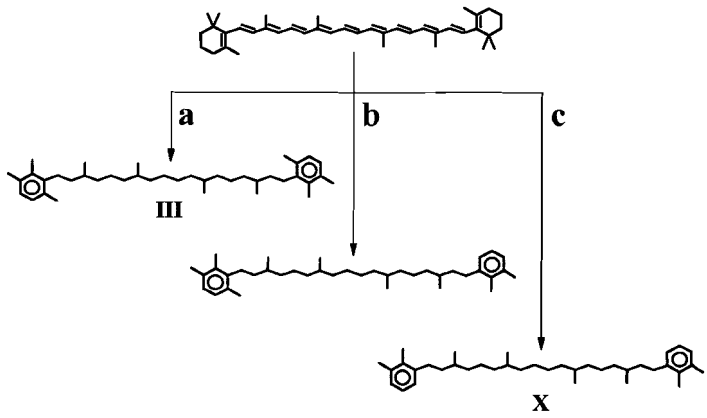

Fig. 9.7. Aromatisation of the 1,1,5-trimethylcyclohex-5-enyl moieties of β-carotene accompanied by (**a** and **b**) the 1,2-shift of a geminal methyl group and/or (**b** and **c**) a rearrangement involving elimination of a methyl group can theoretically result in three different compounds. Reduction of the double bonds in the isoprenoid chain is not indicated.

sents only 16% of the quantitated diagenetic products of β-carotene.

Aromatisation of a terminal 1,1,5-trimethylcyclohex-5-enyl moiety of β-carotene can proceed *via* (i) a 1,2-shift of a geminal methyl group or (ii) elimination of a methyl group. In a North Sea oil, aromatic diagenetic products of β-carotene were identified that had been formed predominantly by a 1,2-shift of a geminal methyl group (Koopmans *et al.*, 1996c). In the present study, however, the diagenetic products of β-carotene with aromatic end groups have been formed exclusively by a rearrangement of methyl groups involving elimination of a methyl group. This discrepancy may be explained by the different mechanisms inferred in the literature for laboratory aromatisation of compounds with rings containing quaternary carbon atoms (Fu and Harvey, 1978). A 1,2-shift of a geminal methyl group proceeds *via* an ionic mechanism, in which the first step is the transfer of a hydride ion to the aromatisating agent, *e.g.* a quinone (Braude *et al.*, 1954). Elimination of a geminal methyl group is associated with a radical mechanism, in which the abstraction of a H atom in an allylic or benzylic position is the first step. It should be stressed, however, that the diagenetic aromatisation reaction of β-carotene in the Green River Shale does not only involve elimination of a geminal methyl group, because formally there is also a shift of a methyl group. It is not clear if the elimination and the shift of the methyl groups are part of the same mechanism, nor is it clear if this mechanism is ionic or radical. Interestingly, no compounds were identified with one 1,1,5-trimethylcyclohexyl moiety and one aromatised end group, although these do occur in the North Sea oil studied earlier (Koopmans *et al.*, 1996c). This may suggest that aromatisation of one 1,1,5-trimethylcyclohex-5-enyl moiety of β-carotene during

diagenesis of the Green River Shale induced aromatisation of the other 1,1,5-trimethyl-cyclohex-5-enyl moiety.

An intriguing alternative possibility for the formation of compounds **X-XVII**, **XX-XXV** is an origin from a C_{38} diaromatic 'carotenoid' with a 1,2-dimethyl substitution pattern for both aromatic end groups (**XXXII**). This would explain the uniformity of the aromatic substitution patterns for the aromatic end groups, and the observation that in all identified compounds **X-XVII**, **XX-XXV** both end groups are aromatic. However, to the best of our knowledge **XXXII** has never been observed in organisms or sediments. Moreover, the high abundance of β-carotane, and the presence of compounds **V**, **VII-IX**, which are clearly diagenetic products of β-carotene, seem to suggest that the compounds **X-XVII**, **XX-XXV** originate from β-carotene. However, an origin from the C_{38} 'carotenoid' **XXXII** cannot be fully excluded.

β-Carotane makes up the bulk of the diagenetic products of β-carotene (Table 9.1). This suggests that reduction of the double bonds of β-carotene is an important diagenetic pathway for the formation of β-carotane. The reduction of β-carotene can be envisaged in two ways, *i.e.* direct and indirect (Fig. 9.8). Direct reduction implies the poorly understood (Brassell, 1992) reaction of β-carotene with hydrogen as inferred in the early literature (*e.g.* Murphy *et al.*, 1967; Schaeflé *et al.*, 1977). Repeta (1989) noted a correlation between carotenoid reduction and methanogenesis, although the exact relationship is not clear. Indirect reduction implies the reaction of β-carotene with reduced inorganic sulphur species during early diagenesis, and the subsequent thermally induced cleavage of C-S bonds to yield (partly) hydrogenated β-carotene (cf. Hartgers *et al.*, 1994c). This route is potentially important, because in some immature samples the β-carotane carbon skeleton is present almost exclusively in a sulphur-bound form (Kohnen *et al.*, 1991c; Adam *et al.*, 1993). Recently, Sinninghe Damsté *et al.* (1995c) proposed a similar sulphurisation/desulphurisation route for the reduction of tetrahymanol to gammacerane. Koopmans *et al.* (1996a) showed in an artificial maturation study of an immature marlstone from the Gessoso-solfifera Formation that the portion of the isorenieratane carbon skeleton sequestered by sulphur decreased progressively with increasing maturation temperature. It seems that the indirect route *via* the reaction with reduced inorganic sulphur was not very important during early diagenesis of the Green River Shale, since desulphurisation of the polar fraction yielded only 20 μg β-carotane/g TOC, representing *c.* 1% of the total amount of β-carotane carbon skeletons. However, the possibility that the Green River Shale, which has an estimated vitrinite reflectance value of 0.44%, has already passed through a 'sulphur stage' cannot be fully excluded (cf. Koopmans *et al.*, 1996b). For comparison, in a sample from the Gessoso-solfifera Formation that was artificially matured for 72 h at 300°C, corresponding to a vitrinite reflectance value of *c.* 0.4%, the relative amount of sulphur-bound isorenieratane (**III**) was only 14% whereas it was 100% in the unheated sample (Koopmans *et al.*, 1996a).

The timing of the reduction of β-carotene can be estimated by comparison with maturation studies of isorenieratene (**IV**), which showed that expulsion of toluene and

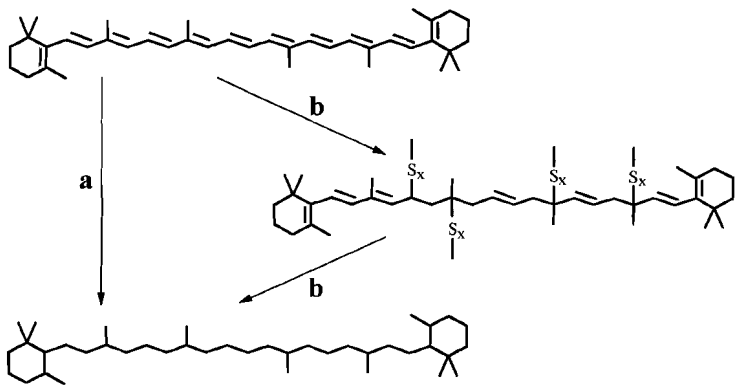

Fig. 9.8. Reduction of β-carotene can occur either (**a**) directly, or (**b**) indirectly *via* a sulphurisation/desulphurisation pathway.

m-xylene and cyclisation of the polyene isoprenoid chain both occur during early diagenesis (Koopmans *et al.*, 1996a). The early diagenetic expulsion of toluene and *m*-xylene from β-carotene is supported by kinetic calculations based on laboratory heating experiments (Byers and Erdman, 1983). The high abundance of β-carotane compared to the 'expulsion product' lexane (**V**) in the Green River Shale suggests that at least disturbance of the conjugated double bond system of β-carotene was a competing process during early diagenesis.

Geological preservation of carotenoids

The geological preservation potential of carotenoids is generally considered to be low (Mackenzie, 1984; Brassell, 1993). This is probably prompted by the inherent presence of multiple functional groups (mainly double bonds), which are potentially labile sites. Intact carotenoids have indeed not been found in sedimentary rocks older than *c.* 20 Ma (Cardoso *et al.*, 1978), although the carbon skeleton of carotenoids has been recognised in sedimentary rocks as old as *c.* 450 Ma (Koopmans *et al.*, 1996a).

Erdman (1961) was the first to recognise the potential importance of carotenoids as precursors of crude oils. He pointed out that the generation of toluene and *m*-xylene from the thermal degradation of carotenoids can contribute to crude oils, in which these aromatics are commonly the most abundant compounds (Martin *et al.*, 1963).

Recently, a whole range of dia- and catagenetic products of the diaromatic carotenoid isorenieratene was identified in a number of sedimentary rocks ranging from Ordovician to Miocene (Koopmans *et al.*, 1996a). It was hypothesised that similar products could be formed from other carotenoids, because the reactions responsible for the formation of these compounds were all related to the conjugated double system, a fea-

ture (by definition) of all carotenoids. The diagenetic derivatives of β-carotene identified in this study indicate that these reactions are indeed not restricted to isorenieratene. It remains to be discovered if similar products can be formed from oxygen-containing carotenoids.

9.5 Conclusions

A number of novel aromatic diagenetic products of β-carotene has been identified in a sample from the Mahogany Zone of the Green River Formation. These compounds have been formed by (i) cyclisation and aromatisation of the polyene isoprenoid chain, (ii) expulsion of toluene and *m*-xylene from the polyene isoprenoid chain, (iii) aromatisation of the terminal 1,1,5-trimethylcyclohex-5-enyl moieties resulting in 1,2-dimethylbenzene end groups, and (iv) reduction of double bonds. These compounds are similar to the diagenetic derivatives of the diaromatic carotenoid isorenieratene reported earlier (Koopmans *et al.*, 1996a). Despite the presence of these aromatic compounds, β-carotane is still the most abundant derivative of β-carotene, formed *via* reduction of β-carotene. These results suggest that the geological preservation potential of carotenoids is larger than previously thought.

9.6 Acknowledgements

Drs. M.D. Lewan and T.E. Ruble are gratefully acknowledged for providing the sample from the Green River Shale. Dr. P. Albrecht is thanked for providing the standards of renieratane and octadecahydrorenierapurpurin. We thank Shell International Exploration and Production for providing a research studentship to MPK. Mr. W.G. Pool, Mrs. M. Dekker and Mrs. M.M. Klapwijk are thanked for analytical assistance. Mr. T.A. Daws is thanked for Rock-Eval measurements. This work was partly supported by a PIONIER grant to JSSD from the Netherlands Organisation for Scientific Research (NWO).

Appendix I

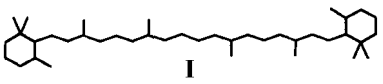

I

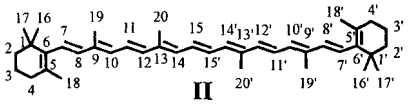

II

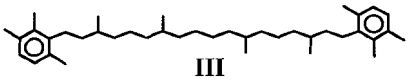

III

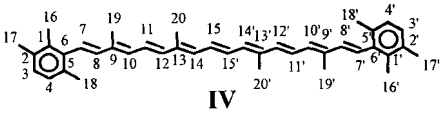

IV

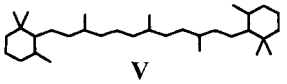

V

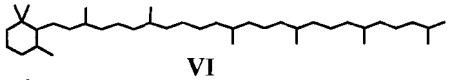

VI

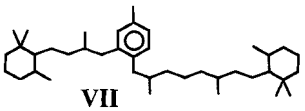

VII

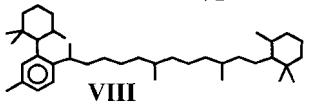

VIII

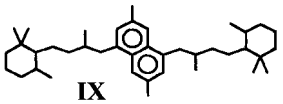

IX

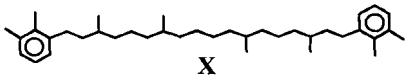

X

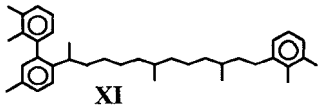

XI

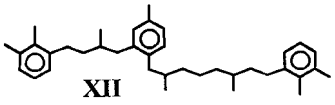

XII

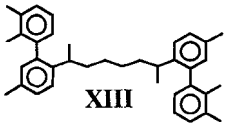

XIII

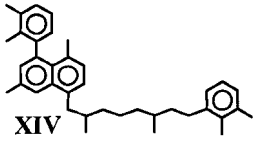

XIV

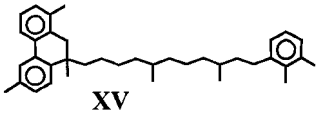

XV

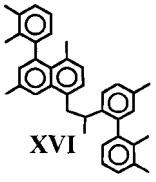

XVI

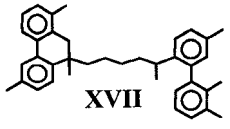

XVII

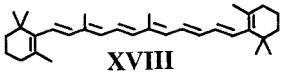

XVIII

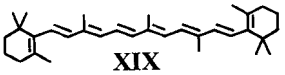

XIX

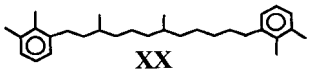

XX

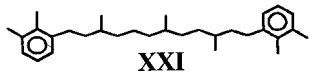

XXI

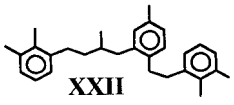

XXII

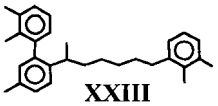

XXIII

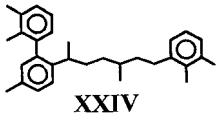

XXIV

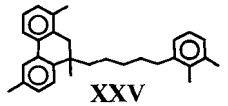

XXV

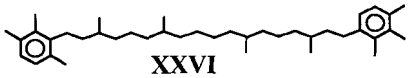

XXVI

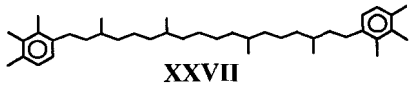

XXVII

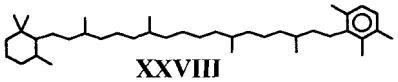

XXVIII

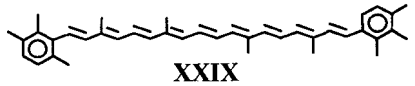

XXIX

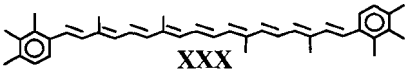

XXX

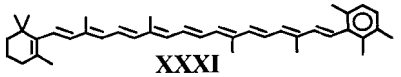

XXXI

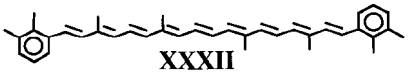

XXXII

Appendix II. Details of structural identifications of **VII-XVII**, **XX-XXV**.

Structure	*Formula*	$M^{+\cdot}$	*Diagnostic fragment ions (intensity)*	*Cyclisation* [a]	*Further details*
VII	$C_{40}H_{70}$	550(35)	69[b](72), 119[c](100), 300[d](6), 370[d](3)	11-15'	
VIII	$C_{40}H_{70}$	550	nd[e]	7-12	
IX	$C_{40}H_{64}$	544(100)	69[b](20), 183[f](40)	11-15', 15-11'	
X	$C_{38}H_{62}$	518(4)	119[g](38), 120[d](100)	No	Mass spectrum in Fig. 9.4**a**
XI	$C_{38}H_{54}$	510(12)	119[g](15), 193[h](12), 208[i](10), 223[j](100)	7-12	Mass spectrum in Fig. 9.4**b**
XII	$C_{38}H_{54}$	510(11)	119[g](100), 120[d](40), 159(11), 173(21)	11-15'	
XIII	$C_{38}H_{46}$	502(14)	193[h](18), 208[i](12), 223[j](100)	7-12, 12'-7'	Mass spectrum in Fig. 9.4**c**
XIV	$C_{38}H_{48}$	504(65)	119[g](41), 243[h](31), 258[i](13), 273[j](100)	7-12, 11-15'	
XV	$C_{38}H_{52}$	508(11)	119[g](17), 191[h](6), 206[i](8), 221[k](100)	7-12, 13-16	
XVI	$C_{38}H_{40}$	496(29)	193[h](10), 208[i](6), 223[j](38), 243[h](28), 258[i](9), 273[l](100)	7-12, 11-15', 12'-7'	Mass spectrum in Fig. 9.4**d**
XVII	$C_{38}H_{44}$	500(12)	191[h](7), 206[i](12), 221[k](100), 223[j](15)	7-12, 13-16, 12'-7'	
XX	$C_{30}H_{46}$	406(7)	119[g](58), 120[d](100)	No	Mass spectrum in Fig. 9.5**a**
XXI	$C_{31}H_{48}$	420(5)	119[g](47), 120[d](100)	No	Mass spectrum in Fig. 9.5**b**
XXII	$C_{30}H_{38}$	398(16)	119[g](100), 159(29), 173(53)	11-9'	Mass spectrum in Fig. 9.5**c**; see for NMR Sinninghe Damsté *et al.* (1996).
XXIII	$C_{30}H_{38}$	398(17)	119[g](18), 193[h](18), 208[i](10), 223[j](100)	7-12	Mass spectrum in Fig. 9.5**d**
XXIV	$C_{31}H_{40}$	412(13)	119[g](25), 120[d](10), 193[h](20), 208[i](11), 223[j](100)	7-12	
XXV	$C_{30}H_{36}$	396(8)	191[h](3), 206[i](12), 221[k](100)	7-12, 13-16	

[a] Carbon atoms connected by a C-C bond formed by cyclisation are indicated by their carbon number (cf. **II** in Appendix I).

[b] Cleavage through the 1,1,5-trimethylcyclohexyl moiety.

[c] Cleavage β to both sides of the additional aromatic ring (cf. Sinninghe Damsté *et al.* , 1991).

[d] McLafferty rearrangement.

[e] Not determined due to coelution with **VII**.

[f] Cleavage β to both sides of naphthalene moiety.

[g] Cleavage β to benzene ring.

[h] Loss of two $\cdot CH_3$'s from the main fragment ion, indicating severely hindered rotation around a C-C single bond (cf. Wolf, 1993; Wolf *et al.* , 1995;

Koopmans et al., 1996a).

[i] Loss of $\bullet CH_3$ from the main fragment ion, indicating severely hindered rotation around a C-C single bond (cf. Wolf, 1993; Wolf *et al.* , 1995; Koopmans *et al.* , 1996a).

[j] Cleavage β to biphenyl moiety.

[k] Cleavage β to 9,10-dihydrophenanthrene moiety.

[l] Cleavage β to naphthalene moiety.

REFERENCES

Abbott G.D., Wang G.Y., Eglinton T.I., Home A.K. and Petch G.S. (1990) The kinetics of sterane biological marker release and degradation processes during the hydrous pyrolysis of vitrinite kerogen. *Geochim. Cosmochim. Acta* **54**, 2451-2461.

Adam P., Schmid J.C. and Albrecht P. (1991) 2α and 3β steroid thiols from reductive cleavage of macromolecular petroleum fraction. *Tetrahedron Lett.* **32**, 2955-2958.

Adam P., Schmid J.C., Mycke B., Strazielle C., Connan J., Huc A., Riva A. and Albrecht P. (1993) Structural investigation of nonpolar sulphur cross-linked macromolecules in petroleum. *Geochim. Cosmochim. Acta* **57**, 3395-3419.

Aizenshtat Z., Krein E.B., Vairavamurthy M.A. and Goldstein T.P. (1995) Role of sulfur in the transformations of sedimentary organic matter: A mechanistic overview. In *Geochemical Transformations of Sedimentary Sulfur* (Edited by M.A. Vairavamurthy and M.A.A. Schoonen), *ACS Symposium Series 612*, pp. 16-37. Amer. Chem. Soc., Washington.

Alexander R., Kagi R.I. and Woodhouse G.W. (1981) Geochemical correlation of Windalia oil and extracts of Winning Group (Cretaceous) potential source rocks, Barrow Subbasin, Western Australia. *A.A.P.G. Bull.* **65**, 235-250.

Allen J. and Creaney S. (1991) Oil families of the Western Canada Basin. *Bull. Can. Petr. Geol.* **39**, 107-122.

Anders D.E. and Robinson W.E. (1971) Cycloalkane constituents of the bitumen from Green River Shale. *Geochim. Cosmochim. Acta* **35**, 661-678.

Anders D.E., Doolittle F.G. and Robinson W.E. (1973) Analysis of some aromatic hydrocarbons in a benzene-soluble bitumen from Green River shale. *Geochim. Cosmochim. Acta* **37**, 1213-1228.

Aquino Neto F.R., Trendel J.M., Restle A., Connan J. and Albrecht P.A. (1983) Occurrence and formation of tricyclic and tetracyclic terpanes in sediments and petroleums. In *Advances in Organic Geochemistry 1981* (Edited by M. Bjorøy *et al.*), pp. 659-667. Wiley, London.

Arthur M.A. and Sageman B.B. (1994) Marine black shales: Depositional mechanisms and environments of ancient deposits. *Annu. Rev. Earth Planet. Sci.* **22**, 499-551.

Barakat A.O. and Rullkötter J. (1994) Occurrence and identification of C_{33}, C_{37}, and C_{38} organic sulphur compounds in sediment extracts. *Energy Fuels* **8**, 1168-1174.

Barth T., Borgund A.E. and Hopland A.L. (1989) Generation of organic compounds by hydrous pyrolysis of Kimmeridge oil shale - Bulk results and activation energy calculations. *Org. Geochem.* **14**, 69-76.

Baskin D.K. and Peters K.E. (1992) Early generation characteristics of a sulfur-rich Monterey kerogen. *A.A.P.G. Bull.* **76**, 1-13.

Behar F., Derenne S. and Largeau C. (1995) Closed pyrolyses of the isoprenoid algaenan of *Botryococcus braunii, L* race: Geochemical implications for derived kerogens. *Geochim. Cosmochim. Acta* **59**, 2983-2997.

Benalioulhaj S., Sterner B.C., Philp R.P. and Landais P. (1993) Assessment of biomarkers characteristic of hypersalinity using artificial maturation on sediments from diverse evaporitic environments. In *Organic Geochemistry* (Edited by K. Øygard), pp. 532-535. Falch Hurtigtrykk, Oslo.

Ben-Amotz A., Shaish A. and Avron M. (1989) Mode of action of the massively accumulated β-carotene of *Dunaliella bardawil* in protecting the alga against damage by excess irradiation. *Plant Physiol.* **91**, 1040-1043.

Bishop A.N. and Abbott G.D. (1993) The interrelationship of biological marker maturity parameters and molecular yields during contact metamorphism. *Geochim. Cosmochim. Acta* **57**, 3661-3668.

Bjorøy M., Hall P.B., Hustad E. and Williams J.A. (1992) Variation in stable carbon isotope ratios of individual hydrocarbons as a function of artificial maturity. In *Advances in Organic Geochemistry 1991* (Edited by C.B. Eckardt, J.R. Maxwell, S.R. Larter and D.A.C. Manning), *Org. Geochem.* **19**, 89-105.

Blumer M. and Thomas D.W. (1965) "Zamene," isomeric C_{19} monoolefins from marine zooplankton, fishes, and mammals. *Science* **148**, 370-371.

Blumer M., Mullin M.M. and Thomas D.W. (1963) Pristane in zooplankton. *Science* **140**, 974.

Blumer M., Robertson J.C., Gordon J.E. and Sass J. (1969) Phytol-derived C_{19} di- and triolefinic hydrocarbons in marine zooplankton and fishes. *Biochemistry* **8**, 4067-4074.

Boon J.J., van der Meer F.W., Schuyl P.J.W., de Leeuw J.W. and Schenck P.A. (1978) 1. Organic geochemical analyses of core samples from Site 362, Walvis Ridge, DSDP Leg 40. In *Initial Reports of the Deep-Sea Drilling Project* (Edited by H.F. Bolli, W.B.F. Ryan *et al.*), Vol. 40, Supplement, pp. 627-637. U.S. Government Printing Office, Washington.

Brassell S.C. (1992) Biomarkers in recent and ancient sediments: The importance of the diagenetic continuum. In *Organic Matter: Productivity, Accumulation, and Preservation in Recent and Ancient Sediments* (Edited by J.K. Whelan and J.W. Farrington), pp. 339-367. Columbia University Press, New York.

Brassell S.C. (1993) Applications of biomarkers for delineating marine palaeoclimatic fluctuations during the Pleistocene. In *Organic Geochemistry: Principles and Applications* (Edited by M.H. Engel and S.A. Macko), pp. 699-738. Plenum Press, New York.

Brassell S.C., Eglinton G. and Maxwell J.R. (1983) The geochemistry of terpenoids and steroids. *Biochem. Soc. Trans.* **11**, 575-586.

Brassell S.C., Brereton R.G., Eglinton G., Grimalt J., Liebezeit G., Marlowe I.T., Pflaumann U. and Sarnthein M. (1986a) Palaeoclimatic signals recognized by chemometric treatment of molecular stratigraphic data. In *Advances in Organic Geochemistry 1985* (Edited by D. Leythaeuser and J. Rullkötter), *Org. Geochem.* **10**, 649-660.

Brassell S.C., Lewis C.A., de Leeuw J.W., de Lange F. and Sinninghe Damsté J.S. (1986b) Isoprenoid thiophenes: Novel products of sediment diagenesis? *Nature* **320**, 160-162.

Brassell S.C., Marlowe I.T., Pflaumann U. and Sarnthein M. (1986c) Molecular stratigraphy: A new tool for climatic assessment. *Nature* **320**, 129-133.

Brassell S.C., Sheng Guoying, Fu Jiamo and Eglinton G. (1988) Biological markers in lacustrine Chinese oil shales. In *Lacustrine Petroleum Source Rocks* (Edited by A.J. Fleet, K. Kelts and M.R. Talbot), pp. 299-308. Geological Society Special Publication No. 40. Blackwell Scientific Publications, Oxford.

Braude E.A., Jackman L.M. and Linstead R.P. (1954) Hydrogen transfer. Part II. The dehydrogenation of 1:4-dihydronaphthalene by quinones. Kinetics and mechanism. *J. Chem. Soc.*, 3548-3563.

Braude E.A., Jackman L.M., Linstead R.P. and Lowe G. (1960) Hydrogen transfer. Part XII. Dehydrogenation of "blocked" hydroaromatic compounds by quinones. *J. Chem. Soc.*, 3123-3132.

Bray E.E. and Evans E.D. (1961) Distribution of *n*-paraffins as a clue to recognition of source beds. *Geochim. Cosmochim. Acta* **22**, 2-15.

Britton G., Liaaen-Jensen S. and Pfander H. (1995) Carotenoids today and challenges for the future. In *Carotenoids Volume 1A: Isolation and Analysis* (Edited by G. Britton, S. Liaaen-Jensen and H. Pfander), pp. 13-26. Birkhäuser Verlag, Basel.

Brooks J.D., Gould K. and Smith J. (1969) Isoprenoid hydrocarbons in coal and petroleum. *Nature* **222**, 257-259.

Buchardt B. and Lewan M.D. (1990) Reflectance of vitrinite-like macerals as a thermal maturity index for Cambrian-Ordovician Alum Shale, southern Scandinavia. *A.A.P.G. Bull.* **74**, 394-406.

Burnham A.K. (1989) On the validity of the Pristane Formation Index. *Geochim. Cosmochim. Acta* **53**, 1693-1697.

Burnham A.K. and Sweeney J.J. (1989) A chemical kinetic model of vitrinite maturation and reflectance. *Geochim. Cosmochim. Acta* **53**, 2649-2657.

Byers J.D. and Erdman J.G. (1983) Low temperature degradation of carotenoids as a model for early diagenesis in Recent sediments. In *Advances in Organic Geochemistry 1981* (Edited by M. Bjorøy *et al.*), pp. 725-732. Wiley, London.

Cardoso J.N., Wardroper A.M.K., Watts C.D., Barnes P.J., Maxwell J.R., Eglinton G., Mound D.G. and Speers G.C. (1978) Preliminary organic geochemical analyses; Site 391, leg 44 of the Deep Sea Drilling Project. In *Init. Rpt. Deep Sea Drilling Proj. Leg 44* (Edited by W.E. Benson *et al.*), pp. 617-624. US Govt. Printing Office.

Chappe B., Michaelis W., Albrecht P. and Ourisson G. (1979) Fossil evidence for a novel series of archaebacterial lipids. *Naturwissenschaften* **66**, 522-523.

Chicarelli M.I., Aquino Neto F.R. and Albrecht P. (1988) Occurrence of four stereoisomeric tricyclic terpane series in immature Brazilian shales. *Geochim. Cosmochim. Acta* **52**, 1955-1959.

Chou M.-I.M. and Wood K.V. (1986) New aromatic biomarkers and possible maturity indicators found in New Albany Shale extracts. *Org. Geochem.* **9**, 351-356.

Clark J.P. and Philp R.P. (1989) Geochemical characterization of evaporite and carbonate depositional environments and correlation of associated crude oils in the Black Creek Basin, Alberta. *Bull. Can. Petr. Geol.* **37**, 401-416.

Claxton M.J., Patience R.L. and Park P.J.D. (1993) Molecular modelling of bond energies in potential kerogen sub-units. In *Organic Geochemistry* (Edited by K. Øygard), pp. 198-201. Falch Hurtigtrykk, Oslo.

Clayton J.L. and Koncz I. (1994) Petroleum geochemistry of the Zala Basin, Hungary. *A.A.P.G. Bull.* **78**, 1-22.

Clayton J.L., Warden A., Daws T.A., Lillis P.G., Michael G.E. and Dawson M. (1992) Organic geochemistry of black shales, marlstones, and oils of Middle Pennsylvanian rocks from the northern Denver and southeastern Powder River Basins, Wyoming, Nebraska, and Colorado. *U.S. Geol. Sur. Bull.* 1917-K, pp. 1-44.

Collister J.W., Summons R.E., Lichtfouse E. and Hayes J.M. (1992) An isotopic biogeochemical study of the Green River oil shale. In *Advances in Organic Geochemistry 1991* (Edited by C.B. Eckardt, J.R. Maxwell, S.R. Larter and D.A.C. Manning), *Org. Geochem.* **19**, 265-276.

Comet P.A., McEvoy J., Giger W. and Douglas A.G. (1986) Hydrous and anhydrous pyrolysis of DSDP Leg 75 kerogens - A comparative study using a biological marker approach. *Org. Geochem.* **9**, 171-182.

Connan J. (1974) Diagenèse naturelle et diagenèse artificielle de la matière organique a éléments végétaux prédominants. In *Advances in Organic Geochemistry 1973* (Edited by B.P. Tissot and F. Bienner), pp. 73-95. Éditions Technip, Paris.

Conte M.H., Volkman J.K. and Eglinton G. (1994) Lipid biomarkers of the Haptophyta. In *The Haptophyte Algae* (Edited by J.C. Green and B.S.C. Leadbeater), Systematics Association Special Volume No. 51, pp. 351-377. Clarendon Press, Oxford.

Day W.C. and Erdman J.G. (1963) Ionene: A thermal degradation product of β-carotene. *Science* **141**, 808.

Demaison G.J. and Moore G.T. (1980) Anoxic environments and oil source bed genesis. *A.A.P.G. Bull.* **64**, 1179-1209.

Derenne S., Largeau C., Berkaloff C., Rousseau B., Wilhelm C. and Hatcher P.G. (1992) Non-hydrolysable macromolecular constituents from outer cell walls of *Chlorella fusca* and *Nanochlorum eucaryotum*. *Phytochemistry* **31**, 1923-1929.

Didyk B.M., Simoneit B.R.T., Brassell S.C. and Eglinton G. (1978) Organic geochemical indicators of palaeoenvironmental conditions of sedimentation. *Nature* **272**, 216-222.

Doering W.v.E., Sotiriou-Leventis C. and Roth W.R. (1995) Thermal interconversions among 15-*cis*-, 13-*cis*-, and *all-trans*-β-carotene: Kinetics, Arrhenius parameters, thermochemistry, and potential relevance to anticarcinogenicity of *all-trans*-β-carotene. *J. Am. Chem. Soc.* **117**, 2747-2757.

Douglas A.G., Sinninghe Damsté J.S., Fowler M.G., Eglinton T.I. and de Leeuw J.W. (1991) Unique distributions of hydrocarbons and sulphur compounds released by flash pyrolysis from the fossilised alga *Gloeocapsomorpha prisca*, a major constituent in one of four Ordovician kerogens. *Geochim. Cosmochim. Acta* **55**, 275-291.

van Duin A.C.T., Hollanders B., Smits R.J.A., Baas J.M.A., van de Graaf B., Koopmans M.P. and de Leeuw J.W. (1996) Molecular mechanics calculation of the rotational barriers of 2,2',6-trialkylbiphenyls to explain their GC-elution behaviour. *Org. Geochem.* **24**, 587-591.

Durand B. (1980) Sedimentary organic matter and kerogen. Definition and quantitative importance of kerogen. In *Kerogen. Insoluble Organic Matter from Sedimentary Rocks* (Edited by B. Durand), pp. 13-34. Éditions Technip, Paris.

Dzou L.I.P., Noble R.A. and Senftle J.T. (1995) Maturation effects on absolute biomarker concentration in a suite of coals and associated vitrinite concentrates. *Org. Geochem.* **23**, 681-697.

Edmunds F.S. and Johnstone R.A.W. (1965) Constituents of cigarette smoke. Part IX. The pyrolysis of polyenes and the formation of aromatic hydrocarbons. *J. Chem. Soc.*, 2892-2897.

Eglinton G. and Hamilton R.J. (1967) Leaf epicuticular waxes. *Science* **156**, 1322-1335.

Eglinton T.I. and Douglas A.G. (1988) Quantitative study of biomarker hydrocarbon releases from kerogen during hydrous pyrolysis. *Energy Fuels* **2**, 81-88.

Eglinton T.I., Rowland S.J., Curtis C.D. and Douglas A.G. (1986) Kerogen-mineral reactions at raised temperatures in the presence of water. In *Advances in Organic Geochemistry 1985* (Edited by D. Leythaeuser and J. Rullkötter), *Org. Geochem.* **10**, 1041-1052.

Eglinton T.I., Douglas A.G. and Rowland S.J. (1988a) Release of aliphatic, aromatic and sulphur compounds from Kimmeridge kerogen by hydrous pyrolysis: A quantitative study. In *Advances in Organic Geochemistry 1987* (Edited by L. Mattavelli and L. Novelli), *Org. Geochem.* **13**, 655-663.

Eglinton T.I., Philp R.P. and Rowland S.J. (1988b) Flash pyrolysis of artificially matured kerogens from the Kimmeridge Clay, U.K. *Org. Geochem.* **12**, 33-41.

Eglinton T.I., Sinninghe Damsté J.S., Kohnen M.E.L. and de Leeuw J.W. (1990a) Rapid estimation of the organic sulphur content of kerogens, coals and asphaltenes by pyrolysis-gas chromatography. *Fuel* **69**, 1394-1404.

Eglinton T.I., Sinninghe Damsté J.S., Kohnen M.E.L., de Leeuw J.W., Larter S.R. and Patience R.L. (1990b) Analysis of maturity-related changes in the organic sulfur composition of kerogens by flash pyrolysis-gas chromatography. In *Geochemistry of Sulfur in Fossil Fuels* (Edited by W.L. Orr and C.M. White), *ACS Symposium Series 249*, pp. 529-565. Amer. Chem. Soc., Washington.

Ensminger A., van Dorsselaer A., Spyckerelle C., Albrecht P. and Ourisson G. (1974) Pentacyclic triterpenes of the hopane type as ubiquitous geochemical markers: Origin and significance. In *Advances in Organic Geochemistry 1973* (Edited by B. Tissot and F. Bienner), pp. 245-260. Éditions Technip, Paris.

Enzell C.R. and Wahlberg I. (1980) Carotenoids. In *Biochemical Applications of Mass Spectrometry* (Edited by G.R. Waller and O.C. Dermer), pp. 407-438. Wiley, New York.

Erdman J.G. (1961) Some chemical aspects of petroleum genesis as related to the problem of source bed recognition. *Geochim. Cosmochim. Acta* **22**, 16-36.

Evans R.J. and Felbeck Jr. G.T. (1983) High temperature simulation of petroleum formation - I. The pyrolysis of Green River Shale. *Org. Geochem.* **4**, 135-144.

Farrimond P., Eglinton G. and Brassell S.C. (1986) Alkenones in Cretaceous black shales, Blake-Bahama Basin, western North Atlantic. In *Advances in Organic Geochemistry 1985* (Edited by D. Leythaeuser and J. Rullkötter), *Org. Geochem.* **10**, 897-903.

Fowler M.G. (1992) The influence of *Gloeocapsomorpha prisca* on the organic geochemistry of oils and organic-rich rocks of late Ordovician age from Canada. In *Early Organic Evolution: Implications for Mineral and Energy Resources* (Edited by M. Schidlowski *et al.*), pp. 336-356. Springer-Verlag, Berlin.

Fowler M.G., Snowdon L.R., Brooks P.W. and Hamilton T.S. (1988) Biomarker characterisation and hydrous pyrolysis of bitumens from Tertiary volcanics, Queen Charlotte Islands, British Columbia, Canada. In *Advances in Organic Geochemistry 1987* (Edited by L. Mattavelli and L. Novelli), *Org. Geochem.* **13**, 715-725.

Fowler M.G., Hamblin A.P., MacDonald D.J. and McMahon P.G. (1993) Geological occurrence and geochemistry of some oil shows in Nova Scotia. *Bull. Can. Petr. Geol.* **41**, 422-436.

Freeman K.H., Hayes J.M., Trendel J.-M. and Albrecht P. (1990) Evidence from carbon isotope measurements for diverse origins of sedimentary hydrocarbons. *Nature* **343**, 254-256.

Freeman K.H., Boreham C.J., Summons R.E. and Hayes J.M. (1994) The effect of aromatization on the isotopic compositions of hydrocarbons during early diagenesis. *Org. Geochem.* **21**, 1037-1049.

Fresenius P. (1989) *Organic Chemical Nomenclature: Introduction to the Basic Principles*. Ellis Horwood Ltd., Chichester.

Fu Jiamo, Sheng Guoying and Liu Dehan (1988) Organic geochemical characteristics of major types of terrestrial petroleum source rocks in China. In *Lacustrine Petroleum Source Rocks* (Edited by A.J. Fleet, K. Kelts and M.R. Talbot), pp. 279-289. Geological Society Special Publication No. 40. Blackwell Scientific Publications, Oxford.

Fu P.P. and Harvey R.G. (1978) Dehydrogenation of polycyclic hydroaromatic compounds. *Chem. Rev.* **78**, 317-361.

Fukushima K., Yasukawa M., Muto N., Uemura H. and Ishiwatari R. (1992) Formation of C_{20} isoprenoid thiophenes in modern sediments. *Org. Geochem.* **18**, 83-91.

Gallegos E.J. (1975) Terpane-sterane release from kerogen by pyrolysis gas chromatography-mass spectrometry. *Anal. Chem.* **47**, 1524-1528.

Gelin F., Gatellier J.-P.L.A., Sinninghe Damsté J.S., Metzger P., Derenne S., Largeau C. and de Leeuw J.W. (1993) Mechanisms of flash pyrolysis of ether lipids isolated from the green microalga *Botryococcus braunii* race *A. J. Anal. Appl. Pyrol.* **27**, 155-168.

Gelin F., de Leeuw J.W., Sinninghe Damsté J.S., Derenne S., Largeau C. and Metzger P. (1994) Scope and limitations of flash pyrolysis-gas chromatography/mass spectrometry as revealed by the thermal behaviour of high-molecular-weight lipids derived from the green microalga *Botryococcus braunii. J. Anal. Appl. Pyrol.* **28**, 183-204.

Gelin F., Sinninghe Damsté J.S., Harrison W.N., Maxwell J.R. and de Leeuw J.W. (1995) Molecular indicators for palaeoenvironmental change in a Messinian evaporitic sequence (Vena del Gesso, Italy): III. Stratigraphic changes in the molecular structure of kerogen in a single marl bed as revealed by flash pyrolysis. *Org. Geochem.* **23**, 555-566.

Gelin F., Boogers I., Noordeloos A.A.M., Sinninghe Damsté J.S., Hatcher P.G. and de Leeuw J.W. (1996a) Novel resistant microalgal polyethers: The major sink of organic carbon in the marine environment? *Geochim. Cosmochim. Acta.* **60**, 1275-1280.

Gelin F., Sinninghe Damsté J.S., Harrison W.N., Reiss C., Maxwell J.R. and de Leeuw J.W. (1996b) Variations in origin and composition of kerogen constituents as revealed by analytical pyrolysis of immature kerogens before and after desulphurization. *Org. Geochem.* **24**, 705-714.

Goodwin T.W. (1980) *The Biochemistry of the Carotenoids. Volume I. Plants.* Chapman and Hall, London.

Goossens H., de Leeuw J.W., Schenck P.A. and Brassell S.C. (1984) Tocopherols as likely precursors of pristane in ancient sediments and crude oils. *Nature* **312**, 440-442.

Goossens H., Due A., de Leeuw J.W., van de Graaf B. and Schenck P.A. (1988a) The Pristane Formation Index, a new molecular maturity parameter. A simple method

to assess maturity by pyrolysis/evaporation-gas chromatography of unextracted samples. *Geochim. Cosmochim. Acta* **52**, 1189-1193.

Goossens H., de Lange F., de Leeuw J.W. and Schenck P.A. (1988b) The Pristane Formation Index, a molecular maturity parameter. Confirmation in samples from the Paris Basin. *Geochim. Cosmochim. Acta* **52**, 2439-2444.

Goossens H., de Leeuw J.W., Rijpstra W.I.C., Meyburg G.J. and Schenck P.A. (1989) Lipids and their mode of occurrence in bacteria and sediments - I. A methodological study of the lipid composition of *Acinetobacter calcoaceticus* LMD 79-41. *Org. Geochem.* **14**, 15-25.

de Graaf W., Sinninghe Damsté J.S. and de Leeuw J.W. (1992) Laboratory simulation of natural sulphurisation: I. Formation of monomeric and oligomeric isoprenoid polysulphides by low-temperature reactions of inorganic polysulphides with phytol and phytadienes. *Geochim. Cosmochim. Acta* **56**, 4321-4328.

de Graaf W., Sinninghe Damsté J.S. and de Leeuw J.W. (1995) Low-temperature addition of hydrogen polysulfides to olefins: Formation of 2,2'-dialkyl polysulfides from alk-1-enes and cyclic (poly)sulfides and polymeric organic sulfur compounds from α,ω-dienes. *J. Chem. Soc. Perkin Trans. I*, 635-640.

van Graas G., de Leeuw J.W. and Schenck P.A. (1981) Kerogen of Toarcian shales of the Paris Basin. A study of its maturation by flash pyrolysis techniques. *Geochim. Cosmochim. Acta* **45**, 2465-2474.

van Graas G., Baas J.M.A., van de Graaf B. and de Leeuw J.W. (1982) Theoretical organic geochemistry. I. The thermodynamic stability of several cholestane isomers calculated by molecular mechanics. *Geochim. Cosmochim. Acta* **46**, 2399-2402.

Gransch J.A. and Posthuma J. (1974) On the origin of sulphur in crudes. In *Advances in Organic Geochemistry 1973* (Edited by B. Tissot and F. Bienner), pp. 727-739. Éditions Technip, Paris.

Greiner A.C., Spyckerelle C. and Albrecht P. (1976) Aromatic hydrocarbons from geological sources - I. New naturally occurring phenanthrene and chrysene derivatives. *Tetrahedron* **32**, 257-260.

Greiner A.C., Spyckerelle C., Albrecht P. and Ourisson G. (1977) Aromatic hydrocarbons from geological sources. Part V. Mono- and di-aromatic hopane derivatives. *J. Chem Research (M)*, 3829-3871.

Grice K., Schwark L., Schaeffer P., Eckardt C.B. and Maxwell J.R. (1995) Stable carbon isotopic compositions and distributions of biomarkers in the Permian Kupferschiefer. In *Organic Geochemistry: Developments and Applications to Energy, Climate, Environment and Human History* (Edited by J.O. Grimalt *et al.*), pp. 61-64. A.I.G.O.A., San Sebastian.

Guthrie J.M. and Pratt L.M. (1995) Geochemical character and origin of oils in Ordovician reservoir rock, Illinois and Indiana, USA. *A.A.P.G. Bull.* **79**, 1631-1649.

Hall P.B. and Douglas A.G. (1983) The distribution of cyclic alkanes in two lacustrine deposits. In *Advances in Organic Geochemistry 1981* (Edited by M. Bjorøy *et al.*), pp. 576-587. Wiley, London.

Hartgers W.A., Sinninghe Damsté J.S. and de Leeuw J.W. (1991) Mechanisms of hydrocarbon formation during flash pyrolysis of kerogen. *Prepr. Am. Chem. Soc., Div. Fuel Chem.* **36**, 790-795.

Hartgers W.A., Sinninghe Damsté J.S., Koopmans M.P. and de Leeuw J.W. (1993) Sedimentary evidence for a diaromatic carotenoid with an unprecedented aromatic substitution pattern. *J. Chem. Soc., Chem. Commun.*, 1715-1716.

Hartgers W.A., Sinninghe Damsté J.S. and de Leeuw J.W. (1994a) Geochemical significance of alkylbenzene distributions in flash pyrolysates of kerogens, coals and asphaltenes. *Geochim. Cosmochim. Acta* **58**, 1759-1775.

Hartgers W.A., Sinninghe Damsté J.S., Requejo A.G., Allan J., Hayes J.M. and de Leeuw J.W. (1994b) Evidence for only minor contributions from bacteria to sedimentary organic carbon. *Nature* **369**, 224-227.

Hartgers W.A., Sinninghe Damsté J.S., Requejo A.G., Allan J., Hayes J.M., Ling Y., Xie T.-M., Primack J. and de Leeuw J.W. (1994c) A molecular and carbon isotopic study towards the origin and diagenetic fate of diaromatic carotenoids. In *Advances in Organic Geochemistry 1993* (Edited by N. Telnæs, G. van Graas and K. Øygard), *Org. Geochem.* **22**, 703-725.

Harvey G.R., Boran D.A., Chesal L.A. and Tokar J.M. (1983) The structure of marine fulvic and humic acids. *Mar. Chem.* **12**, 119-132.

ten Haven H.L., de Leeuw J.W., Peakman T.M. and Maxwell J.R. (1986) Anomalies in steroid and hopanoid maturity indices. *Geochim. Cosmochim. Acta* **50**, 853-855.

ten Haven H.L., de Leeuw J.W., Rullkötter J. and Sinninghe Damsté J.S. (1987) Restricted utility of the pristane/phytane ratio as a palaeoenvironmental indicator. *Nature* **330**, 641-643.

ten Haven H.L., Rullkötter J., Sinninghe Damsté J.S. and de Leeuw J.W. (1990) Distribution of organic sulfur compounds in Mesozoic and Cenozoic sediments from the Atlantic and Pacific Oceans and the Gulf of California. In *Geochemistry of Sulfur in Fossil Fuels* (Edited by W.L. Orr and C.M. White), *ACS Symposium Series 249*, pp. 613-632. Amer. Chem. Soc., Washington.

ten Haven H.L., Eglinton G., Farrimond P., Kohnen M.E.L., Poynter J.G., Rullkötter J. and Welte D.H. (1992) Variations in the content and composition of organic matter in sediments underlying active upwelling regimes: A study from ODP Legs 108, 112 and 117. In *Upwelling Systems: Evolution Since the Early Miocene* (Edited by C.P. Summerhayes, W.L. Prell and K.C. Emeis), pp. 229-246. Geological Society Special Publication No. 64. The Geological Society, London.

Hayes J.M. (1993) Factors controlling ^{13}C contents of sedimentary organic compounds: Principles and evidence. *Mar. Geol.* **113**, 111-125.

Hayes J.M., Freeman K.H., Popp B.N. and Hoham C.H. (1990) Compound-specific isotope analysis: A novel tool for reconstruction of ancient biogeochemical processes. In *Advances in Organic Geochemistry 1989* (Edited by B. Durand and F. Behar), *Org. Geochem.* **16**, 1115-1128.

Hefter J., Hauke V., Richnow H.H. and Michaelis W. (1995) Alkanoic subunits in sulfur-rich geomacromolecules. Information from stepwise chemical degradation and compound-specific isotopic analysis. In *Geochemical Transformations of Sedimentary Sulfur* (Edited by M.A. Vairavamurthy and M.A.A. Schoonen), *ACS Symposium Series 612*, pp. 93-109. Amer. Chem. Soc., Washington.

Ho T.Y., Rogers M.A., Drushel H.V. and Koons C.B. (1974) Evolution of sulfur compounds in crude oils. *A.A.P.G. Bull.* **58**, 2338-2348.

Hoefs M.J.L., van Heemst J.D.H., Gelin F., Koopmans M.P., van Kaam-Peters H.M.E., Schouten S., de Leeuw J.W. and Sinninghe Damsté J.S. (1995) Alternative biological sources for 1,2,3,4-tetramethylbenzene in flash pyrolysates of kerogen. *Org. Geochem.* **23**, 975-979.

Hoering T.C. and Navale V. (1987) A search for molecular fossils in the kerogen of Precambrian sedimentary rocks. *Precambrian Res.* **34**, 247-267.

Hofmann I.C., Hutchison J., Robson J.N, Chicarelli M.I. and Maxwell J.R. (1992) Evidence for sulphide links in a crude oil asphaltene and kerogens from reductive cleavage by lithium in ethylamine. In *Advances in Organic Geochemistry 1991* (Edited by C.B. Eckardt, J.R. Maxwell, S.R. Larter and D.A.C. Manning), *Org. Geochem.* **19**, 371-387.

Hofmann P., Huc A.Y., Carpentier B., Schaeffer P., Albrecht P., Keely B., Maxwell J.R., Sinninghe Damsté J.S., de Leeuw J.W. and Leythaeuser D. (1993) Organic matter of the Mulhouse Basin, France: A synthesis. *Org. Geochem.* **20**, 1105-1123.

Horsfield B. and Düppenbecker S.J. (1991) The decomposition of Posidonia Shale and Green River Shale kerogens using microscale sealed vessel (MSSV) pyrolysis. *J. Anal. Appl. Pyrol.* **20**, 107-123.

Horsfield B., Disko U. and Leistner F. (1989) The micro-scale simulation of maturation: Outline of a new technique and its potential applications. *Geol. Rundsch.* **78**, 361-374.

Hufnagel H. (1984) Oil shale in Jordan. *Geol. Jb., Rh. A* **75**, 295-311.

Hughes W.B., Holba A.G. and Dzou L.I.P. (1995) The ratios of dibenzothiophene to phenanthrene and pristane to phytane as indicators of depositional environment and lithology of petroleum source rocks. *Geochim. Cosmochim. Acta* **59**, 3581-3598.

Hunt J.M., Lewan M.D. and Hennet R.J.-C. (1991) Modeling oil generation with time-temperature index graphs based on the Arrhenius equation. *A.A.P.G. Bull.* **75**, 795-807.

Huseby B., Ocampo R., Bauder C., Callot H.J., Rist K. and Barth T. (1996) Study of the porphyrins released from the Messel oil shale kerogen by hydrous pyrolysis experiments. *Org. Geochem.* **24**, 691-703.

Hussler G., Connan J. and Albrecht P. (1984) Novel families of tetra- and hexacyclic aromatic hopanoids predominant in carbonate rocks and crude oils. *Org. Geochem.* **6**, 39-49.

Ishiwatari M. (1980) Thermal reaction of β-carotene. Part 1. *J. Anal. Appl. Pyrol.* **2**, 153-167.

Jiang Z.S. and Fowler M.G. (1986) Carotenoid-derived alkanes in oils from northwestern China. In *Advances in Organic Geochemistry 1985* (Edited by D. Leythaeuser and J. Rullkötter), *Org. Geochem.* **10**, 831-839.

Johnson J.E., Blizzard R.H. and Carhart H.W. (1948) Hydrogenolysis of alkyl halides by lithium aluminium hydride. *J. Am. Chem. Soc.* **70**, 3664-3665.

Johnson R. (1981) Stratigraphic evidence for a deep Eocene Lake Uinta, Piceance Creek Basin, Colorado. *Geology* **9**, 55-62.

Jones D.M., Douglas A.G. and Connan J. (1988) Hydrous pyrolysis of asphaltenes and polar fractions of biodegraded oils. In *Advances in Organic Geochemistry 1987* (Edited by L. Mattavelli and L. Novelli), *Org. Geochem.* **13**, 981-993.

van Kaam-Peters H.M.E., de Leeuw J.W. and Sinninghe Damsté J.S. (1997a) Palaeoenvironmental controls on the preservation of organic matter in the Kimmeridge Clay Formation as revealed by biomarkers, molecular stable carbon isotope analysis, and pyrolysis. *Geochim. Cosmochim. Acta*. Submitted.

van Kaam-Peters H.M.E., de Leeuw J.W. and Sinninghe Damsté J.S. (1997b) Palaeoenvironmental reconstruction of a Kimmeridgian lagoonal system in the French southern Jura. In preparation.

Katz B.J. (1995) The Green River Shale: An Eocene carbonate lacustrine source rock. In *Petroleum Source Rocks* (Edited by B.J. Katz), pp. 309-324. Springer Verlag, Berlin.

Keely B.J., Sinninghe Damsté J.S., Betts S.E., Ling Y., de Leeuw J.W. and Maxwell J.R. (1993) A molecular stratigraphic approach to palaeoenvironmental assessment and the recognition of changes in source inputs in marls of the Mulhouse Basin (Alsace, France). *Org. Geochem.* **20**, 1165-1186.

Keely B.J., Blake S.R., Schaeffer P. and Maxwell J.R. (1995) Distributions of pigments in the organic matter of marls from the Vena del Gesso evaporitic sequence. *Org. Geochem.* **23**, 527-539.

Kenig F., Hayes J.M., Popp B.N. and Summons R.E. (1994) Isotopic biogeochemistry of the Oxford Clay Formation (Jurassic), UK. *J. Geol. Soc., Lond.* **151**, 139-152.

Kenig F., Sinninghe Damsté J.S., Frewin N.L. and de Leeuw J.W. (1995) Molecular indicators for palaeoenvironmental change in a Messinian evaporitic sequence (Vena del Gesso, Italy). II: High-resolution variations in abundances and ^{13}C contents of free and sulphur-bound carbon skeletons in a single marl bed. *Org. Geochem.* **23**, 485-526.

Kimble B.J., Maxwell J.R., Philp R.P., Eglinton G., Albrecht P., Ensminger A., Arpino P. and Ourisson G. (1974) Tri- and tetraterpenoid hydrocarbons in the Messel oil shale. *Geochim. Cosmochim. Acta* **38**, 1165-1181.

Kingston E.E., Eichholzer J.V., Lyndon P., MacLeod J.K. and Summons R.E. (1988) An unexpected γ-hydrogen rearrangement in the mass spectra of di-*ortho*-substituted alkylbenzenes. *Org. Mass Spectrom.* **23**, 42-47.

Klemme H.D. and Ulmishek G.F. (1991) Effective petroleum source rocks of the world: Stratigraphic distribution and controlling depositional factors. *A.A.P.G. Bull.* **75**, 1809-1851.

Kohnen M.E.L., Sinninghe Damsté J.S., ten Haven H.L. and de Leeuw J.W. (1989) Early incorporation of polysulphides in sedimentary organic matter. *Nature* **341**, 640-641.

Kohnen M.E.L., Peakman T.M., Sinninghe Damsté J.S. and de Leeuw J.W. (1990a) Identification and occurrence of novel C_{36}-C_{54} 3,4-dialkylthiophenes with an unusual carbon skeleton in immature sediments. In *Advances in Organic Geochemistry 1989* (Edited by B. Durand and F. Behar), *Org. Geochem.* **16**, 1103-1113.

Kohnen M.E.L., Sinninghe Damsté J.S., Kock-van Dalen A.C., ten Haven H.L., Rullkötter J. and de Leeuw J.W. (1990b) Origin and diagenetic transformations of C_{25} and C_{30} highly branched isoprenoid sulphur compounds: Further evidence for the formation of organically bound sulphur during early diagenesis. *Geochim. Cosmochim. Acta* **54**, 3053-3063.

Kohnen M.E.L., Sinninghe Damsté J.S., Rijpstra W.I.C. and de Leeuw J.W. (1990c) Alkylthiophenes as sensitive indicators of palaeoenvironmental changes: A study of a Cretaceous oil shale from Jordan. In *Geochemistry of Sulfur in Fossil Fuels* (Edited by W.L. Orr and C.M. White), *ACS Symposium Series 249*, pp. 444-485. Amer. Chem. Soc., Washington.

Kohnen M.E.L., Sinninghe Damsté J.S., ten Haven H.L., Kock-van Dalen A.C., Schouten S. and de Leeuw J.W. (1991a) Identification and geochemical significance of cyclic di- and trisulphides with linear and acyclic isoprenoid carbon skeletons in immature sediments. *Geochim. Cosmochim. Acta* **55**, 3685-3695.

Kohnen M.E.L., Sinninghe Damsté J.S., Kock-van Dalen A.C. and de Leeuw J.W. (1991b) Di- or polysulphide-bound biomarkers in sulphur-rich geomacromolecules as revealed by selective chemolysis. *Geochim. Cosmochim. Acta* **55**, 1375-1394.

Kohnen M.E.L., Sinninghe Damsté J.S. and de Leeuw J.W. (1991c) Biases from natural sulphurization in palaeoenvironmental reconstruction based on hydrocarbon biomarker distributions. *Nature* **349**, 775-778.

Kohnen M.E.L., Schouten S., Sinninghe Damsté J.S., de Leeuw J.W., Merritt D.A. and Hayes J.M. (1992a) Recognition of paleobiochemicals by a combined molecular sulfur and isotope geochemical approach. *Science* **256**, 358-362.

Kohnen M.E.L., Schouten S., Sinninghe Damsté J.S., de Leeuw J.W., Merritt D.A. and Hayes J.M. (1992b) The combined application of organic sulphur and isotope geochemistry to assess multiple sources of palaeobiochemicals with identical carbon skeletons. In *Advances in Organic Geochemistry 1991* (Edited by C.B. Eckardt, J.R. Maxwell, S.R. Larter and D.A.C. Manning), *Org. Geochem.* **19**, 403-419.

Kohnen M.E.L., Sinninghe Damsté J.S., Baas M., Kock-van Dalen A.C. and de Leeuw J.W. (1993) Sulphur-bound steroid and phytane carbon skeletons in geomacromolecules: Implications for the mechanism of incorporation of sulphur into organic matter. *Geochim. Cosmochim. Acta* **57**, 2515-2528.

König W.A., Gehrcke B., Runge T. and Wolf C. (1993) Gas chromatographic separation of atropisomeric alkylated and polychlorinated biphenyls using modified cyclodextrins. *J. High Res. Chrom.* **16**, 376-378.

Koopmans M.P., Sinninghe Damsté J.S., Lewan M.D. and de Leeuw J.W. (1995) Thermal stability of thiophene biomarkers as studied by hydrous pyrolysis. *Org. Geochem.* **23**, 583-596.

Koopmans M.P., Köster J., van Kaam-Peters H.M.E., Kenig F., Schouten S., Hartgers W.A., de Leeuw J.W. and Sinninghe Damsté J.S. (1996a) Diagenetic and catagenetic products of isorenieratene: Molecular indicators for photic zone anoxia. *Geochim. Cosmochim. Acta* **60**, 4467-4496.

Koopmans M.P., de Leeuw J.W., Lewan M.D. and Sinninghe Damsté J.S. (1996b) Impact of dia- and catagenesis on sulphur and oxygen sequestration of biomarkers as revealed by artificial maturation of an immature sedimentary rock. *Org. Geochem.* Accepted.

Koopmans M.P., Schouten S., Kohnen M.E.L. and Sinninghe Damsté J.S. (1996c) Restricted utility of aryl isoprenoids as indicators for photic zone anoxia. *Geochim. Cosmochim. Acta* **60**, 4873-4876.

Koopmans M.P., de Leeuw J.W. and Sinninghe Damsté J.S. (1997a) Novel cyclised and aromatised diagenetic products of β-carotene in the Green River Shale. *Org. Geochem.* Submitted.

Koopmans M.P., Schaeffer-Reiss C., de Leeuw J.W., Lewan M.D., Maxwell J.R., Schaeffer P. and Sinninghe Damsté J.S. (1997b) Sulphur and oxygen sequestration of n-C_{37} and n-C_{38} unsaturated ketones in an immature kerogen and the release of their carbon skeletons during early stages of thermal maturation. *Geochim. Cosmochim. Acta.* Submitted.

Koopmans M.P., Rijpstra W.I.C., Klapwijk M.M., de Leeuw J.W., Lewan M.D. and Sinninghe Damsté J.S. (1997c) A thermal and chemical degradation approach to decipher pristane and phytane precursors in sedimentary organic matter. In preparation.

Koopmans M.P., Rijpstra W.I.C., de Leeuw J.W., Lewan M.D. and Sinninghe Damsté J.S. (1997d) Artificial maturation of an immature sulphur- and organic-rich limestone from the Ghareb Formation, Jordan. *Org. Geochem.* Submitted.

Köster J., Wehner H. and Hufnagel H. (1988) Organic geochemistry and organic petrology of organic rich sediments within the 'Hauptdolomit' formation (Triassic, Norian) of the Northern Calcareous Alps. In *Advances in Organic Geochemistry 1987* (Edited by L. Mattavelli and L. Novelli), *Org. Geochem.* **13**, 377-386.

Köster J., Rospondek M., Zubzycki A., Kolouba M., de Leeuw J.W. and Sinninghe Damsté J.S. (1995a) A molecular organic geochemical study of black shales associated with diatomites from the Oligocene Menilite Shale (Flysch Carpathians, SE Poland). In *Organic Geochemistry: Developments and Applications to Energy,*

Climate, Environment and Human History (Edited by J.O. Grimalt *et al.*), pp. 87-89. A.I.G.O.A., San Sebastian.

Köster J., Schouten S., Sinninghe Damsté J.S. and de Leeuw J.W. (1995b) Reconstruction of the depositional environment of Toarcian marlstones (Allgäu Formation, Tyrol/Austria) using biomarkers and compound specific carbon isotope analysis. In *Organic Geochemistry: Developments and Applications to Energy, Climate, Environment and Human History* (Edited by J.O. Grimalt *et al.*), pp. 76-78. A.I.G.O.A., San Sebastian.

Köster J., van Kaam-Peters H.M.E., Koopmans M.P., de Leeuw J.W. and Sinninghe Damsté J.S. (1997) Sulphurisation of homohopanoids: Effects on carbon number distribution, speciation and 22S/22R epimer ratios. *Geochim. Cosmochim. Acta.* Submitted.

Krein E.B. and Aizenshtat Z. (1994) The formation of isoprenoid sulfur compounds during diagenesis: Simulated sulfur incorporation and thermal transformation. *Org. Geochem.* **21**, 1015-1025.

Krein E.B. and Aizenshtat Z. (1995) Proposed thermal pathways for sulfur transformations in organic macromolecules: Laboratory simulation experiments. In *Geochemical Transformations of Sedimentary Sulfur* (Edited by M.A. Vairavamurthy and M.A.A. Schoonen), *ACS Symposium Series 612*, pp. 110-137. Amer. Chem. Soc., Washington.

Kuhn R. and Winterstein A. (1933) Ketten-Verkürzung und Cyclisierung beim thermischen Abbau natürlicher Polyen-Farbstoffe. *Ber. Deut. Chem. Ges.* **66**, 1733-1741.

Landais P., Michels R., Poty B. and Monthioux M. (1989) Pyrolysis of organic matter in cold-seal pressure autoclaves. Experimental approach and applications. *J. Anal. Appl. Pyrol.* **16**, 103-115.

Larter S.R. (1984) Application of analytical pyrolysis techniques to kerogen characterization and fossil fuel exploration/exploitation. In *Analytical Pyrolysis: Techniques and Applications* (Edited by K.J. Voorhees), pp. 212-275. Butterworths, London.

de Leeuw J.W., van der Meer F.W., Rijpstra W.I.C. and Schenck P.A. (1980) On the occurrence and structural identification of long chain unsaturated ketones and hydrocarbons in sediments. In *Advances in Organic Geochemistry 1979* (Edited by A.G. Douglas and J.R. Maxwell), pp. 211-217. Pergamon Press, Oxford.

de Leeuw J.W., Rijpstra W.I.C. and Schenck P.A. (1981) The occurrence of C_{30}, C_{31} and C_{32} alkan-1,15-diols and alkan-15-one-1-ols in Unit I and Unit II of Black Sea sediments. *Geochim. Cosmochim. Acta* **45**, 2281-2285.

Leif R.N. and Simoneit B.R.T. (1995) Ketones in hydrothermal petroleums and sediment extracts from Guaymas Basin, Gulf of California. *Org. Geochem.* **23**, 889-904.

Lewan M.D. (1983) Effects of thermal maturation on stable organic carbon isotopes as determined by hydrous pyrolysis of Woodford Shale. *Geochim. Cosmochim. Acta* **47**, 1471-1479.

Lewan M.D. (1985) Evaluation of petroleum generation by hydrous pyrolysis experimentation. *Phil. Trans. R. Soc. Lond. A* **315**, 123-134.

Lewan M.D. (1993a) Identifying and understanding suppressed vitrinite reflectance through hydrous pyrolysis experiments. *Tenth Annual Meeting of the Society for Organic Petrology, Abstracts and Program*, v. 10, pp. 1-3.

Lewan M.D. (1993b) Laboratory simulation of petroleum formation: Hydrous pyrolysis. In *Organic Geochemistry: Principles and Applications* (Edited by M.H. Engel and S.A. Macko), pp. 419-442. Plenum Press, New York.

Lewan M.D. (1997) Experiments on the role of water in petroleum formation. *Geochim. Cosmochim. Acta*. Submitted.

Lewan M.D., Winters J.C. and MacDonald J.H. (1979) Generation of oil-like pyrolysates from organic-rich shales. *Science* **203**, 897-899.

Lewan M.D., Bjorøy M. and Dolcater D.L. (1986) Effects of thermal maturity on steroid hydrocarbons as determined by hydrous pyrolysis of Phosphoria Retort Shale. *Geochim. Cosmochim. Acta* **50**, 1977-1987.

Li M., Larter S.R., Taylor P., Jones D.M., Bowler B. and Bjorøy M. (1995) Biomarkers or not biomarkers? A new hypothesis for the origin of pristane involving derivation from methyltrimethyltridecylchromans (MTTCs) formed during diagenesis from chlorophyll and alkylphenols. *Org. Geochem.* **23**, 159-167.

Liaaen-Jensen S. (1965) Bacterial carotenoids. XVIII. Aryl-carotenes from *Phaeobium*. *Acta Chem. Scand.* **19**, 1025-1030.

Liaaen-Jensen S. (1978a) Chemistry of carotenoid pigments. In *The Photosynthetic Bacteria* (Edited by R.K. Clayton and W.R. Sistrom), pp. 233-247. Plenum Press, New York.

Liaaen-Jensen S. (1978b) Marine carotenoids. In *Marine Natural Products* (Edited by D.J. Faulkner and W.H. Fenical), pp. 1-73. Academic Press, New York.

Liaaen-Jensen S. (1990) Artifacts of natural carotenoids - Unintended carotenoid synthesis. In *Carotenoid Chemistry and Biology* (Edited by N.I. Krinsky, M.M. Matthews-Roth and R.F. Taylor), pp. 149-165. Plenum, New York.

Ling C.C.K. and Harris M.M. (1964) The mechanism of racemisation of 2,2'-di-iodobiphenyl. *J. Chem. Soc.*, 1825-1835.

Mackenzie A.S. (1984) Applications of biological markers in petroleum geochemistry. In *Advances in Petroleum Geochemistry Vol. 1* (Edited by J. Brooks and D. Welte), pp. 115-214. Academic Press, London.

Mackenzie A.S., Patience R.L., Maxwell J.R., Vandenbroucke M. and Durand B. (1980) Molecular parameters of maturation in the Toarcian shales, Paris Basin, France - I. Changes in the configurations of acyclic isoprenoid alkanes, steranes and triterpanes. *Geochim. Cosmochim. Acta* **44**, 1709-1721.

Mackenzie A.S., Hoffmann C.F. and Maxwell J.R. (1981a) Molecular parameters of maturation in the Toarcian shales, Paris Basin, France - III. Changes in aromatic steroid hydrocarbons. *Geochim. Cosmochim. Acta* **45**, 1345-1355.

Mackenzie A.S., Lewis C.A. and Maxwell J.R. (1981b) Molecular parameters of maturation in the Toarcian shales, Paris Basin, France - IV. Laboratory thermal alteration studies. *Geochim. Cosmochim. Acta* **45**, 2369-2376.

March J. (1985) *Advanced Organic Chemistry: Reactions, Mechanisms, and Structure*. John Wiley & Sons, Inc., New York.

Marlowe I.T., Brassell S.C., Eglinton G. and Green J.C. (1984) Long chain unsaturated ketones and esters in living algae and marine sediments. In *Advances in Organic Geochemistry 1983* (Edited by P.A. Schenck, J.W. de Leeuw and G.W.M. Lijmbach), *Org. Geochem.* **6**, 135-141.

Marlowe I.T., Brassell S.C., Eglinton G. and Green J.C. (1990) Long-chain alkenones and alkyl alkenoates and the fossil coccolith record of marine sediments. *Chem. Geol.* **88**, 349-375.

Martin R.L., Winters J.C. and Williams J.A. (1963) Composition of crude oils by gas chromatography: Geological significance of hydrocarbon distribution. *Proc. 6th World Petr. Cong., Frankfurt* **5**, 231-260.

McCaffrey M.A., Simoneit B.R.T., Aquino Neto F.R. and Moldowan J.M. (1994) Functionalized biological precursors of tricyclic terpanes: Information from sulfur-bound biomarkers in a Permian Tasmanite. *Org. Geochem.* **21**, 481-487.

McCracken A.D. and Nowlan G.S. (1989) Conodont paleontology and biostratigraphy of Ordovician carbonates and petroliferous carbonates on Southampton, Baffin, and Akpatok islands in the eastern Canadian Arctic. *Can. J. Earth Sci.* **26**, 1880-1903.

McLafferty F.W. and Stauffer D.B. (1989) *The Wiley/NBS Registry of Mass Spectral Data, Vol. 1.* Wiley, New York.

van de Meent D., Brown S.C., Philp R.P. and Simoneit B.R.T. (1980) Pyrolysis-high resolution gas chromatography and pyrolysis gas chromatography-mass spectrometry of kerogens and kerogen precursors. *Geochim. Cosmochim. Acta* **44**, 999-1013.

Mello M.R., Telnæs N., Gaglianone P.C., Chicarelli M.I., Brassell S.C. and Maxwell J.R. (1988) Organic geochemical characterisation of depositional palaeoenvironments of source rocks and oils in Brazilian marginal basins. In *Advances in Organic Geochemistry 1987* (Edited by L. Mattavelli and L. Novelli), *Org. Geochem.* **13**, 31-45.

Michaelis W. and Albrecht P. (1979) Molecular fossils of archaebacteria in kerogen. *Naturwissenschaften* **66**, 420-422.

Michels R., Landais P., Philp R.P. and Torkelson B.E. (1995) Influence of pressure and the presence of water on the evolution of the residual kerogen during confined, hydrous, and high-pressure hydrous pyrolysis of Woodford Shale. *Energy Fuels* **9**, 204-215.

Mislow K. (1966) *Introduction to Stereochemistry.* W.A. Benjamin, Inc., New York.

Moldowan J.M., Lee C.Y., Sundararaman P., Salvatori T., Alajbeg A., Gjukic B., Demaison G.J., Slougui N.-E. and Watt D.S. (1992) Source correlation and maturity assessment of select oils and rocks from the Central Adriatic Basin (Italy and Yugoslavia). In *Biological Markers in Sediments and Petroleum* (Edited by J.M. Moldowan, P. Albrecht and R.P. Philp), pp. 370-401. Prentice Hall, Englewood Cliffs.

Monthioux M. (1988) Expected mechanisms in nature and in confined-system pyrolysis. *Fuel* **67**, 843-847.

Monthioux M., Landais P. and Monin J.-C. (1985) Comparison between natural and artificial maturation series of humic coals from the Mahakam delta, Indonesia. *Org. Geochem.* **8**, 275-292.

Monthioux M., Landais P. and Durand B. (1986) Comparison between extracts from natural and artificial maturation series of Mahakam delta coals. In *Advances in Organic Geochemistry 1985* (Edited by D. Leythaeuser and J. Rullkötter), *Org. Geochem.* **10**, 299-311.

Morris R.J. and Brassell S.C. (1988) Long-chain alkanediols: Biological markers for cyanobacterial contributions to sediments. *Lipids* **23**, 256-258.

Murphy M.T.J., McCormick A. and Eglinton G. (1967) Perhydro-β-carotene in the Green River Shale. *Science* **157**, 1040-1042.

Mycke B., Narjes F. and Michaelis W. (1987) Bacteriohopanetetrol from chemical degradation of an oil shale kerogen. *Nature* **326**, 179-181.

Navale V. (1992) A study of chemical transformation of glycerol ether lipids to hydrocarbons by flash and hydrous pyrolysis. *J. Anal. Appl. Pyrol.* **23**, 121-133.

Navale V. (1994) Comparative study of low and high temperature hydrous pyrolysis products of monoglyceryl diether lipid from archaebacteria. *J. Anal. Appl. Pyrol.* **29**, 33-43.

Nelson B.C., Eglinton T.I., Seewald J.S., Vairavamurthy A. and Miknis F.P. (1995) Transformations in organic sulphur speciation during maturation of Monterey Shale: Constraints from laboratory experiments. In *Geochemical Transformations of Sedimentary Sulfur* (Edited by M.A. Vairavamurthy and M.A.A. Schoonen), *ACS Symposium Series 612*, pp. 138-166. Amer. Chem. Soc., Washington.

O'Mara M.M. (1977) Combustion of PVC. *Pure & Appl. Chem.* **49**, 649-660.

Orr W.L. (1986) Kerogen/asphaltene/sulfur relationships in sulfur-rich Monterey oils. *Org. Geochem.* **10**, 499-516.

Oschmann W. (1991) Distribution, dynamics and palaeoecology of Kimmeridgian (Upper Jurassic) shelf anoxia in Western Europe. In *Modern and Ancient Continental Shelf Anoxia* (Edited by R.V. Tyson and T.H. Pearson), pp. 381-395. Geological Society Special Publication No. 58. The Geological Society, London.

Ostroukhov S.B., Arefev O.A., Makushina V.M., Zabrodina M.N. and Petrov Al.A. (1982) Monocyclic aromatic hydrocarbons with isoprenoid chains. *Neftekhimiya* **22**, 723-788. In Russian.

Ourisson G., Albrecht P. and Rohmer M. (1982) Predictive microbial biochemistry - from molecular fossils to procaryotic membranes. *Trends Biochem. Sci.* **7**, 236-239.

Overmann J., Cypionka H. and Pfennig N. (1992) An extremely low-light-adapted phototrophic sulfur bacterium from the Black Sea. *Limnol. Oceanogr.* **37**, 150-155.

Payzant J.D., Montgomerey D.S. and Strausz O.P. (1983) Novel terpenoid sulfoxides and sulfides in petroleum. *Tetrahedron Lett.* **24**, 651-654.

Payzant J.D., Cyr T.D., Montgomerey D.S. and Strausz O.P. (1988) Studies on the structure of the terpenoid sulfide type biological markers in petroleum. In *Geochemical Biomarkers* (Edited by T.F. Yen and J.M. Moldowan), pp. 133-147. Harwood Academic Publishers, Chur.

Peakman T.M., ten Haven H.L., Rechka J.R., de Leeuw J.W. and Maxwell J.R. (1989) Occurrence of (20R)- and (20S)-$\Delta^{8(14)}$ and Δ^{14} 5α(H)-sterenes and the origin of 5α(H),14β(H),17β(H)-steranes in an immature sediment. *Geochim. Cosmochim. Acta* **53**, 2001-2009.

Pedersen T.F. and Calvert S.E. (1990) Anoxia vs. productivity: What controls the formation of organic-carbon-rich sediments and sedimentary rocks? *A.A.P.G. Bull.* **74**, 454-466.

Peters K.E. and Moldowan J.M. (1993) *The Biomarker Guide: Interpreting Molecular Fossils in Petroleum and Ancient Sediments.* Prentice Hall, New Jersey.

Peters K.E., Moldowan J.M., Driscole A.R. and Demaison G.J. (1989) Origin of Beatrice oil by co-sourcing from Devonian and Middle Jurassic source rocks, Inner Moray Firth, United Kingdom. *A.A.P.G. Bull.* **73**, 454-471.

Peters K.E., Moldowan J.M. and Sundararaman P. (1990) Effects of hydrous pyrolysis on biomarker thermal maturity parameters: Monterey phosphatic and siliceous members. *Org. Geochem.* **15**, 249-265.

Philp R.P., Gilbert T.D. and Russell N.J. (1982) Characterization by pyrolysis-gas chromatography-mass spectrometry of the insoluble organic residues derived from the hydrogenation of *Tasmanites* sp. oil shale. *Fuel* **61**, 221-226.

Philp R.P., Chen J.H., Fu J.M. and Sheng G.Y. (1992) A geochemical investigation of crude oils and source rocks from Biyang Basin, China. *Org. Geochem.* **18**, 933-945.

Powell T.G. and McKirdy D.M. (1973) Relationship between ratio of pristane to phytane, crude oil composition and geological environment in Australia. *Nature* **243**, 37-39.

Prahl F.G. and Wakeham S.G. (1987) Calibration of unsaturation patterns in long-chain ketone compositions for palaeotemperature assessment. *Nature* **330**, 367-369.

Prahl F.G., Muehlhausen L.A. and Zahnle D.L. (1988) Further evaluation of long-chain alkenones as indicators of paleoceanographic conditions. *Geochim. Cosmochim. Acta* **52**, 2303-2310.

Prahl F.G., de Lange G.J., Lyle M. and Sparrow M.A. (1989) Post-depositional stability of long-chain alkenones under contrasting redox conditions. *Nature* **341**, 434-437.

Quandt I., Gottschalk G., Ziegler H. and Stichler W. (1977) Isotope discrimination by photosynthetic bacteria. *FEMS Microbiol. Lett.* **1**, 125-128.

Radke M., Schaeffer R.G. and Leythaeuser D. (1980) Composition of soluble organic matter in coals: Relation to rank and liptinite fluorescence. *Geochim. Cosmochim. Acta* **44**, 1787-1800.

Rashid M.A. (1979) Pristane-phytane ratios in relation to source and diagenesis of ancient sediments from the Labrador Shelf. *Chem. Geol.* **25**, 109-122.

Rechka J.A. and Maxwell J.R. (1988a) Characterisation of alkenone temperature indicators in sediments and organisms. In *Advances in Organic Geochemistry 1987* (Edited by L. Mattavelli and L. Novelli), *Org. Geochem.* **13**, 727-734.

Rechka J.A. and Maxwell J.R. (1988b) Unusual long chain ketones of algal origin. *Tetrahedron Lett.* **29**, 2599-2600.

Regtop R.A., Crisp P.T., Ellis J. and Fookes C.J.R. (1986) 1-Pristene as a precursor for 2-pristene in pyrolysates of oil shale from Condor, Australia. *Org. Geochem.* **9**, 233-236.

Repeta D.J. (1989) Carotenoid diagenesis in recent marine sediments: II. Degradation of fucoxanthin to loliolide. *Geochim. Cosmochim. Acta* **53**, 699-707.

Repeta D.J. (1993) A high resolution historical record of Holocene anoxygenic primary production in the Black Sea. *Geochim. Cosmochim. Acta* **57**, 4337-4342.

Repeta D.J., Simpson D.J., Jorgensen B.B. and Jannasch H.W. (1989) Evidence for anoxygenic photosynthesis from the distribution of bacteriochlorophylls in the Black Sea. *Nature* **342**, 69-72.

Requejo A.G. (1994) Maturation of petroleum source rocks - II. Quantitative changes in extractable hydrocarbon content and composition associated with hydrocarbon generation. *Org. Geochem.* **21**, 91-105.

Requejo A.G., Allan J., Creany S., Gray N.R. and Cole K.S. (1992) Aryl isoprenoids and diaromatic carotenoids in Paleozoic source rocks and oils from the Western Canada and Williston basins. *Org. Geochem.* **19**, 245-264.

Requejo A.G., Sassen R., Kennicutt II M.C., Kvedchuk I., McDonald T., Denoux G., Comet P. and Brooks J.M. (1995) Geochemistry of oils from the northern Timan-Pechora Basin, Russia. *Org. Geochem.* **23**, 205-222.

Revill A.T., Volkman J.K., O'Leary T., Summons R.E., Boreham C.J., Banks M.R. and Denwer K. (1994) Hydrocarbon biomarkers, thermal maturity, and depositional setting of tasmanite oil shales from Tasmania, Australia. *Geochim. Cosmochim. Acta* **58**, 3803-3822.

Ricci M.P., Merritt D.A., Freeman K.H. and Hayes J.M. (1994) Acquisition and processing of data for isotope-ratio-monitoring mass spectrometry. *Org. Geochem.* **21**, 561-571.

Richnow H.H., Jenisch A. and Michaelis W. (1992) Structural investigations of sulphur-rich macromolecular oil fractions and a kerogen by *sequential* chemical degradation. In *Advances in Organic Geochemistry 1991* (Edited by C.B. Eckardt, J.R. Maxwell, S.R. Larter and D.A.C. Manning), *Org. Geochem.* **19**, 351-370.

Richnow H.H., Jenisch A. and Michaelis W. (1993) The chemical structure of macromolecular fractions of a sulfur-rich oil. *Geochim. Cosmochim. Acta* **57**, 2767-2780.

Risatti J.B., Rowland S.J., Yon D.A. and Maxwell J.R. (1984) Stereochemical studies of acyclic isoprenoids - XII. Lipids of methanogenic bacteria and possible contributions to sediments. In *Advances in Organic Geochemistry 1983* (Edited by P.A. Schenck, J.W. de Leeuw and G.W.M. Lijmbach), *Org. Geochem.* **6**, 93-104.

de Rosa M. and Gambacorta M. (1988) The lipids of archaebacteria. *Prog. Lipid Res.* **27**, 153-175.

Rowland S.J. (1990) Production of acyclic isoprenoid hydrocarbons by laboratory maturation of methanogenic bacteria. *Org. Geochem.* **15**, 9-16.

Rowland S.J. and Volkman J.K. (1982) Biogenic and pollutant aliphatic hydrocarbons in *Mytilus edulis* from the North Sea. *Mar. Environ. Res.* **7**, 117-130.

Rowland S.J., Rockey C., Al-Lihaibi S.S. and Wolff G.A. (1993) Incorporation of sulphur into phytol derivatives during simulated early diagenesis. *Org. Geochem.* **20**, 1-5.

Ruble T.E., Bakel A.J. and Philp R.P. (1994) Compound specific isotopic variability in Uinta Basin native bitumens: Paleoenvironmental implications. *Org. Geochem.* **21**, 661-671.

Rullkötter J. and Michaelis W. (1990) The structure of kerogen and related materials. A review of recent progress and future trends. In *Advances in Organic Geochemistry 1989* (Edited by B. Durand and F. Behar), *Org. Geochem.* **16**, 829-852.

Rullkötter J., Aizenshtat Z. and Spiro B. (1984) Biological markers in bitumens and pyrolyzates of Upper Cretaceous bituminous chalks from the Ghareb Formation (Israel). *Geochim. Cosmochim. Acta* **48**, 151-157.

Rullkötter J., Landgraf M. and Disko U. (1988) Gas chromatographic and mass spectrometric characterization of isomeric alkylthiophenes (C_{20}) and their occurrence in deep sea sediments. *J. High Res. Chrom. Chrom. Commun.* **11**, 633-638.

Rullkötter J., Littke R. and Schaefer R.G. (1990) Characterization of organic matter in sulfur-rich lacustrine sediments of Miocene age (Nördlinger Ries, southern Germany). In *Geochemistry of Sulfur in Fossil Fuels* (Edited by W.L. Orr and C.M. White), *ACS Symposium Series 249*, pp. 149-169. Amer. Chem. Soc., Washington.

Safe S. and Hutzinger O. (1971) Chlorine randomization between phenyl groups in the electron impact-induced fragmentation of polychlorinated biphenyls. *J. Chem. Soc., Chem. Comm.*, 446-448.

Safe S. and Hutzinger O. (1972) The mass spectra of polychlorinated biphenyls. *J. Chem. Soc. Perkin I*, 686-691.

Safe S. and Hutzinger O. (1973) *Mass Spectrometry of Pesticides and Pollutants.* CRC Press, Cleveland.

Sanger J.E. (1988) Fossil pigments in paleoecology and paleolimnology. *Palaeogeogr. Palaeoclimatol. Palaeoecol.* **62**, 343-359.

Sauer J. and Sustmann R. (1980) Mechanistische Aspekte der Diels-Alder-Reaktion: Ein kritischer Rückblick. *Angew. Chem.* **92**, 773-801.

Saxby J.D., Bennett A.J.R., Corcoran J.F., Lambert D.E. and Riley K.W. (1986) Petroleum generation: Simulation over six years of hydrocarbon formation from torbanite and brown coal in a subsiding basin. *Org. Geochem.* **9**, 69-81.

Schaeffer P., Harrison W.N., Keely B.J. and Maxwell J.R. (1995a) Product distributions from chemical degradation of kerogens from a marl from a Miocene evaporitic sequence (Vena del Gesso, N. Italy). *Org. Geochem.* **23**, 541-554.

Schaeffer P., Reiss C. and Albrecht P. (1995b) Geochemical study of macromolecular organic matter from sulfur-rich sediments of evaporitic origin (Messinian of Sicily) by chemical degradations. *Org. Geochem.* **23**, 567-581.

Schaeflé J., Ludwig B., Albrecht P. and Ourisson G. (1977) Hydrocarbures aromatiques d'origine geologique. II. Nouveaux carotenoïdes aromatiques fossiles. *Tetrahedron Lett.* **41**, 3673-3676.

Scheer H. (1991) Structure and occurrence of chlorophylls. In *Chlorophylls* (Edited by H. Scheer), pp. 3-30. CRC Press, Boca Raton.

Schidlowski M., Matzigkeit U. and Krumbein W.E. (1984) Superheavy organic carbon from hypersaline microbial mats. Assimilatory pathway and geochemical implications. *Naturwissenschaften* **71**, 303-308.

Schmid J.C., Connan J. and Albrecht P. (1987) Identification of long-chain dialkylthiacyclopentanes in petroleum. *Nature* **329**, 54-56.

Schoell M., Hwang R.J., Carlson R.M.K. and Welton J.E. (1994) Carbon isotopic composition of individual biomarkers in gilsonites (Utah). *Org. Geochem.* **21**, 673-683.

Schouten S., van Driel G.B., Sinninghe Damsté J.S. and de Leeuw J.W. (1993) Natural sulphurization of ketones and aldehydes: A key reaction in the formation of organic sulphur compounds. *Geochim. Cosmochim. Acta* **57**, 5111-5116.

Schouten S., de Graaf W., Sinninghe Damsté J.S., van Driel G.B. and de Leeuw J.W. (1994) Laboratory simulation of natural sulphurization: II. Reaction of multi-functionalized lipids with inorganic polysulphides at low temperatures. In *Advances in Organic Geochemistry 1993* (Edited by N. Telnæs, G. van Graas and K. Øygard), *Org. Geochem.* **22**, 825-834.

Schouten S., Eglinton T.I., Sinninghe Damsté J.S. and de Leeuw J.W. (1995a) Influence of sulphur cross-linking on the molecular-size distribution of sulphur-rich macromolecules in bitumen. In *Geochemical Transformations of Sedimentary Sulfur* (Edited by M.A. Vairavamurthy and M.A.A. Schoonen), *ACS Symposium Series 612*, pp. 80-92. Amer. Chem. Soc., Washington.

Schouten S., Sinninghe Damsté J.S., Baas M., Kock-van Dalen A.C., Kohnen M.E.L. and de Leeuw J.W. (1995b) Quantitative assessment of mono- and polysulphide-linked carbon skeletons in sulphur-rich macromolecular aggregates present in bitumens and oils. *Org. Geochem.* **23**, 765-775.

Schouten S., Sinninghe Damsté J.S., Kohnen M.E.L. and de Leeuw J.W. (1995c) The effect of hydrosulphurisation on stable carbon isotopic compositions of free and sulphur-bound lipids. *Geochim. Cosmochim. Acta* **59**, 1605-1609.

Schouten S., Sinninghe Damsté J.S. and de Leeuw J.W. (1995d) A novel triterpenoid carbon skeleton in immature sulphur-rich sediments. *Geochim. Cosmochim. Acta* **59**, 953-958.

Schouten S., Sinninghe Damsté J.S. and de Leeuw J.W. (1995e) The occurrence and distribution of low-molecular-weight sulphoxides in polar fractions of sediment extracts and petroleum. *Org. Geochem.* **23**, 129-138.

Schouten S., Schoell M., Sinninghe Damsté J.S., Summons R.E. and de Leeuw J.W. (1996) Molecular biogeochemistry of Monterey sediments (Naples Beach, USA) II: Carbon isotopic compositions of free and sulphur-bound carbon skeletons. In *CMOGS volume* (Edited by C.M. Isaacs and J. Rullkötter), Columbia University Press. In press.

Schwark L. and Püttmann W. (1990) Aromatic hydrocarbon composition of the Permian Kupferschiefer in the Lower Rhine Basin, NW Germany. *Org. Geochem.* **16**, 749-761.

Seifert W.K. and Moldowan J.M. (1980) The effect of thermal stress on source-rock quality as measured by hopane stereochemistry. In *Advances in Organic Geochemistry 1979* (Edited by A.G. Douglas and J.R. Maxwell), pp. 229-237. Pergamon Press, Oxford.

Seifert W.K. and Moldowan J.M. (1986) Use of biological markers in petroleum exploration. In *Methods in Geochemistry and Geophysics Vol. 24* (Edited by R.B. Johns), pp. 261-290. Elsevier Science Publishers, Amsterdam.

Shaish A., Ben-Amotz A. and Avron M. (1992) Biosynthesis of β-carotene in *Dunaliella. Meth. Enzymol.* **213**, 439-444.

Shi Ji-Yang, Mackenzie A.S., Alexander R., Eglinton G., Gowar A.P., Wolff G.A. and Maxwell J.R. (1982) A biological marker investigation of petroleums and shales from the Shengli oilfield, the People's Republic of China. *Chem. Geol.* **35**, 1-31.

Sikes E.L. and Volkman J.K. (1993) Calibration of alkenone unsaturation ratios ($U_{37}^{k'}$) for paleotemperature estimation in cold polar waters. *Geochim. Cosmochim. Acta* **57**, 1883-1889.

Sinninghe Damsté J.S. and de Leeuw J.W. (1987) The origin and fate of C_{20} and C_{15} isoprenoid sulphur compounds in sediments and oils. *Int. J. Environ. Anal. Chem.* **28**, 1-19.

Sinninghe Damsté J.S. and de Leeuw J.W. (1990) Analysis, structure and geochemical significance of organically-bound sulphur in the geosphere: State of the art and future research. In *Advances in Organic Geochemistry 1989* (Edited by B. Durand and F. Behar), *Org. Geochem.* **16**, 1077-1101.

Sinninghe Damsté J.S., ten Haven H.L., de Leeuw J.W. and Schenck P.A. (1986) Organic geochemical studies of a Messinian evaporitic basin, northern Apennines (Italy) - II. Isoprenoid and *n*-alkyl thiophenes and thiolanes. In *Advances in Organic Geochemistry 1985* (Edited by D. Leythaeuser and J. Rullkötter), *Org. Geochem.* **10**, 791-805.

Sinninghe Damsté J.S., Kock-van Dalen A.C., de Leeuw J.W. and Schenck P.A. (1987a) The identification of 2,3-dimethyl-5-(2,6,10-trimethylundecyl)thiophene, a novel sulphur-containing biological marker. *Tetrahedron Lett.* **28**, 957-960.

Sinninghe Damsté J.S., Kock-van Dalen A.C., de Leeuw J.W., Schenck P.A., Sheng Guoying and Brassell S.C. (1987b) The identification of mono-, di- and trimethyl 2-methyl-2-(4,8,12-trimethyltridecyl)chromans and their occurrence in the geosphere. *Geochim. Cosmochim. Acta* **51**, 2393-2400.

Sinninghe Damsté J.S., de Leeuw J.W., Kock-van Dalen A.C., de Zeeuw M.A., de Lange F., Rijpstra W.I.C. and Schenck P.A. (1987c) The occurrence and identification of series of organic sulphur compounds in oils and sediment extracts I. A study of Rozel Point Oil (U.S.A.) *Geochim. Cosmochim. Acta* **51**, 2369-2391.

Sinninghe Damsté J.S., Kock-van Dalen A.C. and de Leeuw J.W. (1988a) Identification of long-chain isoprenoid alkylbenzenes in sediments and crude oils. *Geochim. Cosmochim. Acta* **52**, 2671-2677.

Sinninghe Damsté J.S., Rijpstra W.I.C., de Leeuw J.W. and Schenck P.A. (1988b) Origin of organic sulphur compounds and sulphur containing high molecular weight substances in sediments and immature crude oils. In *Advances in Organic Geochemistry 1987* (Edited by L. Mattavelli and L. Novelli), *Org. Geochem.* **13**, 593-606.

Sinninghe Damsté J.S., Eglinton T.I., de Leeuw J.W. and Schenck P.A. (1989a) Organic sulphur in macromolecular sedimentary organic matter: I. Structure and origin of sulphur-containing moieties in kerogen, asphaltenes and coal as revealed by flash pyrolysis. *Geochim. Cosmochim. Acta* **53**, 873-889.

Sinninghe Damsté J.S., van Koert E.R., Kock-van Dalen A.C., de Leeuw J.W. and Schenck P.A. (1989b) Characterisation of highly branched isoprenoid thiophenes occurring in sediments and immature crude oils. *Org. Geochem.* **14**, 555-567.

Sinninghe Damsté J.S., Rijpstra W.I.C., Kock-van Dalen A.C., de Leeuw J.W. and Schenck P.A. (1989c) Quenching of labile functionalised lipids by inorganic sulphur species: Evidence for the formation of sedimentary organic sulphur compounds at the early stages of diagenesis. *Geochim. Cosmochim. Acta* **53**, 1343-1355.

Sinninghe Damsté J.S., Rijpstra W.I.C., de Leeuw J.W. and Schenck P.A. (1989d) The occurrence and identification of series of organic sulphur compounds in oils and sediment extracts. II. Their presence in samples from hypersaline and non-hypersaline depositional environments and their possible application as source, palaeoenvironmental and maturity indicators. *Geochim. Cosmochim. Acta* **53**, 1323-1341.

Sinninghe Damsté J.S., Eglinton T.I., Rijpstra W.I.C. and de Leeuw J.W. (1990a) Characterization of organically bound sulfur in high-molecular-weight, sedimentary organic matter using flash pyrolysis and Raney Ni desulfurization. In *Geochemistry of Sulfur in Fossil Fuels* (Edited by W.L. Orr and C.M. White), *ACS Symposium Series 249*, pp. 486-528. Amer. Chem. Soc., Washington.

Sinninghe Damsté J.S., Kohnen M.E.L. and de Leeuw J.W. (1990b) Thiophenic biomarkers for palaeoenvironmental assessment and molecular stratigraphy. *Nature* **345**, 609-611.

Sinninghe Damsté J.S., Kock-van Dalen A.C., Albrecht P.A. and de Leeuw J.W. (1991) Identification of long-chain 1,2-di-*n*-alkylbenzenes in Amposta crude oil from the Tarragona Basin, Spanish Mediterranean: Implications for the origin and fate of alkylbenzenes. *Geochim. Cosmochim. Acta* **55**, 3677-3683.

Sinninghe Damsté J.S., Betts S.E., Ling Y., Hofmann P.M. and de Leeuw J.W. (1993a) Hydrocarbon biomarkers of different lithofacies of the Salt IV Formation of the Mulhouse Basin, France. *Org. Geochem.* **20**, 1187-1200.

Sinninghe Damsté J.S., Hartgers W.A., Baas M. and de Leeuw J.W. (1993b) Characterization of high-molecular-weight organic matter in marls of the Salt IV Formation of the Mulhouse Basin. *Org. Geochem.* **20**, 1237-1251.

Sinninghe Damsté J.S., Keely B.J., Betts S.E., Baas M., Maxwell J.R. and de Leeuw J.W. (1993c) Variations in abundances and distributions of isoprenoid chromans and long-chain alkylbenzenes in sediments of the Mulhouse Basin: A molecular sedimentary record of palaeosalinity. *Org. Geochem.* **20**, 1201-1215.

Sinninghe Damsté J.S., Wakeham S.G., Kohnen M.E.L., Hayes J.M. and de Leeuw J.W. (1993d) A 6,000-year sedimentary molecular record of chemocline excursions in the Black Sea. *Nature* **362**, 827-829.

Sinninghe Damsté J.S., van Duin A.C.T., Hollander D., Kohnen M.E.L. and de Leeuw J.W. (1995a) Early diagenesis of bacteriohopanepolyol derivatives: Formation of fossil homohopanoids. *Geochim. Cosmochim. Acta* **59**, 5141-5157.

Sinninghe Damsté J.S., Frewin N.L., Kenig F. and de Leeuw J.W. (1995b) Molecular indicators for palaeoenvironmental change in a Messinian evaporitic sequence (Vena del Gesso, Italy). I: Variations in extractable organic matter of ten cyclically deposited marl beds. *Org. Geochem.* **23**, 471-483.

Sinninghe Damsté J.S., Kenig F., Koopmans M.P., Köster J., Schouten S., Hayes J.M. and de Leeuw J.W. (1995c) Evidence for gammacerane as an indicator of water column stratification. *Geochim. Cosmochim. Acta* **59**, 1895-1900.

Sinninghe Damsté J.S., Köster J., Baas M., Koopmans M.P., van Kaam-Peters H.M.E., Geenevasen J.A.J. and Kruk C. (1995d) Cyclisation and aromatisation of carotenoids during sediment diagenesis. *J. Chem. Soc., Chem. Commun.*, 187-188.

Sinninghe Damsté J.S., Baas M., Koopmans M.P. and Geenevasen J.A.J. (1996) Cyclisation, aromatisation and expulsion reactions of β-carotene during sediment diagenesis. *J. Chem. Soc., Chem. Commun.* Submitted.

Sirevåg R. and Ormerod J.G. (1970) Carbon dioxide fixation in green sulphur bacteria. *Biochem. J.* **120**, 399-408.

Sirevåg R., Buchanan B.B., Berry J.A. and Troughton J.H. (1977) Mechanisms of CO_2 fixation in bacterial photosynthesis studied by the carbon isotope technique. *Arch. Microbiol.* **112**, 35-38.

Siskin M., Brons G., Katritzky A.R. and Balasubramanian M. (1990) Aqueous organic chemistry. 1. Aquathermolysis: Comparison with thermolysis in the reactivity of aliphatic compounds. *Energy Fuels* **4**, 475-482.

Smith J.W., Batts B.D. and Gilbert T.D. (1989) Hydrous pyrolysis of model compounds. *Org. Geochem.* **14**, 365-373.

Snowdon L.R. (1980) Petroleum source potential of the Boundary Creek Formation. *Bull. Can. Petr. Geol.* **28**, 46-58.

Stalker L., Farrimond P. and Larter S.R. (1994) Water as an oxygen source for the production of oxygenated compounds (including CO_2 precursors) during kerogen maturation. In *Advances in Organic Geochemistry 1993* (Edited by N. Telnæs, G. van Graas and K. Øygard), *Org. Geochem.* **22**, 477-486.

Starnes Jr. W.H. and Edelson D. (1979) Mechanistic aspects of the behaviour of molybdenum (VI) oxide as fire-retardant additive for poly(vinyl chloride). An interpretive review. *Macromolecules* **12**, 797-802.

Summons R.E. and Powell T.G. (1986) Chlorobiaceae in Palaeozoic seas revealed by biological markers, isotopes and geology. *Nature* **319**, 763-765.

Summons R.E. and Powell T.G. (1987) Identification of aryl isoprenoids in source rocks and crude oils: Biological markers for the green sulphur bacteria. *Geochim. Cosmochim. Acta* **51**, 557-566.

Summons R.E. and Powell T.G. (1992) Hydrocarbon composition of the Late Proterozoic oils of the Siberian Platform: Implications for the depositional environment of source rocks. In *Early Organic Evolution: Implications for Mineral and Energy Resources* (Edited by M. Schidlowski *et al.*), pp. 296-307. Springer-Verlag, Berlin.

Tegelaar E.W., de Leeuw J.W., Derenne S. and Largeau C. (1989) A reappraisal of kerogen formation. *Geochim. Cosmochim. Acta* **53**, 3103-3106.

Theilacker W. and Hopp R. (1959) Spaltung des Naphthidins und des 2.3.2'.3'-Tetramethylbenzidins in optische Antipoden. *Chem. Ber.* **92**, 2293-2301.

Thierstein H.R., Geitsenauer K.R. and Molfino B. (1977) Global synchroneity of late Quaternary coccolith datum levels: Validation by oxygen isotopes. *Geology* **5**, 400-404.

Tissot B.P., Califet-Debyser Y., Deroo G. and Oudin J.L. (1971) Origin and evolution of hydrocarbons in Early Toarcian shales, Paris Basin, France. *A.A.P.G. Bull.* **55**, 2177-2193.

Tomic J., Behar F., Vandenbroucke M. and Tang Y. (1995) Artificial maturation of Monterey kerogen (Type II-S) in a closed system and comparison with Type II kerogen: Implications on the fate of sulfur. *Org. Geochem.* **23**, 647-660.

Tribovillard N.-P., Gorin G.E., Belin S., Hopfgartner G. and Pichon R. (1992) Organic-rich biolaminated facies from a Kimmeridgian lagoonal environment in the French

Southern Jura mountains - A way of estimating accumulation rate variations. *Palaeogeogr., Palaeoclimatol., Palaeoecol.* **99**, 163-177.

Tüdös F., Kelen T., Nagy T.T. and Turcsányi B. (1974) Polymer-analogous reactions of polyenes in poly(vinyl chloride). *Pure & Appl. Chem.* **38**, 201-226.

Vai G.B. and Ricci Lucchi F. (1977) Algal crusts, autochtonous and clastic gypsum in a cannibalistic evaporite basin: A case history from the Messinian of Northern Apennines. *Sedimentology* **24**, 211-244.

Valisolalao J., Perakis N., Chappe B. and Albrecht P. (1984) A novel sulfur containing C_{35} hopanoid in sediments. *Tetrahedron Lett.* **25**, 1183-1186.

Vetter W., Englert G., Rigassi N. and Schwieter U. (1971) Spectroscopic methods. In *Carotenoids* (Edited by O. Isler), pp. 189-266. Birkhäuser Verlag, Basel.

Volkman J.K. and Maxwell J.R. (1986) Acyclic isoprenoids as biological markers. In *Biological Markers in the Sedimentary Record* (Edited by R.B. Johns), pp. 1-42. Elsevier, New York.

Volkman J.K., Eglinton G., Corner E.D.S. and Forsberg T.E.V. (1980a) Long chain alkenes and alkenones in the marine coccolithophorid *Emiliania huxleyi*. *Phytochemistry* **19**, 2619-2622.

Volkman J.K., Eglinton G., Corner E.D.S. and Sargent J.R. (1980b) Novel unsaturated straight chain C_{37}-C_{39} methyl and ethyl ketones in marine sediments and a coccolithophore *Emiliania huxleyi*. In *Advances in Organic Geochemistry 1979* (Edited by A.G. Douglas and J.R. Maxwell), pp. 219-227. Pergamon Press, Oxford.

Volkman J.K., Barrett S.M., Dunstan G.A. and Jeffrey S.W. (1992) C_{30}-C_{32} alkyl diols and unsaturated alcohols in microalgae of the class Eustigmatophyceae. *Org. Geochem.* **18**, 131-138.

Volkman J.K., Barrett S.M., Blackburn S.I. and Sikes E.L. (1995) Alkenones in *Gephyrocapsa oceanica*: Implications for studies of palaeoclimate. *Geochim. Cosmochim. Acta* **59**, 513-520.

Vorob'yeva N.S., Zemskova Z.K., Punanov V.G. and Petrov A.A. (1993) Higher carotinoid petroleum hydrocarbons. *Petrol. Chem.* **33**, 277-282.

Wakeham S.G. (1990) Algal and bacterial hydrocarbons in particulate organic matter and interfacial sediment of the Cariaco trench. *Geochim. Cosmochim. Acta* **54**, 1325-1336.

Wakeham S.G., Sinninghe Damsté J.S., Kohnen M.E.L. and de Leeuw J.W. (1995) Organic sulfur compounds formed during early diagenesis in Black Sea sediments. *Geochim. Cosmochim. Acta* **59**, 521-533.

Watts C.D., Maxwell J.R. and Kjøsen H. (1977) The potential of carotenoids as environmental indicators. In *Advances in Organic Geochemistry 1975* (Edited by R. Campos and J. Goñi), pp. 391-413. Enadimsa, Madrid.

Weres O., Newton A.S. and Tsao L. (1988) Hydrous pyrolysis of alkanes, alkenes, alcohols and ethers. *Org. Geochem.* **12**, 433-444.

Wignall P.B. (1994) *Black Shales*. Clarendon Press, Oxford.

Winters J.C., Williams J.A. and Lewan M.D. (1983) A laboratory study of petroleum generation by hydrouspyrolysis. In *Advances in Organic Geochemistry 1981* (Edited by M. Bjorøy *et al.*), pp. 524-533. Wiley, London.

de Wit R. and Caumette P. (1995) An overview of the brown-coloured isorenieratene-containing green sulphur bacteria (Chlorobiaceae). In *Organic Geochemistry: Developments and Applications to Energy, Climate, Environment and Human History* (Edited by J.O. Grimalt *et al.*), pp. 908-909. A.I.G.O.A., San Sebastian.

Wolf C. (1993) Synthese von chiralen o,o'-substituierten Biphenylen und Untersuchung ihrer Racemisierungsreaktionen mit der dynamischen Gaschromatographie. Diploma thesis, University of Hamburg.

Wolf C., König W.A. and Roussel C. (1995) Influence of substituents on the rotational energy barrier of atropisomeric biphenyls - Studies by polarimetry and dynamic gas chromatography. *Liebigs Ann.*, 781-786.

Yawanarajah S.R., Kruge M.A., Mastalerz M. and Sliwinski W. (1993) Organic geochemistry of Permian organic-rich sediments from the Sudetes area, SW Poland. *Org. Geochem.* **20**, 267-281.

Yu Xinke, Fan Pu and Philp R.P. (1990) Novel biomarkers found in South Florida Basin. *Org. Geochem.* **15**, 433-438.

ACKNOWLEDGEMENTS

I would like to take this opportunity to sincerely thank Jan de Leeuw and Jaap Sinninghe Damsté for their guidance, constructive criticism and stimulating advice during the past five years. I greatly appreciated the opportunity to take a three months leave to travel through China. Mike Lewan at the US Geological Survey in Denver guided me through the hydrous pyrolysis experiments. He and his family made sure my stay was a pleasant one, and I keep the warmest memories. I am indebted to Irene Rijpstra, who did much of the experimental work on the Ghareb Formation. Many thanks also to Marianne Baas, who isolated several sedimentary carotenoid derivatives. Finally, I would like to thank everybody who, one way or the other, lent a helping hand during my Ph.D. Thanks!

CURRICULUM VITAE

Martin Koopmans was born on Wednesday April 27, 1966 in Amsterdam. After finishing his secondary education ('ongedeeld Atheneum') at the Veenlanden College in Mijdrecht in 1984, he went to Amsterdam to study Chemistry at the Free University. He did a major in Physical Chemistry in the group of Prof. C.A. de Lange at the University of Amsterdam, and obtained his *Doctorandus* degree in May 1991. In January 1992, he started his research in the Organic Geochemistry group at the Delft University of Technology. He continued his work at the Netherlands Institute for Sea Research (NIOZ), Texel, first as 'onderzoeker in opleiding', and then as Postdoc. This thesis describes the results of his work at Delft and Texel.